AD-A079 757 OREGON UNIV EUGENE DEPT OF PHYSICS F/G 7/4
TURBULENCE AND STATISTICAL MECHANICS.(U)
NOV 79 R J DONNELLY AFOSR-76-2880
UNCLASSIFIED AFOSR-TR-79-1357 NL

1 OF 3
AD-
A079757

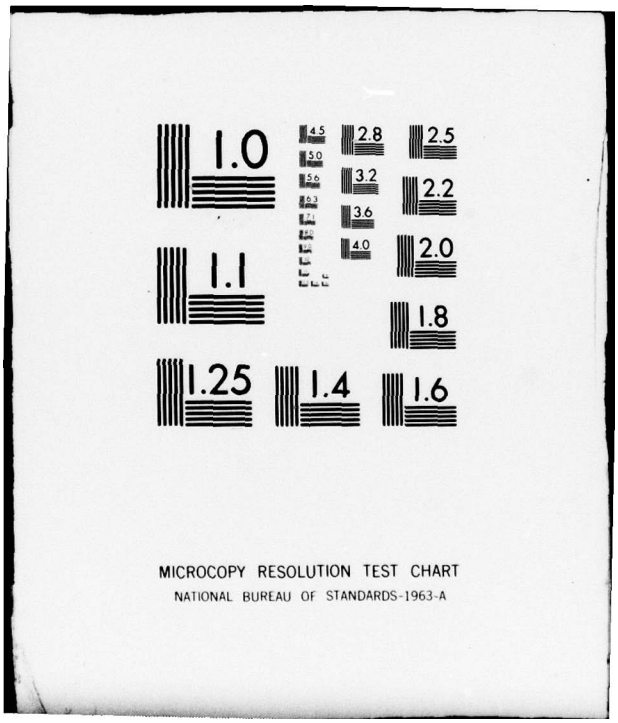
1.0
1.1
1.25
1.4
1.6
1.8
2.0
2.2
2.5
2.8
3.2
3.6
4.0
4.5
5.0
5.6
6.3
MICROCOPY RESOLUTION TEST CHART
NATIONAL BUREAU OF STANDARDS-1963-A

(19) REPORT DOCUMENTATION PAGE

READ INSTRUCTIONS BEFORE COMPLETING FORM

(18) 1. REPORT NUMBER: AFOSR-TR-79-1357

2. GOVT ACCESSION NO.

3. RECIPIENT'S CATALOG NUMBER

4. TITLE (and Subtitle)

(6) Turbulence and Statistical Mechanics,

5. TYPE OF REPORT & PERIOD COVERED
Final Report
July 1, '76 - Sept. 30, '79

6. PERFORMING ORG. REPORT NUMBER

7. AUTHOR(s)

(10) Russell J./Donnelly

8. CONTRACT OR GRANT NUMBER(s)

(15) AFOSR-76-2880

9. PERFORMING ORGANIZATION NAME AND ADDRESS
Department of Physics
University of Oregon
Eugene, OR 97403

10. PROGRAM ELEMENT, PROJECT, TASK AREA & WORK UNIT NUMBERS
(16) 61102F (17) 2301/A5

11. CONTROLLING OFFICE NAME AND ADDRESS
Air Force Office of Scientific Research/NP
Building 410, Bolling AFB
Washington, D.C. 20332

(11)

12. REPORT DATE
1 Nov[illegible]79

13. NUMBER OF PAGES
256

14. MONITORING AGENCY NAME & ADDRESS (if different from Controlling Office)

(12) 257

15. SECURITY CLASS. (of this report)
unclassified

15a. DECLASSIFICATION/DOWNGRADING SCHEDULE

16. DISTRIBUTION STATEMENT (of this Report)

Approved for public release;
distribution unlimited.

17. DISTRIBUTION STATEMENT (of the abstract entered in Block 20, if different from Report)

(9) Final rept. 1 Jul 76-30 Sep 79,

18. SUPPLEMENTARY NOTES

19. KEY WORDS (Continue on reverse side if necessary and identify by block number)

Superfluid, turbulence, helium II, quantized vortex lines, equations of motion, elementary excitations

20. ABSTRACT (Continue on reverse side if necessary and identify by block number)

This report summarized research during the period July 1, 1976 to October 1, 1979 directed to understanding turbulence in superfluid helium heat transport. This study showed, for the first time, how to create a reasonably homogeneous turbulent flow in a test section of a heat flow channel. The first systematic study of the power spectrum of turbulent fluctuations was completed. Several theoretical studies of helium II were also published, treating elementary excitations, temperature dependent energy levels, equations of motion and restricted geometries.

DD FORM 1 JAN 73 1473 EDITION OF 1 NOV 65 IS OBSOLETE

FINAL REPORT:

TURBULENCE AND STATISTICAL MECHANICS

Research supported by the Air Force Office of Scientific Research under grant number AFOSR-76-2880C from July 1, 1976 - September 30, 1979.

Report prepared by R. J. Donnelly
Department of Physics
University of Oregon, Eugene, Oregon 97403

October 29, 1979

TABLE OF CONTENTS

FINAL TECHNICAL REPORT

TURBULENCE AND STATISTICAL MECHANICS

The Physics of Fluids group at the University of Oregon has been fortunate in having research support from the Air Force Office of Scientific Research for a number of years. The period covered by this report is July 1, 1976 to September 30, 1979, during which time our grant was numbered AFOSR-76-2880.

The purpose of this brief introduction is to trace through the period of the grant several of the principal ideas that have guided our work. The body of this report consists of publications supported by AFOSR, with related publications added which round out our total activities and make the report more complete for the interested reader. On July 15, 1975 we issued the predecessor to this report which covered the period from January 1, 1971 to June 30, 1975. Obviously a number of ideas from that earlier period find their fulfilment in the present report.

I. EXPERIMENTAL RESEARCH ON LIQUID HELIUM

Turbulence in classical fluids is considered one of the greatest unsolved problems in physics and has been receiving a great deal of attention from the physics community. Years ago Feynman observed that quantized vortex lines in helium II might form a turbulent tangle. This was investigated experimentally by Vinen in a series of papers in the 1950's; moreover, Vinen proposed a simple theoretical model of this turbulence which is still in widespread use. Much of the quantitative work on turbulence in He II has been obtained in narrow channels by a number of investigators, particularly Tough and his collaborators. Wider channels have been the subject of more recent work by Northley, Moss and their students. Moss was the first to observe low frequency fluctuations in turbulent counterflow, which raised in our minds the hope that methods similar to those

used in classical turbulence might be used with helium II, including power spectra, phase and coherence measurements.

With direct cooperation from Professor Moss we established some experimental work in fluctuations in wide channel of both ion and second sound probes. We experienced considerable trouble in obtaining reproducible results with ion probes, and gradually turned our attention to second sound resonances in channels of size of order 1cm x 1cm x 10cm. The use of several transducer pairs along such a channel revealed that the attenuation of second sound, and hence the vortex line density was quite inhomogeneous--being considerably larger at the heater end than the open end of the channel. Efforts to smooth this inhomogeneity by means of grids such as in wind tunnels, were generally unsuccessful.

After many trials we finally found that a very long (1cm x 1cm x 40cm) channel had a reasonably homogeneous section near the middle. At the same time we became concerned about the accuracy of the continuous second sound resonance techniques we were using: how reliable is the attenuation information about the vortex line density local to the probe (about a $1cm^3$ volume) when the whole channel is in resonance?

The solution to the question above was to resort to a pulse technique which completely avoids the channel resonance problem. Preliminary results with this new technique, and a history of our earlier work with ion and second sound probes is contained in Michael Cromar's thesis:

"Turbulence in Helium II Counterflow in Wide Channels" by Michael William Cromar, Ph. D. thesis, University of Oregon, 1977 (unpublished).

The first published report was contained in the proceedings of LT15:

Reprint 1*: "Turbulent Counterflow: Vortex Line Density," R.M. Ostermeier, M.W. Cromar, P. Kittel and R. J. Donnelly, J. de Physique C6 Supp #8, Vol. 39 pp. 160-162, (1978).

*Reprints included in Appendix.

This was followed by a more complete account

Reprint 2: "Steady State Vortex-Line Density in Turbulent He II Counterflow," by R.M. Ostermeier, M.W. Cromar, P. Kittel and R. J. Donnelly, Phys. Rev. Lett. 41, 1123-1126 (1978).

The above papers have to do completely with equilibrium flow. The dynamical properties must include a description of fluctuations as well. We were able to modify the pulse technique in such a way as to allow a local measurement of low frequency fluctuations. This recently completed work is contained in

Reprint 3: "Fluctuations in Turbulent He II Counterflow," by R.M. Ostermeier, M.W. Cromar, P. Kittel and R. J. Donnelly (to be submitted).

II. RESEARCH ON THE EQUATIONS OF MOTION OF He II

Ultimately one believes that the description of turbulent flow must find some description from the equations of motion of the fluid. More than thirty years after Landau's original work the problem of the equations of motion of He II is still an open question. A statement of the question itself was included in our last AFOSR report in an Annual Review of Fluid Mechanics article by P.H. Roberts and R.J. Donnelly. The resolution of the question based on the most general principals of continuum mechanics has been considered by R.N. Hills and P.H. Roberts. Their work, still under active development, includes the effects of healing and relaxation missing in the original Landau-Khalatnikov treatment as well as addressing the problem of vortices in rotating helium II. Four contributions are included here:

Reprint 4: "Healing and Relaxation in Flows of Helium II - I; Generalization of Landau's Equations," by R.N. Hills and P.H. Roberts, Int. J. Engng. Sci. 15, pp. 305 - 316 (1977).

Reprint 5: "Healing and Relaxation in Flows of Helium II - II; First, Second and Fourth Found," by R.N. Hills and P.H. Roberts, J. Low Temp. Phys. 30, 709 - 727 (1978).

Reprint 6: "Healing and Relaxation in Flows of Helium II - III; Pure Superflow," by R.N. Hills and P.H. Roberts, J. Phys. C. 11, 4485-4499 (1978).

Reprint 7: "Superfluid Mechanics for a High Density of Vortex Lines," by R.N. Hills and P.H. Roberts, Archive for Rational Mechanics and Analysis 66, 43-71 (1977)

Actual calculation of the predictions of these theories requires a precise knowledge of the thermodynamics and elementary excitation spectrum of He II at all temperatures and pressures. The calculation of the healing length, for example, requires knowledge of the free energy of helium II evaluated at non-equilibrium values of e_s . The way in which this is done is described in

Reprint 8: "Calculation of the Static Healing Length in Helium II;" by P.H. Roberts, R.N. Hills and R.J. Donnelly, Physics Letters 70A, 437-440 (1979).

III. Research on the Thermodynamic Properties of HeII

The development of precise data on HeII discussed above has been a long-time concern to our group. Not only is the data sometimes hard to find, it is important for many purposes to know how to integrate over the excitation spectrum to calculate new quantities, such as the healing length described in Reprint 8 above. For temperatures above 1K, however, nearly all quantities of interest in the excitation spectrum are both pressure-and temperature-dependent. The simple statistical mechanics of non-interacting excitations cannot be used to calculate thermodynamic properties and new expressions had to be found. The method and final expressions for handling this problem are discussed in

Reprint 9: "A Theory of Temperature-Dependent Energy Levels: Thermodynamic Properties of HeII," by Russell J. Donnelly and Paul H. Roberts, J. Low Temp. Phys. 27, 687-736 (1977).

The direct application of this theory to the calculated thermodynamic properties of He II resulted in extensive sets of tables:

Reprint 10: "The Calculated Thermodynamic Properties of Superfluid Helium-4" by J.S. Brooks and R.J. Donnelly, J. Phys. Chem. Ref. Data 6, 51-104 (1977).

The preparation of these tables pointed up the problem of the absence of data in a number of regions of temperature and pressure, particularly below 1K. New experiments on thermodynamics and inelastic neutron scattering were called for:

Reprint 11: "Need for More Precise Thermodynamic and Neutron Scattering Data on Liquid Helium," by R.J. Donnelly and P.H. Roberts, J. Phys. C. 10, L683-L685 (1977).

IV. Theories of Elementary Excitations in He II.

The properties of ^{3}He-^{4}He solutions form a vast area of research in themselves. We have addressed the problem of calculating the shifts of roton energies due to the addition of ^{3}He in dilute quantities and have used the dielectric model developed several years ago:

Reprint 12: "Dielectric Model of Roton Interactions in Dilute Solutions of ^{3}He in ^{4}He," by R.J. Donnelly, R.W. Walden and P.H. Roberts, J. Low Temp. Phys. 31, 375-387 (1978).

In the same issue of the Journal of Low Temperature Physics we examined the binding of rotons to impurities such as ^{3}He particles, the positive helium ion and the negative electron bubble:

Reprint 13: "Bound States of Rotons to Impurities in He II," by P.H. Roberts, R.W. Walden and R.J. Donnelly, J. Low Temp. Phys. 31, 389-408 (1978).

V. Superfluidity in Narrow Channels.

Several years ago Donnelly and Roberts advanced several theories on the nucleation of quantized vortices by the moving superfluid. Recently there has been very substantial theoretical and experimental work on the properties of thin films, particularly work stimulated by the ideas of Kosterlitz and Thouless on two dimensional systems. It seemed useful to examine the predictions of the older nucleation theories to channel flow. The investigation showed that it is

necessary to assume a free energy barrier to vortex nucleation which is present irrespective of any superflow. Flow then modifies the barrier, and decay of superflow results. This investigation appeared recently in Physical Review Letters:

Reprint 14: "Superflow in Restricted Geometries," by R.J. Donnelly, R.N. Hills and P.H. Roberts, Phys. Rev. Letters 42 725-728 (1979).

VI. Infrared Detectors

Our group has been active in upper atmosphere research, principally with NASA support. In one important instance, however, the low temperature facilities at Oregon were important in the development of an ^{3}He-cooled infrared bolometer detector. The construction of the cryostat is described in the next paper:

Reprint 15: "Portable ^{3}He Detector Cryostat for the Far Infrared" by J.V. Radostitz, I.G. Nolt, P. Kittel and R.J. Donnelly, Rev. Sci. Instrum. 49, 86-88 (1978).

Personnel Associated with the Reserach Effort

1) Russell J. Donnelly, Professor of Physics, principal investigator.
2) Paul H. Roberts, Professor of Mathematics, University of Newcastle upon Tyne. Professor Roberts was elected a Fellow of the Royal Society of London in 1979.
3) Roger N. Hills, Senior Lecturer in Mathematics, Herriot-Watt University, Edinburgh
4) James V. Radostitz, Research Associate, constructed the apparatus and assisted in the experimental set-up.
5) Richard M. Ostermeier, Research Associate. Dr. Ostermeier is now at Shell Development Corp., Houston, Texas.
6) Peter Kittel, Research Associate. Dr. Kittel is now with NASA Ames Research Center in Mountain View California
7) Michael W. Cromar obtained his Ph.D. for the work described above and is now

at the National Bureau of Standards, Boulder, Colorado.

8) Robert Walden obtained his Ph.D. in 1978 for research in fluid dynamics, and is now at Bell Laboratories, Murray Hill, New Jersey.

Conferences and related activities

The results of this research have been reported at several conferences. Richard Ostermeier presented the turbulence work at LT15. Research has been regularly reported at the Washington meeting of the American Physical Society each April, and in 1978, Russell Donnelly presented an invited paper at a Symposium of the Division of Fluid Dynamics.

In July of 1979, the Fourth Oregon Conference on Liquid Helium was held at Timberline Lodge, Mount Hood, Oregon. The work described here was reported by P.H. Roberts and R.J. Donnelly.

In October 1978, Russell Donnelly was a Senior Visiting Fellow of the Science Research Council(UK) and gave lectures at Newcastle, Edinburgh, St. Andrews, Birmingham, Manchester, Sussex and London.

Acknowledgements

Our project monitors at AFOSR during the period of this grant were Dr. William Dunnill and Dr. Thomas Collins. We are grateful to them for their encouragement and support.

Much of the research reported here has had concurrent support. In particular Russell Donnelly has had a grant for the Division of Materials Research, National Science Foundation and Paul Roberts and R.N. Hills have had grants from the Science Research Council of the United Kingdom.

APPENDIX

TURBULENT COUNTERFLOW : VORTEX LINE DENSITY

R.M. Ostermeier, M.W. Cromar, P. Kittel and R.J. Donnelly

Department of Physics, University of Oregon, Eugene, Oregon 97403 USA

Résumé.- Une technique de "pulse 2e son" a été développée comme preuve locale de la "vorticité" générée dans un "counterflow" thermique dans l'hélium II. Les mesures de densité des vortex obtenues en utilisant cette technique sont présentées.

Abstract.- A second sound burst technique has been developed as a local probe of vorticity generated in thermal counterflow in He II. Measurements of the steady-state vortex line density obtained using this technique are presented.

Turbulent counterflow in wide channels (∿1cm) was first studied in detail by Vinen /1/ using a resonant second sound technique to measure steady-state and transient properties averaged over the length of the channel. From his observations he envisioned the turbulence as a homogeneous, isotropic tangle of quantized vortex line satisfying the dynamical balance equation

$$\frac{dL}{dt} = \frac{1}{2}\chi_1 B \frac{\rho_n}{\rho} v L^{3/2}\left(1 - \frac{\alpha}{L^{1/2}d}\right) - \frac{\chi_2 \kappa}{2\pi} L^2 \qquad (1)$$

where L is the vortex line density, v is the counterflow velocity, χ_1, χ_2, and B are the usual temperature dependent Vinen/1/ parameters. The factor in parentheses accounts for the finite size of the channel (d = diam., $\alpha \sim 1$), and implies a critical counterflow velocity for the transition from laminar to turbulent flow. This model has been successful in explaining most experimental results on thermal counterflow. One notable exception concerns the assumption of isotropy. Ashton and Northby /2/ discovered that the vortex tangle moves in the direction of the normal fluid with a drift velocity proportional to v. Though this result contradicts an assumption of Vinen's theory, it is not surprising in view of the natural anisotropy of the counterflow velocity. A new theory developed by Schwarz /3/ takes this into account and gives a vortex line drift velocity in agreement with experiment. Implicit in the data analysis of Ashton and Northby the theory of Schwarz, and the Vinen model is the assumption of homogeneity. Actually, there is reason to believe that L may not be uniform along the length of a channel. Induced temperature and pressure gradients will, of course, produce slight inhomogeneity ; but more important is the problem of how turbulence is initiated /1/. For example, one might expect an enhanced vortex line density near the heater if it is an intrinsic source of turbulence. Measurements of the vortex line density profile were motivated also by the observation of Ladner, Childers and Tough /4/ of a third flow regime at higher heat currents.

The channel used in our experiments has a 1 cm square cross-section and runs down the center of a brass rod 3 cm in diameter and 41 cm long. Its bottom end is open to the bath. The upper end houses a heater which is insulated from the channel walls by a Delrin support. The heater consists of a 9 mm square OFHC copper plate backed with ∿100Ω of manganin wire. Ten pairs of capacitive-type transducers /5/ (∿6 mm diameter) are spaced along the channel's length as shown in figure 1.

To provide a local probe of the vorticity (necessary for a profile measurement) we developed a second sound burst technique as schematized in figure 1. A burst generator excites the transmitting transducer, with the burst interval adjusted to allow for complete decay of all echoes. The received signal is preamplified and passed into a lock-in operated in the fast phase-sensitive mode. The burst frequency and phase are adjusted to maximize the output of the lock-in which corresponds essentially to the RMS of the received signal. The first trace in figure 1 shows, from left to right, the pick-up burst, and a series of burst echoes. The second trace is the lock-in output. The third trace is a series of time delay adjustable 20 μs pulses which mark the points in time that the lock-in output is sampled by the computer. Since the relative attenuation (between $\dot{Q}$ on and $\dot{Q}$ off) for a single transit across the channel is generally quite small, measu-

rements on the echoes allow considerable improvement in the uncertainty without substantially diminishing the local nature of the probe.

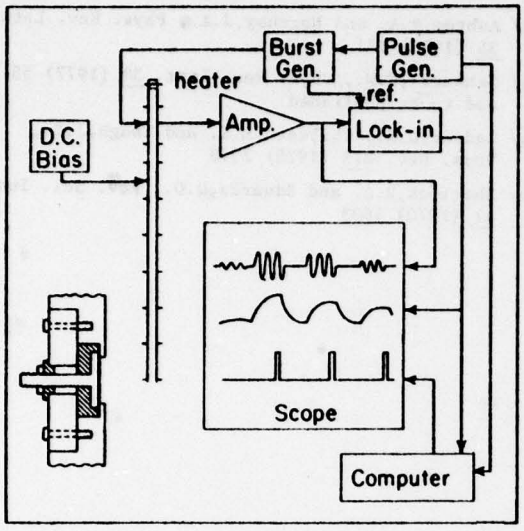

Fig. 1 : A schematic of the counterflow channel and the associated electronics. A cross-section of the second sound transducer is shown in the lower left-hand corner.

Since the attenuation $\beta \sim L$, eq. (1) can be written in the steady state as

$$\beta/\dot{Q}^2 = \gamma\{1 + \sqrt{1 - \dot{Q}_{C1}/\dot{Q}}\}^2 \qquad (2)$$

where, according to the Vinen theory, γ is a function of temperature only and $\dot{Q}_{C1}$, the critical heat current, is a function of temperature and channel width. In figure 2 we plot our data at 1.35 K as $\beta/\dot{Q}^2$ vs $\dot{Q}$ for four of the transducer pairs. Concentrating first on $\dot{Q} \lesssim 100$ mW/cm^2 we note that near the open end at 40 cm a two parameter fit (γ and $\dot{Q}_{C1}$) of eq. (2) provides excellent agreement with our data. If we assume different values of γ and $\dot{Q}_{C1}$, a similar good fit can be obtained at 20 cm. As one approaches the heater to within 5 and especially 2.5 cm, it becomes impossible to fit the data to the functional form of eq. (2). Thus γ and Q_{C1} not only depend strongly on the distance from the heater X, but the shape of the vortex line density profile changes with $\dot{Q}$ as well. This is particularly evident when comparing data for $\dot{Q}$ = 80 mW/cm^2 with that for 35 mW/cm^2 as shown in figure 3. At 80 mW/cm^2 there occurs over the length of the channel a gradual decrease in β of $\sim$50 %, whereas at 35 mW/cm^2 there is a sharp inhomogeneity localized near the heater.

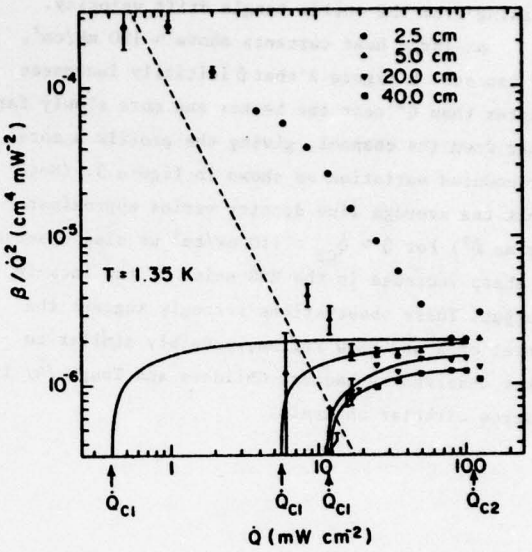

Fig. 2 : A plot of $\beta/\dot{Q}^2$ at T = 1.35 K for 4 transducer pairs located at various distances from the heater. The solid curves are eq. (2) fitted to the 4 sets of data at $\dot{Q}_{C1}$ and 100 mW/cm^2. $\dot{Q}_{C2}$ indicates the onset of a new secondary flow.

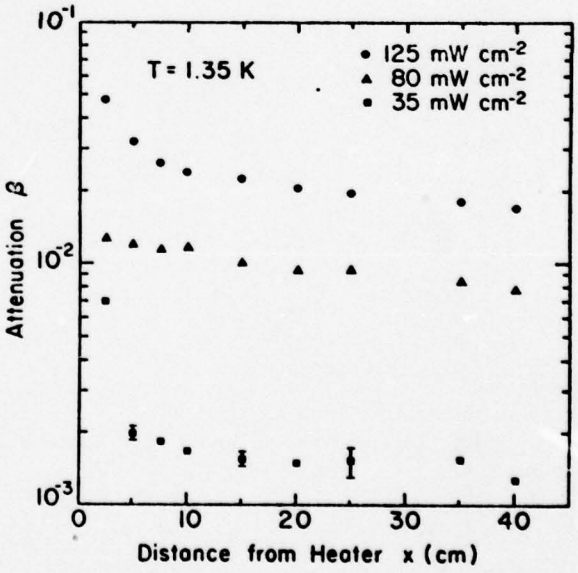

Fig. 3 : The attenuation β versus distance from the heater X for various $\dot{Q}$ at T = 1.35 K.

The observed dependences of β and Q_{C1} on X and the profile on $\dot{Q}$ have no ready explanation in existing theory. An understanding of these phenomena may lie in the aforementioned intrinsic pro-

duction of vorticity by the heater, end effects and/or presence of a convection term in eq. (1) arising from the vortex tangle drift velocity.

At large heat currents above $\sim$ 100 mW/cm^2, we can see in figure 2 that β initially increases faster than $\dot{Q}^2$ near the heater and more slowly farther down the channel, giving the profile a more pronounced variation as shown in figure 3. (Note that the average line density varies approximately as $\dot{Q}^2$) For $\dot{Q} > \dot{Q}_{C2} \simeq$ 110 mW/cm^2 we also observe a sharp increase in the RMS noise of the lock-in output. These observations strongly suggest the onset of a new flow regime, possibly similar to that observed by Ladner, Childers and Tough /4/ in narrow circular channels.

References

/1/ Vinen,W.F., Proc. Roy. Soc. A240 (1957a) 114 A240 (1975b) 128, A242 (1957c) 443, A243 (1957d) 400

/2/ Ashton,R.A. and Northby,J.A., Phys. Rev. Lett. 35 (1975) 171

/3/ Schwarz ,K.W., Phys. Rev. Lett. 38 (1977) 551 and to be published

/4/ Ladner,D.R., Childers,R.K. and Tough,J.T., Phys. Rev. B13 (1975) 2918

/5/ Sherlock,R.A. and Edwards,D.O., Rev. Sci. Instr. 41 (1970) 1603

Steady-State Vortex-Line Density in Turbulent He II Counterflow

R. M. Ostermeier, M. W. Cromar,[a] P. Kittel,[b] and R. J. Donnelly
Department of Physics, University of Oregon, Eugene, Oregon 97403
(Received 22 August 1978)

We have measured the steady-state vortex-line density in turbulent counterflow using a second-sound-burst technique as a local probe. Contrary to the Vinen theory and previous assumptions, we find substantial line-density inhomogeneity and strong departures from the predicted heat-current dependence. Anomalous behavior of the line density at higher heat currents provides evidence for a new secondary flow state.

In a classic series of experiments Vinen[1] was the first to study in detail the nature of turbulent counterflow in wide (~ 1 cm) channels. Using a resonant second-sound technique he measured the steady-state and transient attenuation averaged over the length of the channel. On the basis

of his observations he envisioned turbulent He II as consisting of a homogeneous, isotropic tangle of quantized vorticity satisfying the dynamical balance equation[2]

$$\frac{dL}{dt}=\frac{\chi_1 B\rho_n}{2\rho} v L^{3/2}\left[1-\frac{\alpha}{dL^{1/2}}\right]-\frac{\chi_2\kappa}{2\pi}L^2, \qquad (1)$$

where L is the vortex-line density, v is the counterflow velocity, B is the mutual friction parameter, and χ_1 and χ_2 are parameters of order unity. The term in brackets accounts for the finite width of the channel (d = diam, $\alpha \sim 1$), and implies a critical counterflow velocity for the transition from laminar to turbulent flow.

This model has been successful in explaining temperature difference[3] and average steady-state line-density[2] behavior. However, serious problems do remain. As Vinen recognized, the model does not explain the initiation of turbulence. His introduction into Eq. (1) of a phenomenological term to account for this deficiency provides no real insight into this problem and is questionable in view of the theory's inadequacy in dealing with transient phenomena. More recently the assumption of isotropy has come under attack. Ashton and Northby[4] observed that the vortex tangle moves with a drift velocity proportional to v—a result not too surprising considering the intrinsic anisotropy of counterflow. Schwarz[5] has attempted to remedy the theoretical situation in his development of an equation for the vorticity distribution function. His theory accurately predicts the average steady-state line density and its motion down the channel, but it too does not treat the problem of vortex initiation.

Besides these difficulties, the Vinen model (as well as Schwarz's theory and other theoretical discussions and data analyses) assumes homogeneous turbulent flow. Actually there are a number of reasons to believe that turbulent counterflow may be inhomogeneous. The channel walls will almost certainly influence the line density in a more complicated fashion than described by Eq. (1). Consideration of the annihilation, polarization, and concentration of vorticity in the central stream of the flow suggests a diminishing line density down the channel. A more interesting possibility involves creation of turbulence. Since the buildup of turbulence from thermally excited vorticity is energetically unlikely,[2] it is conceivable that the heater plays a more direct role in vorticity creation. If this is the case, a study of the line density in the vicinity of the heater might prove useful in understanding this phenomenon.

Finally, the observation of a new secondary flow in circular capillary tubing[6] and the absence of such a state in Vinen's observations suggest that this state might manifest itself in wide channels as a modification of the line-density distribution.

To test these ideas we have carried out a study of the local behavior of the line density in steady turbulent counterflow. Our counterflow channel is 1 cm square in cross section and runs down the center of a brass bar 3.8 cm in diameter and 40.5 cm long. Its bottom end is open to the bath. At the top end the heater, consisting of a 2-mm × 9-mm–square oxygen-free, high conductivity copper plate backed by ~ 100 Ω of Manganin wire, is inlaid in a Delrin support that insulates it from the channel walls. Ten pairs of capacitive-type second-sound transducers[7] (6 mm diam) are spaced along the channel's length as shown in Fig. 1.

To provide a local probe of vorticity a second-sound-burst technique was developed. A burst generator excites the transmitting transducer, with the burst interval adjusted to allow decay of echoes. The received signal is preamplified, filtered, and amplified by a lockin operated in the fast phase sensitive mode. The burst frequency and lockin phase control are adjusted to maximize lockin output. The first trace in Fig. 1 shows, from left to right, the pickup burst, the first received burst, and a series of burst echoes. The second trace is the lockin output corresponding essentially to the rms received signal.

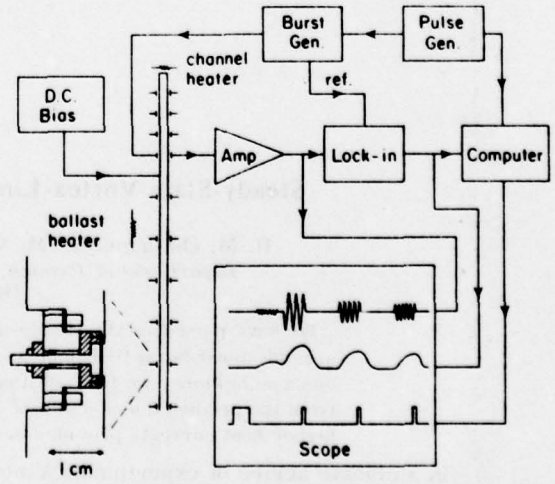

FIG. 1. A schematic of the counterflow channel and the electronics for the second-sound-burst technique. A cross section of the capacitive-type second-sound transducer is shown at the lower left.

The third trace is a series of time-delay–adjustable 20-μsec pulses preceded by a 200-μsec pulse. These pulses mark the points in time when the lockin output is sampled by the computer. The echoes are analyzed since the relative attenuation due to superfluid turbulence is, for a single transit across the channel, generally quite small. Measurements on the echoes thus allow considerable improvement in uncertainty without significantly diminishing the local nature of the probe. A more complete description of this technique will be published elsewhere.

Since second-sound attenuation $\beta \sim L$ and heat current $\dot{Q} \sim v$, Eq. (1) can be written in the steady state as

$$\beta/\dot{Q}^2 = (\gamma/4)[1 + (1 - \dot{Q}_{c1}/\dot{Q})^{1/2}]^2, \qquad (2)$$

where γ is, according to the Vinen theory, a function of temperature only, and $\dot{Q}_{c1}$, the critical heat current, depends on channel width and temperature. In Fig. 2 we have plotted our data at 1.45 K for $\beta/\dot{Q}^2$ vs $\dot{Q}$ at four positions down the channel. The data indicate three regions of distinctive behavior. Concentrating first on values of $\dot{Q} \gtrsim \dot{Q}_{c2} \sim 100$ mW we note that near the channel's open end at 40 cm a two-parameter fit (γ and $\dot{Q}_{c1}$) of Eq. (2), indicated by the solid line, provides good agreement with the data. A similar good fit, using different parameter values, can be had at 25 cm. Closer to the heater the situation changes considerably. At 5 cm, $\beta/\dot{Q}^2$ follows Eq. (2) at higher heat currents, but a distinct deviation occurs at about 17 mW below which $\beta/\dot{Q}^2$ increases with decreasing $\dot{Q}$. This marks the onset of a new region of behavior which occurs at higher heat currents as the heater is approached. At 2.5 cm, for example, the deviation begins at about 70 mW and continues to the lowest $\dot{Q}$ for which β is measurable.

The difference in behavior between these two regimes is evident also in Figs. 3(a) and 3(b) where line-density profiles are shown for $\dot{Q} = 35$ and 80 mW, respectively. The enhanced vorticity near the heater at lower heat currents decreases rapidly with x, dropping by a factor of 6–8 in 2.5 cm. Farther from the heater and/or at higher heat currents the line density diminishes by about a factor of 2 down the length of the channel. This gradual falloff may be associated with wall effects. The enhanced density near the heater is possibly related to vorticity creation by the heater. This is suggested by the rapid decay, the almost linear $\dot{Q}$ dependence of the line density, and the more pronounced behavior of this effect at lower heat currents.

The third region, as indicated by the open sym-

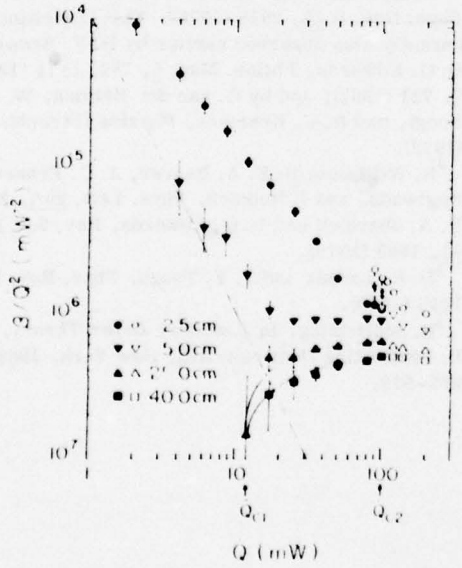

FIG. 2. $\beta/\dot{Q}$ vs $\dot{Q}$ at 1.45 K for four positions down the channel. The solid lines are Eq. (2) fitted to the 25- and 40-cm data. The open symbols are data taken in the presence of a new secondary flow whose onset is at $\dot{Q}_{c2} \sim 100$ mW. The light dashed line indicates a rough estimate of the experimental resolution.

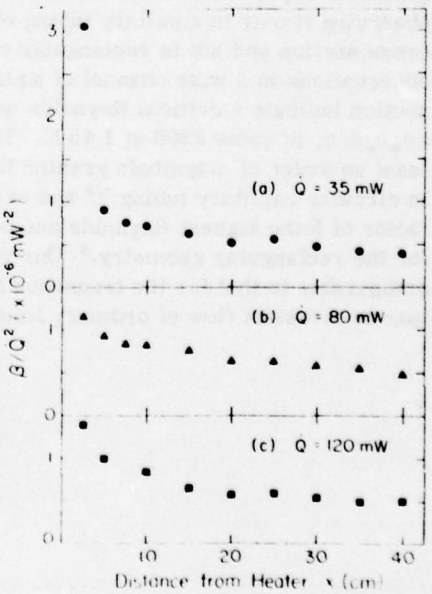

FIG. 3. $\beta/\dot{Q}^2$ vs distance from the heater at 1.45 K for $\dot{Q}$ = 35, 80, and 120 mW.

bols in Fig. 2, is characterized by an anomalous shift in line density accompanied by an increase in the signal rms noise. At 1.45 K the onset of this region occurs at $\dot{Q}_{c2} \simeq 100$ mW independent of x. The shift in attenuation, most evident at 2.5 cm and 100 mW, can occur spontaneously in either direction, i.e., between the closed and open symbols. At higher heat currents $\beta/\dot{Q}^2$ assumes only values shown as open symbols. For $\dot{Q}$ slightly below $\dot{Q}_{c2}$ (for example, 90 mW at 2.5 cm) the larger attenuation can be induced by mechanical vibration of the cryostat immediately prior to data collection, but this enhanced density eventually decays. Similar behavior, though not as pronounced, is observed at 5 cm. Farther down the channel this phenomenon manifests itself only weakly as enhanced signal rms noise and a gradual reduction in $\beta/\dot{Q}^2$ with $\dot{Q}$.

The line-density profile above $\dot{Q}_{c2}$ is shown in Fig. 3(c) for 120 mW. Comparison of this profile with that at 80 mW$<\dot{Q}_{c2}$ [Fig. 3(b)] shows that immediately above $\dot{Q}_{c2}$ a more rapid decline in line density down the channel occurs. Also the average $\beta/\dot{Q}^2$ appears to decrease slightly above $\dot{Q}_{c2}$. This is in contrast to the interpretation of Ladner *et al.*[6] of their high-$\dot{Q}$ pressure and temperature difference data which suggests an increase in this quantity.

Ladner, Childers, and Tough[8] noted a strong geometry dependence in the second transition, observing it only in capillary tubing of circular cross section and not in rectangular tubing. Our observations in a wide channel of square cross section indicate a critical Reynolds number $R = \rho_n v_n d/\eta_n$ of about 2800 at 1.45 K. This is at least an order of magnitude greater than observed in circular capillary tubing,[6,8] and exceeds by a factor of 5 the highest Reynolds numbers explored for the rectangular geometry.[8] Our value of R is comparable to that for the transition from laminar to turbulent flow of ordinary fluids in square channels,[9] and suggests that the transition at $\dot{Q}_{c2}$ is the analogous transition for the normal-fluid component. If this interpretation is correct, the observed gradual decrease in R with temperature may indicate an inhibiting effect of the superfluid vorticity on the transition.

We acknowledge useful discussions with F. Moss, K. Schwarz, and J. Tough. This work has been supported by National Science Foundation Grant No. DMR 76-21814, and by U. S. Air Force Office of Scientific Research Grant No. AFOSR-76-2880C.

---

[a]Present address: Department of Physics, University of Rochester, Rochester, N. Y. 14627.

[b]Present address: NASA Ames Research Center, Moffett Field, Calif. 94035.

[1]W. F. Vinen, Proc. Roy. Soc. London, Ser. A 240, 114, 128 (1957).

[2]W. F. Vinen, Proc. Roy. Soc. London, Ser. A 242, 443 (1957), and 243, 400 (1957).

[3]R. K. Childers and J. T. Tough, Phys. Rev. B 13, 1040 (1976).

[4]R. A. Ashton and J. A. Northby, Phys. Rev. Lett. 35, 171 (1975).

[5]K. W. Schwarz, Phys. Rev. Lett. 38, 551 (1977), and to be published.

[6]D. R. Ladner, R. K. Childers, and J. T. Tough, Phys. Rev. B 13, 2918 (1975). This transition was apparently also observed earlier by D. F. Brewer and D. O. Edwards, Philos. Mag. 6, 775, 1174 (1961), and 7, 721 (1962); and by G. van der Heijden, W. J. P. de Boogt, and H. C. Kramers, Physica (Utrecht) 59, 473 (1972).

[7]R. Williams, S. E. A. Beaver, J. C. Fraser, R. S. Kagiwada, and I. Rudnick, Phys. Lett. 29A, 279 (1969); R. A. Sherlock and D. O. Edwards, Rev. Sci. Instrum. 41, 1603 (1970).

[8]D. R. Ladner and J. T. Tough, Phys. Rev. B 17, 1455 (1978).

[9]H. Schlichting, in *Boundary Layer Theory*, edited by H. Schlichting (McGraw-Hill, New York, 1968), pp. 575–578.

FLUCTUATIONS IN TURBULENT HE II COUNTERFLOW

R. M. Ostermeier [a], M. W. Cromar [b], P. Kittel [c]
and R. J. Donnelly

Department of Physics
University of Oregon
Eugene, Oregon 97403

Abstract

We have measured the power spectral density and the mean square of vortex line density fluctuations in steady turbulent counterflow using a second sound burst technique as a local probe. Our results are compared with previous measurements and theoretical predictions.

(P.A.C.S. 67.40.Hf)

In recent years considerable experimental and theoretical effort has been directed at understanding steady turbulent counterflow. The dynamical aspects of turbulent He II, however, have not received nearly as much attention. The first investigations were those of Vinen [1] who studied transient behavior using a resonant second sound technique. Propagation of turbulent wave fronts in narrow channels has been investigated by a number of authors including Mendelssohn et al.[2] and Peshkov and Tkachenko.[3] More recently Moss and coworkers [4,5] have provided a new and powerful experimental method by investigating fluctuations in the vortex line density. Following this approach Piotrowski and Tough [6] have studied the fluctuating motion of an airfoil suspended in turbulent counterflow.

In this paper we present measurements of the power spectral density (PSD) and the mean square (MS) of vortex line density fluctuations in steady turbulent He II counterflow. We believe our results to be more reliable than previous measurements for at least three reasons. First, the experiments were carried out using a local probe designed to measure vortex line density fluctuations directly. Second, measurements were made at different positions along a relatively high aspect ratio (1 cm square by 40 cm long) channel. Third, our data acquisition and analyses were superior to that then available in earlier work.

The apparatus and second sound burst technique were similar to that used in our line density measurements[7]. However, burst echoes were suppressed in order to maximize the available frequency range for optimal PSD determination. Since second sound attenuation (in non-turbulent HeII) increases as f^2

(f=frequency),[8] this was accomplished by operating at higher burst frequencies. Thus repetition rates up to 160 Hz could be attained without signal overlap.

As shown in Fig. 1 the burst excites the transmitting transducer and the received signal is preamplified, bandpass filtered, and amplified by a lock-in operated in the fast phase sensitive mode. The lock-in output, as shown in the second trace, is then sampled by computer at every burst as specified by the pulses in the third trace. This is done for 100 seconds thus yielding time series consisting of approximately 16000 data points each. Since computer memory was limited to transformation of 1024 point time series, the data were analyzed to produce one low frequency and approximately 16 high frequency PSDs. This procedure also allowed an estimation of aliasing effects[9]. These arose from the inability to effectively filter the fluctuation modulated signal, the bandwidth of which was about 160 Hz centered at anywhere from 50 to 100 KHz, the typical burst frequency.

Two sets of spectra with heat current $\dot{Q} = 0$ and 100 mW are shown in Fig. 2. These data taken at T=1.25K and x=25 cm from the heater, represent averages of twenty five 16000 point time series. Conversion of the measured second sound burst amplitude PSD, $S_A(f)$, to the vortex line density PSD, $S_L(f)$, follows from $A=A_o \exp(-\Sigma L)$ where $\Sigma=\pi\kappa Bd/16\, u_2$. For small fluctuations this gives

$$S_L(f) = \{S_A(f)/A^2 - S_{Ao}(F)/A_o^2\}/\Sigma^2, \quad (1)$$

assuming zero correlation between fluctuations in A_o and L. Here L is the randomly oriented line density, A_o is the amplitude of the received second sound signal for $\dot{Q} = 0$, κ is the quantum of circulation, B is the mutual

friction parameter, d is the channel width, and u_2 is the second sound velocity. For a given heat current the aliasing is easily estimated from the degree of overlap between low and high frequency PSDs.[9] At $\dot{Q}$=100 mW, for example, aliasing is rather negligible until above about 10 Hz where background noise dominates the signal.

There were three general features observed in the power spectral densities. First, for all heat currents investigated up to 280 mW all of the additional power above background occurred at low frequencies, usually below about 10Hz. Second, a low frequency plateau was always present in the spectra at sufficiently high heat currents. Finally, every PSD exhibited a roll-off at increasing frequencies with increasing $\dot{Q}$. These features are illustrated in Fig. 3 where smoothed spectra, taken at T=1.25K and x=25.0 cm, are shown for $\dot{Q}$ ranging from 17 to 140 mW.

Our data differ from Hoch et al.[4] mainly in the 1/f behavior they observed at low frequencies. This may be attributable to a combination of relatively low heat currents investigated and insufficiently low frequencies examined by them in order to have detected a plateau at those heat currents. We also did not observe a well defined $1/f^3$ roll-off at higher frequencies as they did. Instead we found the power of the roll-off varied from about 2 to 4, generally increasing with $\dot{Q}$. This roll-off is also inconsistent with the exponential dependence deduced by Piotrowski and Tough [6] in their experiments. The disagreement probably indicates a complicated relation between the fluctuating forces acting on their probe and the local vortex line density.

Observations of line density inhomogeneity[7] suggest that low aspect ratio channels used in previous experiments[4-6] may have effected these earlier

results. For example, in this work we observed that the $\dot{Q}$ dependence of the spectra was generally more erratic and anomalous near the heater than farther down the channel. This is illustrated in Fig. 4 where we have plotted the MS fluctuation, $\langle \delta L^2 \rangle$, versus $\dot{Q}$ for T=1.25K and x=2.5 and 25.0 cm. In Fig. 4a we note an abrupt increase in $\langle \delta L^2 \rangle$ at about 100 mW. This is consistent with the observed anomalous increase in line density at this same critical heat current, $\dot{Q}_{c2}$, and our suggestion that this may indicate the onset of turbulent normal fluid flow.[7] Associated with this behavior are hysteretic effects as evidenced by the upper point at 50 mW. This datum was taken immediately after those at higher heat currents as indicated by the dashed line and arrow. At lower heat currents the $\dot{Q}$ dependence of the data at 2.5 cm is rather ill-defined in comparison with that observed farther down the channel as seen in Fig. 4b. Here the solid line through the data indicates a $\dot{Q}^2$ dependence. In contrast to the data at 2.5 cm, there is no substantial effect evident at $\dot{Q}_{c2} \cong 100$ mW, though there is some slight relative reduction of $\langle \delta L^2 \rangle$ above $\dot{Q}_{c2}$ again consistent with our observations of L.[5] This general behavior described for the data at 25.0 cm prevails over most of the length of the channel, from within about 10 cm of the heater to the open end.

Since steady-state line density measurements[7,10] suggest some validity of Vinen's phenomenological theory[11] sufficiently far from the heater, it is useful to compare predictions of that theory with the measured PSDs. Assuming line density fluctuations much smaller than the steady-state L, Vinen's dynamical balance equation[11] can be linearized to form a Langevin equation. It then follows that

$$S_L(f) = g_o \, S_v(f)/\{1 + (f/fo)^2\}, \quad (2)$$

where $g_o \sim \dot{Q}^2$, $f_o \sim \dot{Q}^2$, and $S_v(f)$ is the counterflow velocity fluctuation PSD. A similar result is also obtained from Schwarz's theory [12]. If $S_v(f)$ is assumed to be flat over the bandwidth of interest, we get the dashed curves shown in Fig. 3 corresponding to the indicated values of $\dot{Q}$. We also find that $\langle \delta L^2 \rangle \sim \dot{Q}^4$ as shown by the dashed line in Fig. 4b.

Although the predicted roll-off frequency, f_o, is of the correct order of magnitude, the discrepancies between theory and experiment with regard to plateau amplitude, roll-off slope, and $\langle \delta L^2 \rangle$ suggest that the dynamical aspects of Vinen's and Schwarz's theory may be incomplete. This is corroborated to some extent by the inconsistency Vinen noted between his observations of transient phenomena and his theory.[11] On the other hand there is reason to believe that fluctuations in the velocity may contribute to the observed spectra. In considering this possibility Northby[13] has deduced an expression for $S_L(f)$ from the two fluid equations and Vinen's dynamic balance equation. Taking into account feedback between fluctuations of the velocity and the line density he finds

$$S_L(f) \sim a/\{(c-f^2)^2 + b\, f^2\}, \qquad (3)$$

where a, b, and c are specified but complicated functions of $\dot{Q}$. We note that Eqn. (3) possesses the general features exhibited by our PSD data; namely a plateau at low frequencies relatively insensitive to $\dot{Q}$, a roll-off at higher frequencies with roll-off frequency and slope increasing with $\dot{Q}$, and also the observed $\dot{Q}$ dependence of $\langle \delta L^2 \rangle$. Although a detailed and systematic study comparing Eqn. (3) with our data has not yet been completed[14] a preliminary analysis[15] suggests that Northby's feedback model may have some basis of validity at least sufficiently far from the heater.

We acknowledge useful discussions with F. Moss, J. Northby, K. Schwarz, and J. Tough; and the assistance of Brian Lee in taking some of the data. This work was supported by NSF Grant DMR 78-10782 and Air Force Grant AFOSR-76-2880. One of us (R.M.O.) thanks Shell Oil Company for support during the preparation of this manuscript.

REFERENCES

(a) Present Address: Shell Oil Co., P. O. Box 991, Houston, TX 77001.

(b) Present Address: Dept. of Physics, University of Rochester, Rochester, NY 14627.

(c) Present Address: NASA Ames Research Center, Moffett Field, CA 94035.

1. W. F. Vinen, Proc. Roy. Soc. A240, 128 (1957).

2. K. Mendelssohn and W. A. Steele, Proc. Roy. Soc. 73, 144 (1959); and S. M. Bhagat, P. R. Critchlow, and K. Mendelssohn, Cryogenics 4, 166 (1964).

3. V. P. Peshkov and V. K. Tkachenko, J. Exp. Theor. Phys. 41, 1427 (1961).

4. H. Hoch, L. Busse, and F. Moss, Phys. Rev. Lett. 34, 384 (1975).

5. J. Mantese, G. Bischoff, and F. Moss, Phys. Rev. Lett. 39, 565 (1977).

6. C. Piotrowski and J. T. Tough, Phys. Rev. B18, 2066 (1978).

7. R. M. Ostermeier, M. W. Cromar, P. Kittel, and R. J. Donnelly, Phys. Rev. Lett. 41, 1123 (1978).

8. J. Wilks, The Properties of Liquid and Solid Helium, (Oxford University, London, 1967), p.191.

9. R. K. Otnes and L. Enochson, Digital Time Series Analysis, (John Wiley & Sons, New York, 1972), p.35.

10. W. F. Vinen, Proc. Roy. Soc. A240, 114 (1957).

11. W. F. Vinen, Proc. Roy. Soc. A242, 443 (1957) and A243, 400 (1957).

12. K. W. Schwarz, Phys. Rev. Lett. 38, 551 (1977) and Phys. Rev. B18, 245 (1978).

13. J. A. Northby, Phys. Rev. B18, 3214 (1978).

14. (In preparation).

15. J. A. Northby, private communication.

FIGURE CAPTIONS

Figure 1: A schematic of the counterflow channel and electronics for the second sound burst technique. Burst echoes have been suppressed as explained in the text. In the lock-in output the pick-up has been eliminated and the received signal maximized by adjusting burst frequency and lock-in phase control.

Figure 2: The power spectral density of the amplified second sound burst amplitude, $S_A(f)$, versus frequency for $\dot{Q}$ = 0 and 100 mW. The data were taken at T = 1.25K and x = 25.0 cm. The low and high frequency curves represent averages of 25 and approx. 400 individual spectra, respectively.

Figure 3: $S_L(f)$ versus frequency for $\dot{Q}$ = 17, 35, 70, and 140 mW; respectively. The data were taken at T = 1.25K and x = 25.0 cm. The dashed curves correspond to Eq. (2) evaluated at the same heat currents with $S_v(f)$ a constant adjusted to fit the 70 mW data at low frequencies.

Figure 4a: $\langle \delta L^2 \rangle$ versus $\dot{Q}$ at T = 1.25K and x = 2.5 cm. The dashed line indicates hysteresis as explained in the text.

Figure 4b: $\langle \delta L^2 \rangle$ versus $\dot{Q}$ at T = 1.25K and x = 25.0 cm. The solid and dashed lines indicate a $\dot{Q}^2$ and $\dot{Q}^4$ dependence, respectively.

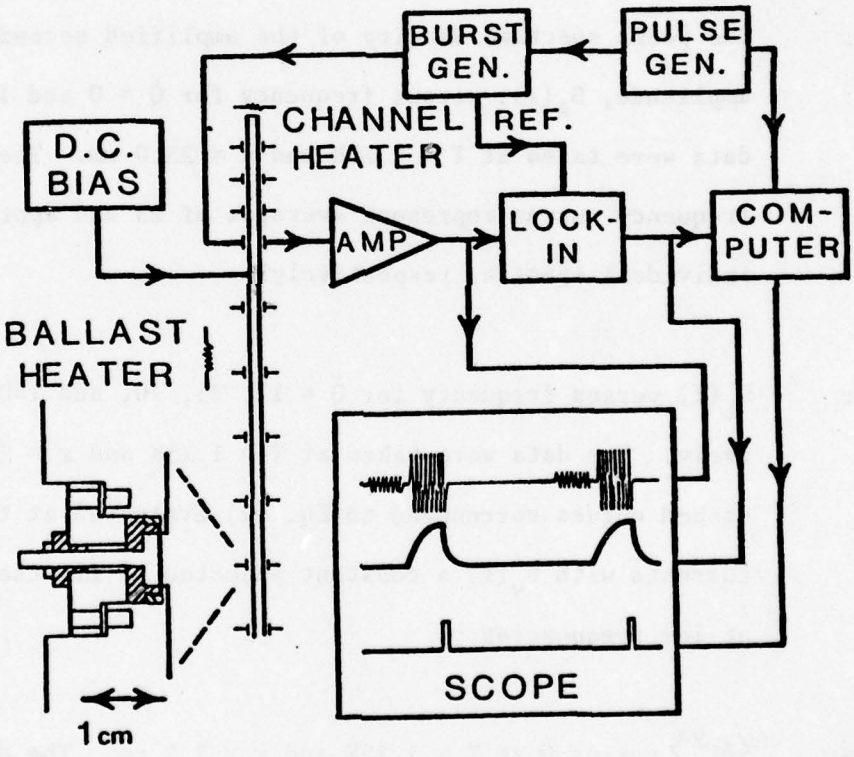
BURST GEN.
PULSE GEN.
CHANNEL HEATER
REF.
D.C. BIAS
AMP
LOCK-IN
COM-PUTER
BALLAST HEATER
SCOPE
1 cm

FIG. 1

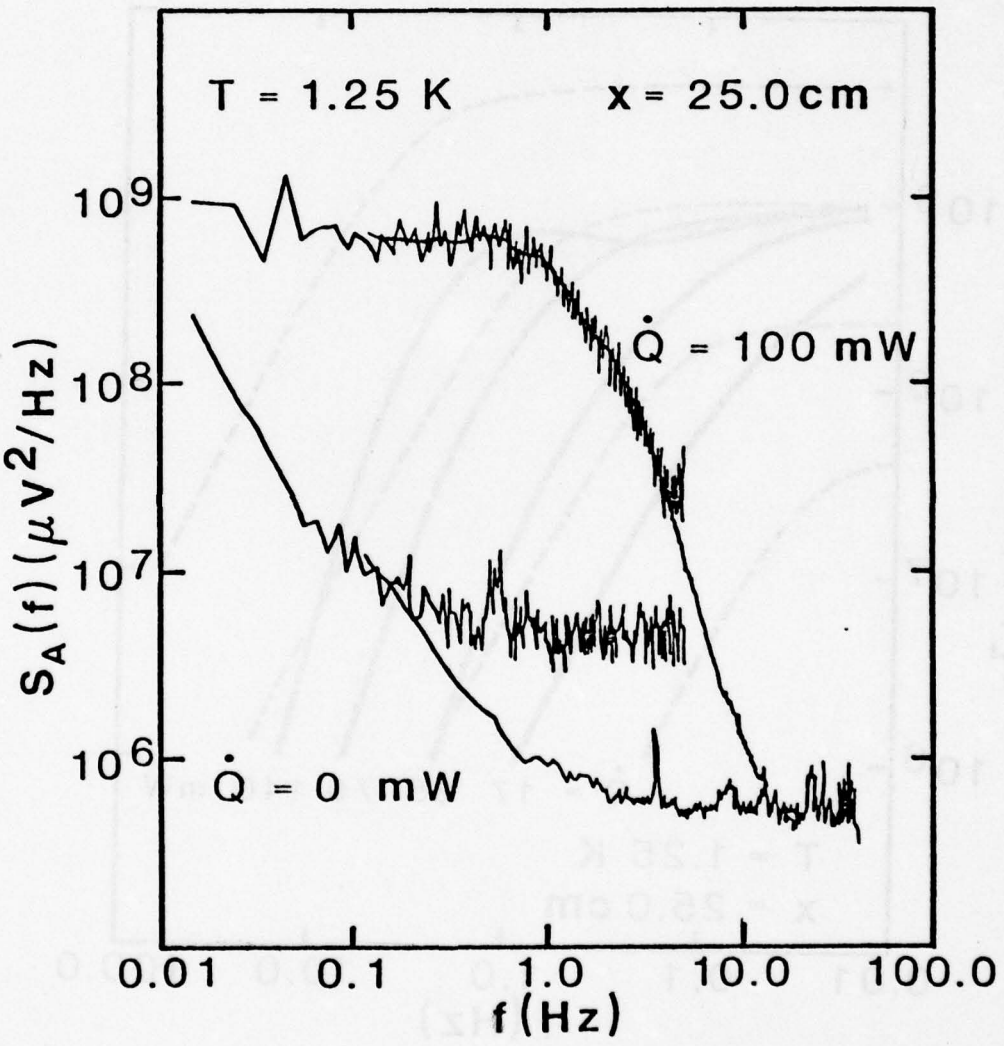
T = 1.25 K
x = 25.0cm
10^9
10^8
10^7
10^6
$S_A(f)$ (μV^2/Hz)
$\dot{Q}$ = 100 mW
$\dot{Q}$ = 0 mW
0.01
0.1
1.0
10.0
100.0
f (Hz)

FIG. 2

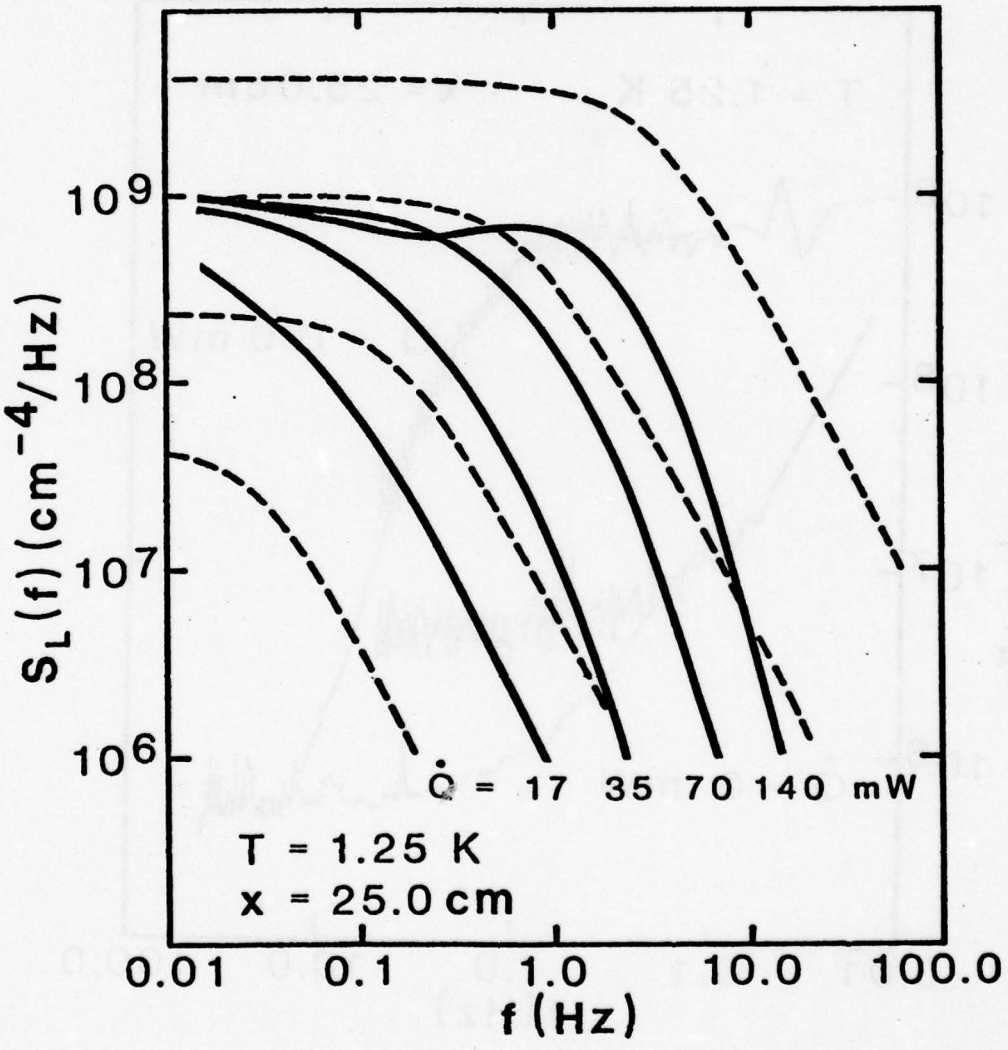
10^9
10^8
10^7
10^6
$S_L(f)$ (cm^{-4}/Hz)
Q = 17 35 70 140 mW
T = 1.25 K
x = 25.0 cm
0.01
0.1
1.0
10.0
100.0
f (Hz)

FIG. 3

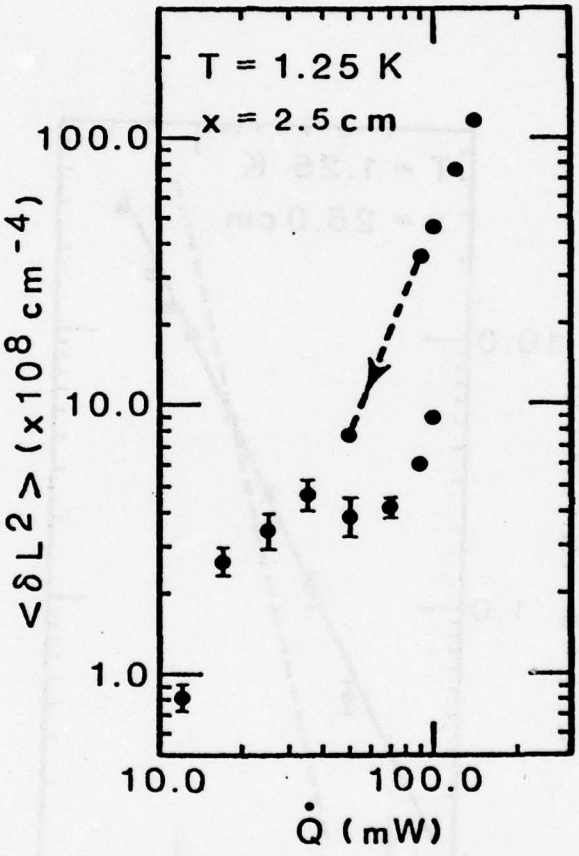
T = 1.25 K
x = 2.5 cm
100.0
10.0
1.0
10.0
100.0
$\dot{Q}$ (mW)
$\langle \delta L^2 \rangle$ ($\times 10^8$ cm^{-4})

FIG. 4A

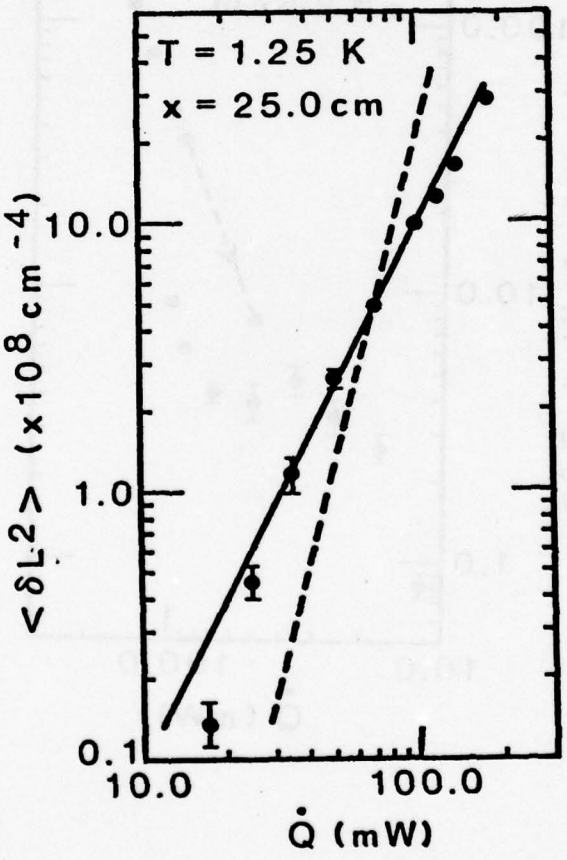
T = 1.25 K
x = 25.0 cm
10.0
1.0
0.1
10.0
100.0
$\dot{Q}$ (mW)
$\langle \delta L^2 \rangle$ ($\times 10^8$ cm^{-4})

FIG. 4B

Int. J. Engng Sci., 1977, Vol. 15, pp. 305–316. Pergamon Press. Printed in Great Britain

HEALING AND RELAXATION IN FLOWS OF HELIUM II—I

GENERALIZATION OF LANDAU'S EQUATIONS

R. N. HILLS
Mathematics Department, Heriot-Watt University, Edinburgh, Scotland

and

P. H. ROBERTS
Department of Applied Mathematics, The University, Newcastle-upon-Tyne, England

Abstract—The Landau 2-fluid equations for the motion of helium II are often criticised on two grounds: they ignore healing of the wave function, and they require the superfluid percentage to change instantaneously when the thermodynamic state is altered. In 1970 Khalatnikov[4] proposed a way of incorporating relaxation effects associated with conversion between superfluid and normal fluid. Using this as our starting point and employing the techniques of modern continuum mechanics, we develop a thermodynamically acceptable generalization that incorporates both healing and relaxation phenomena.

1. INTRODUCTION

ALTHOUGH the Landau equations have, for a generation, dominated the theory of the macroscopic behaviour of helium II, it has been recognized for a number of years that they contain unsatisfactory elements that cause them to misrepresent certain types of phenomena, particularly near the λ-point. The two most serious omissions of the Landau theory are, perhaps, healing and relaxation processes.

Healing causes the wave-function to fall to zero at, for example, (infinite potential) walls confining the fluid. A 2-fluid model ought to recognize this by requiring the superfluid density, ρ^s, to tend to zero at such a boundary. The Landau theory fails to do so. This may account for some of the difficulties that have been experienced in reconciling aspects of film flow with Landau's equations (see, e.g. Putterman[1], Section 41; Rudnick[2]). There is further evidence in support of a condition on ρ^s when one considers the energy associated with the superfluid vortex. By Landau's law of irrotationality the superfluid velocity becomes large as the singularity of vorticity is approached and, in classical terms, the energy per unit length of vortex will be infinite. This suggests that healing occurs at the vortex core and that the superfluid density tends to zero so rapidly that, despite the rising velocity, the energy is finite.† However, the boundary conditions stating that the superfluid density tends to zero appears to be in conflict with the 2-fluid model. The characteristic distance over which healing effects are important, the so-called "healing length", increases as the λ-point is approached. Thus the neglect of healing can lead to serious difficulties near the λ-point.

Another feature of the Landau equations is their insistance that conversion processes between normal and superfluid occur instantaneously. Given the thermodynamic state (as defined by density ρ, temperature T and $\mathbf{w}$, say), ρ^n and ρ^s are known. No matter how rapidly the thermodynamic state changes, ρ^n and ρ^s instantly take the values appropriate to that state: there is no relaxation. It is generally accepted that, though physically implausible, this feature of the Landau equations will not usually lead to serious error, simply because the relaxation time, τ, of the conversion between species is typically very small compared with the macroscopic time scales over which the gross features of the flow change. This attitude is not easily defended for small $T_\lambda - T$, because τ becomes large as the λ-point is approached. Dispersion of first and second sound then occurs, not merely at ultra-high frequencies.

These shortcomings of the Landau equations led Khalatnikov and others to seek

†In the case of the quantum vortices, this statement could be contested by invoking a different physical mechanism: localization. Since strictly ρ^s is a decreasing function of $|\mathbf{w}|$, where $\mathbf{w} = \mathbf{v}^n - \mathbf{v}^s$ is the relative velocity of the superfluid, the superfluid concentration decreases as the core of a vortex is approached: see Ref. [3].

generalizations that evaded such criticisms. The most recent of these works (Khalatnikov[4]) sought to develop a continuum theory by expansion in the order parameter for small $T_\lambda - T$. The main emphasis was laid on relaxation processes, the aspects dealing with healing being abandoned during the analysis. Our work not only generalizes Khalatnikov's theory of relaxation but also retains the healing phenomenon. We use the methods of modern continuum mechanics, and in particular recent ideas in the theory of mixtures (Müller[5]). However, in one respect our theory differs from the traditional treatments. It is usual in the constitutive theory of binary mixtures to regard the total density as the independent variable and to postulate for the concentration or the mass supply of one of the constituents. In this paper we wish to discuss healing phenomena by both allowing a constitutive dependence on superfluid density gradients and imposing the condition that the superfluid density vanishes at a solid boundary. It seems, therefore, more natural to reverse the usual roles played by the total and superfluid densities and regard the superfluid density as the independent variable and postulate constitutive equations for the *total* density. This step means that the conservation of mass eqn (1.3) will now determine the superfluid density rather than the total density as in classical treatments. Despite this difference in formulation, the theory still correctly reduces to a Landau form when healing and relaxation are neglected and, as in the Landau theory, irrotational flow is always a possible solution of the superfluid momentum equation under conservative forcing.

We collect here for easy reference the final governing equations. The notation of the paper is explained in detail in Section 2 but here we shall employ the following.

Notation

ρ^s = superfluid density, v_i^s = superfluid velocity,
Ω^s = potential of external body force per unit mass b_i^s $(= \Omega_{,i}^s)$,
ϕ^s = superfluid velocity potential $(v_i^s = \phi_{,i}^s)$,
$m^s = \partial\rho^s/\partial t + (\rho^s v_i^s)_{,i}$ = superfluid mass supply, r = heat supply function,
ρ = total density, A = an energy function, S = entropy, (1.1)
$w_i = v_i^n - v_i^s$ = relative velocity, T = temperature, p = pressure,
K = thermal conductivity ≥ 0, Φ = thermodynamical potential,
α_1, α_2 = coefficients of bulk viscosity and shear viscosity of normal fluid $(\alpha_2 \geq 0, \alpha_1 + \frac{1}{3}\alpha_2 \geq 0)$,

η = healing coefficient, Λ = relaxation coefficient (≥ 0),
D_{ij}^n = rate-of-deformation tensor for normal fluid $= \frac{1}{2}(v_{i,j}^n + v_{j,i}^n)$.

The analogous quantities to $(1.1)_1$–$(1.1)_5$ for the normal fluid are obvious. The equations are

$$\rho = \rho^n + \rho^s. \tag{1.2}$$

Conservation of mass

$$\frac{\partial \rho}{\partial t} + (\rho^n v_i^n + \rho^s v_i^s)_{,i} = 0. \tag{1.3}$$

Superfluid Bernouilli equation

$$\frac{\partial \phi^s}{\partial t} + \frac{1}{2}v^{s2} - \Omega^s + A + \rho\left(\frac{\partial A}{\partial \rho} + \frac{\partial A}{\partial \rho^s}\right) - \eta\rho_{,ii}^s - \frac{1}{2}\frac{\mathrm{d}\eta}{\mathrm{d}\rho^s}\rho_{,i}^s\rho_{,i}^s = f(t). \tag{1.4}$$

Total momentum equation

$$\frac{\partial}{\partial t}(\rho^n v_i^n + \rho^s v_i^s) + (\rho^n v_i^n v_j^n + \rho^s v_i^s v_j^s)_{,j} = \rho^n \Omega_{,i}^n + \rho^s \Omega_{,i}^s - p_{,i} + \Sigma_{ij,j}, \tag{1.5}$$

$$p = \rho^2 \frac{\partial A}{\partial \rho} + \rho\rho^s \frac{\partial A}{\partial \rho^s} - \eta\rho^s\rho_{,ii}^s - \frac{1}{2}\left(\eta + \rho^s \frac{\mathrm{d}\eta}{\mathrm{d}\rho^s}\right)\rho_{,i}^s\rho_{,i}^s,$$

$$\Sigma_{ij} = \alpha_1 D_{rr}^n \delta_{ij} + \alpha_2 D_{ij}^n - \eta\rho_{,i}^s\rho_{,j}^s.$$

Energy equation

$$\rho r - T\left\{\frac{\partial}{\partial t}(\rho S) + (\rho v_i^n S)_{,i}\right\} - (KT_{,i})_{,i} + \Lambda m^{*2} + \alpha_1 D_{rr}^n D_{pp}^n + \alpha_2 D_{ij}^n D_{ij}^n = 0. \tag{1.6}$$

Constitutive theory

$$A = A(\rho, \rho^*, T), \quad \eta = \eta(\rho^*), \quad \Lambda = \Lambda(\rho^*, T), \quad S = -\partial A/\partial T,$$
$$\rho\frac{\partial A}{\partial \rho^*} + \left\{\frac{1}{2}w^2 - \eta\rho^*_{,ii} - \frac{1}{2}\left(\frac{\mathrm{d}\eta}{\mathrm{d}\rho^*}\right)\rho^*_{,i}\rho^*_{,i} + \Lambda m^*\right\} = 0. \tag{1.7}$$

In (1.1)–(1.7), a suffix following a comma denotes differentiation with respect to the corresponding Cartesian coordinate: repeated suffices are summed. The expression (Γ, say) in braces in the last eqn of (1.7) is evidently a function of ρ, ρ^* and T by the first eqn of (1.7). It follows that ρ may be written, if desired, as a function of ρ^*, T and Γ.

The boundary conditions required to complete the theory depend on the nature of the surface under consideration. We will discuss only the case $\eta \neq 0$ since, if $\eta = 0$, the conditions differ in no way from those customarily applied to the Landau equations (e.g. see [1]).

Consider a stationary rigid surface ∂B with unit normal $\mathbf{n}$. Regarding the wall as an infinite potential barrier, we have

$$\rho^* \to 0 \quad \text{on } \partial B. \tag{1.8}$$

There is no mass flux into the wall so that

$$\mathbf{n} \cdot (\rho^n \mathbf{v}^n + \rho^* \mathbf{v}^*) = 0 \quad \text{on } \partial B. \tag{1.9}$$

When the coefficients of viscosity and thermal conductivity are non-zero, (1.9) is automatically obeyed since

$$\mathbf{n} \cdot \mathbf{v}^n = 0, \quad \rho^* \mathbf{n} \cdot \mathbf{v}^* = 0, \quad \text{on } \partial B. \tag{1.10}$$

Because of (1.8), $(1.10)_2$ does not imply that $\mathbf{n} \cdot \mathbf{v}^* = 0$. In fact $\mathbf{n} \cdot \mathbf{v}^*$ will in general be infinite on ∂B although there are no serious dynamical repercussions since the kinetic energy density

$$\tfrac{1}{2}\rho^*(\mathbf{n} \cdot \mathbf{v}^*)^2 \to \text{finite limit on } \partial B. \tag{1.11}$$

(A similar situation obtains on the vorticity singularity in the vortex core, where $\rho^* \to 0$, $|\mathbf{v}^*| \to \infty$ but $\rho^* v^{*2}$ is finite.)

The relations (1.10) hold even when the heat flux

$$\mathbf{q} \cdot \mathbf{n} = H, \quad \text{on } \partial B, \tag{1.12}$$

from the surface to the fluid is non-zero. If thermal conduction is ignored ($K = 0$), the wall is a source of normal fluid and a sink of superfluid for $H > 0$, and conversely for $H < 0$. Then the quantities set zero in (1.10) become non-zero, although (1.9) still holds. In all these situations, no-slip requires

$$\mathbf{n} \times \mathbf{v}^n = 0, \quad \text{on } \partial B, \tag{1.13}$$

though this restriction too must be lifted if the coefficients α_1, α_2 of viscosity are set zero.

At a free surface, the total stress associated with the normal, $n_j(p\delta_{ij} - \Sigma_{ij})$, should be balanced by the pressure of the vapour above the free surface.

In the present paper the healing and relaxation coefficients are allowed to depend generally on their arguments. However, a study of the two limiting cases $T \to 0$ (see Section 3) and $T \to T_\lambda$ (see Khalatnikov[4]) suggests that a good representation of the healing coefficient is

$$\eta = \frac{\hbar^2}{4m^2\rho^*}, \tag{1.14}$$

where m is the mass of the helium atom. A model of relaxation by Khalatnikov [4] assumes that

$$\Lambda = \frac{\hbar^2}{2m^2\rho^s\xi u_2} \tag{1.15}$$

approximately, where u_2 is the velocity of second sound and ξ is the healing length.

2. BASIC EQUATIONS

We refer the motion of the continuum to a fixed system of rectangular Cartesian axes. Direct tensor notation is used where convenient and also a corresponding suffix notation to denote components. We assume that each of the components of helium II occupies the position $\mathbf{x}$ at time t and we denote the densities and velocities of the normal and superfluid by ρ^n, ρ^s and $\mathbf{v}^n$, $\mathbf{v}^s$ respectively. Also, we use the notation

$$\begin{aligned}
&\rho = \rho^n + \rho^s, && \mathbf{w} = \mathbf{v}^n - \mathbf{v}^s,\\
&m^\alpha = \partial_t\rho^\alpha + \nabla\cdot(\rho^\alpha\mathbf{v}^\alpha), && \mathbf{f}^\alpha = \partial_t\mathbf{v}^\alpha + (\mathbf{v}^\alpha\cdot\nabla)\mathbf{v}^\alpha,\\
&D_{ij}^\alpha = \tfrac{1}{2}(v_{i,j}^\alpha + v_{j,i}^\alpha) \equiv v_{(i,j)}^\alpha, && W_{ij}^n = \tfrac{1}{2}(v_{i,j}^n - v_{j,i}^n) \equiv v_{[i,j]}^n,\\
&\frac{D^\alpha}{Dt} = \partial_t + (\mathbf{v}^\alpha\cdot\nabla), && W_{ij} = W_{ij}^n - W_{ij}^s,
\end{aligned} \tag{2.1}$$

where in (2.1) and throughout a superscript α denotes either n or s and ∂_t denotes differentiation with respect to t with $\mathbf{x}$ held fixed.

The basic governing equations for the mixture have been given, for example, by Hills and Roberts [6]. The equation of mass conservation is

$$m^n + m^s = 0. \tag{2.2}$$

The linear momentum equations in terms of the partial stresses Σ^α are

$$\nabla\cdot\Sigma^\alpha + \rho^\alpha\mathbf{b}^\alpha + \mathbf{g}^\alpha = \rho^\alpha\mathbf{f}^\alpha, \tag{2.3}$$

where $\mathbf{b}^\alpha$ is the applied body forces on each constituent and $\mathbf{g}^\alpha$ is the diffusive force with

$$\mathbf{g}^n + \mathbf{g}^s = -(m^n\mathbf{v}^n + m^s\mathbf{v}^s). \tag{2.4}$$

The equation of moments requires that

$$\hat{\Sigma}^n + \hat{\Sigma}^s = 0, \tag{2.5}$$

where $\hat{\Sigma}^\alpha$ is the axial vector associated with the skew symmetric part of the tensor Σ^α, that is

$$\hat{\Sigma}_i^\alpha = \tfrac{1}{2}e_{ijk}\Sigma_{kj}^\alpha. \tag{2.6}$$

The energy equation for the mixture is

$$\rho r - \rho\frac{DU}{Dt} - \nabla\cdot\mathbf{q} - \frac{1}{2}m^s w^2 + \mathbf{g}^s\cdot\mathbf{w} + tr(\Sigma^n\mathbf{D}^n + \Sigma^s\mathbf{D}^s) + 2\hat{\Sigma}^s\cdot\hat{\mathbf{W}} = 0, \tag{2.7}$$

where U is the internal energy per unit mass of helium II, r the heat supply function per unit mass per unit time, $\mathbf{q}$ the heat flux vector, tr denotes the trace operator and

$$\rho\frac{D}{Dt} = \rho\partial_t + \{(\rho^n\mathbf{v}^n + \rho^s\mathbf{v}^s)\cdot\nabla\}. \tag{2.8}$$

The theory is completed by a statement of the thermodynamical postulate. Previously, in

their studies of the continuum theories of helium II, Hills and Roberts[6] have employed the Clausius–Duhem inequality in this context. However, we might expect in a theory describing healing phenomena new terms which will contribute to the entropy flux. Müller[7] has postulated a thermodynamical inequality with a generalized entropy flux term which is not necessarily equal to the heat flux divided by temperature. In this paper, we adopt the pointwise form of Müller's inequality, viz

$$\rho T\frac{DS}{Dt} - \rho r + T\nabla\cdot\mathbf{k} \geq 0, \tag{2.9}$$

where S is the entropy per unit mass of helium II, T the temperature and $\mathbf{k}$ the entropy flux vector. As in previous studies (Hills and Roberts[6, 8]) we do not explicitly assume heat is carried only by the normal fluid and we refer the reader to the cited works for a full discussion.

If we introduce the Helmholtz free energy F and vector $\boldsymbol{\phi}$ where

$$F = U - ST, \quad \boldsymbol{\phi} = \mathbf{q} - T\mathbf{k}, \tag{2.10}$$

the inequality can be written as

$$-\rho\left\{\frac{DF}{Dt} + S\frac{DT}{Dt}\right\} - \mathbf{k}\cdot\nabla T - \nabla\cdot\boldsymbol{\phi} - \frac{1}{2}m^{s}w^{2} + \mathbf{g}^{s}\cdot\mathbf{w} + tr(\boldsymbol{\Sigma}^{n}\mathbf{D}^{n} + \boldsymbol{\Sigma}^{s}\mathbf{D}^{s}) + 2\hat{\boldsymbol{\Sigma}}^{s}\cdot\hat{\mathbf{W}} \geq 0. \tag{2.11}$$

The fundamental quantities of our theory are assumed to obey certain invariance requirements under a change of observer. If ρ^{n}, ρ^{s}, F, S, g_i^{s}, Σ_{ij}^{n}, Σ_{ij}^{s}, q_i, ϕ_i correspond to the motion in a given frame of reference then we denote the analogous quantities under a change of observer by the same symbol but with an attached asterisk. We assume

$$\begin{aligned} &\rho^{n*} = \rho^{n}, \ \rho^{s*} = \rho^{s}, \ U^{*} = U, \ S^{*} = S, \ T^{*} = T, \\ &\boldsymbol{\Sigma}^{n*} = \mathbf{Q}\boldsymbol{\Sigma}^{n}\mathbf{Q}^{T}, \ \mathbf{q}^{*} = \mathbf{Q}\mathbf{q}, \ \mathbf{g}^{s*} = \mathbf{Q}\mathbf{g}^{s}, \ \boldsymbol{\phi}^{*} = \mathbf{Q}\boldsymbol{\phi}, \end{aligned} \tag{2.12}$$

where $\mathbf{Q}$ is an orthogonal tensor having transpose $\mathbf{Q}^{T}$.

The theory is made determinate by proposing the constitutive equations which will reflect the character of the components. In their development of the constitutive bases for the Landau 2-fluid equations, Hills and Roberts[6] postulated for F, S, ρ^{s}/ρ, $\boldsymbol{\Sigma}^{n}$, $\mathbf{g}^{s}$ and $\mathbf{q}$ assuming that these quantities are general functions of ρ, T, w^{2} and otherwise linear functions of degree one in $\mathbf{D}^{n}$, the gradients of ρ, T, w^{2} and the vector $\mathbf{w}$. However, for the present theory we consider a modified set of postulates. Motivated by the requirement that we impose a boundary condition on ρ^{s}, we take ρ^{s}, not ρ, as the independent variable and postulate constitutive equations for F, S, ρ, $\boldsymbol{\Sigma}^{n}$, $\mathbf{g}^{n}$, $\mathbf{k}$ and $\boldsymbol{\phi}$. The mass conservation equation then becomes an equation for determining the superfluid density ρ^{s} while the momentum eqns (2.4) and the energy eqn (2.7) provide seven equations for determining $\mathbf{v}^{n}$, $\mathbf{v}^{s}$ and T.

Before discussing the constitutive theory, we remind ourselves of some features of the Bose condensate model of helium II. Since this may be applied only at absolute zero, it can provide no information about the way the two components of the mixture interact when $T > 0$. Moreover, the Bose condensate is often considered to be too unrealistic a model of helium, even at $T = 0$, to be trusted. Nevertheless, it appears to portray healing phenomena reliably, and it is the incorporation of healing into the Landau theory that is one of the principal objectives of this paper. Moreover, it is the simplest known model which does so, and our arguments become more transparent than if we had used an expansion in the order parameter, such as that used by Khalatnikov[4], even though such an expansion would generally be considered to represent helium for small $T_{\lambda} - T$ realistically. It must be stressed that our final results do not depend on the Bose condensate model, even though it is motivated by it.

3. PHYSICAL MOTIVATION FOR A CONTINUUM THEORY

The healing phenomenon requires the addition of new terms to the energy densities, the energy flux and the entropy flux. We consider these for the Bose condensate model of helium at

$T = 0$. This model may be regarded as a self-consistent field approximation for the single-particle wave function, $\psi(\mathbf{x}, t)$, which is supposed to obey the non-linear Schrödinger equation

$$i\hbar\partial_t\psi = -\frac{\hbar^2}{2m}\nabla^2\psi + (2m^2V_0|\psi|^2 + W)\psi, \tag{3.1}$$

where $W(\mathbf{x}, t)$ is the externally applied potential, $2m^2V_0\delta(\mathbf{x} - \mathbf{x}_0)$ is the interaction potential between two helium atoms (mass m) situated at x and $\mathbf{x}_0$ and V_0 is a constant of dimensions $M^{-1}L^5T^{-2}$. We may define mass, momentum and energy densities, ρ, j and E, per unit volume by

$$\rho = m|\psi|^2, \quad \mathbf{j} = \left(\frac{\hbar}{2i}\right)(\psi^*\nabla\psi - \psi\nabla\psi^*),$$
$$E = \left(\frac{\hbar^2}{2m}\right)|\nabla\psi|^2 + V_0\rho^2, \tag{3.2}$$

where * denotes the complex conjugate. These are (for $W = 0$) related by

$$\partial_t\rho + \nabla\cdot\mathbf{j} = 0, \quad \partial_t\mathbf{j} + \nabla\cdot\mathbf{\Pi} = 0, \quad \partial_t E + \nabla\cdot\mathbf{Q} = 0, \tag{3.3}$$

where j, $\mathbf{\Pi}$, Q are the mass, momentum and energy fluxes and, according to (3.1),

$$\Pi_{ik} = \frac{\hbar^2}{4m}\left\{\frac{\partial\psi}{\partial x_i}\frac{\partial\psi^*}{\partial x_k} - \psi^*\frac{\partial^2\psi}{\partial x_i\partial x_k} + \frac{\partial\psi^*}{\partial x_i}\frac{\partial\psi}{\partial x_k} - \psi\frac{\partial^2\psi^*}{\partial x_i\partial x_k}\right\} + V_0\rho^2\delta_{ik},$$
$$Q_i = \frac{\hbar^3}{4im^2}\left\{\frac{\partial\psi^*}{\partial x_i}\nabla^2\psi - \frac{\partial\psi}{\partial x_i}\nabla^2\psi^*\right\} + 2V_0\rho j_i. \tag{3.4}$$

Equations (3.2)–(3.4) may be cast in fluid mechanical form by means of the Madelung transformation

$$\psi = \left(\frac{\rho}{m}\right)^{1/2}\exp(im\mathrm{T}/\hbar). \tag{3.5}$$

Then (3.2) gives

$$\mathbf{j} = \rho\mathbf{v} = \rho\nabla\mathrm{T}, \quad E = \frac{1}{2}\rho v^2 + V_0\rho^2 + \frac{\hbar^2}{8m^2\rho}(\nabla\rho)^2, \tag{3.6}$$

the first of which portrays the mass flux, j, as due to an irrotational flow, v, with velocity potential T. The second exhibits the total energy per unit volume as the sum of three parts: the kinetic energy $\frac{1}{2}\rho v^2$, an internal energy which (for the present case of a condensate) is $V_0\rho^2$ and a quantum energy $\hbar^2(\nabla\rho)^2/8m^2\rho$.

In translating the fluxes (3.4) into fluid mechanics form we introduce a stress tensor

$$\Sigma_{ik} = V_0\rho^2\delta_{ik} + \frac{\hbar^2}{4m^2\rho}\left(\frac{\partial\rho}{\partial x_i}\frac{\partial\rho}{\partial x_k} - \rho\nabla^2\rho\delta_{ik}\right). \tag{3.7}$$

The first term is associated with the classical kinetic pressure in the gas which (for the present case of a condensate) is simply $V_0\rho^2$. The final term is the quantum stress. It stands in contrast to that invoked independently by Grant[9] and Putterman[1] which would give instead of (3.7)

$$\bar{\Sigma}_{ik} = V_0\rho^2\delta_{ik} + \frac{\hbar^2}{4m^2\rho}\left(\frac{\partial\rho}{\partial x_i}\frac{\partial\rho}{\partial x_k} - \rho\frac{\partial^2\rho}{\partial x_i\partial x_k}\right). \tag{3.8}$$

The difference between Σ_{ik} and $\bar{\Sigma}_{ik}$ has zero divergence and so does not influence the equations

of motion of the fluid. The form (3.8), although it follows directly from the first of (3.4), does not appear to be as appropriate to the continuum theory for reasons that will not become apparent until later.

With (3.7) we satisfy the last two equations of (3.3) by

$$\Pi_{ik} = \rho v_i v_k + \Sigma_{ik}, \quad Q_i = E v_i + \Sigma_{ik} v_k - \frac{\hbar^2 \dot{\rho}}{4m^2 \rho} \frac{\partial \rho}{\partial x_i}, \tag{3.9}$$

where $\dot{\rho}$ denotes the material derivative $\{\partial_t \rho + (\mathbf{v} \cdot \nabla)\rho\}$ of ρ. In addition to the quantum contribution contained in E and Σ_{ik}, there is a totally unexpected final term in Q_i of quantum origin.

The assumption of an imperfect Bose gas is contained in V_0 terms above. If V_0 is set zero, the conclusions hold for the one particle Schrödinger equation instead.

4. CONSTITUTIVE THEORY

In this section we construct a theory of helium II which, while capable of describing the phenomenon of quantum healing and the relaxation processes associated with the λ-point, reduces to the Landau 2-fluid theory away from the boundaries and the λ-point. The previous section suggests that the constitutive equations should depend on superfluid density gradients and we shall consider only first and second gradients. Moreover, the experiments of Chase[10] indicate that, near the λ-point, there is associated with the material a characteristic time. One way of introducing such a time into a theory is to allow a constitutive dependence on variables such as $D^s\rho^s/Dt$ or m^s. As might be anticipated, the two theories that result from these alternatives are radically different and will be compared at the end of this section. The final term in the expression for E in (3.9) appears to favour $D^s\rho^s/Dt$. However, Section 3 was exclusively concerned with healing and a study of relaxation processes suggests that m^s may be more fundamental.

We generalize the postulates[6] for the Landau 2-fluid model and assume that the free energy F, the entropy S, and the *total density* ρ depend generally on ρ^s, T, w^2, $(\nabla\rho^s)^2$, $\nabla^2\rho^s$ and m^s. Thus, if χ denotes F, S or ρ, we have

$$\chi = \chi(\rho^s, T, w^2, \theta^2, \sigma, m^s), \tag{4.1}$$

where

$$\theta^2 = \rho^s_{,i}\rho^s_{,i} \quad \text{and} \quad \sigma = \rho^s_{,ii}. \tag{4.2}$$

The stress tensors Σ^n and Σ^s are again assumed purely symmetric with extra terms arising from the dependence on density gradients. We have

$$\begin{aligned}
&\Sigma^n_{(ij)} = -p^n\delta_{ij} + \alpha_1 v^n_{r,r}\delta_{ij} + \alpha_2 v^n_{(i,j)} + \alpha_3 \rho^s_{,i}\rho^s_{,j} + \alpha_4 \rho^s_{,ij}, \\
&\Sigma^n_{[ij]} = 0, \\
&\Sigma^s_{(ij)} = -p^s\delta_{ij} + \beta_1 \rho^s_{,i}\rho^s_{,j} + \beta_2 \rho^s_{,ij}, \quad \Sigma^s_{[ij]} = 0,
\end{aligned} \tag{4.3}$$

where the partial pressures p^n, p^s are general functions of the set

$$\mathcal{P} = \{\rho^s, T, w^2, \theta^2, \sigma, m^s\},$$

and the coefficients α_i, β_i are functions of $\mathcal{P}$ but linear in m^s.

In developing their constitutive theory for the Landau 2-fluid model, Hills and Roberts[6] employed the Clausius–Duhem inequality where $\phi = 0$. Their assumptions for the diffusive force $\mathbf{g}^s$ and heat flux vector $\mathbf{q}$ involved gradient terms that are not necessary in the present Müller-type theory. It should be stated that in the context of the Landau 2-fluid theory the governing equations from the two approaches are the same with only the expressions for the partial pressures and diffusive forces differing.† However, it will be seen that for the present

†A similar situation arises with the theory of a mixture of inviscid gases[5, 11].

theory ϕ plays a crucial role. We shall assume

$$g_i^s = \gamma_1 \rho_{,i}^s + \gamma_2 T_{,i} + \gamma_3 w_i,$$
$$k_i = \epsilon_1 \rho_{,i}^s + \epsilon_2 T_{,i} + \epsilon_3 w_i, \tag{4.4}$$

where again the coefficients are functions of $\mathscr{P}$, linear in m^s. Adherence to the principle of equipresence‡ would require a parallel assumption to (4.4) to be made for ϕ. However, with such a postulate an analysis similar to that indicated below rules out any dependence on m^s for the coefficient of $\rho_{,i}^s$. Nevertheless, Section 3 suggests that ϕ should contain a term $\dot{\rho}^s \rho_{,i}^s / \rho^s$, $\dot{\rho}^s \equiv D^s \rho^s / Dt$, and we assume

$$\phi_i = \eta_1 \rho_{,i}^s + \eta_2 T_{,i} + \eta_3 w_i, \tag{4.5}$$

where η_1 depends upon ρ^s, T, w^2, θ^2, σ and is linear in $\dot{\rho}^s$ while η_2, η_3 depend on the set $\mathscr{P}$. We shall write

$$\eta_1 = \eta_1^0 + \dot{\rho}^s \eta_1^1, \quad \dot{\rho}^s = \frac{D^s \rho^s}{Dt}. \tag{4.6}$$

This completes our constitutive assumptions and it is obvious that these assumptions satisfy the invariance requirements (2.12).

We now investigate the implications of the thermodynamical postulate (2.11). In doing so we follow the scheme proposed by Coleman and Noll[12] and regard the heat supply r, the body forces $\mathbf{b}^n$ and $\mathbf{b}^s$ as quantities that can be arbitrarily assigned. Consequently, at any point, there is no restriction upon the choice of

$$\rho^s, T, \mathbf{w}, \mathbf{D}^n, \mathbf{W}^n$$

and the material and spatial derivatives of these quantities implied by the eqns (2.3) and (2.7). However, with the constitutive eqns (4.1), the mass conservation eqn (2.2) gives

$$\frac{\partial \rho}{\partial \rho^s} M(\rho^s) + \frac{\partial \rho}{\partial T} M(T) + \frac{\partial \rho}{\partial w^2} M(w^2) + \frac{\partial \rho}{\partial m^s} M(m^s) + \frac{\partial \rho}{\partial \theta^2} M(\theta^2)$$
$$+ \frac{\partial \rho}{\partial \sigma} M(\sigma) - \mathbf{w} \cdot \nabla \rho^s + \rho^s \nabla \cdot \mathbf{v}^s + \rho^n \nabla \cdot \mathbf{v}^n = 0, \tag{4.8}$$

where

$$M(\chi) \equiv \frac{D\chi}{Dt} + \frac{\rho^s}{\rho} \mathbf{w} \cdot \nabla \chi. \tag{4.9}$$

From the definitions (2.1), we obtain the kinematical results

$$\frac{D\rho^s}{Dt} = m^s + \frac{\rho^n}{\rho} \mathbf{w} \cdot \nabla \rho^s - \rho^s \nabla \cdot \mathbf{v}^s, \tag{4.10}$$

$$\frac{D\theta^2}{Dt} = 2 \nabla \rho^s \cdot \nabla \dot{\rho}^s + \frac{\rho^n}{\rho} \mathbf{w} \cdot \nabla \theta^2 - 2 \nabla \rho^s \cdot \mathbf{D}^s \nabla \rho^s. \tag{4.11}$$

If we regard (4.8) as an equation determining Dw^2/Dt in terms of the other variables and employ the results (4.10), (4.11), the entropy inequality (2.11) can be cast in the form

$$a_1 m^s + a_2 + a_3 \frac{DT}{Dt} + a_4 \frac{Dm^s}{Dt} + a_5 \frac{D\theta^2}{Dt} + a_6 \frac{D\sigma}{Dt} + a_{13} \nabla T \cdot \nabla \rho^s - \epsilon_2 (\nabla T)^2$$
$$+ \mathbf{w} \cdot (a_7 \nabla \rho^s + a_8 \nabla T + a_9 \nabla w^2 + a_{10} \nabla m^s + a_{11} \nabla \theta^2 + a_{12} \nabla \sigma + \gamma_3 \mathbf{w})$$
$$+ a_{14} tr \mathbf{D}^s + a_{15} \nabla \rho^s \cdot \mathbf{D}^s \nabla \rho^s + \beta_2 tr(\mathbf{D}^s \mathbf{P}) + \alpha_1 (tr \mathbf{D}^n)^2 + \alpha_2 tr \mathbf{D}^{n^2} \tag{4.12}$$
$$+ a_{16} tr \mathbf{D}^n + \alpha_4 tr(\mathbf{D}^n \mathbf{P}) + \alpha_3 \nabla \rho^s \cdot \mathbf{D}^n \nabla \rho^s - \eta_2 \nabla^2 T - \nabla \eta_2 \cdot \nabla T$$
$$- \nabla \rho^s \cdot \left(\frac{\partial \eta_1}{\partial \theta^2} \nabla \theta^2 + \frac{\partial \eta_1}{\partial \sigma} \nabla \sigma + \frac{\partial \eta_1}{\partial w^2} \nabla w^2 \right) \geq 0.$$

‡This principle states that a variable present in one constitutive equation is present in all unless proved to the contrary.

When†

$$\mu = \rho \frac{\partial F}{\partial w^2} \Big/ \frac{\partial \rho}{\partial w^2}, \qquad P_{ij} = \rho^* \delta_{ij}, \tag{4.13}$$

the coefficients $a_1 - a_{16}$ take the forms

$$\begin{aligned}
&a_1 = \mu \frac{\partial \rho}{\partial \rho^*} - \rho \frac{\partial F}{\partial \rho^*} - \frac{1}{2} w^2 - \eta_1^1 \sigma - \frac{\partial \eta_1^1}{\partial \rho^*} \theta^2, \quad a_2 = -\left(\eta_1^0 \sigma - \frac{\partial \eta_1^0}{\partial \rho^*} \theta^2 \right), \\
&a_3 = \mu \frac{\partial \rho}{\partial T} - \rho \frac{\partial F}{\partial T} - \rho S, \quad a_4 = \mu \frac{\partial \rho}{\partial m^*} - \rho \frac{\partial F}{\partial m^*}, \quad a_5 = \mu \frac{\partial \rho}{\partial \theta^2} - \rho \frac{\partial F}{\partial \theta^2} - \frac{1}{2} \eta_1^1, \\
&a_6 = \mu \frac{\partial \rho}{\partial \sigma} - \rho \frac{\partial F}{\partial \sigma}, \quad a_7 = \mu \left(\frac{\partial \rho}{\partial \rho^*} - 1 \right) - \rho^n \frac{\partial F}{\partial \rho^*} - \frac{\partial \eta_3}{\partial \rho^*} + \gamma_1, \\
&a_8 = \frac{\mu \rho^*}{\rho} \frac{\partial \rho}{\partial T} - \frac{\partial \eta_3}{\partial T} + \gamma_2 - \epsilon_3, \quad a_9 = \frac{\mu \rho^*}{\rho} \frac{\partial \rho}{\partial w^2} - \frac{\partial \eta_3}{\partial w^2}, \\
&a_{10} = \frac{\mu \rho^*}{\rho} \frac{\partial \rho}{\partial m^*} - \frac{\partial \eta_3}{\partial m^*}, \quad a_{11} = \mu \frac{\partial \rho}{\partial \theta^2} - \rho^n \frac{\partial F}{\partial \theta^2} - \frac{\partial \eta_3}{\partial \theta^2}, \\
&a_{12} = \frac{\mu \rho^*}{\rho} \frac{\partial \rho}{\partial \sigma} - \frac{\partial \eta_3}{\partial \sigma}, \quad a_{13} = -\left(\epsilon_1 + \frac{\partial \eta_1}{\partial T} \right), \\
&a_{14} = \rho^* \left(\mu - \mu \frac{\partial \rho}{\partial \rho^*} + \rho \frac{\partial F}{\partial \rho^*} + \eta_1^1 \sigma + \frac{\partial \eta_1^1}{\partial \rho^*} \theta^2 \right) - p^* + \eta_3, \\
&a_{15} = \beta_1 - 2\left(\mu \frac{\partial \rho}{\partial \theta^2} - \rho \frac{\partial F}{\partial \theta^2} \right), \quad a_{16} = \mu \rho^n - p^n - \eta_3.
\end{aligned} \tag{4.14}$$

It is possible to choose DT/Dt, Dm^*/Dt, $D\theta^*/Dt$ and $D\sigma/Dt$ arbitrarily and independently of all other quantities appearing in the inequality. Hence, $a_3 = a_4 = a_5 = a_6 = 0$. From these results with (4.13) we find

$$\begin{aligned}
F &= F^*(\rho, \rho^*, T, \theta^2), \\
\rho &= \rho(\rho^*, T, w^2, \theta^2, \sigma, m^*),
\end{aligned} \tag{4.15}$$

and‡

$$S = -\frac{\partial F^*}{\partial T}, \quad \eta_1^1 = -2\rho \frac{\partial F^*}{\partial \theta^2}, \tag{4.16}$$

so that

$$F = A(\rho, \rho^*, T) - \frac{\eta_1^1}{2\rho} \theta^2, \quad \rho = \rho(\rho^*, T, w^2, \theta^2, \sigma, m^*). \tag{4.17}$$

Applying the same type of arguments to the residual inequality we find

$$\begin{aligned}
&a_9 = a_{10} = a_{11} = a_{12} = a_{14} = a_{15} = \beta_2 = \eta_2 = 0, \\
&\eta_1 = \eta_1^0(\rho^*, T) + \dot{\rho}^* \eta_1^1(\rho^*, T).
\end{aligned} \tag{4.18}$$

Before we make further deductions from the inequality, we consider the implications of the postulate of irrotationality for the superfluid. By using the constitutive theory and (4.18), we can write the superfluid momentum equation as

$$\rho^* \mathbf{f}^* = -\rho^* \nabla \Phi + a_7 \nabla \rho^* + \left(\rho^* \frac{\partial F}{\partial T} + \gamma_2 - \frac{\partial \eta_3}{\partial T} \right) \nabla T + \gamma_3 \mathbf{w} + \frac{\partial \eta_1^1}{\partial T} (\nabla T \cdot \nabla \rho^*) \nabla \rho^* + \rho^* \mathbf{b}^*, \tag{4.19}$$

†In writing (4.13), we have tacitly assumed that $\partial \rho / \partial w^2 \neq 0$. It may be objected that changes of ρ with w^2 are usually regarded as small to the point of negligibility. This, however, concerns the experimentally accessible derivative $\partial \rho / \partial w^2$ for fixed ρ and T. In (4.13), the variables held fixed are T, θ^2, σ, m^* and ρ^*, a totally different set. There is no obvious reason why the derivative of (4.13), should be small especially when it is remembered that in the Landau theory $(\partial \rho^* / \partial w^2)_{\rho, T} \neq 0$. Further, anticipating (4.17) and (4.25), we find that (4.13), is equivalent to $\mu = (p + \frac{1}{2}\rho^* w^2 + \Lambda \rho^* m^*)/\rho$ which is evidently closely related to the pressure, and is positive unless m^* is extremely large and negative.

‡The variables being held fixed for any partial derivative are implied by the function used, that is $\partial F^*/\partial T = \partial F^*/\partial T|_{\rho^*, w^2}$, etc.

where

$$\Phi = A + \rho\left(\frac{\partial A}{\partial \rho} + \frac{\partial A}{\partial \rho^s}\right) + \eta_1\sigma + \frac{1}{2}\frac{\partial \eta_1^1}{\partial \rho^s}\theta^2. \tag{4.20}$$

The condition that, with conservative body forces, the acceleration $\mathbf{f}^s$ is derivable from a potential implies

$$\gamma_3 = a_7 = 0, \quad \gamma_2 = -\rho^s\frac{\partial F}{\partial T} + \frac{\partial \eta_3}{\partial T}, \quad \eta_1^1 = \eta_1^1(\rho^s). \tag{4.21}$$

Adopting the values (4.21) we see that (4.12) requires

$$a_1 m^s + a_2 \geq 0, \tag{4.22}$$

from which we deduce $\eta_1^0 = 0$. Consequently, if we introduce the variable η by

$$\eta_1^1(\rho^s) \equiv -\eta(\rho^s), \tag{4.23}$$

the equation for ϕ reduces to

$$\phi = -\eta\dot{\rho}^s\nabla\rho^s + \eta_3\mathbf{w}. \tag{4.24}$$

A comparison with Section 3 ($T = 0$) and Khalatnikov[4] ($T \to T_\lambda$) suggests that

$$\eta = \frac{\hbar^2}{4m^2\rho^s}. \tag{4.25}$$

To make further progress we need to be more explicit regarding the coefficient a_1. As a first step we shall assume that the constitutive equations for A and ρ are such that a_1 is linear in m^s, that is

$$a_1 \equiv -\rho\frac{\partial A}{\partial \rho^s} - \frac{1}{2}w^2 + \eta\sigma + \frac{1}{2}\frac{\mathrm{d}\eta}{\mathrm{d}\rho^s}\theta^2 = \Lambda(\rho^s, T)m^s. \tag{4.26}$$

From (4.22) we see that Λ satisfies $\Lambda \geq 0$. The constitutive choice (4.26) is to a large extent motivated by the realization that, when relaxation effects are absent (that is, no dependence on m^s), a_1 is identically zero. This is the case for the Landau 2-fluid theory† and for a theory incorporating only healing phenomena. Equation (4.26) represents an obvious generalization of an equation basic to Khalatnikov's model of relaxation[4]. We observe that, since $A = A(\rho, \rho^s, T)$, the constitutive postulate (4.26) implies that the equation for ρ must have the form

$$\rho = \rho\left(\rho^s, T, \frac{1}{2}w^2 - \eta\sigma - \frac{1}{2}\frac{\mathrm{d}\eta}{\mathrm{d}\rho^s}\theta^2 + \Lambda m^s\right). \tag{4.27}$$

With the assumption (4.26), the reduced inequality requires

$$\begin{gathered} a_8 = a_{13} = a_3 = a_4 = 0, \quad \epsilon_2 \leq 0, \quad \alpha_1 + \tfrac{1}{3}\alpha_2 \geq 0, \qquad \alpha_2 \geq 0, \\ (\alpha_1 + \tfrac{1}{3}\alpha_2)\Lambda m^{s2} - a_{16}^2 \geq 0. \end{gathered} \tag{4.28}$$

By the constitutive assumption, a_{16} depends on m^s but $(4.28)_8$ implies that a_{16} vanishes with m^s

†The Landau equations are usually[6] expressed in terms of the independent variables ρ, T, w^2. These equations can be obtained from the present theory by setting $\eta = \Lambda = 0$ and introducing the Legendre dual transformation $\mathscr{A}(\rho, T, w^2) = A(\rho, \rho^s, T) - (\rho^s w^2/2\rho)$.

Journal of Low Temperature Physics, Vol. 30, Nos. 5/6, 1978

Healing and Relaxation in Flows of Helium II. Part II. First, Second, and Fourth Sound*

R. N. Hills†

Physics Department, University of Oregon, Eugene, Oregon

and P. H. Roberts

Department of Applied Mathematics, The University, Newcastle upon Tyne, England

(Received August 23, 1977)

In Part I of this series, a theory of helium II incorporating the effects of quantum healing and relaxation was developed. In this paper, the propagation of first, second, and fourth sound is discussed. Particular attention is paid to sound propagation in the vicinity of the λ point where the effects of relaxation and quantum healing become important.

1. INTRODUCTION

In Part I of this series[7] the Landau two-fluid equations governing the motion of helium II were generalized to include healing and relaxation. The need to incorporate both these effects for a proper theoretical description was inferred from experimental evidence. For example, there is a disparity between the observed and predicted velocity of third sound, which can be understood, qualitatively at least, by supposing the superfluid density obeys a boundary condition that it vanishes at a wall (see Ref. 14, Section 41). Moreover, the experiments of Chase[4] dealing with the propagation of first sound near the λ point strongly suggest the existence of a relaxation mechanism (for a recent review see Rudnick[15]). It would appear that this mechanism is primarily important in the vicinity of the λ point,‡ while healing embraces the whole temperature range of helium II. In effect, the inclusion of healing recognizes that the superfluid density cannot

*Supported in part by a special research grant GR/A/0556 from the Science Research Council of Great Britain, and (for RNH) by U.S. Air Force grant AFOSR 76-2880 and National Science Foundation grant ENG-76-07354.

†Permanent address: Mathematics Department, Heriot-Watt University, Edinburgh, United Kingdom.

‡Strictly, relaxation could be important over the whole temperature range if the sound frequency were sufficiently high.

0022-2291/78/0300-0709$05.00/0

change significantly over distances short compared with a certain "healing length" ξ; the inclusion of relaxation recognizes that it cannot change significantly over a time short compared with a certain relaxation time τ. Both ξ and τ become infinite as the λ point is approached.

In this paper we study how healing and relaxation processes affect the propagation of first, second, and fourth sound. We leave the study of third-sound waves until later. After setting down the governing equations derived in Part I, we show in Section 2 how an energy function $A(\rho, T, \rho^s)$ required by the theory can be obtained as a function of density ρ, temperature T, and superfluid density ρ^s. This energy function was also an ingredient of an earlier theory of Khalatnikov,[10] which, however, only included the effects of relaxation. In Section 3 we develop the linearized equations governing first and second sound of infinitesimal amplitude, and obtain the effects of healing and relaxation on the dispersion relationship between ω and k, respectively the frequency and wave number of a plane wave. In preparation for the study of wave propagation near the λ point, we summarize in Section 4 the behavior of the relevant physical quantities as T_λ is approached. In Section 5 the dispersion relationship is solved for $T \to T_\lambda$ when both healing and relaxation are present. In Section 6 similar results are derived for fourth sound. We find that the propagation of sound waves is affected by healing and relaxation once ξk and $\omega\tau$ become of order unity or greater.

In a subsequent paper,[8] we examine the effects of healing more closely. In particular, we demonstrate that our theory gives a realistic representation of healing at a plane wall.

Throughout this paper our notation is as follows: ρ^s is the superfluid density, v_i^s is the superfluid velocity, Ω^s is the potential of external body force b_i^s per unit mass ($b_i^s = \Omega_{,i}^s$), ϕ^s is the superfluid velocity potential ($v_i^s = \phi_{,i}^s$), and

$$m^s = \dot{\rho}^s + (\rho^s v_i^s)_{,i} = \text{superfluid mass supply} \tag{1}$$

Similar quantities are defined for the normal fluid (superscript n). In (1) the superposed dot denotes time differentiation holding the spatial variable fixed; a subscript following a comma denotes differentiation with respect to the corresponding Cartesian coordinate: Repeated subscripts are summed. We also have the following: r is the heat supply per unit time, ρ is the total density, A is an energy function, S is the specific entropy, w_i is the relative velocity $v_i^n - v_i^s$, T is the temperature, p is the pressure, K is the thermal conductivity (≥ 0), Φ is the thermodynamic potential per unit mass, α_1 and α_2 are coefficients of viscosity ($\alpha_2 \geq 0$, $\alpha_1 + \frac{1}{3}\alpha_2 \geq 0$), η is the healing coefficient, Λ is the relaxation coefficient (≥ 0), $D_{ij}^n = \frac{1}{2}(v_{i,j}^n + v_{j,i}^n)$ = rate of deformation tensor for normal fluid, and $\sum_{ij}$ is a stress tensor.

In the first paper of this series[7,*] the following equations were obtained:

$$\rho = \rho^n + \rho^s \tag{2}$$

$$\dot{\rho} + (\rho^n v_i^n + \rho^s v_i^s)_{,i} = 0 \tag{3}$$

$$\dot{v}_i^s + v_j^s v_{i,j}^s = (\Omega^s - \Phi)_{,i} \tag{4}$$

$$\dot{(\rho^n v_i^n + \rho^s v_i^s)} + (\rho^n v_i^n v_j^n + \rho^s v_i^s v_i^s)_{,i} = \rho^n \Omega_{,i}^n + \rho^s \Omega_{,i}^s - p_{,i} + \Sigma_{ji,j} \tag{5}$$

$$T[\dot{(\rho S)} + (\rho S v_i^n)_{,i}] = (KT_{,i})_{,i} + \Lambda(m^s)^2 + \alpha_1 D_{rr}^n D_{pp}^n + \alpha_2 D_{ij}^n D_{ij}^n + \rho r \tag{6}$$

$$\rho(\partial A/\partial \rho^s) + \Gamma = 0 \tag{7}$$

$$\Gamma = \tfrac{1}{2}w^2 + \Lambda m^s - \eta \rho_{,jj}^s - \tfrac{1}{2}(d\eta/d\rho^s)\rho_{,j}^s \rho_{,j}^s \tag{8}$$

Equations (3), (5), and (6) are, respectively, the equations of mass, total momentum, and energy balance; (7) and (8) form a constitutive relation governing the healing and relaxation of ρ^s. The viscosities α_1 and α_2 and the thermal conductivity K depend on ρ, T, and ρ^s; the relaxation coefficient Λ is a function of ρ^s and T, while the healing coefficient η depends only on ρ^s. Since the superfluid flow is irrotational, we can integrate the superfluid balance law (4) to obtain the Bernoulli equation

$$\dot{\phi}^s + \tfrac{1}{2}(v^s)^2 + \Phi - \Omega^s = g(t) \tag{9}$$

where the arbitrary function g of time t can be absorbed into ϕ^s if desired. We also have

$$S = -\partial A/\partial T \tag{10}$$

$$\Phi = A + \rho(\partial A/\partial \rho) - (\tfrac{1}{2}w^2 + \Lambda m^s) \tag{11}$$

$$p = \rho^2(\partial A/\partial \rho) - \rho^s(\tfrac{1}{2}w^2 + \Lambda m^s) - \tfrac{1}{2}\eta \rho_{,j}^s \rho_{,j}^s \tag{12}$$

$$\Sigma_{ij} = \alpha_1 D_{rr}^n \delta_{ij} + \alpha_2 D_{ij}^n - \eta \rho_{,i}^s \rho_{,j}^s \tag{13}$$

The energy A depends on ρ, T, and ρ^s alone and we shall assume that it has a minimum with respect to ρ^s at $f(\rho, T)$, say; that is,

$$\left(\frac{\partial A}{\partial \rho^s}\right)_{\rho^s = f(\rho,T)} = 0 \tag{14}$$

Thus f is the equilibrium superfluid density in bulk helium. The only property of A required for linearized equations, such as those governing

*We take this opportunity to correct misprints in Hills and Roberts[7]. K should be replaced by $-K$ in (1.6), (4.37), and (4.43). T should be replaced by Y in (3.5), (3.6), and two lines below (3.6). The derivative of A in (4.44) should be with respect to ρ^s.

first, second, and fourth sound, is

$$A_1 = \rho\left(\frac{\partial^2 A}{\partial(\rho^s)^2}\right)_{\rho^s = f(\rho,T)} > 0 \tag{15}$$

In what follows, we often adopt the models

$$\eta = \zeta/\rho^s, \qquad \Lambda = l/(\rho^s)^{1/2} \tag{16}$$

where $l = l(T)$ and ζ is a constant ($= \hbar^2/4m^2$, where $2\pi\hbar$ is Planck's constant h, and m is the mass of the helium atom). The utility of the model (16) is established by the solutions presented in Hills and Roberts.[8]

2. MODEL FOR THE ENERGY FUNCTION A

The Helmholtz free energy $\mathscr{A}_0(\rho, T)$ of stagnant helium is known accurately; a recent tabulation is included in the compilation of Brooks and Donnelly.[2] Donnelly and Roberts[6] have shown that $\mathscr{A}_0$ can also be obtained satisfactorily as the sum of a ground-state energy $\mathscr{A}_G(\rho)$ and an excitation free energy $\mathscr{A}_E(\rho, T)$ computed from the dispersion curve $\varepsilon(p)$ for the ρ and T concerned. (In this section, p stands for momentum). One may conclude confidently that, to the same accuracy, $\mathscr{A}(\rho, T, w^2)$ could also be computed for moving helium from $\varepsilon(p)$ by the usual prescription [e.g., Ref. 9, Eqs. (1.13) and (2.2)]

$$\mathscr{A}(\rho, T, w^2) = \mathscr{A}_G(\rho) + \mathscr{A}_E(\rho, T, w^2) \tag{17}$$

$$\mathscr{A}_E = -\frac{kT}{\rho}\int \ln(1+n)\, d^3p \tag{18}$$

$$n = \left[\exp\left(\frac{\varepsilon(p) - \mathbf{p}\cdot\mathbf{w}}{kT}\right) - 1\right]^{-1} \tag{19}$$

We shall not follow Donnelly and Roberts[6] by computing $\mathscr{A}_E$ from the most accurate available $\varepsilon(p)$. Instead, we shall, like many authors, be content with the simple Landau approximation in which $\varepsilon(p)$ is represented by a linear phonon branch, with $\partial\varepsilon/\partial p$ the velocity of sound a, and a parabolic roton branch with minimum Δ at momentum p_0. We shall ignore interactions between quasiparticles, although Donnelly and Roberts[6] show that interactions can be well accounted for by permitting $\varepsilon(p)$, or a, p_0, Δ, and the roton effective mass μ, to depend on T as well as ρ. Then, as shown by Khalatnikov [Ref. 9, Eqs. (2.13) and (2.14)]

$$\mathscr{A}_E = \rho^{-1}F_{\rm ph}\left(1 - \frac{w^2}{a^2}\right)^{-2} + \rho^{-1}F_{\rm rot}\left(\frac{kT}{p_0 w}\right)\sinh\frac{p_0 w}{kT} \tag{20}$$

where

$$F_{\rm ph}(\rho, T) = \frac{-4\pi^5}{45}\left(\frac{kT}{ha}\right)^3 kT, \qquad F_{\rm rot}(\rho, T) = \frac{-2p_0^2}{\mu}\left(\frac{2\pi\mu kT}{h^2}\right)^{3/2} \exp\frac{-\Delta}{kT} \tag{21}$$

are the phonon and roton free energies, which depend implicitly on ρ through a, p_0, Δ, and μ; in (21), k and h are the Boltzmann and Planck constants. The normal fluid density, generally given by

$$\rho^n/2\rho = -\partial\mathcal{A}/\partial w^2 \tag{22}$$

is according to (20)

$$\rho^n = -\frac{4F_{\rm ph}}{a^2}\left(1 - \frac{w^2}{a^2}\right)^{-3} - \frac{F_{\rm rot}}{w^2}\left[\cosh\frac{p_0 w}{kT} - \frac{kT}{p_0 w}\sinh\frac{p_0 w}{kT}\right] \tag{23}$$

It is easy to see that ρ^s vanishes at a critical velocity $w = w_c$, which for small T is

$$w_c = a\left[1 - \left(\frac{\pi h}{45\rho a}\right)^{1/3}\left(\frac{2\pi kT}{ha}\right)^{4/3}\right]^{1/2} \tag{24}$$

If $w \ll a$ and $w \ll kT/p_0$, we may expand (20) in a Taylor series

$$\mathcal{A}_E = \rho^{-1}\sum_{n=0}^{\infty} F_n(T) w^{2n} \tag{25}$$

with

$$F_0 = F_{\rm ph} + F_{\rm rot}, \qquad F_1 = \frac{2F_{\rm ph}}{a^2} + \frac{F_{\rm rot}}{6}\left(\frac{p_0}{kT}\right)^2, \qquad F_2 = \frac{3F_{\rm ph}}{a^4} + \frac{F_{\rm rot}}{120}\left(\frac{p_0}{kT}\right)^4, \ldots \tag{26}$$

By assuming that differentiation of (25) does not destroy its convergence for $w \ll a$ and $w \ll kT/p_0$, we find that (22) and (25) imply

$$\rho^n = -2\sum_{n=1}^{\infty} nF_n(T) w^{2(n-1)} \tag{27}$$

which may be inverted to give

$$w^2 = \frac{1}{4F_2}(\rho^s - f) - \frac{3F_3}{32F_2^3}(\rho^s - f)^2 + \frac{9F_3^2 - 4F_2F_4}{128F_2^5}(\rho^s - f)^3 + \ldots \tag{28}$$

where $f(\rho, T) = \rho + 2F_1(\rho, T)$. The quantity $A(\rho, \rho^s, T)$ we require is

related to $\mathscr{A}$ by the Legendre transformation

$$A = \mathscr{A} + (\rho^n/2\rho)w^2 \tag{29}$$

so that by (17), (25), and (28) we have

$$A = A_0(\rho, T) + \frac{A_1(\rho, T)}{2\rho}[\rho^s - f(\rho, T)]^2 + \frac{A_2(\rho, T)}{3\rho^2}[\rho^s - f(\rho, T)]^3 + \cdots \tag{30}$$

where

$$A_0(\rho, T) = \mathscr{A}_G(\rho) + F_0(\rho, T)/\rho, \qquad A_1(\rho, T) = -1/8F_2(\rho, T)$$
$$A_2(\rho, T) = 3\rho F_3(\rho, T)/64[F_2(\rho, T)]^3, \qquad \text{etc.} \tag{31}$$

Since $\mathscr{A}_G < 0$, $F_{ph} < 0$, and $F_{rot} < 0$, it follows that, for all ρ and T,

$$A_0 < 0, \qquad A_1 > 0, \qquad A_2 > 0 \tag{32}$$

The simplest viable model truncates (30) after the quadratic term:

$$A = A_0(\rho, T) + (A_1/2\rho)[\rho^s - f(\rho, T)]^2 \tag{33}$$

The critical velocity is then $w_c = (2A_1 f)^{1/2}$.

Because of the large size of $\mathscr{A}_G$ (see Brooks and Donnelly[2]), the first terms on the right-hand sides of (30) and (33) dominate the remainders. The subsequent convergence of (30) is not rapid in all circumstances. For example, near an infinite potential barrier ($\rho^s \doteqdot 0$) at temperatures near absolute zero ($f \doteqdot \rho$), the ratio of the third term to the second is $\rho|F_3|/4F_2^2 \doteqdot O[\rho h^3 a^5 (kT)^{-4}]$, which is obviously large compared with 1 for sufficiently small T. For this reason we refer to (33) as a "model" for A. Nevertheless, the convergence of (30) should be rapid near the λ point, where $\rho^s - f$ is always small, and this is the regime in which we are mainly interested. Also, (33), like (30), has the necessary attribute that A is stationary (a minimum) for $\rho^s = f$: See (14) and (15).

3. FIRST AND SECOND SOUND

We consider the propagation of infinitesimal disturbances in an equilibrium state with density ρ_0, temperature T_0, and superfluid density $f(\rho_0, T_0)$, all constant. We neglect the effects of viscosity and thermal conductivity. We set $\rho = \rho_0 + \bar{\rho}$, $T = T_0 + \bar{T}$, etc., substitute into the basic equations of Section 1, and neglect the squares and products of $\mathbf{v}^n$, $\mathbf{v}^s$, w, $\bar{\rho}$, and $\bar{T}$ in the usual process of linearization. After suppressing the subscript

zero, we obtain from (1), (3)–(8), and (30)

$$\bar{m}^s = \hat{\rho}^s + \rho^s v^s_{i,i} \tag{34}$$

$$\dot{\hat{\rho}} + \rho^n v^n_{i,i} + \rho^s v^s_{i,i} = 0 \tag{35}$$

$$\rho \dot{v}^s_i = -\bar{\mathscr{P}}_{,i} + \rho S \bar{T}_{,i} + \rho \Lambda \bar{m}^s_{,i} \tag{36}$$

$$\rho^n \dot{v}^n_i + \rho^s \dot{v}^s_i = -\bar{\mathscr{P}}_{,i} + \rho^s \Lambda \bar{m}^s_{,i} \tag{37}$$

$$\rho \dot{\hat{S}} + S\dot{\hat{\rho}} + \rho S v^n_{i,i} = 0 \tag{38}$$

$$A_1(\bar{\rho}^s - \bar{f}) = \eta \bar{\rho}^s_{,ii} - \Lambda \bar{m}^s \tag{39}$$

where we have written for short

$$\mathscr{P} = \rho^2 \partial A / \partial \rho \tag{40}$$

a "thermodynamic pressure" differing from the actual pressure (12) only by $\rho^s \Lambda \bar{m}^s$ in this linearized theory. In (34)–(39) and below, ρ^s and f are used interchangeably, but, of course, $\bar{\rho}^s$ and $\bar{f}$ have to be distinguished.

By (34), (35), and (38) we have

$$\bar{m}^s = \rho^n \hat{\mathscr{P}} / \mathscr{S} \tag{41}$$

where $\mathscr{S} = \rho S / \rho^n$ is the entropy per unit mass of normal fluid. It also follows from (35) and (38) that

$$\rho \dot{\hat{S}} = -\rho^s S (v^n_i - v^s_i)_{,i}, \qquad \rho^n (\dot{v}^n_i - \dot{v}^s_i) = -\rho S \bar{T}_{,i} - \rho^n \Lambda \bar{m}^s_{,i}$$

whence, using (41),

$$\rho \ddot{\hat{S}} = (\rho \rho^s S^2 / \rho^n) \bar{T}_{,ii} + [(\rho^n)^2 \rho^s \Lambda / \rho] \hat{\mathscr{P}}_{,ii} \tag{42}$$

Also, (35), (37), and (41) give

$$\ddot{\hat{\rho}} = \bar{\mathscr{P}}_{,ii} - [(\rho^n)^2 \rho^s \Lambda / \rho S] \hat{\mathscr{P}}_{,ii} \tag{43}$$

Equations (39) and (41) give

$$\bar{\rho}^s - \xi^2 \bar{\rho}^s_{,ii} = \bar{f} - [\tau (\rho^n)^2 / \rho S] \hat{\mathscr{P}} \tag{44}$$

where ξ is the healing length and τ is the relaxation time, defined by

$$\xi^2 = \eta / A_1, \qquad \tau = \Lambda / A_1 \tag{45}$$

We now seek solutions in the form of plane (longitudinal) waves supposing all variables proportional to $\exp[i(kx - \omega t)]$. If ρ, $\mathscr{S}$, and ρ^s are chosen as

independent variables, (43), (42), and (44) now give, respectively,

$$\left(\omega^2-\frac{\partial\mathscr{P}}{\partial\rho}k^2\right)\bar{\rho}-k^2\left(\frac{i\omega\Lambda\rho^s(\rho^n)^2}{\rho S}+\frac{\partial\mathscr{P}}{\partial\mathscr{S}}\right)\bar{\mathscr{P}}-k^2\frac{\partial\mathscr{P}}{\partial\rho^s}\bar{\rho}^s=0 \tag{46}$$

$$\frac{\rho^s S}{\rho\rho^n}\left(\omega^2-\rho S\frac{\partial T}{\partial\rho}k^2\right)\bar{\rho}+\left[\frac{\rho^n}{\rho}\omega^2-\frac{\rho^s S^2}{\rho^n}\frac{\partial T}{\partial\mathscr{S}}k^2+\frac{i\omega\Lambda\rho^s(\rho^n)^2}{\rho^2}k^2\right]\bar{\mathscr{P}}$$

$$-\frac{S}{\rho^n}\left(\omega^2+\rho^s S\frac{\partial T}{\partial\rho^s}k^2\right)\bar{\rho}^s=0 \tag{47}$$

$$\frac{\partial f}{\partial\rho}\bar{\rho}+\left[\frac{\partial f}{\partial\mathscr{S}}+\frac{i\omega\tau(\rho^n)^2}{\rho S}\right]\bar{\mathscr{P}}+\left(\frac{\partial f}{\partial\rho^s}-1-\xi^2k^2\right)\bar{\rho}^s=0 \tag{48}$$

The dispersion relationship linking ω and k^2 is the determinantal condition that these three equations admit a nontrivial solution. The partial derivatives entering (48), which use ρ, $\mathscr{S}$, and ρ^s as independent thermodynamic variables, are not easily interpreted and we therefore consider two other triples, namely ρ, T, ρ^s and ρ, T, Γ where Γ is given by (8). To make it obvious which variables are to be held constant during differentiation, we introduce the following notation. If χ is any one of the dependent thermodynamic functions, we write

$$\chi(\rho,\mathscr{S},\rho^s)=\tilde{\chi}(\rho,T,\rho^s)=\hat{\chi}(\rho,T,\Gamma) \tag{49}$$

so that, for example, $\partial\hat{\chi}/\partial\rho$ means that T and Γ are held fixed and not $\mathscr{S}$ and ρ^s, or T and ρ^s.

When we transform to new variables, certain combinations of derivatives arise with some regularity, for instance

$$\frac{\partial\tilde{S}}{\partial T}-\frac{\partial\tilde{S}}{\partial\rho}\frac{\partial\tilde{\mathscr{P}}}{\partial T}\left(\frac{\partial\tilde{\mathscr{P}}}{\partial\rho}\right)^{-1} \tag{50}$$

These can often be expressed more succinctly in terms of other triples. For example, if $(\mathscr{P},T,\rho^s)$ are used as independent variables in place of (ρ,T,ρ^s), the combination (50) is simply $(\partial S/\partial T)_{\mathscr{P},\rho^s}$. For this reason we introduce two specific heats at constant pressure, $\tilde{c}_{\mathscr{P}}$, $\hat{c}_{\mathscr{P}}$; two adiabatic compressibilities, $\tilde{\kappa}_s$, $\hat{\kappa}_s$; and two coefficients of volume expansion $\tilde{\alpha}_{\mathscr{P}}$, $\hat{\alpha}_{\mathscr{P}}$. In fact we define

$$\tilde{c}_{\mathscr{P}}=T\left(\frac{\partial S}{\partial T}\right)_{\mathscr{P},\rho^s},\qquad \tilde{c}_v=T\left(\frac{\partial\tilde{S}}{\partial T}\right),\qquad \tilde{\gamma}=\frac{\tilde{c}_{\mathscr{P}}}{\tilde{c}_v}$$

$$\tilde{\kappa}_S=\rho^{-1}\left(\frac{\partial\mathscr{P}}{\partial\rho}\right)^{-1}_{S,\rho^s},\qquad \tilde{\kappa}_T=\rho^{-1}\left(\frac{\partial\tilde{\mathscr{P}}}{\partial\rho}\right)^{-1},\qquad \tilde{\alpha}_{\mathscr{P}}=-\rho^{-1}\left(\frac{\partial\rho}{\partial T}\right)_{\mathscr{P},\rho^s},\qquad \tilde{\beta}=\frac{\partial\tilde{\mathscr{P}}}{\partial T} \tag{51}$$

The corresponding definition for the "hatted quantities" with Γ held constant instead of ρ^s are obvious. We wish to stress that we define these functions purely for mathematical convenience and do not imply that they are the corresponding experimentally measured quantities, for which p rather than $\mathscr{P}$ would seem to be the correct pressure to use. In similar fashion we define adiabatic and isothermal speeds of first sound and two closely related velocities of second sound,

$$\tilde{a}_1^2 = \left(\frac{\partial \mathscr{P}}{\partial \rho}\right)_{S,\rho^s}, \qquad \tilde{u}_1^2 = \frac{\partial \tilde{\mathscr{P}}}{\partial \rho}, \qquad \tilde{a}_2^2 = \frac{\rho^s S^2 T}{\rho^n \tilde{c}_{\mathscr{P}}}, \qquad \tilde{u}_2^2 = \frac{\rho^s S^2 T}{\rho^n \tilde{c}_v} \tag{52}$$

and similarly for $\hat{a}_1$, $\hat{a}_2$, $\hat{u}_1$, $\hat{u}_2$. In the usual way we can obtain

$$\tilde{c}_v = \tilde{c}_p - \frac{\tilde{\beta}^2 T}{\rho^2 \tilde{u}_1^2}, \qquad \tilde{a}_1^2 = \tilde{u}_1^2 + \frac{\tilde{\beta}^2 T}{\rho^2 \tilde{c}_v} \tag{53}$$

and similarly for the hatted quantities. Also

$$\tilde{c}_v = \hat{c}_v - \frac{A_1 T}{\rho}\left(\frac{\partial f}{\partial T}\right)_\rho^2 \tag{54}$$

$$\tilde{u}_1^2 = \hat{u}_1^2 + \rho A_1 \left(\frac{\partial f}{\partial \rho}\right)_T^2 \tag{55}$$

Since we expect $\tilde{c}_v$ to be positive, (54) places a restriction on A_1.

Returning now to (46)–(48), we find that the consistency condition is

$$\begin{aligned}(\hat{c}_v/\tilde{c}_v)[\omega^4 - \omega^2 k^2(\hat{a}_1^2 + \hat{u}_2^2) + k^4 \hat{u}_1^2 \hat{u}_2^2] \\ - \xi^2 k^2[\omega^4 - \omega^2 k^2(\tilde{a}_1^2 + \tilde{u}_2^2) + k^4 \tilde{u}_1^2 \tilde{u}_2^2] \\ - i\omega\tau(ad - bc) - i\omega k^4 \tau\eta\rho^s(\rho^n a + \rho^s e)/\rho = 0\end{aligned} \tag{56}$$

where

$$\begin{aligned}a &= \omega^2 - k^2\left(\tilde{a}_1^2 + \frac{\rho^s S T \tilde{\beta}}{\rho \rho^n \tilde{c}_v}\right) \\ b &= -k^2 A_1\left\{\rho^s + \frac{\rho^s T}{\rho \tilde{c}_v}\left(\frac{\partial f}{\partial T}\right)_\rho\left[\frac{\rho S}{\rho^n} + A_1\left(\frac{\partial f}{\partial T}\right)_\rho\right] - \rho\left(\frac{\partial f}{\partial \rho}\right)_T - \frac{\rho^n T \tilde{\beta}}{\rho^2 \tilde{c}_v}\left(\frac{\partial f}{\partial T}\right)_\rho\right\} \\ c &= \frac{\rho^s}{\rho}\omega^2 - k^2\left\{\frac{\rho^n \rho^s}{\rho} A_1\left(\frac{\partial f}{\partial \rho}\right)_T - \frac{\rho^s T}{\rho \tilde{c}_v}\left[\frac{\tilde{\beta}}{\rho} - \frac{\rho^s S}{\rho^n}\right]\left[S - \frac{\rho^n}{\rho} A_1\left(\frac{\partial f}{\partial \rho}\right)_T\right]\right\} \\ d &= -\omega^2 + \frac{k^2 \rho^n \rho^s}{\rho}\left\{A_1 + \frac{T}{\rho \tilde{c}_v}\left[\frac{\rho S}{\rho^n} + A_1\left(\frac{\partial f}{\partial T}\right)_\rho\right]^2\right\} \\ e &= \omega^2 + \frac{k^2 S T}{\tilde{c}_v}\left(\frac{\tilde{\beta}}{\rho} - \frac{\rho^s S}{\rho^n}\right)\end{aligned} \tag{57}$$

The solution of (56) is clearly an arduous task in general. We shall undertake it only in the vicinity of the λ point: See Section 5. However, we note here that it is readily solved when relaxation effects are ignored, particularly in temperature ranges where $\tilde{\gamma} \doteqdot \hat{\gamma} \doteqdot 1$, so that $\tilde{a}_1 = \tilde{u}_1$, $\tilde{a}_2 = \tilde{u}_2$, etc. Then (56) reduces to

$$(\hat{c}_v/\tilde{c}_v)(\omega^2 - \hat{a}_1^2 k^2)(\omega^2 - \hat{a}_2^2 k^2) + k^2\xi^2(\omega^2 - \tilde{a}_1^2 k^2)(\omega^2 - \tilde{a}_2^2 k^2) = 0 \quad (58)$$

It is evident that the two propagation speeds approach $\hat{a}_1$ and $\hat{a}_2$ as $k\xi \to 0$, and $\tilde{a}_1$ and $\tilde{a}_2$ as $k\xi \to \infty$. When $k\xi = O(1)$, the situation is more complicated but we note that if $\hat{u}_2 \ll \hat{u}_1$ and $\tilde{u}_2 \ll \tilde{u}_1$, we have

$$\omega^2 \doteqdot k^2(\hat{c}_v\hat{a}_1^2 + \tilde{c}_v\tilde{a}_1^2 k^2\xi^2)/(\hat{c}_v + \tilde{c}_v k^2\xi^2) \quad (59)$$

and

$$\omega^2 \doteqdot k^2(\hat{c}_v\hat{a}_1^2\hat{a}_2^2 + \tilde{c}_v\tilde{a}_1^2\tilde{a}_2^2 k^2\xi^2)/(\hat{c}_v\hat{a}_1^2 + \tilde{c}_v\tilde{a}_1^2 k^2\xi^2) \quad (60)$$

4. PHYSICAL PROPERTIES AT THE λ TRANSITION

Relaxation processes become significant near the λ transition and can be experimentally detected by the attenuation they create in sound waves. We refer the reader to a recent review of sound propagation by Rudnick.[15] In order to study this phenomenon by the theory of Section 3, we will need to know the asymptotic behavior of the thermodynamic variables as $T \to T_\lambda$. Fortunately, a considerable body of information is available, since helium is one of the few substances that can be studied very close to the transition, a fact that has been fully exploited experimentally (for a recent review, see Ahlers[1]). The use of this knowledge raises certain problems in our theory, which we wish to explore here.

Most properties of helium II are measured in static or quasistatic conditions in which $\Gamma = 0$ or Γ is small. The λ "line" can then be defined unequivocally as $T = \hat{T}_\lambda(\rho)$, where

$$f[\rho, \hat{T}_\lambda(\rho)] = 0 \quad (61)$$

Moreover, since the distinction between p and $\mathscr{P}$ disappears for small Γ, we may unambiguously define $T = \hat{T}_\lambda(\mathscr{P})$ by

$$f\{\rho[\mathscr{P}, \hat{T}_\lambda(\mathscr{P})], \hat{T}_\lambda(\mathscr{P})\} = 0 \quad (62)$$

and believe that $T = \hat{T}_\lambda(\mathscr{P})$ is given by direct physical measurement. All hatted quantities in the theory of Section 3, such as $\hat{c}_\mathscr{P}$, $\hat{c}_v$, $\hat{\gamma}$, $\hat{\kappa}_s$, $\hat{\kappa}_T$, $\hat{\alpha}_\mathscr{P}$, $\hat{\beta}$, $\hat{a}_1$, $\hat{a}_2$, $\hat{u}_1$, $\hat{u}_2$, are required for $\Gamma = 0$ and these are precisely the quantities readily accessible from experiment.

The theory of Section 3 also requires us to consider variations performed so rapidly that ρ^s is almost constant and Γ is large. These are, of course, totally different. It is not impossible for ρ^s to be nonzero at temperatures greater than $\hat{T}_\lambda$ if the variations are executed rapidly enough. We now see that when time variations are important, we have not a λ line but a λ "surface" $T_\lambda(\rho, \Gamma)$, which we may define by

$$\rho^s[\rho, T_\lambda(\rho, \Gamma), \Gamma] = 0 \tag{63}$$

or

$$f[\rho, T_\lambda(\rho, \Gamma)]A_1[\rho, T_\lambda(\rho, \Gamma)] = \Gamma \tag{64}$$

which correctly reduces to (61) when $\Gamma = 0$. The distinction between p and $\mathscr{P}$ may now be important, and, although we may define $T_\lambda(\mathscr{P}, \Gamma)$ in analogy to (62), it is by no means obvious that it is directly measurable. What then is to be done about the quantities $\tilde{c}_p$ to $\tilde{u}_2$ appearing in the theory of Section 3? It seems to us that the only straightforward method open is to define $\tilde{c}_p$ to $\tilde{u}_2$ from $\hat{c}_p$ to $\hat{u}_2$ through general relations of the form

$$\frac{\partial \tilde{\chi}}{\partial \rho} = \frac{\partial \hat{\chi}}{\partial \rho} + \frac{\partial \hat{\chi}}{\partial \Gamma}\frac{\partial \tilde{\Gamma}}{\partial \rho}, \qquad \frac{\partial \tilde{\chi}}{\partial T} = \frac{\partial \hat{\chi}}{\partial T} + \frac{\partial \hat{\chi}}{\partial \Gamma}\frac{\partial \tilde{\Gamma}}{\partial T}, \qquad \frac{\partial \tilde{\chi}}{\partial \rho^s} = \frac{\partial \hat{\chi}}{\partial \Gamma}\frac{\partial \tilde{\Gamma}}{\partial \rho^s} \tag{65}$$

where we can readily obtain the Γ derivatives on the right from (7) and (30), viz.

$$\Gamma = -A_1(\rho^s - f) + O(\rho^s - f)^2 \tag{66}$$

This gives, for $\Gamma = 0$ or $\rho^s = f$,

$$\frac{\partial \tilde{\Gamma}}{\partial \rho} = A_1\left(\frac{\partial f}{\partial \rho}\right)_T, \qquad \frac{\partial \tilde{\Gamma}}{\partial T} = A_1\left(\frac{\partial f}{\partial T}\right)_\rho, \qquad \frac{\partial \tilde{\Gamma}}{\partial \rho^s} = -A_1 \tag{67}$$

It was in this way that relations (54) and (55) were derived. Similar courses are open to us when, for example, $\mathscr{P}$, T, and Γ are the independent variables; cf. (53).

We now attempt to carry out the program mapped out above, starting first with the simplest, hatted, quantities, Let

$$\varepsilon = T_\lambda(\mathscr{P}) - T \tag{68}$$

Clow and Reppy[5] deduced from the behavior of persistent currents near T_λ that

$$f = O(\varepsilon^{2/3}), \qquad \varepsilon \to 0 \tag{69}$$

a result confirmed by subsequent researchers: See Ahlers,[1] Maynard,[12] and Donnelly and Roberts.[6] There appears to be general agreement that (16) is

correct at all ρ^* and since experiments give

$$\xi = O(\varepsilon^{-2/3}), \qquad \tau = O(\varepsilon^{-1}), \qquad \varepsilon \to 0 \tag{70}$$

we see from (45) that

$$A_1 = O(\varepsilon^{2/3}), \qquad \Lambda = O(\varepsilon^{-1/3}), \qquad \varepsilon \to 0 \tag{71}$$

As is well known, $\hat{c}_{\mathscr{P}}$ diverges logarithmically,[3] whereas the compressibility $\hat{\kappa}_T$ remains finite in the experimental range of temperatures. However, it may be shown by an obvious generalization of the so-called Pippard–Buckingham–Fairbank relations (see, for example, Ahlers[1]), using (71), that $\hat{\kappa}_T$ and $\hat{\alpha}_{\mathscr{P}}$ must eventually diverge as $T \to T_\lambda$ since they are proportional to $\hat{c}_{\mathscr{P}}$, i.e.,

$$\hat{c}_{\mathscr{P}}, \hat{\kappa}_T, \hat{\alpha}_{\mathscr{P}} = O(\ln \varepsilon), \qquad \varepsilon \to 0 \tag{72}$$

and we will suppose that

$$\hat{c}_v, \hat{\beta} = O(1), \qquad \varepsilon \to 0 \tag{73}$$

as appears to be consistent with the experimental observations. From (51) and (52) we now obtain

$$\hat{u}_1^2 = O(\ln \varepsilon)^{-1}, \qquad \hat{a}_1^2 = O(1), \qquad \varepsilon \to 0 \tag{74}$$

Differentiating (69) and using (74) and (72), we see that

$$\left(\frac{\partial f}{\partial \rho}\right)_T = O[\varepsilon^{-1/3}(\ln \varepsilon)^{-1}], \qquad \left(\frac{\partial f}{\partial T}\right)_\rho = O(\varepsilon^{-1/3}), \qquad \varepsilon \to 0 \tag{75}$$

Relationships (69)–(75) remain valid if we replace (68) by

$$\varepsilon = T_\lambda(\rho) - T \tag{76}$$

Care is necessary with respect to the first of relations (75). When this is derived from (69) using (76), we must not forget that

$$\left(\frac{\partial \varepsilon}{\partial \rho}\right)_T = \frac{dT_\lambda}{\partial \rho} = \frac{\partial T_\lambda}{\partial \mathscr{P}} \frac{\partial \mathscr{P}}{\partial \rho} = O(\ln \varepsilon)^{-1}, \qquad \varepsilon \to 0 \tag{77}$$

by the first of relations (74); note that $dT_\lambda/d\mathscr{P} = O(1)$. Variable (76) is, of course, more convenient than (68) when applying (65). We now obtain

$$\left.\begin{aligned} \tilde{c}_{\mathscr{P}}, \tilde{\kappa}_T, \tilde{\alpha}_{\mathscr{P}} = O(\ln \varepsilon), \qquad \tilde{c}_v, \tilde{\beta} = O(1) \\ \tilde{u}_1^2 = O(\ln \varepsilon)^{-1}, \qquad \tilde{a}_1^2 = O(1) \end{aligned}\right\} \varepsilon \to 0 \tag{78}$$

exactly as for the hatted quantities; the constants of proportionality are, of course, different.

Relations (72)–(75) and (78) are the basis for our analysis in Section 5 of the dispersion relationship (56) near the λ point. One further subtlety should not be overlooked. In establishing the dispersion relation (56), we encountered derivatives such as

$$\widetilde{\frac{\partial}{\partial T}\left(\frac{\rho S}{\rho^n}\right)} \tag{79}$$

It is tempting, but incorrect, to follow Khalatnikov[10] and use the fact that $\rho^n = \rho - f \to 1$ as $\varepsilon \to 0$ to argue that (79) is asymptotically $\partial\tilde{S}/\partial T$. The derivative is asymptotically

$$\frac{\partial \tilde{S}}{\partial T} - \frac{S}{\rho}\left(\frac{\partial f}{\partial T}\right)_\rho$$

The first term is $O(1)$ by (68) but the second is $O(\varepsilon^{-1/3})$ by the second of relations (75).

5. THE PROPAGATION OF FIRST AND SECOND SOUND NEAR THE λ POINT

The dispersion relationship (56) can be simplified considerably if appeal is made to the asymptotic dependencies of Section 4 to retain only the largest contribution to every coefficient $\omega^p k^q$ as $\varepsilon \to 0$. In this way we obtain

$$\begin{aligned}&\tilde{a}_1^2\tilde{c}_v(i\omega\tau\eta\rho^s - \xi^2\tilde{a}_2^2)k^6\\ &\quad -(i\omega^3\tau\eta\rho^s\tilde{c}_v - \omega^2\xi^2\tilde{a}_1^2\tilde{c}_v - i\omega\tau\tilde{a}_1^2\tilde{a}_2^2\tilde{c}_v + \hat{a}_1^2\hat{a}_2^2\hat{c}_v)k^4\\ &\quad -\omega^2(\xi^2\omega^2\tilde{c}_v + i\omega\tau\tilde{a}_1^2\tilde{c}_v - \hat{a}_1^2\hat{c}_v)k^2 + \omega^4(i\omega\tau\tilde{c}_v - \hat{c}_v) = 0\end{aligned} \tag{80}$$

a relation we now seek to solve for given ω. In (80), $\tilde{a}_2 = \tilde{u}_1\tilde{u}_2/\tilde{a}_1$ and similarly for $\hat{a}_2$. The results depend, of course, very much on the size of ω in relation to ε. For example, if ω is sufficiently large, the term $\hat{c}_v$ in the final parentheses of (80) will be negligible compared with the term $i\omega\tau\tilde{c}_v$ and the roots k^2 will correspondingly assume a different form from the set obtained for small ω, where the $\hat{c}_v$ dominates. It is thus profitable at the outset to identify the ranges of ω in which the coefficients of k in (80) are dominated by one term or another. In conformity with Section 4, we suppose that

$$\begin{aligned}&\hat{c}_v, \tilde{c}_v, \hat{a}_1, \tilde{a}_1 = O(1), \qquad \hat{a}_2, \tilde{a}_2 = O[\varepsilon^{1/3}(\ln\varepsilon)^{-1/2}]\\ &\hat{u}_1, \tilde{u}_1 = O[(\ln\varepsilon)^{-1/2}], \qquad \varepsilon \to 0\end{aligned} \tag{81}$$

and*

$$\rho^s = O(\varepsilon^{2/3}), \quad \eta = O(\varepsilon^{-2/3}), \quad \xi = O(\varepsilon^{-2/3}), \quad \Lambda = O(\varepsilon^{-1/3}),$$
$$\tau = O(\varepsilon^{-1}), \qquad \varepsilon \to 0 \qquad (82)$$

Case A: $\omega \ll O[\varepsilon/(\ln \varepsilon)^{1/2}]$. In each coefficient of k^n the final term dominates and we discover that to leading order

$$k^2 = \frac{\omega^2}{\hat{a}_1^2}, \qquad k^2 = \frac{\omega^2}{\hat{a}_2^2}, \qquad k^2 = -\frac{\hat{a}_1^2\hat{a}_2^2\hat{c}_v}{\tilde{a}_1^2\tilde{a}_2^2\tilde{c}_v}\frac{1}{\xi^2} \qquad (83A)$$

Case AB: $\omega \simeq O[\varepsilon/(\ln \varepsilon)^{1/2}]$. The final terms in the k^6, k^2, and k^0 coefficients are still dominant, but the second and fourth terms in the k^4 coefficient are equally dominant. We obtain

$$k^2 = \omega^2/\hat{a}_1^2, \qquad k^2 = \alpha, \qquad k^2 = \beta \qquad (83AB)$$

where α, β $(\alpha > \beta)$ are the (real) roots of the quadratic equation

$$x^2 - x\left(\frac{\omega^2}{\tilde{a}_2^2} - \frac{\hat{a}_1^2\hat{a}_2^2\hat{c}_v}{\tilde{a}_1^2\tilde{a}_2^2\tilde{c}_v}\frac{1}{\xi^2}\right) - \frac{\hat{a}_1^2\hat{c}_v}{\tilde{a}_1^2\tilde{c}_v}\frac{\omega^2}{\xi^2\tilde{a}_2^2} = 0$$

It is easily seen that $\beta < 0$.

Case B: $O[\varepsilon/(\ln \varepsilon)^{1/2}] \ll \omega \ll O(\varepsilon)$. Again the final terms in the k^6, k^2, and k^0 coefficients are dominant, but now the second term in the coefficient of k^4 is the only one that survives. We find

$$k^2 = \frac{\omega^2}{\hat{a}_1^2}, \qquad k^2 = \frac{\omega^2}{\tilde{a}_2^2}, \qquad k^2 = -\frac{\hat{a}_1^2\hat{c}_v}{\tilde{a}_1^2\tilde{c}_v}\frac{1}{\xi^2} \qquad (83B)$$

Case BC: $\omega = O(\varepsilon)$. In this range the final two terms in the coefficient of k^2 and both terms of the k^0 coefficient assume equal dominance; as in case B, the second terms of the k^6 and k^4 coefficients are all important. Now the roots are

$$k^2 = \frac{\omega^2(\hat{c}_v - i\omega\tau\tilde{c}_v)}{(\hat{a}_1^2\hat{c}_v - i\omega\tau\tilde{a}_1^2\tilde{c}_v)}, \qquad k^2 = \frac{\omega^2}{\tilde{a}_2^2}, \qquad k^2 = \frac{i\omega\tau}{\xi^2} - \frac{\hat{a}_1^2\hat{c}_v}{\tilde{a}_1^2\tilde{c}_v}\frac{1}{\xi^2} \qquad (83BC)$$

Case C: $O(\varepsilon) \ll \omega \ll O(\varepsilon^{1/3}/\ln \varepsilon)$. The second term in each of the coefficients of k^6, k^4, and k^2 is the greatest, while in the k^0 coefficient it is

* The analysis below would be somewhat simpler if we supposed instead that $\Lambda = O(\varepsilon^{-1/3} \ln \varepsilon)$, $\tau = O(\varepsilon^{-1} \ln \varepsilon)$ for $\varepsilon \to 0$. It would be difficult to distinguish experimentally between such laws and the last two relations in (82). Nevertheless, we take the conventional position in (82).

the first that dominates. The result (83BC) is altered to

$$k^2 = \omega^2/\tilde{a}_1^2, \qquad k^2 = \omega^2/\tilde{a}_2^2, \qquad k^2 = i\omega\tau/\xi^2 \tag{83C}$$

Case CD: $\omega = O(\varepsilon^{1/3}/\ln\varepsilon)$. Now both terms in the coefficient of k^6 are of equal order with the other coefficients as in case C. We now find

$$k^2 = \frac{\omega^2}{\tilde{a}_1^2}, \qquad k^2 = \frac{i\omega\xi^2}{\tau\eta\rho^s}\left[1 + \frac{i\xi^2\tilde{a}_2^2}{\omega\tau\eta\rho^s}\right]^{-1}, \qquad k^2 = \frac{i\omega\tau}{\xi^2} \tag{83CD}$$

Case D: $\omega \gg O(\varepsilon^{1/3}/\ln\varepsilon)$. The dominant terms for the coefficients of k^6 and k^0 are the first, and in the coefficients of k^4 and k^2 the first or the second (or both). Thus the roots are, to leading order,

$$k^2 = \omega^2/\tilde{a}_1^2, \qquad k^2 = i\omega\xi^2/\tau\eta\rho^s, \qquad k^2 = i\omega\tau/\xi^2 \tag{83D}$$

The first of the roots (83) corresponds to first sound. We see that if $\omega \gg O(\varepsilon)$, it travels with, to leading order, no dissipation and with the high-frequency adiabatic sound speed $\tilde{a}_1$. If $\omega \ll O(\varepsilon)$, it travels with the low-frequency velocity $\hat{a}_1$. The transition from one speed to the other is effected in the range BC where $\omega = O(\varepsilon)$ and here first sound is dispersed and dissipated. It appears that in all cases the (complex) first-sound speed is well approximated by

$$a = \left[\frac{(\hat{a}_1^2\hat{c}_v - i\omega\tau\tilde{a}_1^2\tilde{c}_v)}{(\hat{c}_v - i\omega\tau\tilde{c}_v)}\right]^{1/2}$$

as indeed Khalatnikov[10] implied. For a discussion of this dispersion relationship, see Landau and Lifshitz,[11] Section 78.

In first sound, superfluid and normal fluid share (to a good approximation) a common motion. Second sound is, however, a temperature wave that relies on conversion between species to supply its thermomechanical restoring force. When the frequency of the wave is large compared with τ^{-1}, or more precisely large compared with $\varepsilon^{1/3}/\ln\varepsilon$, the conversion of species cannot be properly accomplished in the period of the wave, and second sound does not occur. This accounts for the behavior of the second root in the cases CD and D. In the remaining ranges, the second root, which yields second sound, is little affected by relaxation: Note that τ does not appear in leading order before the case CD. There is, then, little attenuation. Dispersion occurs importantly in case AB, which separates the high-frequency second-sound wave, moving with velocity $\tilde{a}_2$, from the low-frequency wave traveling with speed $\hat{a}_2$. In the transition regime AB, the root α corresponds to the second-sound wave and approaches the low- (high-) frequency roots in the limit as ω decreases (increases). Of course, this propagating mode suffers dissipation because of higher order terms not

included in (83AB). In contrast to the results of Khalatnikov[10] for first sound, we have found totally different behavior for second sound. This may be attributed partly to his neglect of healing effects and partly to his treatment of the terms (79).

In each of the above cases, the third root of (83) represents a non-propagating wave that is predominantly associated with healing (and relaxation, for case BC onwards) and gives a $|k|$ that becomes infinite as $\xi \to 0$.

6. FOURTH SOUND

When helium II is contained in a porous solid matrix with pore size much smaller than a viscous penetration length, the normal fluid is locked in position. However, a sound wave is still able to propagate through the motion of the superfluid. This wave is termed fourth sound and was first discussed by Pellam.[13] The governing equations for this wave are obtained by discarding equation (6) due to the viscous domination, setting $v_n = 0$, and then linearizing (3), (4)–(8), and (30) about an equilibrium state as in Section 3. After again suppressing the subscript zero we obtain

$$\bar{m}^s = \hat{\rho}^s + \rho^s v^s_{i,i} \tag{84}$$

$$\dot{\hat{\rho}} + \rho^s v^s_{i,i} = 0 \tag{85}$$

$$\dot{v}^s_i = -\bar{\mu}_{,i} + \rho \Lambda \bar{m}^s_{,i} \tag{86}$$

$$\dot{\hat{\sigma}} = 0 \tag{87}$$

$$A_1(\bar{\rho}^s - \bar{f}) = \eta \bar{\rho}^s_{,ii} - \Lambda \bar{m}^s \tag{88}$$

where we have set

$$\mu = \left(\frac{\partial(\rho A)}{\partial \rho}\right)_{\rho^s, T}, \qquad \sigma = \rho S \tag{89}$$

and again we use ρ^s and f interchangeably but distinguish between $\bar{\rho}^s$ and $\bar{f}$. These equations combine in a straightforward manner to give (87) and

$$\ddot{\bar{\rho}} + \rho^s \Lambda(\dot{\hat{\rho}}^s - \dot{\hat{\rho}})_{,ii} - \rho^s \bar{\mu}_{,ii} = 0 \tag{90}$$

$$\bar{f} - \bar{\rho} + \xi^2 \bar{\rho}^s_{,ii} - \tau(\hat{\rho}^s - \hat{\rho}) = 0 \tag{91}$$

We seek longitudinal plane wave solutions and suppose that all variables are proportional to $\exp[i(kx - \omega t)]$. In view of (87) the most convenient triples to take as independent variables are (ρ, σ, ρ^s) and (ρ, σ, Γ) and we use the notation

$$\chi = \chi'(\rho, \sigma, \rho^s) = \chi''(\rho, \sigma, \Gamma) \tag{92}$$

Then equations (90) and (91) yield

$$\bar{\rho}\left(\rho^s\frac{\partial\mu'}{\partial\rho}k^2-\rho^s\Lambda i\omega k^2-\omega^2\right)+\bar{\rho}^s\rho^s\left(\frac{\partial\bar{\mu}}{\partial\rho^s}k^2+\Lambda i\omega k^2\right)=0 \tag{93}$$

$$\bar{\rho}\left(\frac{\partial f'}{\partial\rho}-i\omega\tau\right)+\bar{\rho}^s\left(\frac{\partial f'}{\partial\rho^s}-1-\xi^2k^2+i\omega\tau\right)=0 \tag{94}$$

The condition for compatibility of these two equations gives the dispersion relationship

$$0=\left(1-\frac{\partial f'}{\partial\rho^s}\right)\left(\rho^s\frac{\partial\mu''}{\partial\rho}k^2-\omega^2\right)+\xi^2k^2\left(\rho^s\frac{\partial\mu'}{\partial\rho}k^2-\omega^2\right)-i\omega\tau\rho^s\eta k^4$$

$$+i\omega\tau\left\{\omega^2-\rho^sk^2\left[\frac{\partial\mu'}{\partial\rho}+\frac{\partial\mu'}{\partial\rho^s}-A_1\frac{\partial f'}{\partial\rho}+A_1\left(1-\frac{\partial f'}{\partial\rho^s}\right)\right]\right\} \tag{95}$$

We can rewrite this equation using the triples (ρ, T, ρ^s) and (ρ, T, Γ) [see (49)] as

$$0=(\hat{c}_v/\tilde{c}_v)(k^2\hat{a}_4^2-\omega^2)+\xi^2k^2(k^2\tilde{a}_4^2-\omega^2)-i\omega\tau\rho^s\eta k^4+i\omega\tau(\omega^2-k^2g) \tag{96}$$

where

$$\tilde{a}_4^2=\frac{\rho^s}{\rho}\left(\tilde{a}_1^2-\frac{2ST\tilde{\beta}}{\rho\tilde{c}_v}\right)+\frac{\rho^n}{\rho}\tilde{u}_2^2,\qquad \hat{a}_4^2=\frac{\rho^s}{\rho}\left(\hat{a}_1^2-\frac{2ST\hat{\beta}}{\rho\hat{c}_v}\right)+\frac{\rho^n}{\rho}\hat{u}_2^2$$

$$g=\tilde{a}_4^2+\frac{\rho^sA_1\hat{c}_v}{\tilde{c}_v}-2A_1\rho^s\left[\left(\frac{\partial f}{\partial\rho}\right)_T+\left(\frac{\partial f}{\partial T}\right)_\rho\left(\frac{\tilde{\beta}T}{\rho^2\tilde{c}_v}-\frac{ST}{\rho\tilde{c}_v}\right)\right] \tag{97}$$

When relaxation effects are ignored we find that

$$k^2=\omega^2(\hat{c}_v+\xi^2\tilde{c}_v k^2)/(\hat{c}_v\hat{a}_4^2+\xi^2k^2\tilde{c}_v\tilde{a}_4^2) \tag{98}$$

so that the propagation speed approaches $\hat{a}_4$ and $\tilde{a}_4$ as $k\xi\to 0$ and $k\xi\to\infty$, respectively, as we would expect.

To discuss the case with relaxation effects present, we need to solve (96) for k^2. With (96) being a quadratic in k^2, there is no difficulty in determining explicitly these roots. However, they are extremely complex and we prefer to obtain the qualitative features of the equation by an asymptotic analysis of the sort in Section 5.

Using the assumed behavior set out in Section 4, we find that $g\doteq\tilde{a}_4^2$ and we write (96) as

$$k^4(\xi^2\tilde{a}_4^2-\rho^s\eta\tau i\omega)+k^2(\hat{c}_v\hat{a}_4^2/\tilde{c}_v-\xi^2\omega^2-i\omega\tau\tilde{a}_4^2)-(\hat{c}_v\omega^2/\tilde{c}_v-i\tau\omega^3)=0 \tag{99}$$

Case A: $\omega \ll O(\varepsilon)$. The dominant terms in each of the coefficients are the first and the roots are

$$k^2 = \frac{\omega^2}{\hat{a}_4^2}, \qquad k^2 = -\frac{\hat{c}_v}{\tilde{c}_v}\frac{\hat{a}_4^2}{\tilde{a}_4^2}\frac{1}{\xi^2} \tag{100A}$$

Case AB: $\omega = O(\varepsilon)$. In this range all three terms in the coefficient of k^2 and both terms in the coefficient of k^0 are of equal importance. The first term in the coefficient of k^4 is the only one we need consider. The roots are

$$k^2 = \frac{\omega^2(\hat{c}_v - i\omega\tau\tilde{c}_v)}{(\hat{c}_v\hat{a}_4^2 - i\omega\tau\tilde{c}_v\tilde{a}_4^2)}, \qquad k^2 = -\frac{(\hat{c}_v\hat{a}_4^2 - i\omega\tau\tilde{c}_v\tilde{a}_4^2)}{\xi^2\tilde{c}_v\tilde{a}_4^2} \tag{100AB}$$

Case B: $O(\varepsilon) \ll \omega \ll O(\varepsilon^{1/3})$. The dominant terms are the first in the coefficient of k^4 and the second in the coefficients of k^2 and k^0. The roots then are

$$k^2 = \omega^2/\tilde{a}_4^2, \qquad k^2 = i\omega\tau/\xi^2 \tag{100B}$$

Case BC: $\omega = O(\varepsilon^{1/3})$. The first and second terms in the coefficient of k^4 are now of equal importance. The dominant terms for the coefficients of k^2 and k^0 are as in the previous case. We find, to leading order,

$$k^2 = \frac{\omega^2}{\tilde{a}_4^2}\left(1 - \frac{i\rho^s\Lambda\omega}{\tilde{a}_4^2}\right)^{-1}, \qquad k^2 = \frac{i\omega\tau}{\xi^2} \tag{100BC}$$

Case C: $\omega \gg O(\varepsilon^{1/3})$. In all the coefficients the second term dominates in this range. The roots are

$$k^2 = i\omega/\rho^s\Lambda, \qquad k^2 = i\omega\tau/\xi^2 \tag{100C}$$

In cases A–BC the first root (100) represents fourth sound. We immediately see that the range AB represents the transition between the low- and high-frequency sound speeds $\hat{a}_4$ and $\tilde{a}_4$. At higher frequency (BC) the wave is dissipated and dispersed until, for frequencies $\omega \gg O(\varepsilon^{1/3})$, the wave will disappear. Since fourth sound is primarily a variation in superfluid density, we might expect this behavior at frequencies sufficiently high for the superfluid density to be unable to change.

The second roots (100A) and (100AB) are associated with healing. However, the second of relations (100AB) marks the transition of this "healing wave" into a "relaxation wave", the second of relations (100BC).

REFERENCES

1. G. Ahlers, in *The Physics of Liquid and Solid Helium*, Part I, K. H. Bennemann, and J. B. Ketterson, eds. (Wiley–Interscience, New York, 1976), Chapter II.

2. J. S. Brooks and R. J. Donnelly, *J. Phys. Chem. Ref. Data* **6**(1), 51 (1977).
3. M. J. Buckingham and W. M. Fairbank, in *Progress in Low Temperature Physics*, C. J. Gorter, ed. (North-Holland, Amsterdam, 1961). Vol. III, p. 80.
4. C. E. Chase, *Phys. Fluids* **1**, 193 (1958).
5. J. R. Clow and J. D. Reppy, *Phys. Rev. Lett.* **16**, 887 (1966).
6. R. J. Donnelly and P. H. Roberts, *Low Temp. Phys.* **27**, 687 (1977).
7. R. N. Hills and P. H. Roberts, *Int. J. Eng. Sci.* **15**, 305 (1977).
8. R. N. Hills and P. H. Roberts, in preparation.
9. I. M. Khalatnikov, *An Introduction to the Theory of Superfluidity* (Benjamin, New York, 1965).
10. I. M. Khalanikov, *Sov. Phys.—JETP* **30**, 268 (1970).
11. L. D. Landau and E. M. Lifshitz, *Fluid Mechanics* (Pergamon Press, Oxford, 1959).
12. J. Maynard, *Phys. Rev. B* **14**, 3868 (1976).
13. I. Rudnick, *'Enrico Fermi' International School of Physics, Course XLII* (1974).
14. S. J. Putterman, *Superfluid Hydrodynamics* (North-Holland, Amsterdam, 1976).
15. I. Rudnick, *'Enrico Fermi' International School of Physics, Course XLII* (1974).

J. Phys. C: Solid State Phys., Vol. 11, 1978. Printed in Great Britain.

Healing and relaxation in flows of helium II
3. Pure superflow

R N Hills† and P H Roberts‡

† Department of Mathematics, Heriot-Watt University, Edinburgh, UK

‡ Department of Applied Mathematics, The University, Newcastle upon Tyne, UK

Received 3 May 1978

Abstract. In part I of this series, a theory of helium II was developed incorporating quantum healing and relaxation effects. In this paper the healing phenomenon is studied for steady superfluid flows in stagnant normal fluid, that is, persistent currents. These include rectilinear flow down uniform pipes, the thinning of films by superfluid motion and rectilinear vortex structure.

1. Introduction

Healing is the term often used to describe the depletion of superfluid density of helium II in the vicinity of boundaries and vortex cores. It is a phenomenon that is thought to be important, for instance in thin films and to be related to the observed reduction of the velocity of third sound riding on that film (e.g. Rudnick and Fraser 1970). Relaxation, a term of universal use in physics, has particular significance in helium II near the λ point where the conversion between superfluid and normal fluid (consequent on changing the thermodynamic state) may occur slowly compared with the period of high frequency second (or first) sound. The resulting relaxation then has measurable effects on the sound propagation.

Unfortunately Landau theory does not contain healing and relaxation effects. There have been several attempts to generalise the Landau equations correctly to include them. One of the most recent of these attempts is our own (Hills and Roberts 1977). It appears to be the simplest of such generalisations possible and has the added advantage that little information need be sought, over and above that required by Landau theory, in order to make concrete predictions. The thermodynamics of the two theories are essentially identical and all that is required for our theory to work is knowledge of a healing parameter and a relaxation parameter.

Since our theory is so readily applied it is also readily tested and we have initiated a programme of research with the object of measuring our theory against experimental data, to determine whether our 'simplest' approach can succeed or whether it lacks physical ingredients that makes necessary its generalisation to a more difficult variant. We have published a discussion of the propagation of first, second and fourth sound (Hills and Roberts 1978a) and in the present paper, the third of the series, we examine some situations involving pure superflow. Other consequences of our theory have been worked out by Johnson (1978a, b) and by Roberts *et al* (1978).

0022-3719/78/0022-4485 $02.00

After setting down the basic equations of our theory (§ 2), we show (§ 3.1) that, even though static and dynamic healing effects will cause the superfluid and total densities to vary across an isothermal system containing a persistent current, our theory will admit such persistent currents in all circumstances. The proof is not trivial since, at first inspection, the problem appears to be overdetermined. In § 3.2 we set up the problem of Poiseuille flow for our theory and, for the particular cases of flow between planes and down a circular pipe, we obtain the relationships between mass flux, superfluid velocity and channel size. We obtain conditions for the absence of superfluidity. In § 4 we address the problem of film thinning and whether, as suggested by Putterman and Rudnick (1971), the stresses associated with healing will break the force of Kontorovich's (1956) argument that a moving film will be thinner than the corresponding static one. For reasons adumbrated by Goodstein and Saffman (1975) we find that this is not the case, although healing in thin films causes differences in detail from Kontorovich's result, even allowing for the average depletion of superfluid density in a thin film. In § 5 we look at the structure of the superfluid vortex in our theory and are able to expose explicitly the pressure gradient that causes vortices to attract and trap ion impurities (e.g. Donnelly and Roberts 1969).

In all these developments (except § 2 and parts of § 3) we adopt a simple quadratic form for the Helmholtz free energy A. We believe that this should be an adequate approximation sufficiently near the λ point. As a later part of our programme, we hope to present results at other temperatures using the full thermodynamic data available (see also Roberts *et al* 1978).

2. Notation and governing equations

We refer the motion to a rectangular Cartesian coordinate system and employ a direct tensor notation. A superposed dot denotes time differentiation holding the spatial variable fixed. Throughout the paper the following notation is employed:

$$\begin{aligned}
&\rho^s = \text{superfluid density; } \boldsymbol{v}^s = \text{superfluid velocity;}\\
&\Omega^s = \text{potential of the superfluid external body force } \boldsymbol{b}^s \text{ per unit mass } (\boldsymbol{b}^s = \nabla\Omega^s);\\
&\phi^s = \text{superfluid velocity potential } (\boldsymbol{v}^s = \nabla\phi^s);\\
&m^s = \dot{\rho}^s + \nabla.(\rho^s\boldsymbol{v}^s) = \text{superfluid mass supply;}\\
&r = \text{heat supply per unit mass per unit time; } \rho = \text{total density;}\\
&A = \text{a specific energy function; } S = \text{specific entropy;}\\
&\Phi = \text{thermodynamic potential per unit mass; } T = \text{temperature;}\\
&p = \text{pressure; } \kappa = \text{thermal conductivity } (\geqslant 0);\\
&\alpha_1, \alpha_2 = \text{coefficients of viscosity } (\alpha_2 \geqslant 0, \alpha_1 + \tfrac{1}{3}\alpha_2 \geqslant 0);\\
&\eta = \text{healing coefficient; } \Lambda = \text{relaxation coefficient } (\geqslant 0);\\
&\boldsymbol{w} = \boldsymbol{v}^n - \boldsymbol{v}^s; \ \boldsymbol{\Sigma} = \text{stress tensor;}\\
&\boldsymbol{D}^n = \text{rate of deformation tensor } D^n_{ij} = \tfrac{1}{2}(v^n_{i,j} + v^n_{j,i}).
\end{aligned} \tag{2.1}$$

The corresponding definitions to (2.1) for the normal fluid are obvious. The governing equations of our theory were derived in Hills and Roberts (1977)† as

$$\rho = \rho^n + \rho^s, \tag{2.2}$$

† See also Hills and Roberts (1978a).

$$\dot{\rho} + \nabla.(\rho^n v^n + \rho^s v^s) = 0, \tag{2.3}$$

$$\dot{v}^s + (v^s.\nabla)v^s = \nabla(\Omega^s - \Phi), \tag{2.4}$$

$$\rho^n \dot{v}^n + \rho^s \dot{v}^s = \rho^n \nabla\Omega^n + \rho^s \nabla\Omega^s - \nabla p - \nabla.\Sigma', \tag{2.5}$$

$$\Sigma'_{ij} = \rho^n v^n_i v^n_j + \rho^s v^s_i v^s_j - \Sigma_{ij}, \qquad \Sigma_{ij} = \alpha_1 D^n_{r,r}\delta_{ij} + \alpha_2 D^n_{ij} - \eta\rho^s_{,i}\rho^s_{,j}, \tag{2.6}$$

$$T\dot{(\rho S)} + \nabla.(\rho S v^n) = \rho r + \nabla.(\kappa\nabla T) + m^{s2} + \alpha_1(\mathrm{tr}D^n)^2 + \alpha_2\mathrm{tr}(D^{n2}), \tag{2.7}$$

$$\rho\frac{\partial A}{\partial \rho^s} + \Gamma = 0, \quad A = A(\rho, T, \rho^s), \quad \Gamma = \tfrac{1}{2}w^2 + \Lambda m^s - \eta\nabla^2\rho^s - \tfrac{1}{2}\frac{\mathrm{d}\eta}{\mathrm{d}\rho^s}(\nabla\rho^s)^2. \tag{2.8}$$

Equations (2.3), (2.5) and (2.6) are the balance equations for total mass, momentum and energy respectively. The equation (2.8) forms a constitutive relation governing the healing and relaxation of ρ^s. Generally the viscosities α_1, α_2 and thermal conductivity κ depend on ρ, T, ρ^s: the relaxation coefficient Λ is a function of ρ^s and T, while the healing coefficient depends only on ρ^s. In what follows we often adopt the models

$$\eta = \zeta/\rho^s, \qquad \Lambda = l/(\rho^s)^{1/2}, \tag{2.9a, b}$$

where $l = l(T)$ and ζ is a constant ($=\hbar^2/4m^2$, where $2\pi\hbar$ is Planck's constant h and m is the mass of the helium atom).

We can derive from (2.4), in the usual way, the superfluid Bernoulli equation

$$\dot{\phi}^s + \tfrac{1}{2}v^{s2} + \Phi - \Omega^s = g(t), \tag{2.10}$$

where the arbitrary function g of time t can be absorbed into ϕ^s if desired. We have also

$$S = -\partial A/\partial T, \qquad p = \rho^2\partial A/\partial\rho - \rho^s(\tfrac{1}{2}w^2 + \Lambda m^s) - \tfrac{1}{2}\eta(\nabla\rho^s)^2, \tag{2.11}$$

$$\Phi = A + \rho\partial A/\partial\rho - (\tfrac{1}{2}w^2 + \Lambda m^s), \tag{2.12}$$

$$\sigma^s_{ij} = -(\rho^s/\rho)[p - \rho^n(\tfrac{1}{2}w^2 + \Lambda m^s)]\,\delta_{ij} - \eta\rho^s_{,i}\rho^s_{,j}, \tag{2.13a}$$

$$\sigma^n_{ij} = -(\rho^n/\rho)[p + \rho^s(\tfrac{1}{2}w^2 + \Lambda m^s)]\,\delta_{ij} + \alpha_1 D^n_{rr}\delta_{ij} + \alpha_2 D^n_{ij}. \tag{2.13b}$$

Hills and Roberts (1978a) developed a Taylor series for the energy function A from the quasi-particle picture which truncated after the first three non-vanishing terms, namely

$$A = A_0(\rho, T) + \frac{A_1(\rho, T)}{2\rho}[\rho^s - f]^2 + \frac{A_2(\rho, T)}{3\rho^2}[\rho^s - f]^3, \tag{2.14}$$

where $f = f(\rho, T)$ is the equilibrium superfluid density in bulk helium. The functions A_0, A_1, A_2 were related to the ground state and excitation free energies and it was found that

$$A_0 < 0, \qquad A_1 > 0, \qquad A_2 > 0. \tag{2.15}$$

The simplest viable model truncates (2.14) after the quadratic term

$$A = A_0(\rho, T) + \frac{A_1(\rho, T)}{2\rho}[\rho^s - f]^2. \tag{2.16}$$

We close this section with a brief mention of the boundary conditions appropriate to pure superflow. Hills and Roberts (1978b) have recently given a fuller and more

general discussion of boundary conditions for helium paying particular attention to the interfacial conditions between a liquid and its vapour when either evaporation or condensation is present. At a solid boundary ∂B we assume that (see Hills and Roberts 1977, Johnson 1978a, b)

$$\rho^s \boldsymbol{n} \cdot \boldsymbol{v}^s = 0, \qquad \rho^s = 0 \qquad \text{on} \quad \partial B. \tag{2.17}$$

At the interface between a liquid and its vapour in thermodynamic equilibrium, we have (see Hills and Roberts 1978a, b)

$$\rho^s = 0, \qquad p + \eta(\nabla\rho^s)^2 = p^g, \qquad \Phi + \tfrac{1}{2}v^{s2} = \Phi^g + \tfrac{1}{2}v^{g2}, \tag{2.18}$$

where a superscript g denotes the quantity associated with the vapour which in this paper is taken to be an inviscid fluid.

3. Superflow solutions

3.1. Persistent currents

One comforting confirmation of the consistency of the above theory comes from seeking hydrostatic solutions or more generally solutions in which only a steady persistent current of the superfluid is present and the material is under the action of a conservative force field $\Omega\,(=\Omega^s = \Omega^n)$. The total momentum equation (2.5) shows that

$$p_{,i} + (\rho^s v_i^s v_j^s + \eta\rho^s{}_{,i}\rho^s{}_{,j})_{,j} = \rho\Omega_{,i}. \tag{3.1}$$

Since the superfluid motion is irrotational, $v^s_{i,j} = v^s_{j,i}$ and from the total mass equation (2.3) $\nabla\cdot(\rho^s\boldsymbol{v}^s) = 0$, we may use (2.12) to rewrite (3.1) as

$$\nabla[\rho^2\partial A/\partial\rho + \tfrac{1}{2}\eta(\nabla\rho^s)^2] - \tfrac{1}{2}(v^s)^2\nabla\rho^s = \rho\nabla\Omega. \tag{3.2}$$

But from the constitutive equation (2.8) we have

$$\rho\partial A/\partial\rho^s - \eta\nabla^2\rho^s - \tfrac{1}{2}(\mathrm{d}\eta/\mathrm{d}\rho^s)(\nabla\rho^s)^2 + \tfrac{1}{2}(v^s)^2 = 0 \tag{3.3}$$

so that, dividing (3.2) by ρ, multiplying (3.3) by $\nabla\rho^s$ and adding, we find

$$\frac{\partial}{\partial\rho}\left(\rho\frac{\partial A}{\partial\rho} + A\right)\nabla\rho + \frac{\partial}{\partial T}\left(\rho\frac{\partial A}{\partial\rho}\right)\nabla T + \frac{\partial}{\partial\rho^s}\left(\rho\frac{\partial A}{\partial\rho} + A\right)\nabla\rho^s = \nabla\Omega. \tag{3.4}$$

However, from (2.10) and (2.12) we have

$$\rho\frac{\partial A}{\partial\rho} + A - \Omega = \text{constant}. \tag{3.5}$$

By taking the gradient of this equation and comparing with (3.4), we see that $\nabla T = 0$ or

$$T = \text{constant}. \tag{3.6}$$

In other words, a necessary condition for the supposed 'hydrostatic' state, with the persistent superflow, is that the helium is isothermal. The variation of ρ and ρ^s over the system can only be found by solving (3.3) and (3.5) in conjunction. We show how this may be done in simple cases below. We note that the result (3.6) is derived without appeal to the postulate (2.14) and is therefore true for all forms of A. No theory that failed to survive the present test could be seriously considered as a model for healing.

3.2. *Healing at a plane wall*

We illustrate the utility of our model for A by a simple example. Let stagnant helium II in complete thermodynamic equilibrium fill the half-space $z > 0$ and be bounded at $z = 0$ by a wall. As we have just seen, T is a constant. We may suppress the temperature dependence everywhere and assume that all quantities spatially depend only on z. In $z > 0$, we must satisfy

$$A + \rho \partial A/\partial \rho = C_1, \tag{3.7}$$

$$\rho^2 \partial A/\partial \rho + \tfrac{1}{2}\eta(\mathrm{d}\rho^s/\mathrm{d}z)^2 = C_2, \tag{3.8}$$

$$\rho \partial A/\partial \rho^s - \eta(\mathrm{d}^2\rho^s/\mathrm{d}z^2) - \tfrac{1}{2}(\mathrm{d}\eta/\mathrm{d}\rho^s)(\mathrm{d}\rho^s/\mathrm{d}z)^2 = 0, \tag{3.9}$$

and

$$\rho^s = 0 \quad \text{on } z = 0, \quad \rho^s \to f \quad \text{as } z \to \infty, \tag{3.10}$$

where C_1 and C_2 are constants. By using (3.7), we can show that (3.8) is the first integral of (3.9) and so we can discard (3.9); (see § 3.1 above). Adopting (2.9) and (2.16), we rewrite (3.7) and (3.8) as

$$A_0 + \rho \partial A_0/\partial \rho - A_1(\partial f/\partial \rho)(R^2 - f) + \tfrac{1}{2}(\partial A_1/\partial \rho)(R^2 - f)^2 = C_1, \tag{3.11}$$

$$2\zeta(\mathrm{d}R/\mathrm{d}z)^2 = C_2 - C_1\rho + \rho A_0 + \tfrac{1}{2}A_1(R^2 - f)^2, \tag{3.12}$$

where A_0, A_1 and f depend on ρ alone and $R^2 = \rho^s$.

The solution of (3.10)–(3.12) is far from trivial. Suppose, however, that

$$f^2 A_1 \ll \rho |A_0|, \tag{3.13}$$

which, as emphasised in Hills and Roberts (1978a), is the only circumstance in which (2.14) and (2.16) are likely to be acceptable. Then, we may proceed by iteration. To leading order, (3.11) gives

$$A_0 + \rho \partial A_0/\partial \rho = C_1, \tag{3.14}$$

which implies to the same accuracy

$$\rho = \text{constant} = \rho_0, \text{ say.} \tag{3.15}$$

The coefficient A_1 in (3.12) is now constant and that equation, together with the boundary conditions (3.10), yield

$$\rho^s = f_0 \tanh^2 Z, \qquad Z = z/2\xi, \tag{3.16}$$

where $f_0 = f(\rho_0)$ etc: and ξ is the *healing length* defined by

$$\xi^2 = \zeta/(fA_1)_0. \tag{3.17}$$

It is interesting to note that the solution (3.16) exhibits non-zero normal stress difference, a phenomenon that is usually associated with viscoelastic materials and their anomalous behaviour. We find that, if the total stress tensor $\boldsymbol{T}$ is defined by

$$T_{ij} = -p\delta_{ij} + \Sigma_{ij}, \tag{3.18}$$

then

$$T_{xx} - T_{yy} = 0, \qquad T_{zz} - T_{yy} = -(fA_1)^2 \operatorname{sech}^4 Z \tag{3.19}$$

and that, even on the plane wall $z = 0$, the second difference is non-vanishing. We will return to this topic in § 3.3.

We can obtain the first correction to (3.15) by substituting (3.16) into (3.11) to obtain

$$\rho = \rho_0 - \frac{\rho_0}{u_0^2}\left(A_1 f \frac{\partial f}{\partial \rho}\right)_0 \operatorname{sech}^2 Z + \tfrac{1}{2}\left(f^2 \frac{\partial A_1}{\partial \rho}\right)_0 \operatorname{sech}^4 Z, \tag{3.20}$$

where u_0 is the isothermal speed of sound defined by

$$u_0^2 = \frac{\partial}{\partial \rho}\left(\rho^2 \frac{\partial A_0}{\partial \rho}\right)_{\rho=\rho_0}. \tag{3.21}$$

By using (3.21) in (3.12), we discover a refinement to (3.16) viz:

$$\rho^s = f_0 \tanh^2 Z - (2\rho/u_0^2 f A_1)_0 \tanh Z \operatorname{sech}^2 Z\left\{\left(A_1 f \frac{\partial f}{\partial \rho}\right)_0^2 Z + \left(f^3 A_1 \frac{\partial f}{\partial \rho}\frac{\partial A_1}{\partial \rho}\right)_0 \tanh Z \right.$$

$$\left. + \left(\tfrac{1}{2} f^2 \frac{\partial A_1}{\partial \rho}\right)_0^2 (\tanh Z - \tfrac{1}{3}\tanh^3 Z)\right\}. \tag{3.22}$$

This process of alternation between (3.11) and (3.12) can evidently be continued indefinitely.

It may be objected that it is inconsistent to carry out the expansion in this way because as each new term is added to (3.20) we ought to add also a new term in the expansion (2.16) of A. The A_2 term of (2.14) should, for instance, enter (3.22), the second term in the braces being replaced by

$$f^3\left(A_1 \frac{\partial f}{\partial \rho}\frac{\partial A_1}{\partial \rho} + \frac{A_2 u_0^2}{3\rho^2}\right)_0 \tanh Z. \tag{3.23}$$

It is often sufficient to take only the leading order of approximation by which we mean results analogous to (3.15) and (3.16).

The solutions of this subsection reflect the crucial role of the postulates (2.14) or (2.16). In a paper now in preparation, (Roberts *et al* 1978) rather than adopt these postulates we have used the tabulations of Brooks and Donnelly (1977) to determine the healing length in stagnant helium directly from the energy spectrum. These results suggest that the models (2.14) and (2.16) cannot be considered too trustworthy far from the λ point.

3.3. Superflow in parallel channels

The method of solution used in the last subsection may readily be adapted to determine the structure of ρ^s in a uniform pipe of arbitrary cross section, $\mathscr{S}$, when there is unidirectional superflow $v^s = ve_x$ along the axis $0x$ of the pipe; it is supposed that there is zero pressure gradient in the pipe, so that the normal fluid is at rest. Since the superfluid moves irrotationally, v is constant over $\mathscr{S}$. Of particular interest is the flux, Q, of superfluid.

Equation (3.7) holds as before while (3.9) requires an additional term $\frac{1}{2}v^2$ on its left-hand side. It is not in general possible to integrate (3.1) in a form like (3.8) although this can be done in § 3.3.1 below. The iteration procedure outlined in § 3.2 can, and will, be used. We will restrict our attention to the leading-order problem.

We scale the equations by introducing

$$v = (\zeta/A_1\rho_\infty^s)^{1/2}, \qquad \rho_\infty^s = f(1 - v^2/2A_1 f), \qquad v = u(2A_1 f)^{1/2}. \tag{3.24}$$

Clearly the *dynamic healing length*, v, reduces to the static healing length ξ when $v = 0$. The density ρ_∞^s is ρ^s in the bulk and is closely approached in the centre of the channel if its dimensions greatly exceed v. We now transform (3.1) by setting

$$\rho^s = \rho_\infty^s R^2, \qquad x_1 = \sqrt{2}\, v s_1, \tag{3.25a, b}$$

where the suffix 1 refers to the coordinates (y, z) in $\mathscr{S}$. We obtain

$$\nabla_1^2 R = R(R^2 - 1), \tag{3.26}$$

where it is understood that differentiations are performed with respect to s_1. We solve (3.26) subject to the healing boundary condition

$$R = 0 \qquad \text{on } C, \tag{3.27}$$

where C is the periphery of $\mathscr{S}$.

The flux down the pipe is

$$Q = \frac{2\zeta v}{A_1} \int_{\mathscr{S}_1} R^2 \, \mathrm{d}^2 s_1. \tag{3.28}$$

Following Mamaladze and Cheishvili (1966) we note that in addition to the case $v = 0$, Q can also vanish for non-zero velocities. To obtain this latter state of *destruction of superflow*, we note that if R is negligible over $\mathscr{S}$ then (3.26) may be written

$$\nabla_1^2 R = -(1/2v^2)R, \tag{3.29}$$

where we have temporarily re-instated x_1 as space variable. The equations (3.29) and (3.27) constitute an eigenvalue system for $1/2v^2$ and the smallest eigenvalue $1/2v_0^2$ determines v_c, the critical v at which superfluidity is destroyed. As we will see from examples below, v_c approaches zero as the scale (a, say) of the pipe is reduced and, no matter what v is, all superfluid is excluded from pipes of scale smaller than some $a_0 > 0$. We will see this more clearly in the following examples.

The lack of isotropy of the stresses (2.13a) due to healing is reflected in parallel flows by a difference in normal stresses that can be readily found in the examples considered below: for the first (see (3.32))

$$T_{xx} = T_{yy}, \qquad T_{zz} - T_{yy} = -\tfrac{1}{2}(\rho_\infty^s)^2 A_1 \left[\frac{2k^2(1-k^2)^2}{(1+k)^2} \frac{snu}{\mathrm{d}n^3 u\, cnu}\right], \qquad u = s/(1+k^2)^{1/2}. \tag{3.30}$$

In the flow of viscoelastic fluids such stress differences give rise to the phenomenon of die swell. The fluid extruded from a pipe swells (or constricts) as it emerges into the atmosphere. For a detailed discussion of the theory see Josephs (1974). It is natural to wonder whether the stress differences (3.30) will cause superflow emerging from a pipe into its vapour to change its cross section similarly and, if so, whether the effect could be detected. It is not hard to show, however, that all surface conditions on the jet emerging from a plane Poiseuille or circular Poiseuille flow (§§ 3.3.1 and 3.3.2 below) are satisfied if the jet continues without change of cross section from pipe to atmosphere. Whether there are other solutions showing die swell which also satisfy all conditions of the problem is problematical but not easily established. Of course, if the thermo-

dynamic potential Φ in the vapour is not continuous with $\Phi + \frac{1}{2}v^2$ at the edge of the jet, the cross section of the jet will change due to evaporation or condensation (see Hills and Roberts 1978b).

3.3.1. Flow between parallel planes. Let the fluid be confined between planes $z = \pm a$, so that $\nabla_1^2 = \mathrm{d}^2/\mathrm{d}s^2$ in (3.26), where $s = z/\sqrt{2v}$ by (3.25*b*). Equation (3.26) may be integrated once to give

$$(\mathrm{d}R/\mathrm{d}s)^2 = \tfrac{1}{2}(R_\mathrm{m}^2 - R^2)(2 - R_\mathrm{m}^2 - R^2), \tag{3.31}$$

where R_m is R at $s = 0$. As Ginzburg and Pitaevskii (1958) and Mamaladze and Cheishvili (1966) have noted, (3.31) may be solved at once in terms of elliptic integrals:

$$R = R_\mathrm{m} cd[s/(1 + k^2)^{1/2}], \qquad R_\mathrm{m} = [2k^2/(1 + k^2)]^{1/2},$$
$$a/2^{1/2}v = (1 + k^2)^{1/2}K(k), \tag{3.32a, b, c}$$

where the argument k ($0 < k < 1$) in cd ($= cn/dn$) is obtained by solving the last of (3.32), in which $K(k)$ is the complete elliptic integral of the first kind.

Since (3.32*c*) is a monotonic increasing function of k for $0 < k < 1$ and $K(0) = \pi/2$, we obtain a critical velocity

$$v_\mathrm{c} = (2A_1 f)^{1/2}[1 - \pi^2\xi^2/2a^2]^{1/2}, \tag{3.33}$$

and see that superfluidity is completely destroyed in channels whose widths are less than $2^{1/2}\pi\xi$. We may regard this as defining the depression of the λ point in channels as

$$\Delta T_\lambda = \frac{\pi^2\xi}{2a^2}\left[\frac{\partial}{\partial T}(A_1 f)\right]^{-1}_{T=T_\lambda}. \tag{3.34}$$

Instead of (3.28), we may compute the flux, $\tilde{Q}$, per unit y length across the channel, i.e.

$$\tilde{Q} = \mathrm{v}\int_{-a}^{a} \rho^s \,\mathrm{d}z = f(2a)(2A_1 f)^{1/2}[2u(1 - u^2)(K(k) - E(k))/(1 + k^2)K(k)], \tag{3.35}$$

where $E(k)$ is the elliptic integral of the second kind. In figure 1 we show the maximum value of $\tilde{Q}$, in units of $f(2a)(2A_1 f)^{1/2}$, attainable for given gap width $2a$, in units of ξ. The corresponding value of v, in units of $(2A_1 f)^{1/2}$, is shown also.

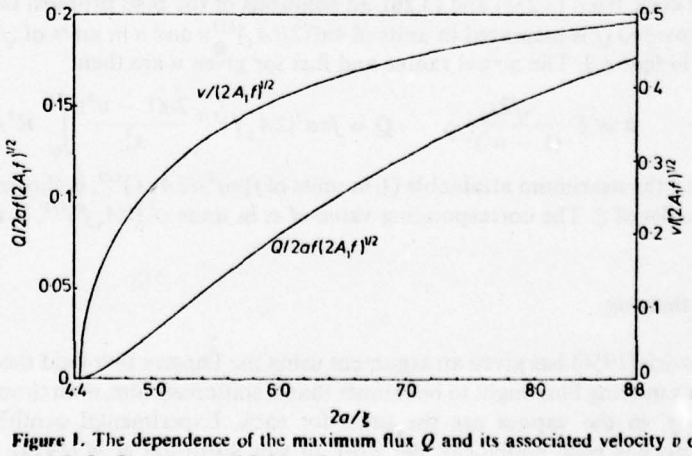

Figure 1. The dependence of the maximum flux Q and its associated velocity v on the gap width $2a$ for flow in a parallel channel.

3.3.2. Flow in a circular pipe. Let the fluid be confined in a pipe $0 \leqslant s \leqslant a$, where (s, θ, x) are cylindrical polar coordinates with axis 0x centred on the pipe. Then (3.26) becomes

$$\frac{d^2R}{ds^2} + \frac{1}{s}\frac{dR}{ds} = R(R^2 - 1), \tag{3.36}$$

which must be solved numerically. The simplest method is to assume a value of $R_m(<1)$ for R at $s = 0$ and integrate until R falls to zero at some $s = s_0 = a/\sqrt{2}v$.

If we assume that $R \ll 1$ throughout the pipe, we can solve (3.36) as $R = R_m J_0(s)$ and the first zero $j_{01} \doteq 2{\cdot}3041$ of the Bessel function J_0 gives

$$v_c = (2A_1 f)^{1/2}[1 - 2j_{01}^2\xi^2/a^2]^{1/2}, \tag{3.37}$$

so that $a_0 = \sqrt{2}\xi j_{01}$, as Mamaladze and Cheishvili (1966) have already noted.

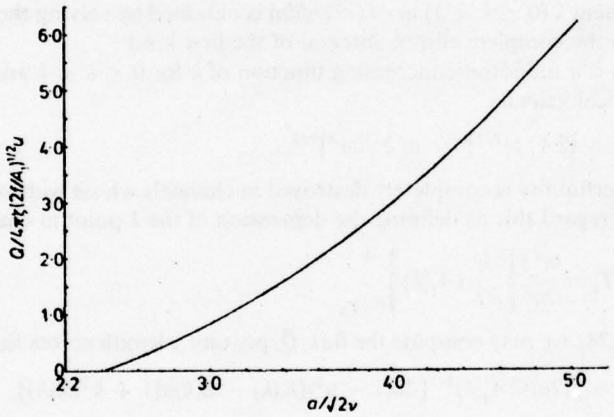

Figure 2. Relationship between the flux Q and the radius a for flow in a circular channel.

As is clear from (3.25*b*) and (3.28), all solutions of the pipe problem fall on one $Q(a)$ curve provided Q is measured in units of $4\pi\zeta(2f/A_1)^{1/2}u$ and a in units of $\sqrt{2}v$. This curve is given in figure 2. The actual radius and flux for given u are then

$$a = \xi\,\frac{\sqrt{2}s_0}{(1-u^2)^{1/2}}, \qquad Q = f\pi a^2(2A_1 f)^{1/2}\,\frac{2u(1-u^2)}{s_0^2}\int_0^{s_0} R^2 s\,ds. \tag{3.38}$$

In figure 3 the maximum attainable Q, in units of $f(\pi a^2)(2A_1 f)^{1/2}$, is shown as a function of a, in units of ξ. The corresponding value of v, in units of $(2A_1 f)^{1/2}$, is also shown.

4. Film thinning

Kontorovich (1956) has given an argument using the Landau two-fluid theory according to which a moving film ought to be thinner than a stationary film, even though conditions 'at infinity' in the vapour are the same for each. Experimental confirmation of his predictions has been equivocal: the work of van Spronson *et al* (1973), Williams and Packard (1974), Graham and Vittoratos (1974) are in accord with Kontorovich's

prediction but Keller (1970) and Telschow *et al* (1975) observe film thicknesses independent of their states of motion. There have been a number of suggestions for theoretically explaining this apparent experimental conflict. Putterman and Rudnick (1971) proposed that an explanation of the Keller and Telschow observations may result from a theory incorporating healing. Goodstein and Saffman (1975) have contested this, making the point that for films with thickness much larger than the healing length,

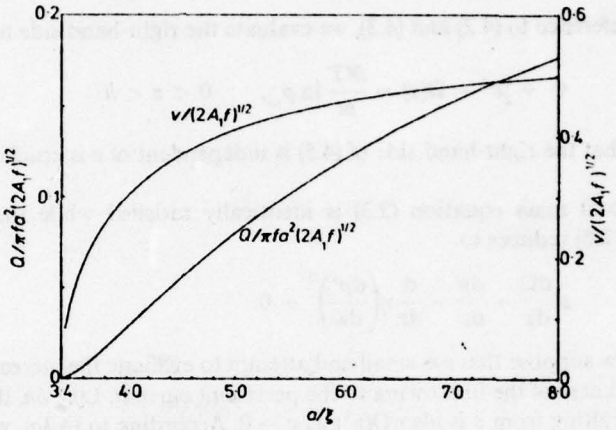

Figure 3. The dependence of the maximum flux Q and its associated velocity v on the radius a for flow in a circular channel.

Kontorovich's argument should again apply at the edge of the healing layer where the superfluid density has its bulk value and should then lead to the same answer. These last named authors sought to explain the thinning and non-thinning by a theory incorporating an intrinsic relaxation time. Recently, however, two studies have been published (Graham 1977, Kwok and Goodstein 1977) which cast serious doubts upon the experiments that report no reduction in thickness. Nevertheless, it is interesting to explore the Putterman and Rudnick suggestion further and study the influence of healing on a moving film. It will be of special interest to see whether there will be departures from Kontorovich's theory for films with thickness of the same order as the healing length.

Consider a superfluid film moving with a steady velocity v in the x direction occupying the region $0 \leqslant z \leqslant h(v)$ and held to the plane wall $z = 0$ under the action of gravity and a van der Waals potential $\Omega^v(z)$. Then, the total potential $\Omega(z)$ is given by

$$\Omega(z) = gz + \Omega^v(z), \qquad \Omega^v(z) = -\alpha/z^3, \tag{4.1}$$

where α is a constant. The thickness is assumed to be small enough that the normal fluid is clamped by viscosity. The film and overlying vapour are at a uniform temperature T, which we again suppress in the analytical details below. The vapour is modelled by an inviscid perfect gas and we assume that it is at rest with pressure p^g and thermodynamic potential Φ^g determined by

$$p^g = p_\infty \exp(m\Omega(z)/kT), \qquad \Phi^g = \frac{\mathscr{R}T}{m} \ln p_\infty + \Omega(z), \tag{4.2a, b}$$

where m is the molecular weight of the vapour, $\mathscr{R}$ the universal gas constant and p_∞ the constant pressure at infinity.

The conditions of phase equilibrium at the liquid–vapour interface are (2.18) viz:

$$\rho^s = 0, \qquad p + \eta(\mathrm{d}\rho^s/\mathrm{d}z)^2 = p^g, \qquad \Phi + \tfrac{1}{2}v^2 = \Phi^g, \qquad \text{on} \quad z = h, \tag{4.3a, b, c}$$

together with the continuity of the temperature. In (4.3) the quantities on the left-hand side are evaluated in the liquid. The superfluid Bernoulli equation (2.10) gives

$$\Phi + \tfrac{1}{2}v^2 - \Omega(z) = \text{constant}, \tag{4.4}$$

and, by reference to (4.2) and (4.3), we evaluate the right-hand side to find

$$\Phi + \tfrac{1}{2}v^2 - \Omega(z) = \frac{\mathscr{R}T}{m}\ln p_\infty, \qquad 0 < z < h. \tag{4.5}$$

The fact that the right-hand side of (4.5) is independent of v is crucial to the subsequent analysis.

The total mass equation (2.3) is identically satisfied while the total momentum equation (2.5) reduces to

$$\rho\frac{\mathrm{d}\Omega}{\mathrm{d}z} - \frac{\mathrm{d}p}{\mathrm{d}z} - \frac{\mathrm{d}}{\mathrm{d}z}\eta\left(\frac{\mathrm{d}\rho^s}{\mathrm{d}z}\right)^2 = 0. \tag{4.6}$$

We now suppose that v is small and attempt to evaluate the increase $\delta h = h(v) - h(0)$ in the thickness of the film owing to the persistent current. Like δh, the Eulerian change δp in p resulting from v is also $O(v^2)$ as $v \to 0$. According to (4.3a), we have

$$\begin{aligned}\Delta\left[p + \eta\left(\frac{\mathrm{d}\rho^s}{\mathrm{d}z}\right)^2\right] &\equiv \delta\left[p + \eta\left(\frac{\mathrm{d}\rho^s}{\mathrm{d}z}\right)^2\right] + \left[\frac{\mathrm{d}}{\mathrm{d}z}\left\{p + \eta\left(\frac{\mathrm{d}\rho^s}{\mathrm{d}z}\right)^2\right\}\right]_{v=0}\delta h \\ &= \delta p^g + \left(\frac{\mathrm{d}p^g}{\mathrm{d}z}\right)_{v=0}\delta h \qquad \text{on} \quad z = h,\end{aligned} \tag{4.7}$$

where Δp denotes the Lagrangian change in p resulting from v. By (4.2a) and (4.6)

$$\Delta\left[p + \eta\left(\frac{\mathrm{d}\rho^s}{\mathrm{d}z}\right)^2\right] = \delta\left[p + \eta\left(\frac{\mathrm{d}\rho^s}{\mathrm{d}z}\right)^2\right] + \rho\left(\frac{\mathrm{d}\Omega}{\mathrm{d}z}\right)_{z=h}\delta h = \rho^g\left(\frac{\mathrm{d}\Omega}{\mathrm{d}z}\right)_{z=h}\delta h, \quad \text{on } z = h. \tag{4.8}$$

We shall assume that $\rho^g \ll \rho$ so that we simply require

$$\Delta\left[p + \eta\left(\frac{\mathrm{d}\rho^s}{\mathrm{d}z}\right)^2\right] = \delta\left[p + \eta\left(\frac{\mathrm{d}\rho^s}{\mathrm{d}z}\right)^2\right] + \rho\left(\frac{\mathrm{d}\Omega}{\mathrm{d}z}\right)_{z=h}\delta h = 0, \qquad \text{on} \quad z = h. \tag{4.9}$$

Consider first the Kontorovich argument. This makes use of the Landau two-fluid theory with

$$\Phi = \Phi(p, T, w^2), \qquad \frac{\partial\Phi}{\partial p} = \frac{1}{\rho}, \qquad \frac{\partial\Phi}{\partial T} = -S, \qquad \frac{\partial\Phi}{\partial w^2} = -\frac{\rho^n}{2\rho}, \qquad w = v^n - v^s. \tag{4.10}$$

Taking the Lagrangian variation of the appropriate Bernoulli equation (2.10) to order v^2 on $z = h$ we get Kontorovich's result

$$\delta h = \frac{\rho^s}{2\rho}\left(\frac{\mathrm{d}\Omega}{\mathrm{d}z}\right)^{-1}_{z=h} v^2. \tag{4.11}$$

Since $\Omega(z)$ decreases with increasing z, δh is negative and the film thins.

We now turn to our theory incorporating healing. From equations (2.12) and (2.13) we have

$$\Phi = A + \rho\frac{\partial A}{\partial \rho} - \tfrac{1}{2}v^2, \qquad p + \eta\left(\frac{\mathrm{d}\rho^s}{\mathrm{d}z}\right)^2 = \rho^2\frac{\partial A}{\partial \rho} - \tfrac{1}{2}\rho^s v^2 + \tfrac{1}{2}\eta\left(\frac{\mathrm{d}\rho^s}{\mathrm{d}z}\right)^2, \tag{4.12a, b}$$

and then (4.5) gives

$$A + \rho\frac{\partial A}{\partial \rho} - \Omega(z) = \frac{\mathscr{R}T}{m}\ln p_\infty. \tag{4.13}$$

Taking the Lagrangian variation, using (4.9), (4.12) and the fact that $\Delta\rho^s = 0$ we obtain

$$\delta h = -\frac{1}{2\rho}\Delta\left[\eta\left(\frac{\mathrm{d}\rho^s}{\mathrm{d}z}\right)^2\right]\left(\frac{\mathrm{d}\Omega}{\mathrm{d}z}\right)^{-1}_{z=h}. \tag{4.14}$$

Clearly everything now depends on the value of $\Delta[\eta(\mathrm{d}\rho^s/\mathrm{d}z)^2]$. To evaluate this we use the solutions of § 3.3 which are based on the model (2.16).

Suppose first that $h \gg v$ where v is the dynamic healing length of (3.24). We see from (3.25*b*) that the superfluid density is given by

$$\rho^s = \rho^s_\infty \tanh^2\left(\frac{z-h}{2v}\right), \qquad \rho^s_\infty = f\left(1 - \frac{v^2}{2fA_1}\right), \tag{4.15}$$

so that with (2.9*a*) we have

$$\eta(\mathrm{d}\rho^s/\mathrm{d}z)^2 = \zeta\rho^s_\infty/v^2, \tag{4.16}$$

and, to order v^2,

$$\Delta\left[\eta\left(\frac{\mathrm{d}\rho^s}{\mathrm{d}z}\right)^2\right] = -fv^2. \tag{4.17}$$

Recalling that ρ^s in (4.11) is the superfluid density in the absence of healing and f is (apart from terms that would produce only v^4 correction to δh) the superfluid density outside the healing layers, we see that (4.14) and (4.17) give (4.11) once more. We conclude therefore that when $v \ll h$, the speculation of Putterman and Rudnick (1971) that the healing terms could remove the thinning predicted by Kontorovich is, as conjectured by Goodstein and Saffman (1975), not correct, at least in so far as our theory is a realistic representation of healing processes. To substantiate the Goodstein and Saffman point when $v \ll h$, condition (4.9) applies with good accuracy at the edge of the healing layer next to the bulk helium and of course (4.13) can equally well be applied there (as anywhere else in the film). The argument then becomes almost identical to that used for the Landau theory. The final term of (4.12*b*) is negligible at the edge of the healing layer, but the penultimate term is to good accuracy $-\frac{1}{2}\rho^s_\infty v^2$, so that we obtain

$$\rho\left[\rho\frac{\partial^2 A}{\partial \rho^2} + 2\frac{\partial A}{\partial \rho}\right]\Delta\rho - \tfrac{1}{2}fv^2 = 0, \tag{4.18}$$

and the result (4.11) follows as before.

If h and v are comparable, instead of (4.15), we have (ignoring compression due to

van der Waals force) the solution (3.26) and

$$\left[\eta\left(\frac{\mathrm{d}\rho^{\mathrm{s}}}{\mathrm{d}z}\right)^2\right]_{z=h} = \frac{4A_1k^2(\rho^{\mathrm{s}}_\infty)^2}{(1+k^2)^2}, \tag{4.19}$$

so that, to first order in v^2,

$$\delta h = \frac{f}{2\rho}\left[\frac{4k^2}{(1+k^2)^2}\right]\left(\frac{\mathrm{d}\Omega}{\mathrm{d}z}\right)^{-1}_{z=h} v^2 \equiv \frac{fC}{2\rho}\left(\frac{\mathrm{d}\Omega}{\mathrm{d}z}\right)^{-1}_{z=h} v^2. \tag{4.20}$$

The reduction in thinning due to the factor C is not correctly interpreted merely as a reduction in the mean density, $\bar{\rho}^{\mathrm{s}}$,

$$\bar{\rho}^{\mathrm{s}} = \frac{1}{h}\int_0^h \rho^{\mathrm{s}}\,\mathrm{d}z = \frac{2\rho^{\mathrm{s}}_\infty}{(1+k^2)}\left(\frac{K-E}{K}\right), \tag{4.21}$$

due to healing. To illustrate the point, we have prepared table 1. The fact that fC cannot

Table 1.

k^2	0	0·05	0·1	0·3	0·5	0·7	0·9	0·95
C	0	0·1814	0·3306	0·7101	0·8889	0·9689	0·9972	0·9993
h/v	4·4429	4·6112	4·7832	5·5272	6·4227	7·6535	10·0513	11·4870
$\bar{\rho}^{\mathrm{s}}/\rho^{\mathrm{s}}_\infty$	0	0·0479	0·0921	0·2410	0·3620	0·4726	0·6016	0·6517

be replaced by $\bar{\rho}^{\mathrm{s}}$ in (4.20) is some support for Putterman and Rudnick's contention that healing effects are not negligible.

5. The rectilinear vortex

As Glaberson *et al* (1968) and Glaberson (1969) have observed, Landau's theory meets an obstacle in vortex dynamics. Considering the rectilinear vortex for simplicity, they noted that, since $v^{\mathrm{s}} \propto \kappa/2\pi r$, where r is the distance from the line, there is a critical distance, r_{c}, within which $w = v^{\mathrm{n}} - v^{\mathrm{s}}$ exceeds the maximum, w_{c}, for which superfluidity exists. In Landau's theory therefore, the core $r < r_{\mathrm{c}}$ of a vortex must contain normal fluid alone, or conceivably helium I. As was shown by Ginzburg and Pitaevskii (1958), however, in their by now classic paper, healing eliminates these abrupt changes (at least so long as we make the choice (2.9a) for η); ρ^{s} decreases monotonically with decreasing r and is $O(r^2)$ for $r \to 0$. Ginzburg–Pitaevskii theory is, however, unable to say more, and this is also true of extensions presented in the recent review by Ginzburg and Sobaynin (1977). There are clearly other questions that deserve answers.

First, one would like to know how the total density varies through the vortex. Second, one may recall that the theory (Donnelly and Roberts 1969) of the most useful experimental technique of ion trapping by vortex lines is based on Landau's theory, and may wonder how its predictions are affected by healing. One should notice here that trapping depends on a gradient of pressure, caused by the Bernoulli effect. In Landau's

theory the Bernoulli reduction in pressure,

$$\tfrac{1}{2}\rho^s v^{s2} = \tfrac{1}{2}\rho^s\left(\frac{\hbar}{mr}\right)^2 = 2f\zeta\left(\frac{R}{r}\right)^2, \qquad \rho^s = fR^2, \tag{5.1}$$

is the only one operative, and this becomes infinite as $r \to 0$: the depth of the trapping well is infinite. To counter this, Donnelly and Roberts (1969) included a substitution energy that recognised that the kinetic energy of the flow would be reduced as the ion approached $r = 0$ because of the volume occupied by the trapped ion. In healing, however, we have an alternative effect that prevents the infinite growth of (5.1). It is readily seen from (2.13) that the total stress normal to the axis is

$$P = p - \Sigma_{rr} = \rho^2 \frac{\partial A}{\partial \rho} - 2f\zeta\left[\left(\frac{R}{r}\right)^2 - \left(\frac{dR}{dr}\right)^2\right]. \tag{5.2}$$

The final healing term in (5.2) grows as $r \to 0$ at exactly the same rate as (5.1), so that their difference is $O(r^2)$.

In computing P, we adopt only the first step of the iteration scheme proposed in § 3, and evaluate $P - p_\infty$ where p_∞ is the pressure at great distances, only to order A_1 in the expansion of the free energy. Our results could, then, only represent the real pressure field near a vortex when $T_\lambda - T$ is small. There would however be no difficulty in principle in performing the calculation for large $T_\lambda - T$ though then full knowledge of $A(\rho, T, \rho^s)$ as a function of ρ^s would be required rather than simply $A_1(\rho, T)$; see Roberts *et al* (1978). For $A_1 f^2 \ll \rho|A_0|$, we can again solve (3.7) approximately as

$$\rho = \rho_0 + \frac{1}{u_0^2}\left[A_1\frac{\partial f}{\partial \rho}(\rho^s - f) - \tfrac{1}{2}\frac{\partial A_1}{\partial \rho}(\rho^s - f)^2\right]_{\rho=\rho_0}. \tag{5.3}$$

Using this to evaluate $\rho^2 \partial A/\partial \rho$ in (5.2), we see that

$$p_\infty - P = \frac{A_1 f^2}{2\rho}(1 - R^2)^2 + 2f\zeta\left[\left(\frac{R}{r}\right)^2 - \left(\frac{dR}{dr}\right)^2\right], \tag{5.4}$$

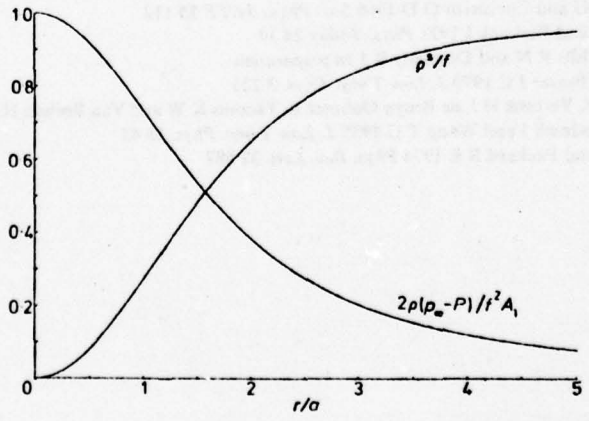

Figure 4. The variation of the superfluid density ρ^s with the distance r from the axis of a rectilinear vortex. The dependence of the total stress P in the radial direction on r is also shown.

where $p_\infty = (\rho^2 \partial A/\partial \rho)_{\rho_0}$. Figure 4 shows $2\rho(p_\infty - P)/A_1 f^2$ as a function of r/a where $a = \sqrt{2\xi} = \sqrt{(2\zeta/fA_1)}$ is the same healing length as was employed by Ginzburg and Pitaevskii (1958). It is clear that P decreases with decreasing r, for all r and reaches its minimum value of $p_\infty - A_1 f^2/2\rho$ at $r = 0$. Also shown in figure 4 is ρ^s/f. This figure was prepared from a fourth-order Runge–Kutta integration.

Finally we should emphasise that the choice (2.9*a*), or of any other $\eta(\rho^s)$ asymptotic to (2.9*a*) as $\rho^s \to 0$, implies either that the vortex circulation is an integral multiple, n, of $\kappa = h/m$ and the superfluid density ρ^s is analytic as $r \to 0$ [$\rho^s = O(r^{2n})$], or that the circulation is non-integral and ρ^s is non-analytic for $r \to 0$. Since the latter possibility is unphysical, in this sense our theory can truly be said to govern a quantum fluid.

References

Brooks J S and Donnelly R J 1977 *J. Phys. Chem. Ref. Data* **6** 51

Donnelly R J and Roberts P H 1969 *Proc. R. Soc.* **312** A 519

Ginzburg V L and Pitaevskii L P 1958 *Sov. Phys.–JETP* **34** 858

Ginzburg V L and Sobaynin A A 1976 *Sov. Phys.-Usp.* **19** 773

Glaberson W I 1969 *J. Low Temp. Phys.* **1** 289

Glaberson W I, Strayer D M and Donnelly R J 1968 *Phys. Rev. Lett.* **21** 1740

Goodstein D L and Saffman P G 1975 *J. Low Temp. Phys.* **18** 435

Graham G M 1977 *J. Low Temp. Phys.* **26** 177

Graham G M and Vitteratos E 1974 *Phys. Rev. Lett.* **33** 1136

Green A E and Naghdi P M 1968 *Int. J. Engng. Sci.* **6** 631

Hills R N and Roberts P H 1977 *Int. J. Engng. Sci.* **15** 305

—— 1978a *J. Low Temp. Phys.* **30** 709

—— 1978b *J. Non-Equilib. Therm.* (in press)

Johnson R S 1978a To appear in *Proc. R. Soc.*

—— 1978b To appear in *Proc. R. Soc.*

Joseph D D 1974 *Arch. Rat. Mech. Anal.* **56** 99

Keller W E 1970 *Phys. Rev. Lett.* **24** 569

Kontorovich V M 1956 *Sov. Phys.–JETP* **3** 770

Kwok D S W and Goodstein D L 1977 *J. Low Temp. Phys.* **27** 187

Landau L D 1941 *Fiz. Zh.* **5** 71

Mamaladze Y G and Cheishvili O D 1966 *Sov. Phys.–JETP* **23** 112

Putterman S J and Rudnick I 1971 *Phys. Today* **24** 39

Roberts P H, Hills R N and Donnelly R J *In preparation*

Rudnick I and Fraser J C 1970 *J. Low Temp. Phys.* **3** 225

van Spronson E, Verbeck H J, de Bruyn Ouboter R, Taconis K W and Van Beehan H 1973 *Phys. Lett.* **A 45** 49

Telschow K, Rudnick I and Wang T G 1975 *J. Low Temp. Phys.* **18** 43

Williams G A and Packard R E 1974 *Phys. Rev. Lett.* **32** 587

Offprint from "Archive for Rational Mechanics and Analysis",
Volume 66, Number 1, 1977, P. 43–71

Printed in Germany

Superfluid Mechanics for a High Density of Vortex Lines

R. N. HILLS & P. H. ROBERTS

Communicated by C. TRUESDELL

Abstract

There are two well known theories to describe the motion and thermodynamics of superfluids when a large number of quantized vortex lines are present and when the phenomena under study are on scales large compared with the vortex line spacing. These works have been criticised on the grounds that their governing equations for the smoothly varying, spatially averaged, fields do not satisfy the accepted invariance principles basic to modern continuum mechanics. This paper demonstrates one way in which such theories can arise from a properly invariant continuum approach and indicates the presence of hitherto unconsidered terms that bring them closer to the generally accepted microscopic picture. The resulting theory has applications both to rotating helium II in the laboratory, and to rotating neutron stars (pulsars).

1. Introduction

According to the current view, helium II is a material which is capable of simultaneously undergoing two motions. With each of these is associated an effective mass, and the sum of these masses is the total mass of the fluid. The velocity fields ascribed to these motions are termed the normal and superfluid velocities, and that portion of the fluid moving with the normal fluid velocity is termed "the normal component". The superfluid component of the mixture is defined similarly. The ideas underlying this two-fluid model were developed by LONDON (1938), TISZA (1938) and LANDAU (1941), but it was LANDAU (1941) who presented the first set of governing equations for the macroscopic description of flows in helium II to be accepted. One of the central postulates of LANDAU's hydrodynamical model is that the superfluid should move irrotationally. Experiments involving steadily rotating buckets of helium suggest, however, that the superfluid can often appear to rotate in some manner, apparently in defiance of LANDAU's law of irrotationality. FEYNMAN (1955) explained this by arguing that the superfluid in the bucket does not rotate in bulk but, rather, such vorticity as it possesses is tightly concentrated into

quantized vortex lines. Picturing the superfluid as a continuum, one must suppose that all the superfluid vorticity is concentrated into singularities of a δ-function character.

The circulation in a quantum vortex line is $\kappa = h/M$ where h is Planck's constant and M is the mass of the helium atom. Higher integral multiples of this circulation, though possible in principle, were rejected by FEYNMAN (1955) from an energy argument. On the continuum picture, a vortex line may be envisaged as having a core of radius a few Ängstroms (10^{-8} cms), in which the density of the superfluid is depleted and falls to zero on the singularity of vorticity. There may also be a local enhancement of the normal fluid density in the core. It appears today that, despite earlier doubts (ANDRONIKASHVILI & TSAKADZE (1965), (1966)), the overall density, ρ, of the fluid is little influenced by the presence or absence of these lines (ANDELIN (1967), SMITH *et al.* (1967)). The vortex lines in the rotating bucket are approximately parallel to its angular velocity, Ω. Their number and spatial distribution have been the subject of several theoretical studies (*e.g.* FETTER (1966), (1967), FETTER & DONNELLY (1966), STAUFFER & FETTER (1968)). They have also recently been photographed by WILLIAMS & PACKARD (1974). Roughly speaking, the distribution of lines is such as to minimize the mean square difference between normal and superfluid velocities, and in consequence there are approximately $n = 2\Omega/\kappa$ vortices per unit cross-sectional area of the bucket. When Ω is large so is n, and the mean spacing between neighbouring lines is small compared with every other length associated with the flow or container. Clearly the superflow will then be of considerable complexity and, particularly when the vortex array is disturbed by wave motions thermally or deliberately produced (HALL (1960)) or by heat currents (CHANG, CROMAR & DONNELLY (1963)), there is little hope of a practical description in complete detail. It is, however, precisely in such circumstances that a theory might be tenable in which the tightly packed vortex array is represented by a continuum, and its associated microscale flow by new macroscale stresses.

There have been a number of simplified theories that aim to describe helium II in the presence of a high density of vortex lines. The work of HALL & VINEN (1956), HALL (1960) and BEKHAREVICH & KHALATNIKOV (1961) (denoted henceforth by HVBK) all envisage a theory relating fields and flows averaged over spatial scales small compared with the macroscale, such as container dimensions, but large compared with the mean vortex spacing. Thus, while the actual superfluid velocity varies rapidly with position on the scale of the vortex separations, the average superfluid velocity, $\boldsymbol{v}^s$, changes smoothly on the macroscale; while the actual superfluid vorticity is either infinite or zero depending on whether a vortex core does or does not pass through the point concerned, the average superfluid vorticity, $\boldsymbol{\omega}^s = \nabla \times \boldsymbol{v}^s$ varies continuously; while when the normal fluid is absent the vortex lines must move with the superfluid in accord with Helmholtz's theorem, the average vortex line velocity, $\boldsymbol{v}^L$, could not be expected to coincide with the average superfluid velocity, $\boldsymbol{v}^s$; and while the actual interactions between elements of vortex lines is non-local in character (*e.g.* see BATCHELOR (1967), §24), it may be expected that the dominant contributions arise from neighbouring lines and would therefore be represented

at high vortex line densities by an average force local in character. No effort was made to derive equations by averaging LANDAU's equations directly, but two plausible consequences of such an averaging were inferred and incorporated as postulates into the theory. The first of these was the recognition (BEKHAREVICH & KHALATNIKOV (1961)) that the rapid circulatory flows round each vortex core would contribute significantly to the energy budget. A term proportional to ω^s was therefore included in the energy density. Second, it was realized that the excitations comprising the normal fluid would collide with the vortex lines to influence the motion of each. HALL (1970), for example, has provided an interesting insight into the nature of this complicated interaction. In the mean HVBK sense, it is represented by a smoothly varying 'diffusive force' that not only causes the normal fluid to move with an average velocity, v^n, different from that in the absence of vortex lines, but also makes the vortex lines move with an average velocity, v^L, that differs from the self-induced velocity they would have in the absence of the normal fluid. HALL & VINEN (1956) based their postulates for this diffusive force on a microscopic picture of the collision process, and the form of v^L was then determined by balancing forces on a vortex core, a reasonable procedure since the inertia of a vortex line is small.

As an example of the governing equations we cite the linear momentum equation for the superfluid in the BK theory†:

$$\rho^s\{\partial_t v^s+(v^s\cdot\nabla)v^s\}=-\rho^s\nabla\Phi-\omega^s\times\operatorname{curl}\lambda\hat{\omega}^s+G, \tag{1.1}$$

where ρ^s is the superfluid density, $\omega^s=\operatorname{curl} v^s$ the superfluid vorticity, Φ a thermodynamic potential and G is

$$G=-B\hat{\omega}^s\times(\omega^s\times A)-B'\omega^s\omega^s\times A+B''(\omega^s\cdot A)\hat{\omega}^s,$$
$$A=\frac{\rho^n\rho^s}{2\rho\omega^s}\left(v^n-v^s-\frac{1}{\rho^s}\nabla\times(\lambda\hat{\omega}^s)\right),\quad \hat{\omega}^s=\omega^s/\omega^s, \tag{1.2}$$

v^n being the normal fluid velocity and ρ^n the normal fluid density. These equations are in conflict with a basic tenet of modern continuum mechanics, the 'principle of material frame indifference'; the material properties must be the same for all observers and quantities such as temperature, the surface forces, the internal energy and the entropy have an intrinsic meaning independent of the observer. The principle is a powerful tool. It can be employed to deduce the continuity and momentum equations, as well as the symmetry of the stress tensor, from the frame indifference of either the total power (NOLL (1963)) or the energy balance (GREEN & RIVLIN (1964)). In constitutive theory it excludes certain quantities from the list of possible independent variables. For example, it can be shown that the stress tensor of a Stokesian fluid cannot depend upon the vorticity tensor (see NOLL (1955)). The principle would similarly rule out equations of the form (1.1) and (1.2). Consider the 'diffusive force' G in (1.1). The vorticity vector for a stationary observer differs from that seen by a rotating observer by 2Υ where Υ is the angular velocity of the rotating frame. The

† See §5, equation (5.14).

principle requires that the G for the two observers should differ only in orientation but, evidently, the form (1.2) does not conform.

On the basis of (1.1) and (1.2), it is frequently claimed that the principle of frame indifference is not universally true and, in particular, that equations obeying such a principle cannot be constructed that explain superfluids in motion. This view gains added force from superficially similar violations in the kinetic theory of gases. Recently, however, TRUESDELL (1977) has exposed the fallacious reasoning behind these criticisms from kinetic theory. It is our principal purpose to show the non-invariant HVBK theories can be replaced by an equally satisfactory, but invariant, alternative.

It should be admitted that occasionally one encounters the view that the HVBK theories *are* invariant *in their present form*. Underlying such statements is a confusion regarding the interpretation to be given to the symbol ω^s appearing in, for example, equation (1.1). In the application of the HVBK theories to specific problems ω^s is unambiguously identified with the vorticity of the superfluid. However, when the equations are claimed to be invariant, ω^s is said to be related to the density of vortex lines, and, since the number of lines should remain unaltered under a change of observer, the ω^s is therefore invariant. This latter view clearly gives to the symbol a meaning other than $\omega^s = \nabla \times v^s$ and it is certainly not obvious that the two interpretations for ω^s are compatible. In our resolution of this dilemma we attach to the symbol ω^s the classical meaning $(\nabla \times v^s)$, but also introduce a continuous axial vector field ζ which we term 'the vortex density vector' ζ. As the name suggests, the magnitude of ζ is proportional to the density of quantized vortex lines. More precisely, if we adopt the usual right-hand rule, we can use the sense of the circulating flow created by any vortex line to give a direction to that line. We may assign a vector to every point of the line, whose magnitude is κ, the circulation, and which is directed along the tangent to the line at that point. Then, if we consider a small element of surface area with unit normal parallel to the i-axis and enclosing a point $\mathscr{P}$, we may picture ζ_i at $\mathscr{P}$ as the sum of the i^{th}-components of all these vectors divided by the area itself. With this physical interpretation in mind, we assume that the vector ζ is frame indifferent and we attempt to develop a theory with ζ as a new fundamental variable. One might hope to recover conservation laws of the form (1.1) and (1.2) but with the crucial difference that ζ replaces ω^s. The resulting equations would be frame indifferent.

This solution of the invariance problem introduces a new difficulty: the theory is no longer complete. An evolutionary equation for ζ is needed, but there is absolutely no guarantee *a priori* that such an equation can ever reinstate the HVBK theories. In §4, however, we discover a properly frame indifferent equation for ζ which, in the inertial frame, admits as a *particular solution*

$$\zeta = \omega^s, \tag{1.3}$$

and in subsequent sections we are able to show how the HVBK theories can result from our more general theory using (1.3).

The experimental evidence suggests that, provided some critical relative velocity between the normal and superfluid is not exceeded, vortex lines do not

appear spontaneously within the fluid (see, for example, ROBERTS & DONNELLY (1974), p. 196ff.). Changes in ζ at a point must then be represented purely by the advection of ζ by the vortex line velocity, v^L, *i.e.*

$$\frac{d}{dt}\int_{\Sigma}\zeta\cdot dS=0 \tag{1.4}$$

for all surfaces, Σ, convected with velocity v^L. The theory we derive must allow (1.4). At the same time, it should be flexible enough to deal with generalizations of interest. In particular, the theory should be capable of dealing naturally with situations where vortex production occurs and in which (1.4) is violated.

The structure of a vortex core, its interaction with its environment and particularly the exchange of material in its interior with the ambient fluid are topics of considerable complexity. On the microscopic level, the circulating superflow created by the vortex line enhances and polarizes rotons in its vicinity (GLABERSON, STRAYER & DONNELLY (1968), GLABERSON (1969)). This leads to the idea that normal fluid is localized by a line (ROBERTS &.DONNELLY (1974)) and that the core of the line may well consist of completely classical fluid (He I). Whether one should regard this fluid and the surrounding excitations as imparting inertia to the line clearly depends on the efficiency or otherwise with which they are exchanged with the ambient flow in which the vortex lies, a topic addressed by HALL (1970) and HILLEL *et al.* (1974). It seems reasonable to suppose that some mass per unit length should be associated with the line and that therefore, in the present continuum description of an array of lines, a mass density, ρ^L, should be associated with the flow v^L and that a mass exchange between all three parts ρ^n, ρ^s, ρ^L of ρ should be envisaged. The vortex fluid, like the super and normal fluids, will be subject to balance laws for linear and angular momentum. Recalling, however, that the dimensions of the core are small, we may anticipate that the inertia of the vortex fluid will be slight. Indeed, we later derive equations of the HVBK type from the general theory by ignoring the inertia of the lines entirely. We should perhaps mention, however, that WANG *et al.* (1975) have recently studied a technique by which vortex lines could be visualized by decorating them with tiny glass beads (of radius of order 10^{-4} cms.). Such beads would clearly enhance the inertia of the lines considerably and so alter the wave properties of the system. It seems that such matters could readily be investigated by slight modification of the theory developed below. It would appear from the work of TSAKADZE & TSAKADZE (1973) that another application of the theory lies in the study of pulsars. These authors demonstrate that there is a possibility of simulating some properties of pulsars by a study of rotating helium II with the quantized vortex lines parallel to the axis of rotation.

To sum up, when a large number of quantized vortex lines are present in helium II, we will adopt a model that is non-classical in the sense that the complete description of the mean flows requires, in addition to the normal and superfluid velocity fields, the specification of the fields v^L and ζ. In the terminology of modern continuum mechanics, the vortex fluid added is a polar material. We shall assume that the fields v^L and ζ contribute to the total energy

of the system and the dissipation occurring within it. It is hoped that, with this approach, many of the salient features of quantized vortices *en masse* will emerge from the subsequent development through the constitutive assumptions. For example, the interaction of the vortices with the normal and superfluid components will appear as a postulate for the supply of linear and angular momentum.

We shall construct the theory using thermodynamic variables associated with the fluid as a whole. The first such formulation of a general mixture theory of non-polar materials was given by GREEN & NAGHDI (1965). More recently, HILLS & ROBERTS (1972) demonstrated that, with a suitable constitutive model, LANDAU's two-fluid equations could be obtained from the general framework built by GREEN & NAGHDI. We shall generalize our earlier paper by adding a polar fluid component. The theory is based on postulated conservation laws for the linear and angular momentum of each constituent, together with a conservation law for the total energy and an entropy production inequality for the mixture as a whole. We hope that by making use of the methods of modern continuum mechanics, we can make abundantly clear precisely what ingredients and assumptions are required to make up a proper theory of the HVBK type. It might seem to the casual reader that our theory relies for its success on a plethora of postulates. We believe, however, that the HVBK theories depend on certainly as many assumptions, though they are not always explicitly stated. One advantage in making the postulates clear is readily appreciated when we generalize the HVBK theories in §5. The need to probe the HVBK theories more deeply has been highlighted by SNYDER (1972) who, in trying to reconcile preliminary experiments on Couette instability with the HVBK theories, was led to believe either that, 'the HVBK theories do not describe the flow ... or that the accepted values of B, B' and λ are grossly incorrect.'

The basic notation of this paper is introduced in §2, and in §3 we postulate the fundamental balance laws and entropy inequality. By taking notice of the constitutive basis of LANDAU's theory for vortex-free helium and by incorporating ideas of HALL & VINEN on the forces of interaction between vortices and normal and superfluid, we select in §4 a constitutive class. The implications of the entropy inequality are studied. In addition we indicate the modifications to the theory that would result if the mixture were assumed incompressible in the sense that the total density, ρ, remains constant.

In §5 we show that theories of the HVBK type can be recovered from our work when the limit $\rho^L \to 0$ is taken. The linear momentum equation for the vortex fluid then becomes a balance of forces as in the work of HV (1956). Although we find it most convenient to compare with the single paper of BEKHAREVICH & KHALATNIKOV rather than with the earlier writings of HALL & VINEN, we do find that, in agreement with the latter writers, the term involving B'' in (1.2) proposed by BEKHAREVICH & KHALATNIKOV (1961) does not arise naturally in our theory. This question is raised again in our attempts to generalize the HVBK theories. We regard these generalizations as the subsidiary objective of our work and they fall into two categories. In the first, we adhere to the conservation of ζ-flux (1.3) and consider modifications to our postulated heat conduction vector and diffusive force for the vortex fluid. These changes are

motivated by the thought that the interaction of heat currents and vortex lines may not hitherto have been adequately included in the theory. One effect of our new terms on the superfluid momentum equation (1.1) is to replace the expression (1.2) for A, by $\tilde{A}$ where

$$\tilde{A}=\frac{\rho^n\rho^s}{2\rho\omega^s}\left[v^n-v^s-\frac{1}{\rho^s}\nabla\times(\lambda\hat{\omega}^s)+\frac{\beta_2}{\rho^s}\nabla T+\frac{\beta_3}{\rho^s}\omega^s\times\nabla T\right], \tag{1.5}$$

and β_2 and β_3 are new diffusive coefficients.

The other category of generalizations briefly considered in § 5 are those that do not preserve ζ-flux, although (1.3) is still allowed. We give two examples. In the first of these we demonstrate one way in which the B'' term can be restored to (1.2), but only at the expense of violating (1.4). Our second example is, we believe, related both to the phenomenon of vortex nucleation and to the diffusive force proposed by GORTER & MELLINK (1949).

Finally, it is perhaps appropriate to catalogue briefly the main accomplishments of this paper. We have shown how the apparently non-invariant HVBK theories can arise from a properly invariant framework and have generalized the HVBK theories to include the inertia of the vortex lines, an effect not negligible in the experiments planned by WANG *et al.* We have demonstrated why a three fluid model is necessary, and for the first time given the constitutive theory for such a model. In doing so we have exposed the interactions between the three components. Finally, we have proposed the addition of new mathematical terms representing neglected physical effects and, for the first time, we have shown how nucleation effects might be incorporated into the theory.

2. Preliminaries

As we have indicated we attempt to model the behaviour of helium II when there is a high density of vortex lines by means of a ternary mixture. Two of the components are called the normal and superfluid and the third the vortex fluid. The motion of the continuum is referred to a fixed system of rectangular Cartesian axes and we assume that each point within the mixture is simultaneously occupied by each of the three components. Direct tensor notation is used where convenient and also a corresponding suffix notation to denote components. Let x^n be the position of a typical particle of the normal fluid at the current time t; then its position at a previous time τ is $x^n(\tau)$ and

$$x^n(\tau)=\chi^n(x^n,\tau,t), \qquad x^n=x^n(t), \qquad -\infty<\tau\leqq t. \tag{2.1}$$

Similarly, for a typical material point of the superfluid and the vortex fluid, we have respectively

$$\begin{aligned} &x^s(\tau)=\chi^s(x^s,\tau,t), \qquad x^s=x^s(t), \qquad -\infty<\tau\leqq t,\\ &x^L(\tau)=\chi^L(x^L,\tau,t), \qquad x^L=x^L(t), \qquad -\infty<\tau\leqq t. \end{aligned} \tag{2.2}$$

The velocity vectors for these materials are

$$v^n(\tau)=\frac{D^n}{D\tau}x^n(\tau), \qquad v^s(\tau)=\frac{D^s}{D\tau}x^s(\tau), \qquad v^L(\tau)=\frac{D^L}{D\tau}x^L(\tau), \tag{2.3}$$

where $\frac{D^n}{D\tau}$ denotes differentiation with respect to τ keeping x^n and t fixed and $\frac{D^s}{D\tau}$ and $\frac{D^L}{D\tau}$ are similar operators for the super and vortex fluids. The acceleration vectors at time τ are denoted by $f^n(\tau)$, $f^s(\tau)$ and $f^L(\tau)$ where

$$f^n(\tau)=\frac{D^n}{D\tau}v^n(\tau), \quad f^s(\tau)=\frac{D^s}{D\tau}v^s(\tau), \quad f^L(\tau)=\frac{D^L}{D\tau}v^L(\tau). \tag{2.4}$$

Associated with the material point of the vortex fluid at time τ there is the vortex density vector, $\zeta(\tau)$, and

$$\zeta(\tau)=\zeta(x^L,\tau,t), \quad \zeta=\zeta(t), \quad -\infty<\tau\leqq t. \tag{2.5}$$

We shall assume that the three material points being considered occupy the same position at the present time t so that $x^n=x^s=x^L$ and at this point we have the three rate fields v^n, v^s, v^L together with the axial vector ζ. The rate of deformation tensor D^n and the vorticity tensor W^n have components

$$D^n_{ij}=\tfrac{1}{2}(v^n_{i,j}+v^n_{j,i}), \quad W^n_{ij}=\tfrac{1}{2}(v^n_{i,j}-v^n_{j,i}), \tag{2.6}$$

where a subscript j following a comma denotes partial differentiation with respect to the space variable x^n_j. The tensors D^s, D^L and W^s, W^L are similarly defined.

At time t the operators of (2.3) can be written as

$$\frac{D^n}{Dt}=\partial_t+(v^n\cdot\nabla), \quad \frac{D^s}{Dt}=\partial_t+(v^s\cdot\nabla), \quad \frac{D^L}{Dt}=\partial_t+(v^L\cdot\nabla), \tag{2.7}$$

where ∂_t denotes partial differentiation with respect to time holding the space variable fixed. If the densities of the normal, super and vortex fluid components are ρ^n, ρ^s, and ρ^L respectively, the total density ρ is given by

$$\rho=\rho^n+\rho^s+\rho^L, \tag{2.8}$$

and we can define the operator $\frac{D}{Dt}$ by

$$\rho\frac{D}{Dt}=\rho^n\frac{D^n}{Dt}+\rho^s\frac{D^s}{Dt}+\rho^L\frac{D^L}{Dt}=\rho\partial_t+[(\rho^n v^n+\rho^s v^s+\rho^L v^L)\cdot\nabla]. \tag{2.9}$$

We shall consider a change of the frame at time τ in which the vectors x^α, ζ^α are transformed into $\tilde{x}^\alpha, \tilde{\zeta}^\alpha$ by a rigid transformation of the form

$$\tilde{x}^\alpha(\tau)=\tilde{a}(\tau)+Q(\tau)[x^\alpha(\tau)-a(\tau)], \quad \tilde{\zeta}(\tau)=Q(\tau)\zeta(\tau), \tag{2.10}$$

where here and throughout the superscript α stands for n, s or L, $\tilde{a}(\tau)$ and $a(\tau)$ are vector functions of τ and $Q(\tau)$ is a time dependent *proper* orthogonal tensor. Under proper orthogonal transformations the distinction between axial and absolute (polar) vectors is lost. However, it will be necessary to distinguish

between these vectors when considering the constitutive theory. The equation $(2.10)_2$ tells us that the vortex number density should remain unaltered under change of observer.

The vectors and tensors of (2.3), (2.4) and (2.6) are defined in terms of the original frame. We denote the analogous quantities for the second frame by the same symbol with a superposed tilde. Then it is easily shown that

$$\tilde{\boldsymbol{D}}^{\alpha}=\boldsymbol{Q}\boldsymbol{D}^{\alpha}\boldsymbol{Q}^{T}, \quad \tilde{\boldsymbol{W}}^{\alpha}=\boldsymbol{Q}\boldsymbol{W}^{\alpha}\boldsymbol{Q}^{T}+\boldsymbol{\Upsilon}, \tag{2.11}$$

where $\boldsymbol{\Upsilon}=\dot{\boldsymbol{Q}}\boldsymbol{Q}^{T}=-\boldsymbol{\Upsilon}^{T}$ and $\boldsymbol{Q}=\boldsymbol{Q}(t)$, *etc.*

3. Balance Laws and Entropy Inequality

For a fixed closed surface A enclosing a volume V we postulate for the linear momentum of each constituent

$$\partial_t \int_V \rho^{\alpha}\boldsymbol{v}^{\alpha}dV+\int_A \rho^{\alpha}\boldsymbol{v}^{\alpha}(\boldsymbol{n}\cdot\boldsymbol{v}^{\alpha})dA=\int_V(\rho^{\alpha}\boldsymbol{F}^{\alpha}+\boldsymbol{G}^{\alpha})dV+\int_A \boldsymbol{T}^{\alpha}\boldsymbol{n}\,dA, \tag{3.1}$$

where the superscript α represents n, s or L. In (3.1) $\boldsymbol{F}^{\alpha}$ is the external body force applied per unit mass to the α-component, $\boldsymbol{T}^{\alpha}$ is the stress tensor associated with the α-component and $\boldsymbol{G}^{\alpha}$ is the density of the supply of linear momentum to the *α-component.*

Next we postulate a moment of momentum equation for each constituent. We assume

$$\begin{aligned}\partial_t \int_V \boldsymbol{x}\times\rho^{\alpha}\boldsymbol{v}^{\alpha}dV+\int_A\{\boldsymbol{x}\times\rho^{\alpha}\boldsymbol{v}^{\alpha}\}(\boldsymbol{n}\cdot\boldsymbol{v}^{\alpha})dA\\ =\int_V \boldsymbol{x}\times(\rho^{\alpha}\boldsymbol{F}^{\alpha}+\boldsymbol{G}^{\alpha})dV+\int_A \boldsymbol{x}\times\boldsymbol{T}^{\alpha}\boldsymbol{n}\,dA+\int_V \boldsymbol{\Gamma}^{\alpha}dV,\end{aligned} \tag{3.2}$$

where $\boldsymbol{\Gamma}^{\alpha}$ is a supply term.

We recall that the changes in ζ are advected with velocity $\boldsymbol{v}^{L}$ and we assume that the balance law for ζ is

$$\partial_t \int_V \lambda\hat{\zeta}dV+\int_A \lambda\hat{\zeta}\boldsymbol{n}\cdot\boldsymbol{v}^{L}dA=\int_V(\Omega^{\zeta}+\eta^{\zeta})dV+\int_A \boldsymbol{T}^{\zeta}\boldsymbol{n}\,dA \tag{3.3}$$

where $\hat{\zeta}=\zeta/\zeta$, Ω^{ζ} and η^{ζ} are the external and intrinsic source terms, $\boldsymbol{T}^{\zeta}$ is a stress tensor associated with the extra kinematical freedom and the coefficient λ in the density term $\lambda\hat{\zeta}$ will be the subject of a constitutive postulate later.

By applying the divergence theorem with the usual conditions of smoothness, we can obtain the pointwise form of the equations (3.1)–(3.3) as

$$\begin{aligned}&\rho^{\alpha}\boldsymbol{f}^{\alpha}=\rho^{\alpha}\boldsymbol{F}^{\alpha}+\boldsymbol{g}^{\alpha}+\nabla\cdot\boldsymbol{T}^{\alpha},\\ &\boldsymbol{\Gamma}^{\alpha}+2\tilde{\boldsymbol{T}}^{\alpha}=0,\\ &\frac{\lambda}{\zeta}\frac{D^{L}\zeta}{Dt}=\gamma^{\zeta}+\Omega^{\zeta}+\nabla\cdot\boldsymbol{T}^{\zeta},\end{aligned} \tag{3.4}$$

where $\hat{T}^\alpha$ is the axial vector associated with the skew-symmetric part of T^α, $\hat{T}^\alpha_i = \frac{1}{2}e_{ijk}T^\alpha_{kj}$, and

$$m^\alpha = \partial_t \rho^\alpha + \nabla\cdot(\rho^\alpha v^\alpha), \quad M^\lambda = \partial_t\left(\frac{\lambda}{\zeta}\right) + \nabla\cdot\left(\frac{\lambda v^L}{\zeta}\right),$$
$$g^\alpha = G^\alpha - m^\alpha v^\alpha, \quad \gamma^\zeta = \eta^\zeta - M^\lambda \zeta. \tag{3.5}$$

For the global postulate for the energy balance we assume

$$\begin{aligned}\partial_t \int_V (\rho U + \tfrac{1}{2}\rho^n v^{n2} + \tfrac{1}{2}\rho^s v^{s2} + \tfrac{1}{2}\rho^L V^{L2} + \lambda\zeta)\,dv + \int_A \{n\cdot(\rho^n v^n + \rho^s v^s + \rho^L v^L)U \\ + \tfrac{1}{2}\rho^n v^{n2}(n\cdot v^n) + \tfrac{1}{2}\rho^s v^{s2}(n\cdot v^s) + \tfrac{1}{2}\rho^L v^{L2}(n\cdot v^L) + \lambda\zeta(n\cdot v^L)\}\,dA \\ = \int_V \{\rho r + \rho^n F^n\cdot v^n + \rho^s F^s\cdot v^s + \rho^L F^L\cdot v^L + \Omega^\zeta\cdot\zeta\}\,dV \\ + \int_A \{v^n\cdot T^n n + v^s\cdot T^s n + v^L\cdot T^L n + \zeta\cdot T^\zeta n - n\cdot q\}\,dA.\end{aligned} \tag{3.6}$$

In (3.6) U is the internal energy per unit mass of helium II, r is the heat supply per unit mass per unit time and q is the heat conduction vector. As such, (3.6) is a generalization of the balance law of GREEN & NAGHDI (1965) when a polar fluid is added to a binary mixture.

In setting down the balances (3.6) and (3.3) we have made a statement regarding the densities of the energy and the number density. Of course, we do not know *a priori* what these densities should be and the relevance of the postulates can only be judged in the light of the predictions of the theory. In this paper we demonstrate at least that the form we have chosen for these densities is closely linked to the HVBK theories. BEKHAREVICH & KHALATNIKOV (1961) included a term $\lambda|\nabla\times v^s|$ in their energy density.

It is perhaps worth noting that the inclusion of $\lambda\zeta$ and $\frac{1}{2}\rho^L v^{L2}$ does not count energy twice. The $\lambda\zeta$ qualitatively represents the energy of the microscopic circulations round the vortex cores, which are averaged out when v^s is formed, and is not contained in $\frac{1}{2}\rho^s v^{s2}$. It is, however, distinct from the kinetic energy of the motion of the mass trapped by, or moving with, the vortices. In § 5 when we consider the limit $\rho^L \to 0$ of negligible line inertia, the energy $\frac{1}{2}\rho^L v^{L2}$ disappears but $\lambda\zeta$ does not.

We are now in a position to apply the standard invariance arguments. We shall assume that under a change of reference frame for the proper orthogonal tensor Q

$$\begin{aligned}&\tilde{\rho}^\alpha = \rho^\alpha, \quad \tilde{U} = U, \quad \tilde{q} = Qq, \quad \tilde{g}^\alpha = Qg^\alpha, \quad \tilde{\Gamma}^\alpha = \Omega\Gamma^\alpha, \\ &\tilde{T}^\alpha = QT^\alpha Q^T, \quad (\tilde{F}^\alpha - \tilde{f}^\alpha) = Q(F^\alpha - f^\alpha), \quad \tilde{\lambda} = \lambda, \quad \tilde{\gamma}^\zeta = Q\gamma^\zeta, \\ &\tilde{T}^\zeta = QT^\zeta Q^T, \quad \widetilde{\left(\Omega^\zeta - \frac{\lambda}{\zeta}\frac{D^L\zeta}{Dt}\right)} = Q\left(\Omega^\zeta - \frac{\lambda}{\zeta}\frac{D^L\zeta}{Dt}\right).\end{aligned} \tag{3.7}$$

Then, by first considering (2.10) with

$$\tilde{a}(\tau) = b\tau, \quad a(\tau) = 0, \quad Q(\tau) = I, \quad -\infty < \tau \leqq t$$

where $\boldsymbol{b}$ is an arbitrary constant vector and $\boldsymbol{I}$ is the unit tensor, we deduce from (3.6), (3.4) and (3.5) the pointwise forms

$$m^n + m^s + m^L = 0, \tag{3.8}$$

$$g^n + g^s + g^L = -(m^n v^n + m^s v^s + m^L v^L). \tag{3.9}$$

If we now consider (2.10) with

$$\tilde{a}(\tau) = a(\tau) = 0, \quad Q = I, \quad \dot{Q} = \Upsilon,$$

where Υ is an arbitrary skew-symmetric tensor, we deduce

$$\Gamma^n + \Gamma^s + \Gamma^L = 0. \tag{3.10}$$

We can use these results to write the pointwise form of the residual energy equation as

$$\rho r - \rho \frac{DU}{Dt} - \tfrac{1}{2} m^s w^2 - \tfrac{1}{2} m^L u^2 - m^\lambda \zeta - \nabla \cdot q + Q = 0, \tag{3.12}$$

where

$$m^\lambda = \partial_t \lambda + \nabla \cdot (\lambda v^L), \tag{3.13}$$

$$Q = g^s \cdot w + g^L \cdot u - \gamma^\zeta \cdot \zeta + \mathrm{tr}(T^n D^n + T^s D^s + T^L D^L + T^\chi Z) + \Gamma^n \cdot \overline{W} + \Gamma^L \cdot \bar{C} \tag{3.14}$$

$$\begin{aligned} &w = v^n - v^s, \qquad c = v^L - v^s, \qquad u = v^n - v^L, \\ &\overline{W} = \overline{W}^n - \overline{W}^s, \quad \bar{C} = \overline{W}^L - \overline{W}^s, \quad Z_{ij} = \zeta_{i,j}, \end{aligned} \tag{3.15}$$

and the trace of a tensor A is denoted by $\mathrm{tr}(A)$.

It is useful at this stage to record that $\dfrac{D\rho}{Dt}, m^s, m^L$ and m^λ can be written as

$$\begin{aligned} \frac{D\rho}{Dt} &= -\rho w \cdot \nabla \left(\frac{\rho^n}{\rho}\right) - \rho c \cdot \nabla \left(\frac{\rho^L}{\rho}\right) - \rho^n \nabla \cdot v^n - \rho^s \nabla \cdot v^s - \rho^L \nabla \cdot v^L, \\ m^s &= \rho \frac{D}{Dt}\left(\frac{\rho^s}{\rho}\right) + \frac{\rho^s}{\rho}\frac{D\rho}{Dt} - \frac{\rho^L}{\rho} c \cdot \nabla \rho^s - \frac{\rho^n}{\rho} w \cdot \nabla \rho^s + \rho^s \nabla \cdot v^s, \\ m^L &= \rho \frac{D}{Dt}\left(\frac{\rho^L}{\rho}\right) + \frac{\rho^L}{\rho}\frac{D\rho}{Dt} + \left(1 - \frac{\rho^L}{\rho}\right) c \cdot \nabla \rho^L - \frac{\rho^n}{\rho} w \cdot \nabla \rho^L + \rho^L \nabla \cdot v^L, \\ m^\lambda &= \rho \frac{D}{Dt}\left(\frac{\lambda}{\rho}\right) + \frac{\lambda}{\rho}\frac{D\rho}{Dt} + \left(1 - \frac{\rho^L}{\rho}\right) c \cdot \nabla \lambda - \frac{\rho^n}{\rho} w \cdot \nabla \lambda + \lambda \nabla \cdot v^L. \end{aligned} \tag{3.16}$$

Because of the curious thermodynamic properties associated with helium II, it might be expected that the choice of the entropy inequality would be all important. Bearing in mind that we are dealing with a mixture theory employing thermodynamical variables for the mixture as a whole, this would seem to be especially true. For a mixture of ideal gases the approach of GREEN & NAGHDI (1965), using the Clausius-Duhem inequality, led to incorrect expressions for the partial pressures according to the kinetic theory. There are two ways of

surmounting this difficulty. GREEN & NAGHDI (1968) introduced a gauge transformation while MÜLLER (1968) used a more general entropy inequality. (For a review of the situation, see ATKIN & CRAINE (1976).) However, for liquid helium the situation is less clear: it is certainly not a mixture of two ideal gases and it is often imprudent even to think of it as a conventional mixture. For example, there is no question of ever being in a position to separate the two components. When in an earlier paper we discussed the Landau two-fluid equations of helium, we used the Clausius-Duhem inequality and we obtained the accepted partial stresses. In the spirit of the generalization of this paper, we again employ the Clausius-Duhem inequality without subsequent gauge transformation*. Thus we have

$$\partial_t \int_V \rho S dV + \int_A n\cdot(\rho^n v^n + \rho^s v^s + \rho^L v^L) S dA - \int_V \frac{\rho r}{T} dV + \int_A \frac{n\cdot q}{T} dA \geqq 0, \quad (3.17)$$

where T denotes the local absolute temperature which is assumed strictly positive and S is the entropy per unit mass of helium II. Looking at the second integral in (3.17) the reader may have qualms that our entropy production inequality conflicts with the accepted picture that, in a heat current, entropy is carried only by the normal fluid. The apparent conflict is illusory. A full discussion is given by HILLS & ROBERTS (1972) who also present an alternative physical picture of heat conduction in a superfluid and deduce the usual equation for entropy conservation from the energy postulate.

From (3.17) and (3.12), with the usual assumptions of smoothness, we get

$$-\rho\left(\frac{DA}{Dt} + S\frac{DT}{Dt}\right) - \tfrac{1}{2}m^s w^2 - \tfrac{1}{2}m^L u^2 - m^\lambda \zeta + Q - \frac{q\cdot\nabla T}{T} \geqq 0, \quad (3.18)$$

where A is the Helmholtz free-energy function defined by

$$A = U - ST. \quad (3.19)$$

The theory is made determinate by proposing constitutive equations which are intended to reflect the character of the components and their mutual interaction. We will postulate equations for $A, S, \lambda, g^s, g^L, \gamma^\zeta$, the symmetric part of the stress T^s, i.e. $T^s_{(ij)}$, Γ^m, Γ^s, T^ζ, q and the concentrations ρ^s/ρ, ρ^L/ρ. With these postulates, the concentration ρ^n/ρ is given by (2.8) and the total density is determined from (3.8). The equations (3.4) provide twelve equations for v^n, v^s, v^L and the vortex density vector ζ. The skew-symmetric stress components $T^L_{[ki]}$ are given by (3.10) and the diffusive force g^n is derived from (3.9). As usual, the temperature distribution is determined from the energy equation (3.12) and the entropy production inequality will, in general, provide restrictions on the constitutive equations.

The specific assumptions made for the constitutive theory are directly influenced by the model of HILLS & ROBERTS (1972) for the Landau two-fluid equations. We again assume that the material has a centre of symmetry. This requires that the relations $(3.7)_{1-8}$ hold for Q a member of the full orthogonal

* Our results could easily be modified to include such gauge transformations. Also we do not claim that the more general Müller inequality has no relevance to helium II. In a forthcoming paper, HILLS & ROBERTS (1977), we have demonstrated that the Müller inequality (or equivalently a non-zero gauge transformation) is essential in order to explain an observed phenomenon in another flow regime of helium.

group. In addition, in place of $(2.10)_2$ and $(3.7)_{9-11}$ we now assume

$$\tilde{\zeta}=sQ\zeta, \quad \tilde{\gamma}^{\zeta}=sQ\gamma^{\zeta}, \quad \tilde{T}^{\zeta}=sQT^{\zeta}Q^{T},$$
$$\widetilde{\left(\Omega^{\zeta}-\frac{\lambda}{\zeta}\frac{D^{L}\zeta}{Dt}\right)}=sQ\left(\Omega^{\zeta}-\frac{\lambda}{\zeta}\frac{D^{L}\zeta}{Dt}\right), \tag{3.20}$$

where $s=\operatorname{sign}\det(Q_{ij})$.

4. Constitutive Theory

The development of the constitutive theory is principally motivated by experiments with rotating helium II. It is natural to hope that the resulting system will reduce to the equations governing the eminently successful Landau two-fluid model of non-rotating helium in the limit of zero vortex-line density, that is, when

$$\rho^{L}\to 0, \quad \zeta\to 0. \tag{4.1}$$

This has been the attitude of all previous authors that have constructed theories of the present type, and it will be our attitude also. Nevertheless, the argument loses force when it is recalled that (although we do not explicitly perform any averaging process) our fields are supposed to be means of corresponding microscopic variables over distances small compared with macroscales, such as container dimensions, but large compared with the intervortex spacing. If the vortex-line density is sufficiently reduced as must happen as the limit (4.1) is taken, such averages lose all meaning. In other words, the regime in which Landau's model and the regime in which the HVBK theories or ours apply are mutually exclusive. By insisting that these theories recover the Landau equations in the limit (4.1), it is implied that, in some ill-defined qualitative sense, they will describe flows in which few vortex lines are present.

The constitutive model of the Landau theory to which our present theory must reduce under (4.1) is (HILLS & ROBERTS (1972))

$$A=A(\rho,T,w^{2}), \qquad S=S(\rho,T,w^{2}), \qquad \frac{\rho^{s}}{\rho}=\frac{\rho^{s}}{\rho}(\rho,T,w^{2}),$$
$$1-\frac{\rho^{s}}{\rho}=-2\frac{\partial\mathscr{A}}{\partial w^{2}}, \qquad S=-\frac{\partial\mathscr{A}}{\partial T}, \qquad \mathscr{A}=A-\frac{(\rho-\rho^{s})}{2\rho}w^{2},$$
$$T^{n}_{(ij)}=-p^{n}\delta_{ij}+\mu_{1}v^{n}_{r,r}\delta_{ij}+2\mu_{2}v^{n}_{(i,j)}, \qquad T^{s}_{(ij)}=-p^{s}\delta_{ij},$$
$$p^{n}=\rho^{n}\left(\rho\frac{\partial\mathscr{A}}{\partial\rho}+\frac{\rho^{s}}{2\rho}w^{2}\right), \qquad p^{s}=\rho^{s}\left(\rho\frac{\partial\mathscr{A}}{\partial\rho}-\frac{(\rho-\rho^{s})}{2\rho}w^{2}\right), \tag{4.2}$$
$$T^{n}_{[ij]}=T^{s}_{[ij]}=0, \qquad p=p^{n}+p^{s}=\rho\frac{\partial\mathscr{A}}{\partial\rho},$$
$$g^{s}=\rho^{s}S\nabla T+p\nabla\left(\frac{\rho^{s}}{\rho}\right)-\tfrac{1}{2}w^{2}\nabla\left[\rho^{s}\left(1-\frac{\rho^{s}}{\rho}\right)\right],$$
$$q=-\beta\nabla T+\rho^{s}TSw.$$

These equations were obtained from a general postulate employing the principle of equipresence†, the entropy production inequality and the condition that the superfluid equation admits irrotational solutions

$$\omega^s \equiv \nabla \times v^s = 0.$$

The coefficients μ_1, μ_2, β are general functions of ρ, T and w^2 and were shown to satisfy

$$\mu_2 \geqq 0, \quad 3\mu_1 + 2\mu_2 \geqq 0, \quad \beta \geqq 0.$$

For the present model we generalize the postulates (4.2) for the free energy A, the entropy S, the coefficient λ and the concentrations ρ^s/ρ and ρ^L/ρ by allowing these quantities to depend generally on density ρ, temperature T, the relative velocities* c and w together with the vortex density ζ. By making use of the invariance requirements $(3.7)_{1-8}$ and (3.20), we can show from the results of SPENCER (1971) that this dependence reduces to a dependence on the set $\mathscr{H}$ where

$$\begin{aligned}\mathscr{H} = \{&\rho, T, w^2, c^2, w\cdot c, \zeta^2, (w\cdot\zeta)^2 - \zeta^2 w^2, (c\cdot\zeta)^2 - \zeta^2 c^2,\\ &(w\cdot\zeta)(c\cdot\zeta) - \zeta^2 (w\cdot c), w\cdot(c\times\zeta)\}.\end{aligned} \tag{4.3}$$

At this stage, rather than be specific regarding the dependence of the functions $g^s, g^L, \gamma^i, T^a_{(kl)}, \Gamma^n, \Gamma^s, T^\zeta_{kl}$ and q, we assume that these functions depend generally on

$$\rho, T, w, c, \zeta, D^n,$$

and possibly the gradients of the quantities of the set $\mathscr{H}$. Then, with (3.16), the entropy production inequality (3.18) becomes

$$-\rho\frac{DA}{Dt} - \rho S\frac{DT}{Dt} - \tfrac{1}{2}\rho w^2 \frac{D}{Dt}\left(\frac{\rho^s}{\rho}\right) - \tfrac{1}{2}\rho u^2 \frac{D}{Dt}\left(\frac{\rho^L}{\rho}\right) - \rho\zeta\frac{D}{Dt}\left(\frac{\lambda}{\rho}\right) + Q' \geqq 0, \tag{4.4}$$

where

$$\begin{aligned}Q' = Q &- \frac{1}{2\rho}\{\rho^L u^2 + \rho^s w^2 + 2\lambda\zeta\}\frac{D\rho}{Dt} - \frac{1}{2\rho}u^2\{(\rho-\rho^L)c - \rho^n w\}\cdot\nabla\rho^L\\ &+ \frac{1}{2\rho}w^2\{\rho^L c + \rho^n w\}\cdot\nabla\rho^s - \frac{1}{\rho}\zeta\{(\rho-\rho^L)c - \rho^n w\}\cdot\nabla\lambda - \tfrac{1}{2}\rho^s w^2\nabla\cdot v^s\\ &- \tfrac{1}{2}(\rho^L u^2 + 2\lambda\zeta)\nabla\cdot v^L - \frac{q\cdot\nabla T}{T}.\end{aligned} \tag{4.5}$$

It is convenient now to introduce a *modified free-energy function* $\mathscr{A}$ defined by

$$\mathscr{A} = A - \frac{1}{2\rho}(\rho-\rho^s)w^2 + \frac{1}{2\rho}\rho^L u^2 + \frac{1}{\rho}\lambda\zeta, \tag{4.6}$$

† This principle proposes that a variable present in one constitutive equation should be present in all unless forbidden by subsequent mathematical analysis.

* It is possible to show using the invariance requirements that a dependence on v^n, v^s, v^L must reduce to a dependence on c and w.

whereupon the inequality (4.4) can be written as

$$-\rho\frac{D\mathscr{A}}{Dt}-\rho S\frac{DT}{Dt}+\tfrac{1}{2}\rho^{L}\frac{Du^{2}}{Dt}-\tfrac{1}{2}(\rho-\rho^{s})\frac{Dw^{2}}{Dt}+\lambda\frac{D\zeta}{Dt}+Q'\geqq 0. \tag{4.7}$$

From the constitutive postulates, we note that $\mathscr{A}$ is a function of the set $\mathscr{H}$, defined by (4.3), and the term Q' is independent of $\frac{D\chi}{Dt}$ where χ is any member of the set $\mathscr{H}$. In studying the implications of the inequality we follow the scheme proposed by COLEMAN & NOLL (1963) and look upon the heat supply r, the body forces $\boldsymbol{F}^{n}$, $\boldsymbol{F}^{s}$, $\boldsymbol{F}^{L}$ and the source Ω^{ζ} as quantities which may be arbitrarily assigned. Then the usual arguments (see for example HILLS & ROBERTS (1972)) allow us to deduce

$$\mathscr{A}=\mathscr{A}(\rho,T,u^{2},w^{2},\zeta),$$

$$S=-\frac{\partial\mathscr{A}}{\partial T},\quad 1-\frac{\rho^{s}}{\rho}=-2\frac{\partial\mathscr{A}}{\partial w^{2}},\quad \rho^{L}=2\rho\frac{\partial\mathscr{A}}{\partial u^{2}},\quad \lambda=\rho\frac{\partial\mathscr{A}}{\partial\zeta}. \tag{4.8}$$

Clearly, the tacit assumption that $1-\frac{\rho^{s}}{\rho}$, ρ^{L} and λ are positive places a restriction on the form of $\mathscr{A}$.

We emphasize that the results (4.8) have been obtained under very broad constitutive assumptions for the diffusive forces $\boldsymbol{g}^{s}$, $\boldsymbol{g}^{L}$, the stress tensors, the heat conduction vector and for γ^{ζ}. However, in order to progress further we need to be more definite regarding these constitutive postulates. One possible course is to use the assumptions we have made in conjunction with the invariance requirements to write down equations which are the most general allowed by the principle of equipresence. The work of SPENCER (1971) shows that the generality of this approach leads to a proliferation of terms which might obscure our present purpose. We prefer to sacrifice this generality in order to obtain a measure of reassurance that our model contains the necessary ingredients.

The model we present has its roots in the postulates (4.2) and in the work of HALL & VINEN (1956). As explained our postulates must reduce to (4.2) in the limit (4.1). This is achieved naturally for the normal and superfluid stress tensors by postulating the same form as (4.2) but with the partial pressures p^{n} and p^{s} modified in a way suggested by the replacement of $\mathscr{A}$ of $(4.2)_{6}$ with $\mathscr{A}$ of (4.6). Thus we obtain

$$\begin{aligned} T^{n}_{(ij)}&=-p^{n}\delta_{ij}+\mu_{1}v^{n}_{r,r}\delta_{ij}+2\mu_{2}v^{n}_{(i,j)}, & T^{n}_{[ij]}&=0,\\ T^{s}_{(ij)}&=-p^{s}\delta_{ij}, & T^{s}_{[ij]}&=0, \end{aligned} \tag{4.9}$$

with

$$\begin{aligned} p^{n}&=\frac{\rho^{n}}{\rho}\left\{\rho^{2}\frac{\partial\mathscr{A}}{\partial\rho}+\tfrac{1}{2}\rho^{s}w^{2}+\tfrac{1}{2}\rho^{L}u^{2}+\lambda\zeta\right\},\\ p^{s}&=\frac{\rho^{s}}{\rho}\left\{\rho^{2}\frac{\partial\mathscr{A}}{\partial\rho}-\tfrac{1}{2}(\rho-\rho^{s})w^{2}+\tfrac{1}{2}\rho^{L}u^{2}+\lambda\zeta\right\}. \end{aligned} \tag{4.10}$$

BK introduced an extra stress for dissipation through vortex motions. This consisted of two parts: a 'pressure' term and a vortex filament tension. In our

theory, we include these through the stress tensor T^L by writing

$$T^L_{(ij)} = -p^L\delta_{ij} + \alpha_1\zeta^2\delta_{ij} + \alpha_2\zeta_i\zeta_j, \tag{4.11}$$

with

$$p^L = \frac{\rho^L}{\rho}\left\{\rho^2\frac{\partial\mathscr{A}}{\partial\rho} + \tfrac{1}{2}\rho^s w^2 - \tfrac{1}{2}(\rho-\rho^L)u^2\right\} - \frac{\lambda}{\rho}(\rho-\rho^L)\zeta. \tag{4.12}$$

We observe that, as before, the total pressure $p = p^n + p^s + p^L$ satisfies

$$p = \rho^2\frac{\partial\mathscr{A}}{\partial\rho}. \tag{4.13}$$

The diffusive forces are perhaps the hardest to postulate since they must correctly represent an extremely complicated microscopic interaction between components. In addition to the terms obtained from generalizing $(4.2)_{13}$, $\boldsymbol{g}^s$ should contain an interaction between superfluid and vortex lines. Following HV (though replacing $\boldsymbol{\omega}^s$ by $\boldsymbol{\zeta}$), we add a term $-\rho^s\boldsymbol{\zeta}\times\boldsymbol{c}$ which is the classical Magnus force, and so obtain

$$\boldsymbol{g}^s = p\nabla\left(\frac{\rho^s}{\rho}\right) + \rho^s S\nabla T + \tfrac{1}{2}u^2\nabla\left(\frac{\rho^L\rho^s}{\rho}\right) - \tfrac{1}{2}w^2\nabla\left\{\rho^s\left(1-\frac{\rho^s}{\rho}\right)\right\} + \boldsymbol{\zeta}\nabla\left(\frac{\lambda\rho^s}{\rho}\right) - \rho^s\boldsymbol{\zeta}\times\boldsymbol{c}. \tag{4.14}$$

In writing $\boldsymbol{g}^L$ we are guided by HV's picture of the interaction of the normal fluid excitations with the vortex core:

$$\boldsymbol{g}^L = p\nabla\left(\frac{\rho^L}{\rho}\right) + \rho^L\alpha_3\nabla T - \tfrac{1}{2}u^2\nabla\left\{\rho^L\left(1-\frac{\rho^L}{\rho}\right)\right\} + \tfrac{1}{2}w^2\nabla\left(\frac{\rho^L\rho^s}{\rho}\right) - \boldsymbol{\zeta}\nabla\left\{\lambda\left(1-\frac{\rho^L}{\rho}\right)\right\}$$
$$+\alpha_4\boldsymbol{\zeta}\times\boldsymbol{c} + \alpha_5\boldsymbol{\zeta}\times\boldsymbol{u} + \alpha_6\boldsymbol{\zeta}\times(\boldsymbol{\zeta}\times\boldsymbol{u}) + \alpha_7\boldsymbol{\zeta}(\boldsymbol{\zeta}\cdot\boldsymbol{u}). \tag{4.15}$$

The term involving α_7 is motivated by the BK theory and was not discussed in the HV development. Other possible terms suggest themselves and would appear in the most general theory consistent with equipresence. We leave a discussion of generalizations of (4.9)–(4.15) until § 5.

The final term of the constitutive equation $(4.2)_{15}$ recognizes the thermo-mechanical transmission of heat in helium II. The way in which this mechanism is influenced by the presence of the vortex lines does not appear to have been given much attention although some recent work of LHUILLIER *et al.* (1972) would appear to have some bearing. At this stage we simply propose

$$\boldsymbol{q} = -\beta_1\nabla T + \rho^s S T\boldsymbol{w} + \rho^L\alpha_{11}T\boldsymbol{u}, \tag{4.16}$$

and leave the question of the interaction of heat currents and vortex lines until § 5.

In constructing the constitutive equations for $\boldsymbol{\gamma}^\zeta$ and T^ζ we recall that we will be required to satisfy the $\boldsymbol{\zeta}$-flux conservation condition (1.4) which may be written

$$\partial_t\int_\Sigma\boldsymbol{\zeta}\cdot d\boldsymbol{S} \equiv \int_\Sigma\left\{\frac{D^L\zeta_i}{Dt} - \zeta_j v^L_{i,j} + \zeta_i v^L_{j,j}\right\}dS_i = 0. \tag{4.17}$$

By comparing (4.17) with the conservation equation $(3.4)_3$, we are led to propose

$$\boldsymbol{\gamma}^\zeta = \alpha_8 \boldsymbol{\zeta} \times \bar{\boldsymbol{C}} + \alpha_9 \boldsymbol{D}^L \boldsymbol{\zeta} + \alpha_{10} \boldsymbol{\zeta} \nabla \cdot \boldsymbol{v}^L, \quad \boldsymbol{T}^\zeta \equiv \boldsymbol{0}. \tag{4.18}$$

The coefficients μ_1, μ_2, α_i $(i = 1, 2, \ldots, 11)$, β_1 are at present assumed general functions of ρ, T, w^2, u^2 and ζ. Then it is easily verified that the equations (4.9)–(4.16) and (4.18) satisfy the invariance requirements $(3.7)_{1-8}$ and (3.20).

If we substitute these constitutive equations into the inequality (4.4) we find that

$$\begin{aligned} &\frac{\beta_1}{T}(\nabla T)^2 + \mu_1 (\operatorname{tr} \boldsymbol{D}^n)^2 + 2\mu_2 \operatorname{tr}(\boldsymbol{D}^{n^2}) + (\alpha_2 - \alpha_9)\boldsymbol{\zeta} \cdot \boldsymbol{D}^L \boldsymbol{\zeta} + (\alpha_1 - \alpha_{10})\zeta^2 \operatorname{tr} \boldsymbol{D}^L \\ &+ (\alpha_4 - \rho^s)\, \boldsymbol{w} \cdot (\boldsymbol{\zeta} \times \boldsymbol{c}) - \alpha_6 (\boldsymbol{\zeta} \times \boldsymbol{u})^2 + \alpha_7 (\boldsymbol{u} \cdot \boldsymbol{\zeta})^2 + \rho^L (\alpha_3 - \alpha_{11})\, \boldsymbol{u} \cdot \nabla \mathrm{T} \geqq 0. \end{aligned} \tag{4.19}$$

Assuming that the coefficients are continuous functions of their arguments, we can deduce by reasoning similar to that of HILLS & ROBERTS (1972)

$$\begin{aligned} &\alpha_1 - \alpha_{10} = 0, \quad \alpha_2 - \alpha_9 = 0, \quad \alpha_4 - \rho^s = 0, \quad \alpha_3 - \alpha_{11} = 0, \\ &\alpha_6 \leqq 0, \quad \alpha_7 \geqq 0, \quad \beta_1 \geqq 0, \quad \mu_2 \geqq 0, \quad 3\mu_1 + 2\mu_2 \geqq 0. \end{aligned} \tag{4.20}$$

To obtain further information about the coefficients α_i, we recall the motivation given in the introduction and we give substance to the terms 'vortex fluid density', 'vortex fluid velocity' and 'vortex density vector' we have used there to describe ρ^L, $\boldsymbol{v}^L$ and $\boldsymbol{\zeta}$. In what follows we shall assume that the prescribed body force $\boldsymbol{F}^s$ and source Ω^ζ are zero. By use of $(4.9)_3$ and (4.14) the superfluid momentum equation $(3.4)_1$ for $\rho^s \neq 0$ becomes

$$\boldsymbol{f}^s = -\nabla \Phi - \boldsymbol{\zeta} \times \boldsymbol{c}, \tag{4.21}$$

where

$$\Phi = \mathscr{A} + p/\rho, \tag{4.22}$$

is the modified Gibbs free energy or thermodynamic potential. Moreover, by use of (4.18) the equation $(3.4)_3$ governing $\boldsymbol{\zeta}$ may be written

$$\frac{\lambda}{\zeta} \frac{D^L \boldsymbol{\zeta}}{Dt} = \alpha_8 \boldsymbol{\zeta} \times \boldsymbol{c} + \alpha_2 \boldsymbol{D}^L \boldsymbol{\zeta} + \alpha_1 \boldsymbol{\zeta} \nabla \cdot \boldsymbol{v}^L. \tag{4.23}$$

This bears a remarkable formal resemblance to the curl of (4.21), viz:

$$\frac{D^L \boldsymbol{\omega}^s}{Dt} = \nabla \times \{(\boldsymbol{\zeta} - \boldsymbol{\omega}^s) \times \boldsymbol{v}^s\} - (\boldsymbol{v}^L \cdot \nabla)(\boldsymbol{\zeta} - \boldsymbol{\omega}^s) + (\boldsymbol{\zeta} \cdot \nabla)\boldsymbol{v}^L - \boldsymbol{\zeta} \nabla \cdot \boldsymbol{v}^L + \boldsymbol{v}^L \nabla \cdot \boldsymbol{\zeta}. \tag{4.24}$$

In fact, if we choose

$$-\alpha_8 = \alpha_2 = -\alpha_1 = \frac{\lambda}{\zeta}, \tag{4.25}$$

and subtract these equations we obtain

$$\frac{D^L}{Dt}(\boldsymbol{\zeta} - \boldsymbol{\omega}^s) = -\nabla \times \{(\boldsymbol{\zeta} - \boldsymbol{\omega}^s) \times \boldsymbol{v}^s\} + (\boldsymbol{v}^L \cdot \nabla)(\boldsymbol{\zeta} - \boldsymbol{\omega}^s) - \boldsymbol{v}^L \nabla \cdot (\boldsymbol{\zeta} - \boldsymbol{\omega}^s) + \tfrac{1}{2}\boldsymbol{\zeta} \times \boldsymbol{\omega}^s, \tag{4.26}$$

which admits the solution

$$\boldsymbol{\zeta} = \boldsymbol{\omega}^s, \tag{4.27}$$

provided of course, as we shall suppose, that this is not in conflict with the boundary conditions. (We return to this topic in our discussion of boundary conditions below.)

The step just taken, of postulating (4.25) and selecting solution (4.27), is analogous to the way the Landau theory is constructed to admit the solution $\omega^s = 0$ in the inertial frame; see HILLS & ROBERTS (1972). Moreover, it is evident that, when (4.25) and (4.27) hold, (4.23) satisfies the condition (1.4) of ζ-flux conservation.

When we adopt (4.25) and (4.27) the governing equations become

$$\partial_t \rho + \nabla\cdot(\rho^n \boldsymbol{v}^n + \rho^s \boldsymbol{v}^s + \rho^L \boldsymbol{v}^L) = 0, \tag{4.28}$$

$$\begin{aligned}\rho^n \boldsymbol{f}^n = {} & \rho^n \boldsymbol{F}^n + m^s w + m^L \boldsymbol{u} - \rho^n \nabla(\Phi + \tfrac{1}{2}w^2) - \{(\rho^n + \rho^s)S + \rho^L \alpha_3\}\nabla T \\ & + \nabla\cdot(\mu_1(\operatorname{tr}\boldsymbol{D}^n)\boldsymbol{I} + 2\mu_2 \boldsymbol{D}^n) - \alpha_5 \boldsymbol{\omega}^s \times \boldsymbol{u} - \alpha_6 \boldsymbol{\omega}^s \times (\boldsymbol{\omega}^s \times \boldsymbol{u}) - \alpha_7 \boldsymbol{\omega}^s (\boldsymbol{\omega}^s \cdot \boldsymbol{u}),\end{aligned} \tag{4.29}$$

$$\boldsymbol{f}^s = -\nabla\Phi - \boldsymbol{\omega}^s \times \boldsymbol{c}, \tag{4.30}$$

$$\begin{aligned}\rho^L \boldsymbol{f}^L = {} & -\rho^L \nabla\{\Phi + \tfrac{1}{2}(w^2 - u^2)\} + \rho^L(\alpha_3 - S)\nabla T - \boldsymbol{\omega}^s \times \nabla \times (\lambda \hat{\boldsymbol{\omega}}^s) + \rho^s \boldsymbol{\omega}^s \times \boldsymbol{c} \\ & + \alpha_5 \boldsymbol{\omega}^s \times \boldsymbol{u} + \alpha_6 \boldsymbol{\omega}^s \times (\boldsymbol{\omega}^s \times \boldsymbol{u}) + \alpha_7 \boldsymbol{\omega}^s (\boldsymbol{\omega}^s \cdot \boldsymbol{u}),\end{aligned} \tag{4.31}$$

$$\begin{aligned}& \rho r - T[\partial_t(\rho S) + \nabla\cdot\{\rho S \boldsymbol{v}^n + \rho^L(\alpha_3 - S)\boldsymbol{u}\}] + \nabla\cdot(\beta_1 \nabla T) + \mu_1(\operatorname{tr}\boldsymbol{D}^n)^2 \\ & \quad + 2\mu_2 \operatorname{tr}(\boldsymbol{D}^{n2}) - \alpha_6(\boldsymbol{\omega}^s \times \boldsymbol{u})^2 + \alpha_7(\boldsymbol{u}\cdot\boldsymbol{\omega}^s)^2 = 0,\end{aligned} \tag{4.32}$$

with the equation (4.23) being superfluous. As can be seen, these equations involve the vector $\boldsymbol{\omega}^s$. Indeed, the superfluid 'momentum' equation (4.30) is precisely that given by HALL & VINEN (1956, eq. 20) [see also BEKHAREVICH & KHALATNIKOV (1961, eq. 27)]. However, it must be emphasized that the system (4.28)–(4.32) represents *a particular solution* in the inertial frame of the general theory of this paper. No violation of the principle of material frame indifference has been perpetrated since our theory has been developed in terms of the objective variable ζ rather than the non-objective variable $\boldsymbol{\omega}^s$.

We now turn to the conditions to be imposed on solutions at a boundary ∂B, and to ensure that these are not in conflict with (4.27) we at once insist that in the inertial frame

$$\zeta = \boldsymbol{\omega}^s \quad \text{on } \partial B. \tag{4.33}$$

Whether we are considering the stress conditions at a free surface, or whether we wish to evaluate the stress or couple on a rigid surface, we need knowledge of the total stress on ∂B. The literature contains two conflicting prescriptions. GREEN & NAGHDI (1968) propose that the total stress $\boldsymbol{T}$ be the sum of the partial stresses $\boldsymbol{T}^\alpha$, where α designates the different components. TRUESDELL & TOUPIN (1960) take instead

$$T_{ij} = \sum_\alpha [T^\alpha_{ij} + \rho^\alpha (v^\alpha_i - v_i)(v^\alpha_j - v_j)], \tag{4.34}$$

where $\boldsymbol{v} = \rho^{-1}\sum_\alpha \rho^\alpha \boldsymbol{v}^\alpha$ is the barycentric velocity. Whenever $\boldsymbol{n}\cdot\boldsymbol{v}^\alpha = U$ on ∂B for all α, the total surface force for both prescriptions become identical. In the

AD-A079 757 OREGON UNIV EUGENE DEPT OF PHYSICS F/G 7/4
TURBULENCE AND STATISTICAL MECHANICS.(U)
NOV 79 R J DONNELLY AFOSR-76-2880
UNCLASSIFIED AFOSR-TR-79-1357 NL

2 OF 3
AD-
A079757

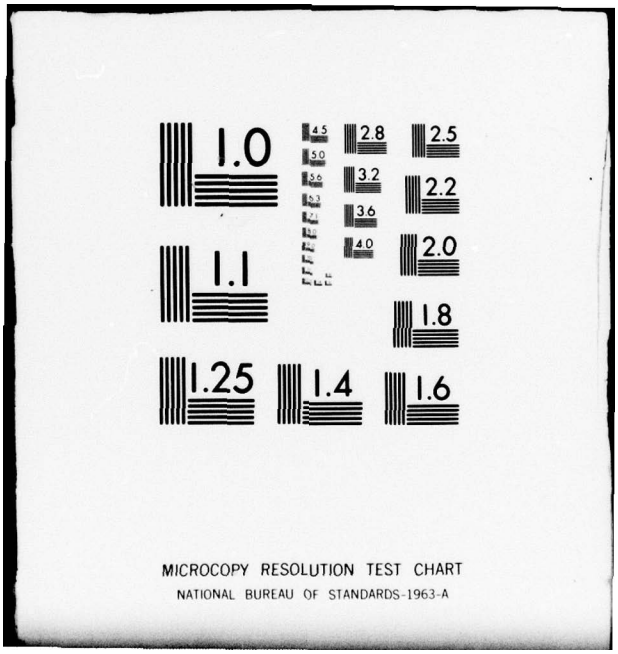
1.0
1.1
1.25
1.4
1.6
1.8
2.0
2.2
2.5
2.8
3.2
3.6
4.0
4.5
5.0
5.6
6.3
7.1
MICROCOPY RESOLUTION TEST CHART
NATIONAL BUREAU OF STANDARDS-1963-A

present application

$$T_{ij}=T_{ij}^{n}+T_{ij}^{s}+T_{ij}^{L}+\frac{\rho^{s}(\rho-\rho^{s})}{\rho}w_i w_j+\frac{\rho^{L}(\rho-\rho^{L})}{\rho}u_i u_j-\frac{\rho^{s}\rho^{L}}{\rho}(w_i u_j-w_j u_i). \quad (4.35)$$

When the viscosities and thermal conductivity of the fluid are neglected, it is not generally true that $\boldsymbol{n}\cdot\boldsymbol{v}^{s}$ and $\boldsymbol{n}\cdot\boldsymbol{v}^{n}$ are zero on ∂B, and the predictions of the TRUESDELL & TOUPIN condition differ from those of GREEN & NAGHDI. Experiments with 'heat currents' in non-rotating helium have long confirmed the correctness of TRUESDELL & TOUPIN's conditions, and the additional stresses $\rho^{n}\rho^{s}w_i w_j/\rho$ required to explain the experiments are usually called 'heat stresses' (see, for example, ROBERTS & DONNELLY (1974)). We imagine that in rotating helium (with zero viscosity and thermal conductivity) the additional heat stresses shown in (4.35) would also be required. From now on, however, we will retain viscosity and thermal conductivity and will find that, as a consequence of (4.38) or (4.41), the difference between the prescriptions evanesces. Ignoring Kapitza resistance, we find that the thermal boundary conditions are

$$T,\ \beta_1\,\boldsymbol{n}\cdot\nabla T \quad \text{continuous on } \partial B, \quad (4.36)$$

if ∂B is thermally conducting and

$$\boldsymbol{n}\cdot\nabla T=0 \quad \text{on } \partial B, \quad (4.37)$$

if it is insulating.

Turning next to the mechanical conditions, suppose first that the surface is rigid and moving with velocity $\boldsymbol{U}$. Bearing in mind the no-slip condition on $\boldsymbol{v}^{n}$ we have

$$\boldsymbol{v}^{n}=\boldsymbol{U}, \quad \boldsymbol{n}\cdot(\boldsymbol{v}^{s}-\boldsymbol{U})=0, \quad \boldsymbol{n}\cdot(\boldsymbol{v}^{L}-\boldsymbol{U})=0 \quad \text{on } \partial B. \quad (4.38)$$

In deriving other conditions we treat the cases $\boldsymbol{n}\cdot\boldsymbol{\omega}^{s}\neq 0$ and $\boldsymbol{n}\cdot\boldsymbol{\omega}^{s}=0$ separately. In the former case it is clear that the physical nature of the boundary will impose further conditions on $\boldsymbol{v}^{L}$. When the surface is 'completely rough' we may expect that the vortex lines will be permanently attached to the points at which they meet ∂B so that

$$(\boldsymbol{n}\cdot\boldsymbol{\omega}^{s})[\boldsymbol{\omega}^{s}\times(\boldsymbol{v}^{L}-\boldsymbol{U})]=0 \quad \text{on } \partial B, \quad (4.39)$$

while for a 'perfectly smooth' surface the lines will always have to meet ∂B perpendicularly, *i.e.*

$$(\boldsymbol{n}\cdot\boldsymbol{\omega}^{s})[\boldsymbol{\omega}^{s}\times\boldsymbol{n}]=0 \quad \text{on } \partial B. \quad (4.40)$$

To emphasize that (4.39) and (4.40) are, and shall be, vacuous when $\boldsymbol{n}\cdot\boldsymbol{\omega}^{s}$ is zero, we have included $\boldsymbol{n}\cdot\boldsymbol{\omega}^{s}$ as a factor in both left-hand sides. In the general case of continuously varying $\boldsymbol{\omega}^{s}$, and ∂B with continuously turning tangent plane, $\boldsymbol{n}\cdot\boldsymbol{\omega}^{s}$ will vanish on ∂B only on isolated curves, arbitrarily close to which (4.39) or (4.40) holds. The experimentalist commonly considers, however, cases in which $\boldsymbol{n}\cdot\boldsymbol{\omega}^{s}$ vanishes over a two-dimensional subspace $\partial B'$ of ∂B, as for example on the curved surface of a cylindrical container rotated about its axis. Moreover, in such a case $\hat{\boldsymbol{\omega}}^{s}$ is unidirectional on $\partial B'$ and, although an unwarrantably long

digression would be required here to support it, a further boundary condition is needed to determine the flow. This condition is $\omega^s=0$, and indicates the existence of a vortex-free region adjacent to $\partial B'$.

For a free surface the corresponding conditions are

$$\begin{gathered} v^n\cdot n=v^s\cdot n=v^L\cdot n=U\cdot n, \\ (T^n+T^s+T^L)\,n=-\Pi n, \\ (n\cdot\omega^s)[n\times\omega^s]=0, \end{gathered} \tag{4.41}$$

where Π is the constant pressure of the vapour above the free surface. The condition $(4.41)_4$ expresses the balance of surface forces normal to the free surface and the last condition insists that the vortex lines should be normal to the free surface. In stating these boundary conditions we have used physical considerations. It is, of course, not yet feasible to state whether these conditions make any flow problem mathematically well-posed in the sense that they ensure existence, uniqueness and continuous dependence. For a further discussion of boundary conditions see KHALATNIKOV (1966, § 16).

In spite of the special nature of the constitutive postulates (4.9)–(4.16) and (4.18), the equations (4.28)–(4.32) represent a complex system of partial differential equations. It is, therefore, appropriate to consider a somewhat simplified theory in which the total mixture is assumed incompressible in the sense that the total density ρ is constant. This will have the effect of filtering out first sound and introducing into the theory a pressure p which is no longer given by a constitutive equation but is instead determined by solving the governing equations subject to the boundary conditions. In addition we simplify the constitutive model. Firstly, we assume that A, S, ρ^s/ρ, ρ^L/ρ and λ are linear functions of u^2, w^2 and ζ and general functions of the temperature T. Then, from (4.8), we deduce

$$\begin{gathered} A=A(T),\quad \frac{\rho^s}{\rho}=\frac{\rho^s}{\rho}(T),\quad \frac{\rho^L}{\rho}=\frac{\rho^L}{\rho}(T),\quad \lambda=\lambda(T), \\ S=S_0+S_1u^2+S_2w^2+S_3\zeta, \end{gathered} \tag{4.42}$$

where

$$S_0=-\frac{dA}{dT},\quad S_1=-\frac{1}{2\rho}\frac{d\rho^L}{dT},\quad S_2=-\frac{1}{2\rho}\frac{d\rho^s}{dT},\quad S_3=-\frac{1}{\rho}\frac{d\lambda}{dT}. \tag{4.43}$$

Moreover, we assume that the constitutive equations (4.9), (4.11), (4.16), (4.18) hold but with

$$\begin{gathered} p^n=\rho^n\mathscr{P},\quad p^s=\rho^s\mathscr{P}-\tfrac{1}{2}\rho^s w^2,\quad p^L=\rho^L\mathscr{P}-\tfrac{1}{2}\rho^L u^2-\lambda\zeta, \\ \mathscr{P}=\frac{p}{\rho}+\frac{1}{2}\frac{\rho^s}{\rho}w^2+\frac{1}{2}\frac{\rho^L}{\rho}u^2+\frac{\lambda}{\rho}\zeta, \end{gathered} \tag{4.44}$$

and

$$g^s=\left[\mathscr{P}\rho^{s\prime}+\rho^sS+\tfrac{1}{2}u^2\frac{\rho^s}{\rho}\rho^{L\prime}-\tfrac{1}{2}\left(1-\frac{\rho^s}{\rho}\right)w^2\rho^{s\prime}+\zeta\frac{\rho^s}{\rho}\lambda'\right]\nabla T-\rho^s\zeta\times c, \tag{4.45}$$

$$g^L = \left[\mathscr{P}\rho^{L\prime} + \rho^L \alpha_3 - \tfrac{1}{2}u^2\left(1-\frac{\rho^L}{\rho}\right)\rho^{L\prime} + \tfrac{1}{2}w^2\frac{\rho^L}{\rho}\rho^{s\prime} - \zeta\left(1-\frac{\rho^L}{\rho}\right)\lambda'\right]\nabla T + \alpha_4\,\zeta\times c + \alpha_5\,\zeta\times u + \alpha_6\,\zeta\times(\zeta\times u) + \alpha_7\zeta(\zeta\cdot u), \tag{4.46}$$

where a dash denotes differentiation with respect to the temperature T. Then the theory can be developed as before and the resulting equations are (4.29)–(4.32) but now with

$$\nabla\cdot(\rho^n v^n + \rho^s v^s + \rho^L v^L) = 0, \tag{4.47}$$

and

$$\Phi = A + \frac{p}{\rho} - \frac{1}{2}\left(1-\frac{\rho^s}{\rho}\right)w^2 + \frac{1}{2}\frac{\rho^L}{\rho}u^2 + \frac{\lambda}{\rho}\omega^s = \mathscr{A} + \frac{p}{\rho}. \tag{4.48}$$

We note that, under isothermal conditions, the densities ρ^n, ρ^s, ρ^L and the coefficient λ become constants. This represents a substantial simplification of the more general theory.

5. Relations with Previous Theories, and Possible Generalizations

The density ρ^L was introduced in §1 to allow for the fluid trapped in and about the vortex core. It was noted that, unless the cores are decorated by necklaces of glass beads in the way proposed by WANG *et al.* (1975), their inertia will be small and we expect that only a small error would be made by setting ρ^L zero. Therefore, we take the limit of the system (2.8), (4.8), (4.13), (4.28)–(4.32) as

$$\rho^L \to 0 \tag{5.1}$$

uniformly, assuming that the velocity field, vortex density field and their gradients remain finite. There result the approximate equations

$$\rho = \rho^n + \rho^s, \tag{5.2}$$

$$\mathscr{A}' = \mathscr{A}'(\rho, T, w^2, \omega^s), \qquad S = -\frac{\partial\mathscr{A}'}{\partial T},$$
$$\rho^n = -2\rho\frac{\partial\mathscr{A}'}{\partial w^2}, \qquad \lambda = \rho\frac{\partial\mathscr{A}'}{\partial\omega^s}, \qquad p' = \rho^2\frac{\partial\mathscr{A}'}{\partial\rho}, \tag{5.3}$$

$$\partial_t\rho + \nabla\cdot(\rho^n v^n + \rho^s v^s) = 0, \tag{5.4}$$

$$\rho^n f^n = \rho^n F^n + m^s w - \rho^n\nabla(\Phi' + \tfrac{1}{2}w^2) - \rho S\nabla T + \nabla\cdot(\mu_1\,\mathrm{tr}(D^n)I + 2\mu_2 D^n) - \alpha_5\,\omega^s\times u - \alpha_6\,\omega^s\times(\omega^s\times u) - \alpha_7\,\omega^s(\omega^s\cdot u), \tag{5.5}$$

$$f^s = -\nabla\Phi' - \omega^s\times c, \tag{5.6}$$

$$0 = -\omega^s\times\nabla\times(\lambda\hat{\omega}^s) + \rho^s\,\omega^s\times c + \alpha_5\,\omega^s\times u + \alpha_6\,\omega^s\times(\omega^s\times u) + \alpha_7\,\omega^s(\omega^s\cdot u), \tag{5.7}$$

$$\rho r - T[\partial_t(\rho S) + \nabla\cdot(\rho S v^n)] + \nabla\cdot(\beta_1\nabla T) + \mu_1(\mathrm{tr}\,D^n)^2 + 2\mu_2(\mathrm{tr}\,D^{n2}) - \alpha_6(\omega^s\times u)^2 + \alpha_7(u\cdot\omega^s)^2 = 0, \tag{5.8}$$

$$\Phi' = A + \frac{p}{\rho} - \frac{1}{2}\frac{\rho^n}{\rho} w^2 + \frac{\lambda}{\rho}\omega^s = \mathscr{A}' + \frac{p'}{\rho}. \tag{5.9}$$

In the limit (5.1), since $\omega^s \neq 0$ in general, equation (5.7) may be solved directly to give

$$\alpha_7 = 0, \quad u = \left(1 - \frac{B'\rho^n}{2\rho}\right) A - \frac{B\rho^n}{2\rho}\hat{\omega}^s \times A, \tag{5.10}$$

where

$$A = v^n - v^s - \frac{1}{\rho^s}\nabla \times (\lambda\hat{\omega}^s), \tag{5.11}$$

$$B = -\frac{2\rho\rho^s\alpha_6\omega^s}{\rho^n\{(\rho^s-\alpha_5)^2 + \alpha_6^2\omega^{s2}\}} > 0, \quad B' = \frac{2\rho}{\rho^n}\left[1 - \frac{\rho^s(\rho^s-\alpha_5)}{(\rho^s-\alpha_5)^2 + \alpha_6^2\omega^{s2}}\right]. \tag{5.12}$$

Again, we assume that the solution does not conflict with the boundary conditions (see later). Since $u = v^n - v^L$, equation $(5.10)_2$ gives v^L explicitly in terms of v^n and v^s. After the limit (5.1) has been taken v^L assumes a partially kinematic character, there being no unique way of deciding what is meant by 'the' velocity of the lines. This arbitrariness is reflected by an indeterminable, but dynamically ineffective, multiple of ω^s which could be added to u in solving (5.7) but which we have chosen to omit from $(5.10)_2$. In the limit

$$|\alpha_5| \to \infty, \quad \alpha_6 \to -\infty \quad \left(B \to 0, \frac{B'\rho^n}{2\rho} \to 1\right)$$

of strong interaction between vortex lines and normal fluid, $(5.10)_2$ gives $u = 0$ $(v^n = v^L)$ as it ought. In the limit of weak interaction $\alpha_5 \to 0$, $\alpha_6 \to 0$ $(B \to 0, B' \to 0)$, it gives $u = A$ which implies that v^L differs from v^s only by a self-induced motion that vortex lines have when bent, reflected here by the final term of (5.11).

Using (5.10), we may rewrite the momentum equations (5.5) and (5.6) as

$$\rho^n f^n = \rho^n F^n + m^s w - \rho^n \nabla(\Phi' + \tfrac{1}{2}w^2) - \rho S \nabla T + \nabla \cdot (\mu_1 (\operatorname{tr} D^n) I + 2\mu_2 D^n) - G, \tag{5.13}$$

$$\rho^s f^s = -\rho^s \nabla \Phi' - \omega^s \times \nabla \times (\lambda\hat{\omega}^s) + G, \tag{5.14}$$

where

$$G = -\frac{B\rho^n\rho^s}{2\rho}\hat{\omega}^s \times (\omega^s \times A) - \frac{B'\rho^n\rho^s}{2\rho}\omega^s \times A. \tag{5.15}$$

The total momentum equation, obtained by adding (5.13) and (5.14), is

$$\begin{aligned} &\partial_t(\rho^n v_i^n + \rho^s v_i^s) + (\rho^n v_i^n v_j^n + \rho^s v_i^s v_j^s)_{,j} \\ &\quad = \rho^n F_i^n - p'_{,i} + \{\mu_1 v^n_{r,r}\delta_{ij} + 2\mu_2 v^n_{(i,j)} + \lambda\hat{\omega}_i^s\omega_j^s - \lambda\omega^s\delta_{ij}\}_{,j}. \end{aligned} \tag{5.16}$$

The energy equation (5.8) may be cast in the form

$$\partial_t(\rho S) + \nabla \cdot \left(\rho S v^n + \frac{q'}{T}\right) = \frac{R}{T}, \tag{5.17}$$

where $q' = -\beta_1 \nabla T$ is the molecular component of the heat conduction vector (4.16) and R includes the dissipation rate from both the viscous and frictional forces, *viz*:

$$R = \rho r + \frac{\beta_1}{T}(\nabla T)^2 + \frac{B\rho^n \rho^s}{2\rho}\omega^s(\hat{\omega}^s \times A)^2 + (\mu_1 + \tfrac{2}{3}\mu_2)(\operatorname{tr} D^n)^2 + 2\mu_2 \operatorname{tr}\{(D^n - \tfrac{1}{3}\operatorname{tr} D^n I)^2\}. \tag{5.18}$$

We now compare these equations with those of BEKHAREVICH & KHALATNIKOV. However, in the original paper of BEKHAREVICH & KHALATNIKOV (1961) the complete system of governing equations is not formally stated, so for ease of reference we shall use the account of the BK paper given in DONNELLY (1967). The relevant equations in DONNELLY are (4.124)–(4.129)†. We observe two differences. Trivially, our Φ' is their Φ. In addition, a term ∇h included in the account of DONNELLY is absent from (5.14). This term arises from the assumption that the stresses acting on the normal and superfluid were as postulated by KHALATNIKOV (1956). It was noted, however, by ROBERTS & DONNELLY (1974) that these could be included only by broadening the constitutive basis of LANDAU's theory in a far from obvious way. In this paper we have postulated viscous stresses appropriate to a Newtonian normal fluid, but it would be a straightforward matter to generalize our approach using the work of ROBERTS & DONNELLY (1974) if this seemed desirable. It is, of course, a simple matter to obtain from (4.42)–(4.48) a simplified HVBK theory for an incompressible fluid.

As with the general theory of §4, we need only consider the mechanical boundary conditions. At a rigid surface ∂B moving with velocity U we assume

$$\zeta = \omega^s, \quad v^n = U, \quad v^s \cdot n = U \cdot n, \tag{5.19}$$

with

$$(n \cdot \omega^s)\,\omega^s \times (v^L - U) = 0 \quad \text{if the surface is rough,} \tag{5.20}$$

and

$$(n \cdot \omega^s)\,\omega^s \times n = 0 \quad \text{if it is smooth.} \tag{5.21}$$

The discussion below again indicates that when ω^s is unidirectional and parallel to a finite area $\partial B'$ of ∂B, then ω^s is zero thereon. If ∂B is a free surface, then the appropriate conditions are

$$\zeta = \omega^s, \quad v^n \cdot n = v^s \cdot n = U \cdot n, \quad (n \cdot \omega^s)(\omega^s \times n) = 0, \quad (T^n + T^s + T^L)\,n = -\Pi n, \tag{5.22}$$

where Π is the constant pressure of the vapour above the free surface. We have not imposed any condition on the component of v^L parallel to ω^s since, as we have seen in obtaining the solution $(5.10)_2$, this component has an associated arbitrariness in the limit $\rho^L \to 0$.

† Equation (4.125) of DONNELLY (1967) contains a typographical error in the sign of the term with coefficient B.

This concludes our discussion of the BK theory. The corresponding comparison with the HV theory is too similar in spirit to be given here.

One may naturally wonder whether, despite their complexity, our equations or those of the HVBK theory, embrace all the fundamental phenomena of highly rotating, or more generally highly vortex laden, flows. The essential feature of the model (4.9)–(4.16), (4.18) is that it allows the solution (4.27) and we feel that any generalization should also allow this solution. In this context, we note that the solution (4.27) is obtained irrespective of the form of the vortex fluid momentum equation. Consequently, there would appear to be a measure of freedom in the postulates we make for g^L and $T^L_{(i,j)}$. However, the entropy inequality (3.18) must be satisfied and this restriction rules out a number of possible generalizations. For example, using the representation theorems given in SPENCER (1971), we might try and add to the expression for g^L the terms

$$\nu_1 \zeta \times (\zeta \times c) + \nu_2 \zeta \times w + \nu_3 \zeta \times (\zeta \times w), \tag{5.23}$$

where, as with the α_i, the coefficients ν_1, ν_2, ν_3 are assumed general functions of ρ, T, w^2, u^2 and ζ. But, by use of (3.18), it is an easy matter to show that $\nu_1 = \nu_2 = \nu_3 = 0$. Nevertheless, some generalizations are possible. Of particular concern is the heat conduction vector (4.16). When, for example, a temperature contrast is set up in a direction perpendicular to the angular velocity vector in a highly rotating flow of helium II, the counter current will be deflected by the vortex lines and impeded by the friction between normal fluid and vortex cores; there will also be corresponding reaction forces on the lines which, if they are not pinned on the end walls, will tend to move. Although some of these effects may already be included in our governing equations, it is by no means obvious that amendments to q and g^L are not required. It seems, therefore, to be of some interest to observe that terms of the right type can be included using the representation results in SPENCER (1971). For example, we may change (4.16) to

$$q = -\beta_1 \nabla T + \rho^s S T w + \rho^L \alpha_{11} T u - \beta_2 T \zeta \times u + \beta_3 T \zeta \times (\zeta \times u) + \beta_4 \zeta \times \nabla T, \tag{5.24}$$

where again the coefficients $\beta_2 - \beta_4$ are assumed general functions of ρ, T, w^2, u^2 and ζ. No concomitant difficulty with the inequality (3.18) arises provided the postulate for the diffusive force g^L is changed to

$$\begin{aligned} g^L = {} & p \nabla \left(\frac{\rho^L}{\rho} \right) + \rho^L \alpha_3 \nabla T - \tfrac{1}{2} u^2 \nabla \left\{ \rho^L \left(1 - \frac{\rho^L}{\rho} \right) \right\} \\ & + \tfrac{1}{2} w^2 \nabla \left(\frac{\rho^L \rho^s}{\rho} \right) - \zeta \nabla \left\{ \lambda \left(1 - \frac{\rho^L}{\rho} \right) \right\} + \alpha_4 \zeta \times c \\ & + \alpha_5 \zeta \times u + \alpha_6 \zeta \times (\zeta \times u) + \alpha_7 \zeta (\zeta \cdot u) + \beta_2 \zeta \times \nabla T + \beta_3 \zeta \times (\zeta \times \nabla T). \end{aligned} \tag{5.25}$$

We observe that, with (5.24) and (5.25), the superfluid equation is unaltered and the solution (4.27) is again possible assuming (4.25). The equations (4.29) and (4.31) are then modified in an obvious manner and the energy equation (4.32) becomes

$$\rho r - T\{\partial_t(\rho S) + \nabla\cdot[\rho S\, v^n + \rho^L(\alpha_3 - S)\, u + \beta_2\, \omega^s \times u - \beta_3\, \omega^s \times (\omega^s \times u) - \beta_4\, \omega^s \times \nabla T]\} + \nabla\cdot(\beta_1 \nabla T) + \mu_1(\operatorname{tr} D^n)^2 + 2\mu_2 \operatorname{tr}(D^n)^2 - \alpha_6(\omega^s \times u)^2 + \alpha_7(u\cdot\omega^s)^2 = 0. \tag{5.26}$$

For the theory obtained by taking the limit (5.1), the effect of making the postulates (5.24) and (5.25) is to replace the vector A in equations (5.15) and (5.16) by the vector $\tilde{A}$ where

$$\tilde{A} = v^n - v^s - \frac{1}{\rho^s}\nabla\times(\lambda\hat{\omega}^s) + \frac{\beta_2}{\rho^s}\nabla T + \frac{\beta_3}{\rho^s}\omega^s\times\nabla T. \tag{5.27}$$

The equation (5.17) becomes

$$\partial_t(\rho S) + \nabla\cdot\left[\rho S\, v^n + \frac{q'}{T} + \beta_2\,\omega^s\times u - \beta_3\,\omega^s\times(\omega^s\times u) - \beta_4\,\omega^s\times\nabla T\right] = \frac{\tilde{R}}{T}, \tag{5.28}$$

where $\tilde{R}$ is obtained by replacing A by $\tilde{A}$ in (5.18).

Recently, a series of experiments have been performed (VIDAL *et al.* (1971), (1974), LYNALL & MEHL (1973)) which indicate that whenever vortices are present in liquid helium, the velocity of second sound decreases. LHUILLIER *et al.* (1972) seek to explain this phenomenon using a simplified model in which the diffusive force of the superfluid equation contains a term proportional to ∇T and the heat flux vector is also modified. In a later paper LHUILLIER & VIDAL (1974) have shown that this approach gives a reasonable agreement between the experimental and theoretical results. An analysis of second sound for the equations of our theory also provides a possible explanation and will be published elsewhere.

We conclude with a brief discussion of questions raised by the addition or removal of vortex lines inside a container of helium. If the speed of a rotating cylinder is altered, we expect the number of vortex lines to change. Mechanisms of vortex production have aroused much interest in the past years with attention being concentrated on processes that tend to bring the normal fluid vorticity ω^n into equality with the mean superfluid vorticity. These are often called nucleation processes (see, for instance, DONNELLY & ROBERTS (1971)). It is evident that continuum theories satisfying (1.4) rely on the walls of the container to supply or absorb vortex lines. Consider the HVBK theories obtained in the limit $\rho^L \to 0$. In the general case in which $n\cdot\omega^s = 0$ only on an isolated curve $\mathscr{C}$ on ∂B, v^L causes the points where the vortex lines meet ∂B to move away or towards $\mathscr{C}$, lengthening or shortening the lines in the process. We note that v^L is determined in these theories from v^n and v^s by (5.10). Hence, implicit in these continuum theories is a mechanism which can create or remove new lines at $\mathscr{C}$. Conceivably, this process could be accommodated by a 'vortex mill' of the kind envisaged by GLABERSON & DONNELLY (1966).

In seeking an alternative mechanism for the creation and destruction of vortex lines, we shall consider two generalizations of the constitutive postulates which relax the ζ-conservation law (1.4), but which preserve the solution (4.27) in an inertial frame and are such that the entropy inequality is still satisfied. When such 'intrinsic mechanisms' are present LANDAU's equations cannot be recovered

in the limit (4.1). The first of these generalizations is probably not a nucleation process in the sense described above. We observe that if the postulates (4.9) are altered according to

$$g^s \to g^s + \rho^s \alpha_{12} u, \quad g^L \to g^L - \rho^s \alpha_{12} A, \quad T^\zeta_{ij} \to -\left(\frac{\lambda}{\zeta}\right) \alpha_{12} e_{ijk} u_k,$$
$$\gamma^\zeta \to \gamma^\zeta - \alpha_{12} \nabla \left(\frac{\lambda}{\zeta}\right) \times u, \quad \alpha_{12} = \alpha_{12}(\rho, T, w^2, u^2, \zeta), \tag{5.30}$$

where A is defined by (5.11), then the entropy inequality is unchanged and (4.21), (4.23) and (4.25) are replaced by

$$f^s = -\nabla \Phi - \zeta \times c + \alpha_{12} u, \tag{5.31}$$

$$\frac{D^L \zeta}{Dt} = \zeta \times \bar{C} + D^L \zeta - \zeta \nabla \cdot v^L + \nabla \times (\alpha_{12} u). \tag{5.32}$$

Following the same procedure as before, we find that these admit the solution (4.27) in the inertial frame, but (4.17) is now

$$\frac{d}{dt} \int_\Sigma \zeta \cdot dS = \int_\Sigma \nabla \times (\alpha_{12} u) \cdot dS, \tag{5.33}$$

so that ζ-flux is not generally conserved.

If we consider this generalization in the limit (5.1), we have in place of (5.7)

$$0 = \omega^s \times [\rho^s A - (\rho^s - \alpha_5) u + \alpha_6 \omega^s \times u] + \alpha_7 (\omega^s \cdot u) \omega^s - \rho^s \alpha_{12} A, \tag{5.34}$$

an equation which can be solved for u to give

$$G = -\frac{\tilde{B} \rho^n \rho^s}{2\rho} \hat{\omega}^s \times (\omega^s \times A) - \frac{\tilde{B}' \rho^n \rho^s}{2\rho} \omega^s \times A + \frac{\tilde{B}'' \rho^n \rho^s}{2\rho} (\omega^s \cdot A) \hat{\omega}^s, \tag{5.35}$$

where

$$\tilde{B} = -\frac{2\rho \rho^s \alpha_6 (\omega^{s2} + \alpha_{12}^2)}{\rho^n \omega^s [(\rho^s - \alpha_5)^2 + \alpha_6^2 \omega^{s2}]}, \tag{5.36}$$

$$\tilde{B}' = \frac{2\rho}{\rho^n} \left[1 - \frac{\rho^s (\rho^s - \alpha_5)(\omega^{s2} + \alpha_{12}^2)}{\omega^{s2} [(\rho^s - \alpha_5)^2 + \alpha_6^2 \omega^{s2}]}\right],$$
$$\tilde{B}'' = \frac{2\rho \rho^s \alpha_{12}}{\rho^n \omega^s [(\rho^s - \alpha_5)^2 + \alpha_6^2 \omega^{s2}]} \left[\rho^s - \alpha_5 - \alpha_6 \alpha_{12} + \frac{\alpha_{12}}{\alpha_7 \omega^{s2}}\right]. \tag{5.36}$$

It is interesting to note that the B'' term in the mutual friction G, shown to be zero in the simplest form of the theory, has for the first time made an appearance. If this is the only method by which this term can arise, it indicates that this effect is present only in experiments in which α_{12} is significant, and in which ζ-flux is not conserved.

The second intrinsic mechanism we consider appears to have a definite relation with nucleation processes. Instead of (5.30), we now generalize the model according to

$$g^s \to g^s + \rho^s \alpha_{13} A, \quad T_{ij}^{\zeta} \to \frac{\lambda}{\zeta} \alpha_{13} e_{ijk} A_k, \quad \gamma^{\zeta} \to \gamma^{\zeta} - \alpha_{13} \nabla \left(\frac{\lambda}{\zeta}\right) \times A,$$
$$\alpha_{13} = \alpha_{13}(\rho, T, w^2, u^2, \zeta), \tag{5.37}$$

where A is again defined by (5.11). To the left-hand side of the entropy inequality must now be added $\rho^s \alpha_{13} A^2$, and we deduce that

$$\alpha_{13} \geqq 0. \tag{5.38}$$

Equations of the form (5.31)–(5.33) follow as before but with $\alpha_{13} u$ replaced by $\alpha_{13} A$. Thus, again, ζ-flux is not preserved but (4.27) holds in the inertial frame. The term $\rho^s \alpha_{13} A$ in the new expression for the diffusive force g^s appears to be related to the force $k \rho^n \rho^s |w|^2 w$ proposed by GÖRTER & MELLINK (1949) from experiments on turbulent heat currents in straight annular channels. This geometry, in which w and A are parallel in an average sense, cannot critically distinguish between these two diffusive forces although it may be possible to use it to provide experimental information about α_{13}. It would evidently be of some interest to compare the predictions of the two diffusive laws in experimental situations in which w and A are not parallel.

To interpret physically the terms added to T_{ij}^{ζ} and γ^{ζ} in (5.37), we consider the evolution of ζ-flux. Taking (4.27) we find

$$\frac{d}{dt} \int_{\Sigma} \omega^s \cdot dS = \int_{\Sigma} \left\{ \alpha_{13} \left[(\omega^n - \omega^s) - \nabla \times \left(\frac{\nabla \times (\lambda \hat{\omega}^s)}{\rho^s} \right) \right] + \nabla \alpha_{13} \times A \right\} \cdot dS. \tag{5.39}$$

We expect α_{13}, like α_{12}, to be sensitively dependent on w and T and to be negligible for slow flows and low temperatures. If, however, we face a situation in which α_{13} is significant, the sign (5.38) of α_{13} is that which favours nucleation. Consider, for example, an experiment with a rotating bucket in which the normal fluid rotates as a solid body with the walls. If we take Σ to be in a plane perpendicular to the rotation axis, (5.39) gives approximately

$$\frac{d}{dt} \int_{\Sigma} \omega^s \cdot dS = \int_{\Sigma} \alpha_{13} (\omega^n - \omega^s) \cdot dS, \tag{5.40}$$

and vortices will be nucleated to bring ω^n and ω^s into coincidence.

It is, of course, possible to combine the modifications (5.30) and (5.37) into a composite law that gives both nucleation and a B'' coefficient. Even these examples do not exhaust the thermodynamically admissible generalizations of the HVBK theories.

Acknowledgement. We wish to thank Professor J.L. ERICKSEN for his comments on an earlier draft of this paper. This paper was supported in part by a special research grant GR/A/0556 from

the Science Research Council of Great Britain. One of us (P.H.R.) is grateful to the U.S. Air Force (Grant AF-AFOSR 71-1999) and the National Science Foundation of the United States (Grant NSF-GH-35898) for partial support during his tenure at the Department of Physics of the University of Oregon at Eugene, Oregon.

References

ANDELIN, J. 1967 Phys. Rev. Lett. **18**, 483.
ANDRONIKASHVILI, E. L., & J. S. TSAKADZE, 1965 JETP Lett. **2**, 177.
ANDRONIKASHVILI, E. L., & J. S. TSAKADZE, 1966 Phys. Lett. **20**, 446.
ATKIN, R. J., & R. J. CRAINE, 1976 Q. Jl. Mech. Appl. Math. **29**, 209.
BATCHELOR, G. K., 1967 *An introduction to fluid dynamics*. Cambridge University Press.
BEKHAREVICH, I. L., & I. M. KHALATNIKOV, 1961 JETP **13**, 643.
CHANG, D. K., M. W. CROMAR & R. J. DONNELLY, 1973 Phys. Rev. Lett. **31**, 433.
COLEMAN, B. D., & W. NOLL, 1963 Arch. Rational Mech. Analysis **13**, 167.
DONNELLY, R. J., 1967 *Experimental superfluidity*. Chicago and London: University of Chicago Press.
DONNELLY, R. J., & P. H. ROBERTS, 1971 Phil. Trans. Roy. Soc. A **271**, 41.
ERINGEN, A. C., 1962 *Nonlinear theory of continuous media*. McGraw-Hill Book Co. Inc.
FETTER, A. L., 1966 Phys. Rev. **152**, 183.
FETTER, A. L., 1967 Phys. Rev. **153**, 285.
FETTER, A. L., & R. J. DONNELLY, 1966 Phys. Fluids **9**, 619.
FEYNMAN, R. P., 1955 *Progress in low temperature physics*, 1 ch. II p. 17. North Holland Pub. Co. (ed. C. J. GORTER).
GLABERSON, W. I., 1969 J. Low Temp. Phys. **1**, 289.
GLABERSON, W. I., & R. J. DONNELLY, 1966 Phys. Rev. **141**, 208.
GLABERSON, W. I., D. M. STRAYER & R. J. DONNELLY, 1968 Phys. Rev. Lett. **21**, 1740.
GORTER, C. J., & J. H. MELLINK, 1949 Physica **15**, 285.
GREEN, A. E., & P. M. NAGHDI, 1965 Int. J. Engng. Sci. **3**, 231.
GREEN, A. E., & P. M. NAGHDI, 1968 Int. J. Engng. Sci. **6**, 631.
GREEN, A. E., & R. S. RIVLIN, 1964 ZAMP **15**, 290.
HALL, H. E., 1960 Phil. Mag. Supp. **9**, 89.
HALL, H. E., 1970 J. Phys. C: Solid State Phys. **3**, 1166.
HALL, H. E., & W. F. VINEN, 1956 Proc. Roy. Soc. A **238**, 215.
HILLEL, A. J., H. E. HALL & P. LUCAS, 1974 J. Phys. C: Solid St. Phys. **7**, 3341.
HILLS, R. N., & P. H. ROBERTS, 1972 J. Inst. Maths. Applics. **9**, 56.
HILLS, R. N., & P. H. ROBERTS, 1977 Int. J. Eng. Sci. **15**, 305.
KHALATNIKOV, I. M., 1956 JETP **3**, 649.
LANDAU, L. D., 1941 J. Phys. USSR **5**, 71.
LONDON, F., 1938 Nature, London. **141**, 643.
LHUILLIER, D., F. VIDAL, M. FRANÇOIS & M. LE RAY 1972 Phys. Lett. **38A**, 161.
LHUILLIER, D., & F. VIDAL, 1974 J. Phys. C: Solid St. Phys. **7**, 1254.
LYNALL, I. H., & J. B. MEHL, 1973 Phys. Lett. **46A**, 115.
MÜLLER, I., 1968 Arch. Rational Mech. Analysis **28**, 1.
NOLL, W., 1955 J. Rational Mech. Anal. **4**, 3.
NOLL, W. 1963. *La methode axiomatique dans les mecaniques classiques et nouvelles*, Colloque International, Paris 1959, p. 47. Gauthier-Villars Paris.
ONSAGER, L., 1949 Nuovo Cimento (Suppl. 2, series 9) **6**, 249.
ROBERTS, P. H., & R. J. DONNELLY, 1974 Annual Review of Fluid Mechanics **6**, 179.
SMITH, E., R. WALTON, H. V. BOHM & J. D. REPPY, 1967 Phys. Rev. Lett. **18**, 637.
SPENCER, A. J. M., 1971 *Continuum physics* Vol. I, p. 240. Academic Press (ed. A. C. ERINGEN).
STAUFFER, D., & A. L. FETTER, 1968 Phys. Rev. **168**, 156.
SNYDER, H. A., 1974 *Low temperature physics LT-13* Vol. I, p. 283. Plenum Press.
TISZA, L., 1938 Nature, London. **141**, 913.
TRUESDELL, C., 1977 Meccanica (in press).
TRUESDELL, C., & R. A. TOUPIN, 1960 *The classical field theories*. Handbuch der Physik III(i). Springer-Verlag (ed. S. FLÜGGE).

TSAKADZE, J.S., & S.J. TSAKADZE, 1973 JETP 37, 918.
VIDAL, F., M. LE RAY & M. FRANCOIS, 1971 Phys. Lett. 36A, 401.
VIDAL, F., M. LE RAY, M. FRANCOIS & D. LHUILLIER, 1974 *Low temperature physics LT-13* Vol. I, p. 334. Plenum Press.
WANG, T., M. SAFFREN & D. ELLEMAN, 1975 Proc. of Space Shuttle Conference, Eugene June 30-July 2 (unpublished).
WILLIAMS, G.A., & R.E. PACKARD, 1974 Phys. Rev. Lett. 33, 280.

Mathematics Department
Heriot-Watt University
Edinburgh
and
School of Mathematics
The University
Newcastle-upon-Tyne

(Received March 28, 1977)

Volume 70A, number 5,6 PHYSICS LETTERS 2 April 1979

CALCULATION OF THE STATIC HEALING LENGTH IN HELIUM II

P.H. ROBERTS [1], R.N. HILLS and R.J. DONNELLY
Institute of Theoretical Science and Department of Physics, University of Oregon, Eugene, OR 97403, USA

Received 28 November 1978

The healing length for stagnant liquid helium II at an infinite plane boundary is calculated from the Hills–Roberts equations. A new thermodynamic function needed to complete the calculation is derived from neutron scattering and thermodynamic data. Results for the healing length are obtained from absolute zero to about a tenth of a degree from the lambda point, and at all pressures. Comparison with experimental evidence is presented.

Experiments on the propagation of third sound in thin, unsaturated films of helium II show that the superfluid behaves as though it had a lower areal density than that given by the product of the superfluid density, ρ^s, and the film thickness at the same temperature, T. Rudnick and his collaborators [1,2] as well as other groups, have associated this reduction in density with "healing", the notion that the superfluid density decreases near a boundary. Hills and Roberts [3–5] have formulated a two-fluid theory to describe healing and relaxation which rests on accepted macroscopic balance laws for mass, momentum and energy together with a postulate for entropy growth. This theory is entirely hydrodynamical, valid over the whole temperature range and allows a constitutive dependence on density gradients. Near T_λ, these equations in a sense contain the Ginzburg–Pitaevskii order parameter model [7]. The boundary condition applicable to ρ^s is not known *a priori* but in this letter we explore the consequences of setting ρ^s equal to zero on an infinite plane boundary and compare the results with available data. The healing length we define is analogous to the "layer thickness" of boundary layer theory.

Consider stagnant helium in complete thermodynamic equilibrium, filling the half-space $z > 0$ above a plane boundary $z = 0$. The governing equations are (see eqs. (3.7)–(3.10), ref. [5])

$$A + \rho(\partial A/\partial\rho) = \Phi_0, \quad A = A(\rho, T, \rho^s), \tag{1}$$

$$\rho^2(\partial A/\partial\rho) + (\hbar^2/8m^2\rho^s)(\mathrm{d}\rho^s/\mathrm{d}z)^2 = P_0, \tag{2}$$

where A is a free energy function, Φ_0 and P_0 are the Gibbs free energy and pressure at great distances from the wall and m is the ^{4}He mass.

It is difficult to solve eqs. (1) and (2) simultaneously for general $A(\rho, T, \rho^s)$: the superfluid density ρ^s can range independently from zero to the bulk value, f ($f = f(\rho, T)$), at large distances from the wall; the total density ρ may itself vary near the wall. According to Brooks and Donnelly [6], however, A is dominated by the ground state free energy $A_G(\rho)$, which is ~ 15 J/g whereas the excitation part A_E is at most 0.4 J/g. This suggests an expansion in small A_E/A_G whereupon eqs. (1) and (2) give

$$(\hbar^2/8m^2\rho^s)(\mathrm{d}\rho^s/\mathrm{d}z)^2 - \rho_0 A_E(\rho_0, T, \rho^s) = -\rho_0 A_E(\rho_0, T, f), \tag{3}$$

where ρ_0 is the value of ρ far from the wall.

We must solve eq. (3) subject to the conditions

$$\rho^s = 0 \quad \text{on} \quad z = 0, \quad \rho^s \to f \quad \text{as} \quad z \to \infty, \tag{4}$$

the latter of which has in essence been incorporated in eq. (3). We obtain

[1] Permanent address: School of Mathematics, University of Newcastle upon Tyne, Newcastle upon Tyne, UK.

$$z = (h^2 f/2\rho m^2)^{1/2} \int_0^R [A(fR^2) - A(f)]^{-1/2}\, \mathrm{d}R, \quad (5)$$

where we have suppressed the suffix on ρ_0, replaced ρ^s by fR^2, and written $A_E(\rho, T, \rho^s)$ as $A(fR^2)$, the other arguments (ρ_0 and T) being constants. We note that for small t, $t = T_\lambda - T$, it should be possible to write to a good approximation

$$A(\rho, T, \rho^s) = A_0(\rho, T) + A_1(\rho, T)[\rho^s - f(\rho, T)]^2/2\rho. \quad (6)$$

In this case eq. (5) yields a familiar solution obtained in the work of Ginzburg–Pitaevskii [7], viz:

$$\rho^s = f \tanh^2(z/D), \quad D = \hbar/m(A_1 f)^{1/2}. \quad (7)$$

There are various possible definitions for the term "healing length". For instance, it can be that value of z for which ρ^s attains 90% of its bulk value, that is $R = \sqrt{0.9}$. We shall use as our measure the "displacement thickness", δ, which is defined to be that distance for which $f\delta$ is the superfluid mass (per unit area of wall) "displaced" from the wall through healing: in other words, the hypothetical density distribution

$$\rho^s = 0, \quad z < \delta,$$
$$= f, \quad z \geqslant \delta, \quad (8)$$

should have the same net superfluid mass as the actual solution. For the density distribution (7) the displacement thickness is D.

For a general energy function A, eq. (5) can be evaluated only by numerical integration and ρ^s will not follow the tanh law (7) except for small t. The displacement thickness is

$$\delta = \int_0^\infty (1 - R^2)\mathrm{d}z = (\hbar^2 f/2\rho m^2)^{1/2} \times \int_0^1 (1 - R^2)[A(fR^2) - A(f)]^{-1/2}\, \mathrm{d}R. \quad (9)$$

No theory of fluid flow can be practically useful until the thermodynamic state functions are available. Neutron scattering and thermodynamic measurements properly analyzed give an excellent account of $A(\rho, T, f)$ but say virtually nothing about $A(\rho, T, \rho^s)$ when $\rho^s \neq f$. It is a principal aim of this letter to see whether one obvious theoretical method of computing $A(\rho, T, \rho^s)$ will yield useful results when used in conjunction with predictions such as eq. (9) of the Hills–Roberts theory.

It is well known that the state functions of the Landau theory depend not only on ρ and T, but also on w^2, where $\boldsymbol{w} = \boldsymbol{v}^n - \boldsymbol{v}^s$ is the relative velocity between components. Also, the normal fluid density $\rho^n (= \rho - \rho^s)$ can be obtained from the Helmholtz free energy $F(\rho, T, w^2)$ by differentiation,

$$\rho^n/2\rho = -\partial F/\partial w^2. \quad (10)$$

For sufficiently small T and density excitations $n(\boldsymbol{p})$, F_E can be accurately obtained by using the classical expression for a non-interacting Bose gas:

$$F_E = (kT/\rho h^3)\int \ln\{1 - \exp[-(\epsilon(p) - \boldsymbol{p}\cdot\boldsymbol{w})/kT]\}\mathrm{d}^3 p, \quad (11)$$

where $\epsilon(p)$ is the energy of a quasiparticle of momentum $\boldsymbol{p}$ in stagnant helium. Donnelly and Roberts [8] have shown that the equilibrium state functions such as $F(\rho, T)$ may be obtained to within a tenth degree of T_λ provided the dependence of $\epsilon(p)$ on T (and, of course, on ρ) is consistently incorporated. When t is sufficiently small or w^2 sufficiently large, the rise of n and the concomitant quasiparticle interactions make eq. (11) suspect.

The energy function A of the Hills–Roberts theory is given by the Legendre transformation

$$A = F_E - w^2 \partial F_E/\partial w^2, \quad (12)$$

and was numerically evaluated using the Brooks–Donnelly tables [6]. However, at low temperatures this scheme suffers a setback. When ρ^n is evaluated for $T \lesssim 0.6$ K, using eqs. (10) and (11), we find that ρ^n achieves its maximum, ρ_L^n, at the Landau velocity, w_L, but $\rho_L^n < \rho$ although $\partial\rho^n/\partial w^2 \to \infty$ as $w \to w_L^-$ (i.e. as $w \to w_L$ from below). The severity of this difficulty is extreme for small T, when eqs. (10) and (11) yield

$$\rho_L^n = p_L^2 (2\pi kT)^{3/2} \zeta(3/2)/(w_L^2 h^3 \mu_L^{1/2}), \quad \mu = \partial^2\epsilon/\partial p^2,$$

where ζ is the Riemann zeta function and w_L and p_L are obtained by solving, in the usual way, $w_L = \epsilon(p_L)/p_L = (\partial\epsilon/\partial p)_L$ for the Landau critical state. Evidently $\rho_L^n \to 0$ as $T \to 0$. To surmount this difficulty we recognize that w_L divides the states of thermal equilibrium, $w < w_L$, from the states $w > w_L$ at

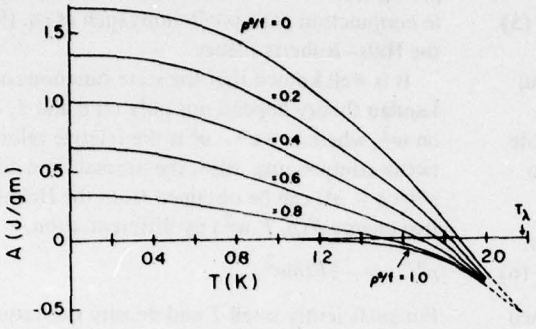

Fig. 1. The free energy function A at density $\rho = 0.1481$ g/cm^3 for six values of ρ^s/f.

which quasiparticle production rates are infinite and equilibrium is impossible. Thus, $w = w_L$ marks a point where any value of ρ^n between ρ^n_L and ∞ is admissable. To evaluate A for $\rho^n > \rho^n_L$ we may simply use the relation $\rho(\partial A/\partial\rho^s) = -w^2/2$ and integrate to get

$$A_E = A_L + w_L^2(\rho^s_L - \rho^s)/2\rho \quad (\rho^s < \rho^s_L). \tag{13}$$

This model allows us to treat the range $T \lesssim 0.6$ K. For $T = 0$ its consequences are particularly elementary. The solution of eqs. (3) and (4), though demanding a careful treatment too lengthy to report here, yields

$$\delta \to h/8mw_L, \quad T \to 0. \tag{14}$$

This remarkably simple result gives $\delta = 2.12$ Å at $T = 0$. Since $w_L \doteq \Delta/p_0$, it demonstrates that δ couples to the reciprocal of the gap (and therefore the structure factor) and not to the interatomic spacing.

Fig. 1 shows A as a function of T and it will be noticed that, for each ρ^s/f, the curve appears to converge on one value A_λ of A at T_λ. The behavior of δ as a function of T for several values of the pressure is shown in fig. 2 [‡1]. We find an increase of ~ 27% in δ on going from 0 to 25 atm. Steingart and Glaberson [9] have shown that the vortex core parameter

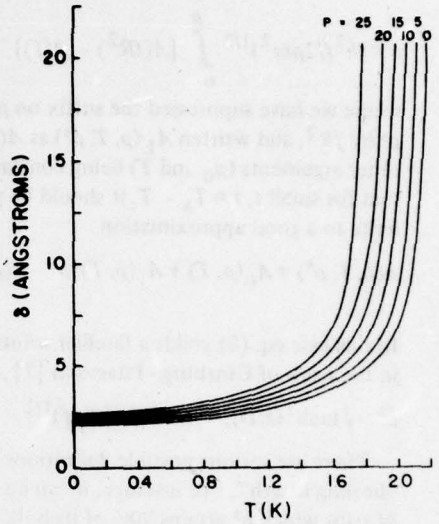

Fig. 2. The displacement thickness δ for six pressures P in atm.

increases by 27 ± 4% over the same pressure range. The vortex core parameter is a dynamic rather than a static healing length. Near $T = 0$, it can be evaluated in a manner analogous to the discussion of eqs. (13) and (14) and yields 0.91 Å or about 0.43δ. In fig. 3 we compare our results for δ with various experiments and the solid curve assumes that healing takes place at both the substrate and the free surface of

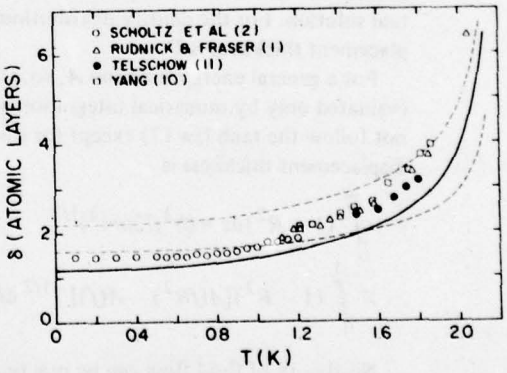

Fig. 3. The total displacement thickness at $P = 0$ compared to the results of various authors. The solid line corresponds to 2δ, i.e. healing on the substrate and the free surface. The lower dashed line corresponds to $1 + \delta$, i.e. healing at the edge of the solid layer and none at the free surface. The upper dashed line corresponds to $1 + 2\delta$, i.e. healing over the solid layer and at the free surface.

[‡1] It may be noticed that, according to eq. (2), it is the total pressure and not the kinetic pressure that is constant through the healing layer. The fact that we have used tabulations at constant P might therefore seem to be dangerous. It may be shown, however, that the resulting error in δ is only of order $A_E\delta/A_G$, and is no worse than the neglect of $(A_E/A_G)^2$ terms already discarded in the derivation of eq. (3).

a film. The agreement is within 20% of the measurements throughout; our calculations, however, have no adjustable parameters.

There is considerable evidence that something of the order of one atomic layer on the substrata is solid. The dashed curves in fig. 3 show that two healing assumptions treating the solid layer as an infinite potential barrier less consistent without calculations than healing on the substrate and free surface. On the present theory it is the increase in ρ^n which reduces ρ^s. The data suggest that the solid acts in much the same way as excess normal fluid in reducing ρ^s.

We are grateful to Professor I.M. Khalatnikov for discussions of this problem. This research was supported under grants NSF ENG 76-07354, NSF DMR 76-21814 and AFOSR 76-2880.

References

[1] I. Rudnick and J.C. Fraser, J. Low Temp. Phys. 3 (1970) 225.
[2] J.H. Scholtz, E.O. McLean and I. Rudnick, Phys. Rev. Lett. 32 (1974) 147.
[3] R.N. Hills and P.H. Roberts, Int. J. Eng. Sci. 15 (1977) 305.
[4] R.N. Hills and P.H. Roberts, J. Low Temp. Phys. 30 (1978) 709.
[5] R.N. Hills and P.H. Roberts, J. Phys. C, to be published.
[6] J.S. Brooks and R.J. Donnelly, J. Phys. Chem. Ref. Data 6 (1977) 51.
[7] V.L. Ginzburg and L.P. Pitaevskii, Sov. Phys. JETP 7 (1958) 858 [Zh. Eksp. Teor. Fiz. 34 (1958) 1240].
[8] R.J. Donnelly and P.H. Roberts, J. Low Temp. Phys. 27 (1977) 687.
[9] M. Steingart and W.I. Glaberson, J. Low Temp. Phys. 8 (1972) 61.
[10] L.C. Yang, Ph.D. Thesis, Dept. of Phys. UCLA (1973).
[11] K. Telschow, quoted in ref. [2].

Journal of Low Temperature Physics, Vol. 27, Nos. 5/6, 1977

A Theory of Temperature-Dependent Energy Levels: Thermodynamic Properties of He II*

Russell J. Donnelly and Paul H. Roberts

Department of Physics and Institute of Theoretical Science, University of Oregon, Eugene, Oregon 97403

(Received November 22, 1976)

The statistical mechanics of interacting bosons is considered for cases where the interactions are sufficiently strong that the observed energy levels are dependent upon temperature. An approximate method is developed to handle the theory when energy levels are known from experiment. The results are applied to the thermodynamic properties of He II using Landau's theory of elementary excitations. This theory is assessed in several levels of approximation, and the results are compared extensively to measured thermodynamic properties. The relationship of neutron inelastic scattering measurements to these problems is discussed.

1. INTRODUCTION

Landau first sketched the S-shaped dispersion curve for the elementary excitations of He II in 1947.[1] While his theory for the thermodynamic and hydrodynamic properties of He II had many notable successes, it was the advent of inelastic neutron scattering measurements which made the basic truth of his assumption on the dispersion curve evident to all. We have recently reviewed the hydrodynamics of He II in an effort to assess the present state of superfluid mechanics and to identify problems which are likely to need more work in the future.[2] This paper is an attempt to do the same for the thermodynamic properties of He II, more from the point of view of an assessment rather than as a comprehensive review; and we shall see that the overall success of the quasiparticle model as applied to thermodynamics leaves much to be desired.

Our interest in the thermodynamic properties goes back to the publication of *Experimental Superfluidity*,[3] which contained a set of tables of most of the known properties of He II, including the results of early neutron

*Research supported by the National Science Foundation and the Air Force Office of Scientific Research under grants NSF DMR 76-21814 and AFOSR 76-2880.

scattering experiments in the form of the Landau parameters of the spectrum. More recently, we have been preparing a comprehensive set of tables of the properties of He II as a function of temperature and pressure, which is to be published in the *Journal of Physics and Chemistry Reference Data*.[4] Since there is nowhere near sufficient experimental data to fill these tables, it was natural to try to use the Landau elementary excitation model as a way to supplement direct thermodynamic measurements by data from inelastic neutron scattering. There is a long history of such attempts. The first systematic neutron studies of He II at the vapor pressure by the Los Alamos group[5] brought forth the reassuring conclusion that the Landau theory was applicable up to temperatures of the order of 1.8 K providing one used the actual dispersion curve for the calculation rather than the Landau approximation of roton and phonon branches.[6] Subsequent thermodynamic studies, such as are surveyed in Wilks' monograph,[7] however, contained disturbing discrepancies, such as differences between neutron and thermodynamic quantities (roton effective mass, for example) which could be as great as a factor of two.

Since that time, neutron scattering measurements have had two principal thrusts. The Chalk River group has extended measurements to higher energy and momentum, revealing a richness in the dispersion spectrum heretofore unsuspected;[8] and the Brookhaven group has produced systematic studies of the roton spectrum over the entire temperature–pressure plane.[9] The latter report, however, which we shall refer to as DGHP, showed that there exist very serious discrepancies between thermodynamic measurements of the entropy at finite temperatures and pressures and the values deduced from neutron studies. The discrepancies are serious enough to render the excitation theory all but useless except for order-of-magnitude estimates. It appears that difficulties arise whenever the linewidth of the scattered neutron group becomes finite, and one is led to suspect that there might be a serious problem with the statistical formulation of the thermodynamics whenever the observed energy levels are broadened. Further complications involve the existence of temperature-dependent energy levels. To appreciate the magnitude of the temperature dependence, note that the roton energy parameter Δ/k (see Fig. 1) changes from 8.54 K at 1.26 K to 4.61 K at 2.1 K.

Aside from linewidth and temperature-dependent energy level problems, other experimental evidence prompted some serious questions. For example, if one plots the molar volume of He II as a function of the number density of phonons at low temperatures, one concludes that the addition of a phonon *expands* the liquid by about 3 Å^3. Conversely, if one plots the molar volume of He II as a function of the number density of rotons at higher temperatures, one concludes that the addition of a roton to the fluid

contracts the liquid by about 3 Å^3.[10,11] The question then arises: Does the $P\delta V$ work involved in the addition of a quasiparticle at pressure P, accompanied by a volume change δV, have to be taken into account explicitly in estimating the energy transfer by a neutron? (As we shall see below, it does not.)

In this paper we shall present a new theory of temperature-dependent energy levels for Bose excitations, which allows the calculation of the thermodynamic properties of He II whenever the exact energies of the elementary excitations are known from experiment. A preliminary letter has already appeared on this subject.[12] With this new theory it will prove possible to deduce quite accurately what the effective values of Δ must be to "explain" the thermodynamic results. Below 1 K, these values of Δ correspond to the neutron data. Above 1 K, these values systematically depart from the parameters deduced from neutron scattering. The discrepancies described above are not resolved in this paper: Some investigators would claim that they never can be. We believe that the experimental results indicate that there exists an "effective sharp dispersion spectrum," which it should be possible to deduce from neutron scattering data. Indeed, Maynard at UCLA, in a related research project (described in Section 10, below) has reached a quite similar conclusion.[13]

The plan of this paper is as follows. We discuss in Section 2 the statistical mechanics of interacting bosons in a manner which is independent of our later considerations of the elementary excitation or quasiparticle picture of He II. The main results on temperature-dependent levels are derived and stated there. Since these results require differentiation of energies with respect to temperature, pressure, and wave number, we discuss ways of representing the spectrum of elementary excitations of He II in Section 3. The actual situation in liquid helium as probed by inelastic neutron scattering is not as simple as one has in mind doing the statistical mechanics. Our experimental knowledge of the dynamic structure factor, quasiparticle energies, and some of the associated experimental problems are outlined in Section 4. The underlying cause of at least some of the temperature dependence and linewidth problems is the long-range interaction between rotons, which is recognized to be dipolar. Section 5 contains a summary of some of the important results on these problems. With a more complete idea of the situation in He II, we compare in Section 6 the results from neutron scattering experiments with the formulas for entropy and the equation of state derived in Section 2. We find the situation at the saturated vapor pressure relatively clear-cut, but at higher pressures and temperatures increasing discrepancies between calculated and observed results are noted. The concept and use of an effective spectrum are reviewed in Section 7. Sections 8 and 9 show the results of calculations with the simple and

generalized Landau approximations to the spectrum, and Section 10 contains a brief discussion of an alternative, but related, approach to the representation of the spectrum.

2. STATISTICAL MECHANICS OF INTERACTING BOSONS

The object of this section is to develop a self-consistent approximation for the statistical mechanics of a set of interacting bosons. It will be supposed that the energy

$$E = E(\mathbf{n}, V) \tag{1}$$

of the system is a known function of the set $\mathbf{n} = (n_1, n_2, \ldots, n_N)$ of occupation numbers of the bosons in N discrete modes (the assumption that N is finite being made purely for presentational convenience). The approximation that will be developed exhibits clearly the single postulate that is needed to interpret and justify the often-used idea of temperature-dependent energy levels. We point out a number of pitfalls that can arise if that idea is applied too superficially. Our treatment has points of similarity with the earlier discussions of Rushbrooke,[14] Elcock and Landsberg,[15] and Bendt *et al.*[6] (BCY). It contains, however, a number of significant differences.

In the first instance, we do not consider that the energy ε_α of level α depends on T, but introduce the more general definition

$$\varepsilon_\alpha(\mathbf{n}, V) = \partial E(\mathbf{n}, V)/\partial n_\alpha \tag{2}$$

which we apply whether the system is in thermal equilibrium or not. In the particular case in which all ε_α are independent of $\mathbf{n}$, (2) implies

$$E = E_0(V) + \sum_\alpha n_\alpha \varepsilon_\alpha(V) \tag{3}$$

a familiar result but one which we cannot use when $\partial\varepsilon_\alpha/\partial n_\beta \neq 0$. Here $E_0(V)$ is the ground state energy.

The probability $\mathscr{P}(\mathbf{n}, V, T)$ that a system at volume V in the ensemble should have occupation numbers $n_1, \ldots, n_N$ in the levels $\varepsilon_1, \ldots, \varepsilon_N$ is

$$\mathscr{P}(\mathbf{n}, V, T) = C^{-1} \exp[-\beta E(\mathbf{n}, V)] \tag{4}$$

where C is chosen so that $\mathscr{P}$, a probability, summed over n, is unity,

$$C = \sum_{\mathbf{n}} \exp[-\beta E(\mathbf{n}, V)] \tag{5}$$

and $\beta = 1/kT$.

Of particular interest are the mean values of quantities such as entropy S, energy E, etc., when thermodynamic equilibrium prevails. We define such means, for any quantity $Q(\mathbf{n}, V)$, by

$$\bar{Q}(V, T) = \sum_{\mathbf{n}} \mathcal{P}(\mathbf{n}, V, T) Q(\mathbf{n}, V) \tag{6}$$

By analogy with the usual expression for $\mathcal{P}$ in Bose statistics, $\mathcal{P}(\mathbf{n}, V, T)$ is the greater, the smaller the n_α. If, however, $\bar{Q}$ increases with n_α, then the terms of (6) making the greatest contribution to $\bar{Q}$ are not those near $\mathbf{n} = 0$. We will suppose, in fact, that in calculating the averages of interest below, the terms making the largest contributions to the relevant sums are those for which the set $\mathbf{n}$ is in the vicinity of some other set $\boldsymbol{\omega}$, and that the terms for which the truncated Taylor expansion

$$E(\mathbf{n}, V) = E(\boldsymbol{\omega}, V) + \sum_\alpha (n_\alpha - \omega_\alpha)\varepsilon_\alpha(\boldsymbol{\omega}, V) \tag{7}$$

is seriously in error make a negligible contribution to these sums. At the moment, the set $\boldsymbol{\omega}$ of (7) is unknown. Later we will suggest a criterion for optimizing the choice of $\boldsymbol{\omega}$.

On substituting (7) into (4), we obtain

$$\mathcal{P}(\mathbf{n}, V, T) = Z^{-1} \prod_\alpha \exp[-\beta n_\alpha \varepsilon_\alpha(\boldsymbol{\omega}, V)] \tag{8}$$

where Z is a partition function

$$Z = \prod_\alpha \sum_{n_\alpha} \exp[-\beta n_\alpha \varepsilon_\alpha(\boldsymbol{\omega}, V)] = \prod_\alpha \{1 - \exp[-\beta \varepsilon_\alpha(\boldsymbol{\omega}, V)]\} \tag{9}$$

We may obtain $\bar{n}_\alpha$ from (6) by a standard argument

$$\begin{aligned} \bar{n}_\alpha &= \sum_\alpha n_\alpha \mathcal{P}(\mathbf{n}, V, T) = \frac{\sum_0^\infty n_\alpha \exp[-\beta n_\alpha \varepsilon_\alpha(\boldsymbol{\omega}, V)]}{\sum_0^\infty \exp[-\beta n_\alpha \varepsilon_\alpha(\boldsymbol{\omega}, V)]} \\ &= -\frac{\partial}{\partial(\beta\varepsilon_\alpha)} \ln \sum_0^\infty \exp[-\beta n_\alpha \varepsilon_\alpha(\boldsymbol{\omega}, V)] = -\frac{1}{\beta}\left[\frac{\partial}{\partial \varepsilon_\alpha} \ln Z\right]_{\boldsymbol{\omega}, V} \end{aligned} \tag{10}$$

Using (9), we obtain

$$\bar{n}_\alpha = \{\exp[\beta \varepsilon_\alpha(\boldsymbol{\omega}, V)] - 1\}^{-1} \tag{11}$$

a result which may also be obtained by maximizing an entropy,

$$S = k \sum_\alpha [(1 + n_\alpha) \ln (1 + n_\alpha) - n_\alpha \ln n_\alpha] \tag{12}$$

for given $\bar{E}$, V, and T. The equilibrium entropy

$$\bar{S} = \sum_\alpha [k \ln (1 + \bar{n}_\alpha) + \bar{n}_\alpha \varepsilon_\alpha(\boldsymbol{\omega}, V)/T] \tag{13}$$

can be obtained by differentiating the Helmholtz free energy $F = -kT \ln Z$ with respect to T, holding V and the set ω constant, or simply by substituting (11) into (12).

What is the optimum choice of ω? We postulate that the best choice of ω is the one that maximizes the equilibrium entropy $\bar{S}$ in (13) holding V, T, and $\bar{E}$ constant. We note that by (2) and (7),

$$\left(\frac{\partial \bar{E}(\bar{\mathbf{n}}, V)}{\partial \omega_\gamma}\right)_V = \sum_\alpha \varepsilon_\alpha(\boldsymbol{\omega}, V)\left(\frac{\partial \bar{n}_\alpha}{\partial \omega_\gamma}\right)_{V,T} + \sum_\alpha (\bar{n}_\alpha - \omega_\alpha)\left(\frac{\partial \varepsilon_\alpha(\boldsymbol{\omega}, V)}{\partial \omega_\gamma}\right)_V \tag{14}$$

while by (11) and (13)

$$\left(\frac{\partial \bar{S}(\bar{\mathbf{n}}, V)}{\partial \omega_\gamma}\right)_V = \frac{1}{T}\sum_\alpha \left(\frac{\partial \bar{n}_\alpha}{\partial \omega_\gamma}\right)_{V,T} \varepsilon_\alpha(\boldsymbol{\omega}, V) \tag{15}$$

It follows that [provided the multipliers are the same as appeared in (8), which can in fact be shown to be the case], the condition for an extremum of $\bar{S}$ is

$$\sum_\alpha (\bar{n}_\alpha - \omega_\alpha)\left(\frac{\partial \varepsilon_\alpha(\boldsymbol{\omega}, V)}{\partial \omega_\gamma}\right)_V = 0 \tag{16}$$

for all γ, i.e.,

$$\omega_\alpha = \bar{n}_\alpha \tag{17}$$

[The possibility that the matrix $\partial \varepsilon_\alpha / \partial \omega_\gamma$ in (16) is singular need not be taken seriously. For example, when ε_α is independent of $\mathbf{n}$, (7) is exact for all choices of $\boldsymbol{\omega}$, and the fact that (17) does not then follow from (16) is physically correct.]

Using (17) with (11), we obtain

$$n_\alpha = \{\exp[\beta \varepsilon_\alpha(\mathbf{n}, V)] - 1\}^{-1} \tag{18}$$

and the equilibrium entropy is

$$S = \sum_\alpha [k \ln(1 + n_\alpha) + n_\alpha \varepsilon_\alpha / T] \tag{19}$$

where we have dropped the overbar on $\bar{S}$, $\bar{n}$, and $\bar{\varepsilon}_\alpha = \varepsilon_\alpha(\bar{\mathbf{n}}, V)$. Note that (18) is identical to the classical expression which holds when ε_α is known and the right side of the equation can be calculated to give n_α at once. When ε_α depends on $\mathbf{n}$ in some assigned way, (7) is not exact and the right-hand side of (18) depends, through ε_α, on $\bar{n}_\alpha$. Thus (18) is an implicit equation for $\bar{n}_\alpha$, which could be solved by iteration and would then give the particular Taylor expansion (7) that maximizes the equilibrium entropy. Once $\bar{n}_\alpha$ has been determined in terms of V and T, all equilibrium fields can be expressed in terms of these variables. In most cases of interest $\varepsilon_\alpha(\mathbf{n}, V)$ is unknown, and

only $\varepsilon_\alpha(\bar{\mathbf{n}}, V)$ is known from experiment; then $\varepsilon_\alpha(\bar{\mathbf{n}}, V)$ is replaced by $\varepsilon_\alpha(T, V)$ and substituted into the right side of (18) to give $\bar{n}_\alpha$ directly, as in the classical case.

A word of caution is appropriate here about the way the theory developed above might be misapplied. Although the optimal choice of ω turned out to be dependent on T, the entire argument supposed ω was fixed. Thus, for example, when obtaining the form (18) for $\bar{n}_\alpha$ using (10) we hold ω constant during differentiation before applying (17). This proviso becomes crucial when differentiating the free energy $F = -kT \ln Z$ to obtain the equilibrium entropy (19). If (17) is applied to (9) before differentiating with respect to T, and $\bar{n}_\alpha$ is treated as a function of T during that differentiation, then a seriously incorrect result for $\bar{S}$ would be obtained instead of (19).

We now switch to continuous variables using the transition

$$\sum_\alpha \to \frac{V}{2\pi^2}\int_0^\infty q^2\,dq \tag{20}$$

and express (19) in terms of variables P and T for comparison with *experiments on* He II:

$$S = (V/2\pi^2)\int_0^\infty [k \ln(1+n) + n\varepsilon/T]q^2\,dq \tag{21}$$

which, on integrating by parts, may be written

$$S = -\frac{V}{2\pi^2}\int_0^\infty \frac{\varepsilon}{3T}\left(\frac{\partial n}{\partial q}\right)_{P,T} q^3\,dq \tag{22}$$

Integration of (22) over T for fixed P gives for the Gibbs free energy

$$\Phi = \Phi_0(P) + \frac{1}{2\pi^2}\int_0^T \frac{V\,dT}{T}\int_0^\infty \frac{\varepsilon}{3}\left(\frac{\partial n}{\partial q}\right)_{P,T} q^3\,dq \tag{23}$$

where $\Phi_0(P)$ is the corresponding ground-state free energy. Writing $V_0 = \Phi_0'$ for the molar volume at absolute zero, we obtain the integral equation of state

$$V = V_0(P) - \frac{1}{2\pi^2}\int_0^T \frac{V\,dT}{T}\int_0^\infty \varepsilon\left[\left(\frac{\partial n}{\partial P}\right)_{T,q} + \frac{\kappa q}{3}\left(\frac{\partial n}{\partial q}\right)_{P,T}\right]q^2\,dq \tag{24}$$

which implies that $\alpha \approx V^{-1}(\partial V/\partial T)_P$ is

$$\alpha = -\frac{1}{2\pi^2 T}\int_0^\infty \varepsilon\left[\left(\frac{\partial n}{\partial P}\right)_{T,q} + \frac{\kappa q}{3}\left(\frac{\partial n}{\partial q}\right)_{P,T}\right]q^2\,dq \tag{25}$$

At first sight the appearance of the $\partial n/\partial q$ terms of (24) and (25) is unexpected. Their necessity follows from both mathematical and physical

reasoning. By the former we note that when differentiating (23) with respect to P we must not forget to differentiate V under the integral sign, and so introduce the isothermal compressibility $\kappa = -V^{-1}(\partial V/\partial P)_T$. The remaining term under the integral sign in (24) follows on integration by parts over q, once use has been made of the fact that, since $n = n(\varepsilon/T)$,

$$\left[\frac{\partial}{\partial P}\left(\frac{\varepsilon}{T}\frac{\partial n}{\partial q}\right)\right]_T = \left[\frac{\partial}{\partial q}\left(\frac{\varepsilon}{T}\frac{\partial n}{\partial P}\right)\right]_T \tag{26}$$

The physical argument recalls that the momentum $\hbar\mathbf{q}_\alpha$, corresponding to state α, arises from $q_i = m_i/L$, where $L = V^{1/3}$ is the mean periodicity of an isotropic substance and m_i is the set of integers defining mode α. Thus, when one replaces $\varepsilon_\alpha(P, T)$ by $\varepsilon(P, T, \mathbf{q})$, one should recognize that the latter is really $\varepsilon(P, T, \mathbf{m}V^{-1/3})$ and that $\mathbf{m}$ rather than $\mathbf{q}$ should be held constant during differentiation. Since $V = V(P, T)$,

$$\left(\frac{\partial \varepsilon}{\partial P}\right)_{T,\mathbf{m}} = \left(\frac{\partial \varepsilon}{\partial P}\right)_{T,q} + \frac{1}{3}\kappa q\left(\frac{\partial \varepsilon}{\partial q}\right)_{P,T} \tag{27}$$

and this is the expression that should replace $(\partial\varepsilon_\alpha/\partial P)_T$ in the discrete analog of (25), viz.

$$\alpha = -\frac{1}{VT}\sum_\alpha \varepsilon_\alpha\left(\frac{\partial n_\alpha}{\partial P}\right)_T \tag{28}$$

when the transition (20) is made. For completeness, (27) and a number of similar relations are listed in Table I.

A wide variety of thermodynamic functions can be derived in the manner just described. These are summarized in Table II, in which E, W, F, and Φ are internal energy, enthalpy, Helmholtz free energy, and Gibbs free energy; and C_V and C_P are the specific heats at constant volume and

TABLE I

Transition from the Discrete to the Continuous

$(\partial\varepsilon_\alpha/\partial T)_V \to (\partial\varepsilon/\partial T)_{V,q}$
$(\partial\varepsilon_\alpha/\partial T)_P \to (\partial\varepsilon/\partial T)_{P,q} - (\alpha q/3)(\partial\varepsilon/\partial q)_{P,T}$
$(\partial\varepsilon_\alpha/\partial V)_T \to (\partial\varepsilon/\partial V)_{T,q} - (q/3V)(\partial\varepsilon/\partial q)_{V,T}$
$(\partial\varepsilon_\alpha/\partial P)_T \to (\partial\varepsilon/\partial P)_{T,q} + (\kappa q/3)(\partial\varepsilon/\partial q)_{P,T}$
$(\partial\varepsilon_\alpha/\partial S)_V \to (\partial\varepsilon/\partial S)_{V,q}$
$(\partial\varepsilon_\alpha/\partial S)_P \to (\partial\varepsilon/\partial S)_{P,q} - (\alpha Tq/3C_P)(\partial\varepsilon/\partial q)_{P,S}$
$(\partial\varepsilon_\alpha/\partial V)_S \to (\partial\varepsilon/\partial V)_{S,q} - (q/3V)(\partial\varepsilon/\partial q)_{V,S}$
$(\partial\varepsilon_\alpha/\partial P)_S \to (\partial\varepsilon/\partial P)_{S,q} + (\kappa C_V q/3C_P)(\partial\varepsilon/\partial q)_{P,S}$

pressure. This table also displays both the summation and integral expressions, since, for the reasons just described, the transition from the former to the latter is not always immediate. In view of the work by Goodstein *et al.*,[16] one point arising from Table II deserves emphasis. The discrete analog of (24) is

$$V = V_0(P) - \int_0^T \sum_\alpha \frac{\varepsilon_\alpha}{T}\left(\frac{\partial n_\alpha}{\partial P}\right)_T dT \tag{29}$$

If ε_α is independent of T, we have, recalling again that $n_\alpha = n_\alpha(\varepsilon_\alpha/T)$,

$$\int_0^T \frac{\varepsilon_\alpha}{T}\frac{\partial n_\alpha}{\partial P}\,dT = \frac{d\varepsilon_\alpha}{dP}\int_0^T \frac{\varepsilon_\alpha}{T^2} n'_\alpha\,dT = -n_\alpha \frac{d\varepsilon_\alpha}{dP} \tag{30}$$

and (29) becomes

$$V = V_0(P) + \sum_\alpha n_\alpha \frac{d\varepsilon_\alpha}{dP} \tag{31}$$

Taken literally, this expression for V implies that, when ε_α depends on P alone, the volume occupied by a boson in energy level α is $d\varepsilon_\alpha/dP$, as conjectured by Donnelly.[10] The present analysis provides a more direct confirmation of this calculation than the external field argument of Goodstein *et al.*,[16] discussed below.

Consider next the effect of applying some "external field" to the system as a result of which the mean occupation number of a particular mode, labeled by p, is held at the population $\tilde{n}_p$, not necessarily close to the $\bar{n}_p$ derived in the theory above.[16] The probability (4) is now replaced by

$$\mathcal{P}(\mathbf{n}, V, T) = C^{-1} \exp\left[-\beta E(\mathbf{n}, V) + \beta\mu n_p\right] \tag{32}$$

where μ is a multiplier or chemical potential, chosen so that for the particular mode p

$$\tilde{n}_p = \sum_{\mathbf{n}} n_p \mathcal{P}(\mathbf{n}, T, V) \tag{33}$$

The normalization constant C follows in analogy with (5). The mean of a quantity Q is still given by (6) but is now evidently a function of V, T, and $\tilde{n}_p$. On adopting (7), we derive results closely similar to those obtained above. For example, (18) holds for all modes except mode p, for which

$$\tilde{n}_p = \{\exp\left[\beta(\varepsilon_p - \mu) - 1\right]\}^{-1} \tag{34}$$

with $\varepsilon_p = \varepsilon_p(\bar{\mathbf{n}}, V) = \varepsilon_p(V, T, \tilde{n}_p)$ and $\mu = \mu(V, T, \tilde{n}_p)$. The entropy (12) reduces in equilibrium not to (19) but to

$$S = k\left[(1+n_p)\ln(1+n_p) - n_p \ln n_p\right] + \sum_\alpha{}' \left[k \ln(1+n_\alpha) + n_\alpha \varepsilon_\alpha/T\right] \tag{35}$$

TABLE II

Expressions for Thermodynamic Quantities

Variable	Summation form	Integral form
S	$\begin{cases} \sum_\alpha \int_0^T \frac{\varepsilon_\alpha}{T}\left(\frac{\partial n_\alpha}{\partial T}\right)_V dT \\ \sum_\alpha \int_0^T \frac{\varepsilon_\alpha}{T}\left(\frac{\partial n_\alpha}{\partial T}\right)_P dT \end{cases}$	$\begin{cases} -\frac{V}{2\pi^2 T}\int_0^\infty \frac{\varepsilon}{3}\left(\frac{\partial n}{\partial q}\right)_{V,T} q^3\, dq \\ -\frac{V}{2\pi^2 T}\int_0^\infty \frac{\varepsilon}{3}\left(\frac{\partial n}{\partial q}\right)_{P,T} q^3\, dq \end{cases}$
C_V	$\sum_\alpha \varepsilon_\alpha\left(\frac{\partial n_\alpha}{\partial T}\right)_V$	$\frac{V}{2\pi^2}\int_0^\infty \varepsilon\left(\frac{\partial n}{\partial T}\right)_{V,q} q^2\, dq$
C_P	$\sum_\alpha \varepsilon_\alpha\left(\frac{\partial n_\alpha}{\partial T}\right)_P$	$\frac{V}{2\pi^2}\int_0^\infty \varepsilon\left[\left(\frac{\partial n}{\partial T}\right)_{P,q} - \frac{\alpha q}{3}\left(\frac{\partial n}{\partial q}\right)_{P,T}\right] q^2\, dq$
F	$F_0(V) - kT\sum_\alpha \ln(1+n_\alpha) - \sum_\alpha \int_0^T n_\alpha\left(\frac{\partial \varepsilon_\alpha}{\partial T}\right)_V dT$	$F_0(V) + \frac{V}{2\pi^2}\int_0^T \frac{dT}{T}\int_0^\infty \frac{\varepsilon}{3}\left(\frac{\partial n}{\partial q}\right)_{V,T} q^3\, dq$
Φ	$\Phi_0(P) - kT\sum_\alpha \ln(1+n_\alpha) - \sum_\alpha \int_0^T n_\alpha\left(\frac{\partial \varepsilon_\alpha}{\partial T}\right)_P dT$	$\Phi_0(P) + \frac{1}{2\pi^2}\int_0^T \frac{V\,dT}{T}\int_0^\infty \frac{\varepsilon}{3}\left(\frac{\partial n}{\partial q}\right)_{P,T} q^3\, dq$
E	$F_0(V) + \sum_\alpha \int_0^T \varepsilon_\alpha\left(\frac{\partial n_\alpha}{\partial T}\right)_V dT$	$F_0(V) + \frac{V}{2\pi^2}\int_0^T dT\int_0^\infty \varepsilon\left(\frac{\partial n}{\partial T}\right)_{V,q} q^2\, dq$

W	$\Phi_0(P)+\sum_\alpha \int_0^T \varepsilon_\alpha \left(\frac{\partial n_\alpha}{\partial T}\right)_P dT$	$\Phi_0(P)+\frac{1}{2\pi^2}\int_0^T V\,dT \int_0^\infty \varepsilon\left[\left(\frac{\partial n}{\partial T}\right)_{P,q}-\frac{\alpha q}{3}\left(\frac{\partial n}{\partial q}\right)_{P,T}\right]q^2\,dq$
P	$P_0(V)+\sum_\alpha \int_0^T \frac{\varepsilon_\alpha}{T}\left(\frac{\partial n_\alpha}{\partial V}\right)_T dT \quad (P_0=-F_0')$	$P_0(V)+\frac{V}{2\pi^2}\int_0^T \frac{dT}{T}\int_0^\infty \varepsilon\left[\left(\frac{\partial n}{\partial V}\right)_{T,q}-\frac{q}{3V}\left(\frac{\partial n}{\partial q}\right)_{V,T}\right]q^2\,dq$
V	$V_0(P)-\sum_\alpha \int_0^T \frac{\varepsilon_\alpha}{T}\left(\frac{\partial n_\alpha}{\partial P}\right)_T dT \quad (V_0=\Phi_0')$	$V_0(P)-\frac{1}{2\pi^2}\int_0^T \frac{V\,dT}{T}\int_0^\infty \varepsilon\left[\left(\frac{\partial n}{\partial P}\right)_{T,q}+\frac{\kappa q}{3}\left(\frac{\partial n}{\partial q}\right)_{P,T}\right]q^2\,dq$
$\alpha T/\kappa$	$\sum_\alpha \varepsilon_\alpha \left(\frac{\partial n_\alpha}{\partial V}\right)_T$	$\frac{V}{2\pi^2}\int_0^\infty \varepsilon\left[\left(\frac{\partial n}{\partial V}\right)_{T,q}-\frac{q}{3V}\left(\frac{\partial n}{\partial q}\right)_{P,T}\right]q^2\,dq$
αTV	$-\sum_\alpha \varepsilon_\alpha \left(\frac{\partial n_\alpha}{\partial P}\right)_T$	$-\frac{V}{2\pi^2}\int_0^\infty \varepsilon\left[\left(\frac{\partial n}{\partial P}\right)_{T,q}+\frac{\kappa q}{3}\left(\frac{\partial n}{\partial q}\right)_{P,T}\right]q^2\,dq$
T	$\sum_\alpha \varepsilon_\alpha \left(\frac{\partial n_\alpha}{\partial S}\right)_V$	$\frac{V}{2\pi^2}\int_0^\infty \varepsilon\left(\frac{\partial n}{\partial S}\right)_{V,q} q^2\,dq$
	$\sum_\alpha \varepsilon_\alpha \left(\frac{\partial n_\alpha}{\partial S}\right)_P$	$\frac{V}{2\pi^2}\int_0^\infty \varepsilon\left[\left(\frac{\partial n}{\partial S}\right)_{P,q}-\frac{\alpha T q}{3C_P}\left(\frac{\partial n}{\partial q}\right)_{P,S}\right]q^2\,dq$
0	$\sum_\alpha \varepsilon_\alpha \left(\frac{\partial n_\alpha}{\partial V}\right)_S$	$\frac{V}{2\pi^2}\int_0^\infty \varepsilon\left[\left(\frac{\partial n}{\partial V}\right)_{S,q}-\frac{q}{3V}\left(\frac{\partial n}{\partial q}\right)_{V,S}\right]q^2\,dq$
	$\sum_\alpha \varepsilon_\alpha \left(\frac{\partial n_\alpha}{\partial P}\right)_S$	$\frac{V}{2\pi^2}\int_0^\infty \varepsilon\left[\left(\frac{\partial n}{\partial P}\right)_{S,q}+\frac{\kappa C_V q}{3C_P}\left(\frac{\partial n}{\partial q}\right)_{P,S}\right]q^2\,dq$

where the prime on the sum indicates that the term $\alpha = p$ is excluded, and we have dropped the tilde over n_p as we have omitted the bar over n_α. The expression for S given at the head of Table II is modified to

$$S = k[(1+n_p)\ln(1+n_p) - n_p \ln n_p] + \sum_\alpha{}' \int_0^T \frac{\varepsilon_\alpha}{T}\left(\frac{\partial n_\alpha}{\partial T}\right)_{V,n_p} dT \tag{36}$$

and other entries in that table are similarly affected. It follows from (18), (34), and (36) that

$$T\,dS = \sum_\alpha \varepsilon_\alpha\, dn_\alpha - \mu\, dn_p \tag{37}$$

Since we have, by (1) and (2),

$$dE = \sum_\alpha \varepsilon_\alpha\, dn_\alpha - P\,dV \tag{38}$$

it follows that

$$dE = T\,dS - P\,dV + \mu\, dn_p \tag{39}$$

By a Legendre transformation, we obtain

$$d\Phi = -S\,dT + V\,dP + \mu\, dn_p \tag{40}$$

Many "Maxwell relations" follow from expressions such as (39) and (40), and similar expressions for dF and dW. We note here that by (40)

$$\left(\frac{\partial V}{\partial n_p}\right)_{P,T} = \left(\frac{\partial^2 \Phi}{\partial n_p \partial P}\right)_T = \left(\frac{\partial \mu}{\partial P}\right)_{T,n_p} \tag{41}$$

and since by (34)

$$\mu = \varepsilon_p - kT\ln(1+n_p) \tag{42}$$

it follows from (41) that

$$\left(\frac{\partial V}{\partial n_p}\right)_{P,T} = \left(\frac{\partial \varepsilon_p}{\partial P}\right)_{n_p,T} \tag{43}$$

Relation (43) holds generally and it might at first sight be supposed that by selecting $\tilde{n}_p$ to be the mean population $\bar{n}_p$ of state p in the absence of the field, and summing over all modes p, (31) would follow generally. This is not the case. The external field may be regarded as a mathematical device that allows $\tilde{n}_p$ to deviate from $\bar{n}_p$ even in statistical equilibrium, so that one can explore what happens when $\tilde{n}_p$ is $\bar{n}_p + 1$ rather than $\bar{n}_p$, say. When such a field is applied, the change in V will indeed be $(\partial\varepsilon_p/\partial P)_{\bar{n}_p,T}$ as implied by (43); but (when ε_α depends on $\mathbf{n}$ or equivalently when $\bar{\varepsilon}_\alpha$ depends on T) this unit change in population of the state p will alter all other energy levels in the system and hence *all* thermodynamic properties, and *all* occupation number

of *all* other levels. The volume changes corresponding to these altered occupation numbers of every level are included in (43). The concept that an elementary excitation expands the fluid by $(\partial\varepsilon_p/\partial P)_T$ depends, however, on the idea that one additional excitation appears in one *particular* mode p, the population of all other modes being unchanged. Clearly this can only be accomplished by an external field in the very special case in which ε_α depends on P alone and not on $\mathbf{n}_\alpha$. And it is *only* in this case that one is justified in summing (43) over all modes to obtain (31). Because of the practical difficulty in realizing, in laboratory conditions, an external field having the above properties, the present "Gedanken experiment" and its consequences such as (43) are of insignificant interest except in the special case $\varepsilon_\alpha = \varepsilon_\alpha(P)$.

We digress to note here that for familiarity of presentation we have begun with the internal energy E as defined in (1), so that the energy levels could be defined as in (2). We could, however, equally well have begun with the enthalpy W,

$$W = W(\mathbf{n}, P) \tag{44}$$

and have written

$$dW = \left(\frac{\partial W}{\partial n_\alpha}\right)_P dn_\alpha + \left(\frac{\partial W}{\partial P}\right)_{n_\alpha} dP = \left(\frac{\partial W}{\partial n_\alpha}\right)_P dn_\alpha + V\,dP \tag{45}$$

Then (36) has the same form except that $(\partial n_\alpha/\partial T)_{V,n_p}$ in the second term is amended to $(\partial n_\alpha/\partial T)_{P,n_p}$; (37) still holds, and defining

$$\varepsilon_\alpha = (\partial W/\partial n_\alpha)_P \tag{46}$$

we have from (45) and (37)

$$dW = T\,dS + V\,dP + \mu\,dn_p \tag{47}$$

The definition of ε_α by (46) is important in neutron inelastic scattering experiments, which are done at constant pressure rather than constant volume: We see that ε_α is precisely defined as the energy transfer to the fluid at constant pressure.

It is apparent that our method of developing the theory of temperature-dependent energy levels depends on an approximation, namely (7). We cannot be dogmatic about the success of the theory until we have found a quantitative measure of the inaccuracies introduced by (7), e.g., by comparing the consequences of (7) with those that follow from the next level of Taylor truncation:

$$E(\mathbf{n}, V) = E(\boldsymbol{\omega}, V) + \sum_\alpha \varepsilon_\alpha(\boldsymbol{\omega}, V)(n_\alpha - \omega_\alpha) + \tfrac{1}{2}\sum_{\alpha,\beta} \phi_{\alpha\beta}(\boldsymbol{\omega}, V)(n_\alpha - \omega_\alpha)(n_\beta - \omega_\beta) \tag{48}$$

where $\phi_{\alpha\beta} = \phi_{\beta\alpha}$ without loss of generality. The labor involved in doing so is formidable. We note, however, that (48) resembles the central postulate

$$E(\mathbf{n}, V) = E_0(V) + \sum_{\alpha} e_\alpha(V) n_\alpha + \tfrac{1}{2} \sum_{\alpha,\beta} f_{\alpha\beta}(V) n_\alpha n_\beta \tag{49}$$

of Fermi liquid theory,[17] where $f_{\alpha\beta} = f_{\beta\alpha}$. Comparison of (48) and (49) shows that

$$E_0(V) = E(\boldsymbol{\omega}, V) - \sum_{\alpha} \varepsilon_\alpha(\boldsymbol{\omega}, V)\omega_\alpha + \tfrac{1}{2} \sum_{\alpha,\beta} \phi_{\alpha\beta}(\boldsymbol{\omega}, V)\omega_\alpha\omega_\beta \tag{50}$$

$$e_\alpha(V) = \varepsilon_\alpha(\boldsymbol{\omega}, V) - \sum_{\beta} \phi_{\alpha\beta}(\boldsymbol{\omega}, V)\omega_\beta \tag{51}$$

and

$$f_{\alpha\beta}(V) = \phi_{\alpha\beta}(\boldsymbol{\omega}, V) \tag{52}$$

Thus (49) is a somewhat special form of (48), namely the case $\boldsymbol{\omega} = 0$, and requires

$$\varepsilon_\alpha(\boldsymbol{\omega}, V) = e_\alpha(V) + \sum_{\beta} f_{\alpha\beta}(V)\omega_\beta \tag{53}$$

The form (7) is less general than (49) in the sense that it requires that $f_{\alpha\beta} = 0$, but it is more general in the sense that ε_α is not necessarily a linear function of $\boldsymbol{\omega}$ as (53) requires. Postulate (49) has the philosophical advantage of specifying $E(\mathbf{n}, V)$ unambiguously, whereas (7) and (48) give slightly different values of $E(\boldsymbol{\omega}, V)$ depending upon the $\boldsymbol{\omega}$ selected for the Taylor expansion.

3. THE SPECTRUM OF ELEMENTARY EXCITATIONS AND ITS REPRESENTATION

Before proceeding with the discussion of excitations in real liquid helium, we shall indicate how our knowledge of the excitation spectrum can be represented in such a way that the expressions of Table II can be used in practice. Every thermodynamic quantity listed there requires a knowledge of $\varepsilon(q)$ and the associated equilibrium population

$$n(q) = h^{-3}\{\exp[\varepsilon(q)/kT] - 1\}^{-1} \tag{54}$$

More significantly, differentials of ε and n over V and T or P and T are needed. Our experimental knowledge of the excitation spectrum comes from an analysis of inelastic neutron scattering data, as will be discussed in Section 4. The errors introduced by direct differentiation of data taken, necessarily, at a few discrete P and T are unacceptable, and it transpires that

the encapsulation of the available data on $\varepsilon(q)$ requires very careful handling. The representation used in this paper is that of Brooks and Donnelly[11,18]; later we shall discuss a different approach by Maynard.[13] It cannot be too strongly emphasized that, while these spectra have been developed with some physical reasoning in mind, the final forms of $\varepsilon(q)$ should be seen as no more than convenient representations of a function in a finite interval, in much the same spirit as the representations of the common transcendental functions listed in Abramowitz and Stegun.[19] The reader who prefers to adopt some different representation that fits the data as well should not obtain significantly different thermodynamic results. The dangers of representing $\varepsilon(q)$ too crudely are well illustrated by a proper comparison of Landau's approximation with experiment as given in Section 8.

At sufficiently low temperatures it is clear from (54) that only the states of lowest energy $\varepsilon(q)$ will be significantly occupied and contribute to the thermodynamics. There are two regions of special significance. The first contains the small-momentum states near (a) in Fig. 1; the second is the region around the energy minimum labeled (c). Though the energy minimum $\varepsilon = \Delta$ at momentum p_0 is large, the density of states is also large, and this gives the "roton minimum" significant statistical weight at all except the lowest temperatures $T < 1$ K, where the "phonon excitations" near $p = 0$ are the more significant. Note that the energies and circular frequencies are connected by $\varepsilon = \hbar\omega$, and the momenta and wave numbers by $p = \hbar q$. Landau showed that a fairly good account of the thermodynamics could be made by a two-branch dispersion curve

$$\varepsilon = u_1 p, \qquad p \simeq 0 \tag{55a}$$

$$\varepsilon = \Delta + (p - p_0)^2/2\mu, \qquad p \simeq p_0 \tag{55b}$$

This is the "simple Landau approximation," originally conceived of as applying for T so small that the quantities u_1, Δ, p_0, and μ in (55a) and (55b) are constants, different of course for each pressure. They are tabulated in Section 8.

The simple Landau approximation may be extended by permitting u_1, Δ, p_0, and μ to be functions of temperature and pressure. Bendt *et al.*[6] recognized that this step was not sufficient to predict thermodynamic variables, and they added a third branch at (b) in Fig. 1, which required a further three constants for its specification, making seven in all. Further piecewise continuous approximations to the dispersion curve were proposed by Brooks and Donnelly[20] and Maynard.[13] At least two continuous representations have been proposed[18,21]; that of Brooks and Donnelly is a simple polynomial in p of degree eight with the constant and quadratic terms omitted. The details of the choice of this function are described in Brooks' thesis.[11] The assumptions used in this method, which seeks to generalize the

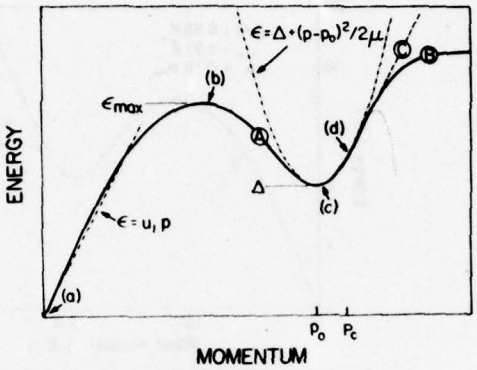

Fig. 1. A schematic diagram of the excitation spectrum for helium II. The simple Landau approximation (55a)–(55b) consists of the phonon and roton branches shown by the linear and parabolic curves. The polynomial for $\varepsilon(p)$ in the appendix gives the solid curve A plus the dotted curve beyond the point (d) (*of momentum* p_c) *where the slope* becomes equal to u_1. The model dispersion curve of the appendix consists of curve A plus the dashed line C, rather than the observed branch B, whose parameters as a function of pressure are as yet unknown.

spectrum for all T and P by the use of known constraints on certain energies and momenta, are discussed in Refs. 11, 18, and particularly in 4. They are summarized in the appendix. An example of such a dispersion curve is given in Fig. 2, compared with neutron scattering data, and Figs. 3a and 3b show how the spectra vary for various T and P. We might call a representation of the complete spectrum with temperature- and pressure-dependent variables "the generalized Landau approximation." Some results of this approach are described in Section 9.

Even when this type of representation has been selected, the handling of the data raises perplexing questions, some which will be described in subsequent sections.

4. THE DYNAMIC STRUCTURE FACTOR AND QUASIPARTICLE ENERGIES

Up to now all our discussions have assumed that the spectra as functions of energy ε for given momentum p are delta functions: We may speak of such spectra as "sharp." Our information on the situation in real liquid helium comes from inelastic neutron scattering measurements, and we shall

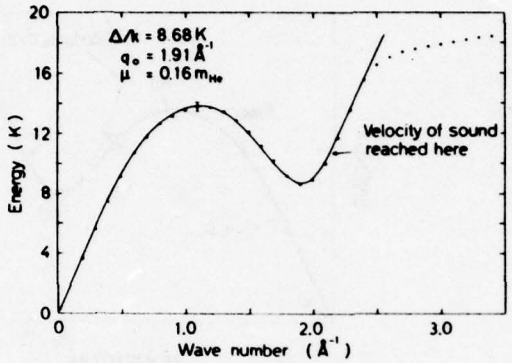

Fig. 2. The experimentally determined excitation spectrum at 1.1 K, SVP. The dots are the neutron scattering data of Cowley and Woods[8]; the solid line is the model dispersion curve of the appendix. The error bar is the smallest experimental error and is not to be associated with any one data point.

attempt to describe some of the procedures used in obtaining these data, which are not generally appreciated by those outside the neutron scattering community. Besides DGHP,[9] the reader is referred to articles by Cowley and Woods,[8,22] which contain comprehensive accounts of the progress and problems in this field.

The most common spectrometers used in neutron inelastic scattering experiments in liquid helium are the triple-axis crystal spectrometer and the time-of-flight spectrometer, the majority of reported measurements using the former. In both cases some general principles are involved, which we shall illustrate by reference to the time-of-flight apparatus of DGHP, since that was the apparatus used to determine the roton parameters of most interest to us in this review. Using the notation of DGHP, the intensity of scattered neutrons measured at an angle θ with respect to the incident beam is called $I_\theta(t)$ since the energy of the neutrons $\hbar^2k^2/2m_n$, m_n being the neutron mass, is given by the time of flight of neutrons over a fixed path. The scattered intensity $I_\theta(\hbar\omega)$, measured in energy units, however, is related to the double differential scattering cross section by the van Hove relation

$$I_\theta(\hbar\omega) \propto d^2\sigma/d\Omega\, dE \propto k_f S(q, \omega) \tag{56}$$

where Ω is the solid angle of scattered neutrons, k_f is the wave number of scattered neutrons, and $S(q, \omega)$ is the dynamic structure factor, which is the Fourier transform of the density–density correlation function characterizing the physical process causing the inelastic scattering of neutrons. The scat-

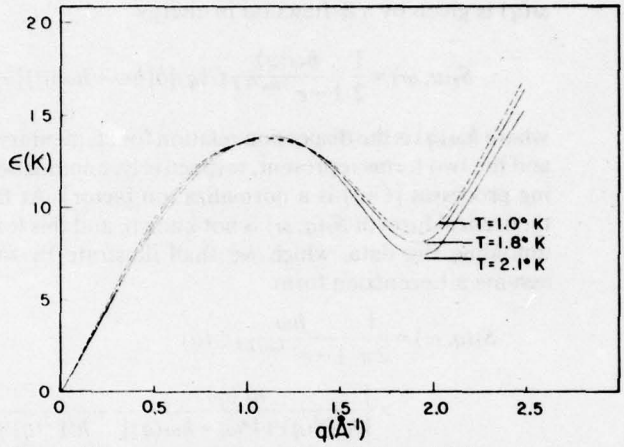

Fig. 3a. The temperature dependence of the model dispersion curves at $P = 0$.

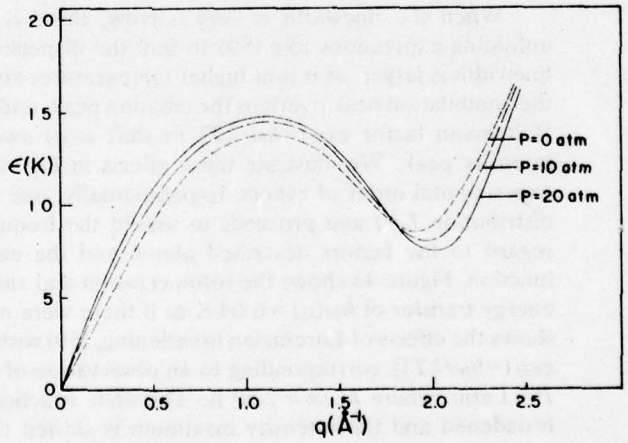

Fig. 3b. The pressure dependence of the model dispersion curves at $T = 1.2$ K.

tered neutron intensity is related not to energy but to time of flight. Those spectra are related by $I_\theta(t) \propto k_f^3 I_\theta(\hbar\omega)$. Thus

$$I_\theta(t) \propto k_f^4 S(q, \omega) \tag{57}$$

Near $T = 0$ the inelastic scattering amplitude of a neutron of incident wave number k_i and final wave number k_f by a single phonon of frequency

$\omega(q)$ is given by a δ-function in energy

$$S_I(q,\omega)=\frac{1}{2}\frac{\hbar\omega(q)}{1-e^{-\hbar\omega/kT}}C(q)\{\delta[\hbar\omega+\hbar\omega(q)]+\delta[\hbar\omega-\hbar\omega(q)]\} \quad (58)$$

where $\hbar\omega(q)$ is the dispersion relation for elementary excitations near $T=0$, and the two terms represent, respectively, annihilation and creation scattering processes [$C(q)$ is a normalization factor]. At finite temperatures, the theoretical form of $S_I(q,\omega)$ is not known, and this leads to an uncertainty in unfolding the data, which we shall illustrate by some examples. DGHP assume a Lorentzian form

$$S_I(q,\omega)=\frac{1}{2\pi}\frac{\hbar\omega}{1-e^{-\hbar\omega/kT}}C(q)$$
$$\times\left\{\frac{\hbar\Gamma(q)}{\hbar^2\Gamma^2(q)+[\hbar\omega+\hbar\omega(q)]^2}+\frac{\hbar\Gamma(q)}{\hbar^2\Gamma^2(q)+[\hbar\omega-\hbar\omega(q)]^2}\right\} \quad (59)$$

where $\hbar\Gamma(q)$ is the half-width at half-maximum (HWHM). Note that (59) has *the same effect as* (58) *in* the limit where $\hbar\Gamma(q)\to 0$.

When the linewidth is very narrow, there is little complication in unfolding expressions like (59) to find the dispersion relation. When the linewidth is larger, as it is at higher temperatures and pressures, the tail of the annihilation peak overlaps the creation peak, and this combines with the Boltzmann factor $\exp(-\hbar\omega/kT)$ to shift $\omega(q)$ away from the scattered intensity peak. We illustrate these effects in Fig. 4 in the reverse of the experimental order of events. Experimentally, one observes the scattered distribution $I_\theta(t)$ and proceeds to unfold the frequencies $\omega(q)$, with due regard to the factors described above and the experimental resolution function. Figure 4a shows the roton creation and annihilation peaks for an energy transfer of $\hbar\omega(q)=6.04$ K as if there were no collisions. Figure 4b shows the effects of Lorentzian broadening, (59) without the factor $\hbar\omega/[1-\exp(-\hbar\omega/kT)]$, corresponding to an observation of DGHP at $T=2.11$ K, $P=1$ atm, where $\hbar\Gamma/k=2.67$ K. The delta functions of Fig. 4a are now broadened and the intensity maximum is shifted to 6.02 K, or down by 0.3%. In Fig. 4c we have included the thermal factor $\hbar\omega/[1-\exp(-\hbar\omega/kT)]$, which almost eliminates the annihilation peak and shifts the intensity maximum to 6.52 K or 8% higher than $\hbar\omega(q)$. Figure 4d shows the added effect of the k_i^4 factor in (57), which leaves the intensity maximum at 6.36 K, or 5.3% higher than $\hbar\omega(q)$. Further adjustment by adding the instrumental resolution function and transforming to the time axis would be required to reproduce the observed spectrum $I_\theta(t)$, but one can already see that the unfolded frequency $\omega(q)$ lies 0.32 K lower than the intensity peak, due principally to the thermal population factor.

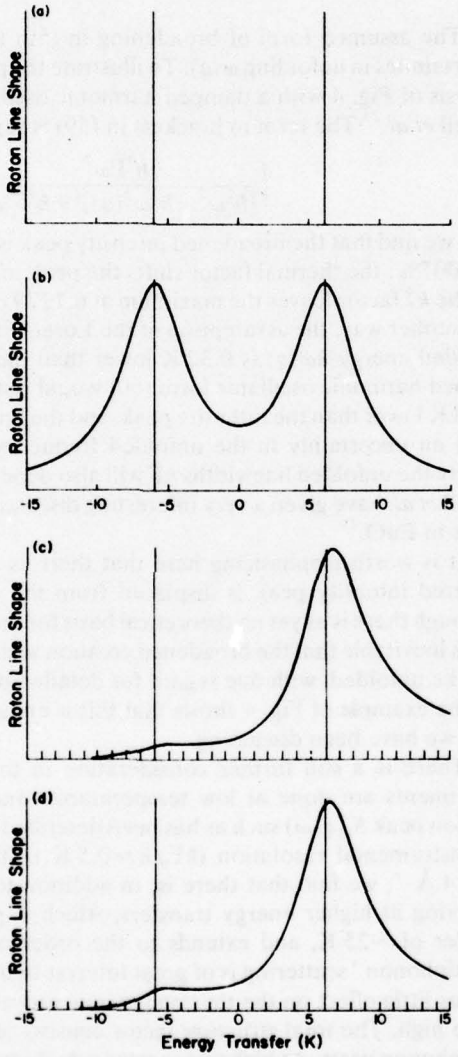

Fig. 4. (a) The line shapes $S(q, \omega)$ at low temperatures, where collisions can be neglected, Eq. (58). (b) Modification of (a) by introducing Lorentzian broadening as in Eq. (59). (c) Further modification of (a) and (b) by introducing the factor $\hbar\omega[1 - \exp(-\hbar\omega/kT)]$ as in Eq. (59). (d) The effect on (c) of adding the factor k_f^4 as in Eq. (57).

The assumed form of broadening in (59) is not unique and leads to uncertainties in unfolding $\omega(q)$. To illustrate the point, we have repeated the analysis of Fig. 4 with a damped harmonic oscillator line shape quoted by Passell *et al.*[23] The term in brackets in (59) is replaced by

$$\left\{\frac{\hbar^3\Gamma\omega^2}{[\hbar^2\omega^2-\hbar^2\omega^2(q)]^2+\hbar^4\Gamma^2\omega^2}\right\} \tag{60}$$

Here we find that the broadened intensity peak is shifted to 6.0404 K, or up by 0.007%; the thermal factor shifts the peak to 6.1657 K, or up by 2.1%; and the k_f^4 factor leaves the maximum at 6.1279 or 1.5% higher than $\hbar\omega(q)$. Put another way, the assumption of the Lorentzian shape in (59) means the unfolded energy $\hbar\omega(q)$ is 0.32 K lower than the intensity peak, while the damped harmonic oscillator form (60) would put the unfolded energy only 0.088 K lower than the intensity peak, and the line shape assumptions alone imply an uncertainty in the unfolded frequency of order 0.23 K or 4%. Clearly the unfolded linewidths $\hbar\Gamma$ will also depend on the assumed shapes. Passell *et al.* have given a very interesting discussion of this problem for spin waves in EuO.[23]

It is worth emphasizing here that there is no mystery as to why the scattered intensity peak is displaced from the underlying energy $\hbar\omega(q)$. Although there is as yet no theoretical basis for the form of $S_I(q,\omega)$ in (59), it seems inevitable that the broadened creation and annihilation contributions must be unfolded, with due regard for detailed balance population factors, and the example of Fig. 4 shows that this is enough to ensure the displacement we have been discussing.

There is a still further consideration in the form of $S(q,\omega)$. When experiments are done at low temperatures, one observes a one-phonon creation peak $S_I(q,\omega)$ such as has been described above, broadened only by the instrumental resolution ($\hbar\Gamma_i/k \approx 0.5$ K in the case of DGHP[9]). For $q \gtrsim 0.4$ Å^{-1}, we find that there is, in addition to the sharp phonon peak, scattering at higher energy transfers, which is peaked around an energy transfer of ~25 K, and extends to the order of 60 K.[8,22] This so-called "multiphonon" scattering is of great interest to the understanding of He II, but has little effect on the thermodynamic properties because the energies are so high. The total structure factor consists of the one-phonon and the multiphonon parts. At high temperatures and pressures, when the widths of the lines are comparable with $\hbar\omega(q)$ itself, the division into one-phonon and multiphonon parts may not be a simple matter.

The "most representative" roton gap is at 1.1 K at the SVP, the conditions adopted for convenience in most preliminary experiments on He II. The neutron determination of Yarnell *et al.*[5] gave $\Delta/k = 8.65 \pm 0.04$ K at 1.1 K, while Cowley and Woods[8] obtained $\Delta/k =$

8.67 ± 0.04 K at the same temperature. DGHP[9] found $\Delta/k = 8.54$ K at $T = 1.26$ K, $P = 1$ atm, which, extrapolated to SVP and $T = 1.1$ K, gives $\Delta/k = 8.66$ K. There is a completely independent way of finding Δ. It is known that Raman scattering from liquid helium at low temperatures gives a peak at 17.022 ± 0.027 K at 1.2 K and 16.97 ± 0.03 K at 0.6 K. This peak is identified by Greytak and his collaborators as a loosely bound state of two rotons.[32,33] An exact quantum mechanical solution to the one model for this state, by Roberts and Pardee,[24] gives the binding energy of the rotons as 0.290 K. Thus the single-roton energy should be $(17.022 + 0.290)/2 = 8.66 \pm 0.02$ at 1.2 K and $(16.97 + 0.29)/2 = 8.63 \pm 0.02$ at 0.6 K, in good agreement with neutron measurements. We note parenthetically that when the linewidth is instrumentally limited ($\hbar\Gamma_i/k \approx 0.5$ K), different assumptions on line shape shift the unfolded peak by less than 0.1%.

5. INTERACTIONS AMONG ELEMENTARY EXCITATIONS IN He II

The evidence from inelastic neutron scattering experiments described in Section 4 is that quasiparticle energies are sharp only at low temperatures. At higher temperatures and pressures, the corresponding peaks, described by $S_t(q, \omega)$, become both broader and shifted downward in energy. The question then is, What can we say about quasiparticle interactions to account for these observations? A recent review of such questions is given in Ref. 22.

Returning to our discussions of Section 2, it is clearly desirable to understand the relationship of $f_{\alpha\beta}$ to the empirically determined departures $\delta\varepsilon_\alpha$ of $\varepsilon_\alpha(\mathbf{n}, P)$ from the zero-temperature energy level $e_\alpha(P)$. To this end, the mode labels α and β appearing in (49) and (50) and the corresponding summations should be understood in a rather general sense. There is danger of error when n_α is regarded as simply the total number of excitations in mode α, for the interaction between two quasiparticles depends not only on their momenta $\mathbf{q}_\alpha$ and $\mathbf{q}_\beta$, but also on their vector separation $\mathbf{r}_\alpha - \mathbf{r}_\beta$. For example, the energy of interaction of two rotons at large distances is often supposed to be dipole–dipole in form,[24,25] i.e.,

$$f_{\alpha\beta} = \frac{\hbar^{-2}V}{4\pi}\left\{\frac{\mathbf{q}_\alpha \cdot \mathbf{q}_\beta}{|\mathbf{r}_\alpha - \mathbf{r}_\beta|^3} - \frac{3[\mathbf{q}_\alpha \cdot (\mathbf{r}_\alpha - \mathbf{r}_\beta)][\mathbf{q}_\beta \cdot (\mathbf{r}_\alpha - \mathbf{r}_\beta)]}{|\mathbf{r}_\alpha - \mathbf{r}_\beta|^5}\right\} \tag{61}$$

It is therefore necessary to regard α as a label describing excitations with momentum $\mathbf{q}_\alpha$ at location $\mathbf{r}_\alpha$ and to extend the series over α and β in (49) and (50) to space (with obvious transitions to integrals when the continuous description is adopted). There is a further complication. The presence of roton $\mathbf{q}_\alpha$ at $\mathbf{r}_\alpha$ tends to polarize the momentum $\mathbf{q}_\beta$ of a second roton lying in

its vicinity at $\mathbf{r}_\beta$. We must then replace (53) by

$$\varepsilon_\alpha(\omega, V) = e_\alpha(V) + \sum_\beta f_{\alpha\beta}\mathcal{F}_2(\mathbf{q}_\alpha, \mathbf{q}_\beta, \mathbf{r}_\alpha, \mathbf{r}_\beta)\omega_\beta \tag{62}$$

where $\mathcal{F}_2$ is the conditional probability density that a quasiparticle $\mathbf{q}_\beta$ is situated at $\mathbf{r}_\beta$ when another with momentum $\mathbf{q}_\alpha$ lies at $\mathbf{r}_\alpha$. (For rotons, $\mathcal{F}_2$ is given to sufficient accuracy by a Maxwell–Boltzmann factor incorporating the interaction potential.) The evaluation of expressions such as (62) is the principal thrust of dielectric theory. For example, the recent calculations of Titulaer and Deutch,[26] developing an earlier theory by Feynman,[27] and of Donnelly and Roberts[28] gave for the roton energy gap

$$\Delta(T, P) = \Delta(0, P) + \frac{p_0^2}{16\pi\rho a^3}\frac{\varepsilon - 1}{2\varepsilon + 1} \tag{63}$$

where a (≈ 1.98 Å at $P = 0$) is a hard-core cutoff for the dipole interaction (61) and $\varepsilon = \rho_s/\rho$ is the effective dielectric constant. The agreement between (63) and experiment is impressive. One notes, for example, that at sufficiently low temperatures, for which $2\varepsilon + 1 \approx 3$, (63)

$$\delta\Delta = \Delta(T, P) - \Delta(0, P) = (-p_0^2/48\pi\rho^2 a^3)\rho_n \tag{64}$$

which is hard to distinguish from the empirical result of Donnelly,[29] who postulated that $\delta\Delta$ is proportional to $\rho_n T/\rho$.

It is possible, as this result by Titulaer and Deutch shows, to postulate an $f_{\alpha\beta}$ such as a cutoff version of (61), and to compute a corresponding $\delta\varepsilon_\alpha$ against temperature. It is considerably harder to reverse the process, i.e., to use an experimentally determined $\varepsilon_\alpha(T)$ to determine the form of $f_{\alpha\beta}$ and we make no attempt to do so here. We note, however, that by postulating the form (7) we have side-stepped some of the difficulties associated with the "dielectric" properties of the fluid, without sacrificing the essential idea of Fermi liquid theory, namely that quasiparticle interactions should be recognized by the quadratic terms in the expansion (49); see (53).

The considerations above make it plausible that energy should depend upon temperature. Physically, for rotons, we picture an individual roton producing a dipolar flow which tends to polarize surrounding rotons; the surrounding rotons react back on the original roton to produce a reverse flow, which lowers its energy by the $\mathbf{p} \cdot \mathbf{v}_s$ interaction. The higher the temperature, the greater the number of neighboring rotons, and hence the greater the "Onsager reaction flow" and correspondingly the greater the lowering of the energy.[10]

What can we say about the observed line broadening? This problem has been considered by Roberts and Donnelly by modeling rotons as point doublets with the dipole moment of rotons obeying the dynamics dictated by

the Landau roton dispersion parabola.[25] Working from this Hamiltonian, they have developed equations of motion for colliding rotons. For the case of zero total momentum, they are able to find the critical impact parameter dividing forward and backward scattering, and hence to estimate the roton–roton scattering cross section to be given by

$$\sigma = \pi\Gamma(\tfrac{1}{3})(p_0^2/8\pi\rho kT)^{2/3} \tag{65}$$

where $\Gamma(\frac{1}{3}) = 2.679$. The average collision frequency for rotons experiencing large-angle collisions is

$$\tau^{-1} = (2kT/\mu)^{1/2}\sigma N_r \tag{66}$$

where N_r is the number density of rotons, and the linewidths (2Γ) may be estimated by the uncertainty principle as $\hbar/k\tau$. Using the result of DGHP[9] that $p_0/\hbar = 3.64\rho^{1/3}$ Å^{-1}, they find the half-width $\hbar\Gamma/k$ to be given by

$$\hbar\Gamma/k = 6.50\times 10^{-34} N_r/\mu^{1/2}\rho^{2/9}T^{1/6} \tag{67}$$

The agreement is quite satisfactory (see Table III), considering: (a) the unfolding difficulties discussed in Section 4—the unfolded values of $\hbar\Gamma$ are sensitive to the assumed line shape; and (b) the theory does not predict a line shape and uses a simple uncertainty argument to obtain the quoted

TABLE III

Comparison of Unfolded Linewidths $\hbar\Gamma/k$ (HWHM) (Reported by DGHP[9]) with the Expression of Roberts and Donnelly, Eq. (67)[25]

P, atm	T, K	$(\hbar\Gamma/k)_{obs}$, K	$(\hbar\Gamma/k)_{calc}$, K
1	2.11	2.7	2.1
1	2.13	3.1	2.3
1	2.15	3.5	2.5
5	1.68	0.7	0.59
5	1.82	1.2	0.99
5	2.05	2.6	2.2
10	1.68	0.81	0.70
10	1.81	1.5	1.2
10	2.00	2.8	2.3
15	1.68	0.93	0.90
15	1.82	1.6	1.5
15	1.95	2.8	2.5
20	1.47	0.7	0.48
20	1.68	1.3	1.1
20	1.90	2.8	2.6
24	1.46	0.7	0.58
24	1.67	1.6	1.4
24	1.82	2.6	2.9

linewidths. Much larger linewidths have been reported by Henshaw and Woods at the vapor pressure, exhibiting a quite different temperature dependence.[30] DGHP[9] have observed that this discrepancy arises because Henshaw and Woods were reporting observed linewidths rather than unfolded linewidths.

Neutron linewidths are often estimated by using the Landau–Khalatnikov roton collision formula, which results from assuming a δ-function interaction for the rotons of amplitude V_0:

$$\tau^{-1} = 2p_0\mu |V_0|^2 N_r \hbar^{-4} \tag{68}$$

where Khalatnikov[31] reports $|V_0|$ to be about 1.9×10^{-38} erg cm^3 from comparison with viscosity data. Generally $|V_0|$ is estimated by a fit to linewidth data. By combining (66) and (68) it is possible to estimate $|V_0|$ from the Roberts–Donnelly approach and give the pressure dependence as well:

$$|V_0|^2 = \frac{\pi\Gamma(\frac{1}{3})\hbar^4}{2p_0\mu}\left(\frac{2kT}{\mu}\right)^{1/2}\left(\frac{p_0^2}{8\pi\rho kT}\right)^{2/3} \tag{69}$$

We list in Table IV values of the pseudopotential $|V_0|$ for future reference at a number of pressures. Its temperature dependence is not great.

Measurements of the linewidth of two-roton bound states[32] are in reasonable accord with neutron linewidths (cf. Fig. 14 of DGHP[9]). At $P = 0$, the observed Raman widths correspond to $|V_0| = 1.73\times10^{-38}$ erg cm^3. The agreement with the value from Table IV is certainly satisfactory, but may be fortuitous: The collision that breaks up the bound state at higher temperatures must be between a roton and the bound pair of rotons. The dynamics of such a collision is likely quite different from that between two rotons. Indeed at 0.6 K, (67) would give a very small linewidth for the collisions, whereas Murray *et al.*[33] report a width of 0.11 K.

It is the general agreement between observed unfolded line widths as shown in Table III and the theory of roton collisions which supports the idea that the broadening of the one-phonon peaks is principally due to collisions, which should produce symmetric broadening. If that is true, then there is some hope that representative sharp frequencies for the phonons might exist.

TABLE IV

Values of the Landau–Khalatnikov Pseudopotential $|V_0|$ for Roton Collisions at 1.2 K

P, atm	0	5	10	15	20	25
$10^{38}\|V_0\|$, erg cm^3	2.69	2.72	2.77	2.82	2.88	2.95

6. COMPARISON OF THE FORMULAS OF TABLE II WITH EXPERIMENT

In order to appreciate the force of the formulas introduced in Section 2, note that by integrating (21) for the entropy over T for fixed P we may write the Gibbs free energy as

$$\Phi = \Phi_0(P) - \frac{kTV}{2\pi^2}\int_0^\infty \ln(1+n)q^2\,dq - \frac{V}{2\pi^2}\int_0^T\int_0^\infty n\left(\frac{\partial\varepsilon}{\partial T}\right)_{P,q} dT\,q^2\,dq \tag{70}$$

a form which clearly separates the classical expression, the first two terms of (70), and the present theory, which includes the third term in $\partial\varepsilon/\partial T$.

To compare the two possibilities, let us calculate $S = -(\partial\Phi/\partial T)_P$ from (70) using neutron scattering data at the vapor pressure. We construct model dispersion curves according to the Brooks–Donnelly scheme of the appendix using the data of Yarnell *et al.*[5] and Henshaw and Woods.[30] The roton energies from these references have been smoothed by a power series in N_r and are presented in Table V. The resulting dispersion curves are as close to the available neutron data as present methods permit.

If we calculate the entropy from the full expression of (70), we obtain the middle curve of Fig. 5, which is seen to be in excellent agreement with the thermodynamically determined entropy of Van den Meijdenberg *et al.*[37] The classical expression for entropy comes from omitting the final term of (70) and using dispersion curve parameters for $T = 0$, which we call ε^0. The result is the lower curve of Fig. 5, which is seen to depart systematically from the data. It might be tempting to use the finite-temperature parameters as a way of "improving" the classical expression for Φ. Such a procedure is obviously mathematically inconsistent; that it is physically of no aid is seen by noting that the upper curve of Fig. 5 results, which also departs systematically from the thermodynamic data.

A similar test may be made with the equation of state, as shown by Fig. 6. The correct expression for the molar volume V is given by (24). If ε_α is independent of T, we have shown that (31) results, which in continuous variables reads

$$V = V_0(P) + \frac{V}{2\pi^2}\int_0^\infty n\left[\left(\frac{\partial\varepsilon}{\partial P}\right)_q + \frac{\kappa q}{3}\left(\frac{\partial\varepsilon}{\partial q}\right)_P\right]q^2\,dq \tag{71}$$

TABLE V

Neutron Determined Values of Δ/k at the Vapor Pressure, from the Data of Refs. 5 and 30, Smoothed

T, K	1.0	1.1	1.2	1.3	1.4	1.5	1.6	1.7	1.8	1.9	2.0	2.1
Δ/k, K	8.614	8.608	8.596	8.577	8.548	8.503	8.444	8.355	8.220	8.006	7.615	6.827

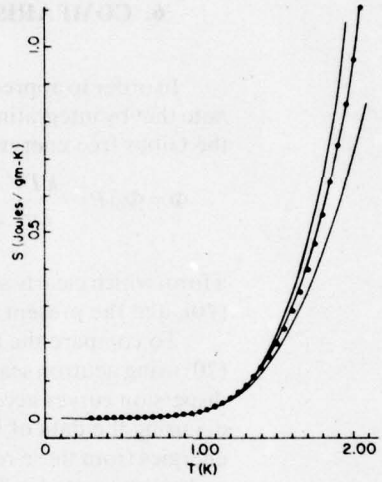

Fig. 5. Experimental data on entropy (Ref. 37) compared to the entropy derived from the new expression for free energy (70) (middle curve), the classical expression consisting of the first two terms of (70) with dispersion parameters at $T = 0$ (lower curve), and the classical expression with finite temperature dispersion data (upper curve).

Here we are at a considerable disadvantage because (24) and (71) require knowledge of $(\partial\varepsilon/\partial P)_q$, which cannot be extracted from existing data at the vapor pressure with satisfactory accuracy. We have, therefore, used a fit to the DGHP[9] neutron data that appears in Eqs. (11) and (12) of Ref. 4 to construct model dispersion curves at $P = 7.5$ atm. The middle curve of Fig. 6 is calculated from our new equation of state, (24). It lies satisfactorily close to the empirical equation of state of Brooks, which is a best fit to all published experimental data on molar volume (some of which are in mutual conflict[11]). Equation (71) has been used to generate the upper curve, which clearly varies too slowly with temperature, and the attempt to use temperature-dependent parameters in an inconsistent way in (71) produces the lower curve, which varies too rapidly with temperature. While the accuracy of these data is not as good as for the entropy, an extensive numerical investigation supports the conclusion that the formulas of Table II are in considerably better agreement with experimental neutron and thermodynamic data than the classical ones, and that a very practical advance has been made in dealing with temperature-dependent energy levels.

While the tests described above indicate that the temperature dependence can be successfully dealt with, there remains a problem when the linewidth becomes large. This is best illustrated in Fig. 7, which shows the entropy calculated from (21) compared with the experimentally determined entropy. Using the neutron data of DGHP[9] to generate the dispersion curves, one can see that at high temperatures and pressures, the calculated entropy lies significantly higher than the measured entropy whenever the

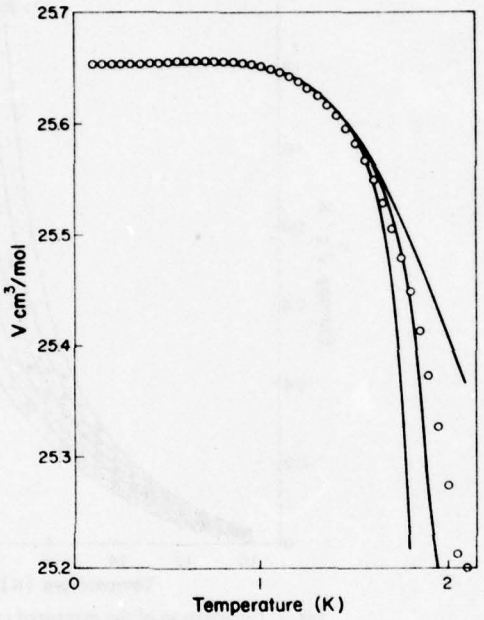

Fig. 6. Molar volume of He II at $P = 7.5$ atm according to the empirical equation of state of Brooks,[11] compared to that derived from the new expression for the molar volume (24) (middle curve). The upper curve is the classical expression (71) with dispersion parameters at $T = 0$. The lower curve is (71) with finite-temperature dispersion data.

lines broaden significantly, as tabulated in Table III. DGHP have noted the same trend in Fig. 17 of their paper[9] (although they performed an extra integration over the linewidth). The molar volume results such as are shown in Fig. 6 become progressively less accurate as the pressure increases.

The question may be asked: Considering how successful the thermodynamic analysis of BCY[6] and indeed our analyses of Figs. 5 and 6 are, why is it that the deconvolved energy levels of DGHP[9] give such poor agreement? There appear to be two reasons for this: First, experiments at the vapor pressure have the smallest linewidth, and hence are least liable to corrections from the effects discussed in Section 4; and second, the DGHP scattering data have been unfolded with the assumed Lorentzian line shape of (59), which, as we have shown, shifts the frequency $\omega(q)$ from the observed intensity maximum. The earlier data on which Table V is based were not subject to such an analysis.

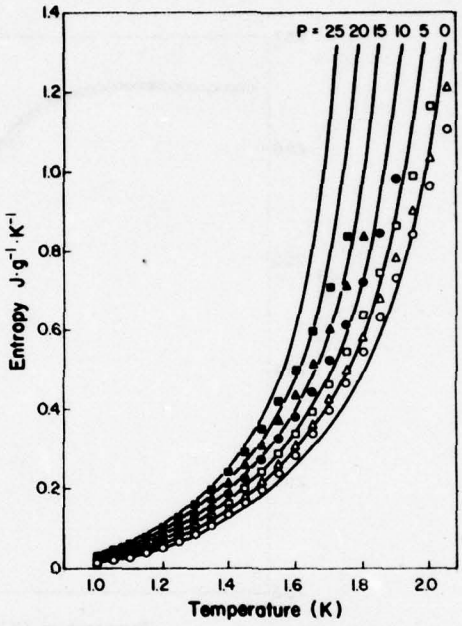

Fig. 7. Comparison of the measured entropy of van den Meijdenberg *et al.*[37] compared with calculations based on Eq. (21) with model dispersion curves generated from the neutron data of DGHP.[9] The calculated entropy (solid lines) lie significantly higher than the data at the higher temperatures and pressures. (○) $P = 0$, (△) $P = 5$, (□) $P = 10$, (●) $P = 15$, (▲) $P = 20$, (■) $P = 25$ atm.

7. AN EFFECTIVE SHARP SPECTRUM FOR THERMODYNAMICS

Since the failure of the neutron data to yield thermodynamically significant energies occurs at higher temperatures and pressures, it is likely that the origin of the discrepancy is uncertainty in the exact energy of the roton minimum. Brooks[11] was the first to suggest that because of the exponential dependence of most quantities on the roton gap, a relatively small adjustment of Δ, keeping all other parts of the dispersion curve the same, could bring the calculated and experimental data into mutual accord. The precise value of μ comes from Δ through the relationship quoted in the appendix. This spectrum assumes that there is some effective sharp frequency (that is, $\Gamma \to 0$) for each value of q; since there is but one adjustment,

the resulting effective spectrum is unique. The effective spectrum at $P = 0$ appears in the appendix and for all P and T in Ref. 4. An extensive numerical investigation has demonstrated the great utility of such a spectrum. We have found:

1. The effective spectrum is capable of yielding accurate thermodynamic results over all pressures, and temperatures to within 0.1 K of $T_\lambda(P)$. All quantities calculated from Table II and this spectrum appear to be in reasonable agreement with experiment, as detailed in Ref. 4.

2. The effective spectrum is consistent with the observed functional form of the spectrum obtained by neutron scattering. It coincides with the neutron spectrum within experimental error at low temperatures, and at high temperatures the difference between the observed and effective values of Δ is less than $\hbar\Gamma$. This is illustrated in Fig. 8.

3. Since the effective spectrum is unique, an exact value of Δ can be chosen by reference to more than one thermodynamic quantity. We have used entropy, expansion coefficient, and normal fluid density.

4. The points listed above and the discussion of interactions in Section 5 allow one to guess that the effective spectrum is probably a reasonable representation of the energies of the elementary excitations of He II.

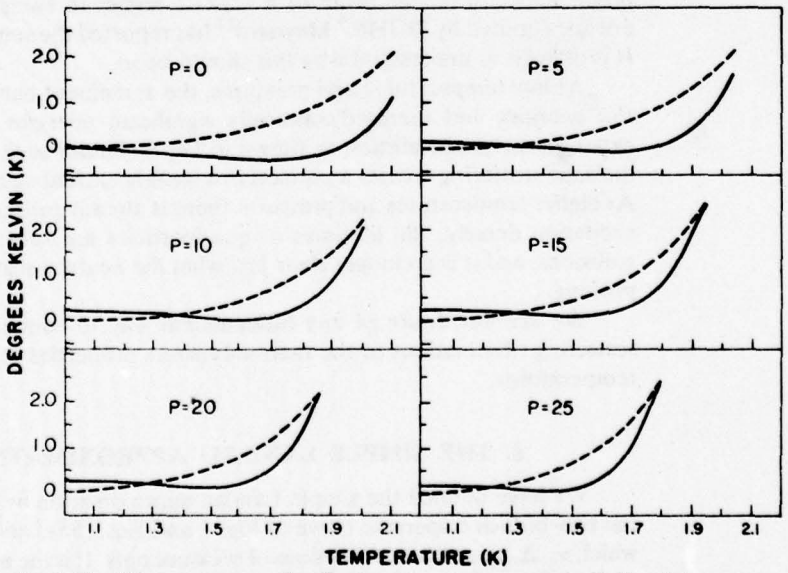

Fig. 8. The difference between the effective roton energy parameter Δ_r/k and the neutron parameter Δ/k (solid lines). The dashed lines are calculations of the half-width $\hbar\Gamma/k$, based on Eq. (67).

The reader may well object that if the spectrum is adjusted to fit the entropy at all temperatures and pressures, Maxwell's equations are sufficient to guarantee the consistency of much of the other thermodynamic data, including the expansion coefficient. The answer to this objection comes by noting that the adjustment concerns only the precise value of one constraint, Δ, on the dispersion curve. At higher temperatures there is substantial occupation of states over most of the dispersion curve, so that it is unlikely that terms such as $\partial\varepsilon/\partial P$ and $\partial\varepsilon/\partial q$ in Table II could accidentally work successfully over such a large part of momentum space. Further, as we have emphasized in Section 3, the representation of the dispersion curve may be accomplished in a number of different ways. We discuss in Section 10 an alternative scheme, which, although quite different in its emphasis and details, yields quite similar results.

DGHP have noted that the thermal weighting factor is the principal cause of the shift of observed frequencies compared to earlier neutron data, and we have illustrated how this comes about in Fig. 4. We have made estimates of the effect of omitting this factor on the quoted roton energies, and it appears that the effective roton energies lie closer to the peaks of the original spectra (of the order of $\hbar^2\Gamma^2/2kT$ higher in energy) than do the energies quoted by DGHP.[9] Maynard[13] has reported the same observation. It is difficult to understand why this should be so.

At low temperatures and pressures, the agreement between the neutron energies and thermodynamically significant energies is well within experimental uncertainties, as shown in Fig. 8. Under such conditions the inelastic scattering creates a phonon in a weakly excited state of the liquid. At higher temperatures and pressures there is already present a substantial excitation density, the lifetimes of quasiparticles are severely limited by collisions, and it is no longer clear just what the neutron scattering event is probing.

We are not aware of any fundamental way to connect the neutron scattering observations to the thermodynamic properties of He II at finite temperatures.

8. THE SIMPLE LANDAU APPROXIMATION

We have defined the simple Landau approximation as a theory using the two-branch dispersion curve of Fig. 1 and Eqs. (55a) and (55b), and in which u_1, Δ, p_0, and μ are functions of pressure only. It is the most frequently used method of obtaining information on the thermodynamics of He II. As we have remarked above, the only consistent parameters to be used are those for $T=0$ when temperature dependence is to be neglected. The relevant parameters are taken from the tables of Brooks and Donnelly for

$T = 0.1$ K, the lowest calculated temperature.[4] We list these parameters in Table VI for the convenience of those using the simple Landau approximation, together with the formulas for the phonon and roton contributions to the excitation density, entropy, specific heat, expansion coefficient, and normal fluid density. Values of Δ in Table VI were obtained by extrapolating neutron scattering and effective spectrum data from higher temperatures. As we shall see, the values of $\partial\Delta/\partial P$ are not well-behaved, but at present there is no way of knowing values of Δ at $T = 0$ more accurately, nor what function of pressure they should be.

The advantage of the simple Landau approximation is its ability to illustrate the physics at hand in a compact way. One of the motivations for our investigation has been the observation that plots of the molar volume V are roughly linear when displayed as a function of the number of phonons per mole ($n_{ph} = N_{ph}V$) at low temperatures, and the number of rotons per mole ($n_r = N_rV$) at high temperatures, as shown in Figs. 9a and 9b. These data suggest that the addition of a phonon will change the molar volume by

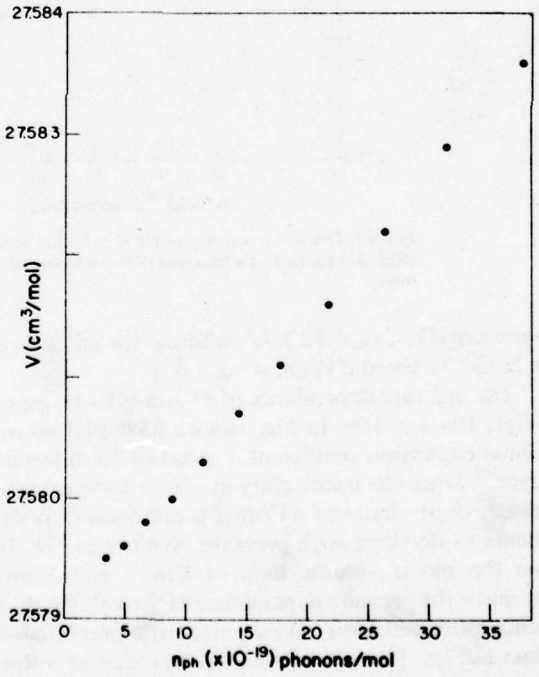

Fig. 9a. The molar volume of He II at low temperature (Ref. 42) plotted as a function of the number of phonons per mole.

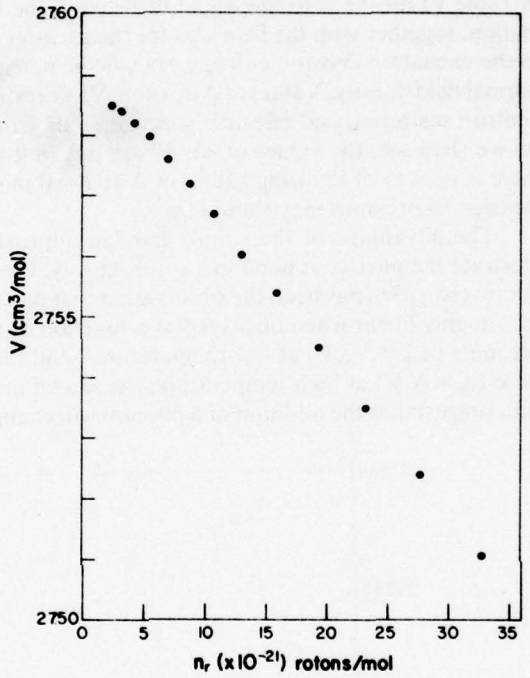

Fig. 9b. The molar volume of He II at higher temperatures (Ref. 42) plotted as a function of the number of rotons per mole.

an amount $dV/dn_{ph} = 12.8$ Å^3, whereas the addition of a roton will contract the liquid by about $dV/dn_r = -2.5$ Å^3.

The pressure dependence of dV/dn in two temperature ranges is shown in Figs. 10a and 10b. In Fig. 10a we have plotted $\alpha(dT/dN_{ph})$, where the thermal expansion coefficient α is taken from the data of Boghosian and Meyer.[38] Since the uncertainty in α is in some cases as large as α itself, the pressure dependence of dV/dn_{ph} is not accurately determined, although it appears to decrease with pressure. We see in Fig. 10b similar data taken from the molar volume data of Elwell and Meyer[39] and analyzed to determine the pressure dependence of the volume change on adding a roton. Within estimated error, dV/dn_r rises with pressure for rotons. The absolute values in Figs. 10a and 10b should be received with caution. For example, determination of dV/dn_r from expansion coefficients gives a similar pressure dependence, but all values are about 1 Å^3 larger than those determined graphically. At $P = 0$, the molar volume result shown in Fig. 9a is 3 Å^3 higher

TABLE VI

Landau Parameters at Absolute Zero and Thermodynamic Formulas for Phonons and Rotons

P, atm	0	2.5	5.0	7.5	10.0	12.5	15.0	17.5	20.0	22.5	25.0
Δ, K[a]	8.712	8.573	8.380	8.189	8.019	7.868	7.732	7.602	7.473	7.343	7.210
μ, m	0.1608	0.1580	0.1543	0.1507	0.1474	0.1445	0.1419	0.1394	0.1369	0.1344	0.1319
q_0, Å^{-1}	1.913	1.931	1.946	1.960	1.972	1.983	1.993	2.002	2.010	2.019	2.026
u_1, m/sec	238.21	257.46	274.22	289.16	302.71	315.15	326.69	337.47	347.60	357.18	366.27
ρ, g/cm^3	0.14513	0.14925	0.15284	0.15603	0.15892	0.16157	0.16403	0.16633	0.16849	0.17053	0.17246
$10^6\kappa$	1.214	1.011	0.8701	0.7665	0.6867	0.6232	0.5712	0.5279	0.4912	0.4597	0.4322

Phonon properties

$$N_{ph} = \pi^{-2}(kT/\hbar u_1)^3\zeta(3), \qquad S_{ph} = [2\pi^4/45\zeta(3)]kVN_{ph}, \qquad C_{ph} = [2\pi^4/15\zeta(3)]kVN_{ph}$$

$$\alpha_{ph} = (16\pi^2k^4T^3/15\hbar^3u_1^3V)[(1/u_1)(\partial u_1/\partial P)_T + \tfrac{1}{3}\kappa]$$

$$\rho_{n\,ph} = [2\pi^4kT/45u_1^2\zeta(3)]N_{ph}, \qquad \zeta(3) = 1.202$$

Roton properties

$$N_r = [2(\mu kT)^{1/2}p_0^2/(2\pi)^{3/2}\hbar^3]\,e^{-\Delta/kT}$$

$$S_r = kVN_r[\tfrac{3}{2} + (\Delta/kT)], \qquad C_r = kVN_r[\tfrac{3}{4} + (\Delta/kT) + (\Delta/kT)^2]$$

$$\alpha_r = -\kappa N_r k\left(\frac{\Delta}{kT} + \frac{3}{2}\right)\left[\frac{1}{2}\frac{\rho}{\mu}\frac{\partial\mu}{\partial\rho} + 2\frac{\rho}{p_0}\frac{\partial p_0}{\partial\rho} - 1 - \frac{\rho}{kT}\frac{\partial\Delta}{\partial\rho}\frac{(\Delta/kT)+\frac{1}{2}}{(\Delta/kT)+\frac{3}{2}}\right]$$

$$\rho_{n,r} = (p_0^2/3kT)N_r$$

[a] Derivatives $\partial\Delta/\partial\rho$ not reliable.

than that determined by expansion coefficients shown in Fig. 10a. The error bars are merely indications of graphical uncertainties.

In the Landau approximation, the long-wavelength part of the spectrum is given by $\varepsilon = u_1 p = u_1 \hbar q$. Now the population of thermal phonons is large near $q = 0.1$ Å^{-1}, where the quantity $\delta\varepsilon/\delta P = \hbar q\, \delta u_1/\delta P \doteq 8$ Å^3 for $T < 1$ K. Similarly, in the roton region, the quantity $\delta\varepsilon/\delta P = \delta\Delta/\delta P \doteq -8$ Å^3 at $T = 1.6$ K. These difference quotients are of the right dimensions, magnitude, and sign to be connected with our observations on thermal expansion. Donnelly[10] postulated from these considerations that the volume change per excitation is equal to the partial derivative $(\delta\varepsilon_\alpha/\delta P)_T$ for each excitation α of the system. In the present notation, his postulate reads

$$\left(\frac{\partial V}{\partial n_\alpha}\right)_{T,P} = \left(\frac{\partial \varepsilon_\alpha}{\partial P}\right)_{T,n_\alpha} \tag{72}$$

[see (43)].

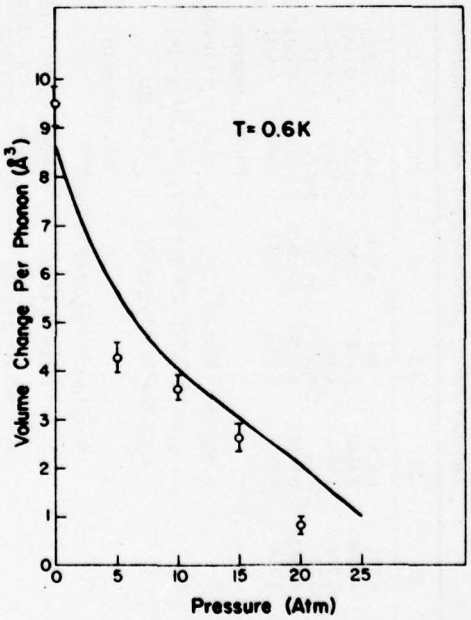

Fig. 10a. The pressure dependence of dV/dn_{ph} from experiment (Ref. 39) and from Eq. (80). Experimental uncertainties are larger than the limits shown, as discussed in the text. The solid line is the result of the simple Landau approximation, Eq. (80).

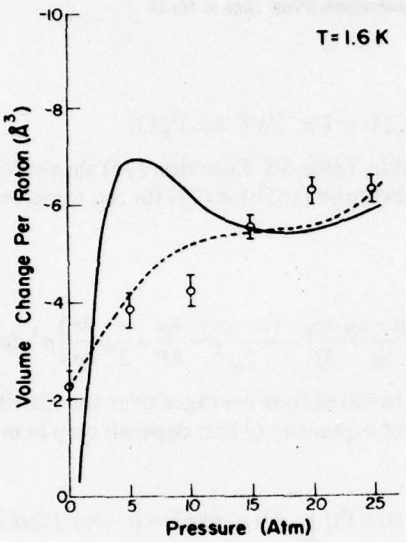

Fig. 10b. The pressure dependence of dV/dn, from experiment (Ref. 38), as discussed in the text. The solid line is the result of the simple Landau approximation, Eq. (80). The maximum is a reflection of uncertainties in the quantity $\partial\Delta/\partial P$ in Table VI. The dashed line is from the exact expression (24).

Making the passage to continuous variables as in the discussion above (27), we recognize that the right-hand side must be $(\partial\varepsilon/\partial P)_{T,n}$, and hence

$$\left(\frac{\partial V}{\partial n}\right)_{T,P} = \left(\frac{\partial \varepsilon}{\partial P}\right)_{T,q} + \frac{1}{3}\kappa q\left(\frac{\partial \varepsilon}{\partial q}\right)_{T,P} \tag{73}$$

The first term on the right appears to be consistent on dimensional grounds; the second, which is much less familiar, may be thought of as due to the excitation pressure increase on adding a phonon. [The second term was recognized by Donnelly, but not as an automatic consequence of (72).] Following a lecture at Caltech in which the postulate above was described by one of us (R.J.D.), Feynman suggested the external field argument stated in Section 2 and subsequently published by Goodstein *et al.*,[16] which puts (72) on a firmer theoretical basis. We have observed in Section 2 that if ε_α is independent of T, (72) can be used to compute the molar volume as in (31) and this leads to (71). When ε_α does depend on T, this simple idea fails and our new expression (24) must be used.

Substituting (55a) in (71) for the phonon branch, we find

$$\begin{aligned} V &= V_0(P) + \frac{V(kT)^4}{(\hbar u_1)^3}\frac{\pi^2}{30}\left(\frac{1}{u_1}\frac{\partial u_1}{\partial P} + \frac{1}{3}\kappa\right) \\ &= V_0(P) + \frac{\pi^4 kT}{30\zeta(3)}\left(\frac{1}{u_1}\frac{\partial u_1}{\partial P} + \frac{1}{3}\kappa\right) n_{\text{ph}} \end{aligned} \tag{74}$$

where

$$n_{ph} = N_{ph} V = V\pi^{-2}(kT/\hbar u_1)^3 \zeta(3) \tag{75}$$

and N_{ph} and $\zeta(3)$ are defined in Table VI. Equation (74) shows at once the linearity noted in Fig. 9a. Substituting (55b) in (71) for the roton branch, we find

$$V = V_0(P) + \frac{V}{2\pi^2\hbar^3} \times \int_0^\infty n\left[\frac{\partial\Delta}{\partial P} - \frac{p-p_0}{\mu}\frac{\partial p_0}{\partial P} - \frac{(p-p_0)^2}{2\mu^2}\frac{\partial\mu}{\partial P} + \frac{\kappa}{3}p\frac{\partial\varepsilon}{\partial p}\right]p^2\,dp \tag{76}$$

The right-hand side of (76) involves four averages over the distribution n. We note that the average $\bar{Q}$ of a quantity Q that depends on $\mathbf{p}$ in magnitude but not direction is

$$\bar{Q} = \int nQ\,d^3p = 4\pi[\exp(-\Delta/kT)]\int_0^\infty Q(p)\exp[-(p-p_0)^2/2\mu kT]p^2\,dp \tag{77}$$

where we have used the Boltzmann distribution for n, a legitimate step since $kT \ll p_0^2/\mu$. In the same approximation we may, with an error of order $\exp(-p_0^2/2\mu kT)$, replace the lower limit of (77) by $-\infty$. By expanding p^2Q in a power series about $p = p_0$, we then obtain an expression for $\bar{Q}$ in powers of $\mu kT/p_0^2$, the first nonvanishing terms of which are

$$\bar{Q} = h^3 N_r\left\{Q(p_0) + \frac{1}{2}\left[\frac{d^2}{dp^2}(p^2Q)\right]_{p=p_0}\frac{\mu kT}{p_0^2} + \cdots\right\} \tag{78}$$

Applied to the four terms of (76), only the first corresponds to nonzero $Q(p_0)$, and for the remaining three the second term of (78) is required. We obtain to leading order

$$V = V_0(P) + \left(\frac{\partial\Delta}{\partial P} - \frac{2}{p_0}\frac{\partial p_0}{\partial P}kT - \frac{1}{2\mu}\frac{\partial\mu}{\partial P}kT + \kappa kT\right)n_r \tag{79}$$

showing the linearity in $n_r = N_r V$ noted in Fig. 9b. Continuing to ignore variations of p_0, μ, Δ, and u_1 with T, when evaluating $\partial N_r/\partial T$, we obtain the expression for the expansion coefficient listed in Table VI which coincides exactly with the expression obtained by Atkins and Edwards.[40] Of course, α may also be obtained directly from (25) as well.

If we consider the entire spectrum to be given by (55a) and (55b), then the total change in volume $\delta V = V - V_0(P)$ may be written

$$\delta V = \left(\frac{\partial V}{\partial n_{ph}}\right)n_{ph} + \left(\frac{\partial V}{\partial n_r}\right)n_r \tag{80}$$

assuming n_{ph} and n_r are small. We see from (80) that strict linearity of δV in n_{ph} will only occur at very low temperatures where $N_r \ll N_{ph}$, and conversely for rotons at high temperatures.

We show as solid lines in Figs. 10a and 10b the calculations of $\delta V/\delta n_{ph}$ and $\delta V/\delta n_r$ obtained from (74), (79), and (80) with $\delta V \simeq V - V_0(P)$ and $\delta n_{ph} = n_{ph}$, etc. They lend some support to Donnelly's original idea of a certain volume per added excitation, and account for the general magnitude and sign of the results. Note that the calculated maximum in Fig. 10b is due to problems in the derivative $(\partial V/\partial P)_{T=0}$ mentioned in connection with the data of Table VI. We show as the dashed line in Fig. 10b $\delta V/\delta n_r$ as computed from the generalized Landau approximation and Eq. (24), the latter being our exact result, which does not use the assumption (31).

The changes in volume δV per quasiparticle are really quite large if one realizes the atomic volume of He II is 45 Å^3 at $P = 0$. At finite pressures, the addition of a phonon will be accompanied by work done by the external source of an amount $P\,\delta V$. For example, if $P = 10$ atm, $\delta V \simeq 4$ Å^3, $P\,\delta V/k = 0.29$ K. Early in our work we had speculated that such corrections to the energy transfer might be needed at finite pressures to obtain correct values of ε_α. The discussion of Section 2 shows that this is not so: ε_α is exactly the energy transfer to the fluid at constant pressure, (46), and is the same ε_α as enters the expressions for the internal energy of the fluid in (1) and (2).

Let us now turn to the assessment of how well the simple Landau theory works for thermodynamic properties. We show in Fig. 11a the entropy calculated from the expressions and values of Table VI, on a logarithmic plot from 0.25 to 2.0 K at $P = 0$. We see that below 1 K the calculated entropy lies somewhat higher than the tabulated entropy. This is because of positive phonon dispersion, a detail which is, of course, absent with a simple phonon branch, Eq. (3a). Above 1 K the simple Landau theory falls progressively lower because the actual roton energy levels are decreasing with increasing temperature. In order to appreciate the magnitude of the discrepancy, we show in Fig. 11b a linear plot of the entropy, which shows that the simple Landau theory is low by 21% at 1.5 K, 33% at 1.9 K, and 42% at 2.05 K. The normal fluid density shows much the same behavior at $P = 0$ and similar discrepancies are present at higher pressures for both quantities.

The discussion of this section shows that the simple Landau approximation is still a useful tool for preliminary analyses of new problems and general orders of magnitude. It should no longer be regarded as having any quantitative significance.

9. THE GENERALIZED LANDAU APPROXIMATION

By the "generalized Landau approximation" we mean a scheme of calculation using a full representation of the dispersion curve, with

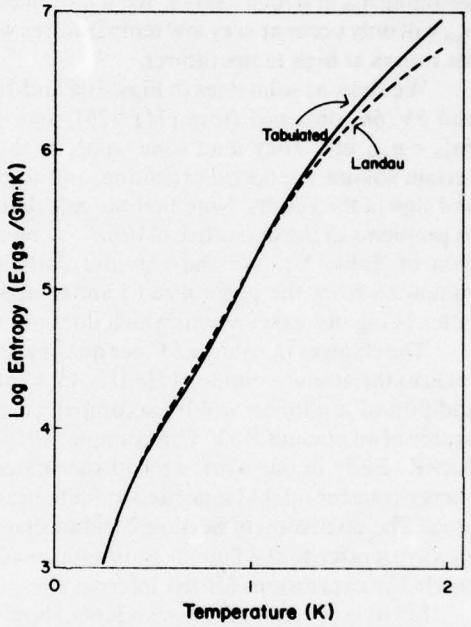

Fig. 11a. The logarithm of the entropy $S_{ph} + S_r$ calculated from the simple Landau approximation as shown in Table VI. The tabulated data are from Ref. 4.

temperature- and pressure-dependent parameters. It is still an approximation because it does not take into account the details of the observed energy levels, such as their linewidths, and because (at least at higher T and P) we need to use the effective spectrum. In spite of these deficiencies, a remarkable amount of information can be calculated from this approximation, using, for example, the coefficients of the model dispersion curves tabulated in Ref. 4.

We show in Fig. 12 the phase velocity ω/q as a function of q for several pressures. We see that the model curve exhibits positive dispersion below 10 atm and is in satisfactory agreement with the data. The low-temperature specific heat is displayed in Fig. 13, and again the effects of dispersion at low temperatures and pressures is seen, and the calculations are in satisfactory agreement with calorimetric data.

We illustrate in Figs. 14–16 the entropy, normal fluid fraction, and expansion coefficient, which again are all in quite reasonable agreement with the experimental data shown. The generalized Landau approximation, together with the formulas of Table II for temperature-dependent energy

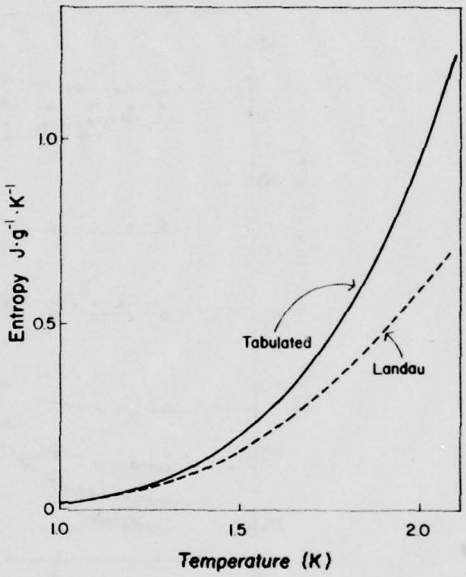

Fig. 11b. A linear plot of the entropy shown in Fig. 11a above 1 K.

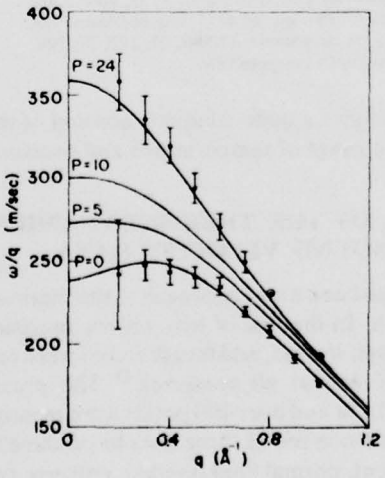

Fig. 12. The phase velocity at 1.2 K for various pressures using the series representation of Brooks and Donnelly.[4] The neutron measurements are: (●) Svensson *et al.*,[34] P = 24 atm; (⊙) Henshaw and Woods,[30] P = 25 atm; (×) Cowley and Woods,[8] $P = 0$ atm. Note that the positive dispersion is greatest at $P = 0$, is nearly absent at $P = 10$, and is completely absent at $P = 24$ atm.

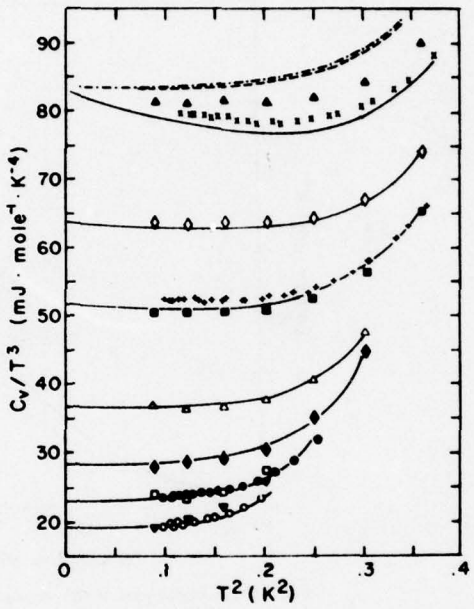

Fig. 13. The specific heat C_V/T^3 as a function of T^2. The solid lines are calculated from the series representation at the pressures (from top to bottom) $P = 0$, 2.5, 5, 10, 15, 20, and 25 atm. The symbols ▲, ◇, ■, △, ◆, □, and ▼ represent the data of Wiebes[35] and are the above respective pressures. The symbols ×, +, ●, and ○ are from the data of Phillips *et al.*[36] and represent the corresponding molar volume 27.580, 26.277, 23.790, and 27.128 cm^3/mole, respectively.

levels, appears to be able to give a quite adequate account of the properties of He II over a remarkable range of temperatures and pressures.

10. DETERMINATION OF THE THERMODYNAMICS OF He II FROM SOUND VELOCITY DATA

Quite recently there has been a new approach to the thermodynamics of He II by a group at UCLA. In the first of two papers, precision measurements of the velocities of first, second, and fourth sound were reported at all temperatures above 1.2 K and at all pressures.[43] The precision of the velocity data was of order 0.2% and over 400 points were measured for each sound mode. Maynard has made use of these data to produce tables of the density, expansion coefficient, normal fluid fraction, entropy, specific heats,

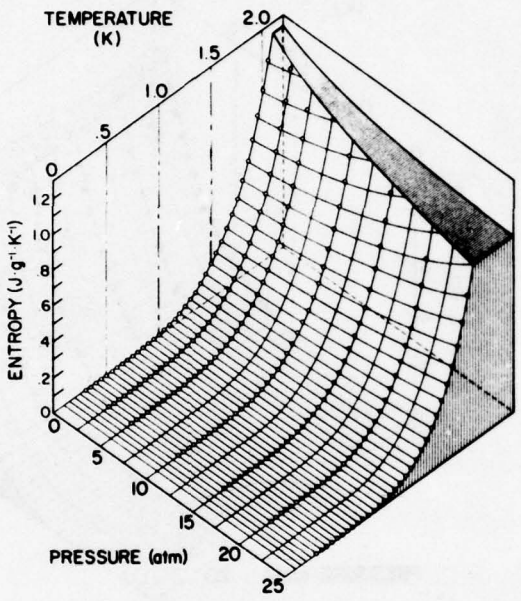

Fig. 14. The entropy of He II as a function of pressure temperature calculated from the series representation of the appendix and the coefficients tabulated in Ref. 4. The data for $0.3 < T < 1.6$ K are from Weibes[35] and those for $1.6 < T < 2.05$ K are from van den Meijdenberg *et al.*[37]

compressibility, and sound velocities.[13] The basic program of the analysis was to first find ρ using u_1, then to use a parametrized dispersion curve and effective spectrum to generate S and ρ_n/ρ, and subsequently to fit u_2 and u_4.

The model dispersion curve consisted of (a) a phonon branch for the region $0 \le q \le 1.1$ Å^{-1} (recall here that $p = \hbar q$):

$$\varepsilon(p) = u_1 p + ap^2 + bp^3 \tag{81}$$

(b) a maxon branch for the region 1.1 Å$^{-1} \le q \le q_0 - 0.1$ Å^{-1}:

$$\varepsilon(p) = \varepsilon_{\max} - c[p - (1.1\text{ Å}^{-1})\hbar]^2 + d[p - (1.1\text{ Å}^{-1})\hbar]^3 \tag{82}$$

(c) a parabolic roton branch for the region $q_0 - 0.1$ Å$^{-1} \le q \le q_c$:

$$\varepsilon(p) = \Delta + (p - p_0)^2/2\mu \tag{83}$$

and (d) a straight line of slope u_1 for $q_c \le q \le 3.0$ Å^{-1}:

$$\varepsilon(p) = [\Delta + (1/2\mu)(p_c - p_0)^2] + u_1(p - p_0) \tag{84}$$

The coefficients a and b were determined by the conditions $\varepsilon(1.1\text{ Å}^{-1}) = \varepsilon_{\max}$ and $(d\varepsilon/dp)_{1.1\text{Å}^{-1}} = 0$; c and d were chosen so that ε and $d\varepsilon/dp$ are

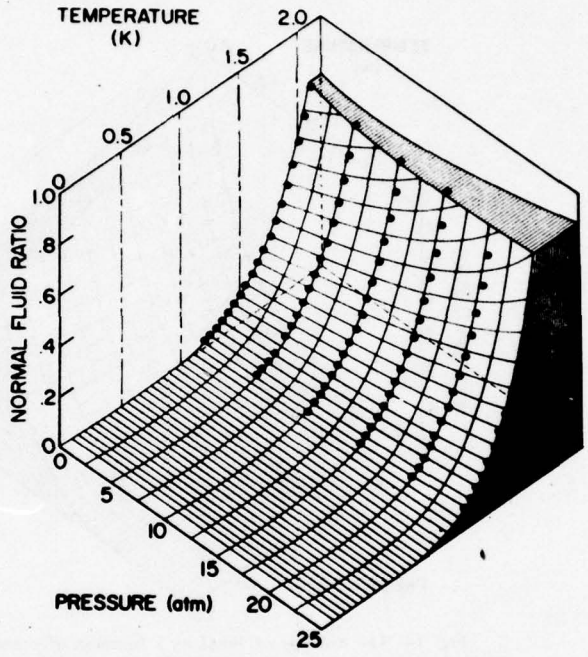

Fig. 15. The normal fluid fraction as a function of temperature for different pressures, calculated from the generalized Landau approximation and the coefficients of Ref. 4. The data are from Maynard.[13]

continuous at the junction between (82) and (83). The parameters p_0 and μ were taken from DGHP[9]; $q_0 = 3.64\rho^{1/3}$ Å^{-1} and $\mu/\mu_\lambda = 1+0.35[1-(T/T_\lambda)^7]$, where μ_λ was taken from a best fit to the data as a function of pressure.

The parameters ε_{max} and Δ were both treated as variables to determine the effective spectrum and were assumed to be given by the expressions

$$\frac{\Delta}{kT} = \frac{\Delta_\lambda}{kT_\lambda} + D_{23}\varepsilon^{2/3} + D_{\ln\varepsilon}\,\varepsilon\ln\varepsilon + D\varepsilon + \varepsilon^2\left[\sum_{n=0}^{3} D_n\varepsilon^n\right] \tag{85}$$

$$\frac{\varepsilon_{max}}{kT} = \frac{\varepsilon_\lambda}{kT_\lambda} + E_{23}\varepsilon^{2/3} + E_{\ln\varepsilon}\,\varepsilon\ln\varepsilon + \varepsilon\frac{T_\lambda}{T}\left[\sum_{n=0}^{3} E_n\varepsilon^n\right] \tag{86}$$

where the expansion parameter was

$$\varepsilon \equiv 1 - T/T_\lambda \tag{87}$$

The quantities Δ_λ and ε_λ were determined from the conditions $S(T_\lambda) = S_\lambda$ and $\rho_n/\rho(T_\lambda) = 1$, where S_λ is known from the work of Ahlers.[44] Ahlers has

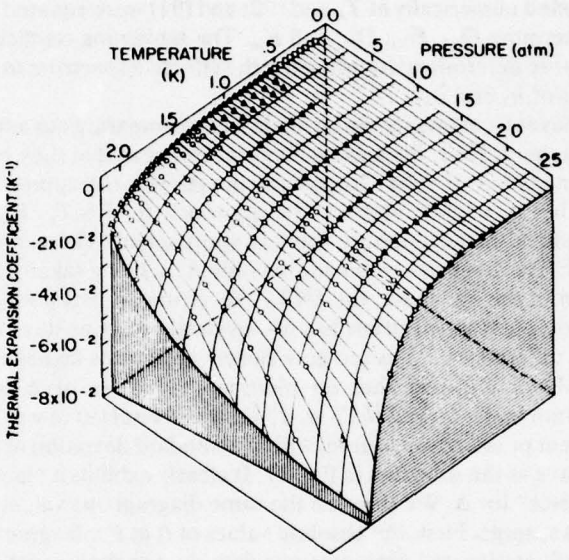

Fig. 16. The thermal expansion coefficient as a function of pressure and temperature. The solid lines are calculated from the expression of Table II. (○) Data of Elwell and Meyer[39]; (▲) Boghosian and Meyer[38]; (△) Van Degrift[41]; and (◇) Kerr and Taylor.[42]

shown that near T_λ (within millidegrees!),

$$S - S_\lambda = A\varepsilon \ln \varepsilon \tag{88}$$

$$\rho_s/\rho = k'\varepsilon^{2/3} \tag{89}$$

The motivation for the terms in ε in (85) and (86) is to produce formulas for S and ρ_s/ρ that fit (88) and (89) as $T \to T_\lambda$. The cubic polynomial terms were needed to extend the fits to lower temperatures.

Maynard adopted forms for S and ρ_s near T_λ suggested by expanding the Landau calculation for small ε:

$$S - S_\lambda = \left(\frac{\partial S}{\partial y} D_{23} + \frac{\partial S}{\partial z} E_{23}\right)\varepsilon^{2/3} + \left(\frac{\partial S}{\partial y} D_{\ln} + \frac{\partial S}{\partial z} E_{\ln}\right)\varepsilon \ln \varepsilon \tag{90}$$

$$\frac{\rho_s}{\rho} = -\left[\frac{\partial(\rho_n/\rho)}{\partial y} D_{23} + \frac{\partial(\rho_n/\rho)}{\partial z} E_{23}\right]\varepsilon^{2/3} - \left[\frac{\partial(\rho_n/\rho)}{\partial y} D_{\ln} + \frac{\partial(\rho_n/\rho)}{\partial z} E_{\ln}\right]\varepsilon \ln \varepsilon \tag{91}$$

where $y = \Delta/kT$ and $z = \epsilon_{max}/kT$. The partial derivatives of S and ρ_n/ρ were evaluated numerically at T_λ and (90) and (91) were equated to (88) and (89) to determine D_{23}, E_{23}, D_{ln}, and E_{ln}. The remaining coefficients in (85) and (86) were determined by adjusting the effective spectrum to fit the observed values of u_2 and u_4.

Several comments can be made when comparing our approach with that of Maynard. First, the approaches are similar in that they each incorporate limiting behavior: The Oregon scheme stresses the approach to $T = 0$, and the UCLA scheme stresses the approach to $T = T_\lambda$. Each method has difficulties as the opposite limit is approached. There are differences in detail: The Oregon system adjusts only Δ, μ being taken to scale with Δ as shown in the appendix; the UCLA spectrum adjusts both Δ and ϵ_{max}; the Oregon phonon spectrum has no quadratic term as does (81). In view of these differences, let us see how closely the results actually compare.

Maynard found that on plotting the values of Δ for his effective spectrum in the form Δ/kT_λ vs. T/T_λ, a universal curve was obtained for 26 different pressures measured, within a standard deviation of 0.2%. We show his curve as the solid line in Fig. 17: It clearly exhibits a "law of corresponding states" for Δ. We show on the same diagram our values of Δ/kT_λ. Two points emerge. First, the absolute values of Δ at $P = 0$ agree to within 0.6%. Second, at elevated pressures our data do not show strict scaling, but the deviations from Maynard's curve lie within the range +0.6% to −1.9% from $T/T_\lambda = 1.0$ to $T/T_\lambda = 0.6$. Below $T/T_\lambda = 0.6$, our values of Δ/kT_λ diverge more strongly for different pressures and give less support to the idea of corresponding states at low temperatures. At $T/T_\lambda = 0.05$, however, the spread in Δ/kT_λ is about 3%, compared to a spread of 17% for Δ/k alone.

The most dramatic scaling obtained by Maynard was for the quantity ρ_s/ρ as a function of T/T_λ. The 400 points on his curve gave the appearance of a single line. We show our calculations for the same quantity in Fig. 18 in the form ρ_s/ρ vs. T/T_λ. The collapse of the data at all pressures to a single curve is a good confirmation of corresponding states for this quantity down to the lowest temperatures where roton properties are significant.

The general agreement between the results of the determination of the effective spectrum and the thermodynamics by the Oregon and UCLA methods is gratifying, and lends support to the idea that the effective spectrum is indeed a unique quantity, independent of the details of the way of deriving it. The results by such different methods also underline our remarks below (54): Provided adequate care is exercised in converting all available data to effective spectra, thermodynamic consequences are almost uninfluenced by the spectral representation that happens to have been selected.

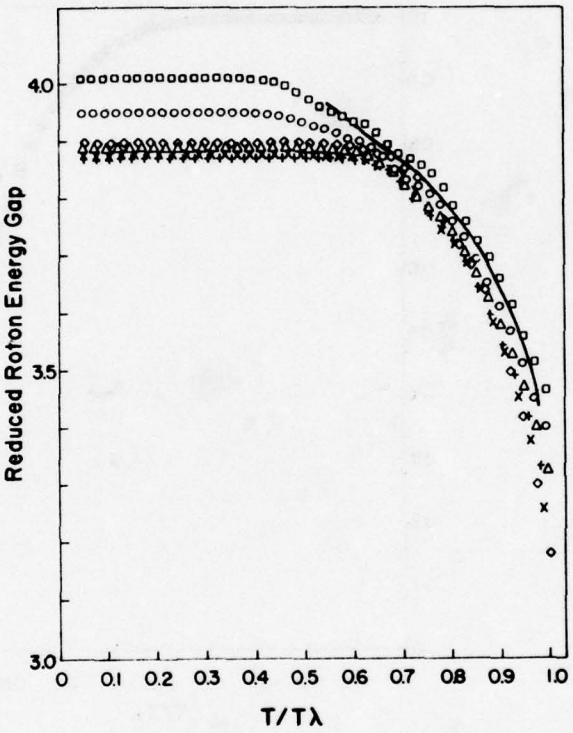

Fig. 17. The reduced roton energy gap Δ_r/kT_λ, as tabulated in Ref. 4, vs. T/T_λ to show the law of corresponding states as suggested by Maynard.[13] The symbols correspond to Δ_r/kT_λ for the following values of P: (□) 0, (○) 5, (△) 10, (+) 15, (×) 20, and (◇) 25 atm. The solid line is Maynard's effective roton parameter.

11. SUMMARY AND CONCLUSIONS

We have presented here a method of handling the statistical mechanics of interacting bosons when the energy states of the system are known to depend parametrically upon the temperature. The basic assumption is the expansion (7) of the internal energy in a Taylor series about a set of occupation numbers, which turn out to be optimally chosen as the mean occupation numbers $\bar{n}_\alpha$. The great merit of this choice is that we can replace the energies $\varepsilon_\alpha(\bar{\mathbf{n}}, V)$ by the experimentally known $\varepsilon_\alpha(T, V)$. Furthermore, the truncation of (48) after two terms is seen by (53) to have partially included the influence of Landau's parameter $f_{\alpha\beta}$ on the energy level α in

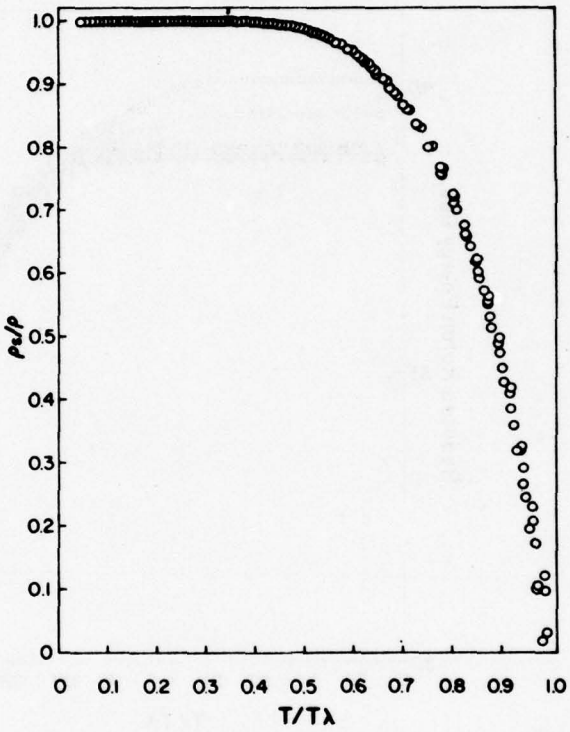

Fig. 18. The superfluid ratio calculated from the tabulations of Ref. 4 against T/T_λ as suggested by Maynard.[13] The data for all pressures collapse to a single line.

the sense of a statistical average. The resulting expressions (Table II) are shown in Section 6 to be of practical use in He II, by comparison with the results of inelastic neutron scattering, in cases where the energy levels are not too broad.

The representation of the energy spectrum can be carried out in a number of different ways, which are discussed in Sections 3 and 8–10. The crudest of these, the simple Landau approximation, is shown in Section 8 to be useful to identify some of the leading temperature-dependent terms, but to be unreliable as far as quantitative thermodynamic calculations are concerned. The results obtained with various, more general Landau approximations that include details from the entire spectrum are shown in Sections 9 and 10 to be far more useful in thermodynamic calculations and to be reasonably independent of the choice of the representation.

When the linewidth becomes broad, the unfolded quasiparticle energies fail to give an accurate account of the thermodynamics. The reason for this failure is not clear, and theoretical work clearly needs to be done to connect inelastic neutron scattering with the thermodynamics at finite temperatures.

The analysis shows that the broadening of the one-phonon peaks can be accounted for satisfactorily by roton–roton collisions, which suggests that some single energy might be thermodynamically significant. By constructing effective spectra with the single adjustment of the roton parameter, keeping all other parts of the dispersion spectra constant, it is possible to determine what the thermodynamically significant roton energies must be. They turn out to lie within a half-width of the observed unfolded neutron energies (Fig. 8). The choice of the effective roton energies can be made at all pressures and at all temperatures to T_λ, and are independent of the details of the spectral representation chosen (Fig. 17). One does not ordinarily expect the concept of a quasiparticle to be particularly useful when the lifetime becomes shortened by collisions. The analysis presented here suggests that the quasiparticle has some validity as a concept throughout the He II region of pressures and temperatures.

APPENDIX. A SERIES REPRESENTATION OF THE EXCITATION SPECTRUM OF HELIUM II[4,11,18]

The series is

$$\varepsilon(p) = u_1 p + a_3 p^3 + a_4 p^4 + a_5 p^5 + a_6 p^6 + a_7 p^7 + a_8 p^8$$

The constraints are

$$\varepsilon(0) = 0; \qquad (d\varepsilon/dp)_{p=0} = u_1$$

(which are automatically satisfied by the series), and

$$\varepsilon(p_{\max}) = \varepsilon_{\max}; \qquad (d\varepsilon/dp)_{p_{\max}} = 0$$

$$\varepsilon(p_0) = \Delta; \qquad (d\varepsilon/dp)_{p_0} = 0; \qquad (d^2\varepsilon/dp^2)_{p_0} = 1/\mu$$

$$(d\varepsilon/dp)_{p_c} = u_1$$

The momenta given above are calculated from

$$p_{\max}/\hbar = 1.1\ \text{Å}^{-1}; \qquad p_0/\hbar = 3.64\rho^{1/3}\ \text{Å}^{-1}; \qquad p_c = \mu u_1 + p_0$$

The maxon energy $\varepsilon_{\max}$ is given at $T = 0$ by

$$[\varepsilon_{\max}(0, \rho_0)/k]E_0 + E_1\rho_0 + E_2\rho_0^2 + E_3\rho_0^3$$

where ρ_0 is the density at $T = 0$. At finite temperatures

$$\varepsilon_{max}(T, \rho) = \varepsilon_{max}(0, \rho_0)(1 - 0.452 \times 10^{-3} T^7)$$

$$E_0 = -216.5672 \text{ K}; \qquad E_1 = 3998.6005 \text{ K g}^{-1} \text{ cm}^3$$

$$E_2 = -23028.6027 \text{ K g}^{-2} \text{ cm}^6; \qquad E_3 = 44199.7232 \text{ K g}^{-3} \text{ cm}^9$$

The coefficients for the series are listed in Ref. 4 with ε in degrees kelvin and p replaced by q in Å^{-1}. A typical spectrum is at $T = 1.2$ K, saturated vapor pressure, where the coefficients a_n are (in K Å^n)

$$u_1 = 18.164108; \qquad a_3 = 44.275581; \qquad a_4 = -160.940887$$

$$a_5 = 209.781281; \qquad a_6 = -135.492432; \qquad a_7 = 43.24568$$

$$a_8 = -5.404290$$

The model dispersion curve consists of the series above for $0 \le p \le p_c$, and by a straight line of slope u_1 beyond p_c, as shown in Figs. 1 and 2.

Note that the values of μ at finite temperatures are scaled as the values of Δ, thus

$$\mu(P, T)/\mu(P, 0) = \Delta(P, T)/\Delta(P, 0)$$

so that once the temperature variation of Δ is determined, that for μ follows directly.

ACKNOWLEDGMENTS

We are grateful to Profs. R. P. Feynman, D. L. Goodstein, W. Halley, R. M. Mazo, and G. H. Wannier for discussions of the theory, to Dr. L. Passell and Dr. O. W. Dietrich for help in understanding the neutron scattering measurements, to Dr. J. S. Brooks for his interest and contributions from the beginning, to Dr. J. Maynard for cooperation in using his measurements and analysis, and to James Gibbons for carrying through the computations.

REFERENCES

1. L. D. Landau, *J. Phys.* **11**, 91 (1947).
2. P. H. Roberts and R. J. Donnelly, *Annual Review of Fluid Mechanics* **6**, 179 (1974).
3. R. J. Donnelly, *Experimental Superfluidity* (Chicago Lectures in Physics Series), notes compiled by W. I. Glaberson and P. E. Parks (Univ. of Chicago Press, 1967).
4. J. S. Brooks and R. J. Donnelly, *J. Phys. Chem. Ref. Data* **6(1)**, in press (1977).
5. J. L. Yarnell, G. P. Arnold, P. J. Bendt, and E. C. Kerr, *Phys. Rev.* **113**, 1379 (1959).
6. P. J. Bendt, R. D. Cowan, and J. L. Yarnell, *Phys. Rev.* **113**, 1386 (1959).
7. J. Wilks, *The Properties of Liquid and Solid Helium* (Clarendon Press, Oxford, 1967).
8. R. A. Cowley and A. D. B. Woods, *Can. J. Phys.* **49**, 177 (1971).
9. O. W. Dietrich, E. H. Graf, C. H. Huang, and L. Passell, *Phys. Rev. A* **5**, 1377 (1972).

10. R. J. Donnelly, in *Quantum Statistical Mechanics in the Natural Sciences*, B. Kursunoglu, S. L. Mintz, and S. M. Widmayer, eds. (Plenum Press, New York, 1974), Vol. 4.
11. J. S. Brooks, The Properties of Superfluid Helium Below 1.6 Degrees Kelvin, Ph.D. Thesis, University of Oregon, Eugene, Oregon (1973); J. S. Brooks and R. J. Donnelly, The Calculated Properties of Helium II. A Technical Report, University of Oregon, Eugene, Oregon (1973).
12. P. H. Roberts and R. J. Donnelly, *Phys. Lett.* **55A**, 443 (1976).
13. J. Maynard, *Phys. Rev. B* **14**, 3868 (1976).
14. G. S. Rushbrooke, *Trans. Faraday Soc.* **36**, 1055 (1940).
15. E. W. Elcock and P. T. Landsberg, *Proc. Phys. Soc. B* **70**, 161 (1957).
16. D. L. Goodstein, J. S. Brooks, R. J. Donnelly, and P. H. Roberts, *Phys. Lett.* **54A**, 281 (1975).
17. L. D. Landau and E. M. Lifshitz, *Statistical Physics* (Addison-Wesley, Reading, Massachusetts, 1969).
18. J. S. Brooks and R. J. Donnelly, *Phys. Lett.* **46A**, 111 (1973).
19. M. Abramowitz and I. E. Stegun, *Handbook of Mathematical Functions* (Dover, New York, 1965).
20. J. S. Brooks and R. J. Donnelly, in *Low Temperature Physics—LT 13*, K. D. Timmerhaus, W. J. O'Sullivan, and E. F. Hammel, eds. (Plenum Press, New York, 1974), Vol. 1.
21. A. Molinari and T. Regge, *Phys. Rev. Lett.* **26**, 1531 (1971).
22. A. D. B. Woods and R. A. Cowley, *Rep. Prog. Phys.* **36**, 1135 (1973).
23. L. Passell, J. Als-Nielsen, and O. W. Dietrich, *Neutron Inelastic Scattering* (IAEA, Vienna, 1972).
24. P. H. Roberts and W. J. Pardee, *J. Phys. A* **7**, 1283 (1974).
25. P. H. Roberts and R. J. Donnelly, *J. Low Temp. Phys.* **15**, 1 (1974).
26. U. M. Titulaer and J. M. Deutch, *Phys. Rev. A* **10**, 1345 (1974).
27. R. P. Feynman, *Phys. Rev.* **94**, 262 (1954); R. P. Feynman and M. Cohen, *Phys. Rev.* **102**, 1189 (1956).
28. R. J. Donnelly and P. H. Roberts, *Phys. Lett.* **43A**, 199 (1973).
29. R. J. Donnelly, *Phys. Lett.* **39A**, 221 (1972).
30. D. G. Henshaw and A. D. B. Woods, *Phys. Rev.* **121**, 1266 (1961).
31. I. M. Khalatnikov, in *The Physics of Liquid and Solid Helium, Part I*, K. H. Bennemann and J. B. Ketterson, eds. (Wiley–Interscience, New York, 1976).
32. T. J. Greytak and J. Yan, in *Proc. 12th Int. Conf. Low Temp. Phys.* (Academic Press of Japan, Kyoto, 1971).
33. C. A. Murray, R. L. Woerner, and T. J. Greytak, *J. Phys. C* **8**, L90 (1975).
34. E. C. Svensson, A. D. B. Woods, and P. Martel, *Phys. Rev. Lett.* **29**, 1148 (1972).
35. J. Wiebes, Caloric Measurements on Liquid and Melting Helium Below 1.5 Kelvin, Ph.D. Thesis, Leiden (1969).
36. N. E. Phillips, C. G. Waterfield, and J. K. Hoffer, *Phys. Rev. Lett.* **25**, 1260 (1970).
37. C. J. N. van den Meijdenberg, K. W. Taconis, and R. De Bruyn Ouboter, *Physica* **27**, 197 (1961).
38. C. Boghosian and H. Meyer, *Phys. Rev.* **152**, 200 (1966); **163**, 206 (1967).
39. D. L. Elwell and H. Meyer, *Phys. Rev.* **164**, 245 (1967).
40. K. R. Atkins and M. H. Edwards, *Phys. Rev.* **97**, 1429 (1955).
41. C. T. Van Degrift, Dielectric Constant, Density, and Expansion Coefficient of Liquid He^4 at Vapor Pressure Below 4.4 K, Ph.D. Thesis, University of California, Irvine (1974).
42. E. C. Kerr and R. D. Taylor, *Ann. Phys.* **26**, 292 (1964).
43. J. Heisermann, J. P. Hulin, J. Maynard, and I. Rudnick, *Phys. Rev. B* **14**, 3862 (1976).
44. G. Ahlers, *Phys. Rev. A* **8**, 530 (1973).

The Calculated Thermodynamic Properties of Superfluid Helium-4

James S. Brooks* and Russell J. Donnelly

Institute of Theoretical Science and Department of Physics, University of Oregon, Eugene, Oregon 97403

Comprehensive tables of the primary thermodynamic properties of superfluid helium-4, such as the specific heat and entropy, are presented as computed from the Landau quasiparticle model, with the aid of inelastic neutron scattering data. The neutron data are represented by continuous functions of temperature, pressure, and wave number and certain excitation properties such as number density, normal and superfluid densities are calculated directly from it. A discussion of the methods used in our computations is included, and comparisons of computed and experimental results are made where applicable. Certain inadequacies of present theoretical methods to describe the thermodynamic properties are reported, and the use of an effective spectrum is introduced to offset some of these difficulties. Considerable experimental effort is also needed to improve the present situation.

Key words: Computed thermodynamic properties; entropy; equation of state; excitation spectrum; helium-4; normal fluid helium-4; phonons; rotons; specific heat; superfluid helium-4.

Contents

List of Figures

* Present affiliation: Dept. of Physics and Astronomy, University of Massachusetts, Amherst, Massachusetts 01002.

List of Auxiliary Tables in Text

List of Tables in Appendix A

Nomenclature

Symbol or expression	Physical quantity	Unit symbol or value
m	Helium-4 mass	6.646×10^{-24} g
k	Boltzmann's constant	1.38054×10^{-23} J·K^{-1}
h, ($\hbar$)	Planck's constant, ($\div 2\pi$)	6.6256×10^{-34} J·s (1.0545×10^{-34} J·s)
P	Pressure	atm (1 atm = $1.01325\cdot10^5$ N·m^{-2})
V	Molar volume	cm^3·mol^{-1}
T	Temperature	K
PVT	Pressure-Volume-Temperature, the equation of state	
SVP	Saturated vapor pressure	
$T_\lambda(P)$	The temperature at which liquid helium-4 becomes a superfluid for a given pressure	K
helium I (He I)	The non-superfluid state of liquid helium-4, $T > T_\lambda$	
helium II (He II)	The superfluid state of liquid helium-4, $T < T_\lambda$	
ρ	Density	g·cm^{-3}
ρ_n	Density of the normal component	g·cm^{-3}
ρ_s	Density of the superfluid component	g·cm^{-3}
ϵ/k	Energy of an excitation $\div$	K
$\omega=\epsilon/\hbar$	Frequency of an excitation	rad·s^{-1}
p	Excitation momentum	g·cm·s^{-1}

Nomenclature—Continued

Symbol or expression	Physical quantity	Unit symbol or value
$q=p/\hbar$	Wave number of excitation	$Å^{-1}$ ($1\ Å^{-1}=10^{10}m^{-1}$)
p_0	Momentum at the roton minimum	$g\cdot cm\cdot s^{-1}$
p_c	Momentum at which $d\epsilon/dp=u_1$	$g\cdot cm\cdot s^{-1}$
$n(p)$	Distribution of excitations as a function of momentum	cm^{-3}
Δ	Roton energy	K
Δ_t	"Thermal" roton energy	K
μ	Roton effective mass	m
μ_t	"Thermal" roton effective mass	m
Γ/k	Half width of scattered neutron distribution $\div k$	K
$S(q,\omega)$	Dynamic structure factor	
S	Entropy	$J\cdot g^{-1}\cdot K^{-1}$
u_1, u_2, u_4	Velocity of first, second, fourth sound	$m\cdot s^{-1}$
u_I, u_{II}	Velocity of first, second sound, uncorrected	$m\cdot s^{-1}$
ϵ_{max}/k	Energy of maxon peak $\div k$	K
N_r	Roton number density	cm^{-3}
N_p	Phonon number density	cm^{-3}
a_n	Coefficients of excitation energy series	$K\cdot Å^n$
α_P	Coefficient of thermal expansion	K^{-1}
κ_T	Isothermal compressibility	$cm^2\cdot dyne^{-1}$
U_G	Grüneisen constant	
L	Latent heat	$J\cdot g^{-1}$
F	Helmholtz free energy	$J\cdot g^{-1}$
Φ	Gibbs free energy	$J\cdot g^{-1}$
W	Enthalpy	$J\cdot g^{-1}$
C_P	Specific heat at constant pressure	$J\cdot g^{-1}\cdot K^{-1}$
C_V	Specific heat at constant volume	$J\cdot g^{-1}\cdot K^{-1}$
$\gamma=C_P/C_V$	Ratio of specific heats	
$V_0, L_0, F_0, \Phi_0, W_0$, etc.	Ground state ($T=0$) values of quantities	
V_E, F_E, Φ_E, W_E, etc.	Finite temperature values of quantities due to excitations only	

1. Introduction

Liquid helium is a rewarding subject for the study of thermodynamic properties, especially because helium II, the lower temperature phase, exhibits the property of superfluidity. The hydrodynamics of this phase are extraordinary: both normal viscous behavior and superflow may be exhibited in closely related experiments. Phenomenologically, one speaks of a "two-fluid" behavior in which the fluid (of density ρ)[1] acts dynamically as if a fraction of effective density ρ_n flows as a normal fluid, and a fraction of effective density $\rho_s=\rho-\rho_n$ flows as an inviscid fluid. This two-fluid motion of helium II leads to some very unusual results, such as the wave-like rather than diffusive propagation of temperature fluctuations (called second sound). Furthermore, the thermodynamic properties are deeply related to the hydrodynamic: for example, the Gibbs free energy is related to the square of the relative velocity between the two fluids. We shall be concerned principally with the static properties of helium II in which all net flow velocities are zero.

On a deeper level, one has the Landau picture [1][2] in which the entire fluid is superfluid at absolute zero. As the temperature[3] is raised, the heat content is described entirely in terms of "elementary excitations" of the superfluid. At low temperatures these are "phonons", at higher temperatures more complex excitations called "rotons" are excited.

The energy $\epsilon\,(=\hbar\omega)$ and momentum $p\,(=\hbar q)$ of the elementary excitations in superfluid helium may be represented by the excitation spectrum (dispersion curve) first proposed by Landau [1] which is shown schematically in figure 1. We will refer again to this

[1] All symbols used in this paper are defined in the section labeled Nomenclature.

[2] Figures in brackets indicate literature references in section 7.

[3] Experiments at liquid helium temperatures almost invariably use the 1958 vapor pressure scale [12]. Caution should be used with earlier data.

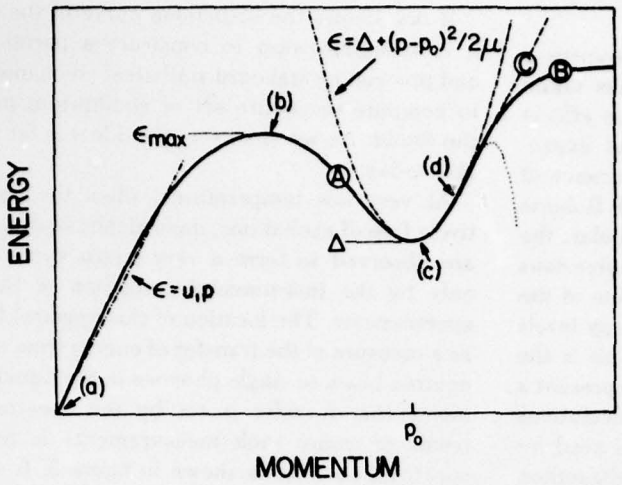

FIGURE 1. A schematic diagram of the excitation spectrum for helium II. Details and labels are discussed in the text.

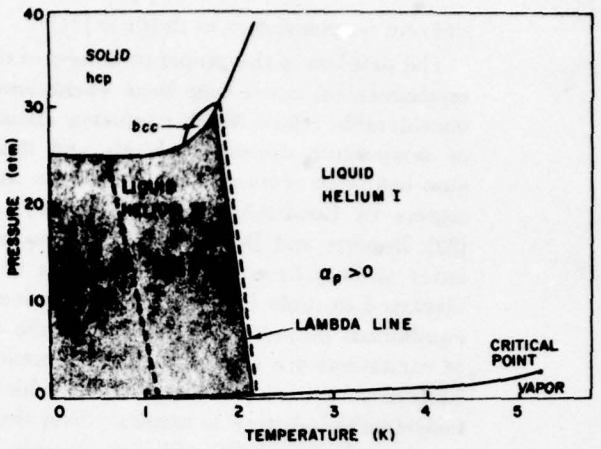

FIGURE 2. A schematic phase diagram for helium-4. The pressure of the liquid-gas transition line has been exaggerated. The hexagonal close-packed and body centered cubic (bcc) phases of the solid are shown, as are the loci of zero thermal expansion (dashed lines).

figure in subsequent sections. In recent years many of the features, and in some cases the entire dispersion curve, have been measured by inelastic thermal neutron scattering techniques for different pressures and temperatures. (See for example references [2–10].) Landau has put forth a simple but elegant theory which allows one to calculate the thermodynamic properties of He II at low temperatures from the excitation spectrum.

The purpose of this paper is to give an account of the equilibrium thermodynamic properties of He II and related quantities such as the velocities of first, second, and fourth sounds and properties of the excitations themselves. These quantities are used in a wide variety of contexts, both experimental and theoretical; and it is often important that the data for different properties be thermodynamically consistent. The ideal solution to this problem would be a critical compilation of experimental properties over the entire $T-P$ plane for He II, and some day this will undoubtedly be possible. At the time this project was begun (1972), the tables in the appendices of the books by Wilks [11] and Donnelly [12] were the most complete available, and far from adequate for the task undertaken here.

Another promising avenue is the use of Landau's theory mentioned above. The thermodynamic properties along the vapor pressure curve have been extracted from neutron scattering measurements with reasonable success by Bendt, Cowan, and Yarnell [10]. We have, then, the possibility that direct thermodynamic measurements can be supplemented by the increasing body of neutron data indicated by the references cited. In particular, we were greatly encouraged by the appearance in 1972 of the landmark study of neutron scattering from rotons by Dietrich, Graf, Huang, and Passell at Brookhaven National Laboratory [3].

The superfluid region of the helium $P-T$ phase diagram is shown schematically as the shaded portion of figure 2. It is to this area that our analysis and subsequent tabulations apply. For all pressures in this shaded region, there is a temperature $T_\lambda(P)$ above which the superfluid properties cease to exist, and one has a classical liquid phase (called helium I). The line which separates these two regions is called the lambda-line, in recognition of the characteristic anomaly in the specific heat observed along this line. In this paper, we do not treat the thermodynamic properties in the immediate vicinity of this line. Such a treatment has, however, been undertaken in an earlier volume of this Journal, by McCarty [13], who has reported on the thermodynamic properties of helium I; and IUPAC Helium-4 tables by Angus, de Reuck, and McCarty [14] are in the process of completion at the time of writing of the present article.

The results described here are the result of a lengthy series of investigations by our research group at the University of Oregon. The first product of our analysis of the Brookhaven data was a report on the Landau parameters [15]. An early attempt at approximating the dispersion curve in a piecewise fashion was reported at LT13 [16]. This proved to be imprecise and was succeeded by the series representation used in this paper [17]. The results of these investigations were summarized in the Ph. D. thesis of J. S. Brooks, which appeared in 1973 [18]. We issued the Tables from that thesis in the form of a University of Oregon Technical Report in December 1973 [19], requesting contributions from other laboratories. We were gratified to receive a number of suggestions, corrections, and reports of new experimental work. In particular, the thesis of Van Degrift on the expansion coefficient [20], and a systematic study of first, second, and fourth sound by Maynard and Rudnick, began at UCLA, have been extremely useful, as has some independent work on dispersion curves by Dr. Maynard [21]. Since this work was submitted, the UCLA measurements have been completed

and sent for publication as shown in [21].

The problem of the proper treatment of the statistical mechanics of interacting Bose excitations has taken considerable effort. Much confusion about the effects of temperature-dependent levels and thermal expansion has been removed with the recent appearance of papers by Goodstein, Brooks, Donnelly, and Roberts [22], Roberts and Donnelly [23, 24]. In particular, the latter authors have developed the set of expressions displayed in table I which allow the calculation of the equilibrium properties of He II when the energy levels of excitations are known from experiment. This is the basis of the present calculated tables, which represent a considerable advance in accuracy over the calculations in our earlier work [18, 19]. For example, the need for an empirical equation of state is eliminated altogether.

The computations reported here have been carried out by James Gibbons on a Hewlett-Packard 2100 A computer.

2. Theoretical Background

Although several authors have discussed the Landau spectrum and theory in detail (see, for example, Wilks [11], Donnelly [12], Keller [25], Khalatnikov [26]) we present here a brief description for completeness. Landau's theory for superfluid helium is based on the assumption that the thermal excitations in the liquid can be described as constituting a weakly interacting gas with the energy spectrum given as the solid line in figure 1. It is also assumed that these excitations obey Bose statistics, and therefore the number density of excitations of a particular momentum, $n(p)$ is given by

$$n(p) = \frac{1}{h^3}\left[e^{\epsilon(p)/kT} - 1\right]^{-1}. \qquad (1)$$

From this expression, we see that the low-lying regions of the energy spectrum will contribute predominantly to the thermodynamic properties, and referring to figure 1 we find that there are two such regions on interest. The first is for small momenta, where the spectrum is approximately linear, and is called the phonon branch. The other is the energy minimum about momentum p_0, which is nearly parabolic and is called the roton branch, or roton minimum. Here the energy is much higher, but the density of states is also very large.

The experimentally observed values of the minimum roton energy Δ are large enough that the Boltzmann distribution is an adequate approximation to eq (1). As a rough guide to thinking of the thermodynamics of helium II, it is sufficient to recognize that below 1 K, the phonon excitations are the more numerous and dominate the thermal properties, whereas at higher temperatures the number of rotons increases exponentially with temperature, and rotons become predominant thermodynamically above 1 K.

If one knows the dispersion curve of the excitations, it is straightforward to construct a partition function and proceed by standard statistical mechanical methods to compute the entire set of equilibrium properties of the liquid. As we shall see, this ideal is far from realizable today.

At very low temperatures, when the liquid is relatively free of excitations, inelastically scattered neutrons are observed to form a very sharp spectrum, limited only by the instrumental resolution of the analyzing spectrometer. The location of this spectral line is taken as a measure of the transfer of energy from the incoming neutron beam to single phonons in the liquid, for a given momentum transfer p set by the spectrometer. The result of many such measurements is an excitation spectrum such as is shown in figure 3. It appears theoretically reasonable, and experimentally fairly certain, that the observed excitation spectrum can be identified with the dispersion curve of the elementary excitations in the fluid at low temperatures.

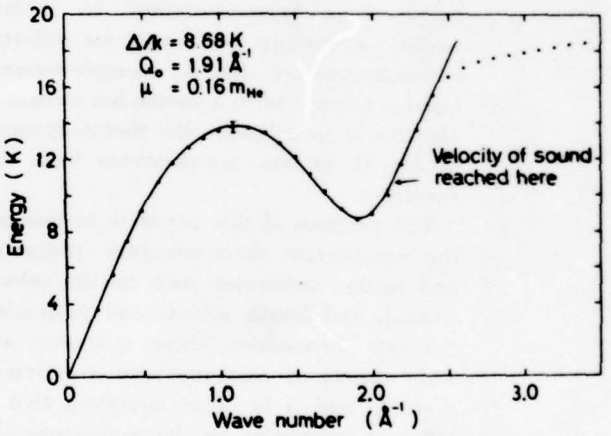

FIGURE 3. The experimentally determined excitation spectrum at 1.1 K, SVP. The dots are the neutron scattering data of Cowley and Woods [2]; the solid line is eqs (20) and (14). The error bar is the smallest experimental error, and is not to be associated with any one data point.

At higher temperatures, however, Yarnell et al. [9], and Henshaw and Woods [5] observed that the widths of the scattered spectra increase rapidly with temperatures. For rotons (at (c) in fig. 1) the linewidths, as measured by the half-width at half maximum Γ, approach the magnitude of the energy itself as T approaches T_λ (i.e., $\Gamma \to \sim \Delta$ as $T \to T_\lambda$). This means, among other things, that the lifetimes of the excitations are decreasing rapidly with increasing temperature. Furthermore, the roton energy Δ is observed to decrease with increasing T and increasing P.

The scattered neutron intensity is proportional to the dynamic structure factor $S(q, \omega)$ which is in turn related to density-density correlations in the fluid. The unfolding of the experimental scattered neutron spectra in terms of assumed forms for $S(q, \omega)$ has been discussed in detail by Dietrich et al. [3]. To the best of

our knowledge at the time of writing, no one has been able to make a rigorous connection between $S(q, \omega)$ at finite temperatures and the energies which enter the thermodynamic calculations. Dietrich et al. [3] have included the linewidth Γ in their thermodynamic calculations in an ad hoc way; perhaps a complete theory will require considerable information on the observed line shape.

If one were to brush aside the considerations of the last paragraph and try to work with the unfolded dispersion curve $\epsilon(q)$, one would still have the problem of treating the statistical mechanics of interacting Bose excitations whose interactions are manifested by an observed dependence of $\epsilon(q)$ on T and P. Bendt, Cowan, and Yarnell [10] argue that when $\epsilon(q)$ is a function of T alone, the entropy should be given by

$$S=\frac{V}{2\pi^2}\int_0^\infty \left[k\ln(1+n)+\frac{n\epsilon}{T}\right]q^2dq, \qquad (2)$$

where n is the Bose distribution function (1). Roberts and Donnelly [23] have presented arguments to show that even at arbitrary T and P, (1) and (2) are still valid provided $\epsilon(q)$ is available from experiment. They have presented a way in which all the thermodynamic properties may be consistently deduced from experimental dispersion curves [24]. We show in table I the expressions which they have derived for the quantities of interest in the present study. In table I we have omitted the subscripts on α_P and κ_T for clarity.

TABLE I. Expressions for thermodynamic quantities

S	$\frac{Vk}{2\pi^2}\int_0^\infty\left[\frac{n\epsilon}{kT}+\ln(1+n)\right]q^2dq$
V	$V_0(P)-\frac{1}{2\pi^2}\int_0^T\frac{VdT}{T}\int_0^\infty\epsilon\left[\left(\frac{\partial n}{\partial P}\right)_{T,q}+\frac{\kappa q}{3}\left(\frac{\partial n}{\partial q}\right)_{P,T}\right]q^2dq$
α_P	$-\frac{1}{2\pi^2T}\int_0^\infty\epsilon\left[\left(\frac{\partial n}{\partial P}\right)_{T,q}+\frac{\kappa q}{3}\left(\frac{\partial n}{\partial q}\right)_{P,T}\right]q^2dq$
F	$F_0(V)+\frac{V}{2\pi^2}\int_0^T\frac{dT}{T}\int_0^\infty\frac{\epsilon}{3}\left(\frac{\partial n}{\partial q}\right)_{V,T}q^3dq$
Φ	$\Phi_0(P)+\frac{1}{2\pi^2}\int_0^T\frac{VdT}{T}\int_0^\infty\frac{\epsilon}{3}\left(\frac{\partial n}{\partial q}\right)_{P,T}q^3dq$
W	$\Phi_0(P)+\frac{1}{2\pi^2}\int_0^T VdT\int_0^\infty\epsilon\left[\left(\frac{\partial n}{\partial T}\right)_{P,q}-\frac{\alpha q}{3}\left(\frac{\partial n}{\partial q}\right)_{P,T}\right]q^2dq$
C_P	$\frac{V}{2\pi^2}\int_0^\infty\epsilon\left[\left(\frac{\partial n}{\partial T}\right)_{P,q}-\frac{\alpha q}{3}\left(\frac{\partial n}{\partial q}\right)_{P,T}\right]q^2dq$
C_V	$\frac{V}{2\pi^2}\int_0^\infty\epsilon\left(\frac{\partial n}{\partial T}\right)_{V,q}q^2dq$

3. Experimental Data Used in the Analysis

In this section the experimental data underlying the Landau theory is discussed.

3.1. Data Obtained by the Inelastic Scattering of Thermal Neutrons from Helium II

The energies and line widths of the elementary excitations of helium II are obtained from examination of inelastically scattered thermal neutrons. The techniques are discussed in detail, for example, in a recent review article by Woods and Cowley [8]. We shall use the measured energy spectrum, following Bendt, Cowan, and Yarnell [10], as the basis for our computations of the thermodynamic properties of helium II from the Landau theory. A completely determined experimental excitation spectrum is shown in figure 3 for $T=1.1$ K, at the SVP. The shape of this spectrum is a complicated function of pressure and temperature, and to use the Landau theory one must first know the detailed spectrum for every value of P and T. A complete set of data for a single pressure and temperature such as is shown in figure 3 is a major experimental undertaking. Hence it is necessary to find a method of estimating the energy spectrum for general P and T accurate enough that derivatives such as appear in table I may be accurately determined. In the sections below, we discuss the salient features of the excitation spectrum obtained from various kinds of experiments, and in section 3.1.e we describe a method of representing the spectrum as a power series in momentum, with pressure- and temperature-dependent coefficients.

3.1.a. The Phonon Branch

For momentum p decreasing to zero, the phonon branch of the energy spectrum approaches linearity, in accordance with theoretical predictions (cf. Feenberg [27]). Here we take the energy spectrum, as indicated at (a) in figure 1, to be

$$\lim_{p\to 0}\epsilon(p)=u_1p, \qquad (3)$$

where u_1 is the velocity of ultrasonic (first) sound, a temperature- and pressure-dependent quantity which may be determined experimentally either from the slope of the excitation spectrum in the zero momentum limit, or more conveniently from experimental first sound data (see section 4.2.a).

The first non-linear terms correcting eq. (3) for small, but non-zero, momenta have been the subject of much controversy in the literature in recent years (see Svensson, Woods, and Martel [7], and references therein). These terms may affect the behavior of, for example, the specific heat at temperatures below 0.45 K, as suggested by Phillips, Waterfield, and Hoffer [28]. We will return to this question in section 3.1.e.

3.1.b. The Maxon Branch

The elementary excitations which have energies at or near the first energy maximum, (b) in figure 1, have come to be called "maxons". This part of the spectrum has been measured at 1.1 K, at the vapor pressure as indicated in figure 3, and the peak position has been determined for various pressures at 1.18 K by Graf, Minkiewicz, Møller, and Passell [6] Measurements have also been made by Henshaw and Woods at the vapor pressure and 25.3 atm [4]. From the existing data on the maxon part of the spectrum, we conclude that the peak energy is density dependent only, since no shift in the peak position in momentum space has been observed. Very little data exists on the temperature dependence of the maxon peak. Figure 1 of Bendt, Cowan, and Yarnell [10] and figure 20 of Cowley and Woods [2] suggest it decreases slowly with temperature. Because the maxon energies are relatively high, their contribution to the thermal properties is very small, and the details of this part of the spectrum are not critical to the computations in this paper.

We represent the density dependence of the maxon energy by the expression

$$\epsilon_{\max}(0, \rho_0)/k = E_0 + E_1\rho_0 + E_2\rho_0^2 + E_3\rho_0^3, \qquad (4a)$$

where ρ_0 is the density at $T=0$ and the coefficients E_n are

$$E_0 = -216.5672 \quad (\mathrm{K})$$

$$E_1 = 3998.6005 \quad (\mathrm{K \cdot g^{-1} \cdot cm^3})$$

$$E_2 = -23028.6027 \quad (\mathrm{K \cdot g^{-2} \cdot cm^6})$$

$$E_3 = 44199.7232 \quad (\mathrm{K \cdot g^{-3} \cdot cm^9})$$

Equation 4a is a fit to the neutron data of Cowley and Woods [2] and Graf et al. [6] and is plotted with the data in figure 4. The rather slow temperature dependence of the peak is represented by

$$\epsilon_{\max}(T, \rho) = \epsilon_{\max}(0, \rho_0)\,(1 - 0.452 \times 10^{-3} T^7). \qquad (4b)$$

Values of $\epsilon_{\max}(T, P)$ are given in table 21, the conversion to pressure being obtained from the equation of state.

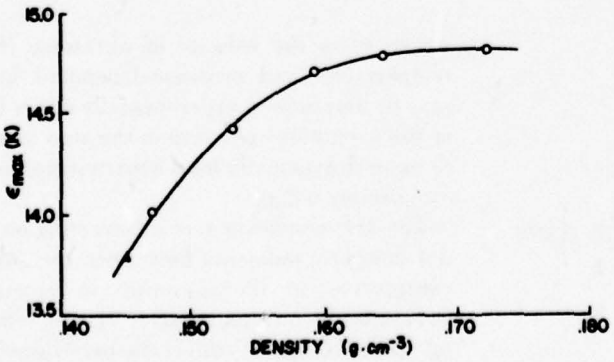

FIGURE 4. The density dependence of the maxon peak. Triangle, Cowley, and Woods [2]; circles, Graf et al. [6]; solid line, eq (4).

3.1.c. The Roton Minimum

The region of the spectrum denoted (c) in figure 1 is called the "roton minimum" and can be very well represented by Landau's parabolic expression

$$\epsilon_{\text{roton}} = \Delta + (p - p_0)^2/2\mu, \qquad (5)$$

where Δ is the minimum roton energy, or energy gap, p_0 is the roton momentum at minimum energy, and μ is the effective mass of excitation near p_0. These three quantities which describe the roton minimum are called the "Landau parameters", and have the typical values at 1.1 K, SVP of $\Delta/k = 8.68$ K, $p_0/\hbar = 1.91$ Å^{-1}, and $\mu = 0.16\ m$. The temperature, pressure, and density dependence of these parameters are best known from the experimental work of Dietrich et al. [3], who find that Δ and μ decrease with increasing temperature and/or pressure, but that p_0 is a function of density only:

$$p_0/\hbar = 3.64\,\rho^{1/3}\ \text{Å}^{-1}. \qquad (6)$$

Values of eq (6) are given in table 24.

Donnelly [15] has provided simple relations for the density dependence of Δ and μ at $T=0$, and also for the relation between Δ and μ at finite temperatures:

$$\Delta(\rho, 0)/k = (16.99 - 57.31\rho)\ (\mathrm{K}), \qquad (7)$$

$$\mu(\rho, 0) = (0.32 - 1.103\rho)\,(m), \qquad (8)$$

and

$$\frac{\mu(\rho, T)}{\mu(\rho, 0)} = \frac{\Delta(\rho, T)}{\Delta(\rho, 0)}. \qquad (9)$$

An expression which describes the temperature and density dependence of $\Delta(\rho,T)/k$ has been given by Brooks and Donnelly [16]:

$$\frac{\Delta(\rho,T)}{k} = \frac{\Delta(\rho,0)}{k} - \frac{\rho_n}{\rho} T \left(1 - \frac{aN_r}{T}\right), \qquad (10)$$

where ρ_n is the normal fluid density and N_r is the roton number density (both quantities will be discussed in section 4). Here, $a = 8.75 \times 10^{-23}$ cm^3·K. Equation (10) gives a good qualitative description of the data of Dietrich et al. [3] to within 20% for Δ[and μ through eq (9)] below the lambda point. These expressions are discussed in detail by Brooks [18].

Recently, motivated by (10), we have performed a least squares fit on the data for Δ and μ, using expres-

sions of the form

$$\Delta(\rho,T)/k = \Delta_1 + \Delta_2\rho + \Delta_3 e^t T/\rho + \Delta_4 e^{2t}\rho + (\Delta_5 + \Delta_6\rho + \Delta_7\rho^2)e^{3t}\ (\mathrm{K}) \qquad (11)$$

and

$$\mu(\rho,T) = U_1 + U_2 e^t T + U_3\rho + U_4 e^t T/\rho + (U_5 + U_6\rho)e^{3t}\ (m), \qquad (12)$$

Here, $t \equiv -\Delta(\rho, 0)/kT$, and the coefficients of eqs (11) and (12) are:

$\Delta_1 = 17.41647$ (K)

$\Delta_2 = -60.48823$ ($\mathrm{K \cdot g^{-1} \cdot cm^3}$)

$\Delta_3 = -0.5307478$ ($\mathrm{g \cdot cm^{-3}}$)

$\Delta_4 = 1.817261 \times 10^4$ ($\mathrm{K \cdot g^{-1} \cdot cm^3}$)

$\Delta_5 = -1.351398 \times 10^7$ (K)

$\Delta_6 = 1.621499 \times 10^8$ ($\mathrm{K \cdot g^{-1} \cdot cm^3}$)

$\Delta_7 = -5.062661 \times 10^8$ ($\mathrm{K \cdot g^{-2} \cdot cm^6}$)

and

$U_1 = 0.3420601$ (m)

$U_2 = 1.239037$ ($m \cdot \mathrm{K^{-1}}$)

$U_3 = -1.238153$ ($m \cdot \mathrm{g^{-1} \cdot cm^3}$)

$U_4 = -0.2234561$ ($m \cdot \mathrm{K^{-1} \cdot g \cdot cm^{-3}}$)

$U_5 = -13429.95$ (m)

$U_6 = 632197.06$ ($m \cdot \mathrm{g^{-1} \cdot cm^3}$)

The experimental roton energy gap and effective mass are shown in figures 5 and 6 with the results of eqs (11) and (12) respectively. Although eqs (11) and (12) suggest an expansion in terms of the roton number density, no particular theoretical significance can be attached to the terms in these equations.

We will see in section 3.1.f below that the experimental values of Δ and μ described in this section will have to be adjusted slightly to obtain the accurate thermodynamic information from the Landau theory.

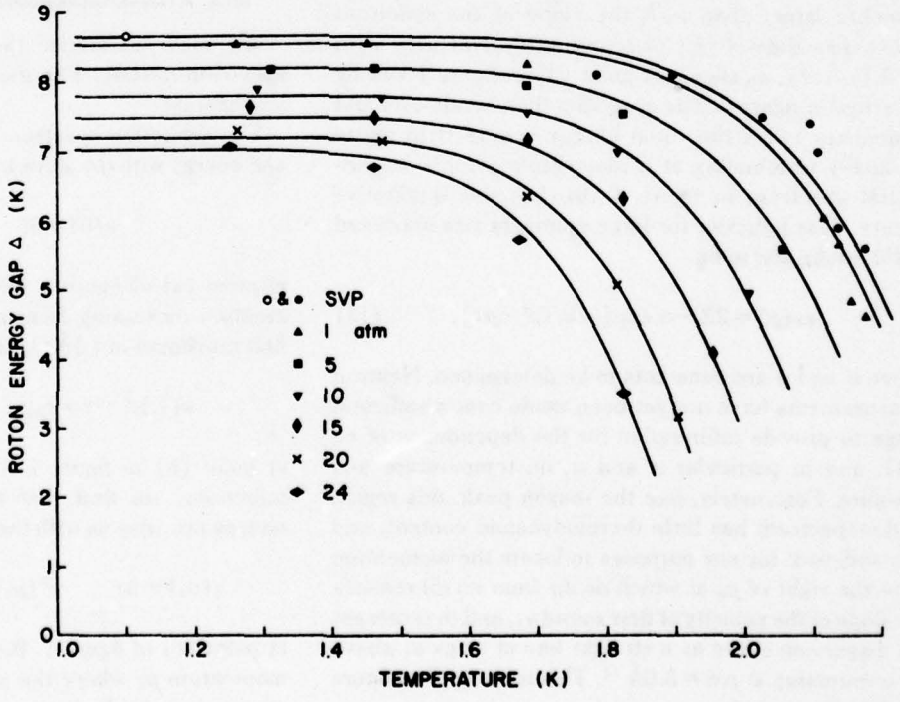

FIGURE 5. Least squares fit of eq (11) to the experimental roton energy gap Δ. Data at SVP, Henshaw and Woods [5] (solid circles), Cowley and Woods [2] (open circle); data at higher pressures, Dietrich et al. [3].

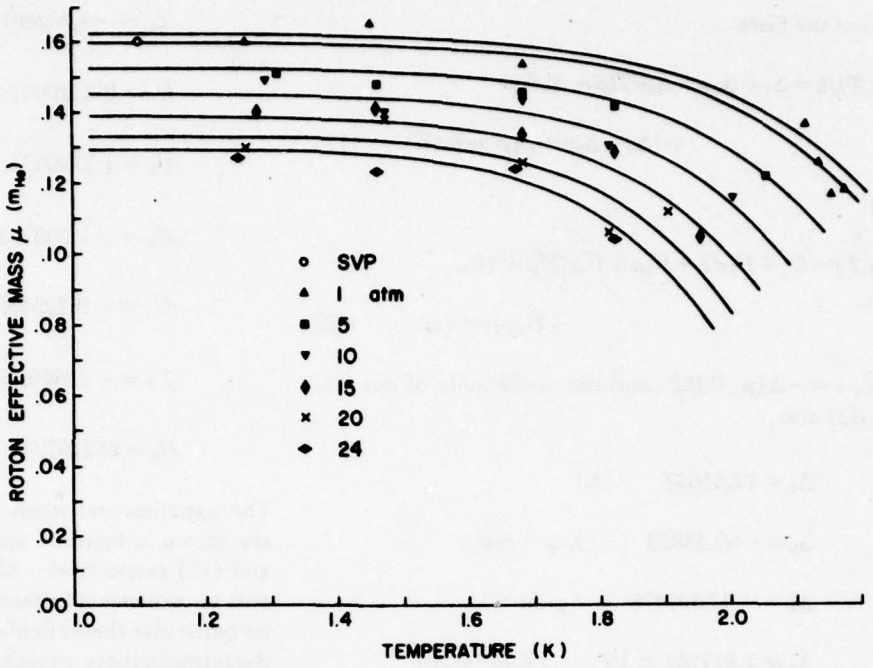

FIGURE 6. Least squares fit of eq (12) to the experimental roton effective mass μ. Data point at SVP, Cowley and Woods [2]: data at higher pressures, Dietrich et al. [3].

3.1.d. The Shoulder Beyond the Roton Minimum

Recent neutron scattering experimental results (Graf, Minkiewicz, Møller, and Passell [6] indicate that for momenta larger than $p_0/\hbar$ the slope of the spectrum approaches the velocity of sound at a momentum $p_c/\hbar$ ($\simeq 2.15$ Å^{-1}), as shown at point (d) in figure 1 and by the arrow in figure 3. The spectrum then bends over and approaches twice the roton energy (curve B in figure 1), finally terminating at a momentum p'. The experimental spectrum in figure 3 also has this qualitative feature. This behavior for large momenta was predicted by Pitaevskii [29] to be

$$\epsilon_P(p) = 2\Delta - \alpha \exp[-a/(p'-p)], \qquad (13)$$

where α and a are constants to be determined. Neutron measurements have not yet been made over a sufficient range to provide information for the dependence of eq (13), and in particular α and a, on temperature and pressure. Fortunately, like the maxon peak, this region of the spectrum has little thermodynamic content, and it is sufficient for our purposes to locate the momentum p_c to the right of p_0 at which $d\epsilon/dp$ from eq (5) reaches the slope of the velocity of first sound u_1, and to represent the dispersion curve as a straight line of slope u_1 above p_c, terminating at $p/\hbar = 3.0$Å^{-1}. This is curve C in figure 1, which is given by

$$\epsilon(p) = u_1\,(p - p_c) + \epsilon(p_c) \qquad p \geq p_c, \qquad (14)$$

where

$$p_c = \mu u_1 + p_0. \qquad (15)$$

This approximation is also indicated in figure 3 as the straight line above $p_c/\hbar \simeq 2.15$Å^{-1}.

3.1.e. A Polynomial Representation for the Excitation Spectrum

We may summarize the behavior of the excitation spectrum described in the previous sections in the following way:

The excitation spectrum starts out at zero momentum and energy with the slope u_1. Hence

$$\epsilon(0) = 0; \qquad \epsilon'(0) = u_1, \qquad (16)$$

at point (a) of figure 1. Here $\epsilon'(p) = d\epsilon(p)/dp$. For momentum increasing from zero, the spectrum attains its first maximum at 1.1Å^{-1}, and

$$\epsilon(1.1\text{Å}^{-1}) = \epsilon_{max}; \qquad \epsilon'(1.1\text{Å}^{-1}) = 0, \qquad (17)$$

at point (b) in figure 1. Continuing down to the roton minimum, we find that the parabolic representation near p_0 provides us with the relations

$$\epsilon(p_0) = \Delta; \qquad \epsilon'(p_0) = 0; \qquad \epsilon''(p_0) = 1/\mu, \qquad (18)$$

at point (c) of figure 1. Beyond the roton minimum, for momentum p_c where the slope approaches the velocity at sound, we finally have

$$\epsilon'(p_c) = u_1 \qquad (19)$$

at point (d) in figure 1.

Clearly, eqs (16) through (19) represent the most important features of the excitation spectrum. We have discovered, partially guided by theoretical considerations (see Feenberg [27]), that a polynomial in momentum without a quadratic term

$$\epsilon(p)/k = u_1 p + a_3 p^3 + a_4 p^4 + a_5 p^5 + a_6 p^6 + a_7 p^7 + a_8 p^8, \quad (20)$$

is an excellent representation for the excitation spectrum in the momentum interval $0 \leq p \leq p_c$, and that by using eq (14) for the interval $p_c/\hbar \leq p/\hbar \leq 3.0$ Å^{-1}, one has a continuous expression for the spectrum which may be used to great advantage in the computation of thermodynamic properties based upon the Landau theory. Note that if eq (20) is continued above p_c, it diverges negatively, as indicated by the dotted line in figure 1. Hence care must be used to apply eq (14) above p_c.

The coefficients a_n of eq (20) may be obtained for any temperature and pressure by applying the conditions imposed by eqs (16) through (19), which in turn will depend on T and P. Since there is no constant term, and the first coefficient must be u_1, the problem of determining the coefficients a_n is reduced to solving six equations with six unknowns, at any temperature and pressure.

The degree to which eqs (20) and (14) fit the neutron scattering data is shown as the solid line in figure 3 at 1.1 K, SVP, and again by the solid lines in figure 7 at 1.1 K, at SVP, and at 25.3 atm. The experimental values were used in eqs (16) through (19) to obtain these plots. One can appreciate from figure 7 how the spectrum changes with pressure.

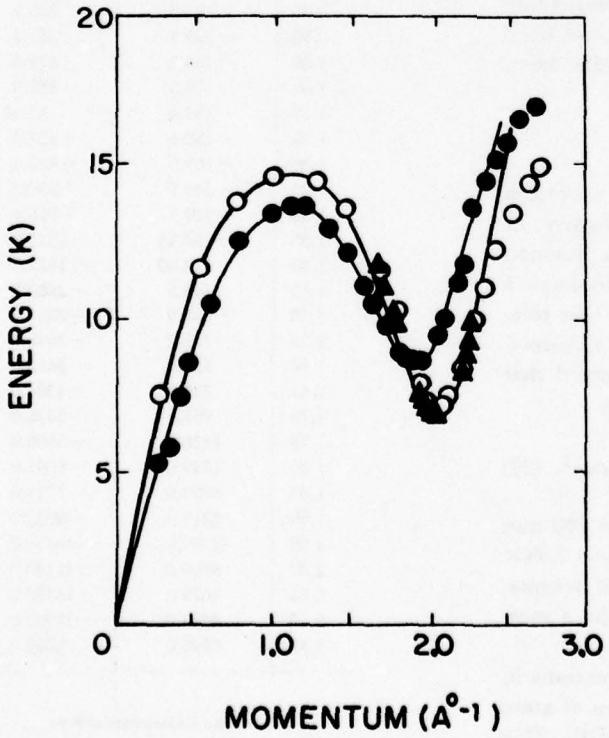

FIGURE 7. The excitation spectrum at two pressures at 1.1 K. Dots, SVP, open circles, 25.3 atm, Henshaw and Woods [4]; triangles, 1.25 K, 24.26 atm, Dietrich et al. [3]; solid lines, eqs (20) and (14).

As mentioned in section 3.1.a, a controversy surrounds the exact form that eq (20) should have for small momenta. We make here several comments concerning our choice of eq (20). First, we found that a series with no quadratic term was by far the best fit to the neutron data. A detailed comparison of several series is given by Brooks [18]. Secondly, one can see by inspection of the results of such calculations that the coefficient of the first nonlinear term a_3 changes sign upon increasing pressure. We find this to be consistent with the results of Phillips et al. [28] (see Brooks and Donnelly [17]). Finally, the form of eq (20) has prompted us to make some calculations concerning the low temperature behavior of the second sound velocity (Brooks and Donnelly [30]). The second sound velocity is quite sensitive to the leading terms in (20) and a careful measurement would serve as a check on the form we have chosen [30].

3.1.f. The Effective Sharp Spectrum for Thermodynamics

If we use the neutron model dispersion curves described in the previous section to compute, say, the entropy from table I, we discover that the agreement with the calorimetrically determined entropy is quite good at low temperatures for all pressures. At higher temperatures, however, the calculated entropy lies markedly higher. For example, at the vapor pressure, the calculated entropy exceeds the experimental by 17% at ~2.1 K; at 15 atmospheres the calculated entropy is 11% high at ~1.9 K, and at 20 atmospheres it is 23% high at ~1.8 K. This same trend may be seen in figure 17 of Dietrich et al. [3] who, however, made a correction to the formula for S by an additional integration over the linewidth. The departures between calculated and measured entropy occur at about the same value of $(T_\lambda - T)$ at all pressures, and correspond to the temperatures at which the linewidths of the scattered neutron distributions start to grow rapidly. The resulting problem in interpretation has been referred to in section 2 above.

Following Brooks [18] we have investigated the idea of constructing an effective dispersion spectrum, which represents the energies which yield thermodynamic results in accord with experiment. This is done by noting that the only constraint among eqs (16)–(19) which can be varied at all readily within experimental uncertainty is the exact value of Δ in (18) [and also of μ since it is computed from eq (9)]. We therefore allow Δ to float, retaining all other constraints as before, and produce a dispersion curve identical with the neutron data except for the precise value of Δ, computing μ from eq (9). This spectrum assumes there is some effective sharp frequency (that is, $\Gamma \to 0$) for each value of q; since there is but one adjustment, the resulting effective

spectrum is unique. An extensive numerical investigation has demonstrated the great utility of such a spectrum.

We find:

(1) The effective spectrum is capable of yielding accurate thermodynamic results over all pressures and temperatures up to $\sim (T_\lambda - 0.1\ \mathrm{K})$. All quantities calculated from table I and this spectrum appear to be in reasonable agreement with experiment.

(2) The effective spectrum is consistent with the observed functional form of the spectrum determined by neutron scattering. It coincides with the neutron spectrum within experimental error at low temperatures, and at high temperatures the difference between the observed and effective values of Δ is such that $(\Delta_{\mathrm{effective}} - \Delta_{\mathrm{neutron}}) < \Gamma$.

(3) Because the effective spectrum is unique, the exact value of Δ can be chosen by reference to more than one thermodynamic quantity. We have used entropy, expansion coefficient, and normal fluid density.

(4) The points listed above allow one to guess that the effective spectrum is probably a reasonable representation of the energies of elementary excitations of helium II.

3.2. The Thermodynamic Data

In order to use the formulas provided by the Landau theory, we need an equation of state to relate the pressure, volume (or density), and temperature, and from which we may obtain the velocity of first sound. Likewise, to test the results of our computations, we need calorimetric data, primarily entropy and specific heat. We now discuss these experimental data.

3.2.a. The Equation of State

Many of the parameters of the excitation spectrum depend on the density, and terms in the density, or molar volume, appear in expressions of the Landau theory (table I). It is therefore imperative to have a suitable equation of state or "*PVT*" relation. Our relationship is based upon the work of Abraham, Eckstein, Ketterson, Kuchnir, and Roach [31], who showed that as $T \to 0$, the equation of state can be written

$$P = A_0(\rho - \rho_0) + A_1(\rho - \rho_0)^2 + A_2(\rho - \rho_0)^3, \quad (21)$$

where ρ_0 is the density at $P = 0$, $T = 0$; $A_0 = 560$ atm $\mathrm{g^{-1}cm^3}$, $A_1 = 1.097 \times 10^4$ atm $\mathrm{g^{-2}cm^6}$, and $A_2 = 7.33 \times 10^4$ atm $\mathrm{g^{-3}cm^9}$. The "ground state" molar volume, $V_0(P) \equiv V(0, P)$ is calculated from eq. (21) by a root-searching technique.

Before the methods which led to the expressions in table I were developed, an empirical equation of state generalizing (21) was developed by Brooks [18]. This empirical equation of state was based on (21) and the data of Boghosian and Meyer [32], Elwell and Meyer [33], and Kerr and Taylor [34]. It was sufficiently accurate to give a good account of the density and isothermal compressibility, but was not sufficiently accurate to calculate the expansion coefficient.

Since this work was begun, a thesis has appeared by Craig Van Degrift [20] which employs the dielectric method for determining the density and expansion coefficient at the vapor pressure. Dr. Van Degrift has kindly supplied to us a table of data corrected to zero pressure. We have abstracted some of his data in table II. His complete results are in the process of preparation for publication. We should like to encourage the acquisition of data of comparable accuracy at a series of higher pressures.

TABLE II. Density differences and expansion coefficients corrected to $P = 0$ as determined by Van Degrift [20]. $\rho_0 = 0.145119$ g/cm³

T	$(\rho - \rho_0)/\rho_0 \times 10^6$	$\alpha_P(K^{-1}) \times 10^6$
0.30	− 2.255	29.49
0.35	− 4.122	45.96
0.40	− 6.931	67.28
0.45	− 10.94	93.93
0.50	− 16.42	126.3
0.55	− 23.67	164.5
0.60	− 32.95	207.7
0.65	− 44.49	254.2
0.70	− 58.37	300.5
0.75	− 74.46	342.1
0.80	− 92.40	373.3
0.85	− 111.5	387.9
0.90	− 130.8	380.2
0.95	− 149.1	345.4
1.00	− 164.8	279.8
1.05	− 176.5	181.0
1.10	− 182.4	47.48
1.15	− 180.6	− 122.3
1.20	− 169.5	− 330.4
1.25	− 146.9	− 580.2
1.30	− 110.7	− 876.4
1.35	− 58.43	− 1223.0
1.40	12.50	− 1622.0
1.45	104.5	− 2062.0
1.50	218.9	− 2511.0
1.55	356.7	− 3045.0
1.60	524.0	− 3652.0
1.65	722.8	− 4304.0
1.70	955.7	− 5015.0
1.75	1226.0	− 5806.0
1.80	1539.0	− 6699.0
1.85	1899.0	− 7724.0
1.90	2315.0	− 8922.0
1.95	2797.0	− 10360.0
2.00	3360.0	− 12140.0
2.05	4025.0	− 14480.0
2.10	4833.0	− 17990.0
2.15	5896.0	− 25880.0

3.2.b. The Calorimetric Data

The most fundamental calorimetric property directly accessible experimentally is the entropy S, which can be measured in an unusual way by employing the thermo-

mechanical effect. The entropy is calculated from the relation

$$S = \frac{1}{\rho}\frac{\Delta P}{\Delta T}, \tag{22}$$

where ΔP and ΔT are the differences in pressure and temperature between two chambers of helium II connected by a superleak. This relation, which is a direct result of the two fluid nature of superfluid helium, is discussed in the standard references [11, 12, 25, 26].

The specific heat C may be obtained by conventional calorimetric methods, and the entropy may be computed from the results by the relation

$$S = \int_0^T \frac{C}{T}\, dT. \tag{23}$$

The entropy is available from the thermomechanical effect data of Van den Meijdenberg, Taconis, and De Bruyn Ouboter [35] in the temperature range $1.15 \leq T \leq 2.05$ K and pressure range $0 \leq P \leq 25$ atm. The specific heat capacity measurements of Wiebes [36] cover the same range of pressure, but the temperature range $0.3 \leq T \leq 1.65$ K. We have used these two sets of data in our analysis, since they cover nearly the entire superfluid phase, and are in reasonable mutual agreement.

The specific heat has also been measured by Phillips, Waterfield, and Hoffer [28]. Through the kindness of Professor Phillips and Dr. Hoffer we have had access to some of their original calorimetric measurements, which are in satisfactory agreement with those of Wiebes (see, for example, Brooks and Donnelly [17], figure 2). The publication of the final data from these experiments is still awaited.

4. Computational Methods and Comparison of Computed Values With Experiment

In this section we discuss the way in which each of the tabulated properties given in Appendix A is obtained, and describe to what degree of accuracy the computed values agree with the corresponding experimental data. Direct references are made to the tables.

4.1. Generation of the Effective Spectrum

We discussed in section 3.1.f above, the concept of an effective sharp spectrum for thermodynamics. It differs from the spectrum of section 3.1.e. only in allowing the value of $\epsilon(p_0) = \Delta$ to float, its exact value being chosen by comparison of the calculated quantities with experiment. In the original tables computed by Brooks [18], the procedure was to adjust Δ and thus the effective mass through eq (9), so that the calculated entropy agrees with the experimental entropy at all temperatures and pressures at which the roton part of the spectrum contributes significantly. This method had the disadvantage that even with quite accurate values of S, the expansion coefficient calculated from $(\partial S/\partial P)_T$ could be quite poor. Dr. Jay Maynard of UCLA drew our attention to the fact that the normal fluid density (cf. section 4.4.b.) is weighted heavily toward higher momenta, and hence is also a useful measure of the effective roton gap. We decided, therefore, that for the generation of the effective spectrum for this work, we would endeavor to employ a method which would incorporate all available thermodynamic evidence: from entropy, expansion coefficient, and normal fluid density.

James Gibbons undertook the job of computing the effective spectrum. This proved to be an arduous task because of the great sensitivity of the thermodynamics to minor changes of the spectrum in the vicinity of the roton minimum. The first step was a weighted fit to experimental values of S and α, making use of the Maxwell relations $(\partial V/\partial T)_P = -(\partial S/\partial P)_T$. This produced a set of polynomials in the pressure at 0.1 K temperature intervals. Since the tables are tabulated in 0.05 K intervals, this data was interpolated by a second degree polynomial in temperature fitted to three local points to find the best fit to data at 0.05 K intervals. A new set of polynomials in pressure were then generated from $T =$ 1 K to $T = 2.2$ K in 0.05 K intervals. Special care had to be taken near the lambda line because of the existence of large high-order derivatives. An iterative root-searching method was then used to find what one could call $\Delta(S, \alpha)$ from eq (2), in all cases calculating μ from eq (9).

The second step was to interpolate the experimental data on ρ_n/ρ, which also exists chiefly on 0.1 K increments, by a procedure analogous to that used for S and α. The end result of a similar root search was a set of values named $\Delta(\rho_n/\rho)$, at 0.05 K intervals.

The third step was to adjust the values of Δ at zero pressure to the compromise $[\Delta(\rho_n/\rho) + \Delta(S, \alpha)]/2$, retaining the curvature of the polynomials determined in the first step at higher pressures. The result of this step might be called $\Delta(S, \alpha, \rho_n/\rho)$.

The fourth and final step was a smoothing operation on the energy data of step three by means of a power series in N_r, the roton number density. This step was essential to encourage the monotonic behavior of the values of Δ as T is reduced below 1 K. Once the smoothed table of Δ was available, μ was calculated by eq (9). We have named these final values of Δ the "thermal" roton gap Δ_t, and the corresponding thermal effective masses μ_t. They are listed in tables 22 and 23. Having obtained Δ_t and μ_t, the effective spectrum (20) is computed by the methods described in section 3.1.e. In eqs (16) and (19), the isothermal velocity of sound was used, eq (24) below. The errors resulting from this approximation are negligible. Attempts to use eq (25) for u_t led to severe problems in numerical instability.

It is interesting to note that the differences between

the neutron roton energy gap and the thermal roton gap Δ_t are not random but systematic. We find that, in general, Δ_t lies above Δ at higher temperatures and pressures. The two agree within experimental uncertainties at low temperatures. The differences $(\Delta_t - \Delta) \ll \Gamma$ except at temperatures near the lambda line. Γ may be calculated from the expression of Roberts and Donnelly [37]:

$$\Gamma/k = 0.65 \times 10^{-33} N_r / (\mu^{1/2} \rho^{2/9} T^{1/6}) \text{ K}.$$

At the vapor pressure, the neutron determinations of Yarnell et al. [9] give $\Delta/k = 8.65 \pm 0.04$ K at 1.1 K, while Cowley and Woods [2] obtained $\Delta/k = 8.67 \pm 0.04$ K at the same temperature, and Dietrich et al. [3] find $\Delta/k = 8.54$ K at $T = 1.26$ K, $P = 1$ atm, which extrapolated to zero pressure gives $\Delta/k = 8.64$ K. There is a completely independent way of finding Δ. It is known that Raman scattering from liquid helium at low temperatures gives a peak at 16.97 ± 0.03 K. This peak has been identified by Greytak and his collaborators as a loosely bound state of two rotons [38]. An exact quantum mechanical solution to one model for this state by Roberts and Pardee [39] gives the binding energy of the rotons as 0.290 K. Thus the roton energy should be $(16.97 + 0.290)/2 = 8.63 \pm 0.015$ K, in good agreement with the neutron measurements. We find $\Delta_t = 8.622$ K at 1.1 K, $P = 0$, in satisfactory agreement with all methods.

4.2. The Equation of State

The integral expression for V in table I is, in contrast to our earlier empirical equation of state [18, 19], completely consistent with the expressions for α_P and κ_T. By making use of the empirical equation of state [19], the equation of state for our tables 1 and 2 was obtained in a single iteration. One can also start from absolute zero data for V and κ_T and iterate to find substantially the same results. As we mentioned in section 3.2.a above, $V_0(P)$ comes from eq (21).

The low temperature behavior of the molar volume is shown in figure 8, plotted in the form $V_E(T, P) = V(T, P) - V(0, P)$ vs. temperature for 2.5 atmosphere increments in pressure. A nonlinear scale has been deliberately chosen to emphasize the characteristic maximum in the molar volume near 1 K. We show in figure 9 the entire temperature and pressure range of V, plotted with the data of Boghosian and Meyer [32], and Elwell and Meyer [33]. The deviations of our equation of state from the experimental data used in our analysis varies across the P–T plane. If we define a fractional deviation for the molar volume $\Delta V = (V_{\text{calculated}} - V_{\text{measured}})/V_{\text{measured}}$, we can get a rough idea of the variations by averaging ΔV over temperature at each pressure and denoting the result by $\overline{\Delta V}$ expressed in percent. The results are given in tabular form below, separated to display positive and negative deviations at six pressures, and we see that the temperature-averaged deviations are at most +0.42%–0% from the data.

P (atm)	0	5	10	15	20	25
$\pm(\overline{\Delta V})$%	0.01	0.17	0.19	0.29	0.39	0.42
$-(\overline{\Delta V}$(%	0	0	0	0	0	0

4.2.a. The Velocity of Sound

There are several other quantities which may be calculated from the equation of state, such as the isothermal velocity of sound:

$$u_{1,T}^2 = \left(\frac{\partial P}{\partial \rho}\right)_T = (\rho \kappa_T)^{-1}, \tag{24}$$

where κ_T is defined in (26) below. A first order correction for thermal expansion using computed values of $\gamma = C_P/C_V$ (discussed in section 4.3.e.) gives

$$u_1^2 = \left(\frac{\partial P}{\partial \rho}\right)_S = \frac{\gamma}{\rho \kappa_T}.$$

The actual expression used for the calculations reported here carries a higher order correction for thermal expansion [40, 41]

$$u_1^2 = u_I^2 + \frac{\gamma - 1}{\gamma} \frac{u_I^2 u_{II}^2}{u_I^2 - u_{II}^2}, \tag{25}$$

where u_{II} is defined in section 4.4.c. below. The corrected velocity of first sound u_1 is given in table 3 and illustrated in figure 10. At $T = 0$ K, the deviations from the data of Abraham et al. [31] are less than 0.09%. At higher temperatures, (> 1 K), the deviations $\Delta u_1 = (u_{1\,\text{calc}} - u_{1\,\text{meas}})/u_{1\,\text{meas}}$ from some preliminary data of Maynard and Rudnick [21] are as follows:

P (atm)	0	5	10	15	20	25
$+(\overline{\Delta u_1})$%	0.8	0.3	0.5	0.8	1.0	0.5
$-(\overline{\Delta u_1})$%	0	0	0	0	0	1.2

Below 1.6 K, the deviations are much less than 1%. Only the highest few temperatures depart significantly from the data.

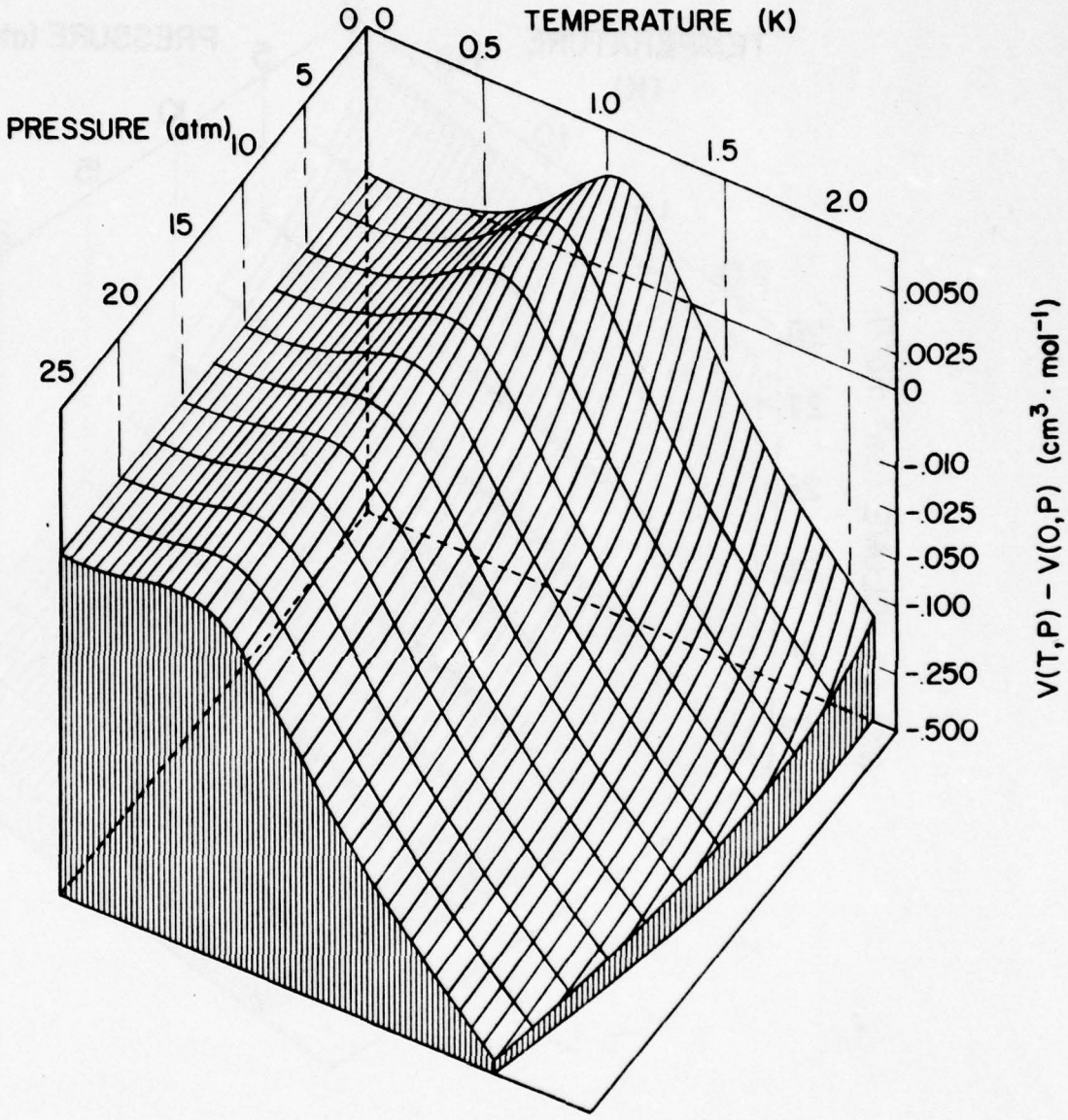

FIGURE 8. The relative change in molar volume given by the expression in table I. The nonlinear scale is chosen to emphasize the locus of maximum molar volume, or zero thermal expansion.

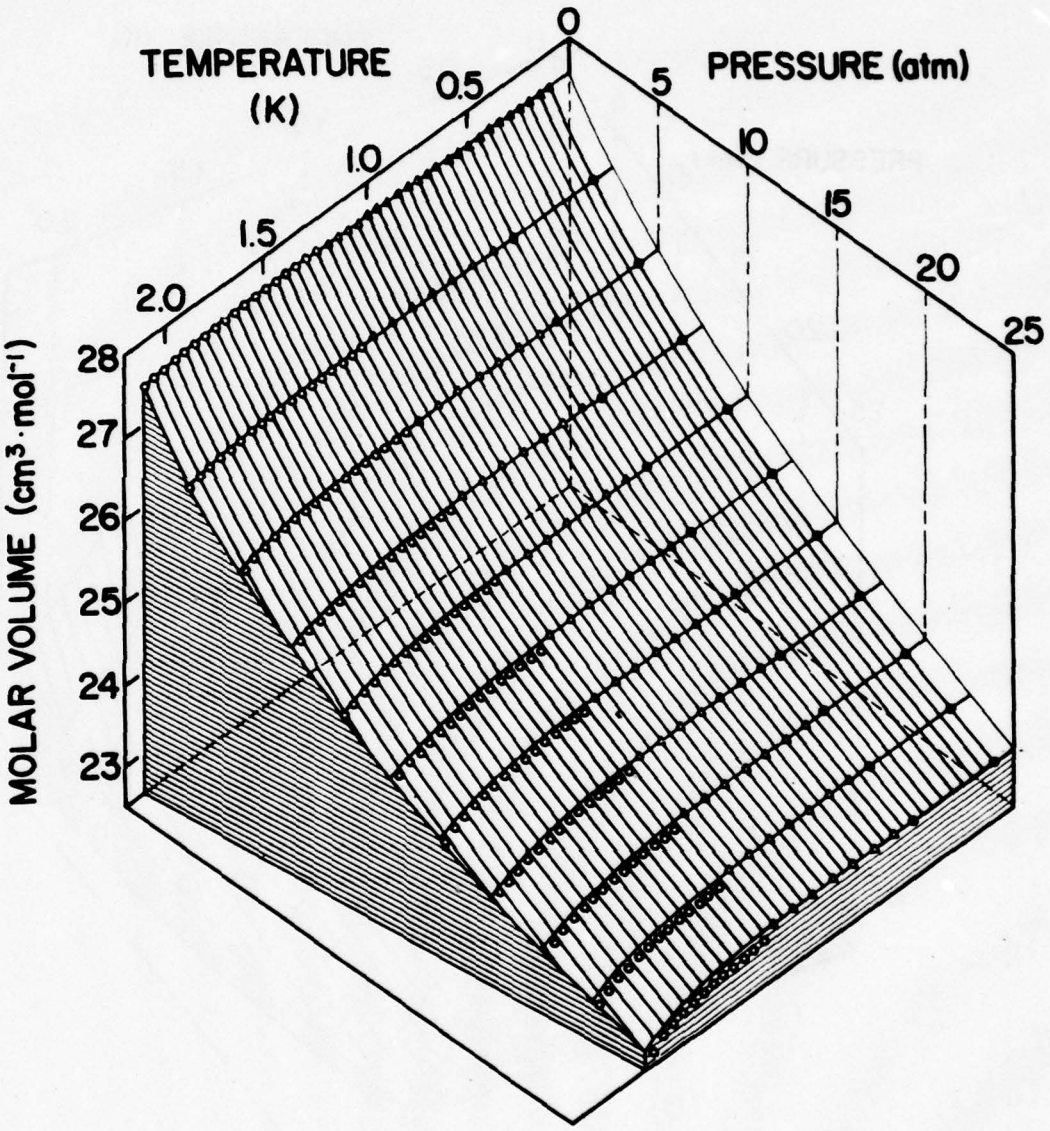

FIGURE 9. The P–V–T surface of helium II. Solid lines come from the expression in table I; open circles, Elwell and Meyer [33]; open triangles, Boghosian and Meyer [32]; solid circles, Abraham et al. [31]; solid triangles, Kerr and Taylor [34]. The deviation between calculation and the data may be seen as a difference perpendicular to the P–T plane. The experimental data have been numerically interpolated to 5 atm intervals in pressure.

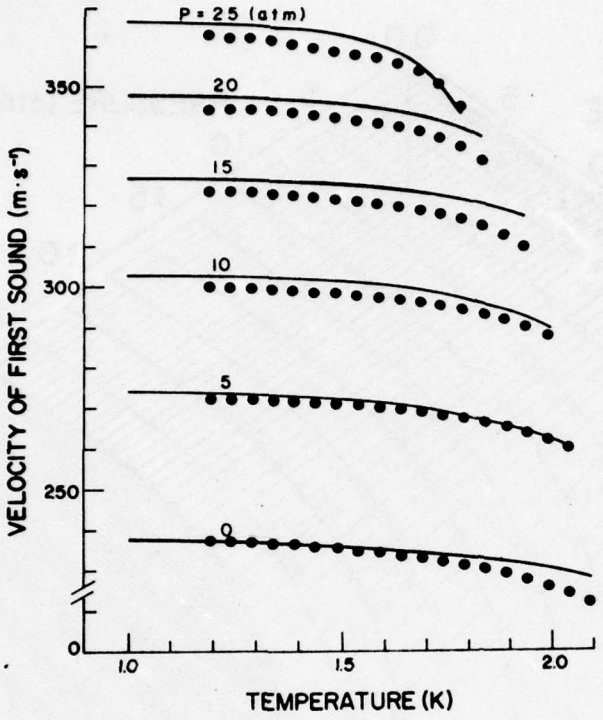

FIGURE 10. The velocity of first sound as a function of temperature for different pressures calculated from eq (25). Data points from Heiserman et al. [21].

4.2.b. The Isothermal Compressibility

The isothermal compressibility, which is defined as

$$\kappa_T \equiv -\frac{1}{V}\left(\frac{\partial V}{\partial P}\right)_T, \tag{26}$$

is obtained by noting that $V(T, P) = V(O, P) + \delta V(T, P)$ from table I. The derivative $(\partial V/\partial P)$ is calculated separately for the two terms, resulting in more reliable results than differentiating the total molar volume directly. The results are in table 4.

The first term $\kappa_T(0)$ can be compared directly with the data of table V of Boghosian and Meyer [32]. The deviations $\Delta\kappa \equiv (\kappa_{calc} - \kappa_{meas})/\kappa_{meas}$ range from +4.1% to −5.0%. However, we believe that our data, derived from the later measurements of Abraham et al. [31], are considerably more reliable. Since the contribution from the temperature dependent part of V is so small, the the deviations quoted are the dominant ones at all temperatures up to 1.25 K, the highest reported by Boghosian and Meyer [32].

Elwell and Meyer [33] report measurements of κ_T in the range above 1.2 K. Comparing with their tables IV and V, we find the pressure averaged deviations $\Delta\kappa$ to be +0, −2.4% at 1.3 K; and +0, −2.0% at 1.8 K.

Our computed values of the compressibility are not sufficiently accurate near the lambda line to exhibit the peak structure observed by Grilly [42].

4.2.c. The Grüneisen Constant

Another quantity which appears in expressions for the ultrasonic attenuation and dispersion in helium II is the Grüneisen constant, defined as

$$U_G \equiv \left(\frac{\rho}{u_1}\right)\left(\frac{\partial u_1}{\partial \rho}\right)_T. \tag{27}$$

It is listed in table III below; the values at $T = 0$ K are in agreement with the $T = 0.1$ K data of Abraham et al. [31] at all pressures, to within ± 0.25%.

TABLE III. The Grüneisen constant U_G

T(K)	P(atm)					
	0	5	10	15	20	25
0.0	2.843	2.608	2.460	2.356	2.276	2.212
0.5	2.842	2.608	2.460	2.356	2.275	2.213
1.0	2.842	2.624	2.466	2.339	2.270	2.194

4.2.d. The Coefficient of Thermal Expansion

The thermal expansion coefficient is a temperature derivative of the equation of state:

$$\alpha_P \equiv \frac{1}{V}\left(\frac{\partial V}{\partial T}\right)_P. \tag{28}$$

It is, however, directly calculated from the integral expression of Roberts and Donnelly given in table I.

We experienced great difficulty with α_P because it is a very small quantity which passes through zero near 1 K. Our calculations, listed in table 5 and illustrated in figure 11, are sufficiently accurate to give a good account of the locus of zero expansion indicated by the dashed line in figure 2. We have also managed to keep the deviations from growing rapidly above 1.6 K as they did in our earlier work [18, 19]. The temperature-averaged deviations $\Delta\alpha_P = (\alpha_{P\,calculated} - \alpha_{P\,measured})/\alpha_{P\,measured}$ follow:

P(atm)	0	5	10	15	20	25
$+(\overline{\Delta\alpha_P})\%$	14	16	34	0.8	1.1	1.6
$-(\overline{\Delta\alpha_P})\%$	16	3.2	8	9	10	11

Except for the vapor pressure, where the systematic work of Van Degrift exists, the experimental situation on α_P is quite unsatisfactory and the data often in mutual conflict. A systematic study over the entire T–P plane would be of great benefit in reducing the deviations listed above.

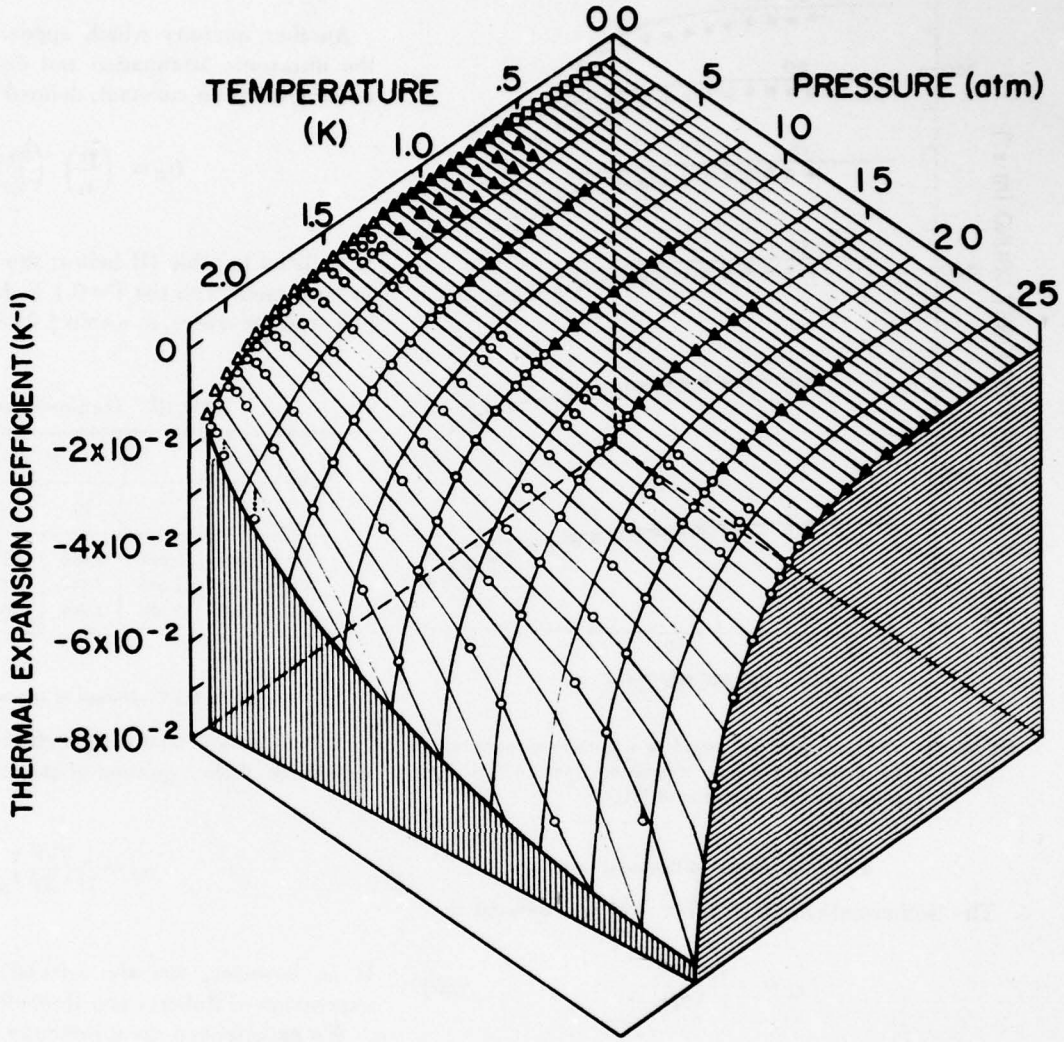

FIGURE 11. The thermal expansion coefficient as a function of pressure and temperature. The solid lines are calculated from the expression in table I; circles, Elwell and Meyer [33]; solid triangles, Boghosian and Meyer [32]; open triangles, Van DeGrift [20]; open diamonds, Kerr and Taylor [34].

4.3. The Fundamental Thermodynamic Functions

In this section we describe our use of the Landau theory and the effective spectrum to compute the thermodynamic properties of helium II.

4.3.a. The Entropy

The entropy is the fundamental quantity used to find the effective spectrum. Deviations, then, reflect imperfections in the data itself as well as the effective spectrum. The temperature averaged deviations $\Delta S = (S_{calc} - S_{meas})/S_{meas}$ are as follows:

P(atm)	0	5	10	15	20	25
$+(\overline{\Delta S})\%$	0.7	1.5	1.2	0.5	0.6	0.2
$-(\overline{\Delta S})\%$	3.9	2.6	2.4	2.5	2.8	2.0

The entropy is listed in table 9 and plotted in figure 12.

4.3.b. The Helmholtz Free Energy

Table I shows that the Helmholtz free energy F consists of a ground state part $F_0(V)$ and an excitation part F_E given by the double integral over the spectrum. $F_0(V)$ can be determined by integrating the expression $dF_0 = -PdV$. The results give F_0 at $T = 0$ K to within an additive constant $L_0[L_0 = F(0, 0) = \Phi(0, 0)]$ where L_0 is the latent heat of vaporization extrapolated to zero temperature, and is approximately $14.6 J \cdot g^{-1}$ (from Keesom [43]). L is a measure of the energy required to separate the atoms of the liquid to infinity.

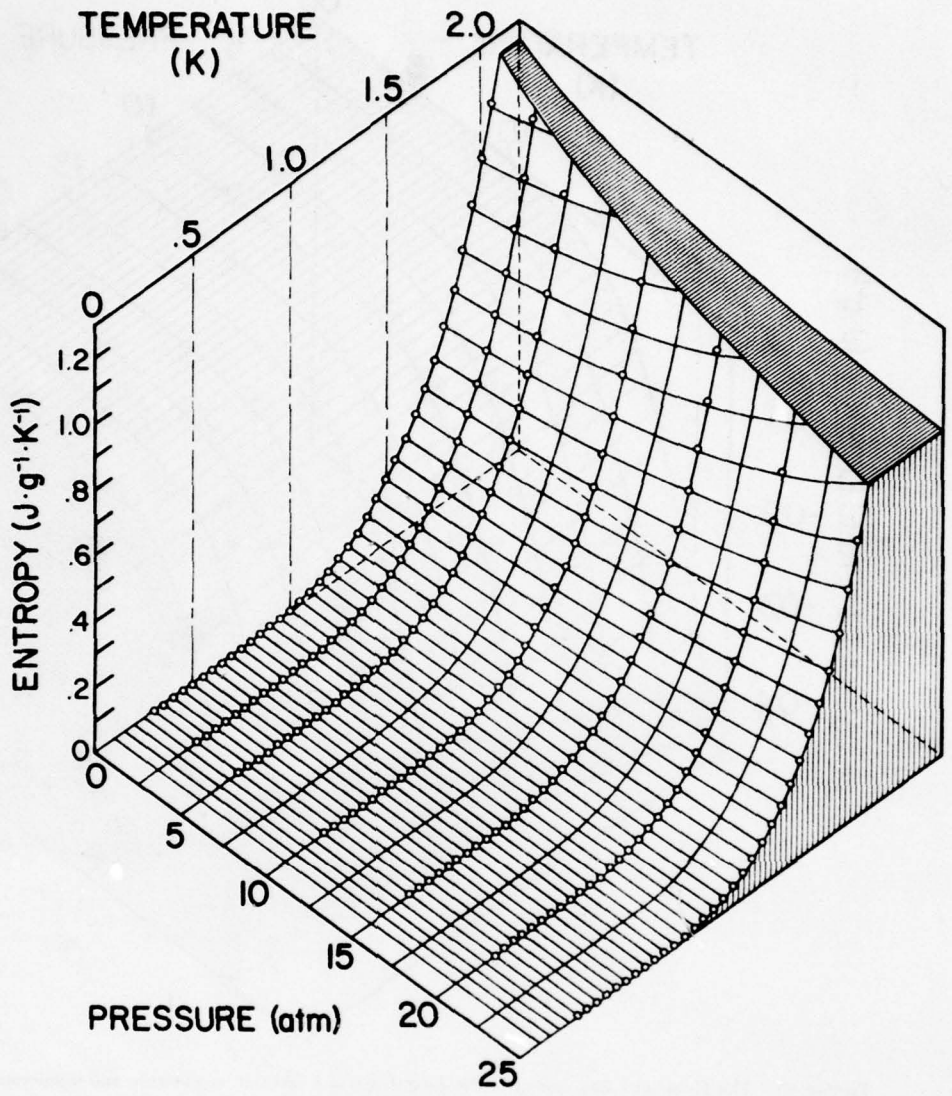

FIGURE 12. The entropy of helium II as a function of pressure and temperature calculated from equation (2). The data for $0.3 \leq T \leq 1.6$ K is from Wiebes [36], and for $1.6 \leq T \leq 2.05$ K is from Van der Meijdenberg et al. [35].

TABLE IV. The ground state Helmholtz free energy $\Delta F_0(P) = [F(0, P) - F(0, 0)]$ J·g^{-1}

P(atm)	0	2.5	5	7.5	10	12.5
$F_0(V)$ (J·g^{-1})	0	0.023254	0.082368	0.16671	0.26980	0.38737
P(atm)		15	17.5	20	22.5	25
$F_0(V)$ (J·g^{-1})		0.51645	0.65490	0.80111	0.95385	1.1122

The Helmholtz free energy is not a directly accessible quantity, and no comparison with experimental data can be readily made. However, table IV comes from the equation of state of Abraham et al. [31] and should be quite accurate. The excitation free energy is tabulated in table 6 and plotted in figure 13. The derivative $(\partial n/\partial q)$ in the expression for F in table I is taken at constant volume. We approximated it by constant pressure. In order to check the accuracy of our calculation, we computed $-(\partial F/\partial T)$ at constant pressure and compared it to S. Except at the highest temperatures and pressures, the error in our procedure is generally less than 1% and never more than 2.2%.

4.3.c. The Gibbs Free Energy

The Gibbs free energy Φ has a ground state part $\Phi_0(P)$ and an excitation part $\Phi_E(P, T)$ given by the double integral in table I. $\Phi_0(P)$ can be determined by integrating the expression $d\Phi = VdP$. The results determine Φ_0 at $T = 0$ K to within an additive constant L_0 as described in section 4.3.b. above.

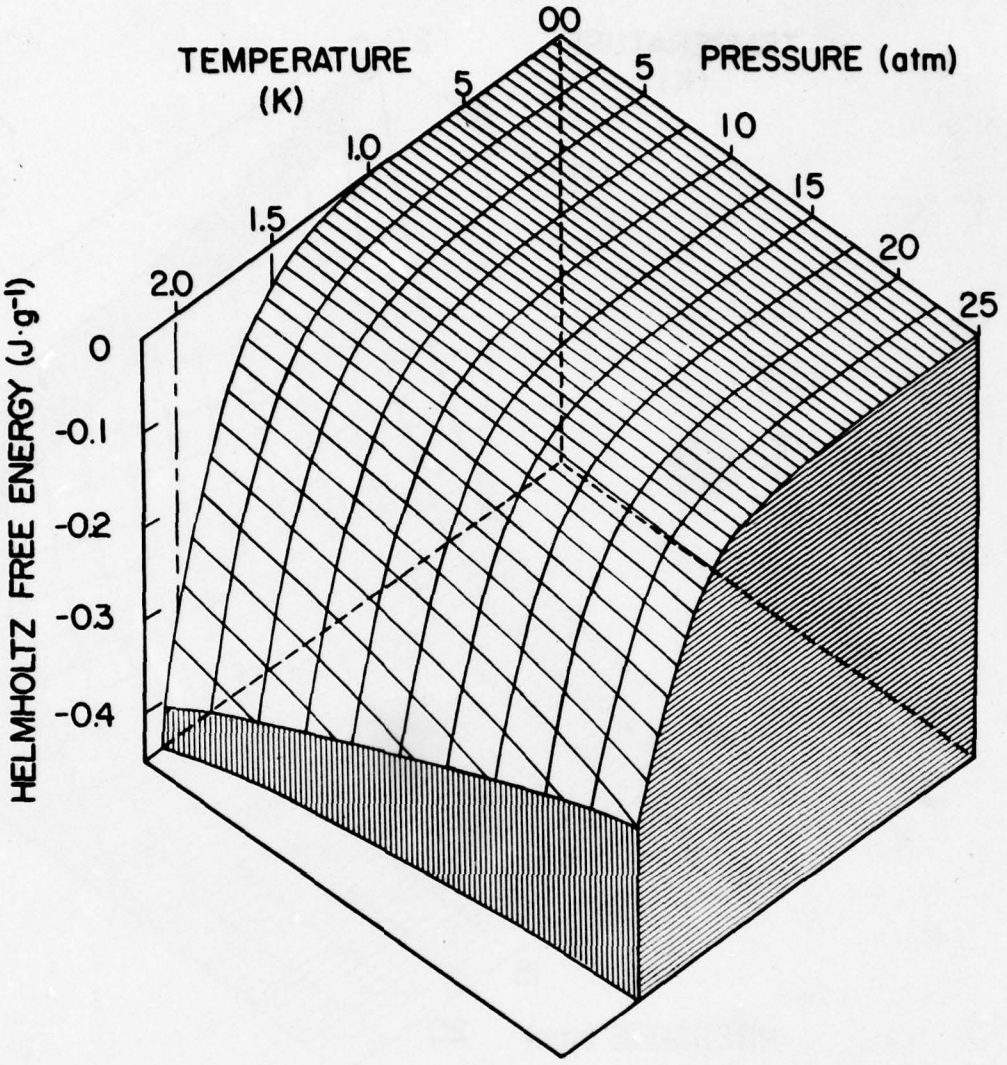

FIGURE 13. The Helmholtz free energy of the excitations as a function of pressure and temperature. The Gibbs free energy has substantially the same appearance.

TABLE V. The ground state Gibbs free energy $\Phi_0(P) = [\Phi(0, P) - \Phi(0, 0)]$ J·g^{-1}

P(atm)	0	2.5	2	7.5	10	12.5
$\Phi_0(P)$J·g^{-1}	0	1.7205	3.3972	5.0373	6.6457	8.2263
P(atm)	15		17.5	20	22.5	25
$\Phi_0(P)$J·g^{-1}	9.7821		11.316	12.829	14.323	15.800

The Gibbs free energy is not directly accessible experimentally. The data of table V come from integration of the equation of state of Abraham et al. [31] and hence should be reliable. The excitation part of the Gibbs free energy is tabulated in table 7: the appearance of this energy surface is similar to the Helmholtz energy in figure 13. We have checked the integration by comparing $(\partial\Phi/\partial T)_P$ to S. The differences are less than 0.3% over most of the T–P plane and never exceed 1%.

4.3.d. The Enthalpy

The enthalpy W has a ground state part $W_0(P)$ and an excitation part $W_E(P, T)$ as given by the double integral in table I. The ground state part $W_0(P) = \Phi_0(P)$ is tabulated in table V in section 4.3.c. above. The enthalpy of the excitations is tabulated in table 8 and illustrated in figure 14.

We have cross-checked our tabulations with the equivalent expression $\int_0^T C_P dT$. We find the differences are less than 1.7% at most temperatures and pressures. The enthalpy, then, should have the same basic accuracy as the specific heat, as discussed in section 4.3.e below.

4.3.e. The Specific Heat

The specific heat at constant pressure,

$$C_P = T(\partial S/\partial T)_P, \tag{29}$$

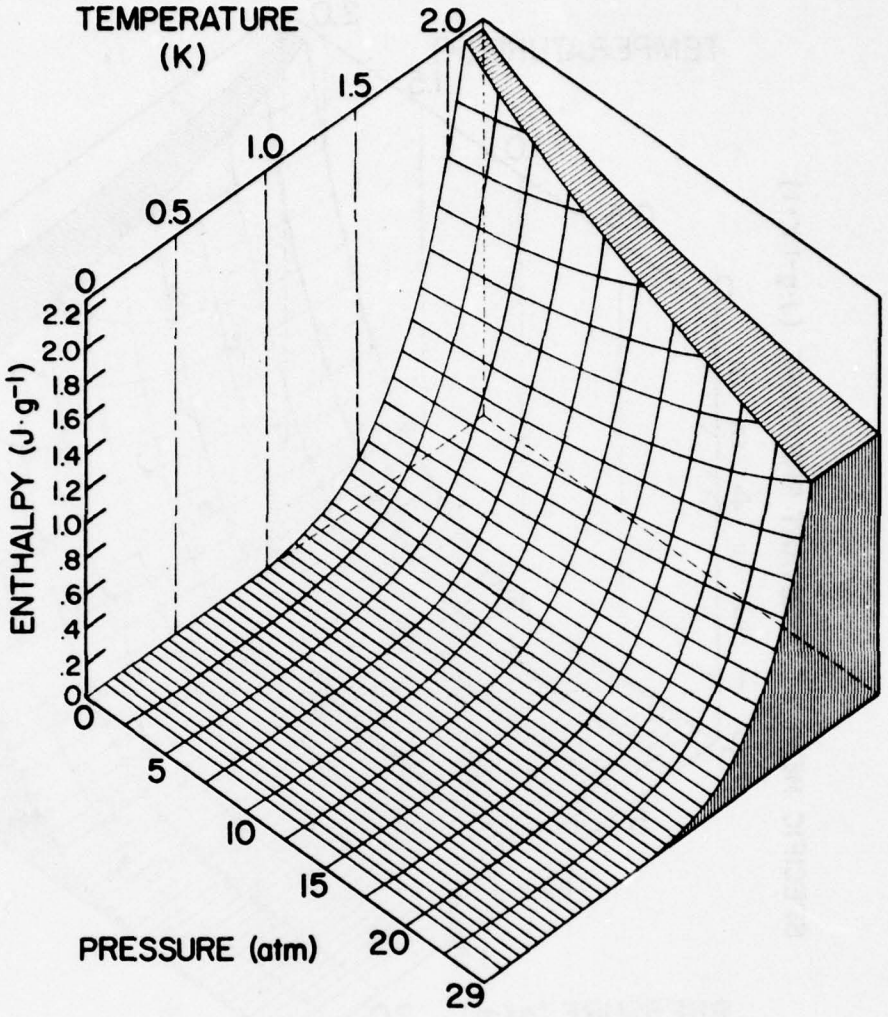

FIGURE 14. The enthalpy of the excitations as a function of pressure and temperature, as calculated from the expression in table I.

is obtained by the integral expression in table I. Below 1 K this worked satisfactorily; above 1 K we experienced difficulty in getting a smooth table. We therefore used (29) directly, selecting five local entropy values, fitting a quadratic function by least squares, and finding $\partial S/\partial T$ from that function. The resulting values are listed in table 10 and plotted in figure 15.

The deviations $\Delta C_P = (C_{P\,\mathrm{calc}} - C_{P\,\mathrm{meas}})/C_{P\,\mathrm{meas}}$ have been compared with the data of Wiebes [36] for $T \leq 1.6$ K.

P(atm)	0	5	10	15	20	25
$+(\overline{\Delta C_P})\%$	2.2	1.5	1.4	0.88	1.0	2.0
$-(\overline{\Delta C_P})\%$	6.5	3.0	2.2	2.3	3.3	2.8

The ratio of specific heats is compiled from

$$\gamma = \frac{C_P}{C_V} = \left[1 - \frac{\alpha_P^2 T}{\rho C_P \kappa_T}\right]^{-1} \qquad (30)$$

The term in α_P^2 is subject to an accumulation of errors and is perhaps as much as 50% in error in some regions. Values of γ are tabulated in table 12.

The specific heat at constant volume $C_V = C_P/\gamma$ is listed in table 11. Although γ is quite uncertain, the correction is generally small. Comparing with the data of Wiebes [36], we find the deviations are as follows ($T \leq 1.6$ K):

P(atm)	0	5	10	15	20	25
$+(\overline{\Delta C_V})\%$	2.2	1.6	1.4	1.0	2.2	2.7
$-(\overline{\Delta C_V})\%$	6.5	2.9	2.1	2.3	3.2	2.6

Table I shows an integral expression for C_V. We have used the correction of eq (30) rather than our theoretical expression because the latter involves a derivative at constant volume.

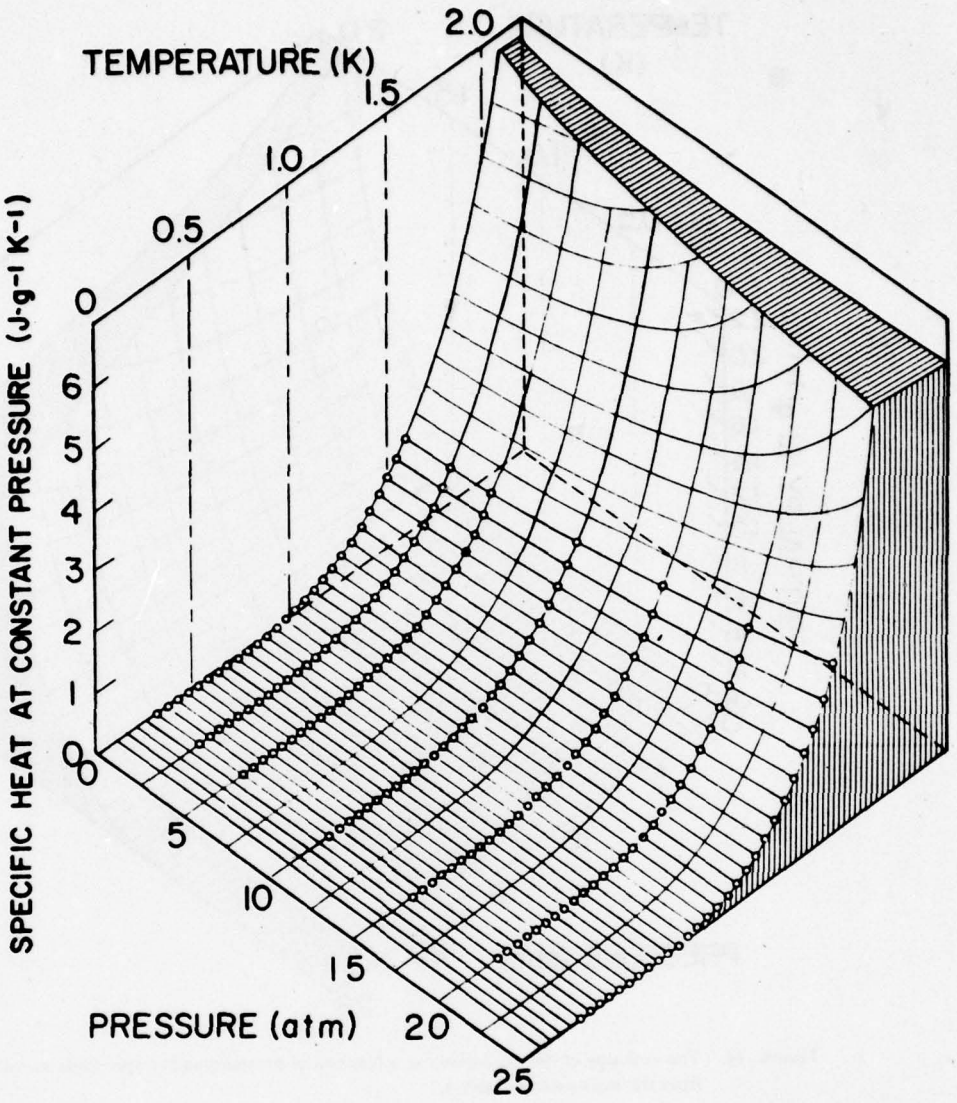

FIGURE 15. The specific heat at constant pressure as a function of pressure and temperature, calculated from the expression in table I. Data, Wiebes, [36].

4.4. Superfluid Properties

4.4.a. The Excitation Number Densities

The density of thermal excitations, calculated by numerical integration, has been separated into a phonon part N_p and a roton part N_r by defining (quite arbitrarily) excitations with wave number less than 1.1 Å^{-1} phonons. For phonons, we have for the number density [from eq (1)]

$$N_p = \int_0^{q_{max}} n(q)d^3q, \tag{31}$$

and for rotons

$$N_r = \int_{q_{max}}^{q_f} n(q)d^3q, \tag{32}$$

where q_{max}=1.1 Å^{-1}, q_f=3.0 Å^{-1}. Tabulations of N_p and N_r appear in tables 13 and 14, respectively. No comparison of the results can be made since the number densities are not directly accessible experimentally.

4.4.b. The Normal Fluid and Superfluid Densities

The normal fluid density may be computed from Landau's expression

$$\rho_n = \frac{\hbar^2}{6\pi^2 kT}\int_0^{3\text{Å}^{-1}} \frac{\exp[\epsilon(q)/kT]}{[\exp(\epsilon(q)/kT)-1]^2}\, q^4 dq, \tag{33}$$

and the computed values appear in table 15. From the equation of state, we may obtain the superfluid density by subtraction of ρ_n,

$$\rho_s = \rho - \rho_n,$$

and one may also obtain the ratios ρ_n/ρ and ρ_s/ρ. The quantities ρ_n/ρ, ρ_s, and ρ_s/ρ appear in tables 16, 17, and 18 respectively, and ρ_n/ρ is plotted in figure 16.

The calculations can be compared with a variety of experiments. At the vapor pressure, the deviations $\Delta\rho_n = (\rho_{n\,calc} - \rho_{n\,meas})/(\rho_{n\,meas})$ from the data of Tough et al. [44] are $\overline{\Delta\rho_n} = -0.78\%, +3.1\%$, with most of the latter error occurring at 2 K and above. Comparing with some unpublished data of Maynard (based on second and fourth sound measurements [21]), one finds the following:

P(atm)	0	5	10	15	20	25
$+(\overline{\Delta\rho_n/\rho})\%$	3.1	2.7	2.5	3.8	3.6	8.0
$-(\overline{\Delta\rho_n/\rho})\%$	0	2.8	4.0	3.5	5.8	5.0

The oscillating disk data of Romer and Duffy [45], principally above 1.6 K, averages about 4–7% low compared to our calculations.

4.4.c. The Velocity of Second Sound

The velocity of second sound, neglecting thermal expansion, is

$$u_{II}^2 = \left(\frac{\rho_s}{\rho_n}\right)\frac{TS^2}{C_V},$$

where u_{II} was used to correct the velocity of first sound in section 4.2.a above. Allowing for thermal expansion, the velocity of second sound is given by [40, 41].

$$u_2^2 = u_{II}^2 - \left(\frac{\gamma - 1}{\gamma}\right)\left[\frac{u_I^2\, u_{II}^2}{u_I^2 - u_{II}^2}\right] \tag{34}$$

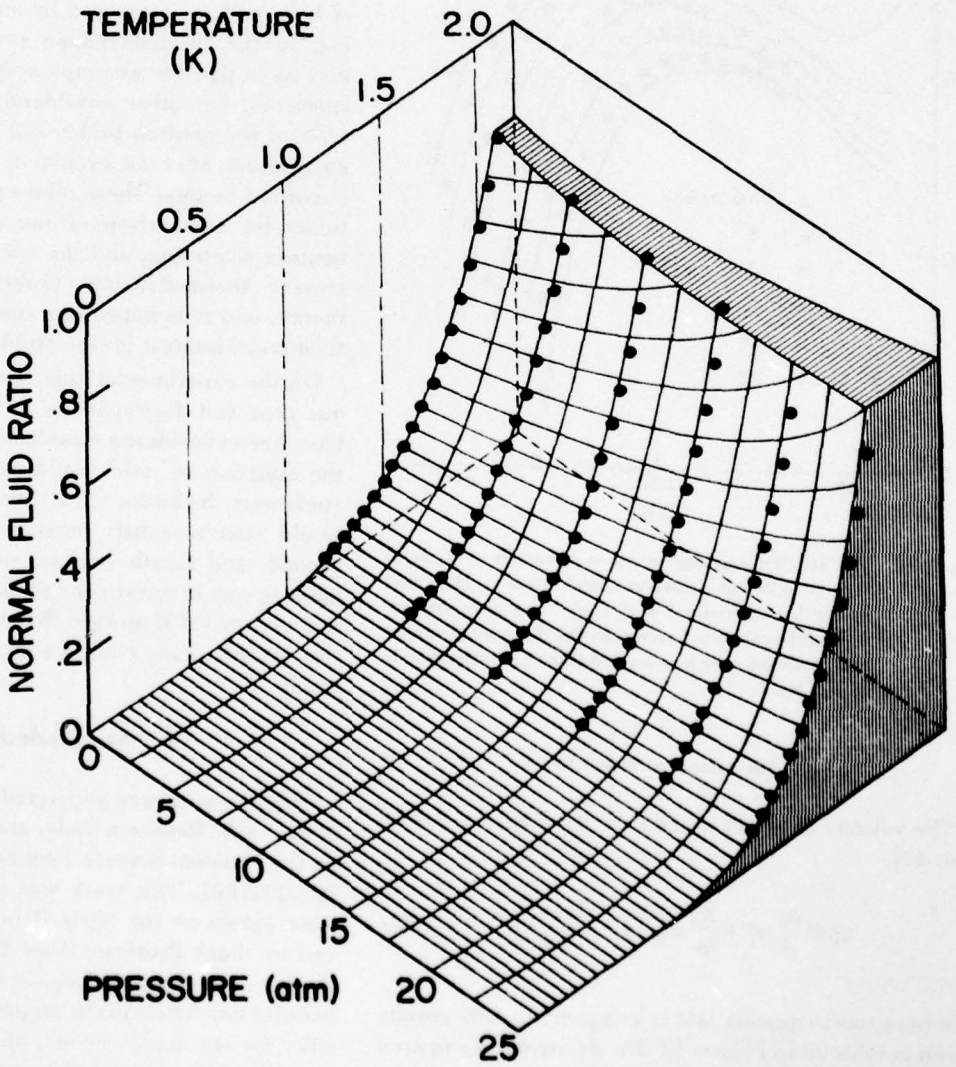

FIGURE 16. The normal fluid fraction as a function of temperature for different pressures calculated from eq (33). The data points are from Maynard [21].

We have used equation (34) to compute u_2, with results given in table 19 and figure 17. The data shown in figure 17 is that of Heiserman et al. [21]. Comparison of our results with the data of [21] is as follows:

P(atm)	0	5	10	15	20	25
$+(\overline{\Delta u_2})\%$	0	0.5	0.1	0.6	0.9	0.8
$-(\overline{\Delta u_2})\%$	2.1	1.7	2.4	4.6	4.2	4.8

Below 0.8 K, the calculated values show marked effects of phonon dispersion, as discussed by Brooks and Donnelly [30].

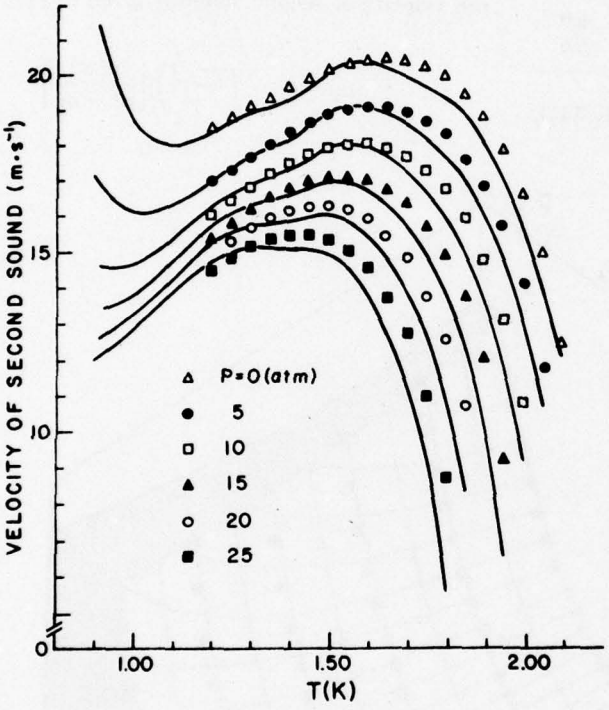

FIGURE 17. The velocity of second sound as a function of temperature, at different pressures. Solid lines, eq (34); data points, from Heiserman et al. [21]. Some of the unevenness of the calculated curves may be the result of numerical problems; note how many derived quantities appear in eq (34).

4.4.d. The Velocity of Fourth Sound

The velocity of fourth sound is, to good approximation [40, 41]

$$u_4^2 = \frac{\rho_s}{\rho} u_1^2 + \frac{\rho_n}{\rho} u_{II}^2 \left[1 - \frac{2\alpha_P u_1^2}{\gamma S}\right]. \qquad (35)$$

We have used equation (35) to compute u_4, with results given in table 20 and figure 18. The deviations, compared with the data of Heiserman et al. [21] are:

P(atm)	0	5	10	15	20	25
$+(\overline{\Delta u_4})\%$	0.3	0.5	0.9	6.4	1.5	1.4
$-(\overline{\Delta u_4})\%$	0.4	5.3	6.4	0.2	0.5	2.4

5. Conclusions

We have provided tables of the thermodynamic and superfluid properties of helium II computed, when possible, by theoretical methods. Due to inadequacies in the present theory, we were not able to achieve absolute agreement with the experimental data in all cases. The accuracy of our computed values is, however, generally very good, and we hope that the tables will provide a ready reference for theoretical and experimental research in helium II.

Perhaps the most interesting outcome of this research, other than the tables, is the result that there appears to be no theory at present which can accurately relate the energy and momentum of the elementary excitations of helium II, as measured by inelastic neutron scattering, to the thermodynamic properties. The problem may be in part the assumption of zero line width for the spectrum, but other considerations such as the time scale of the neutron probe, and the re-establishment of equilibrium after an excitation is created, may prove important factors. These tables provide a unique opportunity for comparison of the spectrum measured by neutron scattering, and the spectrum which yields the correct thermodynamic properties via the Landau theory, and it is hoped that our analysis will stimulate theoretical interest in this problem.

On the experimental side, we see that there are serious gaps and discrepancies in some of the data which have been considered established for many years. Even the equation of state would benefit from a systematic study over the entire (T, P) plane. An ideal experiment would simultaneously measure the velocities of first, second, and fourth sounds, and the expansion coefficient in one cryostat over all pressures and all temperatures from 0.3 K upward. When such data are available, the present study could be repeated with considerable profit.

6. Acknowledgments

This research was supported by the Air Force Office of Scientific Research under grant AFOSR-76-2880 and by the National Science Foundation under grant DMR-72-3221/A01. This work was begun when the authors were guests at the Niels Bohr Institute, Copenhagen, and we thank Professor Aage Bohr for the hospitality of the Institute. We would also like to thank Mr. James Gibbons for much help in the preparation of the computer results for our initial report, and for the entire task of preparing the present tables using recent data and the

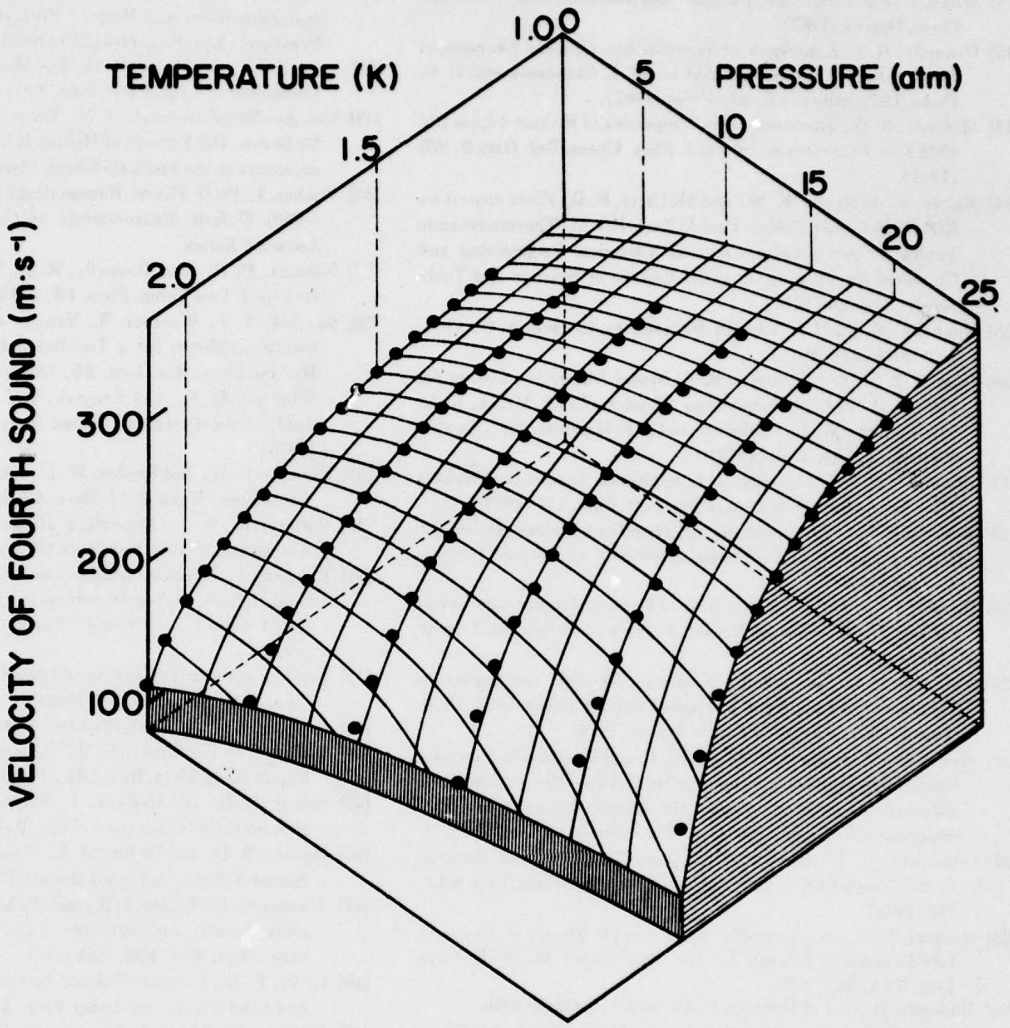

FIGURE 18. The velocity of fourth sound as a function of pressure and temperature calculated from eq (35). The data points are from Heiserman et al. [21].

formulae of table I. We are indebted to Professors D. L. Goodstein, R. P. Feynman, R. M. Mazo, and P. H. Roberts for discussions and collaboration on the theory. Professor I. Rudnick, Dr. Jay Maynard, and Dr. C. Van Degrift have made data available to us in advance of publication. We have appreciated the support and patience of the editors and staff of this Journal in the preparation of the manuscript.

7. References

[1] Landau, L. D., The Theory of Superfluidity of Helium II, J. Phys. **5**, 71 (1941); On the Theory of Superfluidity of Helium II, J. Phys. **11**, 91 (1947).

[2] Cowley, R. A., and Woods, A. D. B., Inelastic Scattering of Thermal Neutrons From Liquid Helium, Can. J. Phys. **49**, 177 (1971).

[3] Dietrich, O. W., Graf, E. H., Huang, C. H., and Passell, L., Neutron Scattering by Rotons in Liquid Helium, Phys. Rev. A **5**, 1377 (1972); also unpublished data provided by O. W. Dietrich.

[4] Henshaw, D. G., and Woods, A. D. B., Modes of Atomic Motions in Liquid Helium by Inelastic Scattering of Neutrons, in *Proc. Seventh Int. Conf. on Low Temperature Physics*, G. M. Graham and A. C. Hollis Hallet, eds., p. 539, University of Toronto Press, Toronto (1961).

[5] Henshaw, D. G., and Woods, A. D. B., Modes of Atomic Motions in Liquid Helium by Inelastic Scattering of Neutrons, Phys. Rev. **121**, 1266 (1961).

[6] Graf, E. H., Minkiewicz, V. J., Møller, H. B., and Passell, L., Neutron-Scattering Study of Collective Excitations in Superfluid Helium, Phys. Rev. A **10**, 1748 (1974).

[7] Svensson, E. C., Woods, A. D. B., and Martel, P., Phonon Dispersion in Liquid Helium under Pressure, Phys. Rev. Lett. **29**, 1148 (1972).

[8] Woods, A. D. B., and Cowley, R. A., Structure and Excitations of Liquid Helium, Rep. Prog. Phys. **36**, 1135 (1973).

[9] Yarnell, J. L., Arnold, G. P., Bendt, P. J., and Kerr, E. C., Excitations in Liquid Helium: Neutron Scattering Measurements, Phys. Rev. **113**, 1379 (1959).

[10] Bendt, P. J., Cowan, R. D., and Yarnell, J. L., Excitations in Liquid Helium: Thermodynamic Calculations, Phys. Rev. **113**, 1386 (1959).

[11] Wilks, J., *The Properties of Liquid and Solid Helium*, Clarendon Press, Oxford (1967).

[12] Donnelly, R. J., *Experimental Superfluidity*, Chicago Lectures in Physics Series, notes compiled by W. I. Glaberson and P. E. Parks, University of Chicago Press (1967).

[13] McCarty, R. D., Thermodynamic Properties of Helium 4 from 2 to 1500 K at Pressures to 10^8 Pa, J. Phys. Chem. Ref. Data **2**, 923 (1973).

[14] Angus, S., de Reuck, K. M., and McCarty, R. D., *Final Report on IUPAC Helium-4 Tables. Part I: Text*, IUPAC Thermodynamic Tables Project Centre, Dept. of Chemical Engineering and Chemical Technology, Imperial College of Science and Technology, London (1975).

[15] Donnelly, R. J., The Landau Parameters in Helium II, Phys. Lett. **39A**, 221 (1972).

[16] Brooks, J. S., and Donnelly, R. J., Model Dispersion Curves for Helium II, in *Low Temperature Physics—LT13*, Vol. 1, K. D. Timmerhaus, W. J. O'Sullivan, and E. F. Hammel, eds., Plenum Publishing, New York (1974).

[17] Brooks, J. S., and Donnelly, R. J., Excitation Spectrum of Helium II: A Series Representation, Phys. Lett. **46A**, 111 (1973).

[18] Brooks, J. S., *The Properties of Superfluid Helium Below 1.6 Degrees Kelvin*, Ph.D. Thesis, University of Oregon, Eugene, Oregon (1973).

[19] Brooks, J. S., and Donnelly, R. J., *The Calculated Properties of Helium II. A Technical Report*, University of Oregon, Eugene (1973).

[20] Van Degrift, C. T., Dielectric Constant, Density, and Expansion Coefficient of Liquid He^4 at Vapor Pressure Below 4.4 K, Ph.D. Thesis, University of California, Irvine (1974).

[21] Heiserman, J., Hulin, J. P., Maynard, J., and Rudnick, I., Precision Sound Velocity Measurements in He II, Phys. Rev. (submitted); Maynard, J., Determination of the Thermodynamics of He II from Sound Velocity Data, Phys. Rev. (submitted).

[22] Goodstein, D. L., Brooks, J. S., Donnelly, R. J., and Roberts, P. H., Quasiparticles and Thermal Expansion, Phys. Lett. **54A**, 281 (1975).

[23] Roberts, P. H., and Donnelly, R. J., Simple Theory of Temperature-Dependent Energy Levels: Application to He II Phys. Lett. **55A**, 443 (1976).

[24] Donnelly, R. J., and Roberts, P. H. (paper in preparation).

[25] Keller, W. E., *Helium-3 and Helium-4*, Plenum Press, New York (1969).

[26] Khalatnikov, I. M., *An Introduction to the Theory of Superfluidity*, W. A. Benjamin, New York (1965).

[27] Feenberg, E., Comments on Long-Wavelength Excitations and Structure Functions in the Theory of Liquid ^{4}He at $T=0$, Phys. Rev. Lett. **26**, 301 (1971); also *Theory of Quantum Fluids*, Academic Press, New York (1969).

[28] Phillips, N. E., Waterfield, C. G., and Hoffer, J. K., Calorimetric Evidence for Positive Phonon Dispersion in Liquid Helium-4, Phys. Rev. Lett. **25**, 1260 (1970).

[29] Pitaevskii, L. P., Properties of the Spectrum of Elementary Excitations Near the Disintegration Threshold of the Excitations, J. Exptl. Theoret. Phys. (USSR) **36**, 1168 (1959). Engl. trans.: Soviet Phys. JETP **9**, 830 (1959).

[30] Brooks, J. S., and Donnelly, R. J., Influence of Phonon Dispersion on the Velocity of Second Sound in He II, Phys. Rev. A **9**, 1444 (1974).

[31] Abraham, B. M., Eckstein, Y., Ketterson, J. B., Kuchnir, M., and Roach, P. R., Velocity of Sound, Density, and Grüneisen Constant in Liquid ^{4}He, Phys. Rev. **A1**, 250 (1970); Errata, Phys. Rev. **A2**, 550 (1970).

[32] Boghosian, C., and Meyer, H., Density, Coefficient of Thermal Expansion, and Entropy of Compression of Liquid He^4 Under Pressure Below 1.4 °K, Phys. Rev. **152**, 200 (1966); Errata, Phys. Rev. **163**, 206 (1967).

[33] Elwell, D. L., and Meyer, H., Molar Volume, Coefficient of Thermal Expansion, and Related Properties of Liquid He^4 Under Pressure, Phys. Rev. **164**, 245 (1967).

[34] Kerr, E. C., and Taylor, R. D., The Molar Volume and Expansion Coefficient of Liquid He^4, Ann. Phys. **26**, 292 (1964).

[35] Van den Meijdenberg, C. J. N., Taconis, K. W., and Ouboter, R. De Bruyn, The Entropy of Helium II Under Pressure from Measurements on the Fountain Effect, Physica **27**, 197 (1961).

[36] Wiebes, J., Ph.D. Thesis, Kammerlingh Onnes Laboratory, Leiden (1969). *Caloric Measurements on Liquid and Melting Helium below 1.5 Kelvin.*

[37] Roberts, P. H., and Donnelly, R. J., Scattering and Binding of Rotons, J. Low Temp. Phys. **15**, 1 (1974).

[38] Greytak, T. J., Woerner, R., Yan, J., and Benjamin, R., Experimental Evidence for a Two-Roton Bound State in Superfluid Helium, Phys. Rev. Lett. **25**, 1547 (1970); and Murray, C. A., Woerner, R. L., and Greytak, T. J., High Resolution Raman Study of the Two-Roton Bound State, J. Phys. **C8** (6), L90–94 (1975).

[39] Roberts, P. H., and Pardee, W. J., Bound States of the Two-roton Schrödinger Equation, J. Phys. **A7**, 1283 (1974).

[40] Putterman, S. J., *Superfluid Hydrodynamics*, North-Holland/American Elsevier, New York (1974), Chapter I, Section 7.

[41] Rudnick, I., Physical Acoustics at UCLA in the Study of Superfluid Helium, in *New Directions in Physical Acoustics*, International School of Physics "Enrico Fermi." XLIII Corso (In press).

[42] Grilly, E.R., Compressibility of Liquid He^4 as a Function of Pressure, Phys. Rev. **149**, 97 (1966).

[43] Keesom, W. H., *Helium*, Elsevier, Amsterdam (1942).

[44] Tough, J. T., McCormick, W. D., and Dash, J. G., Viscosity of Liquid He II, Phys. Rev. **132**, 2373 (1963).

[45] Romer, R. H., and Duffy, R. J., Normal-Fluid Densities in Liquid Helium II Under Pressure, Phys. Rev. **186**, 255 (1969).

[46] Maurer, R. D., and Herlin, M. A., Pressure Dependence of Second Sound Velocity in Liquid Helium II, Phys. Rev. **81**, 444 (1951).

[47] Watson, G. E., Reppy, J. D., and Richardson, R. C., Low Temperature Density and Solubility of He^3 in Liquid He^4 Under Pressure, Phys. Rev. **188**, 384 (1969).

[48] Grilly, E. R., Pressure-Volume-Temperature Relations in Liquid and Solid ^{4}He, J. Low Temp. Phys. **11**, 33 (1973).

[49] Whitney, W. M., and Chase, C. E., Ultrasonic Velocity and Dispersion in Liquid Helium II from 0.15 to 1.8 °K, Phys. Rev. **158**, 200 (1967).

[50] Atkins, K. R., and Stasior, R. A., First Sound in Liquid Helium at High Pressures, Can. J. Phys. **31**, 1156 (1953).

[51] Vignos, J. H., and Fairbank, H. A., Sound Measurements in Liquid and Solid He^3, He^4, and He^3-He^4 Mixtures, Phys. Rev. **147**, 185 (1966).

[52] Barmatz, M., and Rudnick, I., Velocity and Attenuation of First Sound Near the λ Point of Helium, Phys. Rev. **170**, 224 (1968).

[53] Atkins, K. R., and Edwards, M. H., Coefficient of Expansion of Liquid Helium II, Phys. Rev. **97**, 1429 (1955).

[54] Kierstead, H. A., Lambda Transformation of Liquid He^4 at High Pressures, Phys. Rev. **153**, 258 (1967).

[55] Harris-Lowe, R. F., and Smee, K. A., Thermal Expansion of Liquid Helium II, Phys. Rev. **A2**, 158 (1970).

[56] Mills, R. L., and Sydoriak, S. G., Thermal Expansion of Compressed He II, Ann. Phys. **34**, 276 (1965).

[57] Mueller, K. H., Pobell, F., and Ahlers, G., Thermal Expansion Coefficient and Universality Near the Superfluid Transition of ^{4}He Under Pressure (to be published).

[58] Kierstead, H. A., Lambda Curve of Liquid He^4, Phys. Rev. **162**, 153 (1967).

[59] Kramers, H. C., Wasscher, J. D., and Gorter, C. J., The Specific Heat of Liquid Helium between 0.25 and 1.9 °K, Physica **18**, 329 (1952).

[60] Hercus, G. R., and Wilks, J., The Specific Heat of Liquid Helium II as a Function of Pressure, Phil. Mag. **45**, 1163 (1954).
[61] Lounasmaa, O. V., and Kojo, E., The Specific Heat C_V of Liquid Helium Near the λ-curve at Various Densities, Ann. Acad. Scien. Fennicae A VI; Physica **36**, 1 (1959).
[62] Scott, S. A., Guyon, E., and Rudnick, I., Specific Heat and Superfluid Density of Liquid Helium in Porous Media, J. Low Temp. Phys. **9**, 389 (1972).
[63] Ahlers, G., Heat Capacity near the Superfluid Transition in He^4 at Saturated Vapor Pressure, Phys. Rev. **A3**, 696 (1971).
[64] Ahlers, G., Thermodynamics and Experimental Tests of Static Scaling and Universality near the Superfluid Transition in He^4 Under Pressure, Phys. Rev. **A8**, 530 (1973).
[65] Dash, J. G., and Taylor, R. D., Hydrodynamics of Oscillating Disks in Viscous Fluids: Density and Viscosity of Normal Fluid in Pure He^4 from 1.2 °K to the Lambda Point, Phys. Rev. **105**, 7 (1957).
[66] Clow, J. R., and Reppy, J. D., Persistent-Current Measurements of the Superfluid Density and Critical Velocity, Phys. Rev. **A5**, 424 (1972).
[67] Greywall, D. S., and Ahlers, G., Second Sound Velocity and Superfluid Density in He^4 Under Pressure near T Lambda, Phys. Rev. **A7**, 2145 (1973).
[68] De Klerk, D., Hudson, R. P., and Pellam, J. R., Second Sound Propagation below 1 °K, Phys. Rev. **93**, 28 (1954).
[69] Peshkov, V. P., Second Sound in Helium II, J. Exptl. Theoret. Phys. (USSR) **38**, 799 (1960). English translation: Soviet Phys. JETP **11**, 580 (1960).

Appendix A

Tables of the Calculated Properties of Helium II

A short statement concerning the use of these tables is appropriate here. There are seven important points to remember:

(i) As a rule-of-thumb, the tables can be expected to be most accurate below 1.6 K.

(ii) The tables may be less reliable near the lambda-line, and certainly no attempt should be made to use them in scaling relations.

(iii) All numbers are the result of continuous functions, and each number has been given as many figures as space allows to provide a continuous tabulation for numerical analysis. The large number of figures for the power series in table 25 is needed since these coefficients are highly correlated. Similarly, accurate derivatives of thermodynamic variables need many significant figures. In all other cases, the values should be rounded to two or three figures as indicated by the tabulations of average deviations in the relevant sections of the text. The notation .34753+05 indicates that the number 0.34753 is to be multiplied by 10^{+5}, etc.

(iv) The highest temperature for which data is listed in each pressure column is governed by the temperature at which the calculated normal fluid density starts to exceed the total density $\rho_n/\rho = 1$ and represents the "lambda-line" of the model calculation.

(v) When unusual accuracy is required, the original data must be consulted. An annotated bibliography is given in Appendix B as an initial guide.

(vi) Data at "$P = 0$" are generally measured SVP. The corrections are generally insignificant since SVP at 2.10 K is only 0.04 atm.

(vii) Several units in common use in low temperature physics have S.I. equivalents:

$$1 \text{ atm} = 1.01325 \times 10^5 \text{ Nm}^{-2}$$

For ^{4}He: 1 mol = 4.0026 g

$$1 \text{ Å} = 10^{-10} \text{ m}$$

$$1 \text{ Å}^{-1} = 10^{10} \text{ m}^{-1}$$

TABLE 1. Density (g cm^{-3})

Temp. (K)	Pressure (atm)										
	.00	2.50	5.00	7.50	10.00	12.50	15.00	17.50	20.00	22.50	25.00
.10	.14513E+00	.14925E+00	.15284E+00	.15603E+00	.15892E+00	.16157E+00	.16403E+00	.16633E+00	.16849E+00	.17053E+00	.17246E+00
.15	.14513E+00	.14925E+00	.15284E+00	.15603E+00	.15892E+00	.16157E+00	.16403E+00	.16633E+00	.16849E+00	.17053E+00	.17246E+00
.20	.14513E+00	.14925E+00	.15284E+00	.15603E+00	.15892E+00	.16157E+00	.16403E+00	.16633E+00	.16849E+00	.17053E+00	.17246E+00
.25	.14513E+00	.14925E+00	.15284E+00	.15603E+00	.15892E+00	.16157E+00	.16403E+00	.16633E+00	.16849E+00	.17053E+00	.17246E+00
.30	.14513E+00	.14925E+00	.15284E+00	.15603E+00	.15892E+00	.16157E+00	.16403E+00	.16633E+00	.16849E+00	.17053E+00	.17246E+00
.35	.14513E+00	.14925E+00	.15284E+00	.15603E+00	.15892E+00	.16157E+00	.16403E+00	.16633E+00	.16849E+00	.17053E+00	.17246E+00
.40	.14513E+00	.14925E+00	.15284E+00	.15603E+00	.15892E+00	.16157E+00	.16403E+00	.16633E+00	.16849E+00	.17053E+00	.17246E+00
.45	.14513E+00	.14925E+00	.15283E+00	.15603E+00	.15892E+00	.16157E+00	.16403E+00	.16633E+00	.16849E+00	.17053E+00	.17246E+00
.50	.14513E+00	.14925E+00	.15283E+00	.15603E+00	.15892E+00	.16157E+00	.16403E+00	.16633E+00	.16849E+00	.17053E+00	.17246E+00
.55	.14513E+00	.14925E+00	.15283E+00	.15603E+00	.15892E+00	.16157E+00	.16403E+00	.16633E+00	.16849E+00	.17053E+00	.17246E+00
.60	.14513E+00	.14925E+00	.15283E+00	.15603E+00	.15892E+00	.16157E+00	.16403E+00	.16633E+00	.16849E+00	.17053E+00	.17246E+00
.65	.14512E+00	.14925E+00	.15283E+00	.15603E+00	.15892E+00	.16157E+00	.16403E+00	.16633E+00	.16849E+00	.17053E+00	.17246E+00
.70	.14512E+00	.14925E+00	.15283E+00	.15602E+00	.15892E+00	.16157E+00	.16403E+00	.16633E+00	.16849E+00	.17053E+00	.17246E+00
.75	.14512E+00	.14925E+00	.15283E+00	.15602E+00	.15892E+00	.16157E+00	.16403E+00	.16633E+00	.16849E+00	.17053E+00	.17247E+00
.80	.14512E+00	.14924E+00	.15283E+00	.15602E+00	.15892E+00	.16157E+00	.16403E+00	.16633E+00	.16849E+00	.17053E+00	.17247E+00
.85	.14512E+00	.14924E+00	.15283E+00	.15603E+00	.15892E+00	.16157E+00	.16403E+00	.16633E+00	.16849E+00	.17054E+00	.17247E+00
.90	.14511E+00	.14924E+00	.15283E+00	.15603E+00	.15892E+00	.16158E+00	.16404E+00	.16634E+00	.16850E+00	.17054E+00	.17248E+00
.95	.14511E+00	.14924E+00	.15283E+00	.15603E+00	.15893E+00	.16158E+00	.16404E+00	.16634E+00	.16851E+00	.17055E+00	.17249E+00
1.00	.14511E+00	.14925E+00	.15284E+00	.15604E+00	.15893E+00	.16159E+00	.16405E+00	.16635E+00	.16852E+00	.17056E+00	.17251E+00
1.05	.14511E+00	.14925E+00	.15284E+00	.15604E+00	.15894E+00	.16160E+00	.16406E+00	.16636E+00	.16853E+00	.17058E+00	.17252E+00
1.10	.14510E+00	.14925E+00	.15285E+00	.15605E+00	.15895E+00	.16161E+00	.16408E+00	.16638E+00	.16855E+00	.17060E+00	.17255E+00
1.15	.14510E+00	.14926E+00	.15286E+00	.15607E+00	.15897E+00	.16163E+00	.16410E+00	.16640E+00	.16858E+00	.17063E+00	.17258E+00
1.20	.14511E+00	.14926E+00	.15287E+00	.15608E+00	.15899E+00	.16165E+00	.16412E+00	.16643E+00	.16861E+00	.17066E+00	.17262E+00
1.25	.14511E+00	.14927E+00	.15289E+00	.15610E+00	.15901E+00	.16168E+00	.16415E+00	.16647E+00	.16865E+00	.17071E+00	.17267E+00
1.30	.14511E+00	.14929E+00	.15291E+00	.15612E+00	.15904E+00	.16171E+00	.16419E+00	.16651E+00	.16870E+00	.17077E+00	.17273E+00
1.35	.14512E+00	.14930E+00	.15293E+00	.15615E+00	.15907E+00	.16175E+00	.16423E+00	.16656E+00	.16876E+00	.17083E+00	.17282E+00
1.40	.14513E+00	.14932E+00	.15296E+00	.15619E+00	.15911E+00	.16180E+00	.16429E+00	.16663E+00	.16883E+00	.17092E+00	.17291E+00
1.45	.14514E+00	.14934E+00	.15299E+00	.15623E+00	.15916E+00	.16185E+00	.16436E+00	.16670E+00	.16892E+00	.17102E+00	.17303E+00
1.50	.14516E+00	.14937E+00	.15303E+00	.15628E+00	.15922E+00	.16192E+00	.16444E+00	.16680E+00	.16903E+00	.17114E+00	.17317E+00
1.55	.14518E+00	.14941E+00	.15308E+00	.15634E+00	.15929E+00	.16201E+00	.16453E+00	.16691E+00	.16916E+00	.17129E+00	.17335E+00
1.60	.14520E+00	.14944E+00	.15313E+00	.15641E+00	.15938E+00	.16211E+00	.16465E+00	.16704E+00	.16931E+00	.17146E+00	.17356E+00
1.65	.14523E+00	.14949E+00	.15319E+00	.15649E+00	.15948E+00	.16223E+00	.16478E+00	.16719E+00	.16949E+00	.17168E+00	.17382E+00
1.70	.14526E+00	.14954E+00	.15327E+00	.15659E+00	.15960E+00	.16237E+00	.16495E+00	.16738E+00	.16971E+00	.17193E+00	.17413E+00
1.75	.14530E+00	.14960E+00	.15335E+00	.15670E+00	.15974E+00	.16254E+00	.16514E+00	.16760E+00	.16997E+00	.17225E+00	.17457E+00
1.80	.14535E+00	.14967E+00	.15345E+00	.15684E+00	.15991E+00	.16274E+00	.16536E+00	.16786E+00	.17028E+00	.17263E+00	.17512E+00
1.85	.14540E+00	.14975E+00	.15357E+00	.15699E+00	.16011E+00	.16297E+00	.16564E+00	.16818E+00	.17070E+00	.17317E+00	
1.90	.14546E+00	.14984E+00	.15370E+00	.15717E+00	.16032E+00	.16323E+00	.16596E+00	.16860E+00			
1.95	.14553E+00	.14996E+00	.15387E+00	.15738E+00	.16059E+00	.16357E+00	.16641E+00				
2.00	.14561E+00	.15009E+00	.15405E+00	.15762E+00	.16091E+00						
2.05	.14570E+00	.15024E+00	.15427E+00								
2.10	.14582E+00	.15041E+00									

TABLE 2. Molar volume ($cm^3\ mol^{-1}$)

Temp. (K)	Pressure (atm)										
	.00	2.50	5.00	7.50	10.00	12.50	15.00	17.50	20.00	22.50	25.00
.10	.27579E+02	.26818E+02	.26189E+02	.25653E+02	.25186E+02	.24773E+02	.24401E+02	.24064E+02	.23756E+02	.23472E+02	.23208E+02
.15	.27579E+02	.26818E+02	.26189E+02	.25653E+02	.25186E+02	.24773E+02	.24401E+02	.24064E+02	.23756E+02	.23472E+02	.23208E+02
.20	.27579E+02	.26818E+02	.26189E+02	.25653E+02	.25186E+02	.24773E+02	.24401E+02	.24064E+02	.23756E+02	.23472E+02	.23208E+02
.25	.27579E+02	.26818E+02	.26189E+02	.25653E+02	.25186E+02	.24773E+02	.24401E+02	.24064E+02	.23756E+02	.23472E+02	.23208E+02
.30	.27579E+02	.26818E+02	.26189E+02	.25653E+02	.25186E+02	.24773E+02	.24401E+02	.24064E+02	.23756E+02	.23472E+02	.23208E+02
.35	.27580E+02	.26818E+02	.26189E+02	.25653E+02	.25186E+02	.24773E+02	.24401E+02	.24064E+02	.23756E+02	.23472E+02	.23208E+02
.40	.27580E+02	.26818E+02	.26189E+02	.25653E+02	.25186E+02	.24773E+02	.24401E+02	.24064E+02	.23756E+02	.23472E+02	.23208E+02
.45	.27580E+02	.26818E+02	.26189E+02	.25653E+02	.25186E+02	.24773E+02	.24401E+02	.24064E+02	.23756E+02	.23472E+02	.23208E+02
.50	.27580E+02	.26818E+02	.26189E+02	.25653E+02	.25186E+02	.24773E+02	.24401E+02	.24064E+02	.23756E+02	.23472E+02	.23208E+02
.55	.27580E+02	.26818E+02	.26189E+02	.25653E+02	.25187E+02	.24773E+02	.24401E+02	.24064E+02	.23756E+02	.23472E+02	.23208E+02
.60	.27580E+02	.26818E+02	.26189E+02	.25653E+02	.25187E+02	.24773E+02	.24401E+02	.24064E+02	.23756E+02	.23472E+02	.23208E+02
.65	.27580E+02	.26818E+02	.26189E+02	.25654E+02	.25187E+02	.24773E+02	.24401E+02	.24064E+02	.23756E+02	.23472E+02	.23208E+02
.70	.27581E+02	.26819E+02	.26190E+02	.25654E+02	.25187E+02	.24773E+02	.24401E+02	.24064E+02	.23756E+02	.23472E+02	.23208E+02
.75	.27581E+02	.26819E+02	.26190E+02	.25654E+02	.25187E+02	.24773E+02	.24401E+02	.24064E+02	.23756E+02	.23472E+02	.23208E+02
.80	.27582E+02	.26819E+02	.26190E+02	.25654E+02	.25187E+02	.24773E+02	.24401E+02	.24064E+02	.23756E+02	.23471E+02	.23208E+02
.85	.27582E+02	.26819E+02	.26190E+02	.25654E+02	.25186E+02	.24773E+02	.24401E+02	.24064E+02	.23755E+02	.23471E+02	.23207E+02
.90	.27583E+02	.26819E+02	.26190E+02	.25653E+02	.25186E+02	.24772E+02	.24400E+02	.24063E+02	.23754E+02	.23470E+02	.23206E+02
.95	.27583E+02	.26819E+02	.26189E+02	.25653E+02	.25185E+02	.24771E+02	.24400E+02	.24062E+02	.23753E+02	.23469E+02	.23205E+02
1.00	.27583E+02	.26819E+02	.26189E+02	.25652E+02	.25184E+02	.24770E+02	.24398E+02	.24061E+02	.23752E+02	.23467E+02	.23203E+02
1.05	.27584E+02	.26818E+02	.26188E+02	.25651E+02	.25183E+02	.24769E+02	.24397E+02	.24059E+02	.23750E+02	.23465E+02	.23200E+02
1.10	.27584E+02	.26818E+02	.26186E+02	.25649E+02	.25181E+02	.24767E+02	.24395E+02	.24057E+02	.23747E+02	.23462E+02	.23197E+02
1.15	.27584E+02	.26817E+02	.26185E+02	.25647E+02	.25179E+02	.24764E+02	.24392E+02	.24054E+02	.23744E+02	.23458E+02	.23192E+02
1.20	.27584E+02	.26816E+02	.26183E+02	.25644E+02	.25176E+02	.24761E+02	.24388E+02	.24050E+02	.23739E+02	.23453E+02	.23187E+02
1.25	.27584E+02	.26814E+02	.26180E+02	.25641E+02	.25172E+02	.24757E+02	.24384E+02	.24045E+02	.23734E+02	.23447E+02	.23180E+02
1.30	.27583E+02	.26812E+02	.26177E+02	.25637E+02	.25168E+02	.24752E+02	.24378E+02	.24038E+02	.23727E+02	.23439E+02	.23172E+02
1.35	.27582E+02	.26809E+02	.26173E+02	.25633E+02	.25162E+02	.24746E+02	.24371E+02	.24031E+02	.23718E+02	.23430E+02	.23161E+02
1.40	.27580E+02	.26805E+02	.26168E+02	.25627E+02	.25156E+02	.24739E+02	.24363E+02	.24021E+02	.23708E+02	.23418E+02	.23149E+02
1.45	.27578E+02	.26801E+02	.26163E+02	.25620E+02	.25148E+02	.24730E+02	.24353E+02	.24010E+02	.23695E+02	.23405E+02	.23133E+02
1.50	.27574E+02	.26796E+02	.26156E+02	.25612E+02	.25139E+02	.24719E+02	.24341E+02	.23997E+02	.23680E+02	.23388E+02	.23114E+02
1.55	.27571E+02	.26790E+02	.26148E+02	.25602E+02	.25127E+02	.24706E+02	.24327E+02	.23981E+02	.23662E+02	.23367E+02	.23090E+02
1.60	.27566E+02	.26783E+02	.26139E+02	.25591E+02	.25114E+02	.24691E+02	.24310E+02	.23962E+02	.23641E+02	.23344E+02	.23062E+02
1.65	.27561E+02	.26775E+02	.26128E+02	.25577E+02	.25098E+02	.24673E+02	.24290E+02	.23940E+02	.23616E+02	.23315E+02	.23027E+02
1.70	.27555E+02	.26765E+02	.26115E+02	.25561E+02	.25079E+02	.24652E+02	.24266E+02	.23913E+02	.23585E+02	.23280E+02	.22986E+02
1.75	.27547E+02	.26755E+02	.26100E+02	.25543E+02	.25056E+02	.24626E+02	.24238E+02	.23882E+02	.23549E+02	.23237E+02	.22929E+02
1.80	.27539E+02	.26744E+02	.26084E+02	.25521E+02	.25030E+02	.24596E+02	.24205E+02	.23845E+02	.23506E+02	.23186E+02	.22857E+02
1.85	.27528E+02	.26729E+02	.26064E+02	.25495E+02	.24999E+02	.24561E+02	.24165E+02	.23799E+02	.23449E+02	.23114E+02	
1.90	.27516E+02	.26713E+02	.26041E+02	.25467E+02	.24966E+02	.24521E+02	.24118E+02	.23741E+02			
1.95	.27503E+02	.26691E+02	.26014E+02	.25433E+02	.24924E+02	.24470E+02	.24053E+02				
2.00	.27488E+02	.26669E+02	.25982E+02	.25394E+02	.24874E+02						
2.05	.27471E+02	.26641E+02	.25946E+02								
2.10	.27449E+02	.26612E+02									

TABLE 3. First sound velocity ($m\ s^{-1}$)

Temp. (K)	Pressure (atm)										
	.00	2.50	5.00	7.50	10.00	12.50	15.00	17.50	20.00	22.50	25.00
.10	.23821E+03	.25746E+03	.27422E+03	.28916E+03	.30271E+03	.31515E+03	.32669E+03	.33747E+03	.34760E+03	.35718E+03	.36627E+03
.15	.23821E+03	.25746E+03	.27422E+03	.28916E+03	.30271E+03	.31515E+03	.32669E+03	.33747E+03	.34760E+03	.35718E+03	.36627E+03
.20	.23821E+03	.25746E+03	.27422E+03	.28916E+03	.30271E+03	.31515E+03	.32669E+03	.33747E+03	.34760E+03	.35718E+03	.36627E+03
.25	.23821E+03	.25746E+03	.27422E+03	.28916E+03	.30271E+03	.31515E+03	.32669E+03	.33747E+03	.34760E+03	.35718E+03	.36627E+03
.30	.23821E+03	.25746E+03	.27422E+03	.28916E+03	.30271E+03	.31515E+03	.32669E+03	.33747E+03	.34760E+03	.35718E+03	.36627E+03
.35	.23821E+03	.25746E+03	.27422E+03	.28916E+03	.30271E+03	.31515E+03	.32669E+03	.33747E+03	.34760E+03	.35718E+03	.36627E+03
.40	.23821E+03	.25746E+03	.27422E+03	.28916E+03	.30271E+03	.31515E+03	.32669E+03	.33747E+03	.34760E+03	.35718E+03	.36627E+03
.45	.23821E+03	.25746E+03	.27422E+03	.28916E+03	.30271E+03	.31515E+03	.32669E+03	.33747E+03	.34760E+03	.35718E+03	.36627E+03
.50	.23821E+03	.25746E+03	.27422E+03	.28916E+03	.30271E+03	.31515E+03	.32669E+03	.33746E+03	.34760E+03	.35717E+03	.36627E+03
.55	.23821E+03	.25746E+03	.27422E+03	.28916E+03	.30271E+03	.31515E+03	.32668E+03	.33746E+03	.34759E+03	.35717E+03	.36627E+03
.60	.23820E+03	.25745E+03	.27421E+03	.28915E+03	.30270E+03	.31514E+03	.32668E+03	.33745E+03	.34759E+03	.35716E+03	.36626E+03
.65	.23819E+03	.25744E+03	.27420E+03	.28914E+03	.30269E+03	.31513E+03	.32667E+03	.33745E+03	.34758E+03	.35716E+03	.36625E+03
.70	.23817E+03	.25742E+03	.27418E+03	.28912E+03	.30268E+03	.31512E+03	.32666E+03	.33744E+03	.34757E+03	.35715E+03	.36624E+03
.75	.23815E+03	.25739E+03	.27416E+03	.28911E+03	.30266E+03	.31511E+03	.32665E+03	.33742E+03	.34756E+03	.35713E+03	.36622E+03
.80	.23812E+03	.25736E+03	.27413E+03	.28909E+03	.30265E+03	.31510E+03	.32663E+03	.33741E+03	.34753E+03	.35711E+03	.36621E+03
.85	.23806E+03	.25731E+03	.27410E+03	.28907E+03	.30264E+03	.31509E+03	.32662E+03	.33738E+03	.34751E+03	.35709E+03	.36617E+03
.90	.23798E+03	.25725E+03	.27406E+03	.28905E+03	.30263E+03	.31508E+03	.32660E+03	.33735E+03	.34748E+03	.35706E+03	.36611E+03
.95	.23787E+03	.25718E+03	.27402E+03	.28903E+03	.30262E+03	.31508E+03	.32658E+03	.33731E+03	.34744E+03	.35702E+03	.36604E+03
1.00	.23775E+03	.25708E+03	.27396E+03	.28900E+03	.30261E+03	.31507E+03	.32656E+03	.33726E+03	.34737E+03	.35695E+03	.36601E+03
1.05	.23758E+03	.25696E+03	.27388E+03	.28896E+03	.30260E+03	.31506E+03	.32652E+03	.33720E+03	.34731E+03	.35689E+03	.36586E+03
1.10	.23743E+03	.25681E+03	.27378E+03	.28890E+03	.30256E+03	.31504E+03	.32649E+03	.33712E+03	.34725E+03	.35688E+03	.36562E+03
1.15	.23720E+03	.25668E+03	.27366E+03	.28881E+03	.30251E+03	.31500E+03	.32645E+03	.33705E+03	.34714E+03	.35674E+03	.36551E+03
1.20	.23705E+03	.25649E+03	.27350E+03	.28868E+03	.30242E+03	.31494E+03	.32638E+03	.33697E+03	.34707E+03	.35670E+03	.36518E+03
1.25	.23680E+03	.25633E+03	.27335E+03	.28851E+03	.30225E+03	.31476E+03	.32620E+03	.33684E+03	.34696E+03	.35652E+03	.36493E+03
1.30	.23658E+03	.25608E+03	.27316E+03	.28838E+03	.30212E+03	.31461E+03	.32597E+03	.33652E+03	.34674E+03	.35651E+03	.36526E+03
1.35	.23638E+03	.25588E+03	.27293E+03	.28814E+03	.30189E+03	.31438E+03	.32575E+03	.33625E+03	.34636E+03	.35600E+03	.36408E+03
1.40	.23600E+03	.25563E+03	.27273E+03	.28797E+03	.30170E+03	.31413E+03	.32543E+03	.33585E+03	.34600E+03	.35582E+03	.36411E+03
1.45	.23572E+03	.25530E+03	.27240E+03	.28766E+03	.30141E+03	.31386E+03	.32518E+03	.33561E+03	.34578E+03	.35554E+03	.36360E+03
1.50	.23542E+03	.25496E+03	.27207E+03	.28737E+03	.30110E+03	.31351E+03	.32473E+03	.33501E+03	.34545E+03	.35567E+03	.36325E+03
1.55	.23509E+03	.25452E+03	.27163E+03	.28693E+03	.30071E+03	.31315E+03	.32431E+03	.33435E+03	.34450E+03	.35458E+03	.36162E+03
1.60	.23489E+03	.25398E+03	.27108E+03	.28647E+03	.30029E+03	.31273E+03	.32383E+03	.33365E+03	.34378E+03	.35387E+03	.35977E+03
1.65	.23443E+03	.25351E+03	.27044E+03	.28575E+03	.29970E+03	.31227E+03	.32344E+03	.33317E+03	.34303E+03	.35274E+03	.35587E+03
1.70	.23391E+03	.25288E+03	.26974E+03	.28500E+03	.29898E+03	.31167E+03	.32279E+03	.33231E+03	.34229E+03	.35220E+03	.35484E+03
1.75	.23361E+03	.25216E+03	.26869E+03	.28392E+03	.29817E+03	.31109E+03	.32204E+03	.33074E+03	.34002E+03	.34957E+03	.34988E+03
1.80	.23347E+03	.25126E+03	.26746E+03	.28258E+03	.29710E+03	.31061E+03	.32178E+03	.32993E+03	.33901E+03	.34820E+03	.34266E+03
1.85	.23303E+03	.25049E+03	.26634E+03	.28112E+03	.29536E+03	.30887E+03	.32015E+03	.32750E+03	.33652E+03	.34586E+03	
1.90	.23271E+03	.24913E+03	.26506E+03	.27998E+03	.29410E+03	.30749E+03	.31880E+03	.32582E+03			
1.95	.23118E+03	.24813E+03	.26385E+03	.27836E+03	.29219E+03	.30559E+03	.31689E+03				
2.00	.23065E+03	.24598E+03	.26208E+03	.27656E+03	.28984E+03						
2.05	.22871E+03	.24474E+03	.26010E+03								
2.10	.22793E+03	.24309E+03									

TABLE 4. Isothermal compressibility ($cm^2\ dyn^{-1}$) ($1\ cm^2\ dyn^{-1} = 10 m^2\ N^{-1}$)

Temp. (K)	Pressure (atm)										
	.00	2.50	5.00	7.50	10.00	12.50	15.00	17.50	20.00	22.50	25.00
.10	.12143E-07	.10108E-07	.87012E-08	.76651E-08	.68670E-08	.62315E-08	.57122E-08	.52792E-08	.49121E-08	.45966E-08	.43221E-08
.15	.12143E-07	.10108E-07	.87012E-08	.76651E-08	.68670E-08	.62315E-08	.57122E-08	.52792E-08	.49121E-08	.45966E-08	.43221E-08
.20	.12143E-07	.10108E-07	.87012E-08	.76651E-08	.68670E-08	.62315E-08	.57122E-08	.52792E-08	.49121E-08	.45966E-08	.43221E-08
.25	.12143E-07	.10108E-07	.87013E-08	.76652E-08	.68670E-08	.62315E-08	.57122E-08	.52792E-08	.49121E-08	.45966E-08	.43221E-08
.30	.12143E-07	.10108E-07	.87013E-08	.76652E-08	.68671E-08	.62315E-08	.57122E-08	.52793E-08	.49122E-08	.45966E-08	.43221E-08
.35	.12144E-07	.10108E-07	.87014E-08	.76653E-08	.68671E-08	.62315E-08	.57123E-08	.52793E-08	.49122E-08	.45966E-08	.43221E-08
.40	.12144E-07	.10108E-07	.87016E-08	.76654E-08	.68672E-08	.62316E-08	.57123E-08	.52793E-08	.49122E-08	.45966E-08	.43221E-08
.45	.12145E-07	.10109E-07	.87018E-08	.76655E-08	.68673E-08	.62316E-08	.57124E-08	.52793E-08	.49122E-08	.45967E-08	.43222E-08
.50	.12145E-07	.10109E-07	.87021E-08	.76657E-08	.68674E-08	.62317E-08	.57124E-08	.52794E-08	.49123E-08	.45967E-08	.43222E-08
.55	.12146E-07	.10110E-07	.87024E-08	.76659E-08	.68676E-08	.62319E-08	.57125E-08	.52795E-08	.49124E-08	.45968E-08	.43223E-08
.60	.12147E-07	.10110E-07	.87029E-08	.76663E-08	.68678E-08	.62321E-08	.57127E-08	.52796E-08	.49125E-08	.45970E-08	.43224E-08
.65	.12149E-07	.10111E-07	.87036E-08	.76667E-08	.68682E-08	.62323E-08	.57129E-08	.52799E-08	.49128E-08	.45972E-08	.43227E-08
.70	.12151E-07	.10113E-07	.87044E-08	.76673E-08	.68686E-08	.62327E-08	.57133E-08	.52803E-08	.49132E-08	.45976E-08	.43232E-08
.75	.12153E-07	.10114E-07	.87056E-08	.76681E-08	.68692E-08	.62332E-08	.57138E-08	.52808E-08	.49138E-08	.45984E-08	.43241E-08
.80	.12156E-07	.10117E-07	.87071E-08	.76691E-08	.68699E-08	.62338E-08	.57145E-08	.52817E-08	.49149E-08	.45995E-08	.43251E-08
.85	.12162E-07	.10120E-07	.87091E-08	.76704E-08	.68708E-08	.62346E-08	.57155E-08	.52831E-08	.49163E-08	.46010E-08	.43274E-08
.90	.12169E-07	.10125E-07	.87118E-08	.76720E-08	.68719E-08	.62356E-08	.57169E-08	.52850E-08	.49183E-08	.46031E-08	.43304E-08
.95	.12181E-07	.10130E-07	.87150E-08	.76740E-08	.68733E-08	.62369E-08	.57187E-08	.52874E-08	.49212E-08	.46061E-08	.43338E-08
1.00	.12193E-07	.10139E-07	.87196E-08	.76765E-08	.68749E-08	.62386E-08	.57210E-08	.52906E-08	.49250E-08	.46100E-08	.43374E-08
1.05	.12210E-07	.10148E-07	.87252E-08	.76797E-08	.68771E-08	.62407E-08	.57239E-08	.52949E-08	.49292E-08	.46140E-08	.43448E-08
1.10	.12225E-07	.10160E-07	.87325E-08	.76841E-08	.68803E-08	.62435E-08	.57277E-08	.53003E-08	.49341E-08	.46186E-08	.43543E-08
1.15	.12249E-07	.10171E-07	.87405E-08	.76903E-08	.68847E-08	.62478E-08	.57326E-08	.53060E-08	.49411E-08	.46263E-08	.43631E-08
1.20	.12264E-07	.10187E-07	.87518E-08	.76985E-08	.68912E-08	.62533E-08	.57387E-08	.53134E-08	.49483E-08	.46340E-08	.43785E-08
1.25	.12290E-07	.10200E-07	.87625E-08	.77079E-08	.68990E-08	.62614E-08	.57482E-08	.53230E-08	.49594E-08	.46466E-08	.43882E-08
1.30	.12313E-07	.10219E-07	.87749E-08	.77173E-08	.69090E-08	.62724E-08	.57609E-08	.53380E-08	.49722E-08	.46567E-08	.44007E-08
1.35	.12335E-07	.10237E-07	.87919E-08	.77323E-08	.69215E-08	.62843E-08	.57734E-08	.53526E-08	.49905E-08	.46782E-08	.44329E-08
1.40	.12374E-07	.10258E-07	.88069E-08	.77448E-08	.69351E-08	.63007E-08	.57921E-08	.53734E-08	.50100E-08	.46938E-08	.44445E-08
1.45	.12404E-07	.10285E-07	.88299E-08	.77651E-08	.69537E-08	.63189E-08	.58106E-08	.53949E-08	.50349E-08	.47215E-08	.44871E-08
1.50	.12436E-07	.10314E-07	.88535E-08	.77854E-08	.69756E-08	.63429E-08	.58387E-08	.54291E-08	.50646E-08	.47460E-08	.45319E-08
1.55	.12471E-07	.10349E-07	.88859E-08	.78159E-08	.70030E-08	.63683E-08	.58657E-08	.54621E-08	.51051E-08	.47941E-08	.46081E-08
1.60	.12492E-07	.10394E-07	.89247E-08	.78479E-08	.70335E-08	.63991E-08	.58992E-08	.55027E-08	.51488E-08	.48425E-08	.47050E-08
1.65	.12540E-07	.10435E-07	.89707E-08	.78940E-08	.70738E-08	.64352E-08	.59359E-08	.55482E-08	.52065E-08	.49143E-08	.48411E-08
1.70	.12597E-07	.10487E-07	.90205E-08	.79450E-08	.71232E-08	.64818E-08	.59864E-08	.56087E-08	.52730E-08	.49911E-08	.49837E-08
1.75	.12626E-07	.10540E-07	.90908E-08	.80166E-08	.71849E-08	.65327E-08	.60354E-08	.56785E-08	.53696E-08	.51215E-08	.52959E-08
1.80	.12641E-07	.10620E-07	.91803E-08	.81043E-08	.72576E-08	.65854E-08	.60897E-08	.57691E-08	.54986E-08	.53021E-08	.57486E-08
1.85	.12690E-07	.10691E-07	.92707E-08	.81977E-08	.73439E-08	.66673E-08	.61859E-08	.59250E-08	.57100E-08	.55689E-08	
1.90	.12720E-07	.10819E-07	.93726E-08	.82808E-08	.74357E-08	.67849E-08	.63471E-08	.61711E-08			
1.95	.12890E-07	.10908E-07	.94707E-08	.84000E-08	.75874E-08	.69843E-08	.66173E-08				
2.00	.12943E-07	.11100E-07	.96099E-08	.85478E-08	.78040E-08						
2.05	.13169E-07	.11218E-07	.97637E-08								
2.10	.13267E-07	.11360E-07									

TABLE 5. Thermal expansion coefficient (K^{-1})

Temp. (K)	Pressure (atm)										
	.00	2.50	5.00	7.50	10.00	12.50	15.00	17.50	20.00	22.50	25.00
.10	.1138E-05	.7258E-06	.5025E-06	.3682E-06	.2813E-06	.2219E-06	.1795E-06	.1482E-06	.1244E-06	.1054E-06	.9090E-07
.15	.3761E-05	.2419E-05	.1683E-05	.1237E-05	.9469E-06	.7478E-06	.6054E-06	.5001E-06	.4201E-06	.3559E-06	.3071E-06
.20	.8682E-05	.5644E-05	.3952E-05	.2916E-05	.2237E-05	.1770E-05	.1434E-05	.1185E-05	.9964E-06	.8445E-06	.7290E-06
.25	.1646E-04	.1082E-04	.7632E-05	.5657E-05	.4353E-05	.3449E-05	.2799E-05	.2316E-05	.1948E-05	.1652E-05	.1426E-05
.30	.2750E-04	.1833E-04	.1303E-04	.9703E-05	.7491E-05	.5948E-05	.4834E-05	.4004E-05	.3370E-05	.2859E-05	.2470E-05
.35	.4219E-04	.2847E-04	.2041E-04	.1528E-04	.1184E-04	.9424E-05	.7669E-05	.6358E-05	.5353E-05	.4541E-05	.3919E-05
.40	.6075E-04	.4153E-04	.3002E-04	.2260E-04	.1757E-04	.1401E-04	.1140E-04	.9444E-05	.7931E-05	.6694E-05	.5732E-05
.45	.8335E-04	.5770E-04	.4201E-04	.3176E-04	.2471E-04	.1968E-04	.1596E-04	.1312E-04	.1086E-04	.8978E-05	.7407E-05
.50	.1101E-03	.7691E-04	.5623E-04	.4248E-04	.3290E-04	.2596E-04	.2075E-04	.1660E-04	.1314E-04	.1012E-04	.7271E-05
.55	.1408E-03	.9866E-04	.7181E-04	.5365E-04	.4083E-04	.3141E-04	.2408E-04	.1781E-04	.1232E-04	.7153E-05	.1361E-05
.60	.1749E-03	.1214E-03	.8655E-04	.6270E-04	.4572E-04	.3287E-04	.2249E-04	.1297E-04	.3806E-05	-.5229E-05	-.1709E-04
.65	.2112E-03	.1422E-03	.9653E-04	.6493E-04	.4249E-04	.2554E-04	.1069E-04	-.4306E-05	-.1998E-04	-.3601E-04	-.5501E-04
.70	.2497E-03	.1561E-03	.9537E-04	.5402E-04	.2419E-04	.1493E-05	-.1924E-04	-.4238E-04	-.6654E-04	-.9307E-04	-.1279E-03
.75	.2818E-03	.1599E-03	.7569E-04	.2037E-04	-.1767E-04	-.4729E-04	-.7539E-04	-.1098E-03	-.1496E-03	-.1965E-03	-.2399E-03
.80	.3233E-03	.1370E-03	.2509E-04	-.4430E-04	-.9283E-04	-.1319E-03	-.1694E-03	-.2190E-03	-.2785E-03	-.3412E-03	-.4180E-03
.85	.3450E-03	.9061E-04	-.6036E-04	-.1533E-03	-.2133E-03	-.2590E-03	-.3084E-03	-.3799E-03	-.4664E-03	-.5494E-03	-.6761E-03
.90	.3598E-03	-.2966E-05	-.1943E-03	-.3099E-03	-.3864E-03	-.4410E-03	-.5061E-03	-.6013E-03	-.7212E-03	-.8463E-03	-.1005E-02
.95	.3497E-03	-.1128E-03	-.3747E-03	-.5261E-03	-.6157E-03	-.6856E-03	-.7746E-03	-.8950E-03	-.1056E-02	-.1234E-02	-.1389E-02
1.00	.3294E-03	-.2673E-03	-.6053E-03	-.7986E-03	-.9087E-03	-.9983E-03	-.1112E-02	-.1268E-02	-.1474E-02	-.1679E-02	-.1922E-02
1.05	.2495E-03	-.4329E-03	-.8585E-03	-.1105E-02	-.1259E-02	-.1392E-02	-.1517E-02	-.1730E-02	-.1993E-02	-.2176E-02	-.2588E-02
1.10	.1225E-03	-.6585E-03	-.1126E-02	-.1446E-02	-.1668E-02	-.1839E-02	-.2038E-02	-.2287E-02	-.2588E-02	-.2908E-02	-.3292E-02
1.15	.4805E-05	-.8227E-03	-.1404E-02	-.1833E-02	-.2150E-02	-.2405E-02	-.2657E-02	-.2953E-02	-.3309E-02	-.3656E-02	-.4233E-02
1.20	-.2215E-03	-.1086E-02	-.1738E-02	-.2261E-02	-.2684E-02	-.3020E-02	-.3370E-02	-.3768E-02	-.4192E-02	-.4716E-02	-.5387E-02
1.25	-.4523E-03	-.1510E-02	-.2174E-02	-.2649E-02	-.3080E-02	-.3548E-02	-.4096E-02	-.4733E-02	-.5367E-02	-.5922E-02	-.6283E-02
1.30	-.7342E-03	-.1715E-02	-.2578E-02	-.3289E-02	-.3903E-02	-.4480E-02	-.5054E-02	-.5721E-02	-.6516E-02	-.7377E-02	-.8599E-02
1.35	-.1117E-02	-.2387E-02	-.3272E-02	-.4011E-02	-.4662E-02	-.5330E-02	-.6107E-02	-.6942E-02	-.7910E-02	-.8883E-02	-.9883E-02
1.40	-.1387E-02	-.2930E-02	-.4017E-02	-.4904E-02	-.5710E-02	-.6548E-02	-.7456E-02	-.8410E-02	-.9511E-02	-.1067E-01	-.1187E-01
1.45	-.1994E-02	-.3458E-02	-.4748E-02	-.5843E-02	-.6839E-02	-.7914E-02	-.9020E-02	-.1032E-01	-.1181E-01	-.1316E-01	-.1520E-01
1.50	-.2417E-02	-.4111E-02	-.5605E-02	-.6933E-02	-.8210E-02	-.9478E-02	-.1079E-01	-.1237E-01	-.1424E-01	-.1618E-01	-.1885E-01
1.55	-.2937E-02	-.4713E-02	-.6618E-02	-.8284E-02	-.9789E-02	-.1122E-01	-.1267E-01	-.1433E-01	-.1636E-01	-.1886E-01	-.2267E-01
1.60	-.3579E-02	-.5508E-02	-.7717E-02	-.9809E-02	-.1167E-01	-.1340E-01	-.1510E-01	-.1699E-01	-.1948E-01	-.2258E-01	-.2800E-01
1.65	-.3965E-02	-.6625E-02	-.9036E-02	-.1146E-01	-.1389E-01	-.1605E-01	-.1819E-01	-.2062E-01	-.2357E-01	-.2728E-01	-.3294E-01
1.70	-.5155E-02	-.7651E-02	-.1048E-01	-.1351E-01	-.1647E-01	-.1917E-01	-.2176E-01	-.2468E-01	-.2861E-01	-.3375E-01	-.4315E-01
1.75	-.5524E-02	-.7739E-02	-.1172E-01	-.1591E-01	-.1977E-01	-.2270E-01	-.2504E-01	-.2796E-01	-.3297E-01	-.4060E-01	-.5743E-01
1.80	-.6582E-02	-.9490E-02	-.1368E-01	-.1847E-01	-.2307E-01	-.2681E-01	-.3012E-01	-.3466E-01	-.4242E-01	-.5375E-01	-.7711E-01
1.85	-.7929E-02	-.1150E-01	-.1651E-01	-.2106E-01	-.2530E-01	-.2986E-01	-.3538E-01	-.4306E-01	-.5537E-01	-.7240E-01	
1.90	-.8732E-02	-.1440E-01	-.1943E-01	-.2440E-01	-.2978E-01	-.3664E-01	-.4585E-01	-.5877E-01			
1.95	-.1031E-01	-.1659E-01	-.2270E-01	-.2871E-01	-.3652E-01	-.4745E-01	-.6173E-01				
2.00	-.1128E-01	-.1897E-01	-.2610E-01	-.3420E-01	-.4564E-01						
2.05	-.1416E-01	-.2186E-01	-.2949E-01								
2.10	-.1770E-01	-.2344E-01									

AD-A079 757 OREGON UNIV EUGENE DEPT OF PHYSICS F/G 7/4
TURBULENCE AND STATISTICAL MECHANICS.(U)
NOV 79 R J DONNELLY AFOSR-76-2880
UNCLASSIFIED AFOSR-TR-79-1357 NL

3 OF 3
AD-
A079757

END
DATE
FILMED
2-80
DDC

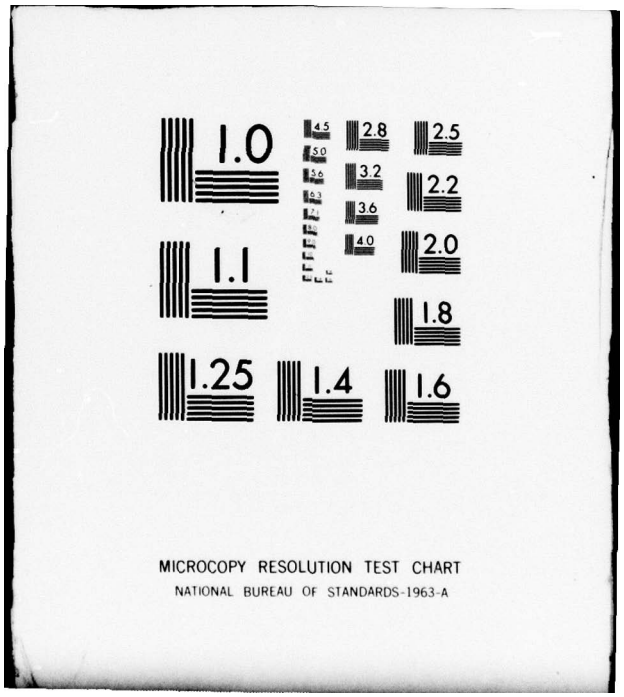
1.0
1.1
1.25
1.4
1.6
1.8
2.0
2.2
2.5
2.8
3.2
3.6
4.0
4.5
5.0
5.6
6.3
7.1
8.0
9.0
MICROCOPY RESOLUTION TEST CHART
NATIONAL BUREAU OF STANDARDS-1963-A

TABLE 6. Helmholtz free energy of excitations (J g^{-1})

Temp. (K)	Pressure (atm)										
	.00	2.50	5.00	7.50	10.00	12.50	15.00	17.50	20.00	22.50	25.00
.10	−.1395E−05	−.1079E−05	−.8744E−06	−.7314E−06	−.6264E−06	−.5463E−06	−.4832E−06	−.4324E−06	−.3907E−06	−.3558E−06	−.3263E−06
.15	−.2092E−05	−.1619E−05	−.1312E−05	−.1097E−05	−.9396E−06	−.8194E−06	−.7248E−06	−.6486E−06	−.5860E−06	−.5337E−06	−.4894E−06
.20	−.3957E−05	−.3067E−05	−.2487E−05	−.2082E−05	−.1784E−05	−.1556E−05	−.1376E−05	−.1232E−05	−.1113E−05	−.1014E−05	−.9295E−06
.25	−.7859E−05	−.6110E−05	−.4963E−05	−.4158E−05	−.3564E−05	−.3110E−05	−.2752E−05	−.2464E−05	−.2226E−05	−.2028E−05	−.1860E−05
.30	−.1489E−04	−.1162E−04	−.9460E−05	−.7935E−05	−.6807E−05	−.5942E−05	−.5260E−05	−.4709E−05	−.4256E−05	−.3877E−05	−.3556E−05
.35	−.2637E−04	−.2066E−04	−.1686E−04	−.1416E−04	−.1216E−04	−.1062E−04	−.9402E−05	−.8420E−05	−.7611E−05	−.6935E−05	−.6361E−05
.40	−.4382E−04	−.3447E−04	−.2819E−04	−.2371E−04	−.2038E−04	−.1781E−04	−.1578E−04	−.1414E−04	−.1279E−04	−.1165E−04	−.1070E−04
.45	−.6897E−04	−.5449E−04	−.4468E−04	−.3765E−04	−.3239E−04	−.2834E−04	−.2513E−04	−.2254E−04	−.2041E−04	−.1864E−04	−.1714E−04
.50	−.1038E−03	−.8236E−04	−.6774E−04	−.5721E−04	−.4933E−04	−.4325E−04	−.3845E−04	−.3459E−04	−.3144E−04	−.2885E−04	−.2671E−04
.55	−.1505E−03	−.1201E−03	−.9915E−04	−.8407E−04	−.7279E−04	−.6413E−04	−.5733E−04	−.5194E−04	−.4763E−04	−.4421E−04	−.4156E−04
.60	−.2120E−03	−.1702E−03	−.1414E−03	−.1207E−03	−.1054E−03	−.9372E−04	−.8473E−04	−.7780E−04	−.7256E−04	−.6873E−04	−.6627E−04
.65	−.2922E−03	−.2365E−03	−.1984E−03	−.1714E−03	−.1517E−03	−.1371E−03	−.1262E−03	−.1184E−03	−.1132E−03	−.1103E−03	−.1098E−03
.70	−.3967E−03	−.3249E−03	−.2766E−03	−.2431E−03	−.2196E−03	−.2030E−03	−.1917E−03	−.1847E−03	−.1818E−03	−.1828E−03	−.1880E−03
.75	−.5345E−03	−.4446E−03	−.3860E−03	−.3475E−03	−.3221E−03	−.3063E−03	−.2974E−03	−.2950E−03	−.2987E−03	−.3089E−03	−.3263E−03
.80	−.7188E−03	−.6098E−03	−.5429E−03	−.5027E−03	−.4797E−03	−.4695E−03	−.4683E−03	−.4767E−03	−.4942E−03	−.5226E−03	−.5618E−03
.85	−.9697E−03	−.8414E−03	−.7706E−03	−.7350E−03	−.7218E−03	−.7253E−03	−.7406E−03	−.7694E−03	−.8117E−03	−.8703E−03	−.9461E−03
.90	−.1315E−02	−.1170E−02	−.1102E−02	−.1081E−02	−.1090E−02	−.1118E−02	−.1162E−02	−.1225E−02	−.1308E−02	−.1415E−02	−.1548E−02
.95	−.1793E−02	−.1636E−02	−.1583E−02	−.1591E−02	−.1635E−02	−.1707E−02	−.1797E−02	−.1912E−02	−.2055E−02	−.2235E−02	−.2449E−02
1.00	−.2458E−02	−.2294E−02	−.2270E−02	−.2325E−02	−.2428E−02	−.2561E−02	−.2720E−02	−.2912E−02	−.3144E−02	−.3425E−02	−.3755E−02
1.05	−.3375E−02	−.3216E−02	−.3238E−02	−.3364E−02	−.3549E−02	−.3771E−02	−.4028E−02	−.4326E−02	−.4679E−02	−.5098E−02	−.5584E−02
1.10	−.4634E−02	−.4491E−02	−.4579E−02	−.4798E−02	−.5093E−02	−.5436E−02	−.5825E−02	−.6266E−02	−.6784E−02	−.7384E−02	−.8076E−02
1.15	−.6335E−02	−.6224E−02	−.6398E−02	−.6736E−02	−.7176E−02	−.7678E−02	−.8241E−02	−.8873E−02	−.9595E−02	−.1043E−01	−.1139E−01
1.20	−.8599E−02	−.8535E−02	−.8813E−02	−.9301E−02	−.9922E−02	−.1063E−01	−.1141E−01	−.1229E−01	−.1328E−01	−.1442E−01	−.1570E−01
1.25	−.1155E−01	−.1156E−01	−.1198E−01	−.1265E−01	−.1349E−01	−.1443E−01	−.1550E−01	−.1668E−01	−.1801E−01	−.1953E−01	−.2122E−01
1.30	−.1534E−01	−.1545E−01	−.1604E−01	−.1693E−01	−.1802E−01	−.1927E−01	−.2066E−01	−.2221E−01	−.2397E−01	−.2597E−01	−.2817E−01
1.35	−.2013E−01	−.2037E−01	−.2116E−01	−.2232E−01	−.2374E−01	−.2536E−01	−.2716E−01	−.2918E−01	−.3144E−01	−.3401E−01	−.3689E−01
1.40	−.2610E−01	−.2651E−01	−.2758E−01	−.2908E−01	−.3088E−01	−.3294E−01	−.3523E−01	−.3779E−01	−.4068E−01	−.4395E−01	−.4756E−01
1.45	−.3353E−01	−.3415E−01	−.3553E−01	−.3745E−01	−.3972E−01	−.4232E−01	−.4523E−01	−.4848E−01	−.5211E−01	−.5622E−01	−.6081E−01
1.50	−.4265E−01	−.4355E−01	−.4534E−01	−.4772E−01	−.5056E−01	−.5379E−01	−.5742E−01	−.6148E−01	−.6606E−01	−.7122E−01	−.7697E−01
1.55	−.5364E−01	−.5488E−01	−.5711E−01	−.6006E−01	−.6359E−01	−.6760E−01	−.7212E−01	−.7715E−01	−.8280E−01	−.8919E−01	−.9642E−01
1.60	−.6674E−01	−.6836E−01	−.7113E−01	−.7476E−01	−.7910E−01	−.8404E−01	−.8954E−01	−.9570E−01	−.1027E+00	−.1105E+00	−.1194E+00
1.65	−.8220E−01	−.8427E−01	−.8765E−01	−.9208E−01	−.9740E−01	−.1035E+00	−.1102E+00	−.1177E+00	−.1262E+00	−.1358E+00	−.1469E+00
1.70	−.1005E+00	−.1030E+00	−.1072E+00	−.1126E+00	−.1190E+00	−.1264E+00	−.1346E+00	−.1438E+00	−.1541E+00	−.1659E+00	−.1795E+00
1.75	−.1219E+00	−.1251E+00	−.1301E+00	−.1366E+00	−.1444E+00	−.1533E+00	−.1633E+00	−.1745E+00	−.1870E+00	−.2014E+00	−.2184E+00
1.80	−.1471E+00	−.1509E+00	−.1568E+00	−.1646E+00	−.1740E+00	−.1849E+00	−.1969E+00	−.2103E+00	−.2254E+00	−.2430E+00	−.2643E+00
1.85	−.1762E+00	−.1810E+00	−.1880E+00	−.1973E+00	−.2086E+00	−.2216E+00	−.2361E+00	−.2523E+00	−.2708E+00	−.2927E+00	
1.90	−.2100E+00	−.2157E+00	−.2241E+00	−.2353E+00	−.2486E+00	−.2640E+00	−.2814E+00	−.3010E+00			
1.95	−.2486E+00	−.2557E+00	−.2657E+00	−.2789E+00	−.2948E+00	−.3133E+00	−.3346E+00				
2.00	−.2930E+00	−.3015E+00	−.3134E+00	−.3291E+00	−.3479E+00						
2.05	−.3440E+00	−.3542E+00	−.3684E+00								
2.10	−.4023E+00	−.4145E+00									

TABLE 7. Gibbs free energy of excitations (J g^{-1})

Temp. (K)	Pressure (atm)										
	.00	2.50	5.00	7.50	10.00	12.50	15.00	17.50	20.00	22.50	25.00
.10	-.1395E-05	-.1079E-05	-.8744E-06	-.7314E-06	-.6264E-06	-.5463E-06	-.4832E-06	-.4324E-06	-.3907E-06	-.3558E-06	-.3263E-06
.15	-.2092E-05	-.1619E-05	-.1312E-05	-.1097E-05	-.9396E-06	-.8194E-06	-.7248E-06	-.6486E-06	-.5860E-06	-.5337E-06	-.4894E-06
.20	-.3957E-05	-.3067E-05	-.2487E-05	-.2082E-05	-.1784E-05	-.1556E-05	-.1376E-05	-.1232E-05	-.1113E-05	-.1014E-05	-.9295E-06
.25	-.7859E-05	-.6110E-05	-.4963E-05	-.4158E-05	-.3564E-05	-.3110E-05	-.2752E-05	-.2464E-05	-.2226E-05	-.2028E-05	-.1860E-05
.30	-.1489E-04	-.1162E-04	-.9460E-05	-.7935E-05	-.6807E-05	-.5942E-05	-.5260E-05	-.4709E-05	-.4256E-05	-.3877E-05	-.3556E-05
.35	-.2637E-04	-.2066E-04	-.1686E-04	-.1416E-04	-.1216E-04	-.1062E-04	-.9402E-05	-.8420E-05	-.7611E-05	-.6935E-05	-.6361E-05
.40	-.4382E-04	-.3448E-04	-.2819E-04	-.2372E-04	-.2038E-04	-.1781E-04	-.1578E-04	-.1414E-04	-.1279E-04	-.1165E-04	-.1070E-04
.45	-.6897E-04	-.5449E-04	-.4468E-04	-.3765E-04	-.3239E-04	-.2834E-04	-.2513E-04	-.2254E-04	-.2041E-04	-.1864E-04	-.1714E-04
.50	-.1038E-03	-.8237E-04	-.6774E-04	-.5721E-04	-.4933E-04	-.4325E-04	-.3845E-04	-.3459E-04	-.3144E-04	-.2885E-04	-.2671E-04
.55	-.1505E-03	-.1201E-03	-.9916E-04	-.8407E-04	-.7279E-04	-.6413E-04	-.5734E-04	-.5194E-04	-.4763E-04	-.4421E-04	-.4156E-04
.60	-.2120E-03	-.1702E-03	-.1414E-03	-.1207E-03	-.1054E-03	-.9373E-04	-.8474E-04	-.7781E-04	-.7256E-04	-.6873E-04	-.6627E-04
.65	-.2922E-03	-.2366E-03	-.1985E-03	-.1714E-03	-.1517E-03	-.1371E-03	-.1262E-03	-.1184E-03	-.1132E-03	-.1103E-03	-.1098E-03
.70	-.3968E-03	-.3249E-03	-.2766E-03	-.2431E-03	-.2196E-03	-.2031E-03	-.1917E-03	-.1847E-03	-.1818E-03	-.1829E-03	-.1880E-03
.75	-.5345E-03	-.4446E-03	-.3861E-03	-.3475E-03	-.3222E-03	-.3064E-03	-.2974E-03	-.2950E-03	-.2987E-03	-.3089E-03	-.3263E-03
.80	-.7189E-03	-.6099E-03	-.5429E-03	-.5028E-03	-.4797E-03	-.4696E-03	-.4683E-03	-.4767E-03	-.4942E-03	-.5226E-03	-.5617E-03
.85	-.9698E-03	-.8415E-03	-.7707E-03	-.7351E-03	-.7219E-03	-.7254E-03	-.7406E-03	-.7694E-03	-.8117E-03	-.8702E-03	-.9460E-03
.90	-.1315E-02	-.1170E-02	-.1103E-02	-.1081E-02	-.1090E-02	-.1118E-02	-.1162E-02	-.1224E-02	-.1307E-02	-.1414E-02	-.1547E-02
.95	-.1793E-02	-.1636E-02	-.1583E-02	-.1591E-02	-.1635E-02	-.1706E-02	-.1796E-02	-.1911E-02	-.2055E-02	-.2234E-02	-.2448E-02
1.00	-.2458E-02	-.2295E-02	-.2270E-02	-.2325E-02	-.2428E-02	-.2561E-02	-.2719E-02	-.2911E-02	-.3143E-02	-.3424E-02	-.3753E-02
1.05	-.3376E-02	-.3217E-02	-.3238E-02	-.3364E-02	-.3548E-02	-.3770E-02	-.4027E-02	-.4325E-02	-.4677E-02	-.5095E-02	-.5580E-02
1.10	-.4634E-02	-.4491E-02	-.4579E-02	-.4797E-02	-.5092E-02	-.5434E-02	-.5823E-02	-.6263E-02	-.6780E-02	-.7379E-02	-.8069E-02
1.15	-.6336E-02	-.6224E-02	-.6397E-02	-.6735E-02	-.7174E-02	-.7674E-02	-.8236E-02	-.8867E-02	-.9587E-02	-.1042E-01	-.1137E-01
1.20	-.8601E-02	-.8535E-02	-.8812E-02	-.9298E-02	-.9918E-02	-.1062E-01	-.1140E-01	-.1228E-01	-.1327E-01	-.1440E-01	-.1568E-01
1.25	-.1155E-01	-.1156E-01	-.1198E-01	-.1264E-01	-.1348E-01	-.1442E-01	-.1548E-01	-.1666E-01	-.1799E-01	-.1950E-01	-.2119E-01
1.30	-.1535E-01	-.1545E-01	-.1604E-01	-.1692E-01	-.1801E-01	-.1925E-01	-.2063E-01	-.2218E-01	-.2393E-01	-.2592E-01	-.2811E-01
1.35	-.2013E-01	-.2036E-01	-.2115E-01	-.2230E-01	-.2372E-01	-.2532E-01	-.2712E-01	-.2912E-01	-.3138E-01	-.3393E-01	-.3680E-01
1.40	-.2610E-01	-.2651E-01	-.2757E-01	-.2906E-01	-.3084E-01	-.3288E-01	-.3516E-01	-.3771E-01	-.4058E-01	-.4383E-01	-.4742E-01
1.45	-.3353E-01	-.3414E-01	-.3551E-01	-.3740E-01	-.3966E-01	-.4223E-01	-.4512E-01	-.4835E-01	-.5196E-01	-.5603E-01	-.6059E-01
1.50	-.4264E-01	-.4353E-01	-.4529E-01	-.4766E-01	-.5046E-01	-.5366E-01	-.5726E-01	-.6128E-01	-.6582E-01	-.7094E-01	-.7664E-01
1.55	-.5364E-01	-.5485E-01	-.5704E-01	-.5995E-01	-.6344E-01	-.6741E-01	-.7187E-01	-.7686E-01	-.8245E-01	-.8878E-01	-.9594E-01
1.60	-.6673E-01	-.6831E-01	-.7102E-01	-.7460E-01	-.7888E-01	-.8375E-01	-.8919E-01	-.9527E-01	-.1021E+00	-.1099E+00	-.1187E+00
1.65	-.8218E-01	-.8419E-01	-.8749E-01	-.9184E-01	-.9708E-01	-.1030E+00	-.1097E+00	-.1171E+00	-.1255E+00	-.1350E+00	-.1459E+00
1.70	-.1004E+00	-.1029E+00	-.1069E+00	-.1122E+00	-.1185E+00	-.1258E+00	-.1338E+00	-.1429E+00	-.1531E+00	-.1646E+00	-.1780E+00
1.75	-.1219E+00	-.1249E+00	-.1298E+00	-.1361E+00	-.1437E+00	-.1525E+00	-.1623E+00	-.1732E+00	-.1856E+00	-.1997E+00	-.2164E+00
1.80	-.1470E+00	-.1507E+00	-.1564E+00	-.1639E+00	-.1731E+00	-.1837E+00	-.1954E+00	-.2085E+00	-.2234E+00	-.2406E+00	-.2615E+00
1.85	-.1761E+00	-.1806E+00	-.1873E+00	-.1963E+00	-.2073E+00	-.2199E+00	-.2341E+00	-.2499E+00	-.2680E+00	-.2893E+00	
1.90	-.2097E+00	-.2152E+00	-.2232E+00	-.2339E+00	-.2468E+00	-.2617E+00	-.2786E+00	-.2977E+00			
1.95	-.2483E+00	-.2549E+00	-.2644E+00	-.2771E+00	-.2923E+00	-.3102E+00	-.3308E+00				
2.00	-.2925E+00	-.3004E+00	-.3116E+00	-.3265E+00	-.3446E+00						
2.05	-.3434E+00	-.3527E+00	-.3660E+00								
2.10	-.4014E+00	-.4124E+00									

TABLE 8. Enthalpy of excitations (J g^{-1})

Temp. (K)	Pressure (atm)										
	.00	2.50	5.00	7.50	10.00	12.50	15.00	17.50	20.00	22.50	25.00
.10	.4174E-05	.3236E-05	.2618E-05	.2190E-05	.1874E-05	.1633E-05	.1443E-05	.1290E-05	.1164E-05	.1058E-05	.9670E-06
.15	.6261E-05	.4855E-05	.3927E-05	.3285E-05	.2811E-05	.2449E-05	.2165E-05	.1936E-05	.1746E-05	.1587E-05	.1450E-05
.20	.1181E-04	.9183E-05	.7449E-05	.6238E-05	.5343E-05	.4660E-05	.4122E-05	.3687E-05	.3328E-05	.3028E-05	.2771E-05
.25	.2337E-04	.1826E-04	.1486E-04	.1247E-04	.1069E-04	.9335E-05	.8262E-05	.7395E-05	.6680E-05	.6082E-05	.5573E-05
.30	.4412E-04	.3467E-04	.2832E-04	.2381E-04	.2045E-04	.1786E-04	.1582E-04	.1417E-04	.1280E-04	.1166E-04	.1069E-04
.35	.7787E-04	.6155E-04	.5046E-04	.4250E-04	.3655E-04	.3196E-04	.2832E-04	.2537E-04	.2294E-04	.2090E-04	.1916E-04
.40	.1290E-03	.1026E-03	.8440E-04	.7126E-04	.6138E-04	.5373E-04	.4766E-04	.4275E-04	.3869E-04	.3531E-04	.3246E-04
.45	.2025E-03	.1621E-03	.1339E-03	.1134E-03	.9799E-04	.8604E-04	.7658E-04	.6897E-04	.6277E-04	.5772E-04	.5359E-04
.50	.3046E-03	.2455E-03	.2041E-03	.1739E-03	.1513E-03	.1339E-03	.1203E-03	.1097E-03	.1014E-03	.9515E-04	.9067E-04
.55	.4436E-03	.3610E-03	.3032E-03	.2616E-03	.2309E-03	.2080E-03	.1909E-03	.1784E-03	.1700E-03	.1652E-03	.1643E-03
.60	.6331E-03	.5226E-03	.4470E-03	.3943E-03	.3572E-03	.3315E-03	.3144E-03	.3047E-03	.3022E-03	.3067E-03	.3191E-03
.65	.8974E-03	.7563E-03	.6648E-03	.6060E-03	.5696E-03	.5493E-03	.5414E-03	.5459E-03	.5626E-03	.5926E-03	.6374E-03
.70	.1278E-02	.1108E-02	.1009E-02	.9573E-03	.9368E-03	.9396E-03	.9594E-03	.9994E-03	.1059E-02	.1143E-02	.1253E-02
.75	.1844E-02	.1652E-02	.1565E-02	.1546E-02	.1569E-02	.1625E-02	.1703E-02	.1813E-02	.1954E-02	.2138E-02	.2364E-02
.80	.2705E-02	.2501E-02	.2461E-02	.2516E-02	.2626E-02	.2781E-02	.2966E-02	.3195E-02	.3477E-02	.3823E-02	.4238E-02
.85	.4008E-02	.3824E-02	.3877E-02	.4065E-02	.4329E-02	.4645E-02	.5001E-02	.5418E-02	.5919E-02	.6513E-02	.7218E-02
.90	.5966E-02	.5841E-02	.6059E-02	.6455E-02	.6953E-02	.7514E-02	.8128E-02	.8828E-02	.9641E-02	.1060E-01	.1171E-01
.95	.8878E-02	.8855E-02	.9306E-02	.1001E-01	.1084E-01	.1175E-01	.1273E-01	.1383E-01	.1507E-01	.1653E-01	.1817E-01
1.00	.1311E-01	.1324E-01	.1401E-01	.1512E-01	.1639E-01	.1776E-01	.1924E-01	.2086E-01	.2270E-01	.2480E-01	.2715E-01
1.05	.1916E-01	.1952E-01	.2066E-01	.2225E-01	.2406E-01	.2603E-01	.2815E-01	.3044E-01	.3306E-01	.3595E-01	.3921E-01
1.10	.2754E-01	.2820E-01	.2977E-01	.3188E-01	.3436E-01	.3706E-01	.3999E-01	.4318E-01	.4671E-01	.5065E-01	.5504E-01
1.15	.3883E-01	.3979E-01	.4179E-01	.4452E-01	.4779E-01	.5144E-01	.5541E-01	.5971E-01	.6442E-01	.6962E-01	.7548E-01
1.20	.5344E-01	.5490E-01	.5751E-01	.6097E-01	.6511E-01	.6979E-01	.7491E-01	.8062E-01	.8684E-01	.9371E-01	.1014E+00
1.25	.7210E-01	.7424E-01	.7768E-01	.8197E-01	.8694E-01	.9259E-01	.9898E-01	.1062E+00	.1144E+00	.1235E+00	.1331E+00
1.30	.9543E-01	.9819E-01	.1024E+00	.1078E+00	.1142E+00	.1215E+00	.1297E+00	.1389E+00	.1492E+00	.1607E+00	.1738E+00
1.35	.1240E+00	.1279E+00	.1335E+00	.1404E+00	.1485E+00	.1575E+00	.1678E+00	.1792E+00	.1921E+00	.2064E+00	.2223E+00
1.40	.1602E+00	.1651E+00	.1723E+00	.1811E+00	.1912E+00	.2027E+00	.2157E+00	.2301E+00	.2462E+00	.2641E+00	.2838E+00
1.45	.2054E+00	.2118E+00	.2205E+00	.2312E+00	.2438E+00	.2581E+00	.2743E+00	.2924E+00	.3131E+00	.3361E+00	.3619E+00
1.50	.2584E+00	.2661E+00	.2767E+00	.2898E+00	.3053E+00	.3230E+00	.3430E+00	.3654E+00	.3908E+00	.4196E+00	.4527E+00
1.55	.3186E+00	.3278E+00	.3406E+00	.3567E+00	.3758E+00	.3976E+00	.4218E+00	.4488E+00	.4789E+00	.5134E+00	.5543E+00
1.60	.3882E+00	.3993E+00	.4145E+00	.4341E+00	.4575E+00	.4843E+00	.5142E+00	.5473E+00	.5842E+00	.6267E+00	.6779E+00
1.65	.4715E+00	.4849E+00	.5034E+00	.5268E+00	.5553E+00	.5884E+00	.6254E+00	.6669E+00	.7132E+00	.7663E+00	.8293E+00
1.70	.5721E+00	.5883E+00	.6100E+00	.6382E+00	.6731E+00	.7138E+00	.7594E+00	.8100E+00	.8670E+00	.9339E+00	.1018E+01
1.75	.6917E+00	.7090E+00	.7331E+00	.7667E+00	.8094E+00	.8597E+00	.9146E+00	.9744E+00	.1042E+01	.1124E+01	.1238E+01
1.80	.8276E+00	.8490E+00	.8785E+00	.9185E+00	.9694E+00	.1029E+01	.1096E+01	.1171E+01	.1258E+01	.1370E+01	.1525E+01
1.85	.9832E+00	.1010E+01	.1048E+01	.1096E+01	.1154E+01	.1222E+01	.1301E+01	.1395E+01	.1511E+01	.1665E+01	
1.90	.1161E+01	.1194E+01	.1240E+01	.1298E+01	.1368E+01	.1451E+01	.1555E+01	.1684E+01			
1.95	.1363E+01	.1402E+01	.1458E+01	.1528E+01	.1613E+01	.1723E+01	.1865E+01				
2.00	.1608E+01	.1654E+01	.1719E+01	.1803E+01	.1911E+01						
2.05	.1891E+01	.1945E+01	.2020E+01								
2.10	.2197E+01	.2262E+01									

TABLE 9. Entropy (J g^{-1} K^{-1})

Temp. (K)	Pressure (atm)										
	.00	2.50	5.00	7.50	10.00	12.50	15.00	17.50	20.00	22.50	25.00
.10	.68889E-05	.53212E-05	.43073E-05	.36013E-05	.30835E-05	.26885E-05	.23779E-05	.21278E-05	.19223E-05	.17507E-05	.16053E-05
.15	.23112E-04	.17910E-04	.14522E-04	.12153E-04	.10411E-04	.90809E-05	.80338E-05	.71898E-05	.64961E-05	.59167E-05	.54258E-05
.20	.54383E-04	.42309E-04	.34379E-04	.28808E-04	.24697E-04	.21551E-04	.19072E-04	.17072E-04	.15427E-04	.14052E-04	.12887E-04
.25	.10534E-03	.82321E-04	.67062E-04	.56275E-04	.48288E-04	.42161E-04	.37325E-04	.33419E-04	.30205E-04	.27517E-04	.25238E-04
.30	.18041E-03	.14169E-03	.11574E-03	.97286E-04	.83563E-04	.73007E-04	.64662E-04	.57914E-04	.52355E-04	.47703E-04	.43757E-04
.35	.28386E-03	.22[illegible]E-03	.18360E-03	.15460E-03	.13295E-03	.11624E-03	.10301E-03	.92302E-04	.83472E-04	.76082E-04	.69818E-04
.40	.41983E-03	.33315E-03	.27388E-03	.23111E-03	.19903E-03	.17422E-03	.15455E-03	.13862E-03	.12552E-03	.11458E-03	.10537E-03
.45	.59254E-03	.47292E-03	.39022E-03	.33023E-03	.28510E-03	.25019E-03	.22257E-03	.20032E-03	.18222E-03	.16740E-03	.15522E-03
.50	.80709E-03	.64828E-03	.53774E-03	.45745E-03	.39716E-03	.35081E-03	.31462E-03	.28606E-03	.26359E-03	.24614E-03	.23324E-03
.55	.10714E-02	.86783E-03	.72633E-03	.62421E-03	.54858E-03	.49184E-03	.44872E-03	.41671E-03	.39395E-03	.37942E-03	.37333E-03
.60	.14006E-02	.11486E-02	.97586E-03	.85450E-03	.76775E-03	.70618E-03	.66321E-03	.63604E-03	.62338E-03	.62473E-03	.64195E-03
.65	.18226E-02	.15219E-02	.13238E-02	.11926E-02	.11070E-02	.10538E-02	.10254E-02	.10205E-02	.10386E-02	.10811E-02	.11493E-02
.70	.23865E-02	.20413E-02	.18328E-02	.17118E-02	.16495E-02	.16304E-02	.16430E-02	.16908E-02	.17725E-02	.18928E-02	.20589E-02
.75	.31649E-02	.27906E-02	.25972E-02	.25218E-02	.25192E-02	.25729E-02	.26656E-02	.28086E-02	.30018E-02	.32620E-02	.35866E-02
.80	.42735E-02	.38840E-02	.37520E-02	.37708E-02	.38804E-02	.40606E-02	.42917E-02	.45890E-02	.49635E-02	.54308E-02	.59979E-02
.85	.58517E-02	.54850E-02	.54647E-02	.56441E-02	.59400E-02	.63147E-02	.67525E-02	.72765E-02	.79173E-02	.86838E-02	.96015E-02
.90	.80843E-02	.77855E-02	.79541E-02	.83705E-02	.89332E-02	.95887E-02	.10319E-01	.11166E-01	.12162E-01	.13343E-01	.14726E-01
.95	.11230E-01	.11042E-01	.11460E-01	.12207E-01	.13127E-01	.14156E-01	.15283E-01	.16562E-01	.18024E-01	.19748E-01	.21696E-01
1.00	.15562E-01	.15531E-01	.16276E-01	.17438E-01	.18815E-01	.20318E-01	.21955E-01	.23770E-01	.25837E-01	.28212E-01	.30896E-01
1.05	.21457E-01	.21648E-01	.22755E-01	.24383E-01	.26280E-01	.28378E-01	.30639E-01	.33093E-01	.35933E-01	.39080E-01	.42648E-01
1.10	.29233E-01	.29716E-01	.31223E-01	.33340E-01	.35858E-01	.38625E-01	.41629E-01	.44939E-01	.48610E-01	.52737E-01	.57356E-01
1.15	.39275E-01	.40009E-01	.41895E-01	.44562E-01	.47776E-01	.51374E-01	.55305E-01	.59588E-01	.64319E-01	.69555E-01	.75456E-01
1.20	.51689E-01	.52846E-01	.55231E-01	.58523E-01	.62507E-01	.67028E-01	.71957E-01	.77447E-01	.83426E-01	.90091E-01	.97621E-01
1.25	.66910E-01	.68645E-01	.71759E-01	.75720E-01	.80318E-01	.85539E-01	.91459E-01	.98205E-01	.10584E+00	.11425E+00	.12317E+00
1.30	.85256E-01	.87415E-01	.91048E-01	.95878E-01	.10165E+00	.10827E+00	.11567E+00	.12389E+00	.13311E+00	.14350E+00	.15539E+00
1.35	.10675E+00	.10981E+00	.11456E+00	.12053E+00	.12752E+00	.13536E+00	.14424E+00	.15420E+00	.16537E+00	.17790E+00	.19172E+00
1.40	.13301E+00	.13679E+00	.14263E+00	.14995E+00	.15848E+00	.16811E+00	.17897E+00	.19108E+00	.20455E+00	.21959E+00	.23620E+00
1.45	.16481E+00	.16958E+00	.17651E+00	.18521E+00	.19538E+00	.20696E+00	.22013E+00	.23477E+00	.25150E+00	.27013E+00	.29107E+00
1.50	.20076E+00	.20644E+00	.21462E+00	.22489E+00	.23703E+00	.25096E+00	.26664E+00	.28423E+00	.30423E+00	.32689E+00	.35275E+00
1.55	.24020E+00	.24688E+00	.25645E+00	.26869E+00	.28315E+00	.29972E+00	.31816E+00	.33871E+00	.36168E+00	.38791E+00	.41876E+00
1.60	.28431E+00	.29219E+00	.30331E+00	.31767E+00	.33491E+00	.35460E+00	.37664E+00	.40100E+00	.42826E+00	.45963E+00	.49733E+00
1.65	.33558E+00	.34472E+00	.35780E+00	.37452E+00	.39481E+00	.41841E+00	.44473E+00	.47423E+00	.50720E+00	.54494E+00	.58951E+00
1.70	.39554E+00	.40654E+00	.42166E+00	.44122E+00	.46522E+00	.49321E+00	.52474E+00	.55989E+00	.59956E+00	.64589E+00	.70314E+00
1.75	.46502E+00	.47641E+00	.49270E+00	.51527E+00	.54382E+00	.57730E+00	.61399E+00	.65402E+00	.69906E+00	.75398E+00	.82798E+00
1.80	.54155E+00	.55525E+00	.57448E+00	.60062E+00	.63384E+00	.67304E+00	.71670E+00	.76541E+00	.82223E+00	.89379E+00	.99186E+00
1.85	.62676E+00	.64369E+00	.66728E+00	.69801E+00	.73486E+00	.77786E+00	.82766E+00	.88645E+00	.95862E+00	.10529E+01	
1.90	.72189E+00	.74187E+00	.77007E+00	.80561E+00	.84859E+00	.89991E+00	.96275E+00	.10406E+01			
1.95	.82613E+00	.84953E+00	.88240E+00	.92403E+00	.97517E+00	.10400E+01	.11228E+01				
2.00	.95098E+00	.97708E+00	.10145E+01	.10630E+01	.11252E+01						
2.05	.10920E+01	.11224E+01	.11643E+01								
2.10	.12394E+01	.12737E+01									

TABLE 10. Specific heat at constant pressure (J g^{-1} K^{-1})

Temp. (K)	Pressure (atm)										
	.00	2.50	5.00	7.50	10.00	12.50	15.00	17.50	20.00	22.50	25.00
.10	.20597E-04	.15930E-04	.12912E-04	.10798E-04	.92471E-05	.80639E-05	.71329E-05	.63825E-05	.57664E-05	.52515E-05	.48151E-05
.15	.68827E-04	.53569E-04	.43498E-04	.36449E-04	.31241E-04	.27256E-04	.24116E-04	.21583E-04	.19494E-04	.17747E-04	.16263E-04
.20	.16143E-03	.12631E-03	.10296E-03	.86430E-04	.74178E-04	.64773E-04	.57348E-04	.51350E-04	.46413E-04	.42283E-04	.38781E-04
.25	.31144E-03	.24535E-03	.20076E-03	.16891E-03	.14516E-03	.12687E-03	.11239E-03	.10068E-03	.91019E-04	.82932E-04	.76069E-04
.30	.53136E-03	.42160E-03	.34640E-03	.29216E-03	.25148E-03	.22000E-03	.19501E-03	.17475E-03	.15803E-03	.14400E-03	.13208E-03
.35	.83310E-03	.66583E-03	.54949E-03	.46471E-03	.40071E-03	.35099E-03	.31141E-03	.27928E-03	.25274E-03	.23051E-03	.21171E-03
.40	.12285E-02	.98942E-03	.82064E-03	.69655E-03	.60240E-03	.52919E-03	.47098E-03	.42402E-03	.38582E-03	.35472E-03	.32915E-03
.45	.17329E-02	.14078E-02	.11761E-02	.10059E-02	.87707E-03	.77784E-03	.70119E-03	.64131E-03	.59557E-03	.56183E-03	.53960E-03
.50	.23752E-02	.19532E-02	.16558E-02	.14404E-02	.12826E-02	.11677E-02	.10838E-02	.10281E-02	.99666E-03	.98835E-03	.10069E-02
.55	.32242E-02	.27072E-02	.23571E-02	.21212E-02	.19642E-02	.18694E-02	.18204E-02	.18147E-02	.18535E-02	.19388E-02	.20859E-02
.60	.44304E-02	.38399E-02	.34844E-02	.32930E-02	.32150E-02	.32157E-02	.32847E-02	.34256E-02	.36485E-02	.39671E-02	.43823E-02
.65	.62771E-02	.56538E-02	.53997E-02	.53745E-02	.55072E-02	.57552E-02	.60901E-02	.65498E-02	.71343E-02	.78674E-02	.87990E-02
.70	.91759E-02	.86499E-02	.86468E-02	.90032E-02	.95489E-02	.10265E-01	.11075E-01	.12077E-01	.13259E-01	.14748E-01	.16499E-01
.75	.13833E-01	.13474E-01	.14016E-01	.15026E-01	.16267E-01	.17726E-01	.19328E-01	.21162E-01	.23312E-01	.25876E-01	.28825E-01
.80	.21063E-01	.21080E-01	.22425E-01	.24426E-01	.26777E-01	.29302E-01	.32026E-01	.35025E-01	.38580E-01	.42565E-01	.47270E-01
.85	.31764E-01	.32527E-01	.35068E-01	.38410E-01	.42238E-01	.46242E-01	.50433E-01	.55051E-01	.60302E-01	.66319E-01	.73260E-01
.90	.47605E-01	.49215E-01	.53157E-01	.58252E-01	.63842E-01	.69707E-01	.75875E-01	.82655E-01	.89970E-01	.98593E-01	.10779E+00
.95	.70011E-01	.72512E-01	.78033E-01	.85181E-01	.92970E-01	.10097E+00	.10956E+00	.11877E+00	.12886E+00	.14021E+00	.15250E+00
1.00	.10505E+00	.10894E+00	.11567E+00	.12423E+00	.13401E+00	.14459E+00	.15595E+00	.16816E+00	.18161E+00	.19624E+00	.21243E+00
1.05	.14650E+00	.15146E+00	.15922E+00	.16929E+00	.18132E+00	.19477E+00	.20941E+00	.22517E+00	.24227E+00	.26070E+00	.28137E+00
1.10	.19817E+00	.20459E+00	.21352E+00	.22518E+00	.23954E+00	.25613E+00	.27428E+00	.29448E+00	.31585E+00	.33932E+00	.36578E+00
1.15	.26074E+00	.26939E+00	.28064E+00	.29408E+00	.30987E+00	.32827E+00	.34953E+00	.37429E+00	.40165E+00	.43169E+00	.46300E+00
1.20	.33524E+00	.34568E+00	.35884E+00	.37496E+00	.39393E+00	.41632E+00	.44217E+00	.47164E+00	.50524E+00	.54295E+00	.58506E+00
1.25	.42129E+00	.43542E+00	.45289E+00	.47325E+00	.49659E+00	.52307E+00	.55397E+00	.58914E+00	.62947E+00	.67528E+00	.72575E+00
1.30	.52646E+00	.54351E+00	.56578E+00	.59192E+00	.62176E+00	.65517E+00	.69371E+00	.73647E+00	.78460E+00	.83890E+00	.89883E+00
1.35	.65761E+00	.67836E+00	.70490E+00	.73720E+00	.77472E+00	.81724E+00	.86570E+00	.91888E+00	.97941E+00	.10472E+01	.11248E+01
1.40	.80938E+00	.83389E+00	.86541E+00	.90353E+00	.94808E+00	.99947E+00	.10579E+01	.11235E+01	.11994E+01	.12852E+01	.13833E+01
1.45	.97047E+00	.99701E+00	.10317E+01	.10766E+01	.11305E+01	.11935E+01	.12629E+01	.13403E+01	.14276E+01	.15292E+01	.16548E+01
1.50	.11339E+01	.11643E+01	.12038E+01	.12567E+01	.13219E+01	.13972E+01	.14801E+01	.15713E+01	.16728E+01	.17935E+01	.19498E+01
1.55	.13177E+01	.13516E+01	.13988E+01	.14612E+01	.15398E+01	.16322E+01	.17334E+01	.18465E+01	.19697E+01	.21151E+01	.22983E+01
1.60	.15517E+01	.15936E+01	.16493E+01	.17230E+01	.18176E+01	.19301E+01	.20568E+01	.21978E+01	.23556E+01	.25439E+01	.27886E+01
1.65	.18508E+01	.18922E+01	.19498E+01	.20351E+01	.21504E+01	.22894E+01	.24412E+01	.26053E+01	.27920E+01	.30307E+01	.33800E+01
1.70	.21893E+01	.22365E+01	.23026E+01	.24026E+01	.25393E+01	.27055E+01	.28878E+01	.30891E+01	.33312E+01	.36629E+01	.41734E+01
1.75	.25493E+01	.26132E+01	.27012E+01	.28223E+01	.29704E+01	.31455E+01	.33524E+01	.36048E+01	.39392E+01	.44235E+01	.51414E+01
1.80	.29321E+01	.30166E+01	.31371E+01	.32816E+01	.34480E+01	.36502E+01	.39229E+01	.42982E+01	.48294E+01	.55658E+01	.65587E+01
1.85	.33395E+01	.34515E+01	.36075E+01	.37832E+01	.39865E+01	.42632E+01	.46753E+01	.52718E+01	.61137E+01	.72245E+01	
1.90	.38692E+01	.39880E+01	.41612E+01	.43727E+01	.46478E+01	.50610E+01	.56810E+01	.65809E+01			
1.95	.45223E+01	.46510E+01	.48294E+01	.50766E+01	.54595E+01	.60556E+01	.69572E+01				
2.00	.52035E+01	.53463E+01	.55206E+01	.58063E+01	.63029E+01						
2.05	.59223E+01	.61268E+01	.63100E+01								
2.10	.66768E+01	.68762E+01									

TABLE 11. Specific heat at constant volume (J g^{-1} K^{-1})

Temp. (K)	Pressure (atm)										
	.00	2.50	5.00	7.50	10.00	12.50	15.00	17.50	20.00	22.50	25.00
.10	.20597E-04	.15930E-04	.12912E-04	.10798E-04	.92471E-05	.80639E-05	.71329E-05	.63825E-05	.57664E-05	.52515E-05	.48151E-05
.15	.68827E-04	.53569E-04	.43498E-04	.36449E-04	.31241E-04	.27256E-04	.24116E-04	.21583E-04	.19494E-04	.17747E-04	.16263E-04
.20	.16143E-03	.12631E-03	.10296E-03	.86429E-04	.74178E-04	.64773E-04	.57348E-04	.51350E-04	.46413E-04	.42283E-04	.38781E-04
.25	.31144E-03	.24535E-03	.20075E-03	.16891E-03	.14516E-03	.12687E-03	.11239E-03	.10068E-03	.91019E-04	.82932E-04	.76069E-04
.30	.53134E-03	.42159E-03	.34639E-03	.29216E-03	.25148E-03	.22000E-03	.19501E-03	.17475E-03	.15802E-03	.14400E-03	.13208E-03
.35	.83306E-03	.66581E-03	.54948E-03	.46471E-03	.40070E-03	.35098E-03	.31140E-03	.27928E-03	.25274E-03	.23051E-03	.21171E-03
.40	.12284E-02	.98937E-03	.82061E-03	.69653E-03	.60239E-03	.52919E-03	.47097E-03	.42401E-03	.38581E-03	.35472E-03	.32915E-03
.45	.17327E-02	.14077E-02	.11760E-02	.10058E-02	.87705E-03	.77782E-03	.70118E-03	.64130E-03	.59556E-03	.56182E-03	.53959E-03
.50	.23749E-02	.19530E-02	.16557E-02	.14403E-02	.12825E-02	.11677E-02	.10838E-02	.10280E-02	.99665E-03	.98834E-03	.10069E-02
.55	.32236E-02	.27068E-02	.23569E-02	.21210E-02	.19642E-02	.18694E-02	.18204E-02	.18147E-02	.18535E-02	.19388E-02	.20859E-02
.60	.44293E-02	.38393E-02	.34840E-02	.32928E-02	.32148E-02	.32156E-02	.32847E-02	.34256E-02	.36485E-02	.39671E-02	.43823E-02
.65	.62754E-02	.56529E-02	.53993E-02	.53742E-02	.55071E-02	.57552E-02	.60901E-02	.65498E-02	.71342E-02	.78673E-02	.87987E-02
.70	.91734E-02	.86487E-02	.86463E-02	.90030E-02	.95489E-02	.10265E-01	.11075E-01	.12077E-01	.13259E-01	.14747E-01	.16498E-01
.75	.13830E-01	.13472E-01	.14016E-01	.15026E-01	.16267E-01	.17726E-01	.19328E-01	.21161E-01	.23310E-01	.25873E-01	.28820E-01
.80	.21058E-01	.21079E-01	.22425E-01	.24426E-01	.26776E-01	.29301E-01	.32024E-01	.35021E-01	.38572E-01	.42554E-01	.47252E-01
.85	.31759E-01	.32527E-01	.35068E-01	.38408E-01	.42234E-01	.46237E-01	.50424E-01	.55037E-01	.60280E-01	.66287E-01	.73208E-01
.90	.47598E-01	.49215E-01	.53154E-01	.58245E-01	.63830E-01	.69690E-01	.75851E-01	.82618E-01	.89913E-01	.98511E-01	.10767E+00
.95	.70005E-01	.72512E-01	.78023E-01	.85160E-01	.92937E-01	.10092E+00	.10950E+00	.11869E+00	.12873E+00	.14003E+00	.15225E+00
1.00	.10504E+00	.10893E+00	.11564E+00	.12418E+00	.13393E+00	.14449E+00	.15582E+00	.16797E+00	.18135E+00	.19588E+00	.21193E+00
1.05	.14650E+00	.15145E+00	.15916E+00	.16919E+00	.18117E+00	.19456E+00	.20916E+00	.22482E+00	.24177E+00	.26007E+00	.28043E+00
1.10	.19816E+00	.20456E+00	.21342E+00	.22498E+00	.23926E+00	.25576E+00	.27380E+00	.29383E+00	.31497E+00	.33814E+00	.36419E+00
1.15	.26074E+00	.26933E+00	.28047E+00	.29375E+00	.30938E+00	.32762E+00	.34867E+00	.37315E+00	.40014E+00	.42974E+00	.46027E+00
1.20	.33523E+00	.34559E+00	.35856E+00	.37445E+00	.39314E+00	.41524E+00	.44072E+00	.46971E+00	.50271E+00	.53958E+00	.58045E+00
1.25	.42128E+00	.43523E+00	.45245E+00	.47252E+00	.49550E+00	.52151E+00	.55174E+00	.58598E+00	.62517E+00	.66976E+00	.71924E+00
1.30	.52642E+00	.54326E+00	.56513E+00	.59076E+00	.61995E+00	.65259E+00	.69020E+00	.73168E+00	.77802E+00	.83001E+00	.88619E+00
1.35	.65752E+00	.67786E+00	.70383E+00	.73540E+00	.77206E+00	.81347E+00	.86039E+00	.91158E+00	.96938E+00	.10339E+01	.11076E+01
1.40	.80923E+00	.83311E+00	.86374E+00	.90075E+00	.94394E+00	.99358E+00	.10497E+01	.11124E+01	.11844E+01	.12653E+01	.13577E+01
1.45	.97015E+00	.99588E+00	.10293E+01	.10725E+01	.11243E+01	.11846E+01	.12506E+01	.13231E+01	.14038E+01	.14981E+01	.16116E+01
1.50	.11334E+01	.11626E+01	.12003E+01	.12508E+01	.13128E+01	.13841E+01	.14619E+01	.15459E+01	.16373E+01	.17451E+01	.18818E+01
1.55	.13169E+01	.13493E+01	.13938E+01	.14525E+01	.15265E+01	.16132E+01	.17076E+01	.18116E+01	.19216E+01	.20479E+01	.21986E+01
1.60	.15506E+01	.15905E+01	.16423E+01	.17105E+01	.17982E+01	.19024E+01	.20192E+01	.21475E+01	.22859E+01	.24456E+01	.26350E+01
1.65	.18494E+01	.18876E+01	.19400E+01	.20176E+01	.21222E+01	.22487E+01	.23854E+01	.25297E+01	.26880E+01	.28851E+01	.31672E+01
1.70	.21868E+01	.22301E+01	.22891E+01	.23776E+01	.24987E+01	.26461E+01	.28063E+01	.29789E+01	.31757E+01	.34372E+01	.38086E+01
1.75	.25464E+01	.26066E+01	.26840E+01	.27871E+01	.29109E+01	.30605E+01	.32422E+01	.34611E+01	.37308E+01	.40964E+01	.45170E+01
1.80	.29278E+01	.30064E+01	.31132E+01	.32333E+01	.33655E+01	.35295E+01	.37607E+01	.40750E+01	.44834E+01	.49978E+01	.54955E+01
1.85	.33332E+01	.34363E+01	.35720E+01	.37195E+01	.38858E+01	.41114E+01	.44494E+01	.49275E+01	.55318E+01	.62190E+01	
1.90	.38614E+01	.39637E+01	.41114E+01	.42858E+01	.45065E+01	.48307E+01	.53017E+01	.59501E+01			
1.95	.45113E+01	.46182E+01	.47604E+01	.49550E+01	.52460E+01	.56713E+01	.62825E+01				
2.00	.51900E+01	.53031E+01	.54286E+01	.56327E+01	.59711E+01						
2.05	.59009E+01	.60686E+01	.61916E+01								
2.10	.66428E+01	.68086E+01									

TABLE 12. Ratio of specific heats (C_P/C_V)

Temp. (K)	Pressure (atm)										
	.00	2.50	5.00	7.50	10.00	12.50	15.00	17.50	20.00	22.50	25.00
.10	.10000E+01	.10000E+01	.10000E+01	.10000E+01	.10000E+01	.10000E+01	.10000E+01	.10000E+01	.10000E+01	.10000E+01	.10000E+01
.15	.10000E+01	.10000E+01	.10000E+01	.10000E+01	.10000E+01	.10000E+01	.10000E+01	.10000E+01	.10000E+01	.10000E+01	.10000E+01
.20	.10000E+01	.10000E+01	.10000E+01	.10000E+01	.10000E+01	.10000E+01	.10000E+01	.10000E+01	.10000E+01	.10000E+01	.10000E+01
.25	.10000E+01	.10000E+01	.10000E+01	.10000E+01	.10000E+01	.10000E+01	.10000E+01	.10000E+01	.10000E+01	.10000E+01	.10000E+01
.30	.10000E+01	.10000E+01	.10000E+01	.10000E+01	.10000E+01	.10000E+01	.10000E+01	.10000E+01	.10000E+01	.10000E+01	.10000E+01
.35	.10000E+01	.10000E+01	.10000E+01	.10000E+01	.10000E+01	.10000E+01	.10000E+01	.10000E+01	.10000E+01	.10000E+01	.10000E+01
.40	.10001E+01	.10000E+01	.10000E+01	.10000E+01	.10000E+01	.10000E+01	.10000E+01	.10000E+01	.10000E+01	.10000E+01	.10000E+01
.45	.10001E+01	.10001E+01	.10001E+01	.10000E+01	.10000E+01	.10000E+01	.10000E+01	.10000E+01	.10000E+01	.10000E+01	.10000E+01
.50	.10001E+01	.10001E+01	.10001E+01	.10001E+01	.10000E+01	.10000E+01	.10000E+01	.10000E+01	.10000E+01	.10000E+01	.10000E+01
.55	.10002E+01	.10001E+01	.10001E+01	.10001E+01	.10000E+01	.10000E+01	.10000E+01	.10000E+01	.10000E+01	.10000E+01	.10000E+01
.60	.10002E+01	.10002E+01	.10001E+01	.10001E+01	.10000E+01	.10000E+01	.10000E+01	.10000E+01	.10000E+01	.10000E+01	.10000E+01
.65	.10003E+01	.10002E+01	.10001E+01	.10000E+01	.10000E+01	.10000E+01	.10000E+01	.10000E+01	.10000E+01	.10000E+01	.10000E+01
.70	.10003E+01	.10001E+01	.10001E+01	.10000E+01	.10000E+01	.10000E+01	.10000E+01	.10000E+01	.10000E+01	.10001E+01	.10001E+01
.75	.10002E+01	.10001E+01	.10000E+01	.10000E+01	.10000E+01	.10000E+01	.10000E+01	.10000E+01	.10001E+01	.10001E+01	.10002E+01
.80	.10002E+01	.10000E+01	.10000E+01	.10000E+01	.10000E+01	.10000E+01	.10001E+01	.10001E+01	.10002E+01	.10003E+01	.10004E+01
.85	.10002E+01	.10000E+01	.10000E+01	.10000E+01	.10001E+01	.10001E+01	.10002E+01	.10003E+01	.10004E+01	.10005E+01	.10007E+01
.90	.10001E+01	.10000E+01	.10000E+01	.10001E+01	.10002E+01	.10002E+01	.10003E+01	.10004E+01	.10006E+01	.10008E+01	.10011E+01
.95	.10001E+01	.10000E+01	.10001E+01	.10003E+01	.10004E+01	.10004E+01	.10006E+01	.10007E+01	.10010E+01	.10013E+01	.10016E+01
1.00	.10001E+01	.10000E+01	.10002E+01	.10004E+01	.10006E+01	.10007E+01	.10008E+01	.10011E+01	.10014E+01	.10018E+01	.10023E+01
1.05	.10000E+01	.10001E+01	.10004E+01	.10006E+01	.10008E+01	.10010E+01	.10012E+01	.10016E+01	.10021E+01	.10024E+01	.10033E+01
1.10	.10000E+01	.10002E+01	.10005E+01	.10009E+01	.10012E+01	.10014E+01	.10018E+01	.10022E+01	.10028E+01	.10035E+01	.10044E+01
1.15	.10000E+01	.10002E+01	.10006E+01	.10011E+01	.10016E+01	.10020E+01	.10025E+01	.10030E+01	.10038E+01	.10045E+01	.10059E+01
1.20	.10000E+01	.10003E+01	.10008E+01	.10014E+01	.10020E+01	.10026E+01	.10033E+01	.10041E+01	.10050E+01	.10063E+01	.10079E+01
1.25	.10000E+01	.10004E+01	.10010E+01	.10015E+01	.10022E+01	.10030E+01	.10040E+01	.10054E+01	.10069E+01	.10083E+01	.10091E+01
1.30	.10001E+01	.10005E+01	.10011E+01	.10020E+01	.10029E+01	.10039E+01	.10051E+01	.10065E+01	.10085E+01	.10107E+01	.10143E+01
1.35	.10001E+01	.10007E+01	.10015E+01	.10024E+01	.10035E+01	.10046E+01	.10062E+01	.10080E+01	.10103E+01	.10129E+01	.10155E+01
1.40	.10002E+01	.10009E+01	.10019E+01	.10031E+01	.10044E+01	.10059E+01	.10078E+01	.10099E+01	.10126E+01	.10157E+01	.10189E+01
1.45	.10003E+01	.10011E+01	.10024E+01	.10038E+01	.10055E+01	.10075E+01	.10099E+01	.10130E+01	.10170E+01	.10208E+01	.10268E+01
1.50	.10004E+01	.10014E+01	.10029E+01	.10047E+01	.10069E+01	.10095E+01	.10124E+01	.10164E+01	.10217E+01	.10277E+01	.10361E+01
1.55	.10006E+01	.10017E+01	.10036E+01	.10060E+01	.10087E+01	.10117E+01	.10151E+01	.10193E+01	.10250E+01	.10328E+01	.10454E+01
1.60	.10007E+01	.10020E+01	.10042E+01	.10073E+01	.10108E+01	.10145E+01	.10186E+01	.10234E+01	.10305E+01	.10402E+01	.10583E+01
1.65	.10008E+01	.10025E+01	.10051E+01	.10087E+01	.10133E+01	.10181E+01	.10234E+01	.10299E+01	.10387E+01	.10504E+01	.10672E+01
1.70	.10011E+01	.10028E+01	.10059E+01	.10105E+01	.10162E+01	.10224E+01	.10290E+01	.10370E+01	.10490E+01	.10656E+01	.10958E+01
1.75	.10011E+01	.10026E+01	.10064E+01	.10127E+01	.10205E+01	.10277E+01	.10340E+01	.10415E+01	.10559E+01	.10798E+01	.11382E+01
1.80	.10014E+01	.10034E+01	.10077E+01	.10149E+01	.10245E+01	.10342E+01	.10431E+01	.10548E+01	.10772E+01	.11137E+01	.11935E+01
1.85	.10019E+01	.10044E+01	.10099E+01	.10171E+01	.10259E+01	.10369E+01	.10508E+01	.10699E+01	.11052E+01	.11617E+01	
1.90	.10020E+01	.10061E+01	.10121E+01	.10203E+01	.10314E+01	.10477E+01	.10715E+01	.11060E+01			
1.95	.10024E+01	.10071E+01	.10145E+01	.10245E+01	.10407E+01	.10678E+01	.11074E+01				
2.00	.10026E+01	.10081E+01	.10169E+01	.10308E+01	.10556E+01						
2.05	.10036E+01	.10096E+01	.10191E+01								
2.10	.10051E+01	.10099E+01									

TABLE 13. Phonon number density (cm^{-3})

Temp. (K)	Pressure (atm)										
	.00	2.50	5.00	7.50	10.00	12.50	15.00	17.50	20.00	22.50	25.00
.10	.20148E+17	.15987E+17	.13244E+17	.11301E+17	.98534E+16	.87335E+16	.78416E+16	.71146E+16	.65106E+16	.60010E+16	.55652E+16
.15	.67739E+17	.53861E+17	.44667E+17	.38138E+17	.33264E+17	.29490E+17	.26483E+17	.24030E+17	.21992E+17	.20271E+17	.18800E+17
.20	.15979E+18	.12738E+18	.10579E+18	.90395E+17	.78882E+17	.69953E+17	.62831E+17	.57019E+17	.52188E+17	.48108E+17	.44618E+17
.25	.31034E+18	.24815E+18	.20642E+18	.17656E+18	.15416E+18	.13676E+18	.12287E+18	.11152E+18	.10208E+18	.94110E+17	.87288E+17
.30	.53296E+18	.42760E+18	.35636E+18	.30513E+18	.26660E+18	.23661E+18	.21263E+18	.19304E+18	.17672E+18	.16294E+18	.15114E+18
.35	.84081E+18	.67700E+18	.56537E+18	.48468E+18	.42379E+18	.37631E+18	.33828E+18	.30717E+18	.28126E+18	.25935E+18	.24058E+18
.40	.12466E+19	.10075E+19	.84324E+18	.72385E+18	.63343E+18	.56276E+18	.50608E+18	.45966E+18	.42095E+18	.38821E+18	.36014E+18
.45	.17628E+19	.14303E+19	.11998E+19	.10314E+19	.90338E+18	.80305E+18	.72245E+18	.65636E+18	.60121E+18	.55452E+18	.51448E+18
.50	.24018E+19	.19564E+19	.16451E+19	.14163E+19	.12417E+19	.11045E+19	.99404E+18	.90336E+18	.82764E+18	.76348E+18	.70842E+18
.55	.31754E+19	.25970E+19	.21892E+19	.18876E+19	.16566E+19	.14745E+19	.13277E+19	.12070E+19	.11061E+19	.10205E+19	.94699E+18
.60	.40958E+19	.33634E+19	.28425E+19	.24549E+19	.21567E+19	.19210E+19	.17306E+19	.15738E+19	.14426E+19	.13312E+19	.12355E+19
.65	.51751E+19	.42673E+19	.36157E+19	.31280E+19	.27510E+19	.24523E+19	.22103E+19	.20108E+19	.18436E+19	.17016E+19	.15794E+19
.70	.64261E+19	.53205E+19	.45201E+19	.39171E+19	.34490E+19	.30768E+19	.27749E+19	.25254E+19	.23161E+19	.21381E+19	.19849E+19
.75	.78612E+19	.65358E+19	.55672E+19	.48332E+19	.42607E+19	.38042E+19	.34329E+19	.31256E+19	.28674E+19	.26476E+19	.24582E+19
.80	.94952E+19	.79260E+19	.67702E+19	.58879E+19	.51970E+19	.46442E+19	.41935E+19	.38199E+19	.35056E+19	.32376E+19	.30066E+19
.85	.11342E+20	.95061E+19	.81415E+19	.70938E+19	.62696E+19	.56079E+19	.50671E+19	.46179E+19	.42394E+19	.39165E+19	.36377E+19
.90	.13419E+20	.11291E+20	.96969E+19	.84647E+19	.74913E+19	.67069E+19	.60646E+19	.55300E+19	.50789E+19	.46934E+19	.43602E+19
.95	.15743E+20	.13300E+20	.11452E+20	.10016E+20	.88760E+19	.79550E+19	.71987E+19	.65681E+19	.60350E+19	.55790E+19	.51842E+19
1.00	.18341E+20	.15552E+20	.13425E+20	.11764E+20	.10440E+20	.93667E+19	.84833E+19	.77453E+19	.71203E+19	.65849E+19	.61207E+19
1.05	.21234E+20	.18070E+20	.15637E+20	.13727E+20	.12200E+20	.10959E+20	.99341E+19	.90765E+19	.83490E+19	.77247E+19	.71830E+19
1.10	.24448E+20	.20879E+20	.18109E+20	.15926E+20	.14176E+20	.12749E+20	.11569E+20	.10579E+20	.97372E+19	.90139E+19	.83853E+19
1.15	.28009E+20	.23999E+20	.20864E+20	.18384E+20	.16389E+20	.14760E+20	.13408E+20	.12271E+20	.11304E+20	.10470E+20	.97448E+19
1.20	.31934E+20	.27459E+20	.23931E+20	.21127E+20	.18866E+20	.17014E+20	.15473E+20	.14176E+20	.13069E+20	.12114E+20	.11281E+20
1.25	.36255E+20	.31289E+20	.27342E+20	.24185E+20	.21631E+20	.19536E+20	.17791E+20	.16318E+20	.15057E+20	.13968E+20	.13016E+20
1.30	.41026E+20	.35519E+20	.31116E+20	.27585E+20	.24719E+20	.22360E+20	.20389E+20	.18723E+20	.17293E+20	.16056E+20	.14971E+20
1.35	.46251E+20	.40196E+20	.35312E+20	.31372E+20	.28164E+20	.25516E+20	.23300E+20	.21421E+20	.19808E+20	.18406E+20	.17177E+20
1.40	.52041E+20	.45375E+20	.39964E+20	.35583E+20	.32005E+20	.29043E+20	.26559E+20	.24446E+20	.22632E+20	.21049E+20	.19661E+20
1.45	.58432E+20	.51110E+20	.45130E+20	.40266E+20	.36284E+20	.32979E+20	.30204E+20	.27837E+20	.25797E+20	.24015E+20	.22445E+20
1.50	.65428E+20	.57404E+20	.50818E+20	.45448E+20	.41037E+20	.37367E+20	.34273E+20	.31633E+20	.29348E+20	.27351E+20	.25579E+20
1.55	.73026E+20	.64297E+20	.57078E+20	.51175E+20	.46309E+20	.42250E+20	.38816E+20	.35881E+20	.33333E+20	.31102E+20	.29111E+20
1.60	.81322E+20	.71851E+20	.63977E+20	.57512E+20	.52163E+20	.47684E+20	.43887E+20	.40626E+20	.37793E+20	.35297E+20	.33063E+20
1.65	.90455E+20	.80183E+20	.71610E+20	.64534E+20	.58663E+20	.53726E+20	.49538E+20	.45921E+20	.42772E+20	.39982E+20	.37474E+20
1.70	.10053E+21	.89391E+20	.80046E+20	.72320E+20	.65879E+20	.60458E+20	.55831E+20	.51828E+20	.48324E+20	.45197E+20	.42345E+20
1.75	.11159E+21	.99502E+20	.89345E+20	.80920E+20	.73886E+20	.67931E+20	.62840E+20	.58415E+20	.54527E+20	.51040E+20	.47796E+20
1.80	.12362E+21	.11062E+21	.99617E+20	.90450E+20	.82770E+20	.76243E+20	.70626E+20	.65724E+20	.61387E+20	.57423E+20	.53652E+20
1.85	.13680E+21	.12284E+21	.11097E+21	.10099E+21	.92624E+20	.85471E+20	.79313E+20	.73893E+20	.69015E+20	.64478E+20	
1.90	.15122E+21	.13628E+21	.12347E+21	.11268E+21	.10357E+21	.95740E+20	.88937E+20	.82856E+20			
1.95	.16704E+21	.15105E+21	.13729E+21	.12567E+21	.11574E+21	.10716E+21	.99557E+20				
2.00	.18452E+21	.16744E+21	.15269E+21	.14006E+21	.12929E+21						
2.05	.20389E+21	.18564E+21	.16976E+21								
2.10	.22513E+21	.20581E+21									

TABLE 14. Roton number density (cm^{-3})

Temp. (K)	Pressure (atm)										
	.00	2.50	5.00	7.50	10.00	12.50	15.00	17.50	20.00	22.50	25.00
.10	.25396E−14	.29891E−14	.90537E−14	.49107E−13	.25799E−12	.11777E−11	.45392E−11	.16808E−10	.61165E−10	.22282E−09	.84183E−09
.15	.12490E−02	.31626E−02	.11525E−01	.41287E−01	.12801E+00	.35257E+00	.86994E+00	.20769E+01	.48902E+01	.11644E+02	.28084E+02
.20	.29191E+04	.58882E+04	.15524E+05	.40309E+05	.94703E+05	.20190E+06	.39665E+06	.76259E+06	.14574E+07	.27769E+07	.53816E+07
.25	.19943E+08	.34950E+08	.75923E+08	.16261E+09	.32148E+09	.58949E+09	.10147E+10	.17089E+10	.28613E+10	.48170E+10	.81674E+10
.30	.72613E+10	.11657E+11	.22187E+11	.41921E+11	.73857E+11	.12257E+12	.19299E+12	.29834E+12	.45741E+12	.70384E+12	.10960E+13
.35	.49805E+12	.74631E+12	.12952E+13	.22398E+13	.36469E+13	.56224E+13	.82872E+13	.12040E+14	.17364E+14	.25126E+14	.36700E+14
.40	.11963E+14	.17060E+14	.27756E+14	.44677E+14	.68271E+14	.10013E+15	.14038E+15	.19465E+15	.26806E+15	.37103E+15	.51508E+15
.45	.14310E+15	.19635E+15	.30210E+15	.46157E+15	.67367E+15	.94422E+15	.12767E+16	.17050E+16	.22706E+16	.30290E+16	.40551E+16
.50	.10496E+16	.13949E+16	.20550E+16	.30076E+16	.42265E+16	.57303E+16	.75258E+16	.97504E+16	.12624E+17	.16362E+17	.21283E+17
.55	.53761E+16	.69608E+16	.98981E+16	.14005E+17	.19079E+17	.25163E+17	.32159E+17	.40798E+17	.51567E+17	.65160E+17	.82940E+17
.60	.21095E+17	.26747E+17	.36886E+17	.50740E+17	.67293E+17	.86638E+17	.10873E+18	.13504E+18	.16722E+18	.20725E+18	.25881E+18
.65	.67172E+17	.83714E+17	.11260E+18	.15101E+18	.19645E+18	.24773E+18	.30525E+18	.37292E+18	.45456E+18	.55497E+18	.67892E+18
.70	.18249E+18	.22330E+18	.29434E+18	.38604E+18	.49229E+18	.61182E+18	.74261E+18	.89530E+18	.10747E+19	.12911E+19	.15573E+19
.75	.43328E+18	.52553E+18	.67821E+18	.87423E+18	.10956E+19	.13419E+19	.16070E+19	.19126E+19	.22666E+19	.26963E+19	.32067E+19
.80	.93329E+18	.11116E+19	.14149E+19	.17921E+19	.22120E+19	.26737E+19	.31695E+19	.37291E+19	.43772E+19	.51441E+19	.60508E+19
.85	.18364E+19	.21681E+19	.27116E+19	.33810E+19	.41244E+19	.49236E+19	.57771E+19	.67287E+19	.78316E+19	.91144E+19	.10629E+20
.90	.33614E+19	.39375E+19	.48574E+19	.59633E+19	.71857E+19	.84895E+19	.98726E+19	.11407E+20	.13160E+20	.15199E+20	.17575E+20
.95	.58313E+19	.67617E+19	.82011E+19	.99335E+19	.11828E+20	.13838E+20	.15976E+20	.18336E+20	.20989E+20	.24079E+20	.27586E+20
1.00	.96233E+19	.11047E+20	.13196E+20	.15764E+20	.18567E+20	.21527E+20	.24686E+20	.28138E+20	.32024E+20	.36471E+20	.41522E+20
1.05	.15278E+20	.17393E+20	.20421E+20	.24021E+20	.27949E+20	.32162E+20	.36651E+20	.41493E+20	.47033E+20	.53194E+20	.60220E+20
1.10	.23329E+20	.26364E+20	.30477E+20	.35294E+20	.40646E+20	.46387E+20	.52553E+20	.59303E+20	.66785E+20	.75216E+20	.84728E+20
1.15	.34436E+20	.38520E+20	.43855E+20	.50152E+20	.57221E+20	.64931E+20	.73273E+20	.82351E+20	.92383E+20	.10356E+21	.11625E+21
1.20	.48941E+20	.54508E+20	.61441E+20	.69537E+20	.78666E+20	.88721E+20	.99604E+20	.11166E+21	.12487E+21	.13967E+21	.15654E+21
1.25	.67653E+20	.75179E+20	.84305E+20	.94527E+20	.10571E+21	.11799E+21	.13165E+21	.14706E+21	.16449E+21	.18387E+21	.20482E+21
1.30	.91255E+20	.10081E+21	.11208E+21	.12500E+21	.13944E+21	.15548E+21	.17314E+21	.19272E+21	.21470E+21	.23964E+21	.26841E+21
1.35	.12006E+21	.13269E+21	.14742E+21	.16389E+21	.18206E+21	.20194E+21	.22406E+21	.24875E+21	.27651E+21	.30785E+21	.34293E+21
1.40	.15683E+21	.17275E+21	.19136E+21	.21218E+21	.23518E+21	.26045E+21	.28857E+21	.31983E+21	.35470E+21	.39403E+21	.43805E+21
1.45	.20336E+21	.22358E+21	.24665E+21	.27250E+21	.30110E+21	.33274E+21	.36816E+21	.40755E+21	.45251E+21	.50318E+21	.56089E+21
1.50	.25783E+21	.28277E+21	.31107E+21	.34284E+21	.37819E+21	.41765E+21	.46153E+21	.51064E+21	.56665E+21	.63067E+21	.70481E+21
1.55	.31940E+21	.34969E+21	.38401E+21	.42295E+21	.46648E+21	.51498E+21	.56857E+21	.62828E+21	.69539E+21	.77274E+21	.86460E+21
1.60	.39045E+21	.42706E+21	.46834E+21	.51549E+21	.56882E+21	.62834E+21	.69446E+21	.76786E+21	.85056E+21	.94654E+21	.10631E+22
1.65	.47590E+21	.51988E+21	.56988E+21	.62674E+21	.69164E+21	.76516E+21	.84682E+21	.93873E+21	.10424E+22	.11626E+22	.13066E+22
1.70	.57947E+21	.63326E+21	.69337E+21	.76226E+21	.84168E+21	.93195E+21	.10333E+22	.11470E+22	.12768E+22	.14303E+22	.16226E+22
1.75	.70382E+21	.76574E+21	.83526E+21	.91784E+21	.10151E+22	.11266E+22	.12494E+22	.13849E+22	.15394E+22	.17289E+22	.19864E+22
1.80	.84507E+21	.92026E+21	.10046E+22	.11039E+22	.12214E+22	.13569E+22	.15085E+22	.16794E+22	.18809E+22	.21374E+22	.24945E+22
1.85	.10072E+22	.10994E+22	.12037E+22	.13242E+22	.14616E+22	.16185E+22	.17989E+22	.20126E+22	.22768E+22	.26272E+22	
1.90	.11939E+22	.13047E+22	.14315E+22	.15763E+22	.17424E+22	.19359E+22	.21698E+22	.24603E+22			
1.95	.14044E+22	.15365E+22	.16886E+22	.18632E+22	.20668E+22	.23163E+22	.26315E+22				
2.00	.16662E+22	.18222E+22	.20028E+22	.22139E+22	.24688E+22						
2.05	.19722E+22	.21591E+22	.23728E+22								
2.10	.22995E+22	.25191E+22									

TABLE 15. Normal fluid density (g cm^{-3})

Temp. (K)	Pressure (atm)										
	.00	2.50	5.00	7.50	10.00	12.50	15.00	17.50	20.00	22.50	25.00
.10	.17497E-08	.11945E-08	.87476E-09	.67253E-09	.53584E-09	.43875E-09	.36709E-09	.31254E-09	.26997E-09	.23603E-09	.20850E-09
.15	.87412E-08	.60088E-08	.44157E-08	.34006E-08	.27113E-08	.22201E-08	.18567E-08	.15796E-08	.13631E-08	.11903E-08	.10500E-08
.20	.27191E-07	.18853E-07	.13920E-07	.10750E-07	.85847E-08	.70367E-08	.58890E-08	.50125E-08	.43267E-08	.37789E-08	.33338E-08
.25	.65232E-07	.45661E-07	.33900E-07	.26262E-07	.21014E-07	.17247E-07	.14447E-07	.12304E-07	.10625E-07	.92839E-08	.81937E-08
.30	.13280E-06	.93920E-07	.70145E-07	.54547E-07	.43758E-07	.35988E-07	.30206E-07	.25791E-07	.22355E-07	.19648E-07	.17517E-07
.35	.24164E-06	.17281E-06	.13010E-06	.10191E-06	.82488E-07	.68707E-07	.58770E-07	.51672E-07	.46848E-07	.44101E-07	.43556E-07
.40	.40748E-06	.29650E-06	.22814E-06	.18479E-06	.15749E-06	.14161E-06	.13420E-06	.13497E-06	.14415E-06	.16392E-06	.19704E-06
.45	.66794E-06	.50857E-06	.42237E-06	.38448E-06	.38156E-06	.40756E-06	.45896E-06	.54128E-06	.66308E-06	.83716E-06	.10821E-05
.50	.11607E-05	.98361E-06	.95820E-06	.10472E-05	.12284E-05	.14956E-05	.18453E-05	.23035E-05	.29171E-05	.37337E-05	.48261E-05
.55	.23363E-05	.22929E-05	.26222E-05	.32542E-05	.41316E-05	.52506E-05	.65878E-05	.82820E-05	.10432E-04	.13182E-04	.16812E-04
.60	.53746E-05	.59092E-05	.73762E-05	.96145E-05	.12434E-04	.15840E-04	.19821E-04	.24639E-04	.30604E-04	.38083E-04	.47788E-04
.65	.12758E-04	.14874E-04	.19169E-04	.25196E-04	.32554E-04	.41051E-04	.50747E-04	.62294E-04	.76359E-04	.93772E-04	.11542E-03
.70	.29073E-04	.34585E-04	.44851E-04	.58536E-04	.74759E-04	.93340E-04	.11399E-03	.13834E-03	.16718E-03	.20217E-03	.24549E-03
.75	.61233E-04	.73621E-04	.94708E-04	.12239E-03	.15425E-03	.19026E-03	.22955E-03	.27525E-03	.32858E-03	.39369E-03	.47146E-03
.80	.12033E-03	.14354E-03	.18344E-03	.23383E-03	.29087E-03	.35454E-03	.42376E-03	.50253E-03	.59442E-03	.70371E-03	.83354E-03
.85	.21939E-03	.26101E-03	.32899E-03	.41381E-03	.50938E-03	.61356E-03	.72620E-03	.85279E-03	.10005E-02	.11732E-02	.13777E-02
.90	.37579E-03	.44501E-03	.55459E-03	.68775E-03	.83697E-03	.99826E-03	.11714E-02	.13650E-02	.15873E-02	.18472E-02	.21514E-02
.95	.61393E-03	.72125E-03	.88514E-03	.10839E-02	.13042E-02	.15407E-02	.17951E-02	.20781E-02	.23981E-02	.27723E-02	.31990E-02
1.00	.95892E-03	.11168E-02	.13510E-02	.16328E-02	.19438E-02	.22763E-02	.26347E-02	.30292E-02	.34758E-02	.39892E-02	.45751E-02
1.05	.14462E-02	.16719E-02	.19893E-02	.23683E-02	.27859E-02	.32386E-02	.37252E-02	.42544E-02	.48623E-02	.55423E-02	.63205E-02
1.10	.21043E-02	.24167E-02	.28327E-02	.33206E-02	.38673E-02	.44589E-02	.50994E-02	.58055E-02	.65919E-02	.74822E-02	.84911E-02
1.15	.29681E-02	.33756E-02	.38975E-02	.45133E-02	.52081E-02	.59704E-02	.68023E-02	.77128E-02	.87252E-02	.98577E-02	.11148E-01
1.20	.40407E-02	.45767E-02	.52329E-02	.59978E-02	.68628E-02	.78211E-02	.88647E-02	.10027E-01	.11308E-01	.12749E-01	.14396E-01
1.25	.53610E-02	.60598E-02	.68948E-02	.78296E-02	.88569E-02	.99896E-02	.11254E-01	.12684E-01	.14308E-01	.16122E-01	.18095E-01
1.30	.69538E-02	.78160E-02	.88172E-02	.99606E-02	.11240E-01	.12664E-01	.14241E-01	.15994E-01	.17971E-01	.20222E-01	.22824E-01
1.35	.88131E-02	.99110E-02	.11174E-01	.12583E-01	.14142E-01	.15852E-01	.17761E-01	.19898E-01	.22310E-01	.25042E-01	.28112E-01
1.40	.11109E-01	.12452E-01	.13998E-01	.15724E-01	.17631E-01	.19736E-01	.22080E-01	.24698E-01	.27633E-01	.30951E-01	.34682E-01
1.45	.13921E-01	.15576E-01	.17438E-01	.19518E-01	.21820E-01	.24374E-01	.27237E-01	.30433E-01	.34091E-01	.38226E-01	.42958E-01
1.50	.17079E-01	.19062E-01	.21286E-01	.23766E-01	.26531E-01	.29616E-01	.33057E-01	.36921E-01	.41340E-01	.46409E-01	.52295E-01
1.55	.20500E-01	.22842E-01	.25461E-01	.28416E-01	.31714E-01	.35398E-01	.39478E-01	.44046E-01	.49195E-01	.55148E-01	.62226E-01
1.60	.24307E-01	.27061E-01	.30126E-01	.33603E-01	.37530E-01	.41919E-01	.46810E-01	.52264E-01	.58433E-01	.65614E-01	.74342E-01
1.65	.28776E-01	.31999E-01	.35610E-01	.39689E-01	.44338E-01	.49607E-01	.55483E-01	.62117E-01	.69644E-01	.78395E-01	.88917E-01
1.70	.34071E-01	.37902E-01	.42140E-01	.46959E-01	.52496E-01	.58799E-01	.65898E-01	.73907E-01	.83087E-01	.93976E-01	.10766E+00
1.75	.40292E-01	.44624E-01	.49428E-01	.55068E-01	.61671E-01	.69252E-01	.77654E-01	.86994E-01	.97683E-01	.11082E+00	.12869E+00
1.80	.47147E-01	.52273E-01	.57957E-01	.64577E-01	.72376E-01	.81380E-01	.91507E-01	.10300E+00	.11660E+00	.13396E+00	.15821E+00
1.85	.54815E-01	.60936E-01	.67771E-01	.75629E-01	.84572E-01	.94804E-01	.10663E+00	.12067E+00	.13809E+00	.16129E+00	
1.90	.63446E-01	.70632E-01	.78754E-01	.87984E-01	.98573E-01	.11093E+00	.12589E+00	.14454E+00			
1.95	.72933E-01	.81325E-01	.90857E-01	.10175E+00	.11446E+00	.13002E+00	.14971E+00				
2.00	.84682E-01	.94402E-01	.10553E+00	.11847E+00	.13405E+00						
2.05	.98195E-01	.10964E+00	.12260E+00								
2.10	.11222E+00	.12547E+00									

TABLE 16. Normal fluid ratio

Temp. (K)	Pressure (atm)										
	.00	2.50	5.00	7.50	10.00	12.50	15.00	17.50	20.00	22.50	25.00
.10	.12056E-07	.80033E-08	.57235E-08	.43103E-08	.33718E-08	.27155E-08	.22379E-08	.18791E-08	.16023E-08	.13841E-08	.12089E-08
.15	.60230E-07	.40259E-07	.28892E-07	.21795E-07	.17061E-07	.13740E-07	.11319E-07	.94970E-08	.80900E-08	.69800E-08	.60880E-08
.20	.18736E-06	.12632E-06	.91080E-07	.68896E-07	.54019E-07	.43552E-07	.35901E-07	.30136E-07	.25680E-07	.22160E-07	.19331E-07
.25	.44947E-06	.30593E-06	.22181E-06	.16832E-06	.13223E-06	.10675E-06	.88073E-07	.73974E-07	.63064E-07	.54443E-07	.47510E-07
.30	.91502E-06	.62928E-06	.45896E-06	.34961E-06	.27535E-06	.22274E-06	.18415E-06	.15506E-06	.13268E-06	.11522E-06	.10157E-06
.35	.16650E-05	.11579E-05	.85123E-06	.65317E-06	.51907E-06	.42525E-06	.35829E-06	.31067E-06	.27806E-06	.25862E-06	.25256E-06
.40	.28077E-05	.19866E-05	.14927E-05	.11844E-05	.99105E-06	.87647E-06	.81818E-06	.81146E-06	.85558E-06	.96126E-06	.11425E-05
.45	.46024E-05	.34076E-05	.27637E-05	.24643E-05	.24011E-05	.25226E-05	.27981E-05	.32544E-05	.39356E-05	.49094E-05	.62743E-05
.50	.79980E-05	.65906E-05	.62699E-05	.67121E-05	.77304E-05	.92572E-05	.11250E-04	.13850E-04	.17314E-04	.21896E-04	.27984E-04
.55	.16099E-04	.15364E-04	.17158E-04	.20858E-04	.26000E-04	.32499E-04	.40164E-04	.49796E-04	.61921E-04	.77306E-04	.97486E-04
.60	.37035E-04	.39595E-04	.48267E-04	.61627E-04	.78250E-04	.98046E-04	.12084E-03	.14814E-03	.18165E-03	.22333E-03	.27709E-03
.65	.87917E-04	.99668E-04	.12543E-03	.16150E-03	.20487E-03	.25409E-03	.30939E-03	.37454E-03	.45321E-03	.54990E-03	.66921E-03
.70	.20034E-03	.23175E-03	.29350E-03	.37521E-03	.47047E-03	.57774E-03	.69495E-03	.83175E-03	.99226E-03	.11855E-02	.14233E-02
.75	.42196E-03	.49333E-03	.61975E-03	.78453E-03	.97070E-03	.11776E-02	.13994E-02	.16548E-02	.19501E-02	.23085E-02	.27334E-02
.80	.82922E-03	.96188E-03	.12004E-02	.14988E-02	.18304E-02	.21943E-02	.25833E-02	.30211E-02	.35276E-02	.41261E-02	.48323E-02
.85	.15119E-02	.17490E-02	.21528E-02	.26524E-02	.32054E-02	.37973E-02	.44268E-02	.51264E-02	.59368E-02	.68779E-02	.79862E-02
.90	.25897E-02	.29821E-02	.36291E-02	.44081E-02	.52665E-02	.61778E-02	.71398E-02	.82044E-02	.94178E-02	.10828E-01	.12469E-01
.95	.42309E-02	.48331E-02	.57920E-02	.69466E-02	.82057E-02	.95339E-02	.10940E-01	.12490E-01	.14227E-01	.16248E-01	.18537E-01
1.00	.66085E-02	.74837E-02	.88402E-02	.10464E-01	.12229E-01	.14084E-01	.16055E-01	.18202E-01	.20616E-01	.23376E-01	.26506E-01
1.05	.99664E-02	.11203E-01	.13016E-01	.15177E-01	.17525E-01	.20035E-01	.22697E-01	.25559E-01	.28833E-01	.32469E-01	.36608E-01
1.10	.14502E-01	.16193E-01	.18532E-01	.21276E-01	.24324E-01	.27579E-01	.31062E-01	.34869E-01	.39079E-01	.43820E-01	.49163E-01
1.15	.20455E-01	.22617E-01	.25497E-01	.28914E-01	.32750E-01	.36919E-01	.41424E-01	.46310E-01	.51708E-01	.57711E-01	.64524E-01
1.20	.27846E-01	.30663E-01	.34228E-01	.38417E-01	.43146E-01	.48350E-01	.53966E-01	.60184E-01	.66985E-01	.74601E-01	.83280E-01
1.25	.36943E-01	.40595E-01	.45091E-01	.50139E-01	.55667E-01	.61734E-01	.68482E-01	.76098E-01	.84718E-01	.94295E-01	.10462E+00
1.30	.47917E-01	.52354E-01	.57652E-01	.63769E-01	.70619E-01	.78231E-01	.86619E-01	.95909E-01	.10635E+00	.11820E+00	.13188E+00
1.35	.60726E-01	.66378E-01	.73046E-01	.80534E-01	.88818E-01	.97874E-01	.10797E+00	.11924E+00	.13194E+00	.14627E+00	.16230E+00
1.40	.76541E-01	.83380E-01	.91479E-01	.10059E+00	.11068E+00	.12179E+00	.13415E+00	.14791E+00	.16329E+00	.18063E+00	.20006E+00
1.45	.95903E-01	.10428E+00	.11392E+00	.12481E+00	.13690E+00	.15031E+00	.16536E+00	.18210E+00	.20127E+00	.22288E+00	.24755E+00
1.50	.11765E+00	.12758E+00	.13901E+00	.15190E+00	.16635E+00	.18251E+00	.20052E+00	.22072E+00	.24383E+00	.27030E+00	.30101E+00
1.55	.14120E+00	.15284E+00	.16620E+00	.18151E+00	.19870E+00	.21795E+00	.23923E+00	.26303E+00	.28982E+00	.32079E+00	.35769E+00
1.60	.16739E+00	.18100E+00	.19655E+00	.21449E+00	.23494E+00	.25785E+00	.28335E+00	.31172E+00	.34378E+00	.38112E+00	.42668E+00
1.65	.19813E+00	.21395E+00	.23218E+00	.25314E+00	.27730E+00	.30479E+00	.33542E+00	.36997E+00	.40911E+00	.45462E+00	.50945E+00
1.70	.23454E+00	.25330E+00	.27457E+00	.29923E+00	.32795E+00	.36080E+00	.39780E+00	.43948E+00	.48722E+00	.54395E+00	.61559E+00
1.75	.27728E+00	.29806E+00	.32180E+00	.35054E+00	.38477E+00	.42431E+00	.46799E+00	.51636E+00	.57167E+00	.64009E+00	.73419E+00
1.80	.32436E+00	.34894E+00	.37697E+00	.41058E+00	.45091E+00	.49778E+00	.55042E+00	.61005E+00	.68084E+00	.77182E+00	.90026E+00
1.85	.37699E+00	.40648E+00	.44034E+00	.48018E+00	.52601E+00	.57877E+00	.63997E+00	.71302E+00	.80422E+00	.92673E+00	
1.90	.43617E+00	.47078E+00	.51109E+00	.55774E+00	.61192E+00	.67572E+00	.75368E+00	.85172E+00			
1.95	.50116E+00	.54155E+00	.58881E+00	.64384E+00	.70897E+00	.78996E+00	.89376E+00				
2.00	.58158E+00	.62796E+00	.68281E+00	.74811E+00	.82823E+00						
2.05	.67397E+00	.72845E+00	.79181E+00								
2.10	.76967E+00	.83239E+00									

TABLE 17. Superfluid density (g cm^{-3})

Temp. (K)	Pressure (atm)										
	.00	2.50	5.00	7.50	10.00	12.50	15.00	17.50	20.00	22.50	25.00
.10	.14513E+00	.14925E+00	.15284E+00	.15603E+00	.15892E+00	.16157E+00	.16403E+00	.16633E+00	.16849E+00	.17053E+00	.17246E+00
.15	.14513E+00	.14925E+00	.15284E+00	.15603E+00	.15892E+00	.16157E+00	.16403E+00	.16633E+00	.16849E+00	.17053E+00	.17246E+00
.20	.14513E+00	.14925E+00	.15284E+00	.15603E+00	.15892E+00	.16157E+00	.16403E+00	.16633E+00	.16849E+00	.17053E+00	.17246E+00
.25	.14513E+00	.14925E+00	.15283E+00	.15603E+00	.15892E+00	.16157E+00	.16403E+00	.16633E+00	.16849E+00	.17053E+00	.17246E+00
.30	.14513E+00	.14925E+00	.15283E+00	.15602E+00	.15892E+00	.16157E+00	.16403E+00	.16633E+00	.16849E+00	.17053E+00	.17246E+00
.35	.14513E+00	.14925E+00	.15283E+00	.15602E+00	.15891E+00	.16157E+00	.16403E+00	.16632E+00	.16848E+00	.17052E+00	.17246E+00
.40	.14513E+00	.14925E+00	.15283E+00	.15602E+00	.15891E+00	.16157E+00	.16403E+00	.16632E+00	.16848E+00	.17052E+00	.17246E+00
.45	.14513E+00	.14925E+00	.15283E+00	.15602E+00	.15891E+00	.16156E+00	.16402E+00	.16632E+00	.16848E+00	.17052E+00	.17246E+00
.50	.14512E+00	.14924E+00	.15282E+00	.15602E+00	.15891E+00	.16156E+00	.16402E+00	.16632E+00	.16848E+00	.17052E+00	.17245E+00
.55	.14512E+00	.14924E+00	.15282E+00	.15601E+00	.15890E+00	.16156E+00	.16402E+00	.16631E+00	.16847E+00	.17051E+00	.17244E+00
.60	.14512E+00	.14923E+00	.15281E+00	.15600E+00	.15889E+00	.16154E+00	.16400E+00	.16630E+00	.16845E+00	.17048E+00	.17241E+00
.65	.14511E+00	.14922E+00	.15280E+00	.15599E+00	.15887E+00	.16152E+00	.16397E+00	.16626E+00	.16841E+00	.17043E+00	.17235E+00
.70	.14509E+00	.14920E+00	.15277E+00	.15595E+00	.15883E+00	.16147E+00	.16391E+00	.16619E+00	.16832E+00	.17033E+00	.17223E+00
.75	.14505E+00	.14916E+00	.15272E+00	.15589E+00	.15875E+00	.16137E+00	.16380E+00	.16606E+00	.16817E+00	.17015E+00	.17201E+00
.80	.14499E+00	.14909E+00	.15263E+00	.15578E+00	.15862E+00	.16122E+00	.16361E+00	.16584E+00	.16791E+00	.16985E+00	.17166E+00
.85	.14489E+00	.14897E+00	.15249E+00	.15560E+00	.15841E+00	.16096E+00	.16332E+00	.16550E+00	.16752E+00	.16940E+00	.17114E+00
.90	.14473E+00	.14878E+00	.15226E+00	.15533E+00	.15809E+00	.16059E+00	.16289E+00	.16500E+00	.16695E+00	.16874E+00	.17039E+00
.95	.14449E+00	.14851E+00	.15194E+00	.15494E+00	.15763E+00	.16006E+00	.16228E+00	.16431E+00	.16617E+00	.16785E+00	.16937E+00
1.00	.14415E+00	.14811E+00	.15148E+00	.15441E+00	.15701E+00	.15935E+00	.16147E+00	.16339E+00	.16512E+00	.16666E+00	.16803E+00
1.05	.14366E+00	.14756E+00	.15085E+00	.15368E+00	.15618E+00	.15841E+00	.16041E+00	.16220E+00	.16377E+00	.16516E+00	.16633E+00
1.10	.14300E+00	.14682E+00	.15002E+00	.15275E+00	.15513E+00	.15722E+00	.15907E+00	.16069E+00	.16209E+00	.16327E+00	.16422E+00
1.15	.14214E+00	.14587E+00	.14897E+00	.15158E+00	.15382E+00	.15575E+00	.15741E+00	.15883E+00	.16001E+00	.16096E+00	.16163E+00
1.20	.14107E+00	.14468E+00	.14765E+00	.15012E+00	.15220E+00	.15394E+00	.15540E+00	.15658E+00	.15750E+00	.15814E+00	.15847E+00
1.25	.13975E+00	.14321E+00	.14601E+00	.14833E+00	.15025E+00	.15183E+00	.15308E+00	.15400E+00	.15458E+00	.15486E+00	.15486E+00
1.30	.13817E+00	.14148E+00	.14412E+00	.14624E+00	.14792E+00	.14922E+00	.15017E+00	.15077E+00	.15101E+00	.15086E+00	.15025E+00
1.35	.13632E+00	.13940E+00	.14180E+00	.14367E+00	.14508E+00	.14611E+00	.14673E+00	.14697E+00	.14679E+00	.14616E+00	.14509E+00
1.40	.13403E+00	.13689E+00	.13902E+00	.14058E+00	.14167E+00	.14231E+00	.14252E+00	.14229E+00	.14159E+00	.14039E+00	.13868E+00
1.45	.13123E+00	.13379E+00	.13563E+00	.13686E+00	.13757E+00	.13778E+00	.13748E+00	.13669E+00	.13528E+00	.13328E+00	.13057E+00
1.50	.12809E+00	.13035E+00	.13184E+00	.13269E+00	.13296E+00	.13266E+00	.13180E+00	.13035E+00	.12821E+00	.12529E+00	.12144E+00
1.55	.12469E+00	.12661E+00	.12774E+00	.12814E+00	.12789E+00	.12701E+00	.12554E+00	.12341E+00	.12055E+00	.11676E+00	.11174E+00
1.60	.12090E+00	.12244E+00	.12315E+00	.12306E+00	.12221E+00	.12065E+00	.11839E+00	.11540E+00	.11154E+00	.10655E+00	.99891E-01
1.65	.11646E+00	.11756E+00	.11776E+00	.11710E+00	.11556E+00	.11315E+00	.10993E+00	.10578E+00	.10059E+00	.94047E-01	.85620E-01
1.70	.11120E+00	.11173E+00	.11134E+00	.10997E+00	.10758E+00	.10417E+00	.99757E-01	.94261E-01	.87445E-01	.78789E-01	.67228E-01
1.75	.10502E+00	.10509E+00	.10417E+00	.10203E+00	.98607E-01	.93958E-01	.88278E-01	.81483E-01	.73189E-01	.62313E-01	.46593E-01
1.80	.98205E-01	.97531E-01	.95785E-01	.92706E-01	.88137E-01	.82107E-01	.74742E-01	.65837E-01	.54659E-01	.39602E-01	.17528E-01
1.85	.90588E-01	.88974E-01	.86133E-01	.81871E-01	.76209E-01	.69000E-01	.59985E-01	.48568E-01	.33617E-01	.12751E-01	
1.90	.82016E-01	.79401E-01	.75336E-01	.69766E-01	.62516E-01	.53236E-01	.41142E-01	.25164E-01			
1.95	.72596E-01	.68847E-01	.63448E-01	.56286E-01	.46985E-01	.34569E-01	.17795E-01				
2.00	.60925E-01	.55930E-01	.49022E-01	.39891E-01	.27802E-01						
2.05	.47502E-01	.40873E-01	.32235E-01								
2.10	.33582E-01	.25265E-01									

TABLE 18. Superfluid ratio

Temp. (K)	Pressure (atm)										
	.00	2.50	5.00	7.50	10.00	12.50	15.00	17.50	20.00	22.50	25.00
.10	.10000E+01	.10000E+01	.10000E+01	.10000E+01	.10000E+01	.10000E+01	.10000E+01	.10000E+01	.10000E+01	.10000E+01	.10000E+01
.15	.10000E+01	.10000E+01	.10000E+01	.10000E+01	.10000E+01	.10000E+01	.10000E+01	.10000E+01	.10000E+01	.10000E+01	.10000E+01
.20	.10000E+01	.10000E+01	.10000E+01	.10000E+01	.10000E+01	.10000E+01	.10000E+01	.10000E+01	.10000E+01	.10000E+01	.10000E+01
.25	.10000E+01	.10000E+01	.10000E+01	.10000E+01	.10000E+01	.10000E+01	.10000E+01	.10000E+01	.10000E+01	.10000E+01	.10000E+01
.30	.10000E+01	.10000E+01	.10000E+01	.10000E+01	.10000E+01	.10000E+01	.10000E+01	.10000E+01	.10000E+01	.10000E+01	.10000E+01
.35	.10000E+01	.10000E+01	.10000E+01	.10000E+01	.10000E+01	.10000E+01	.10000E+01	.10000E+01	.10000E+01	.10000E+01	.10000E+01
.40	.10000E+01	.10000E+01	.10000E+01	.10000E+01	.10000E+01	.10000E+01	.10000E+01	.10000E+01	.10000E+01	.10000E+01	.10000E+01
.45	.10000E+01	.10000E+01	.10000E+01	.10000E+01	.10000E+01	.10000E+01	.10000E+01	.10000E+01	.10000E+01	.10000E+01	.99999E+00
.50	.99999E+00	.99999E+00	.99999E+00	.99999E+00	.99999E+00	.99999E+00	.99999E+00	.99999E+00	.99998E+00	.99998E+00	.99997E+00
.55	.99998E+00	.99998E+00	.99998E+00	.99998E+00	.99997E+00	.99997E+00	.99996E+00	.99995E+00	.99994E+00	.99992E+00	.99990E+00
.60	.99996E+00	.99996E+00	.99995E+00	.99994E+00	.99992E+00	.99990E+00	.99988E+00	.99985E+00	.99982E+00	.99978E+00	.99972E+00
.65	.99991E+00	.99990E+00	.99987E+00	.99984E+00	.99980E+00	.99975E+00	.99969E+00	.99963E+00	.99955E+00	.99945E+00	.99933E+00
.70	.99980E+00	.99977E+00	.99971E+00	.99962E+00	.99953E+00	.99942E+00	.99931E+00	.99917E+00	.99901E+00	.99881E+00	.99858E+00
.75	.99958E+00	.99951E+00	.99938E+00	.99922E+00	.99903E+00	.99882E+00	.99860E+00	.99835E+00	.99805E+00	.99769E+00	.99727E+00
.80	.99917E+00	.99904E+00	.99880E+00	.99850E+00	.99817E+00	.99781E+00	.99742E+00	.99698E+00	.99647E+00	.99587E+00	.99517E+00
.85	.99849E+00	.99825E+00	.99785E+00	.99735E+00	.99679E+00	.99620E+00	.99557E+00	.99487E+00	.99406E+00	.99312E+00	.99201E+00
.90	.99741E+00	.99702E+00	.99637E+00	.99559E+00	.99473E+00	.99382E+00	.99286E+00	.99180E+00	.99058E+00	.98917E+00	.98753E+00
.95	.99577E+00	.99517E+00	.99421E+00	.99305E+00	.99179E+00	.99047E+00	.98906E+00	.98751E+00	.98577E+00	.98375E+00	.98146E+00
1.00	.99339E+00	.99252E+00	.99116E+00	.98954E+00	.98777E+00	.98592E+00	.98395E+00	.98180E+00	.97938E+00	.97662E+00	.97349E+00
1.05	.99003E+00	.98880E+00	.98698E+00	.98482E+00	.98248E+00	.97996E+00	.97730E+00	.97444E+00	.97117E+00	.96753E+00	.96339E+00
1.10	.98550E+00	.98381E+00	.98147E+00	.97872E+00	.97568E+00	.97242E+00	.96894E+00	.96513E+00	.96092E+00	.95618E+00	.95084E+00
1.15	.97955E+00	.97738E+00	.97450E+00	.97109E+00	.96725E+00	.96308E+00	.95858E+00	.95369E+00	.94829E+00	.94229E+00	.93548E+00
1.20	.97215E+00	.96934E+00	.96577E+00	.96158E+00	.95685E+00	.95165E+00	.94603E+00	.93982E+00	.93301E+00	.92540E+00	.91672E+00
1.25	.96306E+00	.95940E+00	.95491E+00	.94986E+00	.94433E+00	.93827E+00	.93152E+00	.92390E+00	.91528E+00	.90570E+00	.89538E+00
1.30	.95208E+00	.94765E+00	.94235E+00	.93623E+00	.92938E+00	.92177E+00	.91338E+00	.90409E+00	.89365E+00	.88180E+00	.86812E+00
1.35	.93927E+00	.93362E+00	.92695E+00	.91947E+00	.91118E+00	.90213E+00	.89203E+00	.88076E+00	.86806E+00	.85373E+00	.83770E+00
1.40	.92346E+00	.91662E+00	.90852E+00	.89941E+00	.88932E+00	.87821E+00	.86585E+00	.85209E+00	.83671E+00	.81937E+00	.79994E+00
1.45	.90410E+00	.89572E+00	.88608E+00	.87519E+00	.86310E+00	.84969E+00	.83464E+00	.81790E+00	.79873E+00	.77712E+00	.75245E+00
1.50	.88235E+00	.87242E+00	.86099E+00	.84810E+00	.83365E+00	.81749E+00	.79948E+00	.77928E+00	.75617E+00	.72970E+00	.69899E+00
1.55	.85880E+00	.84716E+00	.83380E+00	.81849E+00	.80130E+00	.78205E+00	.76077E+00	.73697E+00	.71018E+00	.67921E+00	.64231E+00
1.60	.83261E+00	.81900E+00	.80345E+00	.78551E+00	.76506E+00	.74215E+00	.71665E+00	.68828E+00	.65622E+00	.61888E+00	.57332E+00
1.65	.80187E+00	.78605E+00	.76782E+00	.74686E+00	.72270E+00	.69521E+00	.66458E+00	.63003E+00	.59089E+00	.54538E+00	.49055E+00
1.70	.76546E+00	.74670E+00	.72543E+00	.70077E+00	.67205E+00	.63920E+00	.60220E+00	.56052E+00	.51278E+00	.45605E+00	.38441E+00
1.75	.72272E+00	.70194E+00	.67820E+00	.64946E+00	.61523E+00	.57569E+00	.53201E+00	.48364E+00	.42833E+00	.35991E+00	.26581E+00
1.80	.67564E+00	.65106E+00	.62303E+00	.58942E+00	.54909E+00	.50222E+00	.44958E+00	.38995E+00	.31916E+00	.22818E+00	.99739E-01
1.85	.62301E+00	.59352E+00	.55966E+00	.51982E+00	.47399E+00	.42123E+00	.36003E+00	.28698E+00	.19578E+00	.73265E-01	
1.90	.56383E+00	.52922E+00	.48891E+00	.44226E+00	.38808E+00	.32428E+00	.24632E+00	.14828E+00			
1.95	.49884E+00	.45845E+00	.41119E+00	.35616E+00	.29103E+00	.21004E+00	.10624E+00				
2.00	.41842E+00	.37204E+00	.31719E+00	.25189E+00	.17177E+00						
2.05	.32603E+00	.27155E+00	.20819E+00								
2.10	.23033E+00	.16761E+00									

TABLE 19. Velocity of second sound (m s^{-1})

Temp. (K)	Pressure (atm)										
	.00	2.50	5.00	7.50	10.00	12.50	15.00	17.50	20.00	22.50	25.00
.10	.13824E+03	.14903E+03	.15845E+03	.16693E+03	.17463E+03	.18168E+03	.18821E+03	.19429E+03	.19998E+03	.20534E+03	.21041E+03
.15	.13903E+03	.14936E+03	.15865E+03	.16700E+03	.17466E+03	.18174E+03	.18832E+03	.19450E+03	.20034E+03	.20589E+03	.21119E+03
.20	.13985E+03	.14980E+03	.15877E+03	.16695E+03	.17448E+03	.18146E+03	.18797E+03	.19408E+03	.19984E+03	.20530E+03	.21050E+03
.25	.14077E+03	.15024E+03	.15890E+03	.16688E+03	.17427E+03	.18114E+03	.18758E+03	.19362E+03	.19934E+03	.20476E+03	.20991E+03
.30	.14171E+03	.15067E+03	.15899E+03	.16673E+03	.17393E+03	.18064E+03	.18689E+03	.19270E+03	.19804E+03	.20284E+03	.20692E+03
.35	.14259E+03	.15098E+03	.15882E+03	.16601E+03	.17246E+03	.17801E+03	.18245E+03	.18538E+03	.18628E+03	.18435E+03	.17863E+03
.40	.14296E+03	.15030E+03	.15650E+03	.16092E+03	.16291E+03	.16179E+03	.15746E+03	.14946E+03	.13817E+03	.12410E+03	.10867E+03
.45	.14074E+03	.14484E+03	.14519E+03	.14070E+03	.13179E+03	.11982E+03	.10659E+03	.93018E+02	.79840E+02	.67614E+02	.56589E+02
.50	.13093E+03	.12776E+03	.11801E+03	.10403E+03	.89188E+02	.75449E+02	.63712E+02	.53606E+02	.44868E+02	.37413E+02	.31069E+02
.55	.11028E+03	.99793E+02	.84701E+02	.69596E+02	.56929E+02	.46796E+02	.38917E+02	.32509E+02	.27271E+02	.22983E+02	.19415E+02
.60	.84688E+02	.72151E+02	.58286E+02	.46462E+02	.37493E+02	.30805E+02	.25783E+02	.21869E+02	.18755E+02	.16256E+02	.14268E+02
.65	.62548E+02	.51687E+02	.41006E+02	.32634E+02	.26568E+02	.22213E+02	.19041E+02	.16608E+02	.14723E+02	.13248E+02	.12071E+02
.70	.46564E+02	.38141E+02	.30434E+02	.24637E+02	.20586E+02	.17708E+02	.15663E+02	.14108E+02	.12923E+02	.11970E+02	.11233E+02
.75	.35867E+02	.29636E+02	.24126E+02	.20107E+02	.17353E+02	.15413E+02	.14026E+02	.12987E+02	.12181E+02	.11545E+02	.11050E+02
.80	.28910E+02	.24385E+02	.20442E+02	.17614E+02	.15663E+02	.14308E+02	.13328E+02	.12599E+02	.12013E+02	.11567E+02	.11198E+02
.85	.24600E+02	.21183E+02	.18317E+02	.16281E+02	.14860E+02	.13867E+02	.13146E+02	.12596E+02	.12163E+02	.11813E+02	.11527E+02
.90	.21815E+02	.19251E+02	.17149E+02	.15636E+02	.14577E+02	.13819E+02	.13253E+02	.12810E+02	.12475E+02	.12185E+02	.11975E+02
.95	.20068E+02	.18136E+02	.16566E+02	.15413E+02	.14589E+02	.13996E+02	.13531E+02	.13171E+02	.12882E+02	.12648E+02	.12460E+02
1.00	.18616E+02	.17136E+02	.16024E+02	.15214E+02	.14608E+02	.14137E+02	.13763E+02	.13462E+02	.13214E+02	.13017E+02	.12847E+02
1.05	.18105E+02	.16934E+02	.16091E+02	.15469E+02	.14974E+02	.14572E+02	.14236E+02	.13953E+02	.13729E+02	.13539E+02	.13365E+02
1.10	.17954E+02	.16984E+02	.16309E+02	.15805E+02	.15390E+02	.15031E+02	.14724E+02	.14450E+02	.14225E+02	.14026E+02	.13832E+02
1.15	.18050E+02	.17185E+02	.16580E+02	.16149E+02	.15817E+02	.15530E+02	.15260E+02	.14989E+02	.14739E+02	.14506E+02	.14319E+02
1.20	.18273E+02	.17506E+02	.16966E+02	.16563E+02	.16247E+02	.15965E+02	.15695E+02	.15437E+02	.15174E+02	.14917E+02	.14668E+02
1.25	.18609E+02	.17880E+02	.17349E+02	.16938E+02	.16597E+02	.16302E+02	.16023E+02	.15762E+02	.15503E+02	.15234E+02	.14954E+02
1.30	.18884E+02	.18189E+02	.17645E+02	.17216E+02	.16863E+02	.16556E+02	.16260E+02	.15981E+02	.15706E+02	.15429E+02	.15162E+02
1.35	.19022E+02	.18371E+02	.17860E+02	.17428E+02	.17050E+02	.16703E+02	.16372E+02	.16063E+02	.15748E+02	.15432E+02	.15089E+02
1.40	.19215E+02	.18583E+02	.18079E+02	.17649E+02	.17262E+02	.16895E+02	.16541E+02	.16190E+02	.15819E+02	.15436E+02	.15025E+02
1.45	.19560E+02	.18954E+02	.18455E+02	.17998E+02	.17569E+02	.17151E+02	.16757E+02	.16365E+02	.15967E+02	.15532E+02	.15021E+02
1.50	.19997E+02	.19377E+02	.18855E+02	.18359E+02	.17874E+02	.17402E+02	.16949E+02	.16501E+02	.16043E+02	.15532E+02	.14909E+02
1.55	.20318E+02	.19683E+02	.19120E+02	.18582E+02	.18040E+02	.17496E+02	.16965E+02	.16426E+02	.15882E+02	.15280E+02	.14572E+02
1.60	.20361E+02	.19694E+02	.19100E+02	.18525E+02	.17931E+02	.17321E+02	.16706E+02	.16077E+02	.15421E+02	.14688E+02	.13808E+02
1.65	.20157E+02	.19511E+02	.18927E+02	.18317E+02	.17655E+02	.16964E+02	.16274E+02	.15573E+02	.14818E+02	.13926E+02	.12781E+02
1.70	.19912E+02	.19244E+02	.18623E+02	.17960E+02	.17231E+02	.16455E+02	.15664E+02	.14833E+02	.13894E+02	.12740E+02	.11214E+02
1.75	.19670E+02	.18919E+02	.18205E+02	.17464E+02	.16690E+02	.15860E+02	.14957E+02	.13946E+02	.12753E+02	.11245E+02	.91909E+01
1.80	.19365E+02	.18527E+02	.17690E+02	.16854E+02	.15981E+02	.15012E+02	.13874E+02	.12523E+02	.10868E+02	.87391E+01	.54691E+01
1.85	.18964E+02	.18007E+02	.17035E+02	.16059E+02	.15027E+02	.13823E+02	.12348E+02	.10535E+02	.82274E+01	.47375E+01	
1.90	.18188E+02	.17168E+02	.16094E+02	.14953E+02	.13663E+02	.12079E+02	.10065E+02	.73777E+01			
1.95	.17115E+02	.16005E+02	.14817E+02	.13469E+02	.11807E+02	.96227E+01	.64804E+01				
2.00	.15814E+02	.14546E+02	.13160E+02	.11447E+02	.91281E+01						
2.05	.14131E+02	.12535E+02	.10760E+02								
2.10	.12024E+02	.99886E+01									

TABLE 20. Velocity of fourth sound (m s^{-1})

Temp. (K)	Pressure (atm)										
	.00	2.50	5.00	7.50	10.00	12.50	15.00	17.50	20.00	22.50	25.00
.10	.23821E+03	.25746E+03	.27422E+03	.28916E+03	.30271E+03	.31515E+03	.32669E+03	.33747E+03	.34760E+03	.35718E+03	.36627E+03
.15	.23821E+03	.25746E+03	.27422E+03	.28916E+03	.30271E+03	.31515E+03	.32669E+03	.33747E+03	.34760E+03	.35718E+03	.36627E+03
.20	.23821E+03	.25746E+03	.27422E+03	.28916E+03	.30271E+03	.31515E+03	.32669E+03	.33747E+03	.34760E+03	.35718E+03	.36627E+03
.25	.23821E+03	.25746E+03	.27422E+03	.28916E+03	.30271E+03	.31515E+03	.32669E+03	.33747E+03	.34760E+03	.35718E+03	.36627E+03
.30	.23821E+03	.25746E+03	.27422E+03	.28916E+03	.30271E+03	.31515E+03	.32669E+03	.33747E+03	.34760E+03	.35718E+03	.36627E+03
.35	.23821E+03	.25746E+03	.27422E+03	.28916E+03	.30271E+03	.31515E+03	.32669E+03	.33747E+03	.34760E+03	.35718E+03	.36627E+03
.40	.23821E+03	.25746E+03	.27422E+03	.28916E+03	.30271E+03	.31515E+03	.32669E+03	.33747E+03	.34760E+03	.35718E+03	.36627E+03
.45	.23820E+03	.25746E+03	.27422E+03	.28916E+03	.30271E+03	.31515E+03	.32669E+03	.33746E+03	.34760E+03	.35717E+03	.36627E+03
.50	.23820E+03	.25745E+03	.27421E+03	.28916E+03	.30271E+03	.31515E+03	.32668E+03	.33746E+03	.34759E+03	.35717E+03	.36626E+03
.55	.23820E+03	.25745E+03	.27421E+03	.28915E+03	.30270E+03	.31514E+03	.32667E+03	.33745E+03	.34758E+03	.35716E+03	.36625E+03
.60	.23819E+03	.25744E+03	.27420E+03	.28914E+03	.30269E+03	.31512E+03	.32666E+03	.33743E+03	.34756E+03	.35712E+03	.36621E+03
.65	.23817E+03	.25742E+03	.27418E+03	.28911E+03	.30266E+03	.31509E+03	.32662E+03	.33738E+03	.34750E+03	.35706E+03	.36613E+03
.70	.23814E+03	.25738E+03	.27414E+03	.28907E+03	.30261E+03	.31503E+03	.32655E+03	.33730E+03	.34740E+03	.35694E+03	.36598E+03
.75	.23809E+03	.25733E+03	.27407E+03	.28899E+03	.30252E+03	.31493E+03	.32642E+03	.33715E+03	.34722E+03	.35673E+03	.36573E+03
.80	.23801E+03	.25723E+03	.27397E+03	.28888E+03	.30238E+03	.31476E+03	.32622E+03	.33690E+03	.34693E+03	.35639E+03	.36534E+03
.85	.23787E+03	.25708E+03	.27381E+03	.28869E+03	.30216E+03	.31450E+03	.32591E+03	.33653E+03	.34650E+03	.35588E+03	.36473E+03
.90	.23766E+03	.25687E+03	.27357E+03	.28843E+03	.30185E+03	.31413E+03	.32545E+03	.33599E+03	.34587E+03	.35516E+03	.36387E+03
.95	.23735E+03	.25657E+03	.27324E+03	.28805E+03	.30140E+03	.31360E+03	.32483E+03	.33524E+03	.34501E+03	.35417E+03	.36271E+03
1.00	.23695E+03	.25613E+03	.27277E+03	.28752E+03	.30080E+03	.31289E+03	.32398E+03	.33424E+03	.34384E+03	.35285E+03	.36123E+03
1.05	.23639E+03	.25554E+03	.27214E+03	.28682E+03	.30000E+03	.31196E+03	.32288E+03	.33296E+03	.34238E+03	.35118E+03	.35925E+03
1.10	.23571E+03	.25476E+03	.27129E+03	.28589E+03	.29895E+03	.31077E+03	.32150E+03	.33132E+03	.34056E+03	.34916E+03	.35673E+03
1.15	.23478E+03	.25381E+03	.27023E+03	.28471E+03	.29765E+03	.30928E+03	.31978E+03	.32935E+03	.33827E+03	.34655E+03	.35381E+03
1.20	.23376E+03	.25259E+03	.26888E+03	.28322E+03	.29599E+03	.30743E+03	.31768E+03	.32693E+03	.33555E+03	.34349E+03	.35004E+03
1.25	.23244E+03	.25117E+03	.26725E+03	.28136E+03	.29393E+03	.30514E+03	.31513E+03	.32412E+03	.33234E+03	.33975E+03	.34581E+03
1.30	.23092E+03	.24942E+03	.26534E+03	.27926E+03	.29153E+03	.30238E+03	.31191E+03	.32041E+03	.32829E+03	.33537E+03	.34102E+03
1.35	.22919E+03	.24742E+03	.26300E+03	.27658E+03	.28852E+03	.29900E+03	.30813E+03	.31611E+03	.32333E+03	.32966E+03	.33403E+03
1.40	.22692E+03	.24497E+03	.26025E+03	.27347E+03	.28495E+03	.29489E+03	.30341E+03	.31070E+03	.31727E+03	.32296E+03	.32664E+03
1.45	.22433E+03	.24191E+03	.25679E+03	.26957E+03	.28057E+03	.28996E+03	.29783E+03	.30438E+03	.31003E+03	.31456E+03	.31670E+03
1.50	.22138E+03	.23850E+03	.25293E+03	.26523E+03	.27562E+03	.28427E+03	.29129E+03	.29682E+03	.30166E+03	.30526E+03	.30534E+03
1.55	.21818E+03	.23470E+03	.24862E+03	.26032E+03	.27005E+03	.27792E+03	.28400E+03	.28831E+03	.29178E+03	.29390E+03	.29177E+03
1.60	.21472E+03	.23037E+03	.24368E+03	.25477E+03	.26369E+03	.27061E+03	.27548E+03	.27831E+03	.28020E+03	.28033E+03	.27470E+03
1.65	.21037E+03	.22539E+03	.23779E+03	.24798E+03	.25601E+03	.26179E+03	.26527E+03	.26624E+03	.26570E+03	.26275E+03	.25174E+03
1.70	.20520E+03	.21925E+03	.23069E+03	.23978E+03	.24654E+03	.25084E+03	.25235E+03	.25085E+03	.24742E+03	.24040E+03	.22284E+03
1.75	.19923E+03	.21204E+03	.22234E+03	.23020E+03	.23557E+03	.23796E+03	.23698E+03	.23225E+03	.22499E+03	.21241E+03	.18340E+03
1.80	.19265E+03	.20367E+03	.21233E+03	.21852E+03	.22208E+03	.22231E+03	.21811E+03	.20852E+03	.19419E+03	.16904E+03	.11055E+03
1.85	.18482E+03	.19408E+03	.20069E+03	.20443E+03	.20538E+03	.20274E+03	.19455E+03	.17799E+03	.15145E+03	.95511E+02	
1.90	.17570E+03	.18254E+03	.18695E+03	.18810E+03	.18540E+03	.17753E+03	.16077E+03	.12785E+03			
1.95	.16433E+03	.16940E+03	.17093E+03	.16815E+03	.15993E+03	.14252E+03	.10545E+03				
2.00	.15030E+03	.15150E+03	.14941E+03	.14087E+03	.12235E+03						
2.05	.13180E+03	.12902E+03	.12037E+03								
2.10	.11065E+03	.10084E+03									

TABLE 21. Energy of maxon peak (K)

Temp. (K)	Pressure (atm)										
	.00	2.50	5.00	7.50	10.00	12.50	15.00	17.50	20.00	22.50	25.00
.10	.13816E+02	.14197E+02	.14438E+02	.14592E+02	.14691E+02	.14752E+02	.14789E+02	.14809E+02	.14819E+02	.14822E+02	.14822E+02
.15	.13816E+02	.14197E+02	.14438E+02	.14592E+02	.14691E+02	.14752E+02	.14789E+02	.14809E+02	.14819E+02	.14822E+02	.14822E+02
.20	.13816E+02	.14197E+02	.14438E+02	.14592E+02	.14691E+02	.14752E+02	.14789E+02	.14809E+02	.14819E+02	.14822E+02	.14822E+02
.25	.13816E+02	.14197E+02	.14438E+02	.14592E+02	.14691E+02	.14752E+02	.14789E+02	.14809E+02	.14819E+02	.14822E+02	.14822E+02
.30	.13816E+02	.14197E+02	.14438E+02	.14592E+02	.14691E+02	.14752E+02	.14789E+02	.14809E+02	.14819E+02	.14822E+02	.14822E+02
.35	.13816E+02	.14197E+02	.14438E+02	.14592E+02	.14691E+02	.14752E+02	.14789E+02	.14809E+02	.14819E+02	.14822E+02	.14822E+02
.40	.13816E+02	.14197E+02	.14438E+02	.14592E+02	.14691E+02	.14752E+02	.14789E+02	.14809E+02	.14819E+02	.14822E+02	.14822E+02
.45	.13816E+02	.14197E+02	.14438E+02	.14592E+02	.14691E+02	.14752E+02	.14789E+02	.14809E+02	.14819E+02	.14822E+02	.14822E+02
.50	.13816E+02	.14197E+02	.14438E+02	.14592E+02	.14691E+02	.14752E+02	.14789E+02	.14809E+02	.14819E+02	.14822E+02	.14822E+02
.55	.13816E+02	.14197E+02	.14438E+02	.14592E+02	.14691E+02	.14752E+02	.14789E+02	.14809E+02	.14819E+02	.14822E+02	.14822E+02
.60	.13816E+02	.14197E+02	.14437E+02	.14592E+02	.14690E+02	.14752E+02	.14789E+02	.14809E+02	.14819E+02	.14822E+02	.14821E+02
.65	.13816E+02	.14196E+02	.14437E+02	.14592E+02	.14690E+02	.14752E+02	.14789E+02	.14809E+02	.14818E+02	.14822E+02	.14821E+02
.70	.13815E+02	.14196E+02	.14437E+02	.14592E+02	.14690E+02	.14752E+02	.14788E+02	.14809E+02	.14818E+02	.14821E+02	.14821E+02
.75	.13815E+02	.14196E+02	.14437E+02	.14591E+02	.14690E+02	.14751E+02	.14788E+02	.14808E+02	.14818E+02	.14821E+02	.14821E+02
.80	.13815E+02	.14195E+02	.14436E+02	.14591E+02	.14689E+02	.14751E+02	.14787E+02	.14808E+02	.14817E+02	.14821E+02	.14820E+02
.85	.13814E+02	.14195E+02	.14436E+02	.14590E+02	.14689E+02	.14750E+02	.14787E+02	.14807E+02	.14817E+02	.14820E+02	.14820E+02
.90	.13813E+02	.14194E+02	.14434E+02	.14589E+02	.14687E+02	.14749E+02	.14786E+02	.14806E+02	.14816E+02	.14819E+02	.14818E+02
.95	.13812E+02	.14192E+02	.14433E+02	.14587E+02	.14686E+02	.14748E+02	.14784E+02	.14804E+02	.14814E+02	.14817E+02	.14817E+02
1.00	.13810E+02	.14190E+02	.14431E+02	.14585E+02	.14684E+02	.14745E+02	.14782E+02	.14802E+02	.14812E+02	.14815E+02	.14815E+02
1.05	.13807E+02	.14188E+02	.14428E+02	.14583E+02	.14681E+02	.14743E+02	.14779E+02	.14800E+02	.14809E+02	.14812E+02	.14812E+02
1.10	.13804E+02	.14184E+02	.14425E+02	.14579E+02	.14678E+02	.14739E+02	.14776E+02	.14796E+02	.14806E+02	.14809E+02	.14809E+02
1.15	.13799E+02	.14180E+02	.14420E+02	.14575E+02	.14673E+02	.14734E+02	.14771E+02	.14791E+02	.14801E+02	.14804E+02	.14804E+02
1.20	.13794E+02	.14174E+02	.14414E+02	.14568E+02	.14667E+02	.14728E+02	.14765E+02	.14785E+02	.14795E+02	.14798E+02	.14798E+02
1.25	.13786E+02	.14166E+02	.14406E+02	.14561E+02	.14659E+02	.14720E+02	.14757E+02	.14777E+02	.14787E+02	.14790E+02	.14790E+02
1.30	.13777E+02	.14156E+02	.14397E+02	.14551E+02	.14649E+02	.14710E+02	.14747E+02	.14767E+02	.14777E+02	.14780E+02	.14780E+02
1.35	.13765E+02	.14144E+02	.14384E+02	.14538E+02	.14636E+02	.14698E+02	.14734E+02	.14754E+02	.14764E+02	.14767E+02	.14767E+02
1.40	.13750E+02	.14129E+02	.14369E+02	.14523E+02	.14621E+02	.14682E+02	.14718E+02	.14739E+02	.14748E+02	.14751E+02	.14751E+02
1.45	.13732E+02	.14110E+02	.14350E+02	.14503E+02	.14601E+02	.14662E+02	.14699E+02	.14719E+02	.14728E+02	.14732E+02	.14731E+02
1.50	.13709E+02	.14087E+02	.14326E+02	.14479E+02	.14577E+02	.14638E+02	.14675E+02	.14695E+02	.14704E+02	.14707E+02	.14707E+02
1.55	.13682E+02	.14059E+02	.14297E+02	.14450E+02	.14548E+02	.14609E+02	.14645E+02	.14665E+02	.14675E+02	.14678E+02	.14678E+02
1.60	.13648E+02	.14024E+02	.14262E+02	.14415E+02	.14512E+02	.14573E+02	.14609E+02	.14629E+02	.14639E+02	.14642E+02	.14642E+02
1.65	.13608E+02	.13983E+02	.14220E+02	.14372E+02	.14469E+02	.14530E+02	.14566E+02	.14586E+02	.14596E+02	.14599E+02	.14599E+02
1.70	.13560E+02	.13933E+02	.14170E+02	.14321E+02	.14418E+02	.14478E+02	.14514E+02	.14534E+02	.14544E+02	.14547E+02	.14547E+02
1.75	.13502E+02	.13874E+02	.14109E+02	.14260E+02	.14357E+02	.14417E+02	.14453E+02	.14473E+02	.14482E+02	.14485E+02	.14485E+02
1.80	.13433E+02	.13804E+02	.14038E+02	.14188E+02	.14284E+02	.14344E+02	.14379E+02	.14399E+02	.14409E+02	.14412E+02	.14411E+02
1.85	.13353E+02	.13721E+02	.13953E+02	.14103E+02	.14198E+02	.14257E+02	.14293E+02	.14313E+02	.14322E+02	.14325E+02	
1.90	.13258E+02	.13623E+02	.13854E+02	.14002E+02	.14097E+02	.14156E+02	.14191E+02	.14211E+02			
1.95	.13146E+02	.13508E+02	.13738E+02	.13885E+02	.13978E+02	.14037E+02	.14072E+02				
2.00	.13016E+02	.13375E+02	.13602E+02	.13748E+02	.13840E+02						
2.05	.12865E+02	.13220E+02	.13444E+02								
2.10	.12691E+02	.13041E+02									

TABLE 22. Thermal roton energy gap (K)

Temp. (K)	Pressure (atm)										
	.00	2.50	5.00	7.50	10.00	12.50	15.00	17.50	20.00	22.50	25.00
.10	.87117E+01	.85726E+01	.83799E+01	.81893E+01	.80193E+01	.78676E+01	.77323E+01	.76020E+01	.74729E+01	.73429E+01	.72102E+01
.15	.87117E+01	.85726E+01	.83799E+01	.81893E+01	.80193E+01	.78676E+01	.77323E+01	.76020E+01	.74729E+01	.73429E+01	.72102E+01
.20	.87117E+01	.85726E+01	.83799E+01	.81893E+01	.80193E+01	.78676E+01	.77323E+01	.76020E+01	.74729E+01	.73429E+01	.72102E+01
.25	.87117E+01	.85726E+01	.83799E+01	.81893E+01	.80193E+01	.78676E+01	.77323E+01	.76020E+01	.74729E+01	.73429E+01	.72102E+01
.30	.87117E+01	.85726E+01	.83799E+01	.81893E+01	.80193E+01	.78676E+01	.77323E+01	.76020E+01	.74729E+01	.73429E+01	.72102E+01
.35	.87117E+01	.85726E+01	.83799E+01	.81893E+01	.80193E+01	.78676E+01	.77323E+01	.76020E+01	.74729E+01	.73429E+01	.72102E+01
.40	.87117E+01	.85726E+01	.83799E+01	.81893E+01	.80193E+01	.78676E+01	.77323E+01	.76020E+01	.74729E+01	.73429E+01	.72102E+01
.45	.87117E+01	.85726E+01	.83799E+01	.81893E+01	.80193E+01	.78676E+01	.77323E+01	.76020E+01	.74729E+01	.73429E+01	.72102E+01
.50	.87117E+01	.85726E+01	.83799E+01	.81893E+01	.80193E+01	.78676E+01	.77323E+01	.76020E+01	.74729E+01	.73429E+01	.72102E+01
.55	.87117E+01	.85725E+01	.83799E+01	.81893E+01	.80193E+01	.78676E+01	.77323E+01	.76020E+01	.74729E+01	.73429E+01	.72101E+01
.60	.87116E+01	.85725E+01	.83799E+01	.81893E+01	.80193E+01	.78676E+01	.77323E+01	.76020E+01	.74729E+01	.73429E+01	.72101E+01
.65	.87114E+01	.85723E+01	.83798E+01	.81892E+01	.80193E+01	.78676E+01	.77323E+01	.76020E+01	.74729E+01	.73428E+01	.72101E+01
.70	.87109E+01	.85718E+01	.83795E+01	.81891E+01	.80192E+01	.78676E+01	.77323E+01	.76019E+01	.74728E+01	.73428E+01	.72100E+01
.75	.87098E+01	.85708E+01	.83789E+01	.81889E+01	.80192E+01	.78676E+01	.77323E+01	.76019E+01	.74727E+01	.73426E+01	.72099E+01
.80	.87077E+01	.85689E+01	.83777E+01	.81884E+01	.80190E+01	.78676E+01	.77322E+01	.76018E+01	.74725E+01	.73424E+01	.72096E+01
.85	.87039E+01	.85653E+01	.83757E+01	.81875E+01	.80188E+01	.78677E+01	.77321E+01	.76016E+01	.74721E+01	.73419E+01	.72091E+01
.90	.86976E+01	.85595E+01	.83722E+01	.81861E+01	.80184E+01	.78677E+01	.77319E+01	.76012E+01	.74715E+01	.73412E+01	.72083E+01
.95	.86877E+01	.85503E+01	.83667E+01	.81838E+01	.80177E+01	.78678E+01	.77316E+01	.76007E+01	.74705E+01	.73400E+01	.72070E+01
1.00	.86729E+01	.85366E+01	.83586E+01	.81804E+01	.80168E+01	.78680E+01	.77312E+01	.75999E+01	.74691E+01	.73382E+01	.72051E+01
1.05	.86494E+01	.85148E+01	.83457E+01	.81751E+01	.80154E+01	.78685E+01	.77308E+01	.75991E+01	.74672E+01	.73361E+01	.72030E+01
1.10	.86218E+01	.84893E+01	.83305E+01	.81686E+01	.80135E+01	.78686E+01	.77298E+01	.75973E+01	.74640E+01	.73321E+01	.71985E+01
1.15	.85950E+01	.84673E+01	.83186E+01	.81647E+01	.80131E+01	.78673E+01	.77284E+01	.75912E+01	.74586E+01	.73243E+01	.71891E+01
1.20	.85738E+01	.84464E+01	.83030E+01	.81557E+01	.80075E+01	.78641E+01	.77232E+01	.75860E+01	.74502E+01	.73123E+01	.71722E+01
1.25	.85557E+01	.84234E+01	.82823E+01	.81392E+01	.80009E+01	.78640E+01	.77262E+01	.75868E+01	.74437E+01	.73020E+01	.71634E+01
1.30	.85370E+01	.84088E+01	.82719E+01	.81310E+01	.79892E+01	.78476E+01	.77065E+01	.75661E+01	.74221E+01	.72771E+01	.71241E+01
1.35	.85255E+01	.83901E+01	.82482E+01	.81056E+01	.79646E+01	.78242E+01	.76835E+01	.75385E+01	.73944E+01	.72441E+01	.70942E+01
1.40	.84966E+01	.83598E+01	.82167E+01	.80719E+01	.79279E+01	.77845E+01	.76391E+01	.74925E+01	.73454E+01	.71929E+01	.70399E+01
1.45	.84504E+01	.83111E+01	.81684E+01	.80243E+01	.78790E+01	.77330E+01	.75848E+01	.74337E+01	.72785E+01	.71182E+01	.69550E+01
1.50	.84160E+01	.82737E+01	.81307E+01	.79832E+01	.78365E+01	.76867E+01	.75333E+01	.73777E+01	.72175E+01	.70513E+01	.68762E+01
1.55	.83956E+01	.82501E+01	.81035E+01	.79541E+01	.78005E+01	.76457E+01	.74887E+01	.73306E+01	.71677E+01	.69982E+01	.68140E+01
1.60	.83759E+01	.82274E+01	.80782E+01	.79235E+01	.77641E+01	.76020E+01	.74387E+01	.72725E+01	.71025E+01	.69240E+01	.67276E+01
1.65	.83428E+01	.81909E+01	.80370E+01	.78778E+01	.77126E+01	.75419E+01	.73699E+01	.71922E+01	.70129E+01	.68244E+01	.66191E+01
1.70	.82894E+01	.81317E+01	.79752E+01	.78114E+01	.76384E+01	.74616E+01	.72799E+01	.70952E+01	.69050E+01	.66995E+01	.64689E+01
1.75	.82227E+01	.80682E+01	.79131E+01	.77439E+01	.75630E+01	.73744E+01	.71877E+01	.69996E+01	.68051E+01	.65885E+01	.63261E+01
1.80	.81594E+01	.79973E+01	.78352E+01	.76617E+01	.74730E+01	.72769E+01	.70777E+01	.68746E+01	.66589E+01	.64105E+01	.61073E+01
1.85	.80920E+01	.79210E+01	.77472E+01	.75648E+01	.73766E+01	.71792E+01	.69765E+01	.67559E+01	.65108E+01	.62240E+01	
1.90	.80215E+01	.78419E+01	.76574E+01	.74669E+01	.72696E+01	.70607E+01	.68320E+01	.65780E+01			
1.95	.79480E+01	.77614E+01	.75687E+01	.73688E+01	.71573E+01	.69217E+01	.66558E+01				
2.00	.78425E+01	.76502E+01	.74512E+01	.72422E+01	.70120E+01						
2.05	.77268E+01	.75260E+01	.73215E+01								
2.10	.76284E+01	.74221E+01									

TABLE 23. Thermal roton effective mass (m)

Temp. (K)	Pressure (atm)										
	.00	2.50	5.00	7.50	10.00	12.50	15.00	17.50	20.00	22.50	25.00
.10	.16079E+00	.15803E+00	.15432E+00	.15066E+00	.14739E+00	.14447E+00	.14186E+00	.13935E+00	.13687E+00	.13438E+00	.13185E+00
.15	.16079E+00	.15803E+00	.15432E+00	.15066E+00	.14739E+00	.14447E+00	.14186E+00	.13935E+00	.13687E+00	.13438E+00	.13185E+00
.20	.16079E+00	.15803E+00	.15432E+00	.15066E+00	.14739E+00	.14447E+00	.14186E+00	.13935E+00	.13687E+00	.13438E+00	.13185E+00
.25	.16079E+00	.15803E+00	.15432E+00	.15066E+00	.14739E+00	.14447E+00	.14186E+00	.13935E+00	.13687E+00	.13438E+00	.13185E+00
.30	.16079E+00	.15803E+00	.15432E+00	.15066E+00	.14739E+00	.14447E+00	.14186E+00	.13935E+00	.13687E+00	.13438E+00	.13185E+00
.35	.16079E+00	.15803E+00	.15432E+00	.15066E+00	.14739E+00	.14447E+00	.14186E+00	.13935E+00	.13687E+00	.13438E+00	.13185E+00
.40	.16079E+00	.15803E+00	.15432E+00	.15066E+00	.14739E+00	.14447E+00	.14186E+00	.13935E+00	.13687E+00	.13438E+00	.13185E+00
.45	.16079E+00	.15803E+00	.15432E+00	.15066E+00	.14739E+00	.14447E+00	.14186E+00	.13935E+00	.13687E+00	.13438E+00	.13185E+00
.50	.16079E+00	.15803E+00	.15432E+00	.15066E+00	.14739E+00	.14447E+00	.14186E+00	.13935E+00	.13687E+00	.13438E+00	.13185E+00
.55	.16079E+00	.15803E+00	.15432E+00	.15066E+00	.14739E+00	.14447E+00	.14186E+00	.13935E+00	.13687E+00	.13438E+00	.13185E+00
.60	.16079E+00	.15803E+00	.15432E+00	.15066E+00	.14739E+00	.14447E+00	.14186E+00	.13935E+00	.13687E+00	.13438E+00	.13185E+00
.65	.16078E+00	.15803E+00	.15431E+00	.15065E+00	.14739E+00	.14447E+00	.14186E+00	.13935E+00	.13687E+00	.13438E+00	.13185E+00
.70	.16077E+00	.15802E+00	.15431E+00	.15065E+00	.14739E+00	.14447E+00	.14186E+00	.13935E+00	.13687E+00	.13438E+00	.13185E+00
.75	.16075E+00	.15800E+00	.15430E+00	.15065E+00	.14739E+00	.14447E+00	.14186E+00	.13935E+00	.13687E+00	.13438E+00	.13184E+00
.80	.16071E+00	.15797E+00	.15428E+00	.15064E+00	.14738E+00	.14447E+00	.14186E+00	.13935E+00	.13686E+00	.13437E+00	.13184E+00
.85	.16064E+00	.15790E+00	.15424E+00	.15062E+00	.14738E+00	.14447E+00	.14186E+00	.13934E+00	.13686E+00	.13436E+00	.13183E+00
.90	.16053E+00	.15779E+00	.15418E+00	.15060E+00	.14737E+00	.14447E+00	.14185E+00	.13934E+00	.13685E+00	.13435E+00	.13181E+00
.95	.16035E+00	.15763E+00	.15407E+00	.15055E+00	.14736E+00	.14447E+00	.14185E+00	.13933E+00	.13683E+00	.13433E+00	.13179E+00
1.00	.16007E+00	.15737E+00	.15392E+00	.15049E+00	.14734E+00	.14448E+00	.14184E+00	.13931E+00	.13680E+00	.13430E+00	.13176E+00
1.05	.15964E+00	.15697E+00	.15369E+00	.15039E+00	.14732E+00	.14449E+00	.14183E+00	.13930E+00	.13677E+00	.13426E+00	.13172E+00
1.10	.15913E+00	.15650E+00	.15341E+00	.15028E+00	.14728E+00	.14449E+00	.14181E+00	.13926E+00	.13671E+00	.13418E+00	.13163E+00
1.15	.15864E+00	.15609E+00	.15319E+00	.15020E+00	.14727E+00	.14446E+00	.14179E+00	.13915E+00	.13661E+00	.13404E+00	.13146E+00
1.20	.15824E+00	.15571E+00	.15290E+00	.15004E+00	.14717E+00	.14440E+00	.14169E+00	.13906E+00	.13646E+00	.13382E+00	.13115E+00
1.25	.15791E+00	.15529E+00	.15252E+00	.14973E+00	.14705E+00	.14440E+00	.14175E+00	.13907E+00	.13634E+00	.13363E+00	.13099E+00
1.30	.15756E+00	.15502E+00	.15233E+00	.14958E+00	.14683E+00	.14410E+00	.14139E+00	.13869E+00	.13594E+00	.13318E+00	.13027E+00
1.35	.15735E+00	.15467E+00	.15189E+00	.14912E+00	.14638E+00	.14367E+00	.14096E+00	.13819E+00	.13543E+00	.13257E+00	.12973E+00
1.40	.15682E+00	.15411E+00	.15131E+00	.14850E+00	.14571E+00	.14294E+00	.14015E+00	.13734E+00	.13454E+00	.13164E+00	.12873E+00
1.45	.15597E+00	.15322E+00	.15042E+00	.14762E+00	.14481E+00	.14200E+00	.13915E+00	.13627E+00	.13331E+00	.13027E+00	.12718E+00
1.50	.15533E+00	.15253E+00	.14973E+00	.14686E+00	.14403E+00	.14115E+00	.13821E+00	.13524E+00	.13219E+00	.12904E+00	.12574E+00
1.55	.15495E+00	.15209E+00	.14923E+00	.14633E+00	.14337E+00	.14039E+00	.13739E+00	.13438E+00	.13128E+00	.12807E+00	.12460E+00
1.60	.15459E+00	.15167E+00	.14876E+00	.14577E+00	.14270E+00	.13959E+00	.13647E+00	.13331E+00	.13009E+00	.12672E+00	.12302E+00
1.65	.15398E+00	.15100E+00	.14800E+00	.14493E+00	.14175E+00	.13849E+00	.13521E+00	.13184E+00	.12845E+00	.12489E+00	.12104E+00
1.70	.15299E+00	.14991E+00	.14686E+00	.14370E+00	.14039E+00	.13701E+00	.13356E+00	.13006E+00	.12647E+00	.12261E+00	.11829E+00
1.75	.15176E+00	.14874E+00	.14572E+00	.14246E+00	.13900E+00	.13541E+00	.13187E+00	.12831E+00	.12464E+00	.12057E+00	.11568E+00
1.80	.15059E+00	.14743E+00	.14429E+00	.14095E+00	.13735E+00	.13362E+00	.12985E+00	.12602E+00	.12196E+00	.11732E+00	.11168E+00
1.85	.14935E+00	.14602E+00	.14267E+00	.13917E+00	.13558E+00	.13183E+00	.12799E+00	.12384E+00	.11925E+00	.11390E+00	
1.90	.14805E+00	.14456E+00	.14101E+00	.13737E+00	.13361E+00	.12965E+00	.12534E+00	.12058E+00			
1.95	.14669E+00	.14308E+00	.13938E+00	.13556E+00	.13154E+00	.12710E+00	.12211E+00				
2.00	.14475E+00	.14103E+00	.13722E+00	.13323E+00	.12888E+00						
2.05	.14261E+00	.13874E+00	.13483E+00								
2.10	.14079E+00	.13683E+00									

TABLE 24. Wave number of roton minimum ($Å^{-1}$) (1 $Å^{-1} = 10^{10} m^{-1}$)

Temp. (K)	Pressure (atm)										
	.00	2.50	5.00	7.50	10.00	12.50	15.00	17.50	20.00	22.50	25.00
.10	.19129E+01	.19308E+01	.19462E+01	.19596E+01	.19716E+01	.19826E+01	.19926E+01	.20018E+01	.20104E+01	.20185E+01	.20261E+01
.15	.19129E+01	.19308E+01	.19461E+01	.19596E+01	.19716E+01	.19826E+01	.19926E+01	.20018E+01	.20104E+01	.20185E+01	.20261E+01
.20	.19129E+01	.19308E+01	.19461E+01	.19596E+01	.19716E+01	.19825E+01	.19926E+01	.20018E+01	.20104E+01	.20185E+01	.20261E+01
.25	.19129E+01	.19308E+01	.19461E+01	.19596E+01	.19716E+01	.19825E+01	.19926E+01	.20018E+01	.20104E+01	.20185E+01	.20261E+01
.30	.19129E+01	.19308E+01	.19461E+01	.19596E+01	.19716E+01	.19825E+01	.19925E+01	.20018E+01	.20104E+01	.20185E+01	.20261E+01
.35	.19129E+01	.19308E+01	.19461E+01	.19596E+01	.19716E+01	.19825E+01	.19925E+01	.20018E+01	.20104E+01	.20185E+01	.20261E+01
.40	.19129E+01	.19308E+01	.19461E+01	.19596E+01	.19716E+01	.19825E+01	.19925E+01	.20018E+01	.20104E+01	.20185E+01	.20261E+01
.45	.19129E+01	.19308E+01	.19461E+01	.19596E+01	.19716E+01	.19825E+01	.19925E+01	.20018E+01	.20104E+01	.20185E+01	.20261E+01
.50	.19129E+01	.19308E+01	.19461E+01	.19596E+01	.19716E+01	.19825E+01	.19925E+01	.20018E+01	.20104E+01	.20185E+01	.20261E+01
.55	.19128E+01	.19308E+01	.19461E+01	.19596E+01	.19716E+01	.19825E+01	.19925E+01	.20018E+01	.20104E+01	.20185E+01	.20261E+01
.60	.19128E+01	.19308E+01	.19461E+01	.19595E+01	.19716E+01	.19825E+01	.19925E+01	.20018E+01	.20104E+01	.20185E+01	.20261E+01
.65	.19128E+01	.19308E+01	.19461E+01	.19595E+01	.19716E+01	.19825E+01	.19925E+01	.20018E+01	.20104E+01	.20185E+01	.20261E+01
.70	.19128E+01	.19307E+01	.19461E+01	.19595E+01	.19716E+01	.19825E+01	.19925E+01	.20018E+01	.20104E+01	.20185E+01	.20262E+01
.75	.19128E+01	.19307E+01	.19461E+01	.19595E+01	.19716E+01	.19825E+01	.19925E+01	.20018E+01	.20105E+01	.20186E+01	.20262E+01
.80	.19128E+01	.19307E+01	.19461E+01	.19595E+01	.19716E+01	.19825E+01	.19926E+01	.20019E+01	.20105E+01	.20186E+01	.20263E+01
.85	.19128E+01	.19307E+01	.19461E+01	.19595E+01	.19716E+01	.19826E+01	.19926E+01	.20019E+01	.20106E+01	.20187E+01	.20263E+01
.90	.19128E+01	.19307E+01	.19461E+01	.19596E+01	.19717E+01	.19826E+01	.19927E+01	.20020E+01	.20106E+01	.20188E+01	.20264E+01
.95	.19128E+01	.19307E+01	.19461E+01	.19596E+01	.19717E+01	.19827E+01	.19927E+01	.20021E+01	.20107E+01	.20189E+01	.20265E+01
1.00	.19128E+01	.19307E+01	.19461E+01	.19596E+01	.19718E+01	.19828E+01	.19928E+01	.20022E+01	.20109E+01	.20190E+01	.20267E+01
1.05	.19128E+01	.19307E+01	.19462E+01	.19597E+01	.19718E+01	.19829E+01	.19930E+01	.20023E+01	.20110E+01	.20192E+01	.20269E+01
1.10	.19128E+01	.19308E+01	.19462E+01	.19598E+01	.19719E+01	.19830E+01	.19931E+01	.20025E+01	.20112E+01	.20194E+01	.20271E+01
1.15	.19128E+01	.19308E+01	.19463E+01	.19599E+01	.19721E+01	.19831E+01	.19933E+01	.20027E+01	.20114E+01	.20196E+01	.20274E+01
1.20	.19128E+01	.19309E+01	.19464E+01	.19600E+01	.19722E+01	.19833E+01	.19935E+01	.20029E+01	.20117E+01	.20199E+01	.20277E+01
1.25	.19128E+01	.19309E+01	.19465E+01	.19601E+01	.19724E+01	.19835E+01	.19938E+01	.20032E+01	.20120E+01	.20203E+01	.20281E+01
1.30	.19128E+01	.19310E+01	.19466E+01	.19603E+01	.19726E+01	.19838E+01	.19941E+01	.20036E+01	.20124E+01	.20207E+01	.20285E+01
1.35	.19129E+01	.19311E+01	.19467E+01	.19605E+01	.19729E+01	.19841E+01	.19944E+01	.20040E+01	.20129E+01	.20212E+01	.20290E+01
1.40	.19129E+01	.19312E+01	.19469E+01	.19608E+01	.19732E+01	.19845E+01	.19949E+01	.20044E+01	.20134E+01	.20217E+01	.20296E+01
1.45	.19130E+01	.19313E+01	.19471E+01	.19611E+01	.19736E+01	.19849E+01	.19953E+01	.20050E+01	.20140E+01	.20224E+01	.20303E+01
1.50	.19130E+01	.19315E+01	.19474E+01	.19614E+01	.19740E+01	.19854E+01	.19959E+01	.20056E+01	.20146E+01	.20231E+01	.20311E+01
1.55	.19131E+01	.19317E+01	.19477E+01	.19618E+01	.19745E+01	.19860E+01	.19965E+01	.20063E+01	.20154E+01	.20240E+01	.20320E+01
1.60	.19132E+01	.19319E+01	.19480E+01	.19623E+01	.19750E+01	.19866E+01	.19973E+01	.20071E+01	.20163E+01	.20249E+01	.20330E+01
1.65	.19134E+01	.19322E+01	.19484E+01	.19628E+01	.19757E+01	.19874E+01	.19981E+01	.20081E+01	.20174E+01	.20260E+01	.20342E+01
1.70	.19135E+01	.19325E+01	.19489E+01	.19634E+01	.19764E+01	.19882E+01	.19991E+01	.20092E+01	.20185E+01	.20273E+01	.20356E+01
1.75	.19137E+01	.19328E+01	.19494E+01	.19641E+01	.19772E+01	.19892E+01	.20002E+01	.20104E+01	.20199E+01	.20288E+01	.20371E+01
1.80	.19139E+01	.19332E+01	.19500E+01	.19648E+01	.19782E+01	.19903E+01	.20015E+01	.20118E+01	.20214E+01	.20304E+01	.20389E+01
1.85	.19141E+01	.19337E+01	.19507E+01	.19658E+01	.19793E+01	.19916E+01	.20029E+01	.20134E+01	.20232E+01	.20323E+01	
1.90	.19143E+01	.19342E+01	.19515E+01	.19668E+01	.19806E+01	.19931E+01	.20046E+01	.20153E+01			
1.95	.19146E+01	.19348E+01	.19524E+01	.19680E+01	.19820E+01	.19948E+01	.20065E+01				
2.00	.19150E+01	.19355E+01	.19534E+01	.19693E+01	.19837E+01						
2.05	.19154E+01	.19363E+01	.19546E+01								
2.10	.19158E+01	.19372E+01									

TABLE 25. Coefficients a_1 and a_n of the MDC series (K Å^n)(1 Å = 10^{-10}m)

T (K)	P (atm)	a_1	a_3	a_4	a_5	a_6	a_7	a_8
.20	.00	18.196846	45.108719	−163.085876	211.667572	−136.115967	43.272781	−5.389564
.20	2.50	19.667023	26.523594	−112.360092	152.520172	−100.990311	32.799019	−4.142713
.20	5.00	20.946884	13.519928	−79.787628	116.719101	−80.569763	26.869144	−3.448239
.20	7.50	22.088062	3.969789	−58.034119	94.421631	−68.426041	23.433270	−3.050060
.20	10.00	23.122910	−3.381524	−42.918419	80.189056	−61.114006	21.424671	−2.818585
.20	12.50	24.073158	−9.328510	−31.882721	70.802612	−56.660950	20.251656	−2.684020
.20	15.00	24.954227	−14.386789	−23.284580	64.210098	−53.816437	19.541046	−2.602543
.20	17.50	25.777447	−18.847580	−16.243782	59.369171	−51.980667	19.123726	−2.555310
.20	20.00	26.551479	−22.856491	−10.320194	55.749977	−50.841278	18.909050	−2.531901
.20	22.50	27.283047	−26.474239	−5.339409	53.146721	−50.278160	18.862236	−2.528291
.20	25.00	27.977539	−29.764984	−1.116019	51.340134	−50.162460	18.945549	−2.540059
.40	.00	18.202255	45.046959	−162.938599	211.512787	−136.031036	43.248993	−5.386869
.40	2.50	19.670414	26.481247	−112.258484	152.414948	−100.934372	32.784042	−4.141109
.40	5.00	20.948875	13.491226	−79.717514	116.646820	−80.532272	26.859520	−3.447267
.40	7.50	22.089031	3.967130	−58.038261	94.437393	−68.441177	23.439346	−3.050950
.40	10.00	23.123085	−3.362782	−42.983986	80.277740	−61.172585	21.443634	−2.820991
.40	12.50	24.072704	−9.336058	−31.856209	70.769669	−56.641846	20.246380	−2.683459
.40	15.00	24.953247	−14.393038	−23.257160	64.172882	−53.793556	19.534393	−2.601797
.40	17.50	25.776039	−18.855232	−16.207016	59.316772	−51.946960	19.113453	−2.554100
.40	20.00	26.549694	−22.835377	−10.372450	55.807526	−50.874641	18.918961	−2.533086
.40	22.50	27.280945	−26.463436	−5.355791	53.157700	−50.282394	18.863247	−2.528409
.40	25.00	27.975163	−29.745289	−1.158225	51.381783	−50.184845	18.951885	−2.540795
.60	.00	18.210155	44.947212	−162.696777	211.257385	−135.891357	43.210213	−5.382538
.60	2.50	19.673195	26.448883	−112.187561	152.349792	−100.905060	32.777870	−4.140655
.60	5.00	20.948116	13.472624	−79.654282	116.567139	−80.484283	26.845539	−3.445675
.60	7.50	22.085663	3.966507	−58.007721	94.383545	−68.403625	23.427425	−3.049511
.60	10.00	23.117702	−3.337157	−43.018486	80.294022	−61.174126	21.442753	−2.820804
.60	12.50	24.065712	−9.266668	−32.015945	70.934006	−56.731209	20.271423	−2.686308
.60	15.00	24.944935	−14.323412	−23.403755	64.311218	−53.862968	19.552479	−2.603728
.60	17.50	25.766621	−18.758907	−16.428543	59.542412	−52.067474	19.146423	−2.557751
.60	20.00	26.539330	−22.741051	−10.577082	56.004501	−50.974304	18.944862	−2.535820
.60	22.50	27.269764	−26.344913	−5.630239	53.437424	−50.431076	18.903553	−2.532817
.60	25.00	27.963257	−29.653122	−1.339696	51.538643	−50.255287	18.967911	−2.542256
.80	.00	18.214394	44.885498	−162.573425	211.165649	−135.866547	43.211037	−5.383513
.80	2.50	19.667351	26.488655	−112.289688	152.477020	−100.990265	32.806671	−4.144476
.80	5.00	20.935299	13.580513	−79.899826	116.8[illegible]	−80.625046	26.885708	−3.450315
.80	7.50	22.067688	4.161252	−58.476311	94.87896[illegible]	−68.675858	23.503426	−3.058043
.80	10.00	23.095741	−3.094258	−43.598465	80.898880	−61.500557	21.532032	−2.830614
.80	12.50	24.040565	−8.995251	−32.653259	71.587036	−57.077126	20.364201	−2.696301
.80	15.00	24.917152	−14.022804	−24.107124	65.028442	−54.240[illegible]	19.653042	−2.614472
.80	17.50	25.736622	−18.448452	−17.139606	60.252594	−52.433647	19.241837	−2.567715
.80	20.00	26.507439	−22.400311	−11.365572	56.798393	−51.386284	19.052788	−2.547145
.80	22.50	27.236233	−25.995335	−6.429257	54.231972	−50.8[illegible]	19.008675	−2.543683
.80	25.00	27.928276	−29.267151	−2.238814	52.446419	−50.726234	19.[illegible]992	−2.555119
1.00	.00	18.204235	44.652832	−161.936188	210.556702	−135.624695	43.178589	−5.384238
1.00	2.50	19.639828	26.539146	−112.374146	152.640625	−101.164108	32.884987	−4.156837
1.00	5.00	20.895721	13.968925	−80.890884	117.962906	−81.314407	27.096333	−3.475906
1.00	7.50	22.019199	4.711472	−59.847031	96.367493	−69.508804	23.738297	−3.084483
1.00	10.00	23.040333	−2.439907	−45.208374	82.606598	−62.427147	21.784409	−2.858028
1.00	12.50	23.979599	−8.277168	−34.398270	73.409180	−58.047661	20.623207	−2.723837
1.00	15.00	24.851604	−13.248381	−25.989033	66.995193	−55.289787	19.933578	−2.644359
1.00	17.50	25.667217	−17.631157	−19.118877	62.314148	−53.529625	19.533794	−2.598693
1.00	20.00	26.434711	−21.556465	−13.397085	58.904289	−52.501068	19.348454	−2.578362
1.00	22.50	27.160610	−25.133644	−8.485947	56.346336	−51.947769	19.300289	−2.574163
1.00	25.00	27.850113	−28.360394	−4.412244	54.687294	−51.904831	19.401215	−2.587592

TABLE 25. Coefficients u_i and a_n of the MDC series (K Å^n)(1 Å = 10^{-10} m)—Continued

T (K)	P (atm)	u_1	a_3	a_4	a_5	a_6	a_7	a_8
1.20	.00	18.164108	44.275581	−160.940887	209.781281	−135.492432	43.245468	−5.404290
1.20	2.50	19.572063	26.758766	−112.963913	153.591400	−101.961929	33.197128	−4.202121
1.20	5.00	20.808731	14.826330	−83.174515	120.683197	−82.995148	27.616653	−3.539522
1.20	7.50	21.917927	5.987774	−63.197815	100.143555	−71.676208	24.360001	−3.155261
1.20	10.00	22.927975	−.953682	−49.053604	86.835022	−64.781586	22.437943	−2.930016
1.20	12.50	23.858326	−6.700869	−38.413834	77.752090	−60.422890	21.270164	−2.793734
1.20	15.00	24.722965	−11.594639	−30.183372	71.519653	−57.760544	20.605816	−2.716905
1.20	17.50	25.532345	−15.921318	−23.439617	66.968201	−56.070633	20.225227	−2.673302
1.20	20.00	26.294491	−19.785034	−17.865482	63.712936	−55.125114	20.062019	−2.655275
1.20	22.50	27.015709	−23.259411	−13.246851	61.503365	−54.780006	20.075176	−2.658149
1.20	25.00	27.701077	−26.405735	−9.396870	60.106216	−54.890816	20.220387	−2.676547
1.40	.00	18.072956	45.500061	−164.784180	214.792206	−138.740295	44.278648	−5.532924
1.40	2.50	19.438976	28.420647	−117.804657	159.588531	−105.707138	34.354279	−4.342721
1.40	5.00	20.646286	16.919952	−89.076736	127.769882	−87.295731	28.911419	−3.693208
1.40	7.50	21.733669	8.454481	−70.038254	108.202164	−76.472626	25.777176	−3.320523
1.40	10.00	22.726757	1.779231	−56.529221	95.506714	−69.860260	23.914516	−3.099521
1.40	12.50	23.643452	−3.734785	−46.470146	87.017044	−65.798294	22.817932	−2.969692
1.40	15.00	24.496807	−8.445623	−38.698273	81.261871	−63.381508	22.214680	−2.898664
1.40	17.50	25.296650	−12.555998	−32.553452	77.396759	−62.083504	21.944016	−2.867117
1.40	20.00	26.050594	−16.232990	−27.498936	74.739670	−61.480286	21.876575	−2.859508
1.40	22.50	26.764648	−19.447979	−23.649632	73.455765	−61.685036	22.049335	−2.880445
1.40	25.00	27.443665	−22.335537	−20.564976	72.970154	−62.329536	22.346832	−2.915753
1.60	.00	17.902641	48.812119	−175.371002	228.404266	−147.344147	46.941986	−5.856093
1.60	2.50	19.206341	32.339539	−129.711182	174.417542	−114.864029	37.134735	−4.674360
1.60	5.00	20.369839	21.354656	−102.164581	143.726654	−96.977600	31.805569	−4.033397
1.60	7.50	21.424599	13.275105	−84.012787	125.009552	−86.552719	28.757961	−3.667232
1.60	10.00	22.392326	6.959643	−71.399368	113.254333	−80.433380	27.021046	−3.458503
1.60	12.50	23.288635	1.812648	−62.317459	105.852966	−76.976807	26.089340	−3.346109
1.60	15.00	24.125160	−2.519477	−55.587433	101.279404	−75.224640	25.668606	−3.294540
1.60	17.50	24.910809	−6.211314	−50.637695	98.803894	−74.724228	25.621296	−3.287316
1.60	20.00	25.652557	−9.388725	−47.062798	97.911530	−75.156067	25.849960	−3.312699
1.60	22.50	26.355961	−12.038965	−44.917770	98.682465	−76.574875	26.371922	−3.372718
1.60	25.00	27.025574	−14.073032	−44.509460	101.518951	−79.234451	27.264038	−3.476307
1.80	.00	17.614632	55.727371	−197.996429	257.666931	−165.818451	52.637192	−6.543551
1.80	2.50	18.825653	40.186943	−154.354584	205.484100	−134.100006	42.966637	−5.367590
1.80	5.00	19.923534	29.928108	−128.418213	176.256683	−116.839203	37.751259	−4.731647
1.80	7.50	20.929398	22.472076	−111.735825	158.975952	−107.096619	34.853951	−4.376947
1.80	10.00	21.859222	16.755856	−100.653961	148.854645	−101.841476	33.337959	−4.189687
1.80	12.50	22.725193	12.282404	−93.426895	143.557465	−99.566986	32.729744	−4.111550
1.80	15.00	23.536781	8.741184	−88.975906	141.647369	−99.348129	32.739151	−4.106864
1.80	17.50	24.301491	5.986689	−86.808777	142.483459	−100.781143	33.241653	−4.160482
1.80	20.00	25.025322	3.967886	−86.760010	145.855957	−103.735855	34.196609	−4.267243
1.80	22.50	25.713169	3.099761	−90.202667	153.533234	−109.319916	35.940804	−4.466936
1.80	25.00	26.369068	4.027386	−99.219772	168.126648	−119.121857	38.942955	−4.813305
2.00	.00	17.152634	70.090286	−245.461426	318.905151	−204.214142	64.376389	−7.948897
2.00	2.50	18.221794	55.730057	−204.122437	268.480164	−173.024445	54.714104	−6.756611
2.00	5.00	19.218197	46.419075	−180.144836	240.874268	−156.345490	49.558441	−6.114318
2.00	7.50	20.148487	40.057701	−166.143066	226.299347	−147.931000	46.966454	−5.784702
2.00	10.00	21.020050	35.440361	−157.926758	219.237213	−144.272736	45.848648	−5.634654

Appendix B

Selected Helium Data: A Reference Guide

This appendix is intended to aid the reader in locating original, published experimental data on helium-4. Reference to data not listed herein, such as viscosity, latent heat or vaporization, ion mobilities, etc., may be found in one or more of the general books on helium: Keller [25], Donnelly [12], Wilks [11], and Keesom [43].

Quantity	Symbol	Experimental method	Temperature range (K)	Pressure range (atm)	Comments	Authors
Density or molar volume	ρ or V	Pycnometric	$0.5 \leq T \leq 2.8$	SVP	Detailed measurements near T_λ	Kerr & Taylor [34]
" " "	"	Dielectric constant	$0 < T \leq 4.4$	SVP	" " " "	Van Degrift [20]
" " "	"	" "	$T = 0.05$	$0 \leq P \leq 22$	Also data on ^{3}He-^{4}He mixtures	Watson, Reppy, & Richardson [47]
" " "	"	Ultrasonic	$T \simeq 0.5$	$0 \leq P \leq 23$	Integration of $u_1^2 = \left(\frac{\partial P}{\partial \rho}\right)_T$	Abraham, Eckstein, Ketterson, Kuchnir, & Roach [31]
" " "	"	"	$T < 0.1$	$0 \leq P \leq 24$	" " "	Abraham, Eckstein, Ketterson, Kuchnir, & Roach [31]
" " "	"	Dielectric constant	$0.5 \leq T \leq 1.4$	$0 < P \leq 24.5$		Boghosian & Meyer [32]
" " "	"	" "	$1.25 \leq T \leq 4.2$	$0.5 \leq P \leq 28$	Data also near T_λ, P_λ	Elwell & Meyer [33]
" " "	"	P–V–T measurement	$0.3 \leq T \leq 2.0$	$25 \leq P \leq 37$	Data around melting curve	Grilly [48]
First sound velocity	u_1	Ultrasonic	$0.1 \leq T \leq 1.7$	SVP		Whitney & Chase [49]
" " "	"	"	$T \simeq 0.5$	$0 \leq P \leq 23$		Abraham et al. [31]
" " "	"	"	$T < 0.1$	$0 < P \leq 24$		Abraham et al. [31]
" " "	"	"	$1.0 \leq T^* \leq 2.1$	$0 \leq P \leq 25$		Atkins & Stasior [50]
" " "	"	"	$1.0 \leq T \leq 4.2$	$1 \leq P \leq 150$	Also data on ^{3}He-^{4}He mixtures	Vignos & Fairbank [51]
" " "	"	"	$1.8 \leq T \leq 2.5$	SVP	Data around T_λ	Barmatz & Rudnick [52]
" " "	"	"	$1.2 \leq T < T_\lambda$	$0 \leq P \leq 25$	0.2% precision	Heiserman et al. [21]
Compressibility	κ_T	Indirect	$0.85 \leq T \leq T_\lambda$	SVP	Calculated from u_1 and other data	Atkins & Edwards [53]
"	"	Dielectric constant	$0 \leq T \leq 1.25$	$0 \leq P \leq 24$		Boghosian & Meyer [32]
"	"	" "	$1.3 \leq T \leq 4.0$	$1 \leq P \leq 25$		Elwell & Meyer [33]
"	"	P–V–T measurement	$0.3 \leq T \leq 2.0$	$25 \leq P \leq 35$	Data around melting curve	Grilly [48]
"	"	" "	$1.6 \leq T \leq 2.5$	$1 \leq P < 45$		Grilly [42]
"	"	" "	Near T_λ	Near P_λ		Kierstead [54]
Thermal expansion	α_P	Pycnometric	$0.85 \leq T \leq T_\lambda$	SVP		Atkins & Edwards [53]
" "	"	"	$0.5 \leq T \leq 2.8$	SVP		Kerr & Taylor [34]
" "	"	Dielectric constant	$0.85 \leq T \leq T_\lambda$	SVP		Harris-Lowe & Smee [55]
" "	"	" "	$0 < T \leq 4.4$	SVP		Van Degrift [20]
" "	"	Adiabatic compression and expansion	$0.5 \leq T \leq 1.5$	$3 \leq P \leq 24$		Mills & Sydoriak [56]

Quantity	Symbol	Experimental method	Temperature range (K)	Pressure range (atm)	Comments	Authors
" "	"	Dielectric constant	$0.6 \leq T \leq 1.4$	$0 \leq P \leq 25$		Boghosian & Meyer [32]
" "	"	" "	$1.25 \leq T \leq 4.0$	$0.5 \leq P \leq 28$		Elwell & Meyer [33]
" "	"	Indirect	$0.3 \leq T \leq 1.6$	$0 \leq P \leq 25$	From analysis of entropy	Wiebes [36]
" "	"	P-V-T measurement	$0.3 \leq T \leq 2.0$	$25 \leq P \leq 35$		Grilly [48]
" "	"	" "	Near T_λ	$0 \leq P \leq 25$		Mueller, Pobell, & Ahlers [57]
" "	"	" "	Near T_λ	Near P_λ		Kierstead [58]
Entropy & heat capacity	S, C	Calorimeter	$0.6 \leq T \leq 2.2$	SVP		Kramers, Wasscher, & Gorter [59]
" " "	"	"	$1.0 \leq T \leq 2.0$	$0 < P < 25$	Data ≈ 10% high	Hercus & Wilks [60]
" "	"	"	$1.5 \leq T \leq 2.8$	$0 < P < 25$		Lounasmaa & Kojo [61]
" " "	S only	Thermomechanical effect	$1.15 \leq T \leq 2.0$	$0 \leq P \leq 25$		Van den Meijdenberg, Taconis, & De Bruyn Ouboter [35]
" " "						
"	"	Calorimeter	$0.3 \leq T \leq 1.6$	$0 \leq P \leq 25$		Wiebes [36]
" " "	C only	"	$0.3 \leq T < 0.9$	$0 \leq P < 20$		Phillips, Waterfield, & Hoffer [28]
" " "	C only	"	$1.3 \leq T \leq 2.5$	SVP	Porous media	Scott, Guyon, & Rudnick [62]
" " "	C only	"	Near T_λ	SVP; $0 < P < 26$		Ahlers [63] & [64]
Normal fluid density	ρ_n	Oscillating disks	$1.2 \leq T \leq T_\lambda$	SVP		Dash & Taylor [65].
" " "	"	Wire viscometer	$1.1 \leq T \leq 2.18$	SVP		Tough, McCormick, & Dash [44].
" " "	"	Oscillating disks	$1.45 \leq T \leq T_\lambda$	$5 \leq P \leq 25$		Romer & Duffy [45].
Superfluid density	ρ_s	Persistent current	$1.25 \leq T < T_\lambda$	SVP		Clow & Reppy [66].
" "	"	Fourth sound resonance	$1.1 \leq T \leq T_\lambda$	SVP	Porous media	Scott, Guyon, & Rudnick [62].
" "	"	Second sound resonance	$T \geq 1.6$	$0 \leq P < 30$	Calculated from second sound data, emphasis near λ transition.	Greywall & Ahlers [67].
Second sound velocity	u_2	Heat pulse	$0.015 \leq T \leq 1.0$	SVP		De Klerk, Hudson, & Pellam [68].
" " "	"	Second sound resonance	$0.5 < T < 1.7$	SVP		Peshkov [69].
" " "	"	Heat pulse	$0.95 \leq T < T_\lambda$	SVP $\leq P \leq 25$		Maurer & Herlin [46].
" " "	"	Second sound resonance	$T \geq 1.6$	$0 \leq P < 30$	Emphasis near λ transition	Greywall & Ahlers [67].
" " "	"	" " "	$1.2 \leq T < T_\lambda$	$0 \leq P \leq 25$	0.2% precision	Heiserman et al. [21]
Fourth sound velocity	u_4	Fourth sound resonance	$1.2 \leq T < T_\lambda$	$0 \leq P \leq 25$	0.2% precision	Heiserman et al. [21]
Energy spectrum	$\epsilon(p)$	Inelastic neutron scattering	$T = 1.1$	SVP	$0.55 \leq p/\hbar \leq 2.36$ Å^{-1}	Yarnell, Arnold, Bendt, & Kerr [9].
" "	"	" " "	$T = 1.6, 1.8$	SVP	Roton minimum	" " " "
" "	"	" " "	$T = 1.1$	SVP	$0.25 \leq p/\hbar \leq 2.6$ Å^{-1}	Henshaw & Woods [4].
" "	"	" " "	$T = 1.1$	$P = 25.3$	"	" "
" "	"	" " "	$T = 1.12$	SVP	$0.25 \leq p/\hbar \leq 2.6$ Å^{-1}	Henshaw & Woods [5].
" "	"	" " "	$1.1 \leq T \leq 4.21$	SVP	Roton minimum	" "
" "	"	" " "	$T = 1.1, 2.1$	SVP	$0.20 \leq p/\hbar \leq 3.6$ Å^{-1}	Cowley & Woods [2].
" "	"	" " "	$T = 1.1, 2.3, 4.2$	SVP	$0 < p/\hbar < 0.5$ Å^{-1}	" "
" "	"	" " "	$T = 1.2$	$P = 24$	$0.2 \leq p/\hbar \leq 0.7$ Å^{-1}	Svensson, Woods, & Martel [7].
" "	"	" " "	$1.26 \leq T \leq 4.37$	$1.0 \leq P \leq 24.5$	$1.5 < p/\hbar < 2.3$ Å^{-1}	Dietrich, Graf, Huang, & Passell [3].

J. Phys. C: Solid State Phys., Vol. 10, 1977. Printed in Great Britain.

LETTER TO THE EDITOR

Need for more precise thermodynamic and neutron scattering data on liquid helium

R J Donnelly and P H Roberts

Department of Physics and Institute of Theoretical Science, University of Oregon, Eugene, Oregon 97403

Received 6 October 1977

Abstract. It is shown that even at low temperatures, the dispersion curves derived from existing data on neutron scattering and thermodynamic quantities of HeII have irregularities. Programs of systematic measurement of neutron scattering and thermodynamic data would be of significant benefit to the study of liquid helium.

Until recently, our knowledge of the Landau parameters for HeII was sketchy indeed, and we had only the vaguest notion of the temperature and pressure dependence of the roton energy gap Δ and the association momentum p_0 and effective mass μ (Donnelly 1967). Quantities depending on the Landau parameters vary so rapidly with temperature T and pressure P that attempts to deduce these parameters from thermodynamic data were so inaccurate as to be nearly useless. Comprehensive neutron scattering studies over significant ranges of T and P undertaken at Brookhaven (Dietrich *et al* 1972) together with a careful study of the thermodynamics of temperature dependent energy levels (Donnelly and Roberts 1977) have improved the situation to such a degree that systematic tables of the calculated properties of HeII consistent with neutron and thermodynamic data have been produced (Brooks and Donnelly 1977). Systematic compilations of thermodynamic data from the velocities of first, second and fourth sound have also been published by Maynard (1976). It is not difficult to show however, that in certain regions even these latest tables have deficiencies which will need correction in the future. This Letter is a call for the necessary measurements to be made.

These columns have reported a lively controversy concerning the existence and binding energy of the two-roton bound state (Cowley 1972, Latham and Kobe 1975, Murray *et al* 1975, Woerner and Stephen 1975, Woods *et al* 1977). Precise measurements of the energy of the two-roton state and the Landau parameters necessary to interpret the results have been given by Murray *et al* (1975) and Woods *et al* (1977). The result is that at $\sim 0{\cdot}7$ K and the vapour pressure, the binding energy of the two-roton state is $0{\cdot}27 \pm 0{\cdot}04$K. This is, at first sight, a gratifying result for theory as well. Two quite different calculations, published nearly simultaneously, gave for the binding energy the values $E_B = 1{\cdot}0520 \times 10^{-3} p_0^2/\mu$ (Roberts and Pardee 1974) and $E_B = 1{\cdot}25 \times 10^{-3} p_0^2/\mu$ (Pitaevskiĭ and Fomin 1973). Using the tables of Brooks and Donnelly (1977) at 1 K, this yields $E_B = 0{\cdot}2902$ K for Roberts and Pardee and $E_B = 0{\cdot}345$ K for Pitaevskiĭ and Fomin—satisfactorily close to experiment. The precision determination by Woods *et al* (1977),

however, revises p_o and μ drastically, pushing the theoretical results to $E_B = 0{\cdot}375$ K and 0·446 K, respectively, a shift of 28%, and well beyond the experimental uncertainties. Typically, theories will have characteristic energies, lengths, and times depending on the Landau parameters, such as p_o^2/μ, $(\mu/4\pi\rho)^{1/3}$ and $\mu^{4/3}/(4\pi\rho)^{1/3}p_o$, respectively, where ρ is the density. Uncertainties in these quantities have serious repercussions in comparison with experiment. Since the theories of the bound state give the binding energy in terms of the characteristic energy p_0^2/μ, the pressure dependence of E_B is automatically determined providing the parameters are accurately known as a function of pressure. The pressure dependence of E_B is substantial, as shown from the following results calculated on the theory of Roberts and Pardee (1974) using the tables of Brooks and Donnelly (1977) at $T = 0{\cdot}7$ K:

P(atm)	0	5	10	15	20	25
E_B/k(K)	0·2902	0·3129	0·3363	0·3568	0·3765	0·3970

The values used in the table above involve extrapolations of the data of Dietrich *et al* (1972) below 1 K. With the exception of the single measurement of Woods *et al* (1977), there is no published neutron data on pure ^{4}He below 1 K. This means in particular that the important values of Δ obtained by extrapolating to $T = 0$ K are subject to considerable uncertainty. Evidence that this is so is obtained by calculating the values of $(\partial\Delta/\partial P)_{T=0}$. This has been done by Donnelly and Roberts (1977) and is illustrated in figure 10*b* of their paper. An anomaly of nearly 50% exists in the values of $\partial\Delta/\partial P$ near $P = 5$ atm.

It would be desirable to have neutron scattering data and thermal expansion data over as large a range of T and P as possible, but in particular, straddling the line of zero thermal expansion coefficient, where the PVT surface has a pronounced maximum. Extension of sound measurements such as are reported by Heiserman *et al* (1976) and analysed by Maynard (1976), to as low temperatures as possible, would also be of great value.

We note that in the studies of mixtures of ^{3}He in ^{4}He, such as are reported by Hilton *et al* (1977), the shifts in the spectra relative to pure ^{4}He are often given in place of absolute spectra. This underlines the importance of having a firm idea of the spectrum in pure ^{4}He as a point of departure.

Finally, we would re-emphasise the need for new theoretical work on the lineshape for inelastically scattered neutrons. At relatively high temperatures, where the linewidth of the scattered neutrons is significant, uncertainties in unfolding the underlying energy levels severely limit the usefulness of potentially valuable experimental data (Donnelly and Roberts 1977, Maynard 1977).

We thank the National Science Foundation and Air Force Office of Scientific Research for support of our research program.

References

Brooks J S and Donnelly R J 1977 *J Phys. Chem.* Ref. Data **6** 51–104
Cowely R A 1972 *J Phys C: Solid St. Phys.* **5** L287–91
Dietrich O W, Graf E H, Haung C H and Passell L 1972 *Phys. Rev.* **A5** 1377–91
Donnelly R J 1967 *Experimental Superfluidity* (University of Chicago Press)
Donnelly R J and Roberts P H 1977 *J. Low Temp. Phys.* **27** 687–736
Heiserman J, Hulin J P, Maynard J and Rudnick I 1976 *Phys. Rev.* **B14** 3862–7
Hilton P A, Scherm R and Stirling W G 1977 *J. Low Temp. Phys.* **27** 851
Latham W P and Kobe D H 1975 *J. Phys. C: Solid St. Phys.* **8** L461–3
Maynard J 1976 *Phys. Rev.* **B14** 3868–91
Murray C A, Woerner R L and Greytak T J 1975 *J. Phys. C: Solid St. Phys.* **8** L90–4
Pitaevskiĭ L P and Fomin I A 1973 *Zh. Eksp. Teor. Fiz.* **65** 2516–21
Roberts P H and Pardee W J 1974 *J. Phys. A: Math. Nucl. Gen.* **7** 1283–92
Woerner R L and Stephen M J 1975 *J. Phys. C: Solid St. Phys.* **8** L464–7
Woods A D B, Hilton P A, Scherm R and Stirling W G 1977 *J Phys. C: Solid St. Phys.* **10** L45–9

Journal of Low Temperature Physics, Vol. 31, Nos. 3/4, 1978

Dielectric Model of Roton Interactions in Dilute Solutions of ^{3}He in ^{4}He*

R. J. Donnelly, R. W. Walden, and P. H. Roberts†

Institute of Theoretical Science and Department of Physics, University of Oregon, Eugene, Oregon

(Received October 6, 1977)

The analogy between the theory of superfluidity and the theory of dielectrics can be extended to account for some of the properties of rotons in dilute solutions of ^{3}He in superfluid ^{4}He. These include the normal fluid density ratio and the shifts in energy of roton excitations relative to those of pure ^{4}He.

1. INTRODUCTION

Rotons are those excitations on the single-phonon branch of the ^{4}He dispersion curve $\hbar\omega(p)$ that are near its minimum, situated at $q_0 = p_0/\hbar = 1.91\ \text{Å}^{-1}$. Their interactions are a continuing source of problems and investigations. At large distances, the flow from an isolated roton appears as if it originated from a permanent dipole of moment $\boldsymbol{\mu}_s = \mathbf{p}/4\pi\rho$, where ρ is the density of the fluid,[1] and the group velocity $(\partial\hbar\omega/\partial p)\mathbf{1}_x$ of the roton can be either parallel or antiparallel to the direction $\mathbf{1}_x = \mathbf{p}/p$ of its momentum vector $\mathbf{p}$. Feynman recognized that there is a certain analogy between rotons and electric dipoles.[1] This analogy was developed in detail by Donnelly and Roberts[2] and employed by Titulaer and Deutch[3] to study the temperature dependence of the roton gap and associated thermodynamic properties. The results of the latter study are impressive: Using a single parameter, an assumed cutoff radius a beyond which the roton flow field is assumed to be dipolar, Titulaer and Deutch were able to account for a wide variety of properties of ^{4}He as a function of temperature T and pressure P. (This parameter a was assumed to scale linearly with the cube root of the molar volume.)

*This research is supported in part by National Science Foundation grant DMR 76-21814 and by the Air Force Office of Scientific Research under grant AFOSR 76-2880A.

†Permanent address: School of Mathematics, University of Newcastle upon Tyne, Newcastle upon Tyne, Great Britain.

0022-2291/78/0500-0375$05.00/0

Bardeen *et al.*[4] and Ebner and Edwards[5] have remarked that a ^{3}He atom solvated in ^{4}He is principally distinguished from its surroundings by having an increased atomic volume $(1+\alpha)v_{40}$, where v_{40} is the atomic volume of pure ^{4}He and $\alpha = 0.284$ at low temperatures. The ^{3}He quasiparticle moving at velocity v through the superfluid has a backflow like a sphere moving through an ideal fluid and an induced momentum (δm)v, where δm, the induced or hydrodynamic mass, is half the mass of the displaced fluid.[6] This dipolar flow leads to important quasiparticle interactions, which are reviewed by Ebner and Edwards[5] and Baym.[7]

The purpose of this paper is to extend the dielectric analogy referred to above to calculate contributions to the normal fluid density of ^{3}He solutions and shifts in the roton spectrum due to solvated ^{3}He. In doing so, we shall generalize the analogy of Refs. 1–3 to rotons in the neighborhood of the roton minimum, i.e., to moving rotons. The advantage of this treatment is that no parameters of solvated ^{3}He are required save $1+\alpha$, which we estimate following Ebner and Edwards by noting that the kinetic energy of zero-point motion is inversely proportional to mass.[8] Equating the kinetic energy density (pressure) of the ^{3}He to the surrounding ^{4}He gives $1+\alpha = m_4/m_3 \approx 4/3$. Our central results—(31), (36), and (39)—do not, however, depend on whether we take $\alpha = 1/3$ or the experimental value $\alpha = 0.284$.

2. THE DIELECTRIC ANALOGY FOR PURE ^{4}He

The fundamental variable in the two-fluid theory of helium II is the velocity potential of the superfluid ϕ_s, which is related to the phase of a certain wave function. The superfluid velocity $\mathbf{v}_s$ comes from

$$\mathbf{v}_s = -\nabla\phi_s \tag{1}$$

an equation analogous to the relationship between potential and field in electrostatics,

$$\mathbf{E} = -\nabla\phi_E \tag{2}$$

The mass flux j in helium II is related to the normal and superfluid velocities by

$$\mathbf{j} = \rho_n\mathbf{v}_n + \rho_s\mathbf{v}_s \tag{3}$$

In cases where $\mathbf{v}_n$ and $\mathbf{v}_s$ differ, such as in a counterflow, the velocity

$$\mathbf{w} = \mathbf{v}_n - \mathbf{v}_s \tag{4}$$

can be used to define a flux

$$\mathbf{j}_0 = \rho_n\mathbf{w} \tag{5}$$

and $\mathbf{j}_0$ in turn is related to the mass flux $\mathbf{j}$ by

$$\mathbf{j} = \mathbf{j}_0 + \rho \mathbf{v}_s \tag{6}$$

an equation which is analogous to the relation between displacement, polarization, and field in electrostatics,

$$\mathbf{D} = 4\pi \mathbf{P} + \mathbf{E} \tag{7}$$

In electrostatics, the polarization is found microscopically by calculating the dipole moment per unit volume using statistical mechanics. In helium II, $\mathbf{j}_0$ is calculated from the mean drift momentum density of excitations,

$$\mathbf{j}_0 = \rho_n \mathbf{w} = \int \mathbf{p} n (\varepsilon - \mathbf{p} \cdot \mathbf{w}) \, d^3 p \tag{8}$$

where n is the distribution function for excitations of energy ε and momentum $\mathbf{p}$. For example, for small w (and at high temperatures where rotons dominate), we may expand (8) in powers of $\mathbf{p} \cdot \mathbf{w}$ to give

$$\mathbf{j}_0 = \rho_n \mathbf{w} = (p_0^2 / 3kT) N_r(\Delta) \mathbf{w} \tag{9}$$

which defines the microscopic picture for ρ_n as a function of roton excitation density N_r, which in turn depends on the roton energy gap Δ.

If $\mathbf{w}$ and v_s are constrained to be parallel as in an isotropic dielectric, then (6) and (7) are closely similar. One way to see this is to clamp the normal fluid, such as one does in a superfluid gyroscope, so that

$$\mathbf{v}_n = 0, \qquad \mathbf{w} = -\mathbf{v}_s \tag{10}$$

If a superfluid mass flux $\rho \mathbf{v}_s$ is flowing in such a gyroscope, a net polarization $-(p_0^2/3kT) N_r \mathbf{v}_s = -\rho_n \mathbf{v}_s$ will be produced, leaving a net mass flux $-\rho_n \mathbf{v}_s + \rho \mathbf{v}_s$ or

$$\mathbf{j} = \rho_s \mathbf{v}_s \qquad (\mathbf{v}_n = 0) \tag{11}$$

which resembles

$$\mathbf{D} = \varepsilon \mathbf{E} \tag{12}$$

with ρ_s playing the role of the dielectric constant. The susceptibility $\chi = (\varepsilon - 1)/4\pi$ is analogous to $-\rho_n/\rho$.

If we have a permanent dipole of moment $\boldsymbol{\mu}_E$ in an electric field $\mathbf{E}$, its energy is

$$U_E = -\boldsymbol{\mu}_E \cdot \mathbf{E} \tag{13}$$

Similarly, the energy of an excitation of momentum $\mathbf{p}$ in a flow $\mathbf{v}_s$ is

$$U_s = \mathbf{p} \cdot \mathbf{v}_s \tag{14}$$

Comparing (13) and (14), we see from the sign difference that excitations in helium II tend to line up with their momenta antiparallel to a flow $\mathbf{v}_s$, rather than parallel as in electrostatics.

The free energy per unit volume that must be supplied to establish the superflow $\mathbf{v}_s$ is

$$\Delta F = \tfrac{1}{2}\mathbf{j} \cdot \mathbf{v}_s = \tfrac{1}{2}\rho_s v_s^2 \tag{15}$$

compared to the corresponding expression in electrostatics

$$\Delta F = (1/8\pi)\mathbf{D} \cdot \mathbf{E} = (1/8\pi)\varepsilon E^2 \tag{16}$$

A change in current density in a gyroscope may be due to a change in superflow at constant T, or a change in temperature at constant $\mathbf{v}_s$ (a fixed, quantized circulation):

$$d\mathbf{j} = \rho_s \, d\mathbf{v}_s + \mathbf{v}_s (d\rho_s/dT)_{\mathbf{v}_s} \, dT \tag{17}$$

which, since $d\rho_s/dT < 0$, leads to an *increase* in $\mathbf{j}$ as T is decreased. This is the method of determining ρ_s directly from angular momentum measurements in a superfluid gyroscope, since the angular momentum density will be proportional to $\mathbf{j}$.

Other expressions, such as are contained in Fröhlich's monograph on dielectrics,[9] follow in an obvious way (see especially his discussion of energy and entropy in Chapter I of Ref. 9).

The connection between the variables in the two branches of physics is summarized in Table I, where the explicit connections are for electrostatic variables in esu and variables of helium II in cgs units.

Given the analogy discussed above, one can now apply the powerful tools of dielectric theory to problems in helium II. For example, following Chapter II and Appendix A2 of Fröhlich's monograph,[9] one can define a

TABLE I

Analogous Variables in He II and Electrostatics

Variable in He II	Electrostatic variable (esu)	Explicit connection
ϕ_s	ϕ_E	$\phi_E \to (4\pi\rho)^{1/2}\phi_s$
v_s	E	$E \to (4\pi\rho)^{1/2} v_s$
j	D	$D \to (4\pi/\rho)^{1/2} j$
j_0	P	$P \to j_0/(4\pi\rho)^{1/2}$
ρ_s	ε	$\varepsilon \to \rho_s/\rho$
ρ_n	χ	$\chi \to -\rho_n/(4\pi\rho)$
p	μ_E	$\mu_E \to p/(4\pi\rho)^{1/2}$
μ_s	μ_E	$\mu_E \to \mu_s(4\pi\rho)^{1/2}$
U_s	U_E	$U_E \to -U_s$

"cavity" of radius a and dielectric constant $\varepsilon_s = 1$ containing a permanent point dipole of moment $\boldsymbol{\mu}_E$ at the center of the sphere. The material outside is considered to be a continuum having dielectric constant ε_s and a steady field $\mathbf{E}_\infty$. The dipole polarizes the surrounding medium, which in turn fills the sphere with a uniform "Onsager reaction field"

$$\mathbf{R} = \frac{2(\varepsilon_s - 1)}{2\varepsilon_s + 1} \frac{\boldsymbol{\mu}_E}{a^3} \tag{18}$$

irrespective of the value of $\mathbf{E}_\infty$. The external field $\mathbf{E}_\infty$ is reduced in the sphere to the "cavity field"

$$\mathbf{G} = \frac{3\varepsilon_s}{2\varepsilon_s + 1} \mathbf{E}_\infty \tag{19}$$

whether or not the dipole is present.

Our discussion shows that ε_s is analogous to ρ_s/ρ: We denote $\varepsilon_n = \rho_n/\rho$, so that $\varepsilon_s + \varepsilon_n = 1$. A roton may be considered to be a permanent point dipole of doublet strength $\mathbf{p}/4\pi\rho$ embedded in a sphere of radius a containing pure superfluid ($\varepsilon_s = 1$). Excitations outside are simply considered to be a continuum of dielectric constant ε_s, whose effect is to produce an Onsager reaction flow given by the equation analogous to (18):

$$\mathbf{v}_{sR} = \frac{2(\varepsilon_s - 1)}{2\varepsilon_s + 1} \frac{\mathbf{p}}{4\pi\rho a^3} \tag{20}$$

This flow will, by (14), result in a *reduction* in roton energy of an amount

$$\delta\hbar\omega_4 = -\frac{\varepsilon_n}{3 - 2\varepsilon_n} \frac{p^2}{2\pi\rho a^3} \tag{21}$$

Choosing $a = 3.76$ Å gives quite good agreement with observed changes of roton energy gap Δ with ρ_n/ρ and hence temperature T. Details of this and other related calculations are given by Titulaer and Deutch.[3]

3. A DIELECTRIC CALCULATION OF THE NORMAL FLUID DENSITY OF DILUTE SOLUTIONS OF ^{3}He IN ^{4}He

By way of contrast to the model of the roton discussed above, a solvated ^{3}He atom may be modeled as a bubble of volume $(1+\alpha)v_{40}$, which contains a point mass m_3. This impurity sphere has no permanent dipole moment, but in a flow it will acquire an induced moment. To calculate the polarizability η, note that the relation

$$\boldsymbol{\mu}_E = \eta_E \mathbf{E} \tag{22}$$

from electrostatics is translated into

$$\mu_s = \eta v_s = p/4\pi\rho \tag{23}$$

and since, as we indicated in the introduction, $\mathbf{p} = (\delta m)\mathbf{v}_s$, we have $\eta = \delta m/4\pi\rho$ for a single ^{3}He quasiparticle solvated in ^{4}He.

According to Fröhlich,[9] the Clausius–Mosotti equation relating the dielectric constant ε_s of a pure liquid of nonpolar molecules to the polarizability η_E and number density n is

$$\frac{\varepsilon_s - 1}{\varepsilon_s + 2} = \frac{4\pi}{3}\eta_E n \tag{24}$$

Accordingly, we may expect the "dielectric constant" for ^{3}He particles of number density n_3 to be

$$\frac{1-\varepsilon_s}{2+\varepsilon_s} = \frac{n_3\,\delta m}{3\rho} \tag{25}$$

where again, the change in sign is related to the behavior of dipoles in a superfluid, and $\varepsilon_s \leq 1$. Let us call ε_{nd} the dipolar part of ε_{n3} given by (25),

$$\varepsilon_{nd} = \frac{n_3\,\delta m/\rho_{40}}{1 + n_3\,\delta m/3\rho_{40}} \tag{26}$$

where the subscripts on ρ_{40} indicate that it refers to the density of pure ^{4}He. The total normal fluid ratio for solvated ^{3}He can be written

$$\varepsilon_{n3} = \varepsilon_{nd} + \varepsilon_{np} + \varepsilon_{nT} \tag{27}$$

Here $\varepsilon_{np} = n_3 m_3/\rho$ is simply the classical inertial effect of the point masses m_3, and ε_{nT} is an additional effective mass due to any departure of the ^{3}He spectrum from quadratic. For example, if the ^{3}He spectrum is written

$$\hbar\omega_3(p) = -E_3 + \frac{p^2}{2m_3^*} + \gamma p^4 \tag{28}$$

the last term will lead to a linear temperature dependence of ε_{nT}.[5] If $\varepsilon_3(p)$ has a rotonlike minimum, there will be an exponential dependence of ε_{nT} on T. The neutron data[12] have not yet settled the functional form for $\hbar\omega_3(p)$.

To find ε_{nd}, write $\rho_{40} = m_4/v_{40}$, then $n_3\,\delta m/\rho_{40} = n_3\,\delta m v_{40}/m_4$ and $n_3 v_{40} = X/(1+\alpha X)$ where $X = n_3/(n_3+n_4)$. Approximating $\delta m/m_4 \approx 2/3$, we find to second order in X

$$\varepsilon_{nd} \approx \tfrac{2}{3}X(1 - 5X/9) \tag{29}$$

To connect with results at low temperatures where ε_{nT} may be neglected,

we can write $\rho_{n3} = (\varepsilon_{nd} + \varepsilon_{np})\rho$, where the density of the mixture of N_3 ^{3}He atoms and N_4 ^{4}He atoms in a volume V is

$$\rho = \frac{M}{V} = \frac{N_4 m_4 + N_3 m_3}{N_4 v_{40} + N_3(1+\alpha)v_{40}}$$

$$= \frac{[1 + (n_3/n_4)m_3/m_4]\rho_{40}}{1 + (n_3/n_4)(1+\alpha)} = \frac{(4-X)\rho_{40}}{4(1+\alpha X)} \tag{30}$$

neglecting thermal expansion. To first order in X, we obtain from (29) and (30)

$$\frac{\rho_{n3}}{n_3 m_3} = 1 + \frac{8}{9}\left(1 - \frac{29}{36}X\right) \tag{31}$$

which agrees very well with the concentration dependence of second-sound data of Brubaker *et al.*[10] The magnitude $1\frac{8}{9}$ is 17% low compared with the experimental value 2.28 for $X = 0$. This has no repercussions on our other central results (36) and (39) below.

4. DIELECTRIC CALCULATION OF THE ENERGY SHIFTS OF MOVING ROTONS IN DILUTE SOLUTIONS OF ^{3}He IN ^{4}He

Returning to our model of rotons discussed in Section 2, we shall discuss the effects of adding ^{3}He and allowing the rotons to have a drift velocity with respect to the background fluid. First, we expect a term like (21) due to the surrounding ^{3}He particles. But now we must consider the shifts in energy due to the velocity $\partial(\hbar\omega)/\partial p$ of the roton where both normal and superfluid velocities are involved. The energy for the roton in the presence of a counterflow $\mathbf{w}$ is

$$\hbar\omega(\mathbf{p}, \mathbf{w}) = \hbar\omega(p) - \mathbf{p}\cdot\mathbf{w} \tag{32}$$

In a coordinate system attached to the roton, the normal and superfluid components approach with the same velocity, so that the sign of the velocity is reversed to $-\partial(\hbar\omega)/\partial p$. In the roton sphere, however, the superfluid velocity is reduced to the "cavity" value given by (19):

$$\mathbf{v}_{sc} = -\frac{3\varepsilon_s}{2\varepsilon_s + 1}\left(\frac{\partial\hbar\omega}{\partial p}\right)\mathbf{1}_x \tag{33}$$

But the ^{3}He quasiparticles are impurities having a physical mass m_3 and do not experience the reduction of velocity in the cavity. This is an example of d'Alembert's paradox, which is familiar in other branches of the study of helium II. (For example, ions moving near the core of a quantized vortex line are not carried around by the circulation of the superfluid—they

respond instead to the pressure gradient near the core.) Hence

$$\mathbf{v}_{nc} = -\left(\frac{\partial \hbar\omega}{\partial p}\right)\mathbf{1}_x \tag{34}$$

Thus in the cavity

$$\mathbf{w}_c = \mathbf{v}_{nc} - \mathbf{v}_{sc} = \frac{\varepsilon_s - 1}{2\varepsilon_s + 1}\left(\frac{\partial \hbar\omega}{\partial p}\right)\mathbf{1}_x \tag{35}$$

and the change in energy of the ion is

$$\delta(\hbar\omega_3) \equiv \hbar\omega(p, x) - \hbar\omega(p) = \frac{\varepsilon'_{n3}}{3 - 2\varepsilon'_{n3}}\left[p\left(\frac{\partial \hbar\omega}{\partial p}\right) - \frac{p^2}{2\pi\rho a^3}\right] \tag{36}$$

where the first term of the change comes from (32) and (35) and the second is the reaction flow term (21). We have added a prime to ε'_{n3} to denote omission of the point-mass contribution ε_{np} from Eq. (27), since the point mass does not contribute to the dipolar effects, whereas ε_{nd} and ε_{nT} do.

An interesting contrast arises if we consider the problem of moving rotons in pure ^{4}He. At first sight one might expect a term in $p\,\partial(\hbar\omega)/\partial p$ just as in (36). But a more careful investigation shows that this is not true. To appreciate why, we go back to the cavity flow. Just as before, v_{sc} is reduced to the value given by (33), but the other phonons comprising the normal component of the ^{4}He are excitations of the background fluid and hence their velocity is reduced in the cavity by exactly the same amount. Thus $\mathbf{w}_c \equiv 0$ for pure ^{4}He and the energy shift (21) is valid for all rotons.

As a partial check on (36) we observe that, if we picture any ^{4}He atom present as an impurity sphere of radius a and effective mass (physical mass $4\pi\rho a^3/3$ plus induced mass $2\pi\rho a^3/3$) of $m_4 = 2\pi\rho a^3$ and possessing the classical dispersion curve $\hbar\omega = p^2/4\pi\rho a^3$, we would obtain from (36) a zero change in $\hbar\omega$. This would seem to be a necessary test which any theory such as this must survive.

5. EFFECT OF TEMPERATURE AND ^{3}He ON THE SINGLE-PHONON SPECTRUM

Suppose we measure the dispersion relation for single phonons at some "reference temperature" T_R as close to $T = 0$ K as possible. What is the total effect of raising the temperature and adding ^{3}He? From (21) and (36) we have

$$\hbar\omega(p, T, X) = \hbar\omega(p, T_R, 0) + \frac{\varepsilon'_{n3}}{3 - 2\varepsilon'_{n3}}\left[p\left(\frac{\partial \hbar\omega}{\partial p}\right) - \frac{p^2}{2\pi\rho a^3}\right] - \frac{\varepsilon_n}{3 - 2\varepsilon_n}\frac{p^2}{2\pi\rho a^3} \tag{37}$$

where the ε_n in the last term is ρ_n/ρ for pure ^{4}He. Our discussion in this paper has assumed throughout that the temperature changes are not "too large" or the ^{3}He concentrations "too strong." If we remove these restrictions, many complications arise which are beyond the scope of this simple discussion. For example, one would find that the cutoff parameter a is itself temperature dependent, and it would be necessary to know the complete particle–hole continuum spectrum for mixtures, which is not yet well determined.[12] Let us therefore proceed in the manner of a perturbation calculation. In evaluating (37), we may therefore compute the group velocity $\partial\hbar\omega(p)/\partial p$ from the reference spectrum instead of from the dispersion curve at finite T, and X, etc. Under such conditions, the roton part of the spectrum may be represented by a simple Landau approximation:

$$\hbar\omega(p,0,0)=\Delta_0+(p-p_0)^2/2\mu_0 \tag{38}$$

Noting that $\mu_0/\pi\rho a^3\approx 0.04$ and $p_0^2/6\mu_0 k\approx 46$ K, we find that the effects of solvating ^{3}He and raising the temperature are described by modified Landau parameters Δ_0', μ_0', p_0', where

$$\begin{aligned}
\frac{\Delta_0'-\Delta_0}{p_0^2/6\mu_0}&=-\left[\frac{\varepsilon_{n3}'^2}{3}+\frac{(\varepsilon_{n3}'+\varepsilon_{n4})\mu_0}{\pi\rho a^3}\right]\\
\frac{p_0'-p_0}{p_0}&=\frac{\mu_0'}{\mu_0}\left[-\frac{\varepsilon_{n3}'}{3}+\frac{\mu_0}{3\pi\rho a^3}(\varepsilon_{n3}'+\varepsilon_{n4})\right]\approx-\frac{\varepsilon_{n3}'}{3}\\
\frac{\mu_0'-\mu_0}{\mu_0'}&=-\frac{2\varepsilon_{n3}'}{3}+\frac{\mu_0}{3\pi\rho a^3}(\varepsilon_{n3}'+\varepsilon_{n4})\approx-\frac{2\varepsilon_{n3}'}{3}
\end{aligned} \tag{39}$$

neglecting small quantities. Thus, raising the temperature of pure ^{4}He simply lowers the roton energy, whereas solvating ^{3}He lowers the roton energy, shifts the roton minimum to lower wave numbers, and reduces the effective mass. The shifts in p_0 and μ_0 are first order, whereas the shift in Δ_0 is second order in ε_{n3}'.

In order to compare our results quantitatively with experiment, we shall use the continuous representation of the single-phonon dispersion curve advanced by Brooks and Donnelly[11] and valid in the range $0<q<2.2$ Å^{-1},

$$\frac{\hbar\omega(q)}{k}=u_1 q+\sum_{i=3}^{8}a_i q^i \tag{40}$$

The coefficients are tabulated in Ref. 11. We adopt as a reference spectrum the one for $P=0$, $T_R=0.6$ K. Working near the roton minimum, we obtain the results shown in Table II for the continuous representation of (40) as compared to the simple Landau approximation (39). The agreement is quite satisfactory.

TABLE II

Comparison of Shifts in Landau Parameters Based on Calculations with the Model Spectrum of Brooks and Donnelly[11] and the Simple Landau Approximation ($T = 0.6$ K)

X	$(\Delta_0' - \Delta)/(p_0^2/6\mu_0)$ Spectrum	$(\Delta_0' - \Delta_0)/(p_0^2/6\mu_0)$ Landau
0.06	-2.28×10^{-3}	-2.29×10^{-3}
0.12	-5.56×10^{-3}	-5.64×10^{-3}
0.25	-1.58×10^{-2}	-1.66×10^{-2}
X	$(p_0' - p_0)/p_0$ Spectrum	$(p_0' - p_0)/p_0$ Landau
0.06	-1.23×10^{-2}	-1.33×10^{-2}
0.12	-2.3×10^{-2}	-2.67×10^{-2}
0.25	-4.37×10^{-2}	-5.56×10^{-2}

6. COMPARISON OF CALCULATED SHIFTS WITH RESULTS FROM NEUTRON AND RAMAN SCATTERING

We compare our theory with the experimental results of Hilton *et al.*[12] on the effects of ^{3}He and temperature, by defining

$$\delta\hbar\omega(p) = \delta\hbar\omega_3 + \delta\hbar\omega_4, \tag{41}$$

with

$$\begin{aligned} \delta\hbar\omega_3 &= \hbar\omega(p, T, X) - \hbar\omega(p, T, 0) \\ \delta\hbar\omega_4 &= \hbar\omega(p, T, 0) - \hbar\omega(p, T_R, 0) \end{aligned} \tag{42}$$

We show in Fig. 1a a plot of $\delta\hbar\omega_4$ from Eq. (21) compared with $\hbar\omega(T = 1.55) - \hbar\omega(T = 0.6)$, where ε_n and the coefficients of (40) are taken from Ref. 11. The agreement shown is the result of selecting $a = 3.76$ Å, the sole parameter in this paper. It is gratifying to see that (21) is successful over such a large range of q, and that our extension of the dielectric theory to moving rotons is borne out by the facts.

The effect of adding various concentrations of ^{3}He at low temperatures is shown in Fig. 1b compared with the measured shifts of Hilton *et al.*[12] At low temperatures ε_{n3}' in Eq. (36) is simply ε_{nd} as given by (29) and hence we have plotted

$$\delta\hbar\omega_3 \approx \frac{2}{9}X\left[p\left(\frac{\partial\hbar\omega}{\partial p}\right) - \frac{p^2}{2\pi\rho a^3}\right] \qquad (X, T \to 0)$$

The curves show a dramatic change compared to Fig. 1a. A "hinge" momentum $\hbar q_h$ exists, which is given by (36) as the momentum satisfying $\partial(\hbar\omega)/\partial p = p/2\pi\rho a^3$. This is true for any sufficiently small concentration or

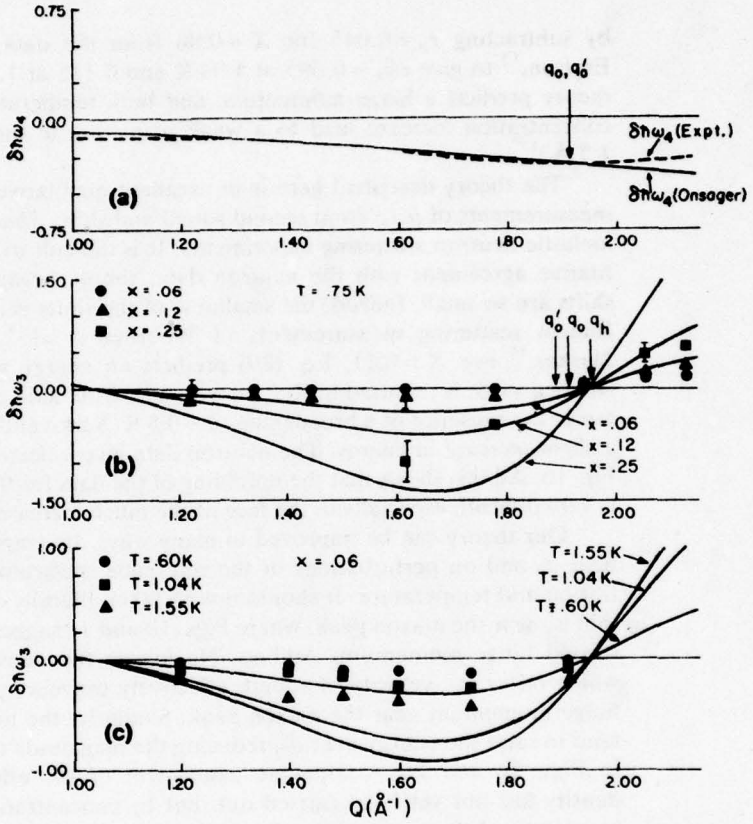

Fig. 1. (a) The difference $\hbar\omega(1.55\,\mathrm{K}) - \hbar\omega(0.6\,\mathrm{K})$ taken from the Brooks–Donnelly tables[11] (dashed line) compared to $\delta\hbar\omega_4$ from Eq. (10) with $a = 3.76$ Å (solid line). This shows the effect of raising the temperature in pure ^{4}He. (b) The shift $\delta\hbar\omega_3$ at $T = 0.75$ K compared to the neutron data of Hilton *et al.*[12] Circles, $X = 0.06$; triangles, $X = 0.12$; squares, $X = 0.25$. Note carefully the distinction between the hinge momentum q_h, the momentum of the reference spectrum q_0, and (for $X = 0.06$ only) the momentum of the shifted spectrum q_0'. (c) The shift $\delta\hbar\omega_3$ at $x = 0.06$ and for $T = 0.60$, 1.04, and 1.55 K compared to the data of Hilton *et al.*[12]

temperature. It should be distinguished carefully from the momentum $\hbar q_0$ of the energy minimum of the unshifted spectrum and from the momentum $\hbar q_0'$ of the minimum of the shifted spectrum, which are also indicated in Fig. 1b.

The shifts for $X = 0.06$ and for $T = 0.6$, 1.04, and 1.55 K are shown in Fig. 1c. Since there is no theory for ε_{nT}, we have estimated ε_{n3}' for Eq. (36)

by subtracting $\varepsilon_p = 0.045$ for $X = 0.06$ from the data of Sobolev and Eselson,[13] to give $\varepsilon'_{n3} = 0.095$ at 1.04 K and 0.115 at 1.55 K. Again, the theory predicts a hinge momentum, and both temperature increase and concentration increase lead to a weak maximum in the shifts near $q = 1.7\ \text{Å}^{-1}$.

The theory described here is in excellent qualitative agreement with measurements of ρ_n/ρ from second sound and shifts $\delta\hbar\omega_3$ and $\delta\hbar\omega_4$ from inelastic neutron scattering experiments. It is difficult to assess the quantitative agreement with the neutron data, simply because the observed shifts are so small. Indeed, the smallness of the shifts is reinforced by the Raman scattering measurements of Woerner *et al.*[14] and Surko and Slusher.[15] For $X = 0.11$, Eq. (39) predicts an energy shift of -0.23 K, whereas none is reported in Ref. 14 within an estimated error of ± 0.05 K, but in the presence of a broadening of ~ 0.5 K. Surko and Slusher[15] report a slight *increase* in energy. The neutron data give a decrease, as shown in Fig. 1b. All this shows that the unfolding of the data for these small effects is very difficult, especially in the face of the much increased linewidth.

Our theory can be improved in many ways. Its emphasis is on shifts near q_0 and on perturbations of the reference spectrum due to concentration and temperature. It should not be taken literally at low momenta, that is, near the maxon peak, where Figs. 1b and 1c suggest formation of a second hinge momentum. Adding ^{3}He lowers the density of the fluid, which raises the velocity of sound, effectively preventing formation of a hinge momentum near the maxon peak. Similarly, the lower density will tend to raise the energy near q_0, reducing the magnitude of the shifts seen in Figs. 1b and 1c. A complete assessment of the effects of changed density has not yet been carried out, but by concentrating on the long-range part of the roton interaction and going to a continuum picture, the dielectric model is capable of giving considerable insight into the problem of roton energy shifts with simplicity and (apart from a) without adjustable parameters. Present theories, as reviewed by Hilton *et al.*, have considerable difficulty in accounting for the experimental results.[12]

ACKNOWLEDGMENTS

We are grateful to Profs. Roger Cowley and John Deutch and to Drs. Paul Hilton and R. N. Hills for discussions of this work.

REFERENCES

1. R. P. Feynman, *Phys. Rev.* **94**, 262 (1954); R. P. Feynman and M. Cohen, *Phys. Rev.* **102**, 1189 (1956).

2. R. J. Donnelly and P. H. Roberts, *Phys. Lett.* **43A**, 199 (1973).
3. U. M. Titulaer and J. M. Deutch, *Phys. Rev.* **10**, 1345 (1974).
4. J. Bardeen, G. Baym, and D. Pines, *Phys. Rev.* **156**, 207 (1967).
5. C. Ebner and D. O. Edwards, *Phys. Rep.* **2C**, 77 (1970).
6. L. D. Landau and E. M. Lifshitz, *Fluid Mechanics* (Pergamon, London, 1959).
7. G. Baym, *Helium Liquids: Proc. 15th Scottish Universities' Summer School in Physics, 1974*, J. G. Armitage and I. E. Farquhar, eds. (Academic Press, London, 1975), Chapter 9.
8. F. London, *Superfluids*, Vol. II (Wiley, New York, 1954).
9. H. Fröhlich, *Theory of Dielectrics* (Oxford, Clarendon Press, 1949).
10. N. R. Brubaker, D. O. Edwards, R. E. Sarwinski, P. Seligmann, and R. A. Sherlock, *Phys. Rev. Lett.* **25**, 715 (1970).
11. J. S. Brooks and R. J. Donnelly, *J. Phys. Chem. Ref. Data* **6**, 51 (1977).
12. P. A. Hilton, R. Scherm, and W. G. Stirling, *J. Low Temp. Phys.* **27**, 851 (1977).
13. V. I. Sobolev and B. N. Eselson, *Soviet Phys.—JETP* **33**, 132 (1971).
14. R. L. Woerner, D. A. Rockwell, and T. J. Greytak, *Phys. Rev. Lett.* **30**, 1114 (1973).
15. C. M. Surko and R. E. Slusher, *Phys. Rev. Lett.* **30**, 1111 (1973).

Journal of Low Temperature Physics, Vol. 31, Nos. 3/4, 1978

Bound States of Rotons to Impurities in He II*

P. H. Roberts,† R. W. Walden, and R. J. Donnelly

Department of Physics and Institute of Theoretical Science, University of Oregon, Eugene, Oregon

(Received October 6, 1977)

Rotons and impurities such as ions or solvated ^{3}He particles can interact via dipolar forces from the flow fields of the roton and the motion of the impurity through the background fluid. Stable bound states of rotons to impurities can occur with near-zero total momentum. We give explicit results of bound-state calculations for solvated ^{3}He, the positive helium ion, and the negative electron bubble.

1. INTRODUCTION

The structure of rotons and roton interactions with other elementary excitations and with solvated impurities in helium II remain fascinating, if very difficult, questions in the phenomenological theory of liquid helium. Fortunately, however, a considerable body of significant information can be had by taking the view that rotons are simply phonons in the general vicinity of the roton minimum at $q_0 = p_0/\hbar \equiv 1.9\ \text{Å}^{-1}$, that they act at great distances as if they had associated with them a permanent point dipole of strength $\boldsymbol{\mu} = \mathbf{p}/4\pi\rho$ and obey a dispersion relation $\varepsilon = \hbar\omega(q)$ which is parabolic near q_0 and otherwise tabulated from neutron scattering data.[1] Their group velocity is taken to be $\mathbf{v} = \partial\varepsilon/\partial\mathbf{p}$. We have explored the consequences of this viewpoint in a variety of calculations. The interaction of rotons with all other quasiparticles of the system has been considered from a thermodynamic viewpoint by Donnelly and Roberts.[2] The roton–roton scattering cross section has been calculated from a Hamiltonian formulation[3]; the binding of rotons has been computed both classically[3] and quantum mechanically.[4] The shifts in the roton spectrum due to interaction with other rotons and with solvated ^{3}He have been treated on a dielectric model.[5,6]

*Research supported by the National Science Foundation and the Air Force Office of Scientific Research under grants NSF DMR 76-21814 and AFOSR 76-2880.

†Permanent address: School of Mathematics, University of Newcastle upon Tyne, Newcastle upon Tyne, England.

0022-2291/78/0500-0389$05.00/0

The interactions of rotons with solvated impurities such as ions and ^{3}He have received a great deal of attention from the point of view of calculating ion mobilities. The possibility of bound states was first considered by Strayer *et al.*,[7] who advanced the view that a moving impurity induced a relative motion near it in which the counterflow velocity $\mathbf{w}=\mathbf{v}_n-\mathbf{v}_s$ achieved considerable magnitude, and the $\mathbf{p}\cdot\mathbf{w}$ interaction would be sufficient to produce a potential well for rotons near the equator of the impurity sphere. This idea was used to estimate the nonlinear drag on a rapidly moving ion and to form the nucleus for the evolution of a quantized vortex ring from such an ion.[7,8]

This paper describes a rather different approach to the problem of bound states to impurities: We take the dynamical approach, using a Hamiltonian formulation. In doing so, we describe the roton as indicated above and consider the impurities as spherical quasiparticles with radii a, effective masses m^*, and dispersion relations $\varepsilon=E+p^2/2m^*$. The effective masses m^* are the sums of their physical masses m and induced masses $m'=\frac{2}{3}\pi\rho a^3$, where ρ is the fluid density. The present approach is semiclassical, but even in the case where such an approach fails, the Hamiltonian may be used as a reasonable starting point for integration of the Schrödinger equation governing the two particles.[4]

The principal result we obtain is that there exist bound states of rotons and impurities of nearly zero total momentum $\mathbf{P}$. The most tightly bound state has exactly $P=0$. Neighboring states extend outward to the roton minimum and beyond, but these are unstable in the sense of having a positive interaction energy, beyond about 0.15 Å^{-1}. We shall discuss the experimental situation and observation of these states in some detail, giving estimates of the energies for their observation. But a rough estimate is obtained simply by adding the energy of a roton Δ to that of the impurity having the same momentum p_0:

$$H\approx p_0^2/2m^*+\Delta$$

where Δ is the roton energy gap.

Rotons are known to bind with other rotons and with impurities. This arises because the roton has a very intense dipole moment and yet can travel very slowly if $q\approx q_0$. The slowness of its motion allows time for interaction to occur and leads to stable bound states as well as to intense scattering. Impurity quasiparticles, on the other hand, have an interaction because of dipolar flow due to their motion through the superfluid. They will not form bound states in themselves. For example, we do not expect to find bound states of two ^{3}He quasiparticles. Instead, they have a weak interaction, which is described by a Fourier-transformed potential $V(q)$

such as was first put forward by Bardeen, Baym, and Pines and amended by others since (see, e.g., Ref. 9).

It is perhaps surprising that the interaction of ion and roton can be described in canonical terms even in classical physics. It may be worth remarking here that the usual treatment requires emendation. It is usually supposed that the acceleration of an ion can be obtained correctly by dividing the applied force by the effective mass m^*. It is sometimes recognized that, strictly, the induced mass of a body in a bounded fluid is not a constant, but depends on its location relative to the walls of the container. It is seldom noted, however, that the induced mass, even in an infinite fluid, is altered when sources are present, as, for example, the dipolar source associated with a roton. We will show below that the proper momentum $\mathbf{p}_2$ conjugate to the position vector $\mathbf{q}_2$ of the ion is not $m^*\mathbf{U}_2$, where $\mathbf{U}_2 = \dot{\mathbf{q}}_2$ is its velocity, but is

$$\mathbf{p}_2 = m^*\mathbf{U}_2 + \tfrac{1}{2}(a/r)^3[\mathbf{p}_1 - 3(\mathbf{p}_1 \cdot \mathbf{r})\mathbf{r}/r^2] \tag{1}$$

where

$$m^* = m + m' = m + \tfrac{2}{3}\pi\rho a^3 \tag{2}$$

and $\mathbf{r} = \mathbf{q}_1 - \mathbf{q}_2$ is the position vector of the roton relative to the ion, $\mathbf{p}_1$ being its momentum.

2. THE INTERACTION HAMILTONIAN

Let (r, θ, ϕ) be spherical polar coordinates centered on the ion, which for simplicity we initially suppose is at rest. In the absence of the ion, a point source of strength M situated at a point P on the z axis ($\theta = 0$) at a distance b ($>a$) from the origin would create a flow $\mathbf{u}$ having the velocity potential

$$\Phi = M/|\mathbf{r} - b\mathbf{1}_z| = (M/b)\sum_0^\infty (r/b)^n P_n(\cos\theta) \tag{3}$$

Here P_n denotes the Legendre function and $\mathbf{1}_z$ is the unit vector in the z direction; the sign convention for Φ is such that the fluid velocity $\mathbf{u}$ is $-\nabla\Phi$. The expanded form of Φ in (3) is, of course, only valid for $r < b$. In the presence of the sphere $r = a$, we require that u_r ($= -\partial\Phi/\partial r$) vanishes on $r = a$. We must therefore add to (3) the potential

$$\hat{\Phi} = \frac{M}{a}\sum_0^\infty \frac{n}{n+1}\left(\frac{a^2}{br}\right)^{n+1} P_n(\cos\theta) \tag{4}$$

a series which converges for all $r > a$. The flow (4) can be regarded as the

reflection of the point source in the surface of the ion. It vanishes for $r \to \infty$ and satisfies Laplace's equation, as it must. It can be represented by an image source at the inverse point ($r = a^2/b$, $\theta = 0$), together with a line of image sources from this inverse point to the origin. The total potential of the flow created by the source can now be written for $r < b$ as

$$\Phi_s = M \sum_0^\infty b^{-n-1} f_n(r) P_n(\cos\theta) \tag{5}$$

where

$$f_n(r) = r^n + \frac{n}{n+1} \frac{a^{2n+1}}{r^{n+1}} \tag{6}$$

The potential Φ_s' for a point source situated at some other point P' with coordinates (b', θ', ϕ'), say, off the z axis can easily be obtained from (5) by a rotation of coordinates and the application of the addition theorem for Legendre functions. It is

$$\Phi_s' = M \sum_0^\infty (b')^{-n-1} f_n(r) \Big[P_n(\cos\theta) P_n(\cos\theta') + 2 \sum_{m=1}^{n} \frac{(n-m)!}{(n+m)!} P_n^m(\cos\theta) P_n^m(\cos\theta') \cos m(\phi - \phi') \Big] \tag{7}$$

where $P_n^m(\cos\theta)$ is the associated Legendre function, normalized in the way suggested by Ferrar. It is simple to obtain from (7) the potential

$$\Phi_D = (\mu_1 \cdot \nabla' \Phi_s')_P \tag{8}$$

of a point doublet source of strength μ_1 situated at a point P, for example, at $r = b$, $\theta = 0$. The prime in (8) indicates that the differentiations are with respect to the coordinate (b', θ', ϕ') of P', and the subscript P indicates that, after this differentiation, we set $b' = b$ and $\theta' = 0$. By (7) and (8) we have

$$\Phi_D = -\mu_{1r} \sum_0^\infty (n+1) b^{-n-2} f_n(r) P_n(\cos\theta) + \mu_{1\theta} \sum_0^\infty b^{-n-2} f_n(r) P_n^1(\cos\theta) \cos(\phi - \phi_0) \tag{9}$$

where $\phi = \phi_0$ is the plane defined by μ_1 and the z axis. We may divide ϕ_D

into the flow potential of the dipole itself and the potential

$$\hat{\Phi}_D = -(\mu_{1r}/ab)\sum_1^\infty n(a^2/br)^{n+1}P_n(\cos\theta)$$

$$+(\mu_{1\theta}/ab)\sum_1^\infty [n/(n+1)](a^2/br)^{n+1}P_n^1(\cos\theta)\cos(\phi-\phi_0) \qquad (10)$$

created by reflection of this flow from the ion. The two series appearing in (10) converge everywhere outside the ion.

The force experienced by the doublet through the reflected flow $\hat{\mu}_D = -\nabla\hat{\Phi}_D$ it creates is

$$\mathbf{f}_1 = -4\pi\rho(\boldsymbol{\mu}_1 \cdot \nabla\hat{\mathbf{u}}_D)_P \qquad (11)$$

where the differentiations are performed with respect to (r, θ, ϕ), and the subscript P indicates that these are replaced by the coordinates of P after differentiation. The velocity $\mathbf{U}_1$ of the doublet is that of the fluid on which it rides, and is therefore

$$\mathbf{U}_1 = (\hat{\mathbf{u}}_D)_P = -(\nabla\hat{\Phi}_D)_P \qquad (12)$$

By straightforward differentiation and series summation, we find (taking $\phi_0 = 0$, without loss of generality)

$$f_{1x} = p_{1x}p_{1z}a^3(3b^2-a^2)/8\pi\rho b^3(b^2-a^2)^3, \qquad f_{1y} = 0$$
$$f_{1z} = -p_{1z}^2a^3(15b^4+4a^2b^2-a^4)/8\pi\rho b^3(b^2-a^2)^4 \qquad (13)$$

$$U_{1x} = -p_{1x}a^3(b^2+a^2)/8\pi\rho b^2(b^2-a^2)^3, \qquad U_{1y} = 0$$
$$U_{1z} = -p_{1z}a^3/2\pi\rho(b^2-a^2)^3 \qquad (14)$$

where $\mathbf{p}_1 = 4\pi\rho\boldsymbol{\mu}_1$ is the momentum corresponding to doublet strength $\boldsymbol{\mu}_1$ (see Section 1).

The force experienced by the sphere through the presence of the doublet may be obtained by integrating the pressure p over the surface of the sphere:

$$\mathbf{f}_2 = -\int_{r=a} p\, d\mathbf{S} \qquad (15)$$

By the momentum theorem, we have

$$p = p_0 + \rho\,\partial\Phi/\partial t - \tfrac{1}{2}\rho(\nabla\Phi)^2 \qquad (16)$$

where p_0 is a constant, which does not contribute to the integral (15). It is straightforward, though tedious, to show that the final term in (16) makes the contribution $-\mathbf{f}_1$ to $\mathbf{f}_2$. To evaluate the force associated with the $\partial\Phi/\partial t$ term, we first consider the general case. Let the velocity potential for

sources lying outside $r = a$ be expanded about $\mathbf{x} = 0$ (the sphere $r = a$ not being present):

$$\Phi = A + B_i x_i + C_{ij}(x^2\delta_{ij} - 3x_i x_j) + \cdots \tag{17}$$

where $C_{ij} = C_{ji}$, and similarly for the higher terms, each of which obeys $\nabla^2\Phi = 0$ individually. In the presence of the sphere, we have

$$\begin{aligned}\Phi = A &+ B_i(1 + a^3/2r^3)x_i + a^3 U_{2i}x_i/2r^3 \\ &+ C_{ij}(1 + 2a^5/3x^5)(x^2\delta_{ij} - 3x_i x_j) + \cdots\end{aligned} \tag{18}$$

In preparation for a later stage in the argument, we have included in (18) the potential required when the sphere moves with velocity $\mathbf{U}_2$ so that $-\nabla\Phi = \mathbf{U}_2$ on $r = a$. Substituting for $\partial\Phi/\partial t$ from (18) into (15), we see that the required contribution to f_{2i} is

$$-\frac{\rho}{2a}\left(3\frac{dB_j}{dt} + \frac{dU_{2j}}{dt}\right)\int x_i x_j\, dS = -\frac{2\pi\rho a^3}{3}\frac{dU_{2i}}{dt} - 2\pi\rho a^3\frac{dB_i}{dt} \tag{19}$$

In what follows, we have no further need of the detailed hydrodynamic description, or a knowledge of the flow at a general point (r, θ, ϕ). We may therefore, without risk of confusion, henceforward denote the position vector of the doublet itself, with respect to the center of the ion, by $\mathbf{r}$. We then have

$$\mathbf{B} = \frac{\mathbf{p}_1}{4\pi\rho r^3} - \frac{3(\mathbf{p}_1 \cdot \mathbf{r})\mathbf{r}}{4\pi\rho r^5} \tag{20}$$

We now also allow the sphere to move, and therefore we add the interaction of the doublet $\frac{1}{2}\mathbf{U}_2 a^3$ at the center of the sphere [cf. Eq. (18)] with the roton doublet. In this way, we obtain the following differential system governing the motion of roton and ion:

$$\begin{aligned}\frac{d\mathbf{p}_1}{dt} = &-\frac{a^3 p_1^2}{8\pi\rho r^4}\frac{3r^4 + 4r^2a^2 - a^4}{(r^2 - a^2)^4}\mathbf{r} - \frac{a^3(\mathbf{p}_1 \cdot \mathbf{r})^2}{4\pi\rho r^6}\frac{6r^4 - 4r^2a^2 + a^4}{(r^2 - a^2)^4}\mathbf{r} \\ &+ \frac{a^3(\mathbf{p}_1 \cdot \mathbf{r})}{8\pi\rho r^4}\frac{3r^2 - a^2}{(r^2 - a^2)^3}\mathbf{p}_1 - \frac{3a^3(\mathbf{p}_1 \cdot \mathbf{r})}{2r^5}\mathbf{U}_2 - \frac{3a^3(\mathbf{U}_2 \cdot \mathbf{r})}{2r^5}\mathbf{p}_1 \\ &- \frac{3a^3(\mathbf{p}_1 \cdot \mathbf{U}_2)}{2r^5}\mathbf{r} + \frac{15a^3(\mathbf{p}_1 \cdot \mathbf{r})(\mathbf{U}_2 \cdot \mathbf{r})}{2r^7}\mathbf{r}\end{aligned} \tag{21}$$

$$\begin{aligned}\frac{d\mathbf{q}_1}{dt} = &\nabla_{p_1}H^{(1)}(p_1) - \frac{a^3(r^2 + a^2)}{8\pi\rho r^2(r^2 - a^2)^3}\mathbf{p}_1 - \frac{a^3(3r^2 - a^2)(\mathbf{p}_1 \cdot \mathbf{r})}{8\pi\rho r^4(r^2 - a^2)^3}\mathbf{r} \\ &+ \frac{3a^3(\mathbf{U}_2 \cdot \mathbf{r})}{2r^5}\mathbf{r} - \frac{a^3}{2r^3}\mathbf{U}_2\end{aligned} \tag{22}$$

$$m_* \frac{d\mathbf{U}_2}{dt} = -\frac{2}{3}\pi\rho a^3 \frac{d\mathbf{U}_2}{dt} - \frac{d}{dt}\left[\frac{a^3}{2r^3}\mathbf{p}_1 - \frac{3a^2(\mathbf{p}_1\cdot\mathbf{r})}{2r^5}\mathbf{r}\right]$$
$$+\frac{a^3 p_1^2}{8\pi\rho r^4}\frac{3r^4+4r^2a^2-a^4}{(r^2-a^2)^4}\mathbf{r} + \frac{a^3(\mathbf{p}_1\cdot\mathbf{r})^2}{4\pi\rho r^6}\frac{6r^4-4r^2a^2+a^4}{(r^2-a^2)^4}\mathbf{r}$$
$$-\frac{a^3(\mathbf{p}_1\cdot\mathbf{r})}{8\pi\rho r^4}\frac{3r^2-a^2}{(r^2-a^2)^3}\mathbf{p}_1 \tag{23}$$

$$\frac{d\mathbf{q}_2}{dt} = \mathbf{U}_2 \tag{24}$$

where $H^{(1)}(p_1)$ is the self-Hamiltonian for the roton. On introducing the momentum (1), these equations assume the canonical forms

$$\frac{dp_{1i}}{dt} = \frac{\partial H}{\partial q_{1i}}, \qquad \frac{dp_{2i}}{dt} = -\frac{\partial H}{\partial q_{2i}}, \qquad \frac{dq_{1i}}{dt} = \frac{\partial H}{\partial p_{1i}}, \qquad \frac{dq_{2i}}{dt} = -\frac{\partial H}{\partial p_{2i}} \tag{25}$$

where $\mathbf{p}_1$ and $\mathbf{p}_2$ are now seen to be momenta conjugate to the position vectors $\mathbf{q}_1$ and $\mathbf{q}_2$ of dipole and ion center respectively, and H is the total Hamiltonian:

$$H = H^{(1)}(p_1) + H^{(2)}(p_2) + H^{(12)}(\mathbf{p}_1, \mathbf{p}_2, \mathbf{q}_1, \mathbf{q}_2) \tag{26}$$

with

$$H^{(1)} = \varepsilon(p_1), \qquad H^{(2)} = p_2^2/2m_*$$
$$H^{(12)} = -\frac{a^3 p_1^2}{16\pi\rho r^2}\frac{r^2+a^2}{(r^2-a^2)^3} - \frac{a^3(\mathbf{p}_1\cdot\mathbf{r})^2}{16\pi\rho r^4}\frac{3r^2-a^2}{(r^2-a^2)^3} \tag{27}$$
$$+\frac{a^6}{8m_* r^6}\left[p_1^2 + \frac{3(\mathbf{p}_1\cdot\mathbf{r})^2}{r^2}\right] - \frac{a^3(\mathbf{p}_1\cdot\mathbf{p}_2)}{2m_* r^3} + \frac{3a^3(\mathbf{p}_1\cdot\mathbf{r})(\mathbf{p}_2\cdot\mathbf{r})}{2m_* r^5}$$

In the applications to helium II that we have principally in mind, the $\varepsilon(p_1)$ in (26) is the familiar dispersion relationship for quasiparticles, often approximated by the Landau spectrum

$$\varepsilon(p) = \Delta + (p-p_0)^2/2\mu \tag{28}$$

Rotons for which $p > p_0$ have parallel momenta and group velocity and are sometimes called "R-rotons" to remind us that in this they share a property with vortex rings; quantum effects make momenta and group velocities antiparallel for rotons for which $p < p_0$, and these have been termed "Q-rotons."

Since H does not contain the time t explicitly, the energy is conserved. Since H involves $\mathbf{q}_1$ and $\mathbf{q}_2$ only in the combination $\mathbf{r}=\mathbf{q}_1-\mathbf{q}_2$, the total linear momentum,

$$\mathbf{P}=\mathbf{p}_1+\mathbf{p}_2 \tag{29}$$

is conserved. It is also easily verified that the total angular momentum

$$\mathbf{M}=\mathbf{q}_1\times\mathbf{p}_1+\mathbf{q}_2\times\mathbf{p}_2 \tag{30}$$

is preserved likewise.

The last two terms of the interaction Hamiltonian (27) evidently give the familiar dipole–dipole reaction between the "backflows" of roton and moving ion. The remaining terms may be thought of as arising from "images" of the dipole in the spherical ion, and are independent of the momentum $\mathbf{p}_2$ of the ion. At distances $r\gg a$, this potential falls off as r^{-6}, like the van der Waals potential. Unlike the van der Waals force, however, our interaction depends on the angle between $\mathbf{p}_1$ and $\mathbf{r}$.

3. A SEARCH FOR BOUND STATES

In this section we seek negative energy states. By this we mean that the total conserved energy is, at every point of the relative orbit, less than the energy $\varepsilon(\mathbf{p}_1)+\mathbf{p}_2^2/2m$ that the roton and ion would have if separated to infinity. In their most general form, we may picture these bound states most easily by placing ourselves in the (accelerated) frame in which the ion is permanently centered on the origin O and the roton describes some path around it. Similar bound states are encountered in the classical theory of roton–roton dynamics[3] and it is there found that the states of greatest binding energy are those in which $\mathbf{P}$ and $\mathbf{M}$ are parallel, and the separation $r=|\mathbf{r}|$ is constant in time, the roton describing a circular path centered on, and in a plane perpendicular to, Oz, the common direction of $\mathbf{P}$ and $\mathbf{M}$. We will confine our search for bound states to solutions of this general type: They are illustrated schematically in Fig. 1.

In this section we work in dimensionless units, using the ion radius a as unit of length, some momentum scale p_0, such as the momentum of the roton minimum in (28), as unit of momentum, and $p_0^2/4\pi\rho a^3$ as unit of energy. The Hamiltonian (26) then becomes

$$H=H_1+H_2p_z+H_3z(\mathbf{p}\cdot\mathbf{r})+H_4(\mathbf{p}\cdot\mathbf{r})^2 \tag{31}$$

We have here written $\mathbf{p}_1=\mathbf{p}$, $\mathbf{p}_2=\mathbf{P}-\mathbf{p}$, and

$$H_1=\varepsilon(p)+\frac{1}{3}\xi P^2+\frac{1}{2}\xi p^2\left(1+\frac{1}{2r^3}\right)^2-\frac{p^2(r^2+1)}{4r^2(r^2-1)^3} \tag{32}$$

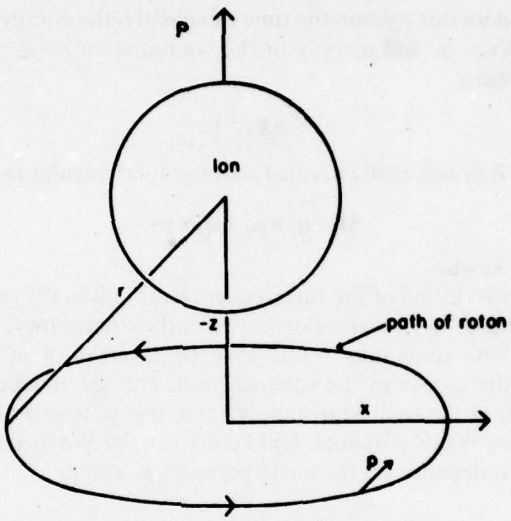

Fig. 1. Coordinates for the study of a roton bound to an impurity sphere.

$$H_2 = -\frac{\xi P}{3}\left(2+\frac{1}{r^3}\right), \qquad H_3 = \frac{\xi P}{r^5} \tag{33}$$

$$H_4 = -\frac{\xi}{r^5}\left(1-\frac{1}{4r^3}\right) - \frac{3r^2-1}{4r^4(r^2-1)^3}, \qquad \xi = \frac{6\pi\rho a^3}{m_*} \tag{34}$$

It is convenient to consider first two special cases. Suppose initially (case A) that the steady state is of zero angular momentum $M \equiv xp_y - yp_x$, so that the roton lies permanently on the axis Oz of symmetry at a fixed distance r either ahead ($z = r, p_z = \pm p$) or behind ($z = -r, p_z = \mp p$) the moving ion. We find that (31) may be written in the form

$$H = \varepsilon(p) + \tfrac{1}{3}\xi[P \mp p(1-r^{-3})]^2 - p^2(r^2-1)^{-3} \tag{35}$$

For a steady state to exist, we require

$$\partial H/\partial r = \partial H/\partial p = 0 \tag{36}$$

which implies that

$$\pm P = p[(1-r^{-3}) + 3r^5/\xi(r^2-1)^4] \tag{37}$$

$$\varepsilon'(p)/p = 2(r^5-1)/(r^2-1)^4 \tag{38}$$

Equation (37) shows that the upper sign must be chosen throughout, i.e., **p** and **P** must be parallel rather than antiparallel. Equation (38) shows that only R-rotons can bind to ions in case A.

It is easy to examine the stability of the states with respect to perturbations in **r** and **p** that are parallel to **P**. Evidently we must satisfy the three inequalities

$$\frac{\partial^2 H}{\partial r^2} \geq 0, \qquad \frac{\partial^2 H}{\partial r^2}\frac{\partial^2 H}{\partial p^2} \geq \left(\frac{\partial^2 H}{\partial r\,\partial p}\right)^2, \qquad \frac{\partial^2 H}{\partial p^2} \geq 0 \tag{39}$$

the first two of which imply the third. The minimum-energy state is the one for which equality holds in the second of (39), and this state is on the verge of instability. Some results are given in Table I and it is hoped that these have relevance to the ^{3}He impurity, the positive ion, and the electron bubble. In obtaining these results, we used the model dispersion curves of Brooks and Donnelly[1] for $T = 1$ K and zero pressure. The total energy H is measured from Δ as origin, and both it and the binding energy $E_B \approx -H_{12}$ are given in degrees kelvin; Δp and ΔP are respectively $p - p_0$ and $P - p_0$.

We next consider (case B) states of zero total momentum P but finite angular momentum M. The orbit is now circular and lies in the "equatorial plane" $z = 0$. Writing $(\mathbf{p}\cdot\mathbf{r})^2 = r^2p^2 - M^2$, we find that the Hamiltonian (36) becomes

$$H = \varepsilon(p) - \tfrac{1}{3}\xi p^2(1 - r^{-3})^2 - p^2(r^2-1)^{-3} + M^2[\xi r^{-5}(1 - \tfrac{1}{4}r^{-3}) + \tfrac{1}{4}r^{-4}(3r^2-1)(r^2-1)^{-3}] \tag{40}$$

Conditions (36) relate r to p for the orbit. They require that

$$\varepsilon'(p)/p = 2(r^2-1)^{-3} - \tfrac{2}{3}\xi(1 - r^{-3})^2 \tag{41}$$

$$-M^2[\xi r^{-6}(5 - 2r^{-3}) + r^{-5}(6r^4 - 4r^2 + 1)(r^2-1)^{-4}] = 2p^2[\xi r^{-4}(1 - r^{-3}) - 3r(r^2-1)^{-4}] \tag{42}$$

Equation (41) shows that a continuum of states is possible, which is limited only by the necessity that M^2, given by (42), should be positive, and by the conditions (39) for stability with respect to displacements of **r** and **p**

TABLE I

Case A: Bound States of Zero Angular Momentum ($M = 0$)

a, Å	m/m_4	m^*/m_4	r, Å	$\Delta p/\hbar$, Å^{-1}	$\Delta P/\hbar$, Å^{-1}	$H - \Delta$, K	E_B, K
2.8	0.75	1.753	9.93	3.19×10^{-3}	-4.92×10^{-3}	-2.613×10^{-4}	7.913×10^{-4}
6.8	2.00	16.37	18.15	6.90×10^{-4}	-3.00×10^{-2}	-8.640×10^{-4}	7.754×10^{-4}
16	0	187.2	40.38	8.0×10^{-5}	-4.04×10^{-2}	3.681×10^{-4}	1.082×10^{-4}

TABLE II

Case B: Bound States of Zero Linear Momentum ($P = 0$)

a, Å	m/m_4	r, Å	$\Delta p/\hbar$, Å^{-1}	$M/\hbar$	$H-\Delta$, K	E_B, K
2.8	0.75	4.88	-1.21×10^{-1}	6.141	10.22	1.352
6.8	2.00	11.05	-9.44×10^{-3}	14.86	1.155	0.1888
16	0	25.69	-7.90×10^{-4}	34.51	0.1005	0.01728

in the plane $z = 0$. Again the maximally bound state is the one on the verge of instability, for which equality obtains in the second of (39). It is found that these are Q-rotons. Results given in Table II are complementary to those of Table I. It will be seen that binding energies are much greater in case B than in case A.

We now transfer our attention to the general case (C) in which neither P nor M is zero. We choose r, z, p, and p_z as independent variables and regard $\mathbf{p}\cdot\mathbf{r}$ as a function of these variables given by

$$(\mathbf{p}\cdot\mathbf{r}-p_z z)^2=(r^2-z^2)(p^2-p_z^2)-M^2 \tag{43}$$

where $M = xp_y - yp_x$ is the constant angular momentum. It follows from (43) that

$$\begin{aligned}
&\frac{\partial}{\partial r}(\mathbf{p}\cdot\mathbf{r})=\frac{r(p^2-p_z^2)}{\mathbf{p}\cdot\mathbf{r}-p_z z}, \qquad \frac{\partial}{\partial p}(\mathbf{p}\cdot\mathbf{r})=\frac{p(r^2-z^2)}{\mathbf{p}\cdot\mathbf{r}-p_z z}\\
&\frac{\partial}{\partial z}(\mathbf{p}\cdot\mathbf{r})=p_z-\frac{z(p^2-p_z^2)}{\mathbf{p}\cdot\mathbf{r}-p_z z}, \qquad \frac{\partial}{\partial p_z}(\mathbf{p}\cdot\mathbf{r})=z-\frac{p_z(r^2-z^2)}{\mathbf{p}\cdot\mathbf{r}-p_z z}
\end{aligned} \tag{44}$$

We use these results to simplify the equations

$$\partial H/\partial r=\partial H/\partial z=\partial H/\partial p=\partial H/\partial p_z=0 \tag{45}$$

determining the orbit, which by (31) are respectively

$$D_1+D_2p_z+D_3z(\mathbf{p}\cdot\mathbf{r})+D_4(\mathbf{p}\cdot\mathbf{r})^2+Q(p^2-p_z^2)=0 \tag{46}$$

$$H_3(\mathbf{p}\cdot\mathbf{r})+Q[p_z(\mathbf{p}\cdot\mathbf{r})-zp^2]=0 \tag{47}$$

$$E_1+Q(r^2-z^2)=0 \tag{48}$$

$$H_2+Q[z(\mathbf{p}\cdot\mathbf{r})-p_z r^2]=0 \tag{49}$$

where

$$Q=[H_3z+2H_4(\mathbf{p}\cdot\mathbf{r})]/(\mathbf{p}\cdot\mathbf{r}-p_z z) \tag{50}$$

$$D_i=r^{-1}\,\partial H_i/\partial r, \qquad E_i=p^{-1}\,\partial H_i/\partial p \qquad (i=1\text{–}4) \tag{51}$$

Excluding cases A and B, (47)–(49) show that either

$$E_1H_3 = 2H_2H_4 \tag{52}$$

a possibility we will exclude (since in no case examined did it give physically realistic solutions), or

$$p_z = -\frac{1}{2H_4}\left[H_3 - \frac{p^2(E_1+2H_4r^2)(E_1H_3-2H_2H_4)}{(H_2+H_3r^2)^2}\right] \tag{53}$$

$$z\mathbf{p}\cdot\mathbf{r} = -\frac{H_2+H_3r^2}{2H_4}\left[1 - \frac{p^2E_1(E_1+2H_4r^2)}{(H_2+H_3r^2)^2}\right] \tag{54}$$

$$Q^{-1} = \frac{1}{2H_4}\left[1 - \frac{p^2(E_1+2H_4r^2)^2}{(H_2+H_3r^2)^2}\right] \tag{55}$$

Substituting these forms back into (46), we discover again that either (52), or cases A or B hold, or that

$$\begin{aligned} &2H_4D_1 - D_2\left[H_3 - \frac{p^2(E_1+2H_4r^2)(E_1H_3-2H_2H_4)}{(H_2+H_3r^2)^2}\right] \\ &\quad -(H_2+H_3r^2)\left[D_3 - D_4\frac{H_2+H_3r^2}{E_1+2H_4r^2}\right]\left[1 - \frac{p^2E_1(E_1+2H_4r^2)}{(H_2+H_3r^2)^2}\right] \\ &= H_3^2 - \frac{p^2(E_1H_3-2H_2H_4)^2}{(H_2+H_3r^2)^2} \end{aligned} \tag{56}$$

This equation, which defines case C, was studied by numerical means. When solutions were obtained, it was first verified that M given by (43) was real, that $|p_z| < p$, and that $|z| < r$, where

$$z^2 = \frac{E_1+2H_4r^2}{2H_4}\left[1 - \frac{p^2E_1(E_1+2H_4r^2)}{(H_2+H_3r^2)^2}\right] \tag{57}$$

When these conditions were met, no further stability tests generalizing (39) were performed, but (31) and (53)–(55) were used to evaluate H and the binding energy. It was found that solutions existed in a torus girdling the ion symmetrically with respect to z. Case B solutions accounted for all the $z = 0$ solutions within the torus, and joined continuously with the case C solutions that lay on either side, $z > 0$ and $z < 0$. In addition, a completely distinct branch of low-angular-momentum C states contained the case A solutions on the z axis. More discussion of the solutions will be given below. We merely report the significant fact that in no case we studied did the binding energy of the case C solutions exceed that of the maximally bound B solution.

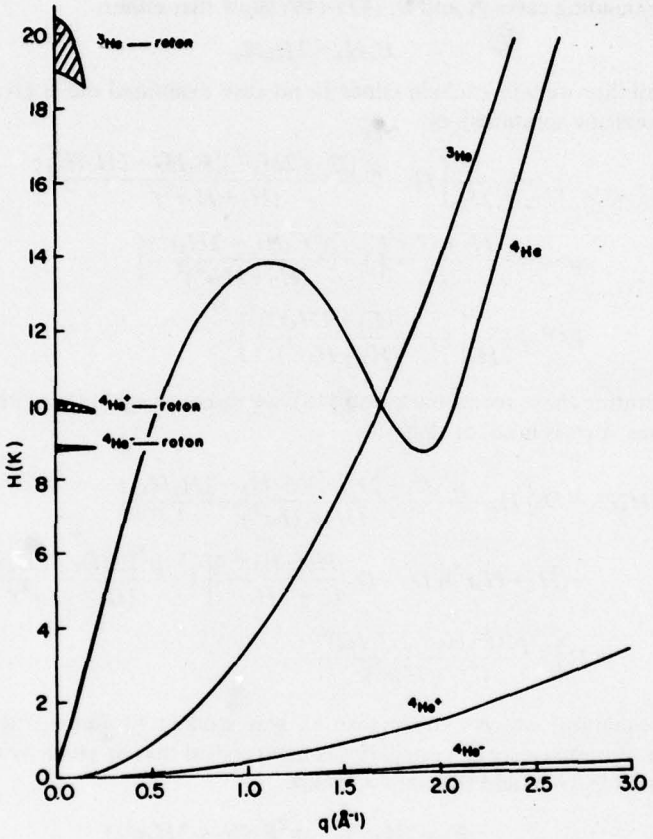

Fig. 2. Dispersion curve for pure ^{4}He compared with the assumed parabolic spectra for ^{3}He, positive, and negative ions with effective masses as given in Table I. The regions of bound states with negative interaction energies are shown for the three impurities near zero momentum.

4. DISCUSSION AND APPLICATION TO EXPERIMENT

As our results in Tables I and II indicate, we are using three impurities as examples of these calculations. We can appreciate the differences in these impurities by examining their free particle dispersion curves in relation to that for the elementary excitations in pure helium II. This is shown in Fig. 2, where the dispersion curve is illustrated for $T = 1$ K.

4.1. ^{3}He Impurities

The curve drawn in Fig. 2 represents $\varepsilon = p^2/2m_3^*$, where $m_3^* = 1.75m_4$ as shown in Table I. Current neutron scattering data show a distinct departure of this curve from parabolic beyond $q = 1.3$ Å^{-1}, but give little information beyond $q = 1.7$ Å^{-1}.[10] For the present considerations we tentatively adopt the parabolic spectrum as the "unperturbed" state of solvated ^{3}He.

For $P = 0$, Table II shows that the most bound state is a roton of angular momentum about $6.1\hbar$ with respect to the ^{3}He atom, circling the equator at $z = 0$ and a radial distance 4.91 Å (or about 2 Å from the

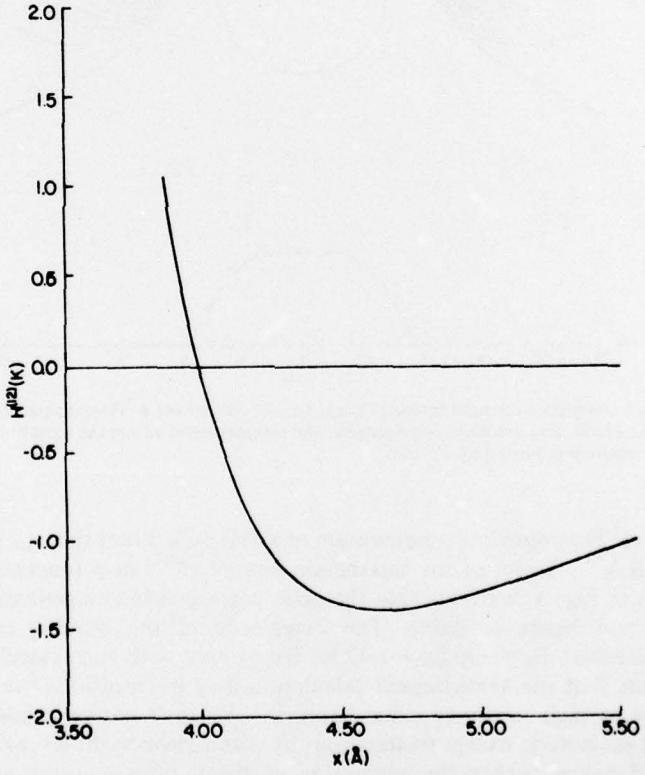

Fig. 3. The energy of the bound roton–^{3}He state of zero total momentum as a function of distance. The stability of the bound state is evident.

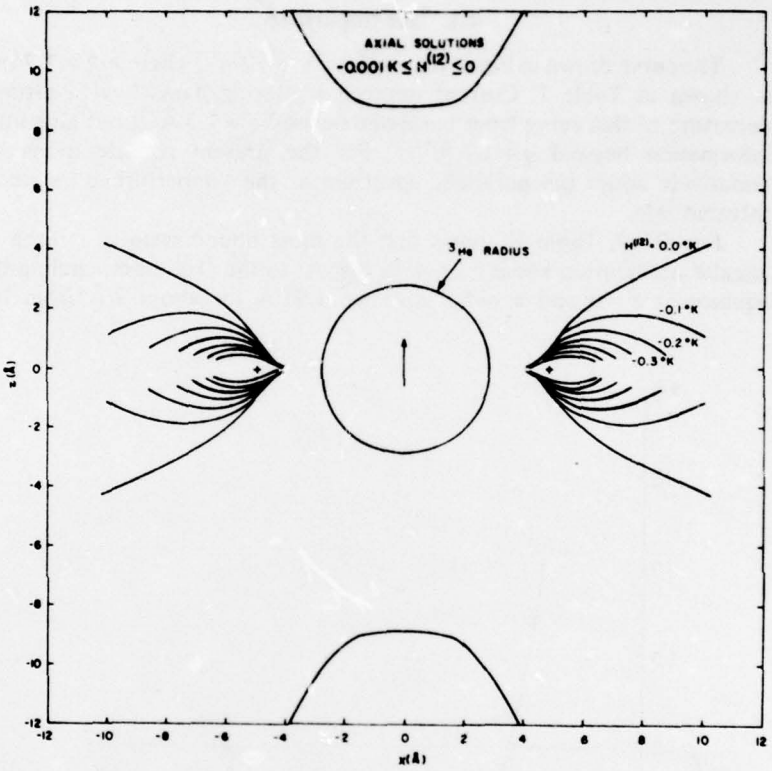

Fig. 4. Contours of constant binding energy for the roton near a ^{3}He quasiparticle. Axial solutions have very small binding energies. The toroidal states adjoin the most bound state at the position indicated by a cross.

surface). The roton has a momentum of about 10% lower than q_0, or about $q = 1.8\,\text{Å}^{-1}$. A plot of the interaction energy $H^{(12)}$ as a function of x is shown in Fig. 3, verifying that the orbit corresponds to a potential minimum and hence is stable. The magnitude of the binding energy is considerable: $E_B = -H^{(12)}_{\max} = 1.42$ K. Experience with such calculations[3,4] suggests that the semiclassical calculation may overestimate the binding energy at such relatively close distances. We shall not speculate on the actual magnitude except to state that by comparison with the calculations quoted below, where the separation of roton from impurity sphere is comfortably larger, we do expect the roton to be bound to the ^{3}He quasiparticle.

A more vivid configuration-space picture of roton orbits about the ^{3}He quasiparticle is shown in Fig. 4. These are plots of constant interaction energy $H^{(12)}$ from case C—the general case. The arrow points in the direction of the total momentum **P** of the complex, which is both the z axis and the direction of motion of the complex. The circle denotes the hydrodynamic radius of the quasiparticle. The states at large values of $|z|/|x|$ correspond to very weakly bound $M \doteq 0$ states resembling case A solutions. Case B solutions occur on the equatorial plane $z = 0$, and the

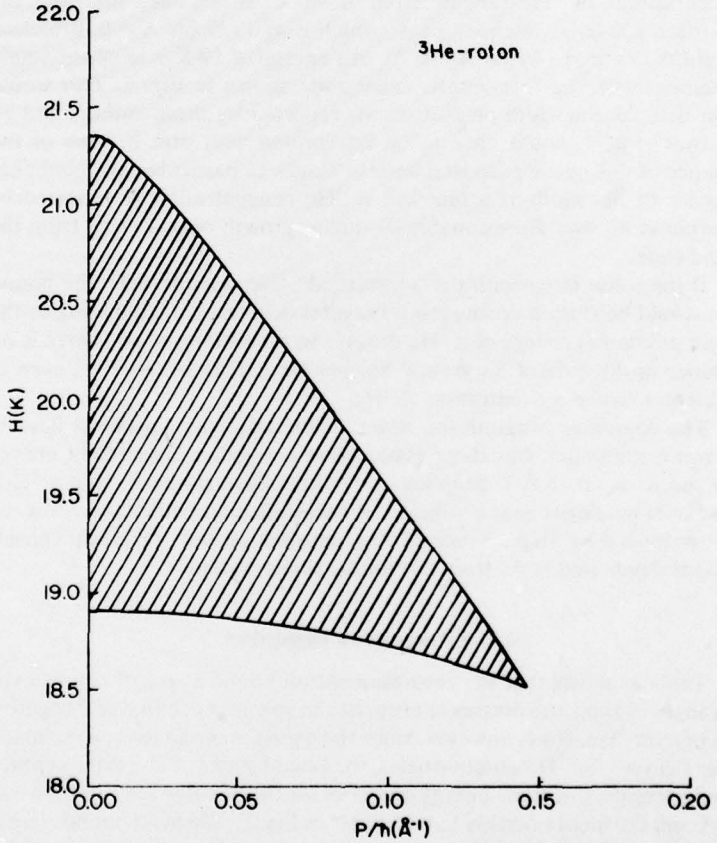

Fig. 5. The region of energy as a function of total momentum P for the ^{3}He–roton-pair containing solutions with negative values of the interaction energy $H^{(12)}$.

particular B solutions denoted by a cross at 4.88 Å, are the most tightly bound states. The remainder of the case C solutions, as we have remarked above, join continuously onto case B and form a torus girdling the equatorial plane of the impurity sphere.

The locus in momentum space of solutions for cases B and C is shown in detail in Fig. 5. For $P \approx 0$ the bound states show a band ranging from about 18.9 to 21.4 K, assuming a roton binds with an "unperturbed" ^{3}He. There is some experimental evidence that these may exist. Surko and Slusher[11] have explored Raman scattering of the two-roton bound state for concentrations of ^{3}He ranging from $X = 0$ to 0.31. They find that the two-roton scattered intensity peak, which is at 17 K for $X = 0$, broadens and shifts to about 19 K at $X = 0.31$. An energy of 19 K is in approximate agreement with the ^{3}He–roton bound state shown in Fig. 5. This would mean that the linewidth measurements reported by these authors and by Woerner *et al.*[12] would have to be interpreted with care in view of the presence of this newly proposed band of states. In particular, the nonlinear behavior of linewidth as a function of ^{3}He concentration X reported by Woerner *et al.* would presumably be due to growth of scattering from the bound state.

If the roton binds with the "perturbed" ^{3}He quasiparticle, the bound state would be shifted downward by several degrees, corresponding to the (as yet unknown) energy of a ^{3}He particle in the vicinity of q_0. There is no evidence in the data of Surko and Slusher for a peak below 19 K even at the highest molar concentration of ^{3}He.

The computer program for case C finds stationary states out beyond the roton minimum, but these states have a negative interaction energy only out to $q = 0.15$ Å^{-1}. Stephen and Mittag have proposed that a ^{3}He–roton state may exist near $q = q_0$.[13] It is very difficult to understand how the state proposed by Stephen and Mittag can exist on the dynamical considerations developed here. It should not be stably bound.

4.2. Charged Ion Impurities

Table II shows that the zero-momentum bound states of rotons exist for ranges of radii and masses appropriate to solvated positive and negative ions in pure ^{4}He. Now, however, since the energies of the ions are so much lower than for the ^{3}He quasiparticles, the bound states of $P \approx 0$ are at much lower energies. Constant-energy contours for the positive ion are shown in Fig. 6 and the locus of stably bound states in Fig. 7. The most bound state is at a distance 4.2 Å from the surface of the impurity sphere, the angular momentum is $14.9\hbar$, and the binding energy $E_B = 0.19$ K. Contours for the negative ion are very similar to Fig. 6 except for scale, with the angular

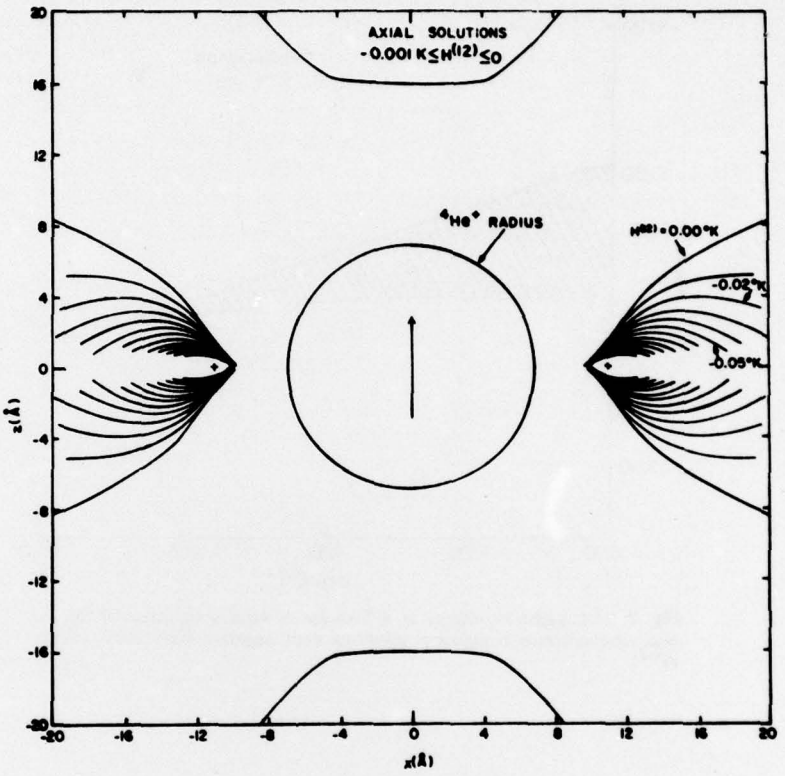

Fig. 6. Contours of constant binding energy for the roton near a positive ion in ^{4}He. The most bound state is indicated by a cross. Except for scale, the results for the negative ion are qualitatively similar.

momentum of the most bound state about $35\hbar$ and $E_B = 0.017$ K, corresponding to a distance of 10 Å from the surface of the negative ion. The locus of stably bound states is shown in Fig. 8.

Contours of bound states of negative $H^{(12)}$ are shown in Figs. 7 and 8. The absolute energy of these states is, of course, dependent on the energies of the ions having their "unperturbed" values.

It seems likely that the ion–roton bound states proposed here exist. If they could be examined experimentally, they would be a rich source of information on roton–impurity interactions. It is not immediately evident how this can be accomplished. Raman scattering from the ion–roton complexes requires a concentration of perhaps 1%, whereas ion beam

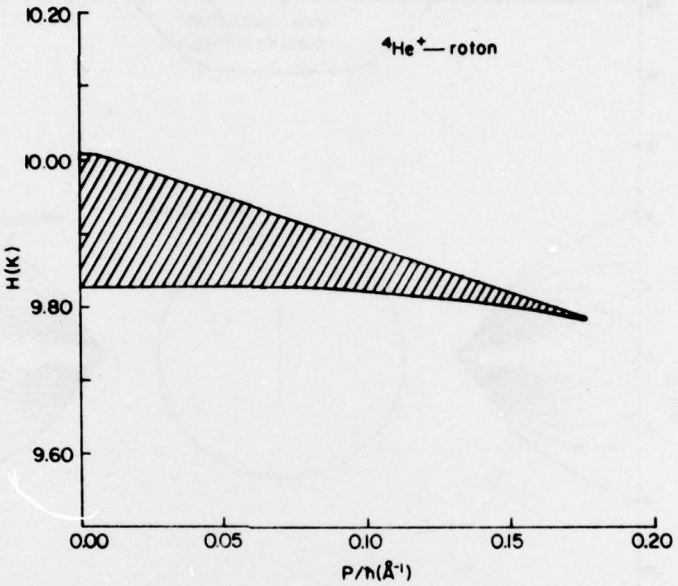

Fig. 7. The region of energy as a function of total momentum P for the positive-ion–roton containing solutions with negative interaction energy $H^{(12)}$.

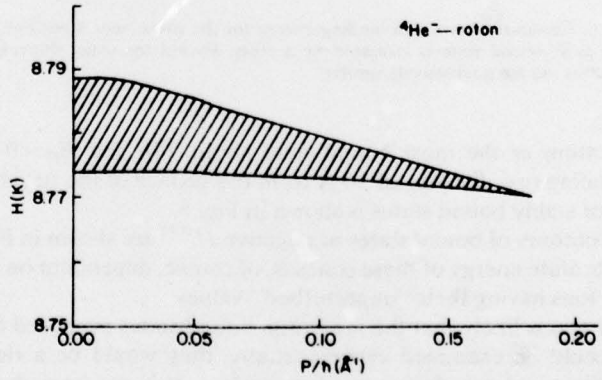

Fig. 8. The region of energy as a function of total momentum P for the negative-ion–roton containing solutions with negative interaction energy $H^{(12)}$.

densities exceeding $10^9\,\mathrm{cm}^{-3}$ are very difficult to achieve. The bound roton–ion complexes are not stable against motion in an electric field, as can be seen from Figs. 7 and 8. Once the total momentum has exceeded about $P = 0.2\ \text{Å}^{-1}$, the states are unstable.

The fraction of impurities having bound rotons is easily estimated from the law of mass action. The dominant quantity in this estimate is $\exp(-H/kT)$. Thus we do not expect a substantial number of impurities to form bound complexes with rotons in equilibrium.

ACKNOWLEDGMENT

We are grateful to James Gibbons for assistance in the early development of the numerical programs.

REFERENCES

1. J. S. Brooks and R. J. Donnelly, *J. Phys. Chem. Ref. Data* **6**, 51 (1977).
2. R. J. Donnelly and P. H. Roberts, *J. Low Temp. Phys.* **27**, 687 (1977).
3. P. H. Roberts and R. J. Donnelly, *J. Low Temp. Phys.* **15**, 1 (1974).
4. P. H. Roberts and W. J. Pardee, *J. Phys. A: Math., Nucl. Gen.* **7**, 1283 (1974).
5. R. J. Donnelly and P. H. Roberts, *Phys. Lett.* **43A**, 199 (1973).
6. R. J. Donnelly, R. W. Walden and P. H. Roberts, *J. Low Temp. Phys.* **31**, 375 (1978).
7. D. M. Strayer, R. J. Donnelly and P. H. Roberts, *Phys. Rev. Lett.* **26**, 165 (1971).
8. R. J. Donnelly and P. H. Roberts, *Phil. Trans. Roy. Soc. A* **271**, 6 (1971).
9. C. Ebner and D. O. Edwards, *Phys. Rep.* **2C**, 78 (1971).
10. P. A. Hilton, R. Scherm, and W. G. Stirling, *J. Low Temp. Phys.* **27**, 851 (1977).
11. C. M. Surko and R. E. Slusher, *Phys. Rev. Lett.* **30**, 1111 (1973).
12. R. L. Woerner, D. A. Rockwell, and T. J. Greytak, *Phys. Rev. Lett.* **30**, 1114 (1973).
13. M. J. Stephen and L. Mittag, *Phys. Rev. Lett.* **31**, 923 (1974).

VOLUME 42, NUMBER 11 PHYSICAL REVIEW LETTERS 12 MARCH 1979

Superflow in Restricted Geometries

R. J. Donnelly, R. N. Hills, and P. H. Roberts[a]
Institute of Theoretical Science and Department of Physics, University of Oregon, Eugene, Oregon 97403
(Received 16 October 1978)

We propose a "competing barrier model" for nucleation of quantized vortices in small channels. The results are compared to experiments on decay of persistent currents, critical velocities, onset temperatures, and the effective superfluid density at onset.

For a number of years experimentalists have tried to use the Iordanskiĭ-Langer-Fisher[1,2] (ILF) theory of fluctuation dissipation for superflow in an unbounded region (intrinsic nucleation) to fit experiments in restricted geometries. Several years ago, two of us (DR)[3] pointed out the necessity of considering a permanent barrier ΔE for flow in a restricted geometry which is present, irrespective of any superflow. For a toroidal channel of circular cross section with zero circulation, DR point out that the probability of nucleating to the wall a vortex of one sign is equal to that for a vortex of opposite circulation. However, when there is a superflow present, the energy barriers for nucleation of the two types of vortex are not the same: For a large superflow the process associated with one type of vortex will completely dominate the other, while for slower flows the nucleation of both types of vortex have to be considered. This is the "competing-barrier model" of nucleation.

In this Letter we show that the competing-barrier model will qualitatively explain experiments on decay of persistent currents as reported, for example, by Hallock and co-workers[4] and Kojima *et al.*[5] We confine ourselves to the broad issues using a simplified one-dimensional nucleation model, neglecting the geometrical differences among various sorts of porous materials and thin films.

The nucleation probability, P, per unit time can be written

$$P = f \exp(-\Delta F/kT), \tag{1}$$

where f is the temperature-dependent attempt frequency discussed and tabulated by DR and ΔF is the barrier height. For the ILF model, ΔF is due to the superflow alone. Here, $\Delta F = \Delta E$ when the superflow $v_s = 0$ and the critical momentum is then p_c. With a flow, the $\vec{p}\cdot\vec{v}_s$ interaction shifts the barrier and (considering only one dimension) we have $\Delta F = \Delta E \pm p_c v_s$ so that (1) becomes

$$P = 2f \exp(-\Delta E/kT) \sinh(p_c v_s/kT). \tag{2}$$

Equation (2) shows that the dimensionless quantity V ($\equiv p_c v_s/kT$), the ratio of ordered flow energy to fluctuation energy, is important.

Suppose the superflow takes place in a toroidal geometry containing n candidates per unit length for nucleation; then (cf. Ref. 3)

$$dv_s/dt = -nP\kappa, \tag{3}$$

where $\kappa \equiv h/m$. Equation (3) can be written nondimensionally as

$$dV/d\tau = -\sinh V \tag{4}$$

by introducing the dimensionless time $\tau = \nu_0 t$ and the nucleation rate ν_0:

$$\nu_0 = \nu \exp(-\Delta E/kT), \quad \nu = 2n\kappa f p_c/kT. \tag{5}$$

Equation (4) has the solution

$$V = \ln[(1 + e^{-\tau} \tanh V_0/2)/(1 - e^{-\tau} \tanh V_0/2)], \tag{6}$$

where V_0 is the value of V at $\tau = 0$. The character of (6) depends on the ranges of V_0 and τ.

For infinitesmal superflows, such as in "Nth sound" ($N = 2, 3, 4$), $V_0 \sim 0$ and (6) gives for all τ

$$V \cong \ln[(1+\tfrac{1}{2}V_0 e^{-\tau})/(1-\tfrac{1}{2}V_0 e^{-\tau})] \cong V_0 e^{-\tau}. \quad (7)$$

Thus all small superflows decay exponentially.

For $V_0 \sim \infty$ and $V \sim \infty$ simultaneously, $e^{-V} \cong \exp(-V_0)+\tau/2$ so that

$$V \cong V_0 \text{ (small } \tau), \quad (8a)$$

$$V \cong \ln(2/\tau) \text{ (large } \tau), \quad (8b)$$

and the dividing case occurs at τ_L obtained by equating the two estimates in (8):

$$\tau_L = 2\exp(-V_0). \quad (9)$$

For fixed τ (>0), V is independent of V_0 in the limit $V_0 \sim \infty$:

$$V \cong \ln\{(1+e^{-\tau})/(1-e^{-\tau})\} = \ln\coth(\tfrac{1}{2}\tau),$$

so that

$$V \cong \ln(2/\tau) \text{ (small } \tau), \quad (10a)$$

$$V \cong 2e^{-\tau} \text{ (large } \tau), \quad (10b)$$

and the dividing case occurs at τ_E obtained by equating the two estimates in (10):

$$\tau_E \cong 1. \quad (11)$$

The dimensionless times τ_L and τ_E are fundamental to our discussion: τ_E is universal and sets the lifetime of all superflows, while τ_L depends on V_0. The flow observed depends on the magnitude of τ. For $\tau \ll \tau_L$ the flow is almost steady; for $\tau_L \ll \tau \ll \tau_E$ the flow shows logarithmic behavior; for $\tau \gg \tau_E$ the flow decays exponentially. The number of decades of logarithmic behavior is given by $\log(\tau_E/\tau_L) \cong 0.43V_0 - 0.37$.

Figure 1 shows several examples of (6), the time evolution of finite superflows. In particular, the flow for $V_0 = 15$ has $\log\tau_L = -6.2$. Larger initial flows are independent of V_0 at $\log\tau = -6.2$, and and experimenter observing at this τ would term $V_0 = 15$ the "saturated critical velocity." Hence, the condition at time τ for a saturated critical velocity is given by $\tau = \tau_L$ and thus the notion of a saturated critical velocity depends crucially on the time of observation.

An experimenter using Nth sound as a probe for evidence of superfluidity would observe nothing for times larger than τ_E. Thus the condition for "onset of superfluidity" is given by $\tau = \tau_E$.

In order to make numerical calculations, we need estimates of ΔE, n, and f. Imagine a channel containing packed powder with a mean open dimension d. A vortex stretched between two grains will have an energy $E_A = (\rho_s \kappa^2 d/4\pi)\ln(d/a)$, where a is the vortex core parameter. When the line is moved into a semicircle, it will just touch the next grain, and then its energy is $E_c = (\rho_s \kappa^2 d/4)\ln(d/a)$. The "barrier" is given by $\Delta E = E_c - E_A$ and $p_c = \frac{1}{2}\rho_s \kappa \pi d^2$. To order one, we adopt for simplicity

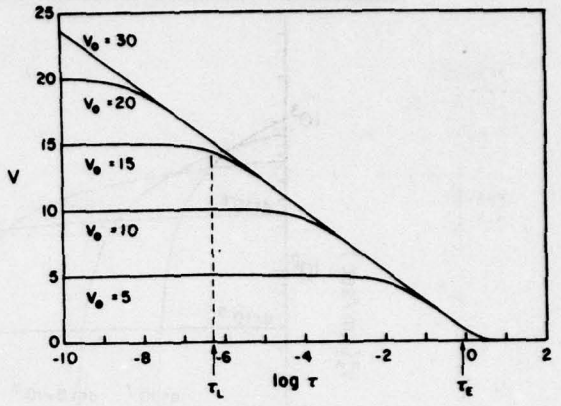

FIG. 1. Plot of Eq. (6) assuming $kT/p_c = 4$ and various values of the initial dimensionless velocity V_0. The dimensionless time showing the beginning of exponential decay τ_E is common to all curves. τ_L is shown for $V_0 = 15$. Initial flows greater than 15 have the same velocity near $\log\tau = -6$; initial flows less than 15 are "steady" for increasing periods as V_0 decreases.

$$\Delta E = (\rho_s \kappa^2 d/4\pi)\ln(d/a), \quad (12a)$$

$$p_c = \rho_s \kappa d^2. \quad (12b)$$

In the same spirit, since the preexponential factors are not important, we assume that n corresponds to one trapped vortex betwen each pair of grains, $n = 1/d$, while a constant value $f = 10^8$ sec^{-1} will suffice. For films we imagine the substrate contains a distribution of trapped vortex lines pinned between protuberances on the substrate. When a trapped line of length of order d moves into semicircle, it will just touch the free surface, forming a vortex of energy E_c as before. Thus the estimates of ΔE, f, and n may be retained for simplicity.

When a saturated current decays according to (8b), the slope of the decay is $dV/d\ln\tau = -1$, or

$$dv_s/d(\log t) = -kT\ln(10)/p_c. \quad (13)$$

Kojima *et al.*[5] observed a decay of 0.63% per decade of a saturated persistent current with $v_s = 67.7$ cm/sec at $t = 1$ sec, $T = 1.3$ K, and $d = 170$–

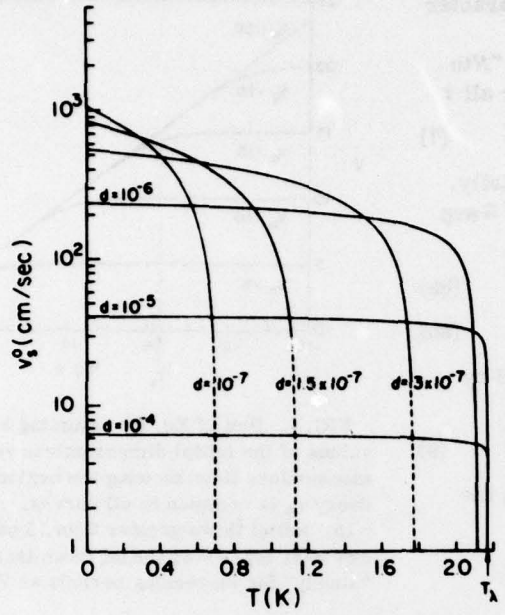

FIG. 2. Saturated velocities obtained from Eq. (14) at $t = 100$ sec for various channel sizes. Flows near onset will show decay as $V_0 \to 1$ (indicated by dashed lines).

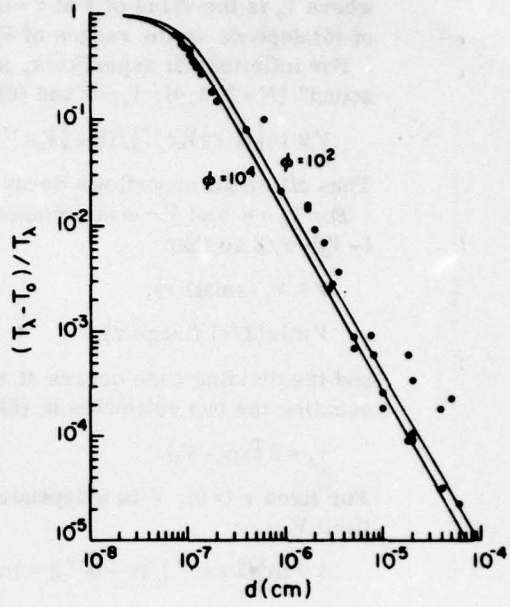

FIG. 3. Onset temperatures T_0 obtained from various channel sizes. Data from many sources.

325 Å. Thus $dv_s/d(\log t) = -6.3\times10^{-3}\times67.7$ or, by (13), $kT/p_c = 0.185$. For $d = 250$ Å we find, using (12b), that $kT/p_c = 0.208$ in good agreement with observation.

The condition that an initial velocity leads to a saturated flow is $\tau = \tau_L$, or $V_0 = \ln(2/\tau)$. Defining v_s^0 as the initial velocity corresponding to V_0, we find from (5) that $\tau = \tau_L$ becomes

$$v_s^0 = \Delta E/p_c - (kT/p_c)\ln(\nu t/2). \quad (14)$$

The first term $\Delta E/p_c = (\kappa/4\pi d)\ln(d/a)$ does not contain temperature explicitly and is a Feynman critical velocity.[6] By itself, it is appropriate only at very low temperatures, since the second term substracts from it, reducing the observed critical velocity. The results shown in Fig. 2 are in order-unity agreement with published results. They show the critical velocity approaching zero near the onset temperature $T_0 < T_\lambda$, to be discussed next.

The condition for the onset of superfluidity is $\tau = \tau_E$. If we express our observation time in terms of frequency $\varphi = t^{-1}$, this condition by (5) is $\nu_0 = \varphi\tau_E$ or

$$[\ln(d/a)/\ln(\nu/\varphi\tau_E)]\,(\rho_s d/T_0) = 4\pi k/\kappa^2, \quad (15)$$

which must be solved by iteration since ν and a are themselves temperature dependent. We show in Fig. 3 the results of T_0 as a function of d compared with the results of many experiments, taking typical values of $\varphi = 10^2$–10^4 Hz. The general agreement is quite satisfactory—below about 0.6 K our results are questionable since the corresponding films are very thin. T_0 increases weakly with φ.

Recently Nelson and Kosterlitz[7] showed that for two-dimensional superfluids the ratio of superfluid mass per unit area near the transition temperature T_0 is given by the exact result,

$$\rho_s(T_0^-)/T_0 = 8\pi k/\kappa^2. \quad (16)$$

Bishop and Reppy[8] and Rudnick[9] have shown that (16) gives a good account of their experiments over a wide range of temperatures and thicknesses identifying $\rho_s(T_0^-)$ with $\bar{\rho}_s d$. We can write (15) in the form (16) by adopting an effective superfluid density at onset:

$$\bar{\rho}_s = \rho_s\{2\ln(d/a)/\ln(\nu/\varphi\tau_E)\}. \quad (17)$$

We illustrate the behavior of $\bar{\rho}_s$ in Fig. 4: It has the usual property of vanishing at $T = 0$ and $T = T_\lambda$. For comparison one can show data quoted by Rudnick derived from third-sound measurements on thin films[9] and by Bishop and Reppy from measurements of $\rho_s(T_0^-)$.[8] Values of $\bar{\rho}_s$ were deduced

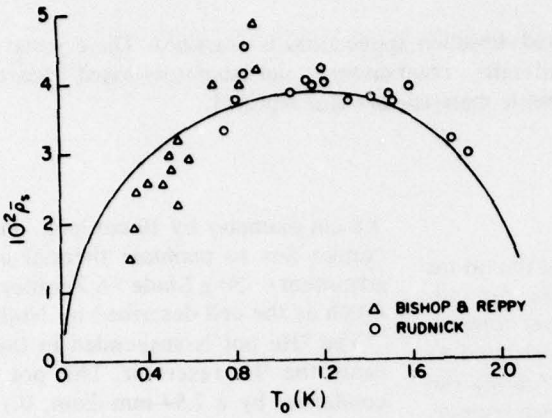

FIG. 4. The effective superfluid density at onset ρ_s calculated from Eq. (17) and compared with experiments of Rudnick (Ref. 9) and Bishop and Reppy (Ref. 8).

assuming the relationship between onset thickness d in atomic layers and T_0 is given by $T_0 = \beta(d - \alpha)$ with $\beta \simeq 1.5$ K per layer and $\alpha \simeq 1.4$ layers for $T_0 < 1$ K.

The works of Nelson and Kosterlitz,[7] Huberman, Myerson, and Doniach,[10] Ambegaokar, Halperin, Nelson, and Siggia,[11] and Myerson[12] address the problem of two-dimensional superfluidity with emphasis on the behavior near the transition. Reference 10 discusses a two-dimensional depairing model and Refs. 10 and 12 give a decay form which fits some of the film data quite well.[4] Reference 11 discusses a vortex depairing and recombination model and provides a detailed discussion of the experiments of Bishop and Reppy.[8] The present theory assumes three dimensions and requires a permanent barrier ΔE. It attempts to include behavior far from critical. Films so thin that the nucleation mechanism discussed above could not operate would have to be treated differently: In particular, the thickness of the film must be considerably greater than the healing length in the present model. We shall address these concerns more fully in a forthcoming article.

Evidence supporting the decay shape shown in Fig. 1 and the dependence of ν_0 and d and T will be presented elsewhere by D. Ekholm and R. B. Hallock, to whom we are indebted for experimental cooperation during the development of this theory. We are also grateful to J. Reppy and I. Rudnick for discussions of their experiments, and to B. Huberman, S. Doniach, E. Siggia, and V. Ambegaokar for the discussions of their theories.

This research was supported by National Science Foundation Grants No. NSF ENG 76-07354 and No. DMR 76-07354 and U. S. Air Force Office of Scientific Research Grant No. 76-2880.

---

[a] Permanent address: School of Mathematics, University of Newcastle upon Tyne, Newcastle upon Tyne, United Kingdom.

[1] S. V. Iordanskiĭ, Zh. Eksp. Teor. Fiz. 48, 708 (1965) [Sov. Phys. JETP 21, 467 (1965)].

[2] J. S. Langer and J. D. Reppy, in *Progress in Low Temperature Physics*, edited by C. J. Gorter (North-Holland, Amsterdam, 1970), Vol. VI, Chap. I.

[3] R. J. Donnelly and P. H. Roberts, Philos. Trans. Roy. Soc. A271, 41 (1970).

[4] K. L. Telschow and R. B. Hallock, Phys. Rev. Lett. 37, 1484 (1976); D. Ekholm and R. B. Hallock, J. Phys. (Paris), Colloq. 39, C6-306 (1978); R. B. Hallock, Bull. Am. Phys. Soc. 23, 536 (1978).

[5] H. Kojima, W. Veith, E. Guyon, and I. Rudnick, in *Low Temperature Physics, LT-13* (Plenum, New York, 1974), Vol. 1, p. 279.

[6] R. P. Feynman, *Progress in Low Temperature Physics*, edited by C. J. Gorter (North-Holland, Amsterdam, 1964), Vol. 1, p. 1.

[7] D. R. Nelson and J. M. Kosterlitz, Phys. Rev. Lett. 39, 1201 (1977).

[8] D. J. Bishop and J. D. Reppy, Phys. Rev. Lett. 40, 1727 (1978).

[9] I. Rudnick, Phys. Rev. Lett. 40, 1454 (1978).

[10] B. A. Huberman, R. J. Myerson, and S. Doniach, Phys. Rev. Lett. 40, 780 (1978).

[11] V. Ambegaokar, B. I. Halperin, D. R. Nelson, and E. D. Siggia, Phys. Rev. Lett. 40, 783 (1978).

[12] R. J. Myerson, Phys. Rev. B 18, 3204 (1978).

Portable ^{3}He detector cryostat for the far infrared

J. V. Radostitz, I. G. Nolt,[a] P. Kittel, and R. J. Donnelly

Department of Physics, University of Oregon, Eugene, Oregon 97403

(Received 26 September 1977)

A portable ^{3}He cryostat for far infrared detection applications is described. The cryostat has been used for a number of years in aircraft- , observatory- , and laboratory-based research. Some related studies of various bolometric materials are also reported.

I. INTRODUCTION

It has been recognized for a number of years that at far infrared wavelengths (100–1000 μm) there are advantages in operating bolometers at the lower temperatures provided by a pumped ^{3}He stage compared to a conventional 2K pumped ^{4}He cryostat.[1] Among the advantages, one can point to a higher resistance temperature factor, $d\ \ln R/dT$, faster response times, and the ability to use larger bolometer elements without compromising the response time. The latter properties arise because at the lower temperature (~0.3 K), the lattice specific heat of the bolometer element is greatly reduced.

The main disadvantage of the ^{3}He cryostat has been the size, weight, and power requirements imposed by the ^{3}He gas system.[1] The high cost of ^{3}He dictates a sealed system for retention of the ^{3}He gas. A first step in the evolution of the present design has been described by Nolt and Martin.[2] That cryostat was the first application of ^{3}He adsorption pump technology to an infrared bolometer cryostat, and the cryostat described here is an outgrowth of this earlier work. The present cryostat has been successfully employed for over six years in airborne-,[3] observatory-,[4] and laboratory-based applications.[5] A somewhat similar system has been independently developed by Chanin and Torre in France.[6] In this article, we describe the design and performance of the cryostat, studies of several bolometric materials made during the development of the cryostat, and the absolute flux calibration of the detector system using a new temperature-modulated cold source method.[5]

II. CRYOSTAT

Our design is shown in Fig. 1 and the specifications are listed in Table I. The ^{4}He Dewar is of welded stainless steel construction with a copper bottom plate affixed by means of a lead O-ring and screws. The outer can and vapor-cooled shielding are of welded aluminum. About ten layers of aluminized Mylar superinsulation was used to provide additional shielding. The condenser, the adsorption pump, and a ^{3}He stage control valve are inside the helium bath. This valve is a standard Hoke valve[7] which has been mass spectrometer leak tested at LN_2 temperatures and modified to be operated by a long screwdriver-like control inserted through the bath vent. The condenser is connected to the external gas storage cell by a capillary. The adsorption pump is 3.8 cm diameter by 10 cm long, and has internal radial copper fins to maintain thermal contact between the adsorbent (~50 g Linde 5A Zeolite) and the pump walls, much as the cell described by Nolt and Martin.[2]

The ^{3}He pot is suspended in the vacuum space beneath the ^{4}He reservoir. This pot is connected to the condenser by a 7.94-mm-diam, 0.15-mm-wall stainless steel tube 7.6 cm long which provides sufficient thermal isolation for the ^{3}He stage. The bolometer and integrating cavity are mounted directly on the ^{3}He pot where the thermal contact between the ^{3}He stage and the bolometer element is made by a 0.2-mm-diam gold wire. At 0.3 K the gold wire and the solder between the wire and the bolometer element are responsible for

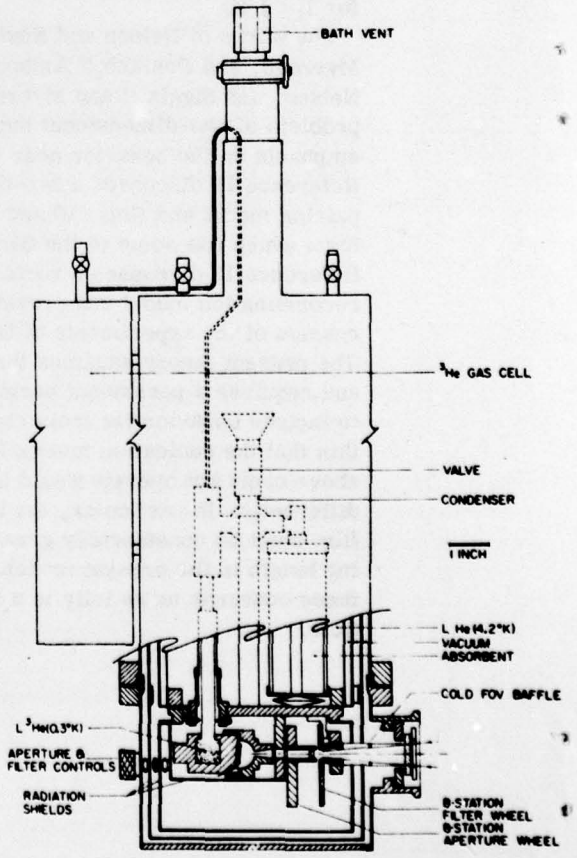

FIG. 1. Cutaway drawing of portable ^{3}He cryostat with bolometer and cooled optics.

 0034-6748/78/4901-0086$00.60

TABLE I. Cryostat specifications.

Quantity	^{4}He	^{3}He
Capacity	2.75 l (liquid)	3 l gas (STP)
Operating temperature	4.2 K	0.31 K
Operating hold time	12 h	>12 h
Weight	10 kg	
Approximate dimensions	15 × 20 × 55 cm	

almost all the heat capacity of our bolometer and thus govern the time constant of the detector.

Access to the photometer section is obtained by removing the bottom shields. Directly in front of the integrating cavity which contains the detector are an aperture wheel and a filter wheel cooled by thermal contact with the copper bottom plate of the cryostat (4.2 K). The positioning of these wheels by screwdriver-like rotors is done from outside the cryostat. The rotors are springloaded so that they are normally disengaged from the wheels to minimize heat leak. The vacuum in the photometer space is maintained by a small (~3 g) adsorption pump mounted on the ^{4}He cold plate.

The cryostat is precooled for several hours by a disposable charge of liquid nitrogen. After the liquid helium transfer, the cool down to 4 K and condensation takes about two hours. Once cold, the apparatus can be restarted in about half an hour. This is possible because the adsorbent cell rapidly outgasses at temperatures above ~10 K. In most applications we maintain the cryostat at liquid nitrogen temperatures between runs. Typical run times are 12 to 16 h, dependent on the radiative heat load.

III. DETECTOR

For bolometers, the ultimate limit of noise equivalent power (NEP) due to Johnson and phonon noise is[8]

$$\mathrm{NEP} \approx 4T(kG)^{1/2}, \tag{1}$$

where T is the temperature, k is Boltzmann's constant, and G is the thermal conductance between the bolometer and its temperature sink. The thermal time constant (τ) of a bolometer is given by the ratio C/G, where C is the total heat capacity of the bolometer. At ^{3}He temperatures, $C \propto T^3$ for the bolometer and $C \propto T$ for the solder and wire (gold) connections between the bolometer and the temperature bath. If the heat capacity of the bolometer dominates and the system has a fixed time constant, then the temperature dependence of the NEP will be

$$\mathrm{NEP} \propto T^{5/2}. \tag{2}$$

However, if the gold and solder have the dominant heat capacity, then

$$\mathrm{NEP} \propto T^{3/2}. \tag{3}$$

In either case, there is a clear advantage in going to lower temperatures.

There is another important advantage in certain applications. This is the ability to clamp the bolometer rigidly in position. We have clamped the bolometer using a layer of 6.4-μm-thick Mylar for electrical and thermal insulation. This thermal insulation is sufficient, probably because the Kapitza resistance through the Mylar is much larger than the thermal resistance of the gold wire link. Clamping the bolometer in this way reduces the possibility of microphonic noise and protects the bolometer from high gravity or vibratory forces.

In selecting a suitable material for a bolometer, we measured the resistance as a function of temperature for a variety of semiconductor samples. The results were analyzed in the way suggested by Zwerdling *et al.*[9] The data were fitted to an expression of the form

$$R = R_0 \exp(T_g/T), \tag{4}$$

where kT_g is the effective energy gap. From this, the esistance-temperature factor

$$\alpha = d \ln R/dT$$
$$= T_g T^{-2} \tag{5}$$

is calculated. The results of our measurements are shown in Fig. 2 and Table II. The material we selected for permanent mounting was sample number 5. The selection was made to maximize α while maintaining a reasonable bolometer resistance. The performance of this detector is summarized in Table III. The optical responsivity and NEP were measured using the cryogenic-temperature modulated source (CTMS) technique.[5] The

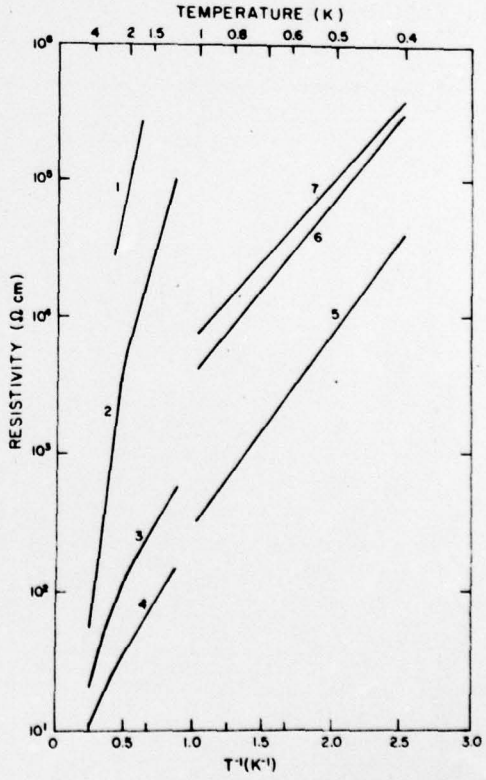

FIG. 2. Resistivity versus inverse temperature plots of tested bolometer materials. The numbers refer to the list of materials in Table II.

TABLE II. Resistance-temperature coefficients

Reference number	Material	Nominal resistivity[a] (Ω cm)	Effective energy gap Tg (K)	$\alpha = d \ln R/dT$ at T_0	
1	Ge:Ga[b]	—	12.0	3.0	2.0
2	Ge:Ga	0.08	8.5	3.8	1.5
3	Ge:InSb	0.18–0.23	4.0	1.8	1.5
4	Ge:(?)	0.2	4.0	1.7	1.5
5	Ge:InSb[c]	—	3.20	20 (24)[e]	0.4
6	Ge:Ga	0.1–0.2	2.9	18	0.4
7	Si:(?)[d]	250 at 4.2 K	2.6	17	0.4

[a] As given by supplier for room temperature.
[b] Infrared Industries, Inc., Tucson, AR.
[c] Present material used in our bolometer.
[d] Molectron, Inc., Sunnyvale, CA.
[e] Calculated from measurements on the same material boule by Drew and Sievers.

TABLE III. Submillimeter detector characteristics

Size	2 × 1.5 × 10 mm
Time constant	4 ms
Thermal conductance	16 mW/K
Optical responsivity	$(2 \pm 1) \times 10^6$ V/W
System noise	50 nV $Hz^{-1/2}$
Optical NEP	$(2.5 \pm 1) \times 10^{-14}$ W $Hz^{-1/2}$
Electrical responsivity	1×10^6 V/W

low NEP confirms the apparent efficient absorption of this bolometer. The measurements suggest that the "optical" NEP may be better than that estimated from electrical measurements. This may be due to the difference between the absorption of energy by the two methods.

On the basis of the experience we have gained from this work, we believe that further advances can be made. Our current efforts are directed toward a ^{3}He cryostat which requires no external power or pumping even while starting up, a ^{3}He cryostat that will work in the absence of gravity, and the use of the CTMS technique to measure the spectral characteristics of the absorptivity of bolometric materials.

ACKNOWLEDGMENT

This research was supported in part by NASA grant NGR 38-003-021 and Air Force grant AFOSR-71-1999.

[a] Present address: Mail Code R31, Environmental Research Laboratories, NOAA, Boulder, Colorado 80302.

[1] H. D. Drew and A. J. Sievers, Appl. Opt. **8**, 2067 (1969).
[2] I. G. Nolt and T. Z. Martin, Rev. Sci. Instrum. **42**, 1031 (1971).
[3] I. G. Nolt, J. V. Radostitz, and R. J. Donnelly, Nature **236**, 444 (1972).
[4] I. G. Nolt, J. V. Radostitz, R. J. Donnelly, R. E. Murphy, and H. C. Ford, Nature **248**, 659 (1974).
[5] I. G. Nolt, J. V. Radostitz, P. Kittel, and R. J. Donnelly, Rev. Sci. Instrum. **48**, 700 (1977).
[6] G. Chanin and J. P. Torre, *Sixth International Cryogenic Eng. Conf.* (IPC Science and Technology Press, Guildford, 1976), pp. 96–98: "Operating Performance of He^3-Cooled Bolometers," preprint.
[7] Hoke valve H4111M2B, Hoke Inc., Cresskill, NJ.
[8] F. J. Low, J. Opt. Soc. Am. **51**, 1400 (1961).
[9] S. Zwerdling, R. A. Smith, and J. P. Theriault, Infrared Phys. **8**, 271 (1968).